LITHIUM IONIC

BANDEIRA LITHIUM PROJECT

ARAÇUAÍ–ITINGA MINAS GERAIS, BRAZIL



NATIONAL INSTRUMENT 43-101 TECHNICAL REPORT—DEFINITIVE FEASIBILITY STUDY UPDATE

Prepared by:

Brian Colin Talbot, BSc (Hons), FAusIMM
Carlos José Evangelista Silva, P.Geo., MSc, AIG
Hugo Ribeiro de Andrade Filho, P.Eng., FAusIMM
Juliano Lima, MAIG (CP)
Porfírio Cabaleiro Rodriguez, P.Eng., BSc, FAIG
João Augusto Hilário de Souza, B.A., MSc., MBA
Noel O´Brien, BE(Met), MBA, FAusIMM
Bernardo Horta de Cerqueira Viana, MBA, FAIG

Effective Date: September 17, 2025

Report Date: October 31, 2025

CONTENTS

1 EXECUTIVE SUMMARY 1-1
1.1 Key Facts 1-1
1.2 Introduction 1-1
1.3 Reliance on Other Experts 1-2
1.4 Property Description and Location 1-2
1.5 Accessibility, Climate, Local Resources, Infrastructure, and Physiography 1-4
1.6 History 1-4
1.7 Geological Setting and Mineralization 1-5
1.8 Deposit Types 1-6
1.9 Exploration 1-7
1.10 Drilling 1-7
1.11 Sample Preparation, Analysis, and Security 1-8
1.12 Data Verification 1-8
1.13 Mineral Processing and Metallurgical Testing 1-9
1.14 Mineral Resources Estimate 1-9
1.15 Mineral Reserve Estimate 1-10
1.16 Mining Methods 1-11
1.17 Recovery Methods 1-12
1.18 Project Infrastructure 1-14
1.19 Market Studies 1-16
1.20 Environmental Studies, Permitting, and Social Impact 1-17
1.21 Capital and Operating Costs 1-18
1.22 Economic Analysis 1-19
1.23 Adjacent Properties 1-21
1.24 Other Relevant Data and Information 1-21
1.25 Interpretation and Conclusions 1-21
1.26 Recommendations 1-22
2 INTRODUCTION 2-1
2.1 Terms of Reference 2-1
2.2 Site Visits 2-1
2.3 Project Overview 2-1
2.4 Qualified Persons 2-2
2.5 Units of Measure and Currency 2-3
3 RELIANCE ON OTHER EXPERTS 3-1
3.1 Marketing 3-1
3.2 Environmental Licensing and Studies 3-1
3.3 Taxation 3-1
3.4 Mineral Rights 3-1
4 PROPERTY DESCRIPTION AND LOCATION 4-1
4.1 Mineral Rights 4-2
4.2 Brazilian Mineral Exploration and Mine Concession 4-2
4.3 Surface Rights 4-2
4.4 Agreements 4-2
4.5 Royalties 4-3
4.5.1 CFEM Royalty 4-3
4.5.2 Landowner's Statutory Royalty 4-3
4.5.3 Royalties Agreements 4-3

4.6 Environmental Liabilities 4-3
4.7 Qualified Person's Comment 4-3
5 ACCESSIBILITY, CLIMATE, LOCAL RESOURCES, INFRASTRUCTURE AND PHYSIOGRAPHY 5-1
5.1 Accessibility 5-1
5.2 Climate 5-3
5.3 Local Resources and Infrastructure 5-5
5.4 Physiography 5-5
6 HISTORY 6-1
6.1 Project History 6-1
6.2 Production History 6-1
7 GEOLOGICAL SETTING AND MINERALIZATION 7-1
7.1 Regional Geology 7-1
7.1.1 Pegmatites 7-4
7.2 Structural Geology 7-8
7.3 Prospective-Exploration Model 7-13
7.4 Bandeira's Mineralization Model 7-18
8 DEPOSIT TYPES 8-1
9 EXPLORATION 9-1
9.1 Rock Chip Sampling 9-1
9.2 Soil Sampling Program 9-2
9.3 Trenching Program 9-3
9.4 Structural Analysis 9-6
9.5 Geophysical Surveys 9-8
10 DRILLING 10-1
10.1 MGLIT Drilling Campaigns 10-1
10.2 Drill Type 10-1
10.3 MGLIT Drilling Campaigns 10-1
10.4 Drill-Collar Monuments 10-1
10.5 Drill-Hole Surveying 10-3
10.6 Core Orientation 10-3
10.7 Drill-Core Chain of Custody 10-4
10.8 Core-Logging Procedures 10-4
10.9 Ore Drilling Intercepts 10-8
10.10 Qualified Person's Comments 10-17
11 SAMPLE PREPARATION, ANALYSIS, AND SECURITY 11-1
11.1 Sampling 11-1
11.2 Sample Preparation, Control, and Custody 11-2
11.3 Density Measurements 11-2
11.4 Sample Preparation 11-3
11.5 Sample Analysis 11-3
11.6 Quality Assurance and Quality Control 11-3
11.6.1 Preparation Blank—Coarse Blank 11-5
11.6.2 Analytical Blank—Fine Blank 11-6
11.6.3 Certified or Standard Reference Material—CRM/SRM 11-8
11.6.4 Crushed Duplicates 11-10
11.6.5 Pulverized Duplicates 11-11
11.6.6 Check Assay 11-12
11.7 Qualified Person's Opinion 11-14

12 DATA VERIFICATION 12-1
12.1 Qualified Person's Verification 12-1
12.2 Qualified Person's Opinion 12-10
13 MINERAL PROCESSING AND METALLURGICAL TESTING 13-1
13.1 Ore Mineralogical Characterization 13-1
13.2 Ore Chemical Analysis 13-2
13.3 Metallurgical Testing 13-3
13.3.1 Preliminary Heavy Liquid Separation Tests at SGS Geosol—HLS Series 1, December 2022 13-7
13.3.2 New Set of HLS Tests—June 2025 13-11
13.3.3 Ore Variability 13-13
13.3.4 Flotation Testing 13-28
13.3.5 Vendor Tests 13-29
13.3.6 Upgrading Fines by Gravity 13-35
13.4 Pilot Plant—Ore Sorter (Steinert) and Dense Media Separation (SGS Geosol) 13-36
13.4.1 Ore Sorter Pilot Plant and HLS 13-36
13.4.2 DMS Pilot Plant (SGS Geosol) Results 13-41
13.5 Conclusions 13-48
14 MINERAL RESOURCE ESTIMATES 14-1
14.1 Drilling Database 14-1
14.2 Geological Modelling 14-2
14.3 Geostatistical Structural Analysis 14-5
14.3.1 Sample Regularization 14-5
14.3.2 Exploratory Data Analysis 14-6
14.3.3 Variographic Analysis 14-9
14.4 Block Model 14-9
14.5 Grade Estimation 14-12
14.6 Estimation Validation 14-13
14.7 Density 14-13
14.8 Classification of Mineral Resources 14-19
15 MINERAL RESERVE ESTIMATES 15-1
15.1 Cut-Off Grade 15-1
15.2 Pit Shell Selection 15-3
15.3 Underground Mineral Reserve Estimates 15-3
16 MINING METHODS 16-1
16.1 Geotechnical Appraisal 16-1
16.1.1 Domaining and Geotechnical Characterization 16-1
16.1.2 Residual Soil and Saprolite Domain 16-7
16.1.3 Sap Rock and Weathered Rock Domain 16-11
16.1.4 Slightly Altered and Fresh Rock Domain 16-14
16.2 Fresh Rock Domains 16-15
16.2.1 Schist Domain (Salinas Formation) 16-15
16.2.2 Pegmatite Domain (Ore) 16-19
16.3 Mining Method 16-21
16.3.1 Open-Pit Geotechnical Design Parameters 16-22
16.3.2 Soil Domain—Bench-Scale Analysis 16-26
16.3.3 Schist Domain—Bench-Scale Analysis 16-29
16.3.4 2-D Limit Equilibrium Analyses—Interramp and Overall Slope Scale 16-33
16.3.5 Underground Mine 16-41
16.3.6 Regional Hydrogeological Context 16-52

16.3.7 Conceptual Hydrogeological Model 16-54
16.3.8 Conditions of Groundwater Flow 16-57
16.4 Mine Planning and Design 16-59
16.4.1 Open-Pit Mining 16-59
16.4.2 Underground Mine 16-62
16.4.3 Mine Design Parameters 16-64
16.4.4 Stope Optimization 16-66
16.4.5 Mining Development 16-71
16.4.6 Stoping Activities 16-74
16.4.7 Mining Schedule 16-74
16.5 Waste-Rock Dump and Dry-Tailings Management 16-84
16.5.1 Waste-Rock Dump Sequencing 16-84
16.5.2 Dry-Tailings Deposition 16-84
16.5.3 Integration of Waste and Tailings Management 16-84
16.6 Mine Equipment 16-87
16.6.1 Mine Production Equipment 16-87
16.6.2 Drilling Equipment 16-87
16.6.3 Loading and Haulage Equipment 16-88
16.6.4 Auxiliary Equipment 16-89
16.6.5 Fleet Sizing 16-90
16.7 Drilling and Blasting Plan 16-91
16.7.1 Longhole Drilling and Blasting 16-91
16.7.2 Slot-Raise Drilling and Blasting 16-91
16.8 Roof Support 16-94
16.8.1 Sublevel Stopes 16-94
16.8.2 Development 16-95
16.9 Backfilling 16-96
16.10 Mine Services 16-96
16.10.1 Ventilation 16-96
16.10.2 Airflow Requirement 16-96
16.10.3 Ventilation Design 16-98
16.10.4 Mine Project Stage—Ventilation Planning 16-100
16.10.5 Mine Production Stage—Ventilation Planning 16-102
16.11 Electric Power System 16-105
16.11.1 Electrical Loads in Underground Mining 16-105
16.11.2 Surface Substation 16-105
16.11.3 Underground Substations 16-109
16.11.4 Service Water 16-110
16.11.5 Water Sources 16-110
16.11.6 Compressed Air 16-111
16.11.7 Communication 16-111
16.11.8 Explosives Storage and Handling 16-112
16.11.9 Fuel Storage and Handling 16-114
16.11.10 Mining Quality Control 16-115
16.11.11 Mine Personnel 16-115
16.12 Safety and Emergency 16-118
16.12.1 Safety and Emergency Measures 16-118

17 RECOVERY METHODS 17-1

17.1 Crushing 17-6
17.2 Fines Thickening and Filtration (−0.60 mm) 17-7
17.3 DMS Modular Circuits 17-8
17.4 Chemical Laboratory 17-9

18 PROJECT INFRASTRUCTURE 18-1
18.1 Plateaus and Accesses 18-1
18.2 Earthworks 18-1
18.2.1 Drainage and Stormwater 18-2
18.3 Process Plant, Operational Area, and Buildings 18-3
18.3.1 Architectural Concept 18-3
18.3.2 Project Areas, Descriptions, and Scope 18-3
18.3.3 Building Sizing 18-7
18.3.4 Processing Plant Layout 18-12
18.3.5 Platework 18-13
18.3.6 Utility Systems 18-13
18.3.7 Raw Water Extraction 18-13
18.3.8 Water Treatment System 18-13
18.3.9 Reclaimed Process Water System 18-13
18.3.10 Sewage Treatment System 18-13
18.3.11 Oily-Effluent Treatment Plant 18-13
18.3.12 Fire Control System 18-14
18.3.13 Compressed-Air Generation and Distribution System 18-14
18.4 Metallic Structures 18-14
18.5 Concrete 18-15
18.6 Electrical 18-16
18.7 Instrumentation, Control, and Automation 18-17
18.8 Telecommunications Systems 18-17
18.8.1 Underground Communication 18-18
18.8.2 System Architecture 18-18
18.8.3 Infrastructure Components 18-18
18.8.4 System Capabilities 18-18
18.8.5 Safety and Redundancy 18-19
18.9 Civils Geotechnical 18-19
18.10 Piping 18-20
18.11 Construction 18-20
18.11.1 Construction Strategy 18-20
18.11.2 General Objectives 18-20
18.11.3 Project's Main Milestones 18-20
18.12 Bandeira Waste Dump and Tailings Storage Facilities 18-23
18.12.1 Reference Documents 18-24
18.12.2 Geotechnical Aspects 18-25
18.12.3 Investigations in the Area 18-26
18.12.4 Main Features of the Storage Facility Foundation 18-27
18.12.5 Seismic Risk 18-27
18.12.6 Cleaning and Treatment of the Foundation 18-29
18.12.7 Internal Drainage and Superficial Drainage 18-30
18.12.8 Geometric Design 18-30
18.12.9 Stack Formation Sequence 18-31
18.12.10 Stability Analysis 18-33
18.12.11 Instrumentation 18-38
18.12.12 Sediment Containment Ponds 18-38
18.12.13 Description of the Bottom Drainage System Project 18-41
18.13 Waste Dumps—Conclusions and Recommendations 18-43
19 MARKET STUDIES AND CONTRACTS 19-1
19.1 Macroeconomic Outlook and Lithium 19-1
19.2 Lithium Price Forecast 19-1

19.3 Contracts 19-2
19.4 Qualified Person's Comment 19-2
20 ENVIRONMENTAL STUDIES, PERMITTING, AND COMMUNITY IMPACTS 20-1
20.1 Regulatory and Permitting Framework 20-1
20.2 Mining and Environmental Licensing Approvals 20-3
20.2.1 Land Access and Occupation 20-6
20.3 Mine Closure 20-8
20.4 Summary of Socio-Environmental Diagnosis 20-9
20.5 Environmental and Social Management Plan 20-10
21 CAPITAL AND OPERATING COSTS 21-1
21.1 Basis of Estimates 21-1
21.1.1 Estimate Price Source 21-1
21.2 Work Breakdown Structure 21-2
21.3 Estimate Plan 21-3
21.4 Capital Cost 21-3
21.4.1 Capital Cost Estimation 21-3
21.4.2 Financial Operation—ECA Equipment Financing (SANDVIK) 21-4
21.4.3 Summary of Main Quantities 21-4
21.4.4 Contingency 21-6
21.4.5 Taxes 21-6
21.4.6 Exclusions 21-6
21.4.7 Mine Capital Cost Estimation 21-6
21.4.8 Underground Development and Infrastructure 21-7
21.4.9 Surface Capital Cost 21-7
21.4.10 Sustaining Capital Cost 21-8
21.5 Operating Costs 21-9
21.5.1 Operating Cost Summary 21-9
21.5.2 Operating Cost Detail 21-9
21.5.3 Labour 21-11
21.5.4 Consumables 21-11
21.5.5 Electrical Energy 21-12
21.5.6 Plant Maintenance 21-12
21.5.7 Plant Services 21-12
22 ECONOMIC ANALYSIS 22-1
22.1 Main Assumptions and Parameters 22-1
22.1.1 Production 22-1
22.1.2 Initial Capital Cost 22-2
22.1.3 Sustaining CAPEX and Mine Closure 22-3
22.1.4 Operating Costs 22-4
22.1.5 Spodumene Concentrate Transportation 22-6
22.1.6 Royalties and Deductions 22-6
22.1.7 Revenue 22-6
22.1.8 Taxation 22-7
22.1.9 Evaluation Base-Date and Exchange Rate 22-10
22.2 Cash-Flow Analysis 22-11
22.3 Sensitivity Analysis 22-11
22.3.1 Sensitivity Analysis to Key Input Variables—After Tax, Unlevered NPV, and IRR 22-12
22.3.2 Sensitivity Analysis—NPV x Discount Rate 22-14
22.4 Financial Projections 22-14

23 ADJACENT PROPERTIES 23-1

24 OTHER RELEVANT INFORMATION 24-1

24.1 Cooperation Agreement with the Government of Minas Gerais 24-1
24.2 Electric Power Connection Agreement 24-1
24.3 Minas Gerais State Tax Exemption 24-1
24.4 Lithium Decree of 1997 24-1

25 INTERPRETATION AND CONCLUSIONS 25-1

25.1 Geology and Mineral Resources 25-1
25.2 Industrial Plant 25-2
25.3 Infrastructure 25-2
25.4 Water Management 25-3
25.5 Underground Mine 25-3
25.6 Geotechnical and Hydrogeology 25-3
25.7 Mineral Reserves Estimate and Mining Methods 25-4
25.8 Environment 25-5
25.9 Capital Cost Estimate 25-5
25.10 Operating Cost Estimate 25-5
25.11 Economic Analysis 25-6

26 RECOMMENDATIONS 26-1

26.1 Geology and Mineral Resource Estimate 26-1
26.2 Mineral Reserves Estimate and Mining Methods 26-1
26.3 Project Infrastructure 26-1
26.3.1 Bridge Over the Piauí River 26-1
26.4 Processing Plant 26-2
26.4.1 Processing Alternatives 26-2
26.5 Environmental Feasibility Assessment 26-2

27 REFERENCES 27-1

28 CERTIFICATE OF AUTHORS 28-1

28.1 Brian Colin Talbot, Chemical Engineer, BSc (Hons), FAusIMM 28-1
28.2 Carlos José Evangelista Silva, P.Geo., MSc, AIG 28-2
28.3 Hugo Ribeiro de Andrade Filho, P.Eng., FAusIMM 28-3
28.4 Juliano Felix de Lima, MAIG (CP) 28-4
28.5 Porfirio Cabaleiro Rodriguez, P.Eng., BSc, FAIG 28-5
28.6 João Augusto Hilário de Souza, B.A.Sc., MBA 28-6
28.7 Noel Mark O'Brien, BE(Met), MBA, FAusIMM 28-7
28.8 Bernardo Horta de Cerqueira Viana, MBA, FAIG 28-8

TABLES

Table 1-1: Qualified Persons, Qualifications, Affiliations, and Site Visits 1-2
Table 1-2: Bandeira Diamond Drill-Hole Summary 1-7
Table 1-3: Bandeira Mineral Resource Estimates (Base-Case Cut-Off Grade of 0.5 % Li_2O) 1-10
Table 1-4: Project Mineral Reserve, Dated September 22, 2025 1-11
Table 1-5: AACE Class 3 Capital Cost Estimate 1-18
Table 1-6: Operating Cost Summary—Per Tonne of Spodumene Concentrate 1-19
Table 1-7: Financial Results Summary 1-20
Table 2-1: Qualified Persons, Qualifications, Affiliations, and Site Visits 2-1
Table 2-2: Qualified Person Areas of Responsibility 2-3
Table 4-1: Project Mineral Rights 4-2

Table 7-1: Main Features of the Orogenic Igneous Supersuites of the Araçuaí Orogen 7-5
Table 7-2: Features of the Main Pegmatite Districts of the Eastern Brazilian Pegmatite Province 7-7
Table 9-1: Summary of Trenches Excavated in the Bandeira Deposit (X, Y, Z Coordinates—UTM Zone 24 South (Sirgas 2000) 9-3
Table 10-1: Bandeira Diamond Drill-Hole Summary 10-1
Table 10-2: Project Drill Collars 10-5
Table 10-3: Project Drill Collars 10-6
Table 10-4: Project Drill Collars 10-7
Table 10-5: Mineralized Intercepts by Bandeira Drill Holes 10-9
Table 10-6: Mineralized Intercepts by Bandeira Drill Holes 10-10
Table 10-7: Bandeira 2022–2024 Diamond Drill Holes 10-11
Table 10-8: Mineralized Intercepts by Bandeira Drill Holes 10-12
Table 10-9: Mineralized Intercepts by Bandeira Drill Holes 10-13
Table 10-10: Mineralized Intercepts by Bandeira Drill Holes 10-14
Table 11-1: QA/QC Program Summary 11-4
Table 13-1: Lithium Minerals Characteristics 13-1
Table 13-2: Average Mineralogical Composition for Seven Metallurgical Drill Holes (XRD, Rietveld Method) 13-2
Table 13-3: Average Chemical Composition for Metallurgical Drill Holes 13-2
Table 13-4: Metallurgical Tests Performed 13-3
Table 13-5: Chemical Analysis for the Seven Drill Holes and Two Composites (Phase 1) 13-13
Table 13-6: Mineralogical Analysis by XRD (Rietveld) for the Seven Drill Holes (Wt%) (Phase 1) 13-14
Table 13-7: Chemical Analysis for the Fifteen Samples (Phase 2) 13-14
Table 13-8: Chemical Analysis for the Samples (Phase 3) 13-14
Table 13-9: HLS Results for Coarse Fraction (−12.7 +6.35 mm) 13-16
Table 13-10: HLS Results for Fine Fraction (−6.35 +0.85 mm) 13-16
Table 13-11: HLS Rougher Step Results 13-24
Table 13-12: HLS Scavenger Step Results 13-25
Table 13-13: Polishing HLS Results 13-25
Table 13-14: HLS Results Simulating the Process Flowsheet 13-27
Table 13-15: Indicative Flotation Results 13-28
Table 13-16: Flotation Locked Cycle Test Results—Eight Cycles 13-28
Table 13-17: Ore Sorter Results for the −31.5 +19.1 mm Size Fraction 13-30
Table 13-18: Ore Sorter Results for the −19.1 + 9.5 mm Size Fraction 13-30
Table 13-19: Ore Sorter Results for the −19.1 +9.5 mm Size Fraction (ITDD-22-054) 13-30
Table 13-20: Ore Sorter Results for the Size Fraction of −19.1 +9.5 mm (ITDD-22-098) 13-31
Table 13-21: Ore Sorter Results for the −31.5 +19.1 mm Size Fraction (ITDD-22-054) 13-31
Table 13-22: Ore Sorter Results for the −31.5 +19 mm Size Fraction (ITDD-22-098) 13-31
Table 13-23: Average CWi Results for the Bond Low-Energy Impact Tests 13-32
Table 13-24: Bond Low-Energy Impact Testwork Statistics 13-32
Table 13-25: Crushability Tests Results 13-33
Table 13-26: HGS Magnetic Separation Chemical Results for the Blended Sample 13-34
Table 13-27: Spirals Results for Fines Concentration 13-35
Table 13-28: Ore Sorter Pilot Plant Results 13-39
Table 13-29: HLS Results for Each Particle-size Range for Spodumene Liberation (Li_2O Dist. %) 13-39
Table 13-30: Accumulated HLS Results by Particle Size 13-39
Table 13-31: Rougher Testwork Results and Metallurgical Recovery 13-48
Table 14-1: Li_2O (%) Spodumene Pegmatite Vein Model Statistics 14-7
Table 14-2: Variographic Parameters 14-9
Table 14-3: Block Model Dimensions 14-9
Table 14-4: Block Model Variables Summary 14-10
Table 14-5: OK Parameters 14-13
Table 14-6: Density Values 14-14
Table 14-7: Financial Assumptions 14-20

Table 14-8: Expected Costs 14-20
Table 14-9: Operational Parameters 14-20
Table 14-10: Cut-Off Grade 14-20
Table 14-11: Bandeira Mineral Resource Estimates (Base-Case Cut-Off Grade of 0.5% Li_2O) 14-21
Table 15-1: Project Mineral Reserves 15-1
Table 15-2: Open Pit Cut-off Grade Calculation 15-2
Table 15-3: Underground Cut-off Grade Calculation 15-2
Table 15-4: Pit Optimization Results 15-3
Table 16-1: Average Orientation of Project Structures 16-5
Table 16-2: Rock Mass Rating Ranges 16-6
Table 16-3: Q-System Rock Mass Quality Range 16-7
Table 16-4: Degree of Weathering of the Rock Mass 16-8
Table 16-5: Consistency According to ISRM Standards 16-9
Table 16-6: Typical FOS Acceptance Criteria Values 16-23
Table 16-7: Summary of Bench-Scale Stability Analysis for All Design Sectors 16-28
Table 16-8: Probability of Failure for the Pit Design Sectors—Markland Test 16-30
Table 16-9: Stability Analysis Results for the Highest Probabilities of Failure in the Pit Design Sectors 16-31
Table 16-10: Parameters Adopted in the 2-D Analyses 16-33
Table 16-11: Min FOS for Open Pit Global-Scale Analysis 16-36
Table 16-12: FOS by Scale for the Open Pit Sections that Present a Minimum FOS <1.5 16-37
Table 16-13: Calculated Hanging-Wall Induced Stresses and Rock Stress Factor A 16-44
Table 16-14: Calculated Modified Stability Number for All Depth Ranges 16-46
Table 16-15: Sensitivity Analysis for Crown Pillar Height 16-49
Table 16-16: Structural Data and Strength Parameters for Discontinuities 16-50
Table 16-17: Rebar Properties Considered in Wedge Limit Equilibrium Assessment 16-51
Table 16-18: Project Ground-Support Recommendation 16-51
Table 16-19: Packer Tests Results 16-55
Table 16-20: Open-Pit Designed Results, Including Waste and Mineral Resources 16-59
Table 16-21: Sublevel Stoping Geotechnical Parameters 16-65
Table 16-22: Optimization Parameters 16-67
Table 16-23: Underground Mineable Stopes 16-68
Table 16-24: Underground Stope Optimization Results 16-70
Table 16-25: First-Pass Parameters in the Stope Optimization 16-70
Table 16-26: Total Production Profile 16-71
Table 16-27: Length of Underground Development Structures (m/a) 16-73
Table 16-28: Mine Scheduling—Development Rates 16-74
Table 16-29: Stoping Activities Specific Values Based on Tonnes per Day 16-75
Table 16-30: Quantities Required for Derived Activities in Drilled Metres 16-75
Table 16-31: Daily Production Rates 16-75
Table 16-32: Time Duration of Each Activity 16-76
Table 16-33: Stope Requirement 16-76
Table 16-34: Mine Scheduling—Production Plan 16-77
Table 16-35: Waste and Tailings Schedule (Tonnes per Year) 16-86
Table 16-36: Mine Production Equipment 16-87
Table 16-37: Fandrill Productivity Parameters and Annual Unit Production 16-88
Table 16-38: Cable Bolter Productivity Parameters and Annual Unit Production 16-88
Table 16-39: Jumbo Productivity 16-88
Table 16-40: Slot Raiseborer Productivity Parameters and Annual Unit Production 16-88
Table 16-41: LHD Productivity Parameters 16-89
Table 16-42: Truck Productivity Parameters 16-89
Table 16-43: Mining Auxiliary Equipment 16-90
Table 16-44: Mining Equipment Fleet Sizing 16-90
Table 16-45: Longhole Drilling and Blasting Plan 16-91

Table 16-46: Slot-Raise Drilling and Blasting Plan 16-92
Table 16-47: Development Drilling and Blasting Plan 16-92
Table 16-48: Design Parameters of the Roof Support Bolting for the Sublevel Stopes 16-94
Table 16-49: Development and Auxiliary Roof-Support Drilling 16-95
Table 16-50: Mesh Installation Design Parameters for Decline 16-95
Table 16-51: Local Ventilation Airflow Requirement Calculation—Loading Activities 16-98
Table 16-52: Local Ventilation Airflow Requirement Calculation—Explosives Charging Activity 16-98
Table 16-53: Main Exhaust System Capacity 16-99
Table 16-54: Underground Mine Administrative and Operations Personnel from Years −2 to 18 16-116
Table 17-1: Operational Parameters 17-4
Table 17-2: ROM Particle-Size Distribution—Underground and Open Pit 17-4
Table 17-3: Process Flowsheet Scenarios Evaluated 17-5
Table 17-4: Average Mass Balance of Mine Life and Metallic Distribution in Relation to Li_2O 17-5
Table 18-1: Power Demand 18-17
Table 18-2: Project's Main Milestones 18-21
Table 18-3: Geometric Parameters of North Dump 18-31
Table 18-4: Geotechnical Parameters 18-34
Table 18-5: ABNT—NBR 13029-2017—Mining—Preparation and Presentation of Waste Disposal in Dump Project 18-34
Table 18-6: Waste Dump Stability Acceptance Criteria 18-35
Table 18-7: Results of Stability Analyses 18-35
Table 18-8: Geometric Characteristics of Designed Surface Drainage Devices—North Dump 18-39
Table 18-9: Summary of Geometric Characteristics of the Designed Bottom Drainage Device 18-41
Table 18-10: Geometric Parameters of South Dump 18-42
Table 20-1: Rural Properties in the Project's ADA 20-7
Table 20-2: Bandeira's Mine Closure Activities and Cost Estimate 20-9
Table 21-1: Sources of Direct and Indirect Cost Estimates 21-2
Table 21-2: Work Breakdown Structure 21-2
Table 21-3: US Dollar and Euro Conversion Rates 21-3
Table 21-4: Initial Capital Cost Summary 21-4
Table 21-5: ECA Equipment Financing Cashflow 21-4
Table 21-6: Summary of Quantities—Start-Up and Replacement Equipment Capital Purchases 21-5
Table 21-7: Project Main Quantities 21-5
Table 21-8: Project Initial CAPEX—Underground Development and Infrastructure 21-7
Table 21-9: Initial CAPEX—Surface Services 21-8
Table 21-10: Initial CAPEX—Surface Supply 21-8
Table 21-11: Sustaining CAPEX 21-8
Table 21-12: LOM Operating Cost Summary—Per Tonne of Spodumene Concentrate 21-9
Table 21-13: LOM Mining Operating Costs 21-9
Table 21-14: LOM Processing OPEX 21-10
Table 21-15: LOM Other OPEX including Sustaining CAPEX and Closure 21-10
Table 21-16: Summary of the Project's Annual Operating Costs ($M) 21-10
Table 21-17: Site Employees—Labour 21-11
Table 21-18: Plant Consumables 21-11
Table 21-19: Annual Plant and Mine Estimated Consumption 21-12
Table 21-20: Equipment Leasing Cost 21-13
Table 22-1: Initial CAPEX ($M) 22-3
Table 22-2: Mining Equipment Financing ($M) 22-3
Table 22-3: Sustaining CAPEX ($M) 22-4
Table 22-4: OPEX—Run-of-Mine Feed ($/t) 22-4
Table 22-5: OPEX per Tonne of 5.2% Li_2O Spodumene Concentrate (SC) 22-5
Table 22-6: Spodumene Concentrate Price (CIF Shanghai) 22-7
Table 22-7: List of Taxes 22-8

Table 22-8: Financial Results Summary 22-11
Table 22-9: Sensitivity for Post-Tax NPV at 8% 22-12
Table 22-10: Sensitivity Post-Tax IRR 22-13
Table 22-11: Sensitivity for Post-Tax, Unlevered NPV x Discount Rate 22-14
Table 22-12: Annual Projections—Production Flow 22-15
Table 22-13: Annual Projections—OPEX, Spodumene Concentrate Transportation, and Other Costs 22-16
Table 22-14: Profit and Loss Statement 22-17
Table 22-15: Project Free Cash Flow—Annual Projections 22-18
Table 25-1: Bandeira Mineral Resource Estimates (0.5% Li_2O Cut-Off) 25-2
Table 25-2: Initial Capital Cost Summary 25-5
Table 25-3: LOM Operating Cost Summary—Per Tonne of Spodumene Concentrate 25-6

FIGURES

Figure 1-1: Location of the Project in the State of Minas Gerais, Brazil 1-3
Figure 1-2: Simplified Process Diagram 1-13
Figure 1-3: Project Master Plan 1-15
Figure 1-4: Spodumene (6% Li_2O) Price History (2018–2024) and Forecast (f) (2025–2032) 1-16
Figure 1-5: Sensitivity for Post-Tax NPV at 8% 1-20
Figure 2-1: Project Location in the State of Minas Gerais, Brazil 2-2
Figure 4-1: Mining Rights of the Project 4-1
Figure 5-1: Access from Belo Horizonte to Araçuaí 5-1
Figure 5-2: Access from Araçuaí to the Port of Vitória 5-2
Figure 5-3: Access from Araçuaí to the Port of Ilhéus 5-3
Figure 5-4: Monthly Meteorological Conditions in Araçuaí, with Low and High Averages (%) 5-4
Figure 5-5: Monthly Maximum and Minimum Temperatures in Araçuaí 5-4
Figure 5-6: Aerial View of Project Area with Future Infrastructure Locations 5-5
Figure 5-7: Site Layout 5-6
Figure 7-1: Simplified Geology of the Araçuaí Orogen 7-1
Figure 7-2: Distributions of U-Pb Ages for Detrital Zircon Grains from Metamorphosed Sedimentary and Volcanic Rocks 7-4
Figure 7-3: Simplified Geologic Map of Araçuaí Origen 7-6
Figure 7-4: Geology of the Araçuaí Pegmatite District 7-9
Figure 7-5: Outcrops and a Drill Core Showing Structures of the Deformation Events D1 and D2 on the Salinas Formation in the Araçuaí Pegmatite District 7-11
Figure 7-6: Location of the Bandeira Deposit in Relation to CBL's Cachoeira Mine and Sigma's Barreiro Deposit 7-14
Figure 7-7: Cachoeira Mine in the Mid-1970s 7-15
Figure 7-8: Cachoeira Pegmatite Swarm in CBL's Mine 7-16
Figure 7-9: Spodumene-Rich Pegmatites (SRP) in CBL's Underground Mine 7-17
Figure 7-10: Old Digging for Gems (A to D) and an Exploration Trench (E and F) 7-18
Figure 7-11: Simplified Map Showing the Distributions of Lithium 7-19
Figure 7-12: Host Rocks of Spodumene-Rich Ore bodies in the Bandeira Deposit 7-20
Figure 7-13: Drill Core Samples from Spodumene-Rich Ore bodies and their Host Rocks in the Bandeira Deposit 7-22
Figure 7-14: Characterization Illustrated Summary for a Typical Spodumene-Rich Pegmatite (SRP) of the Bandeira Deposit 7-23
Figure 8-1: Deposit Type Model for Spodumene-Rich Pegmatite 8-1
Figure 9-1: Bandeira Deposit—Rock Chip Sample 9-1
Figure 9-2: Bandeira Deposit—Soil Geochemical 9-2
Figure 9-3: Bandeira Deposit Trench Sample Map—22 Trenches Sited Preferentially in Soil Anomalies 9-4
Figure 9-4: Project Sample Trenches 9-5
Figure 9-5: Bandeira Target Structural Map Emphasizing the Distribution of Mapped Structures 9-6

Figure 9-6: Fractured Biotite-Schist in the Bandeira Area and Scheme Emphasizing the Interpreted Structures in the Same Outcrop 9-7
Figure 9-7: Location of the Lines and Measuring Stations of the Chargeability and Resistivity Data for Bandeira Area 1 9-8
Figure 9-8: Bandeira IP Depth Model of the Chargeability (Top) and the Actual Resistivity (Bottom) along Line 2 of Area 1 (see Figure 9-7 9-9
Figure 9-9: Bandeira IP Depth Model of the Actual Chargeability (Top) and the Actual Resistivity (Bottom) of Line 3 of Area 1 9-9
Figure 9-10: Conceptual Geological Model from Geophysics Data 9-10
Figure 10-1: Drill Holes and Trenches 10-2
Figure 10-2: Horizontal Projection of Bandeira Drill Holes with Mineralized Intercepts (Scale in Metres) 10-15
Figure 10-3: Oblique View of Drill Holes with Mineralized Intercepts (Scale in Metres) 10-16
Figure 11-1: QA/QC Program 11-4
Figure 11-2: Blank Control Chart—ITAK QG-01 11-5
Figure 11-3: Blank Control Chart—ITAK QF-15 11-6
Figure 11-4: Blank Control Chart—ITAK QF-16 11-7
Figure 11-5: Blank Control Chart—ITAK QF-18 11-7
Figure 11-6: Standard Reference Material Chart—ITAK 1100 11-8
Figure 11-7: Standard Reference Material Chart—ITAK 1101 11-9
Figure 11-8: Standard Reference Material Chart—OREAS 750 11-9
Figure 11-9: Standard Reference Material Chart—OREAS 752 11-10
Figure 11-10: Crushed Duplicates Control 11-11
Figure 11-11: Pulverized Duplicates Control Chart 11-12
Figure 11-12: Check the Assay Control Chart 11-13
Figure 12-1: Field Points During the Site Visit on September 13 and 14, 2023 12-2
Figure 12-2: Spodumene Pegmatites Outcrop and Trench on MGLIT Bandeira Property Site Visit November 25, 2024 12-3
Figure 12-3: Collar Landmarks, September 2023 Site Visit 12-4
Figure 12-4: Collar Landmarks, November 2024 Site Visit 12-5
Figure 12-5: Drilling Rig and Survey Equipment on MGLIT Bandeira Property, September 13, 2023, Site Visit 12-6
Figure 12-6: MGLIT Core Shed Storage in Araçuaí 12-7
Figure 12-7: Workflow, Sampling, QA/QC, and Chain of Custody 12-8
Figure 12-8: Density Measurement and Physical and Digital File Storage 12-9
Figure 12-9: Core Boxes of the Interval Mineralized Spodumene Pegmatite 12-9
Figure 12-10: Bandeira Spodumene Pegmatite Intercept Core Boxes of the Modelled Mineralized Spodumene Zone—Detail of the Spodumene Crystal 12-10
Figure 13-1: Drill-Hole Locations 13-7
Figure 13-2: Bandeira Composite Sample Preparation Procedure 13-8
Figure 13-3: Product Size Distribution After Crushing to P_{100} 12.7 mm 13-9
Figure 13-4: Bandeira Composite Sample Chemical Analysis 13-9
Figure 13-5: HLS Test Flowsheet 13-10
Figure 13-6: Li_2O and Fe Chemical Analysis Results for each HLS Step 13-10
Figure 13-7: Li_2O Recovery and Grade per HLS Step 13-11
Figure 13-8: Sample Preparation for HLS Test 13-12
Figure 13-9: Sequential HLS Test Flowsheet 13-12
Figure 13-10: Sequential HLS Test Results 13-12
Figure 13-11: Sequential HLS Products 13-13
Figure 13-12: Variability Study Drill Holes for Phase 1 HLS Testwork 13-15
Figure 13-13: HLS Metallurgical Recovery as a Function of Feed Grade 13-17
Figure 13-14: HLS Mass Recovery as a Function of Feed Grade 13-17
Figure 13-15: Metallurgical Polynomial Model Adherence 13-18
Figure 13-16: Spodumene Mass Distribution in HLS Test for Coarse Material (−12.7 +6.35 mm) 13-18
Figure 13-17: Spodumene Mass Distribution in HLS Test for Fine Material (−6.35 +0.85 mm) 13-19

Figure 13-18: Montebrasite Mass Distribution in HLS Test for Coarse Material (−12.7 +6.35 mm) 13-19
Figure 13-19: Montebrasite Mass Distribution in HLS Test for Fine Material (−6.35 +0.85 mm) 13-19
Figure 13-20: Petalite Mass Distribution in HLS Test for Coarse Material (−12.7 +6.35 mm) 13-20
Figure 13-21: Petalite Mass Distribution in HLS Test for Fine Material (−6.35 +0.85 mm) 13-20
Figure 13-22: Elbaite Mass Distribution in HLS Test for Coarse Material (−12.7 +6.35 mm) 13-20
Figure 13-23: Elbaite Mass Distribution in HLS Test for Fine Material (−6.35 +0.85 mm) 13-21
Figure 13-24: Variability Additional Drill-Hole Locations (Phase 2 in Blue) 13-22
Figure 13-25: Ore Sorter Results for Lithium and Iron 13-23
Figure 13-26: Comparative Recovery for 2-Stage and 3-Stage Circuits (−12.7 mm +0.5 mm) 13-26
Figure 13-27: HLS Test to Simulate the Flowsheet DMS Operations 13-26
Figure 13-28: Flowsheet HLS Products (left to right: ITDD-23-063, ITDD-23-141, ITDD-23-209, ITDD-23-215) 13-28
Figure 13-29: Ore Sorter Test Procedure Using XRT Sensor 13-29
Figure 13-30: HGS Steinert Magnetic Separation Results 13-33
Figure 13-31: Pilot Plant Flowsheet 13-37
Figure 13-32: Ore Sorter Pilot Plant 13-38
Figure 13-33: HLS Separation for Rougher Stage 13-40
Figure 13-34: DMS Pilot Plant Flowchart 13-42
Figure 13-35: DMS Pilot Plant Second Floor 1/2 13-43
Figure 13-36: DMS Pilot Plant First Floor 2/2 13-44
Figure 13-37: DMS Cyclone 13-45
Figure 13-38: Rougher Coarse Metallurgical Recovery x Li_2O Grade in Concentrate 13-46
Figure 13-39: Rougher Fine Metallurgical Recovery x Li_2O Grade in Concentrate 13-47
Figure 13-40: Rougher Composite Metallurgical Recovery x Li_2O Grade in Concentrate 13-47
Figure 14-1: Drill-Hole Location 14-2
Figure 14-2: Assay Composites Classified by Li_2O >0.3% Grade Limit in Pegmatites Veins (Oblique View NW–SE) 14-3
Figure 14-3: Assay Composites Within the Li_2O >0.3% Limit in Pegmatite Veins Grouped by Separated Lenses and Dykes 14-3
Figure 14-4: Spodumene Grade Shells Modelled with Assay Composites Li_2O >0.3% (Plan View) 14-4
Figure 14-5: Spodumene Grade Shell Model—Assay Composites Li_2O >0.3% (Cross-Section) 14-4
Figure 14-6: Weathering Zone Model (Left, Plan View; Right, Cross-Section View) 14-5
Figure 14-7: Bandeira Assay Interval Length Statistics 14-5
Figure 14-8: Li_2O (%) Box Plots of the Spodumene Pegmatite Vein Model Statistics 14-6
Figure 14-9: Variographic Model—Domains Set NW 14-10
Figure 14-10: Variographic Model—Domains Set SE 14-11
Figure 14-11: Variographic Ellipsoid—Domains Set NW 14-12
Figure 14-12: Variographic Ellipsoid—Domains Set SE 14-12
Figure 14-13: Project Li_2O % Grades Estimation (Plan View) 14-14
Figure 14-14: Project Li_2O % Grades Estimation (Cross-Section) 14-15
Figure 14-15: Estimation Validation—NN-Check of Li_2O 14-15
Figure 14-16: Estimation Validation—NN-Check of Density 14-16
Figure 14-17: Estimation Validation—Swath Plot on the X, Y, and Z Axes for Li_2O Grades 14-17
Figure 14-18: Estimation Validation—Swath Plot on the X, Y, and Z Axes for Density 14-18
Figure 14-19: Resource Classification with RPEEE (Plan View) 14-21
Figure 14-20: Resource Classification with RPEEE (Cross-Section) 14-22
Figure 16-1: Spatial Distribution of Drill Core Geotechnical Logging at the Bandeira's Project—Top Left, Plan; Top Right, Oblique View of Geotechnical Core Logging Holes at the Project Stopes; Bottom Left, Section A–A′ in Plan; Bottom Right, Cross-Section A–A′ (Ore body, Green; Drill Holes, Red) 16-3
Figure 16-2: Left, Underground Mine Plan Showing Stopes Plan and Section B–B′; Right, Cross-Section B–B′ Project Weathering Profile Model (Ore body, Green; Drill Holes, Red) (Drill Holes Vary in Colour According to the Weathering Profile Classification) 16-4
Figure 16-3: Plan (Inset), and Oblique View of Spatial Distribution and Statistical Data Relating to the Project Structural Analysis 16-4

Figure 16-4: Plan (Inset) and Oblique View of Spatial Distribution of Historical Laboratory Tests and Newly Proposed Additional Sampling Positions for Testing as well as the Planned Drill Hole Televiewer Campaign 16-5
Figure 16-5: Plan (Inset) Showing Section C–C′ and Cross-Section C–C′ of the Soil and Saprolite Domains in the Open Pit (Arrow) and Underground Mine Excavations (Light Green) (Drill Holes Coloured According to Degree of Weathering Alteration Grades W1 through W5) 16-7
Figure 16-6: An Example of a Soil and Saprolite Domain within which Different Weathering Profiles can be Identified 16-10
Figure 16-7: Longitudinal Section Along the Axis of Portal 1 16-10
Figure 16-8: Plan (Inset) Showing Section D–D′ and Cross-Section D–D′ of the Sap Rock and Weathered Rock Domain (W4/W3 Open Pit (Arrow) and Underground Mine Excavations (Light Green and Brown) (Drill Holes Coloured According to Degree of Weathering Alteration Grades W1 through W5) 16-11
Figure 16-9: Example of a Sap Rock and Weathered Rock Domain (W3/W4) where Different Weathering Profiles can be Identified 16-13
Figure 16-10: Plan (Inset) Showing Section E–E′ and Cross-Section E–E′ Showing the Planned Underground Mining Excavations, Mostly Within the Competent Rock Mass (W1 and W2) 16-13
Figure 16-11: Plan (Inset) Showing Section E–E′ and Cross-Section E–E′ of the Slightly Altered and Fresh Rock Domain (W1 Purple and W2 Orange) 16-14
Figure 16-12: Project Geotechnical Domains—Left, Cross-Section NW to SE of Ore bodies based on RQD Classification; Right, Plan View of Section F–F′ 16-15
Figure 16-13: Example of Slightly Altered to Fresh Rock Schist Domain (W1/W2) 16-16
Figure 16-14: UCS Results of the Schist Domain—Classified as W1 and W2 16-17
Figure 16-15: A) UCS Tests Performed on Schist Classified as W1 and W2 at Depths <50 m Below Surface; B) UCS Test Results at Depths <50 m Below Surface; C) UCS Tests Performed on Schist Classified as W1 at Depths >50 m Below Surface; D) UCS Test Results at Depths >50 m Below Surface (X-Axis Scales in Metres) 16-18
Figure 16-16: A) UCS for Domain W1/W2 at Depths <50 m (Outliers Removed); B) UCS for the Fresh W1 Domain at Depths >50 m (Outliers Removed) 16-18
Figure 16-17: Oblique View of the Project's 3-D Resource Model 16-19
Figure 16-18: Plan and Section H–H′ (Inset), and Cross-Section H–H′ Illustrating the Different Pegmatite Intrusions and their Respective Mining Methods 16-20
Figure 16-19: Example of Slightly Altered to Fresh Rock Pegmatite (W1/W2) 16-21
Figure 16-20: A) UCS Test Results for the Pegmatite Domain Classified as W1 Related to Depth (X-Axis in Metres); B) Box-and-Whisker Plot for the Range of Pegmatite UCS Strengths N 16-21
Figure 16-21: Association Graph of the RQD in Relation to Depth, Evaluated in the Database 16-24
Figure 16-22: Left, Geological NW–SE Cross-Section (Left) in the Project Property; Right, Plan of NW–SE Section Showing Section Line and Open Pit (Dark Red) in Southeast 16-25
Figure 16-23: Left, Plan Showing Open Pit Design Sectors and Sections; Right, Sector and Section Pit-Slope Angle, Dip, Overall Angle, and Depth 16-25
Figure 16-24: Groundwater Flow Models Applied in Circular Failure Analyses for the Soil Domain, Considering Slopes with a Face Angle of 50° and a Height of 10 m proposed by Hoek and Bray (1981) (GLE = General Limit Equilibrium) 16-27
Figure 16-25: Evaluation of Slope FOS in Diagram 4 in Figure 16-24: Scenario Proposed by Hoek and Bray (1981) Considering Slopes with a Face Angle of 50° and a Height of 20 m (GLE =General Limit Equilibrium; Blue Line is Groundwater Level) 16-27
Figure 16-26: Left, Plan of Project Property showing Four Sectors and Five Sections; Righ,t Example of a Kinematic Analysis Conducted for the Northwest Sector (Dashed Green Outline on Plan), Considering Face Angles of 50° and 85° 16-29
Figure 16-27: Stability Analysis of South Pit Sector E (FOS = 1.0 for Planar Failures); the Main Foliation is the Structure Associated with this FOS in Sector E 16-32
Figure 16-28: Stability Analysis of South Pit Sector E (FOS = 1.1 for Planar Failures in 75° Bench Angle Slopes) 16-32

Figure 16-29: Left, South Pit Sector E Cross-Section Highlighting the Critical Area of the Section (FOS = 1.0 for Planar Failures, with a Face Angle of 85° and a 2 m Bench), Right, Project Property Plan Showing Pit (Pink Outline) 16-33
Figure 16-30: Geometric Parameters Used in the Stability Assessment 16-34
Figure 16-31: Plan of Pit Sectors and Sections (Inset) and Pit Southern Sector Section 4, Stability Analysis Considering the Fully Drained Slope Scenario 16-35
Figure 16-32: Plan of Pit Sectors and Sections (Inset) and Pit Southern Sector Section 4, Stability Analysis of Critical Water Table Scenario 16-35
Figure 16-33: Plan of Pit Sectors and Sections (Inset) and Pit Southern Sector Section 2 Stability Analysis Considering the Critical Water Level and Highlighting the Lowest FOS in the Shallowest Pit Horizon 16-38
Figure 16-34: Plan of Pit Sectors and Sections (Inset) and Pit Southern Sector Section 3 Stability Analysis Considering the Critical Water Level and Highlighting the Lowest FOS in the Shallowest Pit Horizon 16-38
Figure 16-35: Plan of Pit Sectors and Sections (Inset) and Pit Southern Sector Section 5 Stability Analysis Considering the Critical Water Level and Highlighting the Lowest FOS in the Shallowest Pit Horizon 16-39
Figure 16-36: Left, Plan Showing Open Pit Design Sectors and Sections; Right, Proposed Geometry for the Respective Design Sectors 16-40
Figure 16-37: Open Stope Mine Design and Stope Dimensions 16-41
Figure 16-38: Pre-Mining Stress Magnitudes and k-ratio vs. Depth Below Surface 16-43
Figure 16-39: Estimation of Crown and Hanging-Wall Stress for an Open Excavation 16-44
Figure 16-40: Rock Stress Factor A and Resultant Strength-To-Stress Ratios for Depths Ranging from 50 m below Surface to 666 m Below Surface 16-45
Figure 16-41: Estimated Hydraulic Radius Using Calculated N' Numbers for the Concordant and Discordant Ore-Body Hanging Wall 16-46
Figure 16-42: Dilution Estimation and Schematic Section for Sublevel 16-47
Figure 16-43: Cable Bolt Design and Cable Bolting Information for Each 1.5 m Strike Long Section 16-48
Figure 16-44: Span Dipping for Shallow Effective Stopes based on Zone of Influence and Cave and Break Angles 16-48
Figure 16-45: Safety Factor Results for the Schist's Wedge-Limit Equilibrium Assessment in the Underground Development Excavations 16-50
Figure 16-46: Conceptual Model of Regional Groundwater Circulation 16-54
Figure 16-47: Boundary Conditions 16-56
Figure 16-48: Potentiometric Map—Dry—Conceptual Hydrogeological Model Report (July 2025) 16-57
Figure 16-49: Potentiometric Map—Rainy Season Conceptual Hydrogeological Model Report (July 2025) 16-58
Figure 16-50: Geotechnical Parameters for Open Pit 16-60
Figure 16-51: Open-Pit Layout. Section A–A′ is Shown in Cross-Section in Figure 16-52 16-60
Figure 16-52: Cross-Section A-A′ (See Figure 16-51), Showing the Open-Pit Layout (Green Line = Pit Outline; Blue Line = Mineralized Ore body; Brown Line =Topography) 16-61
Figure 16-53: Open Pit Cut-Off Grade Sensitivity Analysis 16-61
Figure 16-54: Underground Mine Portal 16-62
Figure 16-55: Typical Section of the Decline 16-63
Figure 16-56: Schematic Arrangement of the Gallery Position for Top-Down Stope Mining (Drives in Brown within the Projected Stopes in Green) 16-64
Figure 16-57: Schematic Typical Panel of the Project Underground Mine (Green = Main Decline; Blue = Crosscuts; Orange = Developments; Grey = Rib and Sill Pillars; Red = Exhaust Ventilation System; Light Blue = Intake Ventilation System) 16-66
Figure 16-58: Cut-Off Grade Sensitivity Analysis for Underground Mining 16-67
Figure 16-59: Wireframe Plan Viewer 16-68
Figure 16-60: Left, Plan View of Mine Development; Right, Cross-Section of Mine Development 16-69
Figure 16-61: Left, Plan View of Mine Development and Sublevel Stopes; Right, Cross-Section of Mine Development and Sublevel Stopes 16-69
Figure 16-62: Year −2 Mine Sequencing 16-79
Figure 16-63: Year 5 Mine Sequencing 16-80
Figure 16-64: Year 8 Mine Sequencing 16-81
Figure 16-65: Year 11 Mine Sequencing 16-82

Figure 16-66: Year 18 End of Mine Life 16-83
Figure 16-67: Plan View of Waste-Rock Dumps (Dashed Blue Line is the Mining Right Boundary; Dashed Pink Line is the Directly affected area =ADA Area; NATM 1 and 2 are the Portals that Access the Underground Mine 16-85
Figure 16-68: Longhole Drilling 16-91
Figure 16-69: Drilling and Blasting Plan for the Ramps (Red Circles = Charged Holes; Blue = Burn Cut Holes) 16-93
Figure 16-70: Drilling and Blasting Plan for the Drives (Red Circles = Charged Holes; Blue = Burn Cut Holes) 16-93
Figure 16-71: Global Airflow Requirements—Diesel Equipment Plus Personnel vs. Total Annual Tonnage 16-97
Figure 16-72: Total Airflow Requirement 16-97
Figure 16-73: Mine Ventilation System (Exhaust Shafts in Red; Intake Aire in Blue) 16-99
Figure 16-74: Ventilation System Capacity and Requirement for Each Sector Over the LOM 16-100
Figure 16-75: Year -2 Ventilation System 16-101
Figure 16-76: Year −1 Ventilation System 16-101
Figure 16-77: Year 1 Ventilation System 16-102
Figure 16-78: Year 3 Ventilation System 16-103
Figure 16-79: Year 6, Ventilation System 16-103
Figure 16-80: Year 9 Ventilation System 16-104
Figure 16-81: Year 16 Ventilation System 16-105
Figure 16-82: Electrical Substation 16-107
Figure 16-83: Electrical Power Step-Down Diagram 16-108
Figure 17-1: Bandeira Simplified Project Flowchart 17-2
Figure 17-2: Project Flowsheet 17-3
Figure 17-3: Primary Crushing Circuit 17-6
Figure 17-4: Example of Modular Crushing and Classification Plant 17-7
Figure 17-5: Thickening Equipment 17-7
Figure 17-6: Belt Filter 17-8
Figure 17-7: 3-D View of the Concentration Plant 17-8
Figure 18-1: Gatehouse (Portaria Social) and Parking Area (Estacionamento) 18-4
Figure 18-2: Administrative Plateau 18-5
Figure 18-3: Laboratory, Warehouse, Workshop, and Mine Support Plateau 18-6
Figure 18-4: Explosives Magazine Plateau 18-7
Figure 18-5: Administrative Office Building (Left); 3-D Model External and Internal (Right) 18-8
Figure 18-6: Cafeteria Internal Areas—3-D Model 18-10
Figure 18-7: Changing Room Internal Area 3-D Model 18-10
Figure 18-8: 3-D View of the Workshop 18-11
Figure 18-9: Processing Plant Layout (DMS + Crushing + Buildings) 18-12
Figure 18-10: DMS Plant 3-D Model—Steel Structure Equipment 18-15
Figure 18-11: CEMIG Integrator Substation and New Main Substation from 138 kV to 13.8 kV Layout 18-16
Figure 18-12: Preliminary Schedule 18-22
Figure 18-13: Master Plan with North and South Dump Design (Plan View) 18-24
Figure 18-14: Box Plot of the NSPT Values Observed in the Materials Intercepted by the Mided Drilling 18-25
Figure 18-15: Location of the Geotechnical Investigations for the Project 18-26
Figure 18-16: ABNT NBR 15421 (2006) Seismic Zones of Brazil 18-28
Figure 18-17: Brazil Seismic Hazard Heat Map—Peak Acceleration 18-29
Figure 18-18: North Waste and Tailings Dump 18-31
Figure 18-19: Geometries for Forming the Bank Edge 18-32
Figure 18-20: Reached at El. 320 m, Place a Line of Flags 10 m from the Crest, which will be the Edge of Bank 320 18-32
Figure 18-21: Construction Sequence of the Benches—Once the Position of the Berm Is Reached, Mark the Next Berm, Until the Dump is Complete 18-33
Figure 18-22: Stability Analysis of Cross-Section B–B, FOS = 1.26/1.43 18-36
Figure 18-23: Stability Analysis of Cross-Section B–B Seismic Load, FOS = 0.61/1.12 18-37
Figure 18-24: Typical Cross-Section of Hydraulic Devices Consisting of a Trapezoidal Channel with Rockfill Lining 18-40

Figure 18-25: Waste Dump North Cross-Section—Arrangement 18-40
Figure 18-26: Typical Drainage Heap 18-41
Figure 18-27: Typical Bottom Drain Device Cross-Section 18-42
Figure 18-28: Typical Foot Drain Cross-Section 18-42
Figure 18-29: South Dump Design (Plan View) 18-43
Figure 21-1: Câmara de Comercialização de Energia Elétrica (CCEE)—Average Free Market Power Price in the Last 18 Years in Brazil 21-12
Figure 22-1: ROM Feed to Plant over LOM 22-2
Figure 22-2: Spodumene Concentrate Production (5.2% Li_2O) over LOM 22-2
Figure 22-3: Annual OPEX ($M) 22-5
Figure 22-4: Total OPEX ($M) 22-5
Figure 22-5: Gross Revenue and Deductions 22-7
Figure 22-6: Exchange Rate BRL:USD 22-11
Figure 22-7: Sensitivity for Post-Tax NPV at 8% 22-13
Figure 22-8: Sensitivity for Post-Tax IRR 22-13
Figure 22-9: Sensitivity Post-Tax, Unlevered NPV x Discount Rate 22-14

ABBREVIATIONS, ACRONYMS, AND UNITS OF MEASURE

Abbreviations and Acronyms

$	United States dollar
2C	2-litre 4-cylinder
2-D	Two dimensional
3-D	Three dimensional
3T4	Three-quarter ton
AAS	Defined, but never used
AASHTO	United States American Association of State Highway and Transportation Officials
ABNT	Brazilian National Standards Organization (Associação Brasileira de Normas Técnicas)
ADA	Directly Affected Area (Área diretamente afetada)
ADM	Not defined
AFRMM	Additional Charge for Renewal of the Merchant Navy
ANA	National Water Agency (Agência Nacional de Águas)
ANM	National Mining Agency (Agência Nacional de Mineração)
APP	Permanent Preservation Areas (Áreas de Preservação Permanente)
AT	Automation technology
BRA	Brazilian real
BWi	Bond ball mill work index
CAGR	Compound annual growth rate
CAPEX	Capital cost
CAR	Rural Environmental Registry (Cadastro Ambiental Rural)
CBL	Companhia Brasileira de Lítio
CBR	California Bearing Ratio
CBS	Contribution on Goods and Services

CCTV	Closed-circuit television
CECAV	National Center for Research and Conservation of Caves
CEMIG	Minas Gerais Power Plants local power utility (Centrais Elétricas de Minas Gerais)
CENIPA	Center for Investigation and Prevention of Aeronautical Accidents
CETEM	Centro de Tecnologia Mineral
CFEM	Financial Compensation for Mineral Exploration (Contribuição Financeira para Extração Mineral)
CIF	Cost, insurance, and freight
CIM Definition Standards	CIM Definition Standards for Mineral Resources & Mineral Reserves
CIM Guidelines	CIM Estimation of Mineral Resources and Mineral Reserves Best Practice Guidelines
CIM	Canadian Institute of Mining, Metallurgy and Petroleum
CIU	no long form
CL	Low-compressibility inorganic clay
CMD	Cleaning material deposit (unclear is this is a good translation)
COFINS	Contribution to Social Security Financing
CONAMA	National Environmental Council (Conselho Nacional do Meio Ambiente)
COPAM	State Council for Environmental Policy (Conselho de Política Ambiental)
COPANOR	COPASA
COPASA	Companhia de Saneamento de Minas Gerais
CRM	Certified reference material
CSLL	Social Contribution on Net Profit
CWA	no long form
CWi	Bond crushing (impact) work index
CwS	for which I have no gloss
D1	Deformation event
D2	Deformation event
DER	Brazil's Department of Highways
DG	Deformation event
DIFAL	Difference Between Internal and Interstate Rates
DIR	Intermediate waste deposit
DMS	Dense-media separation
DN	Normative Deliberation (Deliberação Normativa)
DNIT	Brazil's National Department of Transportation Infrastructure
DNt	Deformation event
DR/DF	Reference or vendors drawings
DSO	Direct-ship lithium-bearing ores
E	East
EBITDA	Earnings before interest, taxes, depreciation and amortization
EBPP	Eastern Brazilian Pegmatite Province

ECA	either needs definition in 21.4.2 heading or glosses in tables where used
EHSS	Health, safety, environment, and social issues
EIA	Environmental Impact Assessment (Estudo de Impacto Ambiental)
ESG	Environmental, Social, and Governance
ESMS	Environmental and social management system
ESS	Energy storage systems
EV	Electric vehicle
Falcon	Falcon Metais Ltda.
FEAM	State Environmental Agency
FED	Seasonal Deciduous Forest (Floresta Estacional Decidual)
FOS	factors of safety
FTIR	Fourier-transform infrared spectroscopy
G&A	General and administrative
GE21	GE21 Consultoria Mineral
GLE	not spelled out
GPS	not spelled out
HAZID	Hazard Identification (Replace the acronym with spelled out form)
HDPE	High-density polyethylene
HGMS	High Gradient Magnetic Separation
HGS	not spelled out
HLS	Heavy-liquid separation
IBGE	Brazilian Institute of Geography and Statistics
IBS	Tax on Goods and Services
ICMBio	Chico Mendes Institute for Biodiversity Conservation
ICMS	Imposto sobre Circulação de Mercadorias e Serviços
ICP-OES	Inductively coupled plasma–optical emission spectroscopy
IDE SISEMA	Spatial Data Infrastructure of the State Environmental and Water Resources System
IDE	Environmental information
IDW	Inverse distance weighting
IEF-MG	State Forestry Institute (Instituto Estadual de Florestas)
IEPHA	Minas Gerais State Institute of Historical and Artistic Heritage
IGAM	Minas Gerais Institute of Water Management (Instituto Mineiro de Gestão das Águas)
INCRA	National Institute of Colonization and Agrarian Reform (Instituto Nacional de Colonização e Reforma Agrária)
IOF	Tax on Financial Transactions
IP	Induced polarization
IP/IT	Intermediate PT/IT regime
IPHAN	National Institute of Historical and Artistic Heritage
IPI	Tax on Industrialized Products

IRPJ	Corporate Income Tax
IRR	Internal rate of return
ISRM	International Society for Rock Mechanics and Rock Engineering
ISSQN	Municipal Tax on Services of Any Nature
IT	Information technology
L&M Advisory	L&M Assessoria Empresarial S.S. Ltda.
LAC 2	Concomitant Preliminary and Installation License (Licenciamento Ambiental Concomitante)
LAC	Concurrent Environmental License (Licença Ambiental Concomitante)
LCE	Lithium carbonate equivalent
LCT	Lithium-cesium-tantalum
LFP	Lithium-iron-phosphate
LHD	load-haul-dump
LI	Installation License (Licença de Instalação)
Lithium Ionic	Lithium Ionic Corp.
LO	Operating License (Licença de Operação)
LOM	life-of-mine
LP	Preliminary License (Licença Prévia)
LP/HT	Low pressure and high temperature
LTE	long-term evolution
MCC	Motor control centre
MGLIT	MGLIT Empreendimentos Ltda
MME	Ministry of Mines and Energy (Ministério de Minas e Energia)
MOU	Memorandum of Understanding
MP/MT	Medium-pressure and medium-temperature
MPF	Federal Public Prosecutors Office
MSO	mineable stope optimization
N	North
NATM	New Austrian Tunneling Method
NCM	Nickel cobalt manganese
NE	Northeast
NI	National Instrument
NN	Nearest neighbor
NPV	Net present value
NSPT	Blow count
NTU	Overflow turbidity
NW	Northwest
NYF	Niobium–yttrium–fluorine
OK	Ordinary kriging
OPEX	Operating cost

P	Pressure
P100	100% passing
PA	Weighing the sample
PAE	Economic Exploitation Plan (Plano de Aproveitamento Econômico)
PB	Weighing the sample submerged
PCA	Environmental Control Plan (Plano de Controle Ambiental)
PCS	Social Communication Program (Programa de Comunicação Social)
PEA	Preliminary economic analysis
PGA	Peak ground acceleration
PGR	Risk Management Program
PIA	Environmental Intervention Project (Plano de Intervenção Ambiental)
PIS	Social Integration Program
PLC	Programmable logic controllers
PRAD	Degraded Areas Recovery Plan
Project	Bandeira Lithium Project
PSA	Particle-size analysis
PSP	Perthite-spodumene pegmatites
PT	no gloss
P-T	Pressure-temperature
PTP	Perthite-tourmaline pegmatites
PVC	Polyvinyl chloride
Q2	Quarter 2
QA/QC	Quality control and quality assurance
QP	Qualified Person
R$	Brazilian real
RAIPA	Archaeological Heritage Impact Assessment Report (Relatório de Avaliação de Impacto ao Patrimônio Arqueológico)
RAIPI	Impact Assessment Report on Intangible Heritage (Relatório de Avaliação de Impacto ao Patrimônio Imaterial)
RCA	Environmental Control Report (Relatório de Controle Ambiental)
RECAP	Special Regime for the Acquisition of Capital Goods for Exporting Companies (Regime Especial de Aquisição de Bens de Capital para Empresas Exportadoras)
RF	Revenue factor
Rietveld	Total multi-phase spectrum refinement
RIMA	Environmental Impact Report (Relatório de impacto ambiental)
RL	Legal Reserve (Reserva Legal)
RMR	rock mass rating
ROM	run-of-mine
RPEEE	Reasonable prospect for eventual economic extraction
RQD	rock quality designation

R-Tek	R-Tek International DMCC
S	South
S1	Regional schistosity
S2	Regional schistosity
SE	Southeast
SEMAD	Secretariat of Environment and Sustainable Development of Minas Gerais
SGS	SGS Geosol (SGS Geological Services)
SNUC	National System of Nature Conservation Units
SOP	Standard operating procedures
SPO	Spodumene concentrate
SPP	Spodumene-petalite pegmatites
SPT	Standard penetration test
SPT	Standard penetration test
SQUI	Spodumene–quartz intergrowth
SRM	Standard reference materials
SRP	Spodumene-rich pegmatites
SUDENE	Superintendency for Northeast Development (Superintendência do Desenvolvimento do Nordeste)
SW	Southwest
SWOT	Strengths, Weaknesses, Opportunities, and Threats
T	Temperature
TEC	Tarifa Externa Comum
Technical Report	This report
TFRM	Fee for the Control, Monitoring and Inspection of research Mining, Exploration and Utilization of Mining Resources Activities (Taxa de Controle, Monitoramento e Fiscalização das Atividades de Pesquisa, Lavra, Exploração e Aproveitamento de Recursos Minerários)
TIPI	Table of Incidence of the Tax on Industrialized Products (Tabela de incidência do Imposto sobre produtos industrializados)
UC	Conservation Unit
UCS	uniaxial compressive strength
URA	Minas Gerais Department of Regional Environmental Regularization Unit
URA/LM	Eastern Minas Gerais Regional Environmental Unit (Unidades Regionais de Regularização Ambiental do Leste Mineiro)
USD	US dollar
UTM	Mineral Treatment Unit
Valitar	Valitar Participações Ltda
VAT	Value-added tax
W	West
WBS	Work breakdown structure
WLI	Water-level indicator

WTP	Water-treatment plant
WWTP	Wastewater treatment plant
XRD	X-ray diffraction
XRT	X-ray transmission

Units of Measure

°	Degree
°C	Degree Celsius
a	Annum (year)
cm	Centimetre
d	Day
dmt	Dry metric ton
g	Gram
h	Hour
ha	Hectare
k	kilo (thousand)
kbar	Kilobar
kg/h.m^2	Kilogram per hour per square metre
km	Kilometre
kt	Kilotonne
kV	Kilovolt
kv	Vertical seismic coefficient
kVa	Kilovolt-ampere
kWh	Kilowatt hour
L	Litre
µm	Micrometre
M	Million
m	Metre
min	Minute
mm	Millimetre
N	Newton
Pa	Pascal
ppm	Parts per million
R2	Coefficient of determination
s	Second
st	Short ton (2,000 pounds)
t	Tonne
tf/m^2	Tonne force per square metre
wt%	Weight percent

1 EXECUTIVE SUMMARY

1.1 Key Facts

This document, titled *Bandeira Lithium Project, National Instrument (NI) 43-101 Technical Report—Definitive Feasibility Study Update, Araçuaí–Itinga, Minas Gerais, Brazil* (the Technical Report), with an effective date of September 17, 2025, and dated October 31, 2025, presents an update to the Bandeira Lithium Project (the Project) feasibility study update (Horta de Cerqueira Viana, et al., 2025, June 6). The scope of this Technical Report includes revisions to the underground mine design; incorporation of a short-lived open-pit operation within the southern portion of the mineral right; optimization of the process flowsheet for the concentration stage; and updates to capital and operating cost estimates (CAPEX and OPEX, respectively). The Mineral Resource estimates applied in this study were previously published on November 20, 2024, using data from the 2024 drilling campaign (Silva & Bergmann, 2025, March 26).

The updated Mineral Reserves increased the life-of-mine (LOM) from 14 to 18.5 years of operation.

1.2 Introduction

The Project is a hard-rock spodumene concentrate-producing lithium operation near Araçuaí in the state of Minas Gerais, Brazil. The Project scope is a 1.3 Mt/a underground mining operation with a starter pit in the first year of production, supporting a crushing and dense-media separation (DMS) concentrator facility. The average LOM concentrate production is 177 kt/a of 5.2% Li_2O spodumene to be shipped to downstream third-party lithium conversion facilities in the global market.

Lithium Ionic Corp. (Lithium Ionic) is a Canadian-domiciled company and the parent company of the wholly owned subsidiary, MGLIT Empreendimentos Ltda. (MGLIT), the Project developer.

MGLIT holds lithium mineral rights in the Jequitinhonha Valley in Minas Gerais, and in April 2022 started Project exploration activities under Agência Nacional de Mineração (ANM) (National Mining Agency) Mining Rights 832439/2009, 831.116/2016, and 831.117/2016. The Project is on a small portion of the total land package that MGLIT holds and does not include resources from other satellite and exploration deposits.

The Mineral Resource was classified per the Canadian Institute of Mining, Metallurgy and Petroleum (CIM) *CIM Definition Standards for Mineral Resources & Mineral Reserves* (CIM Definition Standards) (CIM, 2014), following the *CIM Estimation of Mineral Resources and Mineral Reserves Best Practice Guidelines* (CIM Guidelines) (CIM, 2019); geostatistical and classical methods; and economic and mining-appropriate parameters relevant to the deposit type.

MGLIT commissioned R-TEK International DMCC (R-Tek), Promon Engenharia, and GE21 to perform engineering studies and generate the CAPEX estimate for the feasibility study update, with Qualified Persons (QP) in mining, mineral processing, CAPEX development, and infrastructure design.

NeoAgro Ambiental was responsible for preparing the baseline studies and the Environmental Impact Assessment, the Relatório de Controle Ambiental and Plano de Controle Ambiental developed for the Project's permitting process, while GE21 consolidated the environmental and social information presented in this Technical Report.

This Technical Report comprises the results of a study to determine the feasibility of mining and processing spodumene-rich pegmatites (SRP) at the Project property. The QPs who signed this Technical Report do not foresee significant risks associated with the operation of the mine and the industrial processing facility that is the subject of this Technical Report.

The Mineral Resource estimate in this Technical Report is updated to include drill data up to November 20, 2024. Thus, it supersedes the previous Mineral Resource estimate (with an effective date of November 13, 2023) (Silvia & Bergmann, 2025).

Table 1-1 presents the QPs responsible for all sections of the Technical Report.

Table 1-1: Qualified Persons, Qualifications, Affiliations, and Site Visits

Name of Qualified Person	Qualifications	Affiliations	Site Visit Dates
Brian Colin Talbot	B.Sc Engineering	R-Tek	August 22 to 23, 2024
Carlos José Evangelista Silva	P.Geo., MSc.	GE21	September 13 and 14, 2023; December 12, 2023; November 26 and 27, 2024
Hugo Ribeiro de Andrade Filho	FAusIMM	GE21	No site visit
Juliano Felix de Lima	P.Geo.	GE21	No site visit
Porfírio Cabaleiro Rodriguez	B.A. Msc, FAIG	GE21	No site visit
João Augusto Hilário de Souza	B.A., Msc., MBA	L&M Advisory	January 17 to 19, 2024
Noel Mark O´Brien	BE (Met), MBA, FAusIMM	R-Tek	No site visit
Bernardo Horta de Cerqueira Viana	MBA, FAIG	GE21	No site visit

Note: L&M Advisory = L&M Assessoria Empresarial S.S. Ltda.

1.3 Reliance on Other Experts

Section 20 was prepared by Bernardo Horta de Cerqueira Viana as QP with the technical support of Branca Horta de Almeida Abrantes.

The financial analysis was prepared by L&M Assessoria Empresarial S.S. Ltda. (L&M Advisory) specialist João Augusto Hilario Souza, who defined the tax and fee assumptions adopted in this Technical Report.

1.4 Property Description and Location

The Project, held under Mining Rights No. 832439/2009, 831.116/2016, and 831.117/2016, covers an area of 174.17 ha in northeast Minas Gerais, near the municipalities of Araçuaí and Itinga, approximately 15 km from Araçuaí, and about 620 km from the state capital, Belo Horizonte (Figure 1-1).

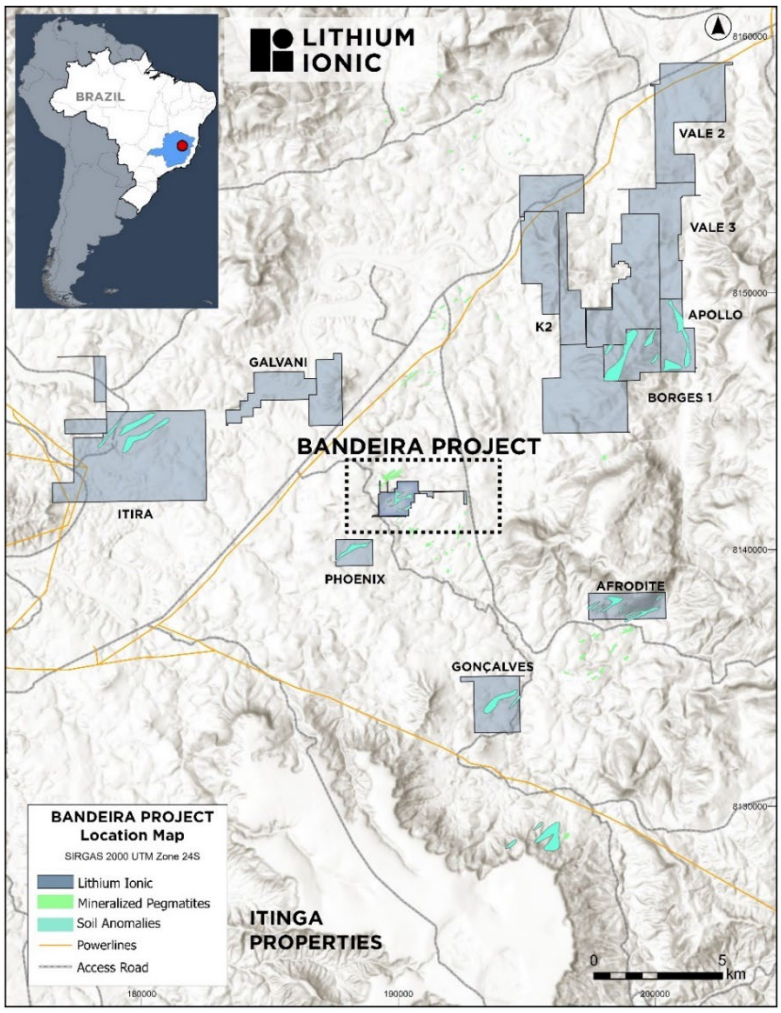


Figure 1-1: Location of the Project in the State of Minas Gerais, Brazil

The site is accessed through an established network of paved highways servicing the region. The Piauí River divides the municipalities of Araçuaí and Itinga, and the mineral asset is near the community of Barreiro, near the left bank of this watercourse.

The Project is in a prolific lithium mining and exploration district otherwise known as Brazil's "Lithium Valley." The Project site is on rural land, adjacent to active hard-rock lithium mines operated by Companhia Brasileira de Lítio (CBL) and Sigma Resources.

The spodumene concentrate produced will be exported through the port of Ilhéus in the south of the state of Bahia, to regions with lithium conversion facilities, such as Asia and North America.

1.5 Accessibility, Climate, Local Resources, Infrastructure, and Physiography

The Project is easily accessed, 3 km from the BR367 federal highway, which connects the city of Gouveia in Minas Gerais with the city of Porto Seguro in Bahia, passing through the cities of Araçuaí and Itinga. It is an asphalt road that recently received an asphalt cover and is in excellent condition.

Araçuaí is served by a municipal airport with a 1,120 m-long asphalt runway, used by small private aircraft. The regional airports with regular flights are Vitória da Conquista, Bahia, 275 km from the Project; Montes Claros, Minas Gerais, 330 km from the Project; and Salinas, Minas Gerais, 120 km from the Project.

The region is characterized by a hot, dry, semi-arid climate. The average temperature is 24.5°C, with an average rainfall of 750 mm. The driest period of the year is June, and the rainiest period is December. There is no harsh cold season. Construction activities and operation can take place year-round, with minor interruptions for a short period of heavy rains. The topography of the region where the Project will be implemented presents hills and valleys with elevation differences of less than 100 m. The Piauí River borders the western side of the operational area. A bridge to be constructed early in the Project timeline will span the river and provide easy access to the full Project area from the nearby highway.

The site staffing plan comprises a local workforce supported by regional cities and communities. Specialist roles will be recruited from further afield as needed. Staff members are to be bused into site from accommodations in nearby Aracuaí and Itinga.

The Araçuaí Campus of the Instituto Federal de Educação, Ciência e Tecnologia do Norte de Minas Gerais (Federal Institute of Education, Science and Technology of North Minas Gerais) and the Araçuaí Instituto Educacional Técnico Polivalente (Polyvalent Technical Educational Institute) can train technicians in surveying, mining, environment, informatics, and occupational safety. In addition, the Serviço Nacional de Aprendizagem Industrial is building a facility in Araçuaí which will train trade skills.

A 138 kV Centrais Elétricas de Minas Gerais (Minas Gerais Power Plants local power utility) transmission line that is supplied by the Irapé hydroelectric plant passes within 3 km of the Project area and will supply low-carbon power to the site.

Authorizations have been granted to intake water from Piaui and Jequitinhonha rivers.

The cities of Araçuaí and Itinga and surrounding region will supply the Project with various services, such as food, transportation, logistics, labour, and accommodation.

1.6 History

MGLIT started its activities in November 2021, with seven mining rights in the municipalities of Araçuaí and Itinga, totalling about 1,300 ha. In May 2022, Lithium Ionic was listed on the Toronto Venture Stock Exchange under the symbol LTH-V.

CBL has actively mined the area to the north of the Project since 1991, using similar underground mining and DMS processing methods. In 2023, Sigma Resources, directly northeast of the Project,

began open pit operations and commissioned its Xuxa DMS concentration plant. Several other exploration companies remain active in the Lithium Valley area.

The Project area was unexplored until initial drilling began with Lithium Ionic and MGLIT in 2022. GE21 completed a preliminary economic analysis (Silva et al., 2023, November 30) based on an SGS NI 43-101-compliant Mineral Resource statement (Dupéré & Sayeed, 2023, August 10).

MGLIT and GE21 published an incremental Mineral Resource estimate update containing Measured and Indicated resources of 27.27 Mt grading 1.34% Li_2O, or 901 kt of lithium carbonate equivalent (LCE)—along with Inferred resources of 18.55 Mt grading 1.34% Li_2O, or 615 kt of LCE (Silva & Bergmann, 2025, March 26).

1.7 Geological Setting and Mineralization

The Project lies in the Middle Jequitinhonha River valley, northeastern Minas Gerais—the Lithium Valley. The region is part of the Eastern Brazilian Pegmatite Province (EBPP), one of the largest pegmatite provinces in the world, covering 150,000 km^2 (see synthesis and references in Pedrosa-Soares et al., 2025). The EBPP resulted from the magmatic and tectono-metamorphic events that formed the Araçuaí Orogen from the Early Ediacaran (ca. 630 Ma) to the Late Cambrian (ca. 490 Ma). The major EBPP pegmatite populations have been grouped into twelve pegmatite districts that include residual pegmatites (representing late silicate melts released by fractional crystallization of parent granites) and/or anatectic pegmatites (formed directly from partial melting of country rocks). Among them, the Araçuaí Pegmatite District includes hundreds of residual pegmatites of the rare-element class (B, Be, Cs, Li, Sn, Ta) and lithium-cesium-tantalum (LCT) family, comprising distinct varieties of spodumene pegmatites

Located in the central part of the Araçuaí Pegmatite District, the Itinga Pegmatite Field comprises the current spodumene mines of CBL and Sigma Lithium, and some of the most important discoveries of lithium deposits in Brazil since the 1950s, both in terms of economic resources and geological potential, such as the Bandeira deposit of MGLIT. The favourable geological conditions for the outstanding abundance of spodumene-rich deposits in the Itinga Field are the large volume of intrusions of lithium-fertile two-mica leucogranites with pegmatoid cupolas, associated with the relatively low-pressure and high-temperature conditions of the regional and contact metamorphisms recorded by the country rocks comprising cordierite-biotite schists locally with andalusite (Pedrosa-Soares et al., 2025). The spodumene ore bodies mined since the early 1990s in CBL's underground mine form a closely spaced swarm of relatively narrow (6 m thick on average) but long (up to 700 m along strike) non-zoned SRP bodies. In the Sigma Lithium properties, where several large SRP bodies are found (e.g., Barreiro, Murial, and Xuxa), an open pit mine is being developed on the Xuxa SRP deposit (15 m thick x 1,800 m long x 500 m). Most SRPs of the Itinga Field are hosted by the regional schistosity S1 (NE strike/NW dip) and the late spaced cleavage S2 (NE strike/SE dip), with some SRP bodies hosted by flat-lying or high-angle dip joints. No significant deformation was found in the SRP ore bodies, except for rare thin fracture zones and late faults with short (centimetre) displacements. These pegmatites imprinted narrow (cm to dm) and discontinuous halos of contact metamorphism and metasomatism in the host schists, replacing biotite by tourmaline and recrystallizing decussate micas, which may obliterate the regional schistosity. These features suggest the post-tectonic emplacement of the SRPs, as with other lithium pegmatites in the region.

Following the regional northeast–southwest structural trend outlined by the SRP swarm mined by CBL, the Bandeira deposit comprises a northeast-striking SRP swarm, including concordant SRP bodies, hosted by the northwest-dipping schistosity (S1), and discordant SRP bodies, emplaced along a southeast-dipping fracture system (the S2 spaced cleavage), as well as a few mineralized pegmatites hosted by late flat-lying joints. The Bandeira SRP ore bodies show sharp contacts with a cordierite-quartz-mica schist that may be enriched in decussate micas, tourmaline, and/or cordierite porphyroblasts, recrystallized along narrow (cm to dm) fringes of contact metamorphism which may also be anomalous in lithium content. The Bandeira pegmatites are tabular bodies with convex, lens-shaped terminations, arranged in a tight and staggered (en-echellon) swarm, locally with branched connections linking ore bodies. Single SRP bodies normally reach hundreds of metres along strike, ranging in thickness from a few decametres to decimetres, with the discordant SRP bodies tending to be thicker than the concordant ones. With known downdip-width up to 800 m, several Bandeira SRP bodies remain open in depth. The Bandeira ore bodies show a rather simple mineralogical assemblage, consisting of medium (3 cm–10 cm) to very coarse-grained (>30 cm) spodumene crystals (up to 30 vol%) within a fine- to medium-grained matrix composed of albite, perthitic microcline, quartz, and muscovite, with generally scarce (<5 vol% in total) accessory (montebrasite, Nb-Sn-Ta oxides) and secondary minerals (cookeite, sericite, zabuyelite, Fe-Mn oxides, clay minerals). Petalite has been found in some drill cores and thin sections, mostly occurring in the SRP matrix as very fine- to fine-grained (sub-millimetric to 1 cm) crystals and, more rarely, in coarse-grained crystals locally found in few core intervals. The thicker SRP bodies generally show a barren external zone rich in albite (which can be rather discontinuous), followed inwards by an internal zone rich in disseminated spodumene (although spodumene may also be more concentrated in some domains than others along the internal zone). The thinner SRP bodies generally lack the external lithium-barren zone, showing disseminated spodumene along the whole ore body. Unidirectional solidification textures outlined by tabular to telescope-shaped spodumene crystals are common in the Bandeira SRP ore bodies. Thin albite-rich pegmatites, barren to poor in lithium, are also found in the Bandeira SRP swarms. The exploration drilling work revealed two main sectors in the Bandeira deposit: the northern swarm, with thicker and longer SRP bodies; and the southern swarm, with smaller SRP bodies.

1.8 Deposit Types

Two Lithium deposits comprise the Araçuaí Pegmatite District:

- The spodumene-rich deposits of the Araçuaí Pegmatite District include the non-zoned to poorly zoned SRPs and spodumene-petalite pegmatite, and the simple-zoned perthite-spodumene pegmatite (Pedrosa-Soares et al., 2025). Among them, the SRP deposits are by far the most important in terms of resource volume, lithium grade, high lithium recovery, and low mining and processing complexities, due to their relatively simple structure and mineralogy, simple and little variable chemistry, and large quantities of spodumene widely disseminated throughout the ore bodies. The proof-of-concept for this are CBL's spodumene mine, producing spodumene through an underground mine since 1992; Sigma's mine, producing spodumene from an open-pit mine since 2023, and all the recently discovered significant spodumene deposits in Brazil, such as MGLIT's Bandeira, Baixa Grande, and Outro Lado SRP deposits. Therefore, the SRP deposit model has proven to be highly efficient in successful knowledge-based exploration of spodumene on formerly unknown to poorly known targets, leading to the discovery of large spodumene deposits by the use of

geological mapping, soil geochemistry, trenching, and continuous core drilling (see details in MGLIT's reports and Pedrosa-Soares et al., 2025).

- The complex-zoned LCT pegmatites with diversified mineralogy, typically displaying a roughly concentric zoning with marginal (granitic), wall (graphic), and intermediate (blocky K-feldspar) zones, and one or more quartz cores, with very variable amounts of secondary units (e.g., fracture fillings, albite-rich replacement bodies, miarolitic cavities, gem-bearing pockets). Despite their relatively large dimensions and recurrent gemstone (mostly colored tourmaline), cassiterite, tantalite, and industrial minerals production, such complex LCT pegmatites may contain little spodumene in internal zones, quartz cores and/or albite-rich units, although none of them has ever been found to be relevant targets for exploration of spodumene in current economic terms (Paes et al., 2016; Pedrosa-Soares et al., 2011, 2025). Therefore, the classical model for complex zoned LCT pegmatites (e.g., Cerný, 1991; Cerný et al., 2012) must be discarded if spodumene is indeed the lithium ore mineral sought in exploration work in the Araçuaí Pegmatite District, although this model can be applied to exploration for lithium-mica (e.g., lepidolite), lithium-phosphate (e.g., montebrasite), and/or petalite.

1.9 Exploration

Since 2022, MGLIT has completed a trench-sampling program, rock-chip sampling programs, structural mapping, and geophysical surveys on the Project property. In all, 44 trenches totalling 2,293 m were completed in 2024 at the Bandeira target.

Some basic field data, such as outcrop attitude (strike and dip), foliation, and cleavage were used to locate several occurrences of spodumene previously unknown or unreported. Since this initial discovery, MGLIT rapidly advanced the Project with diamond drill testing of the targets and the pegmatite system.

1.10 Drilling

All drilling activities conducted within the Bandeira Property until November 20, 2024 (Table 1-2), have been incorporated into the Mineral Resource estimation process. It is important to note that any drill holes completed after this date, and pending sample assay results, have not been considered in the present Mineral Resource statement.

Table 1-2: Bandeira Diamond Drill-Hole Summary

Year	Holes Drilled	Length (m)
2022	49	5,570
2023	207	46,642
2024	41	8,089
Total	297	60,301

1.11 Sample Preparation, Analysis, and Security

Sample intervals in the mineralized zones are defined based on a 1.0 m support. Mineralized samples must have a minimum length of 1.0 m and a maximum length of 1.5 m. In some specific situations, samples shorter than 1.0 m can be generated.

SGS Geosol prepared and analyzed drill core samples. The independent commercial SGS Geosol laboratory facility is certified in ISO 9001, ISO 14001, and ISO 17025. The sample shipment was delivered to its Vespasiano facility, in Minas Gerais, via a parcel transport company.

All samples received at SGS Geosol were inventoried and weighed before processing. Samples were dried at 105°C, crushed to 75% passing a 3 mm sieve, homogenized, split (Jones Riffle Splitter), and pulverized (250 g to 300 g of sample) in a steel mill to 95% passing 150 mesh.

Samples are prepared from NQ-diameter drill cores (47.6 mm). The sampling procedures described in Section 11 reflect MGLIT's current standard operational procedures.

The sample batch composition includes six quality control samples for every 29 regular samples. The quality control composition of the batches comprises:

- Coarse (preparation) and fine (analytical) blanks: 5.2% of the batch, or two blanks per batch, one of each type
- Standards: 5.2% of the batch, or two standards per batch
- Crushed duplicates: 2.6% of the batch, or 1 sample per batch
- Pulverized duplicates: 2.6% of the batch, or 1 sample per batch.

MGLIT has submitted check assay batches for analysis to the ALS Laboratory in Vancouver, British Columbia, Canada. This procedure is used to verify the reliability of the primary laboratory results by cross-checking them with those of a secondary reference laboratory.

The QP finds that the sampling, sample preparation, security, and analytical work carried out by MGLIT and its contractors are appropriate to support a Mineral Resource estimation study. The quality assurance procedures align with industry best practices, and the quality control results fall within acceptable industry standards, attesting to the reliability of the database information.

1.12 Data Verification

Mr. Carlos José E. Silva, an independent QP for geology exploration and Mineral Resource estimate, conducted a site visit at the Project on September 13 and 14, 2023; December 12, 2023; and November 26 and 27, 2024. MGLIT allowed unlimited access to the facilities during the visits.

All verified procedures related to sampling management, storage, logging, sample preparation, and assay were checked, and they are considered to be within acceptable limits and in compliance with mineral industry practices. The rock-type descriptions fit with the checked mineralization style.

1.13 Mineral Processing and Metallurgical Testing

The coarse mineralization exhibited by the Bandeira deposit allows for a simple processing flowsheet featuring DMS. The selected flowsheet is consistent with the region and is used at both CBL and Sigma operations. Based on this, a comprehensive testing program was developed to prove that the DMS process would be suitable for ores originating from the Project.

Metallurgical samples and composites were prepared to represent the bulk ore body and perform variability studies to ensure geo-metallurgical performance is well understood. A variability study was completed to understand mineralogy and validate the process design criteria. All metallurgical samples were sourced from diamond drill-core samples.

Process characterization benchtop testwork was completed at SGS Geosol in Vespasiano, using heavy-liquid separation (HLS) to determine DMS as a viable solution to producing a marketable concentrate. This testwork generated target DMS densities for subsequent testwork program. Initial ore-sorting tests were completed using Tomra equipment, which demonstrated value in a crushing stage gangue removal process to manage mining dilution.

Follow-up pilot plant operation was completed at Steinert (ore sorting) and SGS in Belo Horizonte (DMS). This work processed bulk and specific variability samples to determine ideal operating parameters to support generating a 5.5% Li_2O concentrate.

R-Tek brought a different concept for HLS testing procedure. The sequential cascade HLS starts at a density of 2.5 g/cm^3 and the last stage is at 2.95 g/cm^3. A small variability test program was assembled, with five core diamond drill holes. The results of these HLS tests indicated a bench-scale average lithium oxide recovery of 65.3% can be achieved to generate a concentrate grade of 5.20% Li_2O.

Tests were conducted using magnetic separation, which proved that iron-containing schist can be removed from the final product, with minimal loss of lithium.

1.14 Mineral Resources Estimate

The updated Mineral Resource estimate contains Measured and Indicated resources of 27.27 Mt grading 1.34% Li_2O, containing 901.0 kt of LCE, along with Inferred Mineral Resources of 18.55 Mt grading 1.34% Li_2O, or 615.4 kt of LCE (Table 1-3).

Table 1-3: Bandeira Mineral Resource Estimates (Base-Case Cut-Off Grade of 0.5 % Li_2O)

Category	Resource (Mt)	Grade % Li_2O	Contained LCE (kt)
Measured	3.36	1.38	115
Indicated	23.91	1.33	786
Measured + Indicated	27.27	1.34	901
Inferred	18.55	1.34	615

Source: GE21 (2025).
Notes:

- The Mineral Resource estimate effective date is November 20, 2024.
- Carlos J. E. Silva (MAIG #7868) prepared the Mineral Resource estimate using CIM (2014).
- The report meets the Canadian Securities Administrators' NI 43-101 requirements.
- Mineral Resources are not Mineral Reserves and have no economic viability. There is no certainty that any portion of the Mineral Resource will be converted into a Mineral Reserve.
- Figures are rounded to appropriate levels of precision, and discrepancies may occur due to rounding.
- The spodumene pegmatite domains were modelled using composites with Li_2O grades exceeding 0.3%.
- Grade estimation was conducted using ordinary kriging within Leapfrog Edge 2024.1.3 software.
- The Mineral Resource estimate is confined to the MGLIT Bandeira mining right (ANM) and includes only fresh rock domains.
- The Mineral Resource estimate was restricted by interpreting suitable-grade shells using a 0.5% Li_2O cut-off for underground resources.
- Inferred Mineral Resources are conceptual in nature and can only form the basis for economic analyses with further drilling and evaluation.
- The Mineral Resource estimate may be materially affected by environmental, legal, tax, sociopolitical, permitting, title, marketing, and other relevant factors

The Mineral Resource estimate is based on 297 diamond drill holes comprising 60,301 m of drilling completed between April 2022 and November 20, 2024. This updated Mineral Resource estimate supersedes the November 2023 technical report (Silva et al., 2023, November 30) and April 2024 incremental update (Silva et al.,2024, April 12)

The resource classification was supported by a grade shell representing the underground mining appliance, reasonable prospect for eventual economic extraction, defined through a restricted wireframe based on a grade shell with a cut-off of 0.5% Li_2O, considering an average feed grade of 1.4% Li_2O for the processing plant.

1.15 Mineral Reserve Estimate

The Mineral Reserve estimates for the Project are shown in Table 1-4.

Table 1-4: Project Mineral Reserve, Dated September 22, 2025

Ore Reserve Class	Volume (Mm^3)	Mass (Mt)	Grade (Li_2O %)	Contained LCE (kt)
Proven				
Underground	0.85	2.29	1.12	63.8
Open pit	0.11	0.28	1.10	7.5
Subtotal Proven	0.95	2.57	1.12	71.4
Probable				
Underground	7.29	19.80	1.09	534.2
Open pit	0.31	0.82	1.13	22.9
Subtotal Probable	7.59	20.63	1.09	557.1
Total Proven & Probable	8.54	23.20	1.10	628.5

Notes:

- CIM Definition Standards (2014) were followed for Mineral Reserves estimates.
- Conventional sublevel stoping and open pit mining methods have been proposed
- Figures presented in dry basis
- The Mineral Reserves were calculated considering a cut-off grade of 0.5% Li_2O for underground and 0.3% for open pit.
- For the sublevel stoping mining method, Mineral Reserves volumes and tonnages assume 90% of mine recovery, 21% of total dilution
- Minimum stope width: 2.0 m.
- For the ore from development to work, Mineral Reserves volumes and tonnages assume 100% of mine recovery, 31% of planned dilution, and 10% of operational dilution due to overbreaking.
- For the open pit, Mineral Reserves assumes 100% of mine recovery and 10% of dilution.
- The processing plant is expected to produce at a nominal feed rate of 1.3 Mt/a (dry basis) with a process recovery of 65.3%.
- Figures are rounded to appropriate levels of precision, and discrepancies may occur due to rounding.

Cut-off grades were calculated at 0.3% and 0.5% Li_2O for open pit and underground mine, respectively.

1.16 Mining Methods

The Project's mine design incorporates two distinct mining methods. The primary ore bodies, totalling approximately 22.1 Mt, will be extracted using the sublevel stoping method. In parallel, the southeastern secondary ore body, containing around 1.1 Mt, will be mined by open-pit methods.

The selection of these methods reflects the geometry of the deposit: the open-pit area targets near-horizontal mineralization, whereas the sublevel stoping areas exploit the steeply dipping sections of the ore veins.

Three geomechanical domains were established through geotechnical characterization based on drill-core samples. This process involved identifying main lithotypes, determining fracture patterns, rock quality designation indices, degree of alteration, and spacing of the discontinuities associated with the intervals. The information obtained was sufficient for defining rock resistance properties, supporting geotechnical parameters, and providing the necessary data for the development of mine project work during the feasibility study stage.

The average run-of-mine (ROM) ore production over the LOM is scheduled for 1.3 Mt/a on a dry basis. A gradual increase in ore production will occur over the initial years until reaching the nominal Project capacity in the second year following plant commissioning.

The mine operation schedule will consist of three six-hour shifts per day, with a two-hour interval between shifts for mining ventilation to dissipate blasting gases. The mine will operate 365 days per year 6552 hours of planned production per year.

Access to the underground mine will be through two main ramps at the ore body's footwall, with one of them dividing into two, reaching the sublevel stope portions of the mine.in different locations.

The open pit is forecasted to start in year –1 and finish in year 1 reaching the depletion after 13 The open-pit operation is scheduled to commence in Year –1 and conclude in Year 1, achieving full depletion after approximately 13 months of activity. Although not the sole source of plant feed, the open-pit mine plays a key supporting role during the project’s early phase, supplementing the ore supply and helping sustain production until the underground mine reaches full ramp-up capacity.

The optimization process resulted in a diluted ROM mass of 1.10 Mt of 1.121% Li_2O for the portion mined by the open pit method; a mass of 18.30 Mt of 1.13% Li_2O for the portion mined by the sublevel open-stope method; and a mass of 3.80 Mt at 0.96% Li_2O for the ore originating from development works.

The mine will be supported with a mechanical ventilation system consisting of fans and exhausts. Clean-air supply to the underground mine will be obtained through the ramps, two air-intake raises, and four exhaust raises.

1.17 Recovery Methods

The plant will process 1.3 Mt/a of ROM (average LOM) containing 1.10% Li_2O from the mines to produce 177 kt/a of concentrate containing 5.2% Li_2O (Figure 1-2).

ROM will be comminuted through a primary jaw crusher, a secondary cone crusher, and one tertiary crusher. The crushed ROM will be –16 mm and feed a prep screen to remove −0.6 mm. The fraction between −16 mm + 0.6 mm will be concentrated in a four-stage modular DMS plant. The calculated lithium oxide recovery is 65.3%.

Each modular DMS circuit will consist of protective screens, dense medium cyclones, demagnetising coils, ferrosilicon recovery system and pumps.

The fine material (−0.60 mm) will be dewatered in the thickener, while thickener underflow is dewatered in a belt filter. The filtered fines will be treated as reject material; however, it will be stockpiled separately for concentration applications to be studied in the future, as it contains just below 1% Li_2O.

Crushing will have an availability of 65%. The DMS circuits will have an availability of 85%.

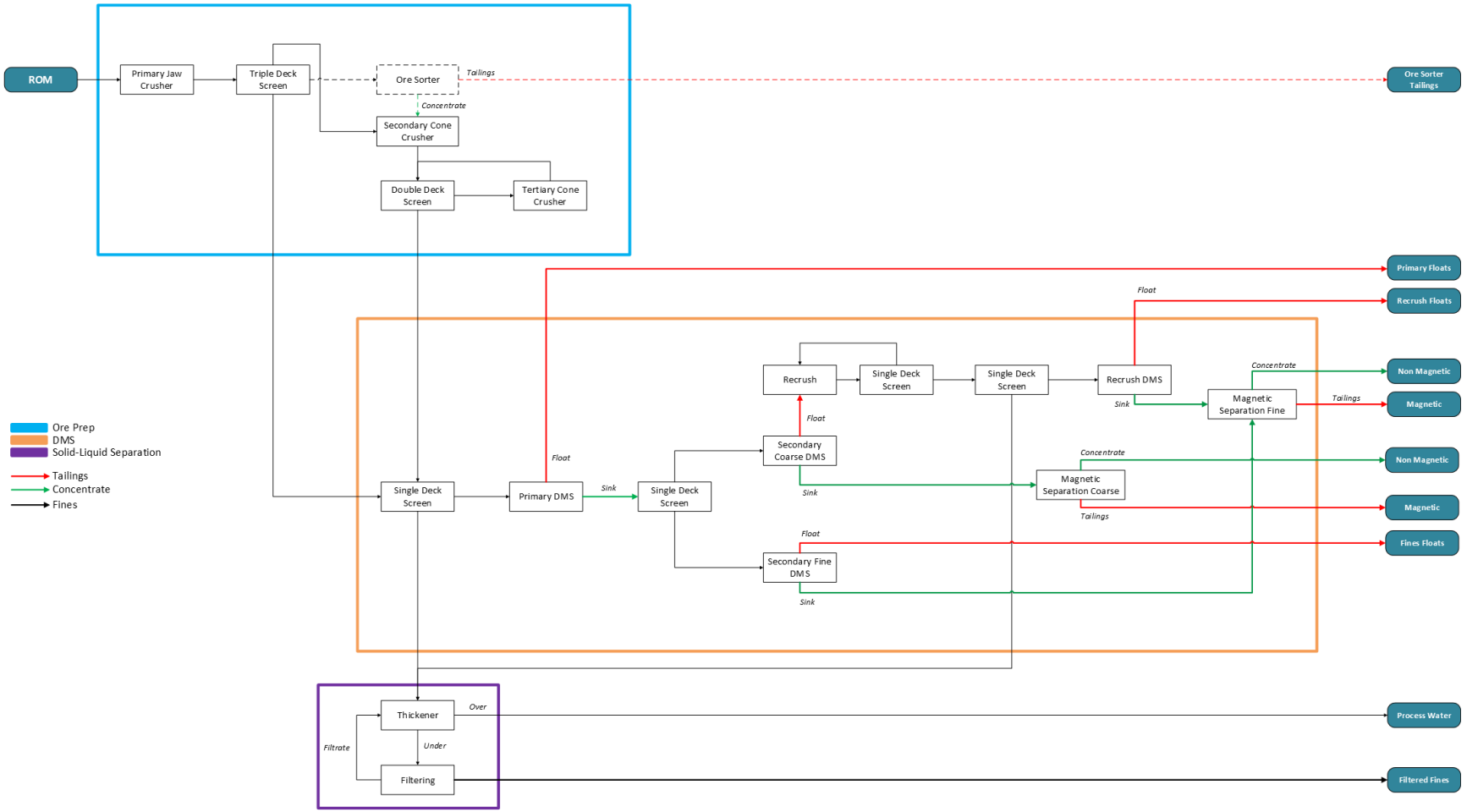


Figure 1-2: Simplified Process Diagram

1.18 Project Infrastructure

The existing regional infrastructure, with easy highway access, readily available low-carbon power, established road and air transportation, and proximity to ports and logistics hubs, provide a good basis for Project development with minimal off-site CAPEX required.

The on-site infrastructure design features all the requirements necessary for supporting the Project. A full complement of semi-modular office, administration, cafeteria, medical, firefighting, warehousing, and maintenance buildings are provided in the initial CAPEX. The site operating philosophy does not include onsite accommodation—employees will be bused to the site.

The plant will be supported with compressed-air facilities, reagent and consumables storage, and supporting maintenance facilities. The plant construction is a compact and lean design, typical of warm climate operations, using minimal enclosures. A tower crane is used instead of overhead gantry cranes for routine and shutdown maintenance.

The mine is supported by an explosives magazine, guarded by a security checkpoint. A ventilation system is designed to support the underground operation. Ancillary services are provided, including a mine dispatch and the standard underground mining safety requirements, such as refuge areas. Two portals are at surface to service access to the two underground ramps.

Tailings (DMS rejects and filtered fines) are to be stored in a dry stack, suitable for the very coarse nature of the DMS plant rejects. Since there will be no fine grinding or flotation, a fine-slurry tailings storage facility is not required. Waste stockpiles have been designed in accordance with geotechnical design criteria provided by external consultants.

Raw water is primarily sourced from the Piauí River, with the Jequitinhonha River an alternative source. Plant process water is reclaimed from thickener and filter operations, and reused as process water. Waste piles and site runoff water is collected via drainage-capture ditches. Potable water and sewage treatment plants are provided and sized to support the on-site workforce. Oil–water separators and effluent treatment are provided to manage mobile equipment wash bays and general maintenance areas.

Site power will be provided by a new 3 km 138 kV transmission line. A new main substation will be built on site to drop the voltage from 138 kV to 13.8 kV. The 13.8 kV will be distributed to the secondary substations in the e-house through overhead distribution networks.

The scope of instrumentation, control, and automation consists of a process control system that enables plant operation. Telecommunications systems will enable the implementation and management of the information technology services required for the plant and supporting site.

The Project infrastructure is planned to ensure safety, operational efficiency, and environmental responsibility, with a focus on utility systems, administrative support, and waste management strategies.

In Figure 1-3, the blue area represents the mining right, the pink area indicates the ADA, the gray areas to the north and south correspond to the waste piles, the light brown area represents the processing plant, and at the center of the image are the NATM portals of the underground mine.

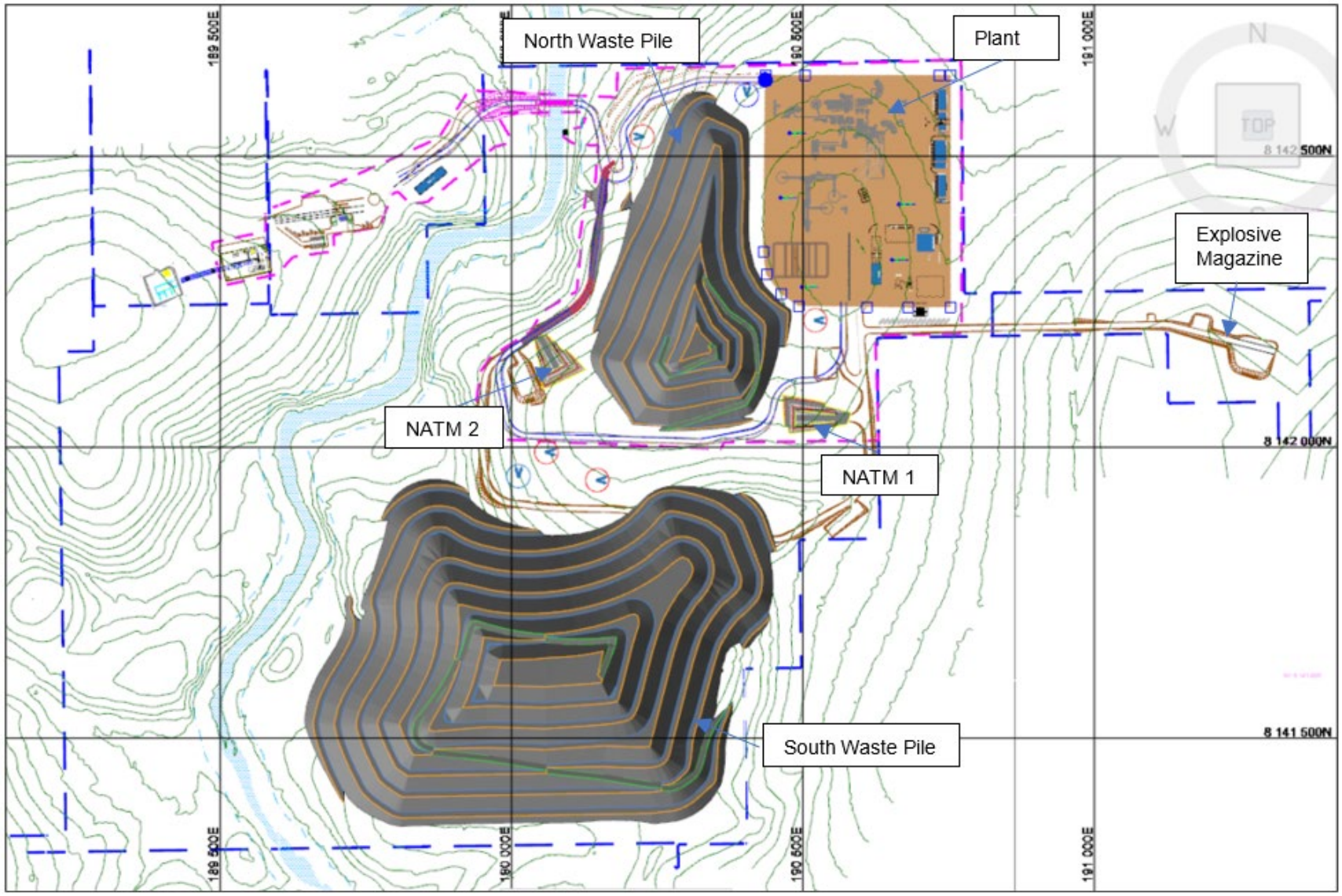


Figure 1-3: Project Master Plan

1.19 Market Studies

Fastmarkets' macroeconomic outlook estimates 2024 lithium salts output at about 1.27 Mt LCE, up approximately 32% year over year, including about 399 kt of hydroxide and 814 kt carbonate. Carbonate is expected to remain the larger share as lithium-iron-phosphate adoption persists, rising at about 11% compound annual growth rate (CAGR) to approximately 1.79 Mt by 2035 and about 65% of total salts. Hydroxide is forecast to grow to 960 kt by 2035 (~12% CAGR). Western markets are positioned as the main hydroxide producers—South America specializes in carbonate, and China has a mixed profile.

Global lithium demand is driven by electrification in transport and stationary storage, reinforced by decarbonization policy and purchase incentives. From 2018 to 2024, demand expanded at about a 25% CAGR. Fastmarkets projects continued growth at a moderate, approximately 18%, CAGR as EV markets mature and policy support becomes more selective.

Fastmarkets forecasts that hydroxide, carbonate, and spodumene prices will average $21.61/kg, $21.66/kg, and $1,716/t, respectively, between 2025 and 2032.

Fastmarkets still expects ongoing volatility in the global lithium market, driven by restocking and destocking cycles, as well as periods of surplus supply followed by supply disruptions and supply deficits later in the decade. The results of this study are shown in Figure 1-4.

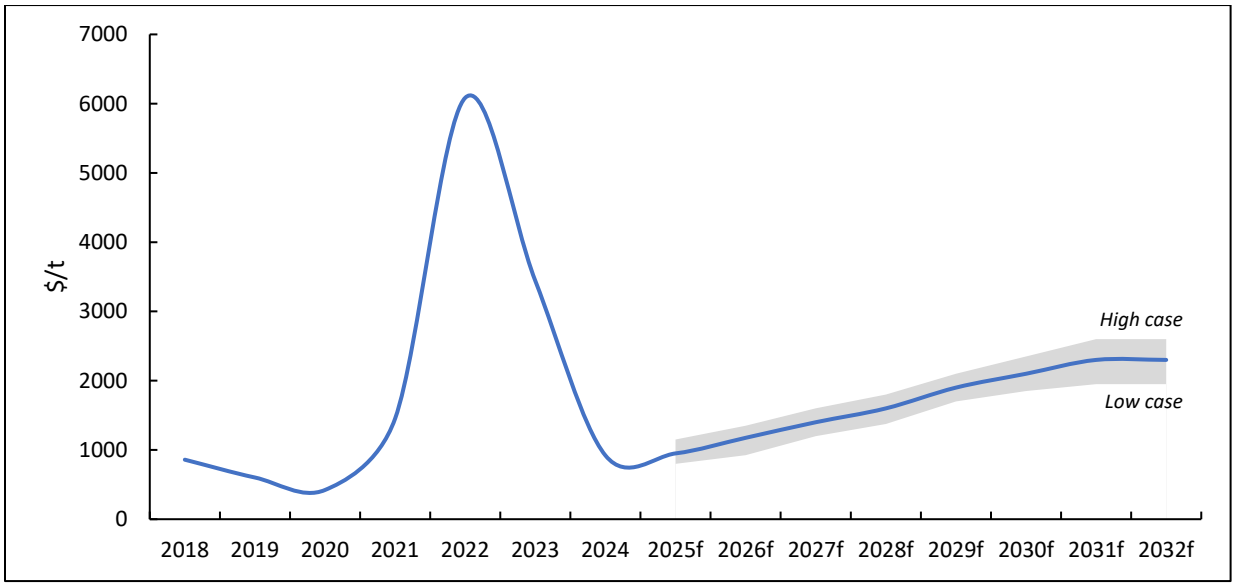


Figure 1-4: Spodumene (6% Li_2O) Price History (2018–2024) and Forecast (f) (2025–2032)

1.20 Environmental Studies, Permitting, and Social Impact

The Project's environmental licensing encompasses both the underground mining operation and the planned open pit. The process follows the framework established by the Licenciamento Ambiental Concomitante (LAC), a concurrent licensing modality that integrates multiple stages of environmental approval into a single, streamlined procedure. This approach ensures regulatory efficiency while maintaining high environmental standards and transparency with authorities and stakeholders.

For the underground mine and process plant, MGLIT was classified in the LAC modality, combining the Preliminary, Installation and Operation Licenses into a single process. Upon granting the combined Preliminary, Installation and Operation License, the Project will be ready for construction and further operation under the same regulatory framework.

Complementary environmental authorizations have been obtained to support Project implementation. These include the river crossing authorization for the installation of the bridge, over the Piauí River and the water use permit for surface abstraction from the same river, both valid for ten years. In addition, the authorization for native vegetation suppression covers areas in an early stage of regeneration within the Atlantic Forest biome, including limited interventions in Permanent Preservation Areas (APPs). This vegetation clearance authorization is directly linked to the main Licenciamento Ambiental Concomitante (LAC) process and will be issued concurrently with the environmental license.

At the federal level, the Project has also advanced in the mining permitting pathway. The Final Exploration Report and Economic Exploitation Plan (PAE) have been submitted to the National Mining Agency (ANM), which will issue the Mining Concession (Portaria de Lavra) and corresponding Servitude Rights once both the PAE and the LAC are approved. These milestones will formalize the Company's right to operate and secure access to the mineral deposit.

As the Project progresses toward construction, a new LAC process will be initiated for the open pit, designed to increase production capacity to approximately 1.5 Mt/a, and establish a tailings storage facility of about 38 hectares.

Parallel permitting processes are also underway for the 138 kV transmission line and Integrating Substation, which require authorizations from the State Forestry Institute (IEF) for vegetation suppression and from the state energy agency, CEMIG, for grid integration.

In terms of water management, the Project already holds a long-term permit for the use of surface water from the Piauí River and has submitted an additional request to the National Water Agency (ANA) for authorization of an alternative supply from the Jequitinhonha River, ensuring operational resilience and redundancy of resources.

At the municipal level, MGLIT is pursuing the necessary permits for two road crossings related to the water pipeline, in coordination with the Municipality of Araçuaí, including the corresponding traffic management and road restoration plans.

Altogether, these authorizations and procedures represent solid progress toward the full implementation of the Project. The current LAC process for the underground operation, combined with the complementary permits already granted, establishes the foundation for construction to begin.

The Project also includes a Conceptual Mine Closure Plan, which defines the measures required to minimize environmental and social impacts associated with the closure phase. The plan establishes corporate guidelines and technical criteria approved by the National Mining Agency (ANM) to ensure that adequate technical and financial conditions are in place for decommissioning. It also outlines the procedures for transitioning the site to post-closure status and defines the criteria for future land use, ensuring long-term environmental stability and compliance with national mine closure standards.

The Project does not have direct impact to any communities or households, and there are no families residing within the Project's footprint or in the immediate area designated for mining and associated infrastructure. The land required for implementation is privately owned, previously used for rural and pasture activities, and free of permanent settlements. As such, no physical or economic displacement is foreseen, and no resettlement measures are required. Environmental assessments also indicate that the Project's physical and biological impacts are low in magnitude, as the activities are located in previously modified areas characterized by early-stage regeneration vegetation, limited fauna occurrence, and the absence of sensitive habitats or protected ecosystems.

1.21 Capital and Operating Costs

The CAPEX estimate includes all the direct and indirect costs, along with the appropriate project contingencies for all the facilities required to bring the Project into production, as defined by this feasibility study update. The labour rate build-up is based on the statutory laws governing benefits to workers in effect in Brazil at the time of the estimate. Brazilian import tariffs have been applied. The estimate does not include any allowances for scope changes, escalation, and exchange-rate fluctuations.

The CAPEX estimate has the level of accuracy for an AACE Class 3 estimate, which requires 20%/+30% accuracy. A contingency rate of 15% was applied for the mine and 10% for the processing plant. All costs are in Q2 2025 US dollars.

Table 1-5: AACE Class 3 Capital Cost Estimate

	Cost ($M)
Mine	59.2
Surface	107.3
Owner's Cost	4.9
Contingency	19.6
Initial CAPEX	**191.0**

The OPEX estimate includes the mine, process plant, and general and administrative costs (G&A). The LOM overall unit OPEX for the Project of ore processed is shown in Table 1-6. Royalty payments are not included in OPEX, but are included in Section 22. All costs are in Q2 2025 US dollars.

Table 1-6: Operating Cost Summary—Per Tonne of Spodumene Concentrate

Description	SPO Concentrate ($/t)
Mining	190
Processing	98
General and Administrative (G&A) Sales	19
Subtotal	307
Capitalized Mining	70
Total Including Capitalized Mining	**378**

Note: SPO = spodumene concentrate.

1.22 Economic Analysis

L&M Advisory updated the economic analysis for the Technical Report. It incorporates increased Mineral Resource and Mineral Reserve and optimized mine and plant design compared to the feasibility study presented in May of 2024.

L&M Advisory's work was based the information Promon provided, and the technical teams from MGLIT and R-Tek. Promon was responsible for the initial CAPEX estimates of the surface infrastructure, and indirect costs.

The technical teams from MGLIT and R-Tek oversaw the initial CAPEX estimates for both open-pit and underground mines, and processing plant. Production plan, mine development, OPEX estimates, sustaining capital, and mine closure costs were also completed by the same team. Additionally, MGLIT provided product sales price projections as part of the market study conducted by the specialized consultancy Fastmarkets.

L&M Advisory was also responsible for estimating tax impacts on the Project, including revenue, CAPEX and OPEX, and profits. The tax rates adopted are in accordance with the current Brazilian tax legislation, as well as the applicable tax benefits at federal and state level.

Table 1-7 summarizes the key elements of the feasibility study financial analysis for the Project, detailed in Section 22. The Project's estimated post-tax, unlevered net present value (NPV) is $1,447.5 million using a discount rate of 8.0%. The post-tax, unlevered Internal Rate of Return (IRR) is 61.2% and the average annual earnings before interest, taxes, depreciation and amortization (EBITDA) is $254 million. The total undiscounted free cash-flow generated over the LOM is $3,392 million and the payback period after the startup of the operations is 2.2 years (26 months).

Based on the assumptions used in this Technical Report, the Project is economically viable, given the significantly positive NPV and IRR as compared to the discount rate adopted.

Table 1-7: Financial Results Summary

Financial Analysis	Unit	Post-Tax
NPV at 8%	$ billion	1.45
Payback[1]	year	2.2
IRR	%	61
Profitability Ratio	%	753
EBITDA[2]	$M	254
Total Cash Flow	**$M**	**3,392**

Notes: IRR = internal rate of return.
[1] Undiscounted, after start-up. [2] Annual average.

A sensitivity analysis was performed for ±30% variations for Spodumene Concentrate (5.2% Li_2O) price, exchange rate, initial CAPEX and OPEX as shown in Figure 1-5.

The Project is most sensitive to spodumene concentrate 5.2% price, followed by exchange rate, initial CAPEX and OPEX. The sensitivity analysis for the NPV and IRR was conducted considering a range of ±30% in the key input variables of the Project's cash flow, as follows:

- Spodumene concentrate price
- Exchange rate BRL/USD
- OPEX
- CAPEX.

Figure 1-5 present the results of the sensitivity analysis for the Project's NPV on an after-tax unlevered basis, and for each of the critical variables. NPV results are reported at a discount rate of 8%.

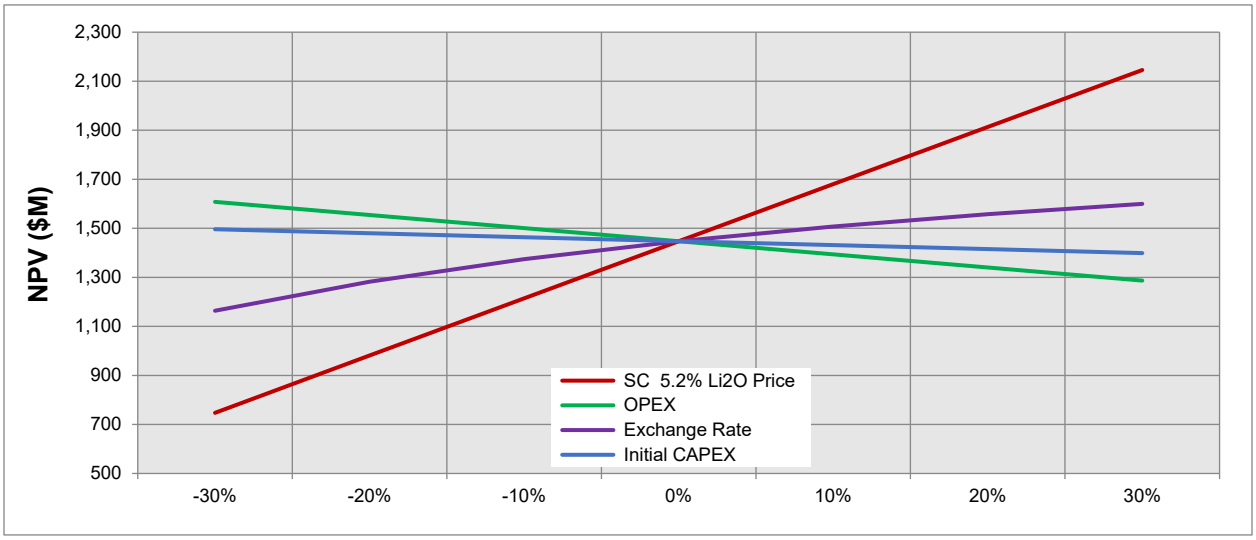


Figure 1-5: Sensitivity for Post-Tax NPV at 8%

1.23 Adjacent Properties

The Bandeira deposit is adjacent to the Cachoeira mine, owned by CBL, and the Xuxa mine, Barreiro, Murial, Nezinho do Chicão, and Lavra do Meio deposits, owned by Sigma Lithium Corporation.

The Araçuaí Pegmatitic District is known for its extensive pegmatite occurrences, including those rich in lithium, gemstones, and ceramic minerals. The Bandeira lithium ore deposit is near the lithium-bearing pegmatites associated with CBL's Cachoeira mine and Sigma Lithium Corporation's Xuxa mine, Barreiro, Murial, Nezinho do Chicão, and Lavra do Meio deposits.

1.24 Other Relevant Data and Information

MGLIT has signed a memorandum of understanding with the Government of the State of Minas Gerais aimed at expediting environmental licensing procedures and advancing other initiatives related to the Project.

In addition, MGLIT has executed a power supply agreement, and all associated projects required for grid connection currently under development.

The lithium decree originally enacted in 1997 to secure the Brazilian domestic market for companies producing lithium within the country was revoked in July 2022.

1.25 Interpretation and Conclusions

The technical work performed by MGLIT, its consultants, and key experts, has resulted in the following conclusions:

- Mineral Resources were estimated and limited to the areas outlined using CIM Guidelines, the Mining Rights polygon that comprises the Bandeira property, and the reasonable prospect for eventual economic extraction. The Project contains 27.27 Mt of 1.34% Li_2O in the Measured and Indicated category, and 18.55 Mt of 1.34% Li_2O in the Inferred category. This Mineral Resource estimate is based on a November 20, 2024, effective date.
- The Mineral Reserve estimate for the deposit demonstrates 2.57 Mt of 1.12% Li_2O, and 20.63 Mt of 1.09% Li_2O of Proven and Probable reserves on a diluted basis, respectively. This estimate is based on the November 2024 Mineral Resource estimate
- The selected mining methods of open pit and sublevel stoping support the orientation of the deposit and the ability to produce an average of 1.3 Mt/a of ROM for processing. The geotechnical characteristics of the ore body support these mining methods.
- The initial CAPEX has been produced at an AACE Class 3 level estimate and encompasses all scope required from start of development in Year −2 through to production. The CAPEX is estimated at $191 million, net of mobile equipment financing. All customary taxes for Brazil and Minas Gerais have been applied.
- The OPEX estimate has been generated using a first-principles buildup, using inputs from local labour costs, maintenance, power, consumables, and other standard costs. The on-site cost is $378/t for 5.2% spodumene concentrate.

- The Project economics show an NPV of $1.45 billion, with a payback of 2.2 years, demonstrating the Project viability, using an externally generated spodumene concentrate benchmark price.
- Risk and sensitivity analyses have been completed for the project. The risk register will be periodically reviewed to capture emerging risks and to revise mitigation measures to minimize potential impacts.
- MGLIT has completed the necessary social and environmental impact studies to build management plans allowing for compliant operation of the Project. The Project area has a low environmental risk, being outside of ecological reserves and areas of environmental sensitivity.

The above statements indicate that the Project has completed a sufficient level of technical study to progress to the next phase of Project engineering and development, targeting a near-term operational strategy.

1.26 Recommendations

The following recommendations are suggested for consideration for further Project improvements:

- With receipt of the LAC permit, follow up with the subsequent submission of the new LAC to support with permitting of the expansion of the Project.
- Carry out an infill-drilling program in the domain of the Indicated resource classification to focus on improving resource delineation
- Perform additional geotechnical drilling to further strengthen geotechnical assumptions for the civil engineering design and construction.
- Commence road improvements and bridge construction over the Piauí River to support mine development and plant construction.
- Complete a Project execution plan including:
  - Detailed project schedule
  - Site safety and entry control
  - Logistics and storage for equipment purchased
  - Study and application for Project Ex Tarifario (duty exemptions)
  - Construction offices
  - Project insurance.
- Study outbound logistics, including port access, storage, and infrastructure.
- Commence a conceptual project design for fines flotation.

2 INTRODUCTION

This report titled *Bandeira Lithium Project, National Instrument 43-101 Technical Report—Definitive Feasibility Study Update, Araçuaí–Itinga, Minas Gerais, Brazil*, with an effective date of September 17, 2025, (the Technical Report), was prepared for MGLIT with the support of key Qualified Person (QP) (Section 2.2).

This National Instrument (NI) 43-101 Technical Report on the Bandeira Lithium Project (the Project) supersedes the first feasibility study (Horta de Cerqueira Viana, et al., 2024, July), which had an effective date of November 13, 2023.

2.1 Terms of Reference

Mineral Resources for the Bandeira deposit are reported using the Canadian Institute of Mining, Metallurgy and Petroleum (CIM) *CIM Definition Standards for Mineral Resources & Mineral Reserves* (CIM Definition Standards) (CIM, 2014). The quality of information, conclusions, and estimates contained this Technical Report is based, in whole or in part, on information available at the time of preparation, internal reports, other technical reports, and other literature, as well as assumptions, conditions, and qualifications specified herein.

2.2 Site Visits

Three NI 43-101 QPs contributing to the Technical Report have made visits to the Project. Table 2-1 presents the QPs responsible for all sections of the Technical Report.

Table 2-1: Qualified Persons, Qualifications, Affiliations, and Site Visits

Name of Qualified Person	Qualifications	Affiliations	Site Visit Dates
Brian Colin Talbot	BSc (Hons), FAusIMM	R-Tek	August 22 to 23, 2024
Carlos José Evangelista Silva	P.Geo., MSc, AIG	GE21	September 13 and 14, 2023; December 12, 2023; November 26 and 27, 2024
Hugo Ribeiro de Andrade Filho	P.Eng., FAusIMM	GE21	No site visit
Juliano Felix de Lima	MAIG (CP)	GE21	No site visit
Porfírio Cabaleiro Rodriguez	P.Eng., BSc, FAIG	GE21	No site visit
João Augusto Hilário de Souza	B.A.Sc., MBA	L&M Advisory	January 17 to 19, 2024
Noel Mark O´Brien	BE (Met), MBA, FAusIMM	R-Tek	No site visit
Bernardo Horta de Cerqueira Viana	MBA, FAIG	GE21	No site visit

Note: L&M Advisory = L&M Assessoria Empresarial S.S. Ltda.

2.3 Project Overview

The Project, in Brazil's "Lithium Valley," in northeast Minas Gerais (Figure 2-1), is a hard-rock spodumene operation in the Araçuaí Pegmatite District. The Project is designed as a predominantly underground mining operation, supported by a streamlined dense-media separation (DMS) and spodumene processing circuit. By leveraging proof-of-concept techniques successfully employed by

neighbouring hard-rock spodumene producers such as CBL and Sigma Lithium, the Project will deliver high-quality spodumene concentrate for shipment through coastal ports, to supply international markets.



Figure 2-1: Project Location in the State of Minas Gerais, Brazil

2.4 Qualified Persons

GE21 Consultoria Mineral (GE21) and R-Tek International DMCC (R-Tek) International prepared this Technical Report. The QPs who sign the technical sections are listed in Table 2-2.

Table 2-2: Qualified Person Areas of Responsibility

Section Name	Qualified Person	Sections
Executive Summary	All	
Introduction	Porfírio Cabaleiro Rodriguez[1]	1.2, 2
Reliance on Other Experts	Porfírio Cabaleiro Rodriguez[1]	1.3, 3
Property Description and Location	Carlos José Evangelista Silva[1]	1.4, 4
Accessibility, Climate, Local Resources, Infrastructure, and Physiography	Carlos José Evangelista Silva[1]	1.5, 5
History	Carlos José Evangelista Silva[1]	1.6, 6
Geology and Mineralization	Carlos José Evangelista Silva[1]	1.7, 7
Deposit Types	Carlos José Evangelista Silva[1]	1.8, 8
Exploration	Carlos José Evangelista Silva[1]	1.9, 9
Drilling	Carlos José Evangelista Silva[1]	1.10, 10
Sample Preparation, Analysis and Quality	Carlos José Evangelista Silva[1]	1.11, 11
Data Verification	Carlos José Evangelista Silva[1]	1.12, 12
Mineral Processing and Metallurgical Testing	Noel O´Brien[3]	1.13, 13
Mineral Resource Estimates	Carlos José Evangelista Silva[1]	1.14, 14
Mineral Reserves Estimate	Hugo Ribeiro de Andrade Filho[1]	1.15, 15
Mining Methods	Hugo Ribeiro de Andrade Filho[1]	1.16, 16
Recovery Methods	Noel O´Brien[3]	1.17, 17
Project Infrastructure	Juliano Lima[1]	1.18, 18
Market Studies and Contracts	Porfírio Cabaleiro Rodriguez[1]	1.19, 19
Environmental, Studies, Permitting, and Social or Community Impacts	Bernardo Horta de Cerqueira Viana[1]	1.20, 20
Capital and Operating Costs	Brian Colin Talbot[3]	1.21, 21.1, 21.2, 21.3, 21.4.1, 21.4.3, 21.4.9, 21.4.10, 21.5
	Hugo Ribeiro de Andrade Filho[1]	1.21, 21.4.2, 21.4.7, 21.4.8,
	João Augusto Hilário de Souza[2]	1.21, 21.4.4, 21.4.5, 21.4.6,
Economy Analysis	João Augusto Hilário de Souza[2]	1.22, 22
Adjacent Properties	Carlos José Evangelista Silva[1]	1.23, 23
Other Relevant Information	Carlos José Evangelista Silva[1]	1.24, 24
Interpretation and Conclusions	All	1.25, 25
Recommendations	All	1.26, 26
References	All	27

Notes: [1] GE21.
[2] L&M Advisory.
[3] R-Tek.

2.5 Units of Measure and Currency

The units of measurement used in this report conform to the International System of Units (metric system). All currency is United States dollars ($) unless otherwise noted.

3 RELIANCE ON OTHER EXPERTS

3.1 Marketing

L&M Advisory's (L&M) carried out the financial analysis in Section 22, in line with the supply and demand expectations of lithium compounds.

3.2 Environmental Licensing and Studies

GE21 reviewed the Project's environmental licensing. Section 20 of this Technical Report describes all components of the environmental licensing and is being used as technical support for the Mineral Resources estimate in Section 14, Mineral Reserves estimate in Section 15, and economic analysis in Section 22.

3.3 Taxation

The financial analysis QP, L&M Assessoria's (L&M Advisory) João Augusto Hilario de Souza is responsible for the assumptions adopted for taxes and fees used in this Technical Report. L&M Advisory implemented all taxes considered—Contribuição Financeira para Extração Mineral (CFEM) (Financial Compensation for Mineral Exploration), Taxa de Controle, Monitoramento e Fiscalização das Atividades de Pesquisa, Lavra, Exploração e Aproveitamento de Recursos Minerários (TFRM), (Fee for the Control, Monitoring and Inspection of research Mining, Exploration and Utilization of Mining Resources Activities), Programa de Integração Social (PIS) (Social Integration Program), Contribuição para o Financiamento da Seguridade Social (COFINS) (Social Security Financing Contribution), Social Contribution on Net Profit (CSLL), Corporate Income Tax (IRPJ) and Tax on operations relating to the circulation of goods and on the provision of the mposto sobre Circulação de Mercadorias e Serviços (ICMS) (Interstate and Intermunicipal Transport and Communication Services)—as well as the federal-level incentive for investment due to the Project's location in areas under the Superintendência do Desenvolvimento do Nordeste (SUDENE) (Superintendency for Northeast Development), which reduces income tax on profit by 75% for 10 years, renewable. All this information was also used to prepare Section 22.

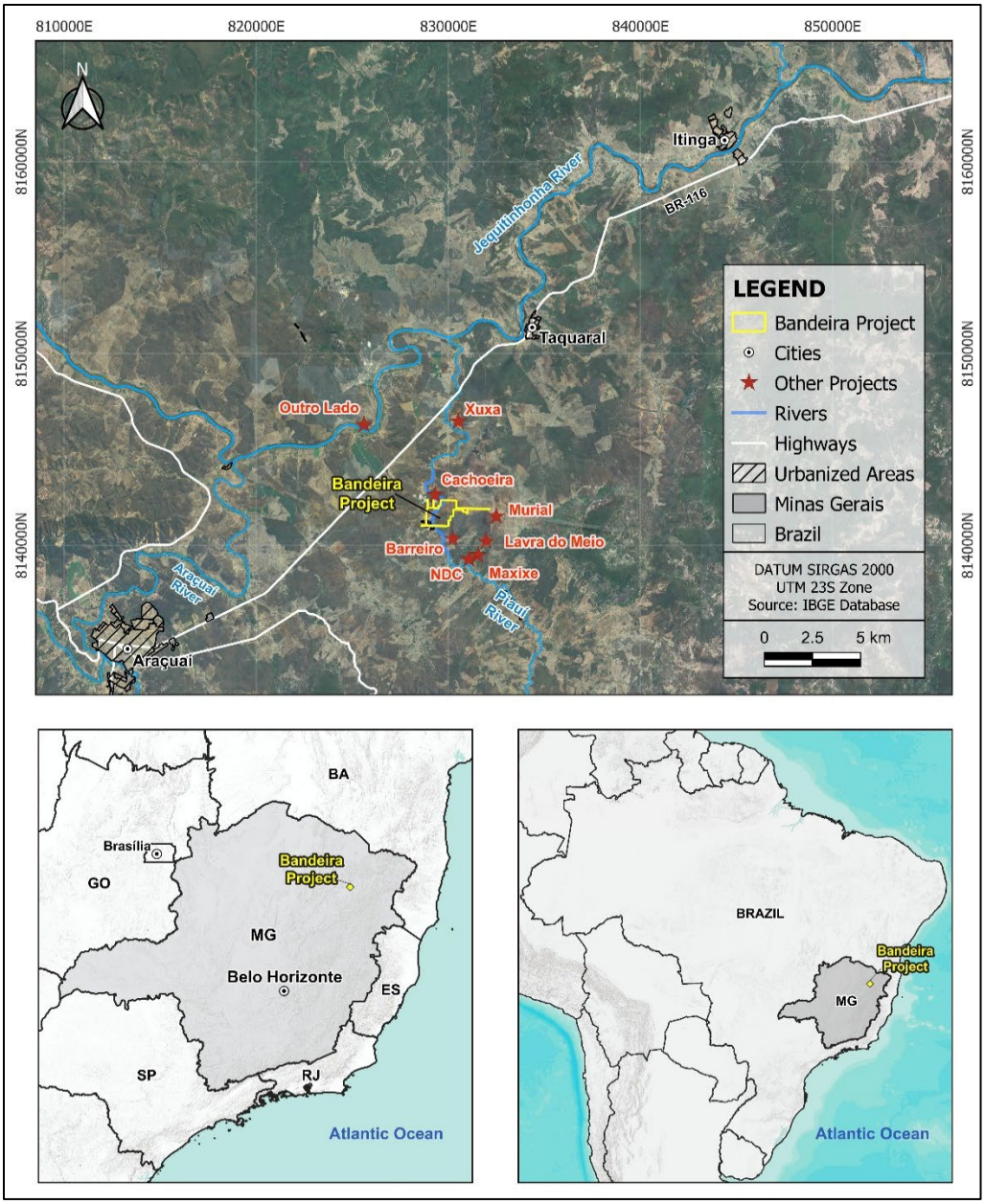
3.4 Mineral Rights

The QPs did not make any assessment of the legal situation of the mining rights of this Project.

William Freire Advogados Associados issued Legal Opinion No. 47/2023—Interested Party: MGLIT Empreendimentos Ltda regarding the mineral rights number ANM 832.439/2009, ANM 831.116/2016, 831.117/2016 stating that the mineral rights are active, allowing MGLIT to perform geological research for lithium ore.

4 PROPERTY DESCRIPTION AND LOCATION

The Project is in the northeastern region of Minas Gerais State, Brazil, within the Jequitinhonha Valley area, approximately 600 km northeast of Belo Horizonte. It is roughly 75 km south of Salinas (population about 42,000) and about 25 km east of Araçuaí (population about 40,000) (Figure 4-1).



Source: GE21s (2024).

Figure 4-1: Mining Rights of the Project

The Project is at latitude 16° 47' S and longitude 41° 53' W (UTM Zone 24S 190117 E 8141940 N) (SIRGAS 2000).

4.1 Mineral Rights

The Project consists of three current mineral rights applicable to mineral exploration research permits covering an area of 174.17 ha (Table 4-1).

Table 4-1: Project Mineral Rights

Claim Number (ANM)	Target Name	Municipality (Mina Gerais)	Area (ha)
832.439/2009	Bandeira	Araçuaí–Itinga	156.77
831.116/2016	Bandeira Leste	Itinga	15.79
831.117/2016	Bandeira Sul	Araçuaí–Itinga	2.27
Total			174.83

Note: ANM = Brazil National Mining Agency.

4.2 Brazilian Mineral Exploration and Mine Concession

Under the Brazilian Constitution, all mineral resources on surface or underground are property of the Federal Government. The Constitution provides companies with the mining rights to the resources under the mining concessions. Mineral rights come under the jurisdiction of the Federal Government, and mining legislation is enacted at the federal level. A company applying for mineral rights must be incorporated under Brazilian law, with management and administrative responsibility directly domiciled in Brazil.

Lithium Ionic has ownership and control of MGLIT Empreendimentos Ltda (MGLIT), its Brazilian subsidiary; MGLIT developed the exploration program and will implement the mine and concentration plant in Brazil.

4.3 Surface Rights

MGLIT has a lease agreement with VALITAR Participações Ltda (VALITAR), the property's landowner. MGLIT is the usufructuary of the properties on which the Project will be implemented, thus having the legal rights of possession and enjoyment of these properties, for the purpose of developing its activities in accordance with Brazilian legislation.

4.4 Agreements

MGLIT has executed usufruct agreements with VALITAR, securing the access and other corresponding rights to the properties for a minimum of 30 years.

4.5 Royalties

4.5.1 CFEM Royalty

The Brazilian Government is entitled to a Compensação Financeira pela Exploração de Recursos Minerais (CFEM) (Compensation Royalty), whereby the holder of a mining concession for lithium mineral is legally obligated to pay the Brazilian government 2.0% of the gross income from its sales. The only deductions allowed are taxes levied on commercial sales.

4.5.2 Landowner's Statutory Royalty

According to Brazilian legislation, landowners are entitled to a royalty in connection with the mineral extraction carried out on their respective properties, in an amount equivalent to 50% of the corresponding CFEM royalty, owed by the holder of the mining concession.

4.5.3 Royalties Agreements

Since the publication of the previous feasibility study with an effective date of November 13, 2023, (Horta, et al., 2024, July 11), a royalty agreement was reached with Appian Capital Advisory LLP. Funds in the amount of $20 million were secured for a royalty of 2.25% on gross revenue for production of ores originating from the Project. This royalty is reflected in the economics of this Technical Report.

4.6 Environmental Liabilities

All Project activities since the exploration and geological research began must comply with federal decree No 99,274/90, which regulates federal law 6,938/81 and establishes the Brazilian Environmental Policy.

The permitting process that encompasses the preliminary licensing and installation was submitted in November 2023.

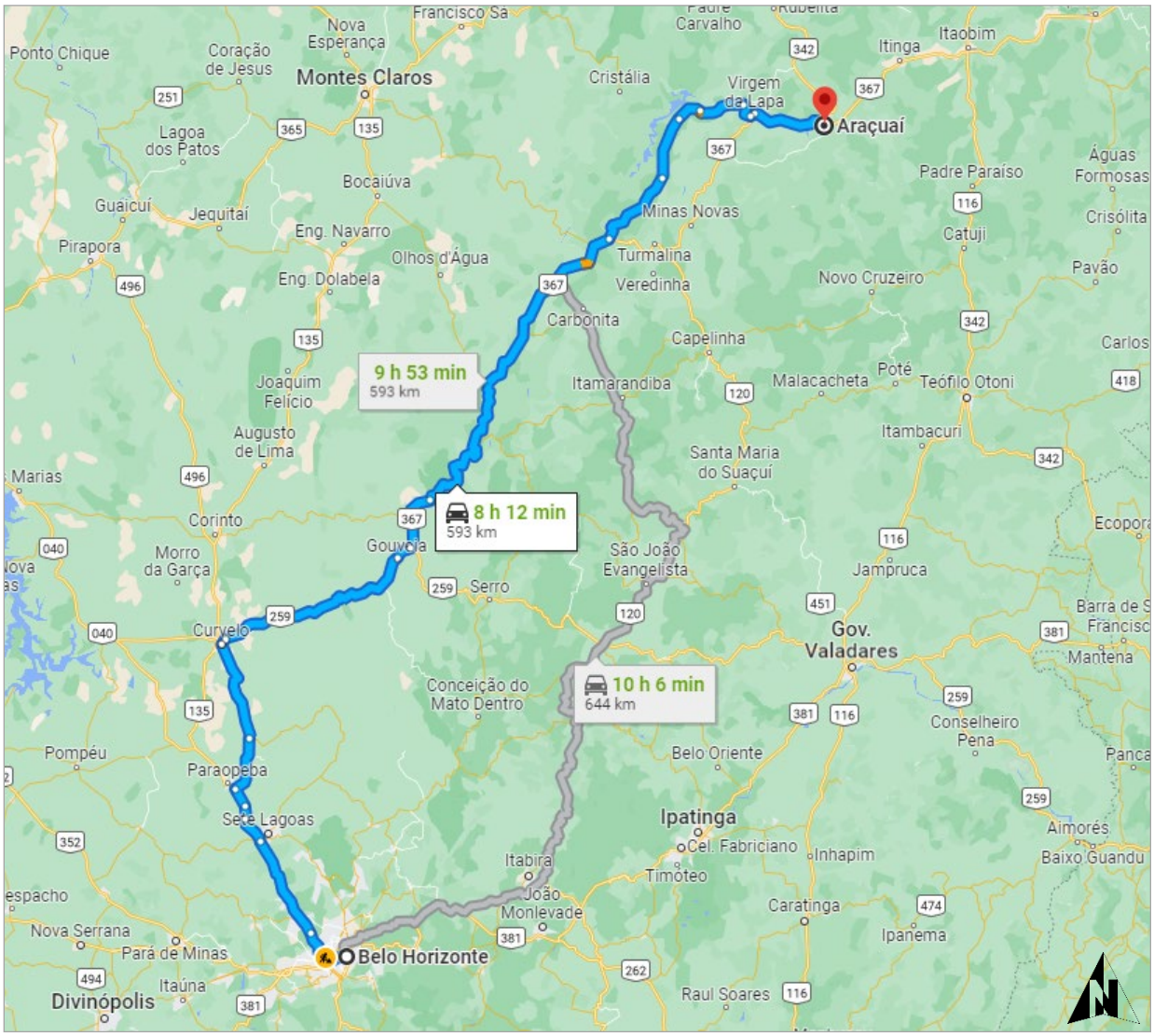
4.7 Qualified Person's Comment

To the extent known, there are no other significant factors and risks that may affect access, title, or the ability to perform work on the Project that not been discussed in this Technical Report.

5 ACCESSIBILITY, CLIMATE, LOCAL RESOURCES, INFRASTRUCTURE AND PHYSIOGRAPHY

5.1 Accessibility

The Project is in northeast Minas Gerais, between the municipality of Itinga and the city of Araçuaí; approximately 15 km from Araçuaí and 620 km northeast of Belo Horizonte (Figure 5-1).

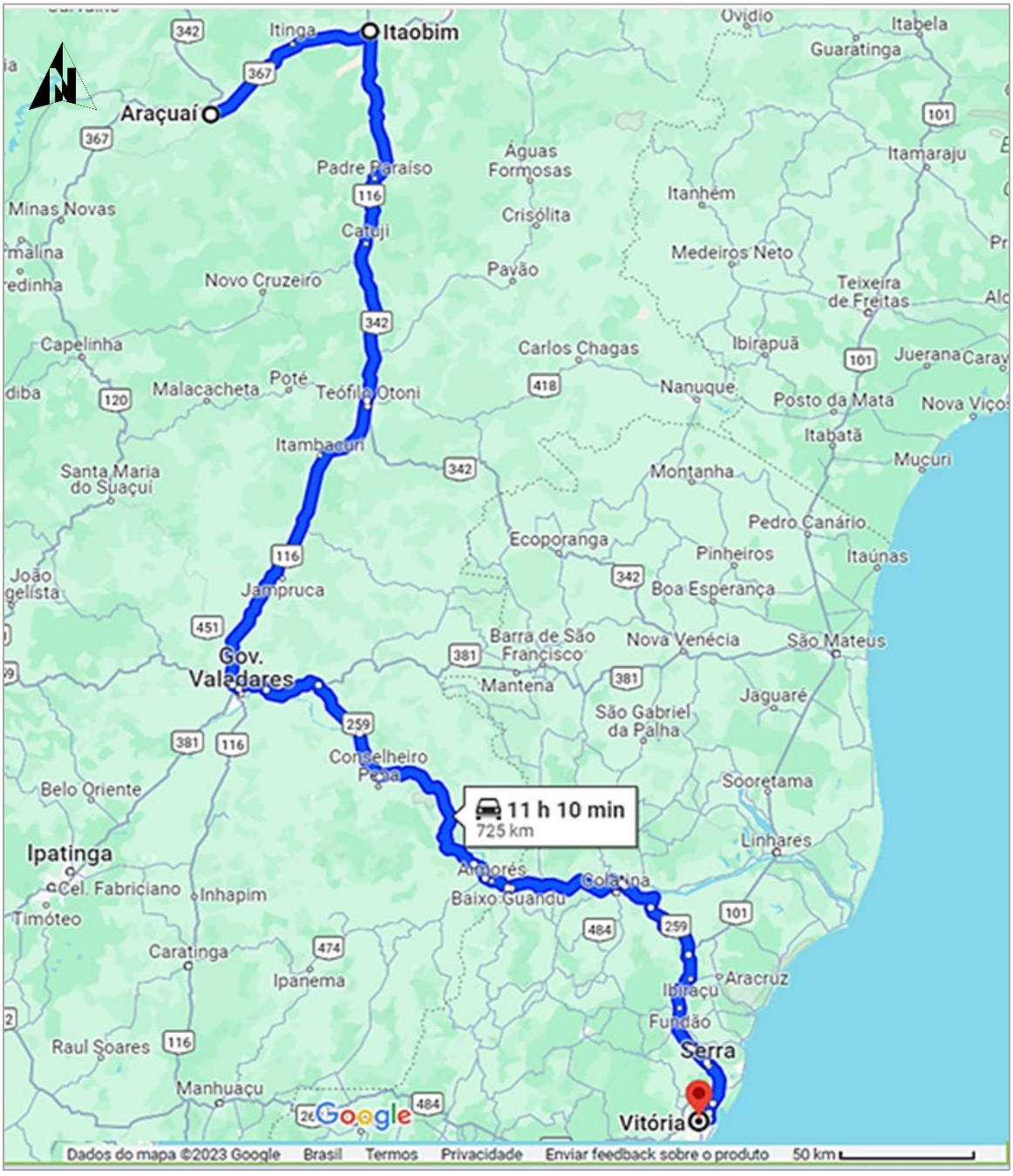


Source: Google Maps (2023).

Figure 5-1: Access from Belo Horizonte to Araçuaí

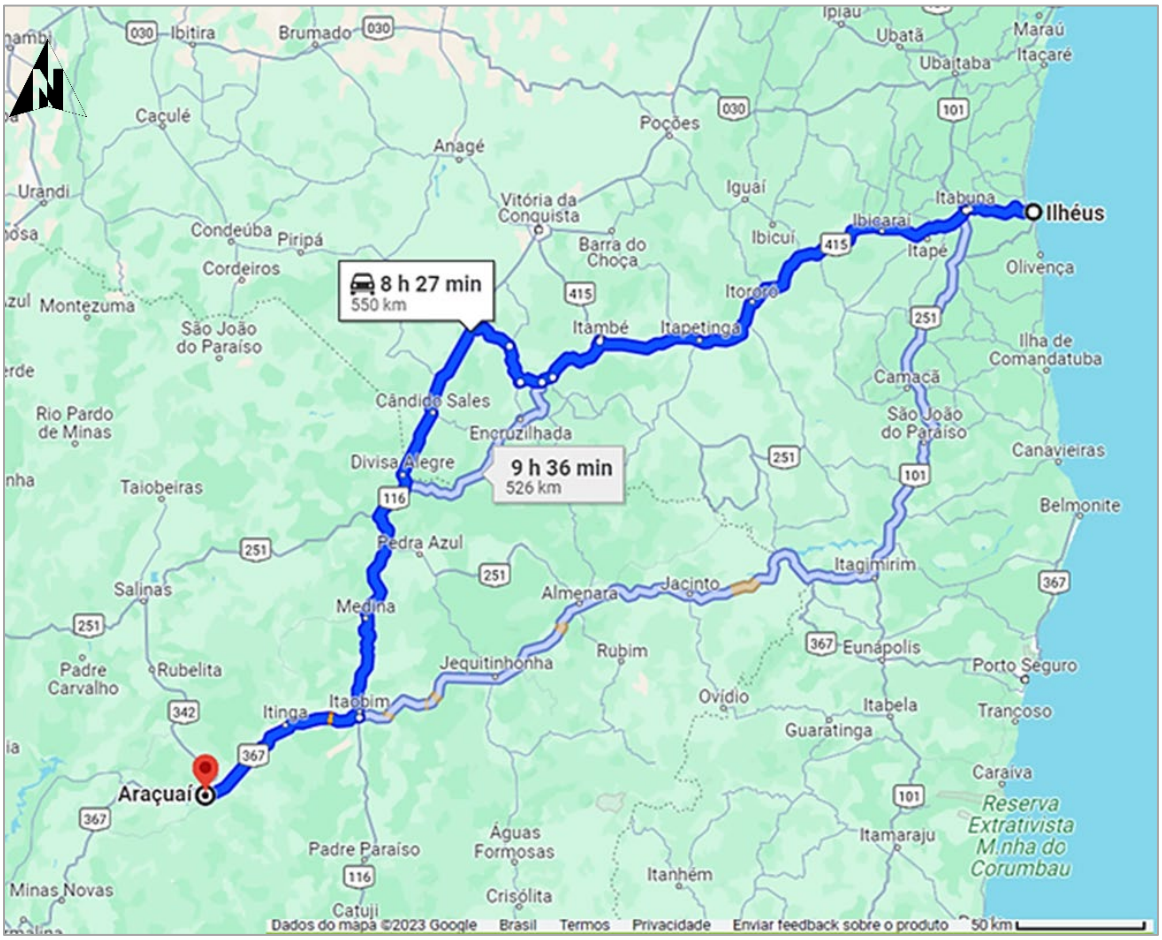
Due to its proximity to the BR-367 national highway, the Project is well-served by a road network. The site is accessible year-round by a good network of highways and airports.

The Project's spodumene production would be exported from the Port of Vitória (Figure 5-2), in the state of Espírito Santo, 725 km from the Project along federal highways BR-367, BR-116 (or -342), and BR-259. Approximately 550 km from the Project, the Port of Ilhéus (Figure 5-3) is another option for exporting the product; it is reached via federal highways BR-367, BR-116, and BR-415, or BR-367, BR-101, and BR-415.



Source: Google Maps (accessed November 22, 2023).

Figure 5-2: Access from Araçuaí to the Port of Vitória



Source: Google Maps (accessed November 22, 2023).

Figure 5-3: Access from Araçuaí to the Port of Ilhéus

5.2 Climate

The region is characterized by a hot, dry, semi-arid climate. The annual average temperature is 24.5°C, with an average annual rainfall of 651.2 mm. The driest period of the year is June, and the wettest is November. There is no harsh cold season. Exploration and mining activities can take place throughout the year. Detailed weather conditions in Araçuaí are given in Figure 5-4 and Figure 5-5.

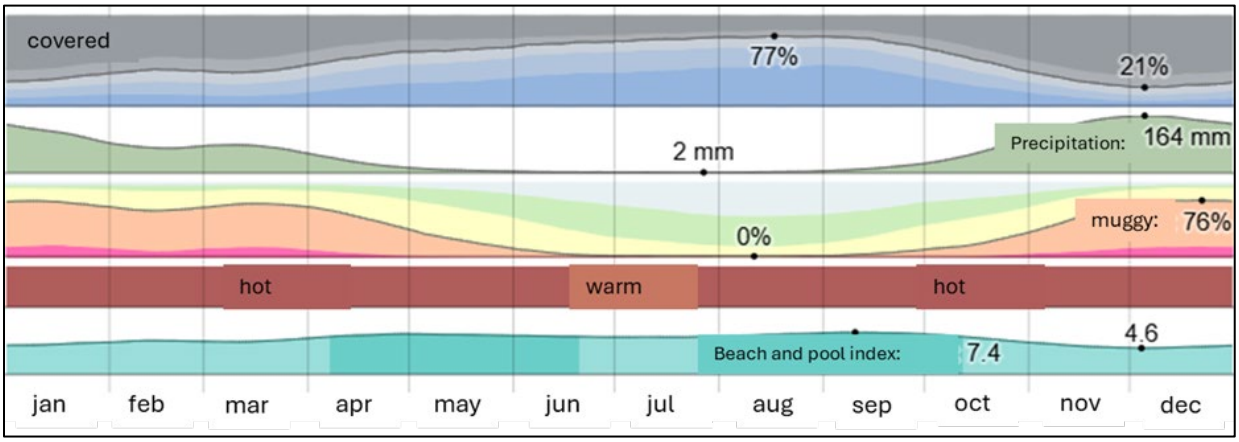
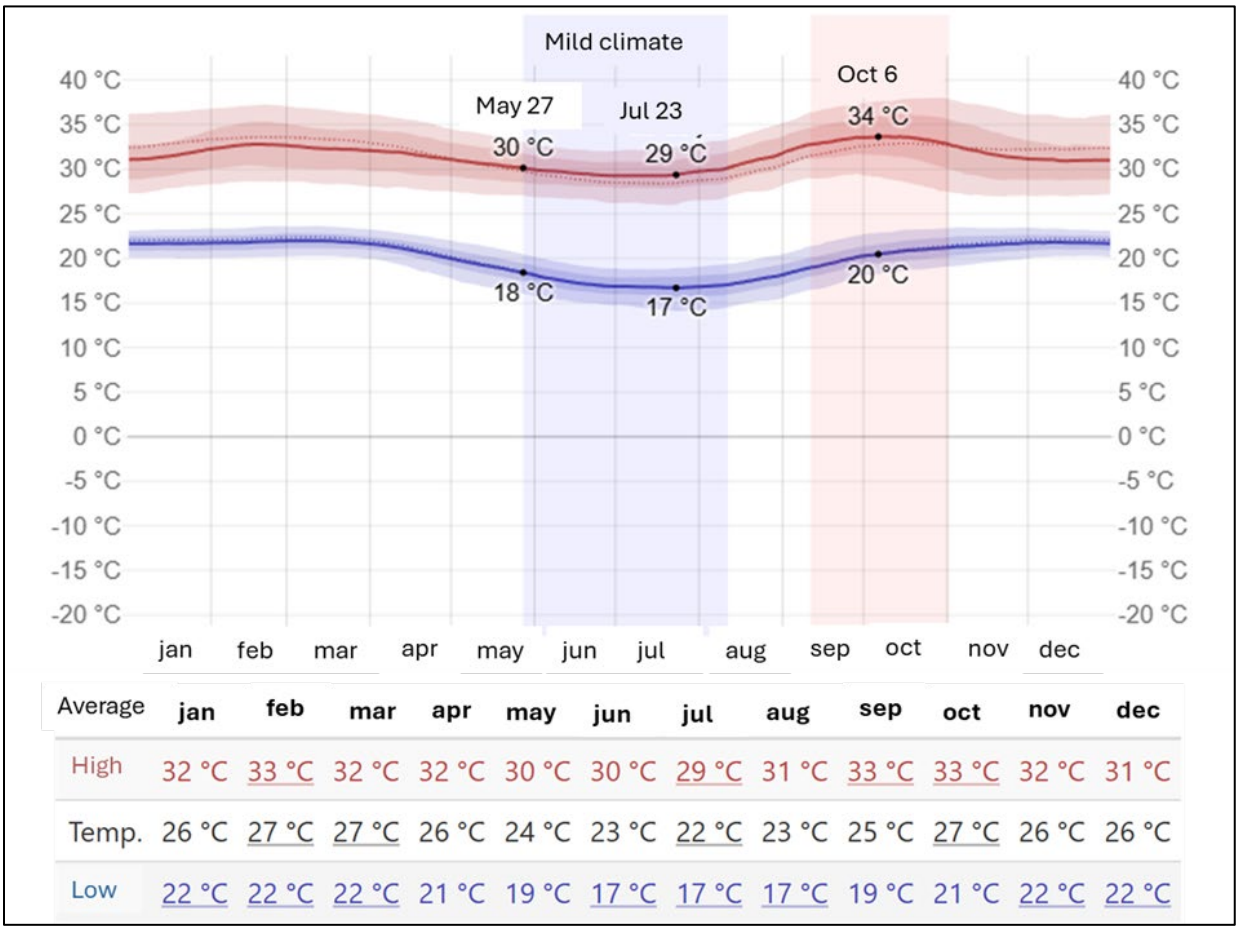


Figure 5-4: Monthly Meteorological Conditions in Araçuaí, with Low and High Averages (%)



Average	jan	feb	mar	apr	may	jun	jul	aug	sep	oct	nov	dec
High	32 °C	33 °C	32 °C	32 °C	30 °C	30 °C	29 °C	31 °C	33 °C	33 °C	32 °C	31 °C
Temp.	26 °C	27 °C	27 °C	26 °C	24 °C	23 °C	22 °C	23 °C	25 °C	27 °C	26 °C	26 °C
Low	22 °C	22 °C	22 °C	21 °C	19 °C	17 °C	17 °C	17 °C	19 °C	21 °C	22 °C	22 °C

Figure 5-5: Monthly Maximum and Minimum Temperatures in Araçuaí

5.3 Local Resources and Infrastructure

Itinga and Araçuaí are the largest cities nearest to the Project, with populations of 14,000 and 40,000 inhabitants, respectively. Araçuaí is served by a small airport and large, commercial mobile phone networks.

In 2022, the average monthly wage in Araçuaí was 1.7 times the minimum wage, and the proportion of unemployed persons was 12.5%.

In Araçuaí 38.3% of households have adequate sanitary facilities; 53.6% of urban households face public roads with trees, and 5.3% of urban households are on public roads with culverts, sidewalks, paving, and curbs.

The nearest medium-sized airport with regular commercial flights is the medium-sized Vitória da Conquista (Bahia), about 297 km north of Araçuaí via BR-367 and BR-116. Another medium-sized airport is Montes Claros, 322 km from Araçuaí, accessed via federal highways BR-342 and BR251. The nearest small airport, with regular commercial flights since December 2023, is in Salinas, around 110 km north of Araçuaí via BR-342.

5.4 Physiography

The topography of the Project area comprises low hills, ravines, and wide valleys, whose elevation differences are less than 100 m. The project occupies areas on both banks of the Piauí River, which will provide raw water to meet the demands of the mine, processing, and concentration plants, as well as other mining facilities (Figure 5-6 and Figure 5-7).



Figure 5-6: Aerial View of Project Area with Future Infrastructure Locations

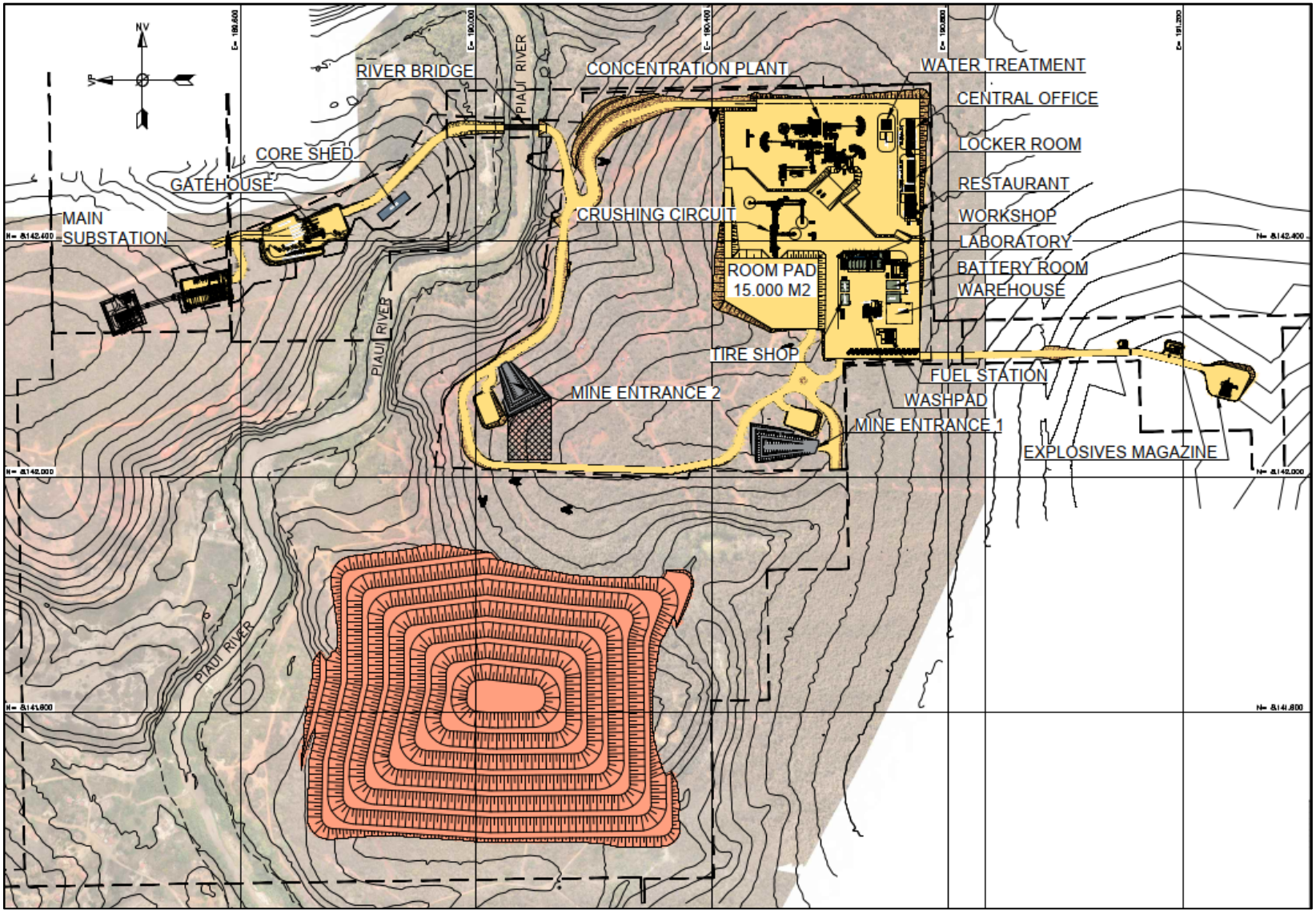


Figure 5-7: Site Layout

6 HISTORY

6.1 Project History

The Project is in a region rich in lithium deposits with other operators present in the area. Prior to 2009, no operation or exploration activity took place in the Project area. From 2009 to 2017, Falcon Metais Ltda. (Falcon) performed initial exploration activities; any fieldwork was completed during this period. In 2020, MGLIT acquired the mineral rights from Falcon. Since 2022, MGLIT has performed several phases of exploration activities and resource estimate updates have been released in 2023 and 2024.

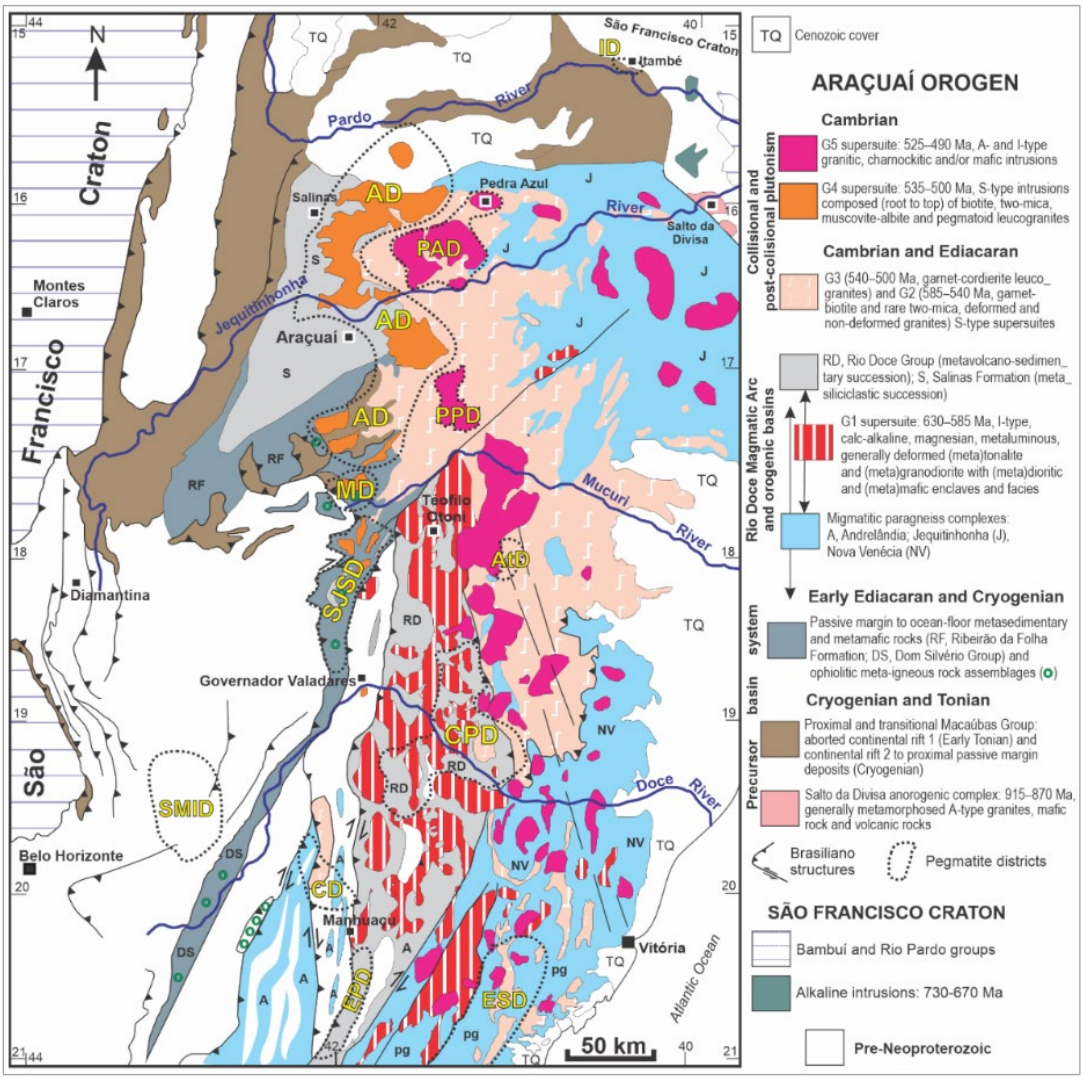
6.2 Production History

Bandeira is a greenfield project and there are no production records for this property. There is evidence of old and deactivated artisanal mines (garimpos) in the area only. There is no evidence of current artisanal or small-miners activity in the area. There has not been any commercial production by Lithium Ionic or its subsidiaries from this property.

7 GEOLOGICAL SETTING AND MINERALIZATION

7.1 Regional Geology

The Project lies in the Eastern Brazilian Pegmatite Province (EBPP), in terranes of the Araçuaí Orogen. The EBPP, one of the largest spegmatitic populations in the world, with about 150,000 km^2, containing 12 pegmatite districts in eastern Minas Gerais (ca. 90% of the whole province), southeastern Bahia, and Espírito Santo States of Brazil.



Notes: Simplified geologic map of the Araçuaí Orogen, highlighting the granite supersuites and pegmatite districts of the Eastern Brazilian Pegmatite Province. Araçuaí (AD); Ataléia (AtD); Caratinga (CD); Conselheiro Pena (CPD); Espírito Santo (ESD); Itambé (ID); Malacacheta (MD); Pedra Azul (PAD); Padre Paraíso (PPD); São José da Safira (SJSD); Santa Maria de Itabira (SMID).

Figure 7-1: Simplified Geology of the Araçuaí Orogen

The EBPP is the most important region in Brazil's history of pegmatite studies, and the development of lithium deposits (Pedrosa-Soares et al. (2025) present a comprehensive synthesis of this province, highlighting spodumene-rich deposits. In the first decades of the 19th century, pioneer naturalists and geologists described pegmatite gem deposits in the Jequitinhonha and Doce river valleys (e.g., Exchwege, Spix, Martius, and Saint-Hilaire). In 1818, Spix and Martius reached the headwaters of the Calhauzinho and Piauí rivers in the Araçuaí region (Figure 7-4, searching for the gemstone's primary sources, which were already mined there, particularly chrysoberyl (then called "chrysolite" locally). They found a "white granite with little mica, but rich in black tourmaline" (i.e., pegmatite).

Brazilian mineralogist José Bonifácio de Andrada discovered and named spodumene (*Journal der Chemie*, 1800), by then pioneer prospectors and gemstone diggers (*garimpeiros* in Brazilian Portuguese) of the Jequitinhonha Valley already called it "rotten chrysolite." In 1866, Charles Hartt described the N45E-trending structure of the mica schists hosting very coarse-grained "granite" veins between Araçuaí and Itinga. Costa Sena (1882) published the first direct reference to spodumene in the Middle Jequitinhonha region (also called "triphane" at that time), after identifying "andalusite, cymophane (chrysoberyl) and triphane with sharp edges, in sands and gravels from streams of the Piauí river valley" and suggested that the primary deposits would also be located there. Luiz Caetano Ferraz (1928) described several spodumene occurrences, among other pegmatite minerals, in the Middle Jequitinhonha Valley.

The importance of pegmatites as economic mineral deposits greatly increased in Brazil from the Second World War, due to the large production of mica, beryl, and quartz to supply the military industry of allied countries, to the end of the Cold War in early 1990s. Glaycon de Paiva (1946) grouped the largest pegmatitic populations of Brazil into provinces—the first definition of the Eastern Brazilian Pegmatite Province. Since then, more than 1,000 pegmatites have been mined there for gemstones, cassiterite, lithium and beryllium ores, Nb-Ta oxides, industrial minerals (K-feldspar, muscovite, albite, quartz), collection and rare minerals, dimension stone, and minerals for esoteric purposes.

Sá (1977) reported historical milestones in the discoveries and mining of lithium deposits in the Araçuaí-Itinga region:

> The discoveries and production of cassiterite, lepidolite, and amblygonite in pegmatites of the Piauí river valley (e.g., Fumal, Generosa, Jenipapo, and Urubu) by the Estanífera do Brasil and Produco companies dated back to the early 1950s. Although spodumene has been known for a long time by gem diggers ("garimpeiros"), who called it "cambalacho" or "crisólita podre" (i.e., rotten chrysolite in reference to its similarity to chrysoberyl), its commercial production only started at the end of the 1960s at the Cachoeira mine (then owned by Companhia Estanífera do Brasil) to supply the increasing demand of the national market. Petalite, formerly called "escória branca" (white scoria) and very often mistaken for feldspar, was correctly identified at the end of the 1960s and immediately mined for exportation by the Companhia Estanífera do Brasil until 1972, followed by Companhia Arqueana de Minérios e Metais Ltda. Around 1977, this mining company has more than twenty distinct pegmatite bodies producing petalite, spodumene, amblygonite, lepidolite, beryl, cassiterite and columbite-tantalite. (Sa, 1977)

Afgouni and Sá (1978, pp. 247–253) predict that "another new use (for that metal) is in lithium batteries for electric cars and, if this application becomes reality, Brazil will be a big consumer, ranking at the

same level as the most developed countries in the world, with the advantage of being one of few countries producing its own raw material." Although this is not yet a full reality, the remarkable increase in lithium ore production in the Jequitinhonha Valley is a result of Arqueana's discoveries of world-class lithium deposits. CBL (Cachoeira mine) bought the assets in the early 1990s, and more recently Sigma Lithium purchased the Xuxa and other spodumene-rich deposits such as Barreiro, Maxixe, and Murial. That heritage continues to drive new companies to the region, whose exploration efforts have led to the discovery of subsurface spodumene deposits in areas lacking outcrops, such as MGLIT's Bandeira deposit.

The EBPP is the result of the magmatic and tectono-metamorphic events that formed the Araçuaí Orogen from the Early Ediacaran (ca. 630 Ma) to the Late Cambrian (ca. 490 Ma). These events comprise the regional deformation, metamorphism and partial melting of sedimentary and volcanic successions deposited in the Tonian-Cryogenian precursor (rift to passive margin) basin system and the Ediacaran orogenic (arc-related) basins (Figure 7-2), as well as of the continental basement (Pedrosa-Soares et al., 2025). These melting events resulted in the production of huge volumes of orogenic granitic rocks and thousands of pegmatites grouped into five supersuites (G1 to G5) (Figure 7-1, Table 7-1).

The sedimentary and volcano-sedimentary successions involved in the tectono-metamorphic-anatectic processes that generated granites and pegmatites show two contrasting distributions of U-Pb ages for detrital grains of zircon (Figure 7-2). One is a classic multimodal age spectrum of a basin system evolved from continental rift to passive margin, represented by the Macaúbas Group and Jequitinhonha Complex. The other age distribution shows a unimodal spectrum typical of orogenic basins largely filled by material from a rather dominant zircon source (e.g., an active magmatic arc), representing the Salinas Formation and Rio Doce Group that host most lithium-bearing pegmatites in the EBPP (Figure 7-1). The Salinas Formation is the main host unit of lithium-rich pegmatites in the whole EBPP, including the spodumene-rich pegmatites of MGLIT's Bandeira deposit; these comprise quartz-mica schist (metapelite) and metawacke (metasandstone) with lenses of calc-silicate rock (metamarl), and meta conglomerate.

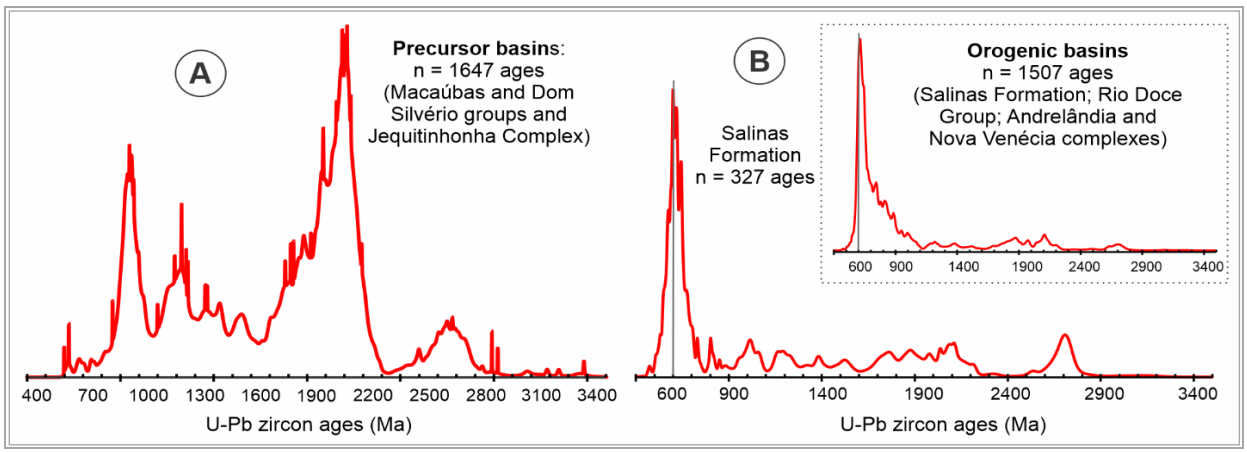
Tectono-metamorphic events and the G1 to G5 granitic supersuites of the Araçuaí Orogen play distinct roles in relation to pegmatite abundance, distribution, genesis, and metallogenetic specialization, imposing important prospecting constraints with regards to metallic potential of distinct pegmatite populations along the EBPP (Figure 7-2).

The G4 is the most important granitic supersuite related to lithium-rich pegmatites, followed by the G2 supersuite, while the G5 and G1 supersuites are related to Be-rich pegmatites generally free of, or poor in lithium-minerals. Tourmaline-bearing pegmatites are widespread in the EBPP, except in some clusters of beryllium-rich and lithium-rich pegmatites. The G4 intrusions and batholiths show the classical distribution of granitic facies, from pluton root to top, found in other lithium-rich pegmatite districts around the world, comprising biotite leucogranite, two-mica leucogranite, muscovite leucogranite, albite leucogranite, and pegmatoid granite. Apatite, beryl, tourmaline, and garnet occur in the pegmatoid granites and muscovite-albite leucogranites (Pedrosa-Soares et al., 2025). The Salinas Formation is also the main host unit of G4 intrusions associated with lithium-rich pegmatites (Figure 7-1).

7.1.1 Pegmatites

Granitic pegmatites represent silica-saturated magmas variably rich in water- and fluorine-bearing fluids, as well as in other hyperfusible (fluxing) components (e.g., Li, Na), crystallized in rather closed chemical systems (Cerný, 1991; London, 2008). The EBPP comprises the two known genetic types of pegmatites, both formed during the evolution of the Araçuaí Orogen: a) the anatectic pegmatites generated directly from the partial melting of country rocks; and b) the residual pegmatites, representing late silicate melts released by fractional crystallization of parental granites. Genetic affiliation and other criteria allow pegmatite districts to be distinguished in the EBPP (Figure 7-2; Table 7-1).

The anatectic pegmatites are coarse-grained quartz-feldspathic bodies (i.e., granitic leucosomes) hosted by migmatitic gneisses and micaschists, mostly formed in the collisional tectono-metamorphic event (585–540 Ma) and in the post-collisional thermal event (540–490 Ma). Therefore, their spatial distribution, and genetic and metallogenetic features are directly related to the melted country rocks. Conversely, the residual pegmatites, especially those enriched in rare elements, have restricted spatial distributions and genetic links directly related to the distinct granite types from which they ultimately inherited their geochemical characteristics and metallogenetic specializations (Figure 7-3; Table 7-2). Therefore, residual pegmatites released from peraluminous, subalkalic-to-alkalic, hydrous, S-type, two-mica leucogranites formed from the partial melting of metasedimentary rocks might have a rather distinct metallogenetic specialization (e.g., richer in Li, Cs, Ta, Sn, and P) in relation to residual pegmatites (e.g., richer in Be, F, and Fe) from metaluminous, high-K calc-alkalic, ferroan, relatively anhydrous, A-type, amphibole-biotite granites formed from the partial melting of mainly igneous rocks. The first case (S-type granites) refers to lithium pegmatites associated with the G4 and G2 supersuites, while the second (A-type granites) stands for the beryllium-rich (but lithium-free) pegmatites comprised by the G5 supersuite (Figure 7-3 Table 7-2).



Source: Adapted from Pedrosa-Soares et al. (2025).

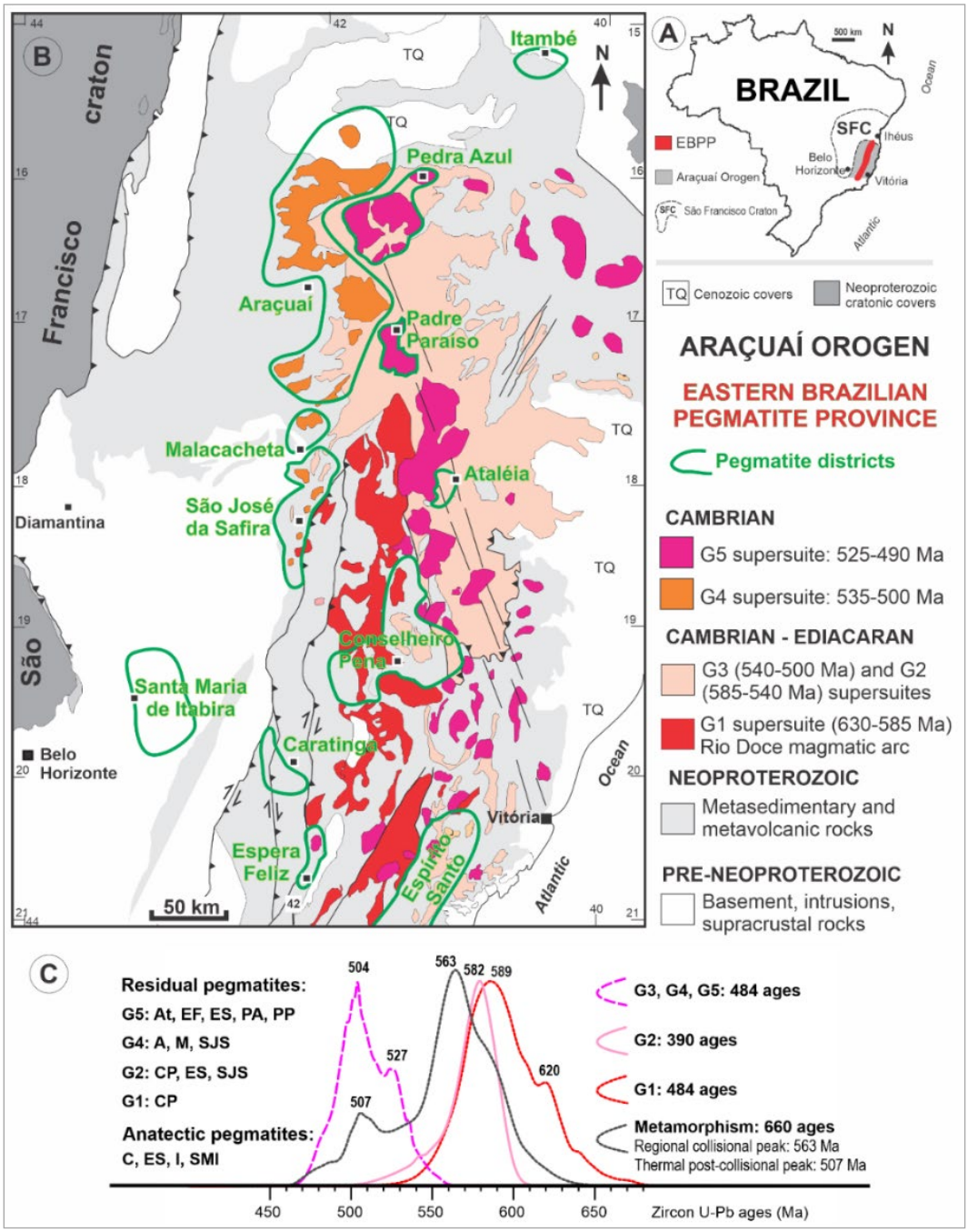
Notes: Araçuaí Orogen within the Eastern Brazilian Pegmatite Province: A, precursor basins (e.g., Macaúbas Group and Jequitinhonha Complex); B, orogenic basins (e.g., Salinas Formation Rio Doce Group).

Figure 7-2: Distributions of U-Pb Ages for Detrital Zircon Grains from Metamorphosed Sedimentary and Volcanic Rocks

Table 7-1: Main Features of the Orogenic Igneous Supersuites of the Araçuaí Orogen

Supersuites	G1	G2	G3	G4	G5
Ages (Ma)	630–585	585–540	540–500	535–500	525–490
Lithotypes	Mostly tonalite and granodiorite, minor diorite to gabbronorite, with biotite, amphibole and/or pyroxenes; poor in pegmatites	Mostly biotite-garnet syenogranite to alkali feldspar granite, garnet-rich monzogranite to tonalite, and garnet-two-mica granite, locally with sillimanite; associated with external rare element pegmatites	Alkali feldspar granite to syenogranite with cordierite and/or garnet and/or sillimanite, free of or poor in biotite; poor in pegmatites	From pluton root to top: biotite granite, two-mica leucogranite, muscovite and/or albite and/or schorlite granite, pegmatoid granite; associated with external rare element pegmatites	Alkali feldspar granite to granodiorite, orthopyroxene-bearing charnockitic rocks, basic (norite) to ultrabasic rocks, and beryl-topaz pegmatites
Field relations	Batholiths and stocks, generally rich in dioritic to mafic enclaves and facies, showing solid-state deformation and migmatization, local well-preserved igneous fabrics, associated with the arc-related metavolcano-sedimentary Rio Doce Group	Batholiths, stocks and stratoid bodies, showing solid-state deformation, metamorphism and migmatization, with common restites and xenoliths of metasedimentary rocks, and localized well-preserved igneous fabrics	Mostly autochthonous, non-deformed patches, veins, and lodes of G3 leucosome, and minor stocks, free of the regional foliation, hosted by migmatites with G2 paleosome	Balloon- to stratoid-shaped intrusions, post-kinematic in relation to the regional ductile foliation, locally imposing late deformation on the regional structural trend (circumscribed intrusions)	Balloon-shaped plutons and multiple intrusions, locally rich in mafic and/or microgranular enclaves with magma mixing features, and norite-rich bodies, post-kinematic in relation to the regional ductile foliation
Geochemical signatures	Metaluminous to slightly peraluminous, magnesian, calcic to alkali-calcic, medium- to high-K, expanded calc-alkaline series	Strongly to weakly peraluminous, calc-alkalic to sub-alkalic (K > Na)	Peraluminous, sub-alkalic (K > Na)	Peraluminous, sub-alkalic (K > Na) to alkalic (Na > K)	Metaluminous to slightly peraluminous, ferroan, high-K calc-alkalic, minor tholeiite
Petrogenetic type	Metaluminous I-type, locally peraluminous I-type	Peraluminous S-type, locally peraluminous I-type	S-type	S-type	A-type and I-type
Tectonic stage	Pre-collisional to early collisional magmatic arc	Late pre-collisional to late collisional	Late collisional to post-collisional	Post-collisional	Post-collisional

Source : Pedrosa-Soares et al. (2025).



Source : Pedrosa-Soares et al. (2025).

Notes: A: Location of Eastern Brazilian Pegmatite Province (EBPP).
B: Simplified geological map highlighting the granite supersuites (G1 to G5) and EBPP pegmatite districts.
C: Distribution of zircon U-Pb ages from orogenic granite supersuites (G1 to G5), regional metamorphism and post-collisional thermal events, correlated to pegmatite districts

Figure 7-3: Simplified Geologic Map of Araçuaí Origen

Table 7-2: Features of the Main Pegmatite Districts of the Eastern Brazilian Pegmatite Province

District Names and Ages (Ma)	Historical and Present-Day Mineral Production, and Rare Minerals	Genetic Affiliation; Class, Subclass, Type, Subtype, and Family[1]	Parent and Host Rocks
Itambé 508 Ma	K-feldspar, quartz crystals, mica, beryl, columbite, monazite	anatectic; muscovite-rare element, REE, allanite-monazite, NYF	biotite-hornblende gneisses, sillimanite-feldspar-mica schists
Pedra Azul 501 Ma	Quartz, beryl (aquamarine), topaz	residual; REE, beryl-topaz, NYF	A-type G5 granites
Padre Paraíso 519 Ma	Quartz, beryl (aquamarine), topaz, quartz crystals, goshenite, chrysoberyl	residual; REE, beryl-topaz, NYF	A- and I-types G5 granites and charnockites
Araçuaí 535–500 Ma	Greenish to pinkish spodumene, petalite, lepidolite, lithium-phosphates, cookeite, cassiterite, columbite-tantalite, industrial minerals (perthitic K-feldspar, albite, muscovite), tourmalines (elbaite, schorlite), beryl ore and gems (aquamarine, morganite), pollucite, quartz crystals, cleavelandite, herderite and other rare phosphates, topaz, bismuthinite	residual; mostly rare element and minor muscovite-rare element, lithium, beryl, complex (spodumene, petalite, lepidolite, elbaite, amblygonite), albite-spodumene (SRP), albite, LCT	S-type G4 leucogranites; low-P/high-T (andalusite, cordierite, sillimanite) to medium-PT (garnet, staurolite, kyanite, sillimanite) mica schists to paragneisses, metasandstones, calc-silicate rocks, meta-ultramafic rocks
Ataléia 502 Ma	Quartz crystals, beryl (aquamarine), topaz, chrysoberyl	residual; REE, beryl-topaz, NYF	A- and I-types G5 granites and charnockites
São José da Safira 545–490 Ma	Tourmalines (elbaite, schorlite), industrial minerals (perthitic K-feldspar, albite, muscovite), beryl ore and gems (aquamarine, heliodor, morganite), lepidolite, lithium -phosphates, spodumene, garnet, cleavelandite, columbite-tantalite, cassiterite, bertrandite, microlite, zircon, rare phosphates	residual; muscovite-rare element and rare element, lithium, beryl, complex (elbaite, lepidolite, lithium -phosphates, spodumene), LCT	S-type G4 and G2 leucogranites; medium-PT (garnet, staurolite, kyanite, sillimanite) mica schists to paragneisses, metasandstones, calc-silicate rocks, meta-ultramafic rocks
Conselheiro Pena 570–545 Ma	Industrial minerals (perthitic K-feldspar, albite, muscovite), tourmalines (elbaite, schorlite), beryl ore and gem, spodumene (kunzite), lepidolite, lithium-phosphates, quartz crystals, cleavelandite, columbite-tantalite, cassiterite, rare phosphates (arrojadite, barbosalite, brasilianite, childrenite, correianevesite, eosphorite, roscherite, vivianite, etc.)	residual; muscovite-rare element and rare element; lithium, beryl, complex (elbaite, lithium-phosphates, lepidolite, spodumene), LCT	S-type G2 (and I-type G1?) granites; medium-PT to intermediate low-P (garnet, staurolite, cordierite, kyanite, sillimanite), mica schists to paragneisses, metasandstones, calc-silicate rocks, meta-ultramafic rocks
Malacacheta 535–500 Ma	Muscovite, beryl, chrysoberyl; alexandrite, sapphire	residual; muscovite-rare element, beryl, LCT; and anatectic to hydrothermal processes	S-type G4 leucogranites; mica schists, meta-ultramafic rocks, migmatites
Santa Maria de Itabira, 545–500 Ma	Emerald, alexandrite, aquamarine, amazonite	quartz-feldspathic hydrothermal deposits, and pegmatites	ultramafic schists, banded iron formations, migmatites
Caratinga, 570 Ma	Kaolin, corundum (sapphire, ruby), beryl	anatectic; abyssal, ceramic	migmatitic paragneisses
Espera Feliz, 500	Quartz crystals, beryl (aquamarine), topaz	residual; REE, beryl-topaz; NYF	G5 granites
Espírito Santo 570–500 Ma	Kaolin, quartz, beryl (aquamarine), topaz, tourmalines (and spodumene?)	anatectic; ceramic; and residual; REE, beryl-topaz, NYF (and LCT?)	migmatitic paragneisses, G5 (and G2?) granites

Notes: [1] Cerný et al. (1991, 2012).
LCT = lithium-cesium-tantalum; NYF = niobium-yttrium-fluorine pegmatites; PT = Pressure Temperature; REE = rare-earth elements.

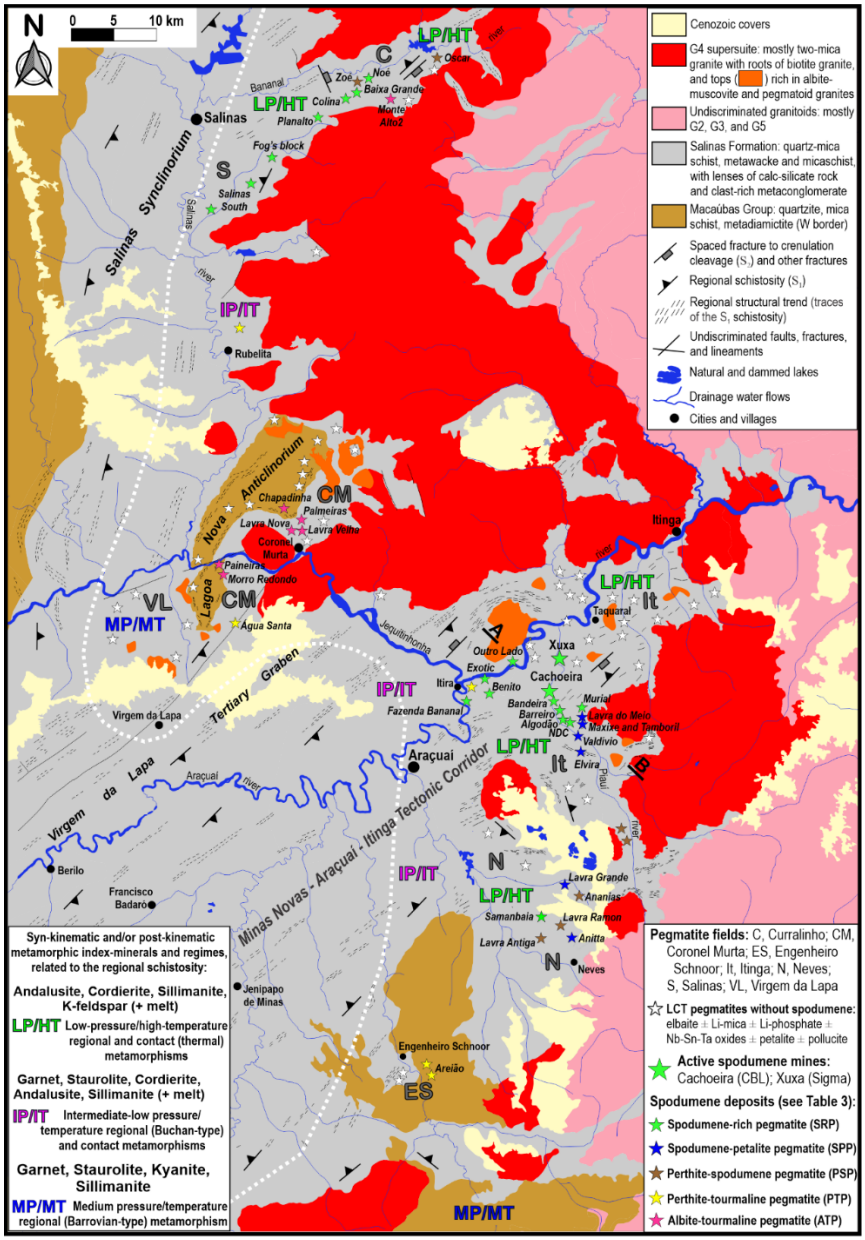
The EBPP comprises twelve pegmatite districts (Pedrosa-Soares et al., 2025), distinguished by mineral production, genetic and metallogenetic affiliation and classification, parental granite type; host rocks and metamorphic regime, and crystallization ages of a relatively large and clustered pegmatite population (Figure 7-3; Table 7-2). Most are districts of residual pegmatites of the rare element class related to the lithium-cesium-tantalum (LCT) or niobium-yttrium-fluorine (NYF) families that, in turn, are associated with distinct types of parental granites. Beryl-topaz (NYF) pegmatites cluster in districts almost completely circumscribed or very close to A-type and I-type G5 intrusions, encompassing granitic and igneous charnockitic (orthopyroxene-bearing) rocks with features of magma mingling-mixing involving mafic melts. Contrastingly, LCT pegmatites, including the spodumene-rich deposits, are found in external aureoles of S-type intrusions composed of two-mica leucogranites with pegmatoid cupolas. Among the LCT districts, the Araçuaí Pegmatite District stands out by having the largest historical and current production of lithium ore and the only world-class spodumene deposits of Brazil, including the CBL and Sigma spodumene mines, and newly discovered deposits like the Bandeira and other spodumene-rich deposits of MGLIT.

The Araçuaí Pegmatite District comprises distinct LCT pegmatites grouped in different pegmatite fields distinguished by their mineral production, pegmatite types and subtypes, and pressure-temperature (P-T) conditions of both the regional and contact metamorphisms (Figure 7-4. For exploration purposes, distinct spodumene pegmatites have been recognized in the Araçuaí District (Figure 7-4), namely: i) spodumene-rich pegmatites (SRP), including the currently most important spodumene deposits of Brazil (e.g., Sigma's SRP Xuxa, Barreiro and other SRP deposits; Bandeira – CBL SRP swarm); ii) spodumene-petalite pegmatites (SPP), such as the Maxixe and Lavra do Meio deposits; iii) perthite-spodumene pegmatites (PSP; e.g., Zoé-Dim); iv) perthite-tourmaline pegmatites (PTP; e.g., Água Santa); and v) albite-tourmaline pegmatites (ATP; e.g., Morro Redondo, Paineiras, Chapadinha). The first three—SRP, SPP, and PSP—are the spodumene-rich deposits that account for almost all spodumene ever found and produced in the Araçuaí District. Spodumene-rich deposits are known in the Curralinho, Itinga, Neves-Tesouras, and Salinas pegmatite fields (Figure 7-4). However, the Itinga Pegmatite Field remains the most important for spodumene production and prospecting, owing to the outstanding abundance of non-zoned to poorly zoned SRP bodies ranging from a few to dozens of metres thick, hundreds to a few thousand metres in length along strike, and dozens to hundreds of metres in down dip width. Many spodumene ore bodies mined by Arqueana, CBL and Sigma, as well as those discovered by MGLIT at Bandeira and other targets, are SRP deposits that may be generally correlated with the albite-spodumene type of Cerný (1991).

7.2 Structural Geology

In the Araçuaí Pegmatite District (Figure 7-4), the present-day structural framework was established after four deformation events (D1, D2, DG, and DNt). Two of them (D1, D2) are directly related to the regional tectono-metamorphic evolution of the Araçuaí Orogen in the Ediacaran-Cambrian. The third deformation event (DG) was caused by the widespread and voluminous intrusions of Cambrian G4 granites that caused contact (thermal) metamorphism and significant structural disturbance on the regional fabrics along areas relatively close to granitic stocks and batholiths (Alkmim et al., 2006; Pedrosa-Soares et al. 1987, 1993, 2011, 2025; Peixoto et al., 2017; Santos et al., 2009). Much later, the last deformation event (DNt) resulted from neotectonics reactivation in the Late Tertiary (Saadi & Pedrosa-Soares, 1990).

The Ediacaran-Cambrian deformation events (D1, D2, and DG) formed the structural framework that passively hosts the rare element pegmatites in the Araçuaí District (Figure 7-4). The much younger neotectonic deformation (DNt) reworked prior structures in upper crustal levels in the Late Tertiary (Miocene), forming normal faults and graben basins (e.g., the Virgem da Lapa Graben, (Figure 7-4) filled by the fluvial to lacustrine sandstone-mudstone piles of the São Domingos Formation that reach more than 100 m thick (Pedrosa-Soares, 1997; Saadi & Pedrosa-Soares, 1990). Locally, neotectonic faults may cut and displace blocks with pegmatite deposits.



Source : Pedrosa-Soares et al., (2025)

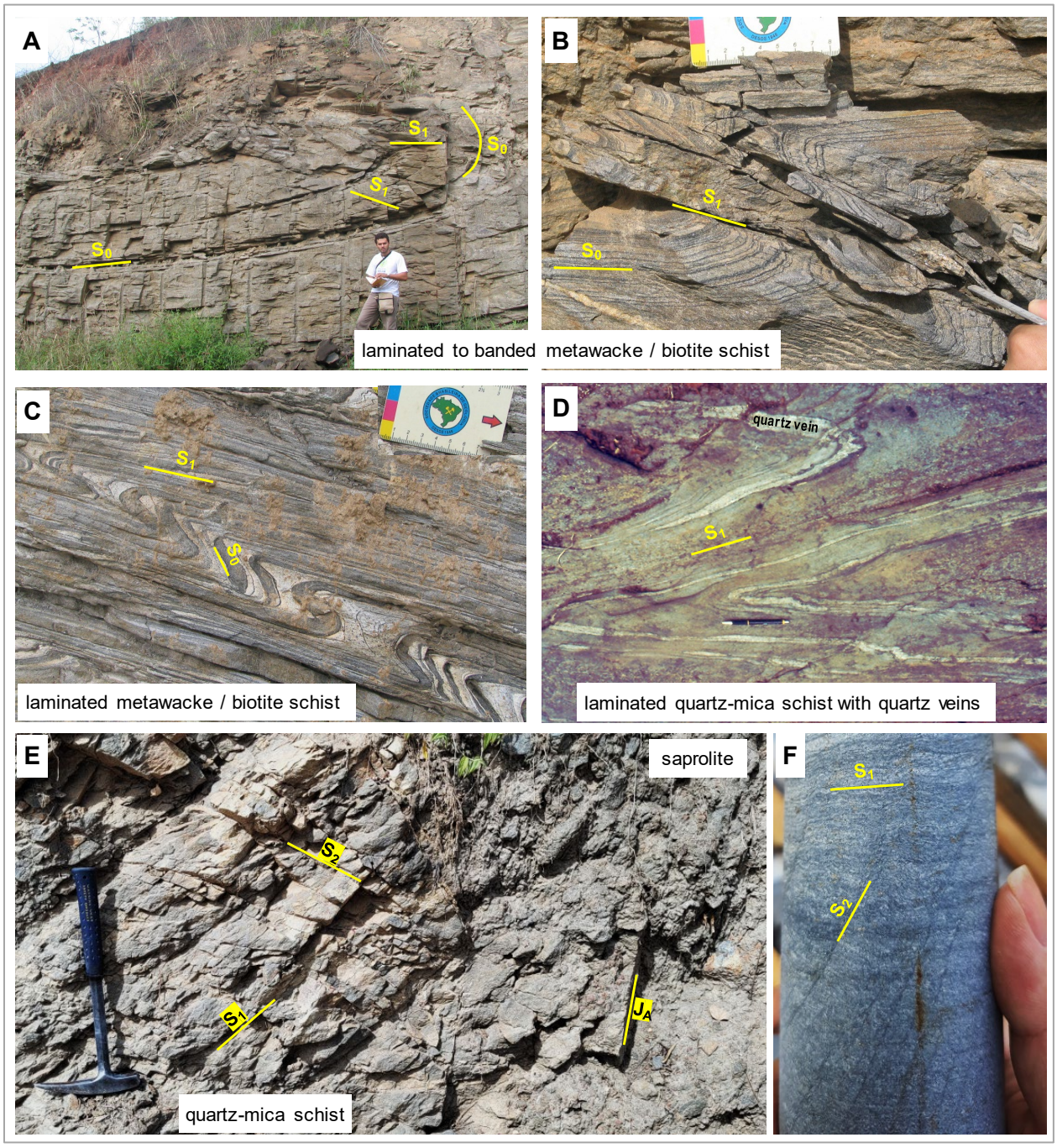
Figure 7-4: Geology of the Araçuaí Pegmatite District

The D1 deformation resulted from regional tectono-metamorphic processes imposed by compressive stresses during the collisional stage (580–540 Ma) of the Araçuaí Orogen. Megascopic to macroscopic D1 structures are asymmetric tight folds with long limbs and short hinges, parasitic folds, and ductile shear zones related to thrust ramps and oblique to transcurrent strike-slip domains. The macroscopic to microscopic D1 structures include the main regional planar structure that evolved from a spaced cleavage to the S1 schistosity (Figure 7-5), which contains the L1 mineral/stretching lineation. S1 is generally (sub)parallel to the layering (S0) along D1 fold limbs, becoming an axial-plane surface in fold hinges (Figure 7-5). Anastomosed and S-C foliations characterize higher strain shear zones syn-kinematic to S1. Although it generally is a very penetrative structure, the S1 foliation also provides host surfaces for pegmatites.

Distinct metamorphic regimes related to the D1 deformation of schists and gneisses rich in micas have been recognized in the region encompassing the Araçuaí Pegmatite District (Costa, 1990; Costa et al., 1984; Pedrosa-Soares et al., 1984, 1993, 1996, 2025; Peixoto et al., 2017; Santos et al., 2009). In the western and southwestern sectors of the region (Figure 7-4), the S1 schistosity shows syn-kinematic (syn-S1) assemblages with iron-rich garnet almandine, staurolite, kyanite and/or sillimanite. Such index-minerals series are typical of a medium pressure and medium temperature (MP/MT) metamorphic regime (Figure 7-4). This, together with quantitative geothermobarometric data, characterize the M1 metamorphic event as a syn-collisional (syn-D1) Barrovian-type (MP/MT) metamorphism dating between 575–550 Ma. P and T increase from about 3.5 kbar at 450°C in the garnet zone at the southwest of Francisco Badaró, passing northeastwards through the staurolite, kyanite, and sillimanite zones, and reaching up to 8.5 kbar at 650°C at the southeast of Coronel Murta (Figure 7-4).

In the northeastern and northern sectors of the region, the S1 schistosity shows syn-kinematic (syn-S1) assemblages with biotite, manganese-rich garnet (spessartine), andalusite, cordierite and/or sillimanite. Such index-minerals series are typical of a low pressure and high temperature (LP/HT) metamorphic regime (Figure 7-4). From the northeastern andalusite zone to the southwest of Itinga, quartz-feldspathic leucosomes with aplitic to pegmatitic textures formed from the breakdown of muscovite along the S1 foliation of cordierite-quartz-mica schists. Northeastwards, through the andalusite-cordierite, cordierite-sillimanite, sillimanite, and K-feldspar zones, increasing metamorphism and partial melting of quartz-mica schists formed migmatitic paragneisses in the eastern tip of the Itinga Pegmatite Field (Figure 7-4).

Regionally, the metamorphic event (M2) records a low-P/high-T metamorphism with pressures from 2 kbar to 5.5 kbar under temperatures from 400°C to 700°C, at around 540–530 Ma. The M2 metamorphism reached partial melting conditions on quartz-mica schists of the Salinas Formation with increasing anatexis rates that formed leucosome-rich migmatites (diatexites) in the easternmost sector of the Araçuaí Pegmatite District. This implies that, in deeper crustal levels, the widespread anatexis on the Salinas Formation could have produced large volumes of S-type granitic magmas in the late collisional to post-collisional stages of the Araçuaí Orogen. Indeed, the time interval of the M2 metamorphism (540–530 Ma) fits well with the oldest ages of G4 granites (535–525 Ma). This, together with the fact that the M2 metamorphism culminated in partial melting of quartz-mica schists and paragneisses in the easternmost Araçuaí Pegmatite District, indicate that the S-type G4 magmas were formed from the anatexis of thick metasedimentary packages in deep levels of the Salinas Formation (Costa, 1990; Deluca, 2019; Pedrosa-Soares et al., 2025; Peixoto et al., 2017).



Notes: A: large tight fold. B: a hinge showing the sedimentary layering (S0) cut by the low-angle dip to flat axial-plane S1 cleavage. C: tight folds with limbs transposed by S1 foliation. D: hinges of tight folds with metamorphic quartz veins in quartz-mica schist. E: spaced cleavage S2 cutting the schistosity S1, and sub-vertical joints (JA) cutting across both S1 and S2 in the Bandeira area. F: S2 spaced foliation marked by recrystallized mica, cutting the S1 schistosity in a drill core sample from the Bandeira deposit.

Figure 7-5: Outcrops and a Drill Core Showing Structures of the Deformation Events D1 and D2 on the Salinas Formation in the Araçuaí Pegmatite District

Along the boundary between the M1 and M2 metamorphic domains (Figure 7-4), the syn-S1 mineral assemblages include almandine and/or staurolite and andalusite and/or cordierite, characterizing an intermediate-low pressure (Buchan-type) metamorphic regime (IP/IT, Figure 7-4) transitional between the M1 Barrovian-type (MP/HT) and the M2 low-P/high-T (LP/HT) metamorphic regimes found in the Araçuaí Pegmatite Districts. Bearing in mind the relations between distinct pegmatite populations, their metallogenetic specializations and metamorphic regimes (Cerný, 1991; Cerný et al., 2012), such metamorphic characterization is of great importance for prospecting different rare element pegmatites, as lithium-rich pegmatites are typically found in terranes with relatively low-P/high-T metamorphism.

The D2 deformation developed from the late collisional to the post-collisional stages of the Araçuaí Orogen, when increasing decompression conditions, imposed by the orogen gravitational collapse, gradually replaced the tangential D1 compressive stresses. In the Araçuaí Pegmatite District, the D2 deformation comprises mostly brittle structures, such as the S2 spaced cleavage, joint families, and normal faults, as well as large open folds (flexures). The spacing between surfaces of the S2 cleavage ranges from less than 1 cm to decimetres (Figure 7-5. Locally, S2 may be very well developed in mica schists, becoming a tight crenulation cleavage to schistosity. The S2 spaced cleavage and other brittle structures, as being more open surfaces than the S1 schistosity, provided host surfaces for lithium-rich pegmatites, generally the thicker ones, in the Itinga Pegmatite Field (Pedrosa-Soares et al., 2025).

The latest Cambrian deformation event (DG) was caused by the intrusion of large volumes of S-type magmas that formed the G4 granites and cut across and disturbed the regional framework imprinted by the D1 and D2 deformations. The DG event deformed the regional structural trend of the host rocks around granitic plutons, forming radial fractures irradiating from the granitic plutons, and imprinting ring-shaped fracture systems that reworked regional structures around the intrusions. All these DG structures can host late orogenic rare element pegmatites.

During emplacement and cooling, the G4 plutons caused contact metamorphism on their country rocks and released residual silicate melts that formed pegmatites that either crystallized within the parental granite or migrated outwards and were hosted by D1, D2, and DG structures of the Salinas Formation and other metasedimentary units. While barren and beryl-bearing pegmatites are found within both parental G4 granites and country rocks, the lithium-bearing pegmatites have been found only in places rather far from (>1 km) granite massifs, emplaced in the Salinas Formation and other metasedimentary units. The G4 batholith emplaced along the whole eastern boundary of the Araçuaí Pegmatite District is formed by multiple coalescent plutons and defines an eastern limit for the occurrence of lithium-bearing pegmatites.

Regionally, the deformational events formed large structures with distinct implications for the occurrence and structural control of pegmatites in the Araçuaí District, such as the Salinas Synclinorium, the Lagoa Nova Anticline, and the Minas Novas–Araçuaí–Itinga Corridor (Figure 7-4). The axial zone of the Salinas Synclinorium shows the best-preserved section of the Salinas Formation, comprising non-deformed to weakly deformed metawacke, metapelite, and metaconglomerate, metamorphosed in the biotite and garnet zones of the low greenschist facies. This low-grade metasedimentary section reaches up to 2 km thick, with no evidence of pegmatite along the synclinorium keel. However, a lithium-rich pegmatite cluster, including SRP bodies, was recently found to the east of the Salinas Synclinorium, along the andalusite-cordierite-bearing, low-pressure/high-temperature metamorphic zone of the Curralinho Pegmatite Field (Figure 7-4). In the case of the Lagoa Nova Anticline, although there are LCT pegmatites emplaced along its structural surfaces, no

SRP was yet found there, probably due to the rather unfavorable pressure-temperature conditions of the regional and contact metamorphisms (between the medium PT [MP/MT] and intermediate PT [IP/IT] regimes). The Minas Novas–Araçuaí–Itinga Corridor, in turn, plays a special role in the understanding of the structural control and the most favourable pressure-temperature conditions for the SRP occurrence in the Araçuaí Pegmatite District. That corridor has been characterized as a flower-shaped transpressive (during D1) to transtensive (during D2) structure (Alkmim et al., 2006; Pedrosa-Soares et al., 1993, 1996, 2025) with the S1 foliation dipping to SE in the NW flank, and to NW in the SE flank (Figure 7-4). In the Itinga Pegmatite Field, the S1 schistosity and S2 spaced cleavage show NE-trending strikes, with the S1 schistosity dipping to NW and the S2 cleavage dipping to SE (if they have not been disturbed by later deformations, i.e., DG and DNt). The S1 foliation, as well as the S2 spaced cleavage and other brittle surfaces (i.e., the flat-lying and subvertical joints) host many lithium-rich pegmatites, with the thicker SRP bodies generally emplaced in more open surfaces of brittle structures.

The regional metamorphism associated with the S1 schistosity gradually increases from southwest to northeast along the corridor, reaching about 3.5 kbar at about 550ºC at the andalusite-cordierite zone in the Piauí river valley, where the contact metamorphism was imposed by G4 granitic intrusions, also under relatively low-pressure conditions. All those tectono-metamorphic and magmatic features favourable to SRP occurrence characterize the Itinga Pegmatite Field, where several of the most important spodumene deposits already found in Brazil are located, such as those of the CBL and Sigma, and MGLIT's spodumene deposits like the Bandeira SRP swarm.

7.3 Prospective-Exploration Model

Pedrosa-Soares et al. (2025) recently characterized different spodumene pegmatites with very distinct importance for lithium prospecting and exploration in the Araçuaí District. Among them, the spodumene-rich deposits only include spodumene-rich pegmatites (SRP), spodumene-petalite pegmatites (SPP), and perthite-tourmaline pegmatites (PTP) (see Section 7.1.1 and Figure 7-4). Indeed, the SRP deposits, such as those currently owned by MGLIT, Sigma, CBL and PLS, account for almost all the spodumene ore ever found and produced in the Araçuaí District. Therefore, if the aim is to find potentially economic spodumene deposits, it is of overwhelming importance to conceive a specific prospective-exploration model based on mines and surface exposures of spodumene-rich pegmatites, as Pedrosa-Soares et al. (2025) describe.

The Bandeira spodumene deposit is immediately southeast of CBL's Cachoeira underground mine, which has produced spodumene ore since the early 1990s (Figure 7-6). This mine has played a major role in the understanding of the mineralogical, petrographic, geochemical, and structural features of spodumene-rich pegmatites (SRP) in the Araçuaí Pegmatite District (Afgouni & Marques, 1997; Afgouni & Sá, 1978; Chaves et al., 2018; Correia-Neves et al., 1986; Dias, 2015; Luiz, 2023; Pedrosa-Soares et al., 2009, 2011, 2025; Quéméneur & Lagache, 1999; Romeiro, 1998; Romeiro & Pedrosa-Soares, 2005; Sá, 1977). The Cachoeira pegmatite swarm has been mined since the 1970s by the Arqueana Company (Figure 7-7), followed by CBL's production of spodumene ore at an industrial scale since 1993 (Figure 7-8). This mine, therefore, provided solid information for the prospective model that was successfully applied to the exploration of the Bandeira deposit (Figure 7-6).

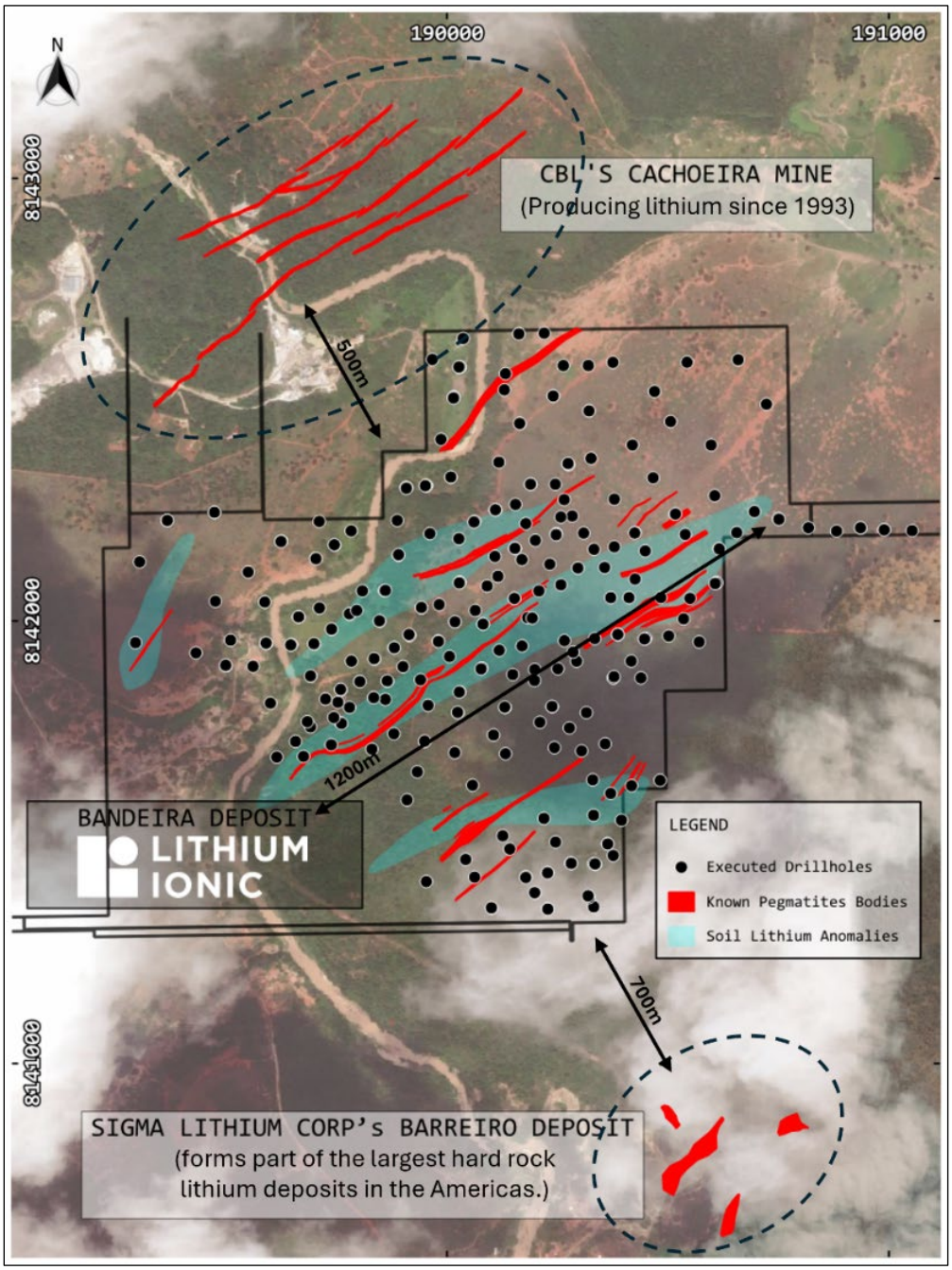
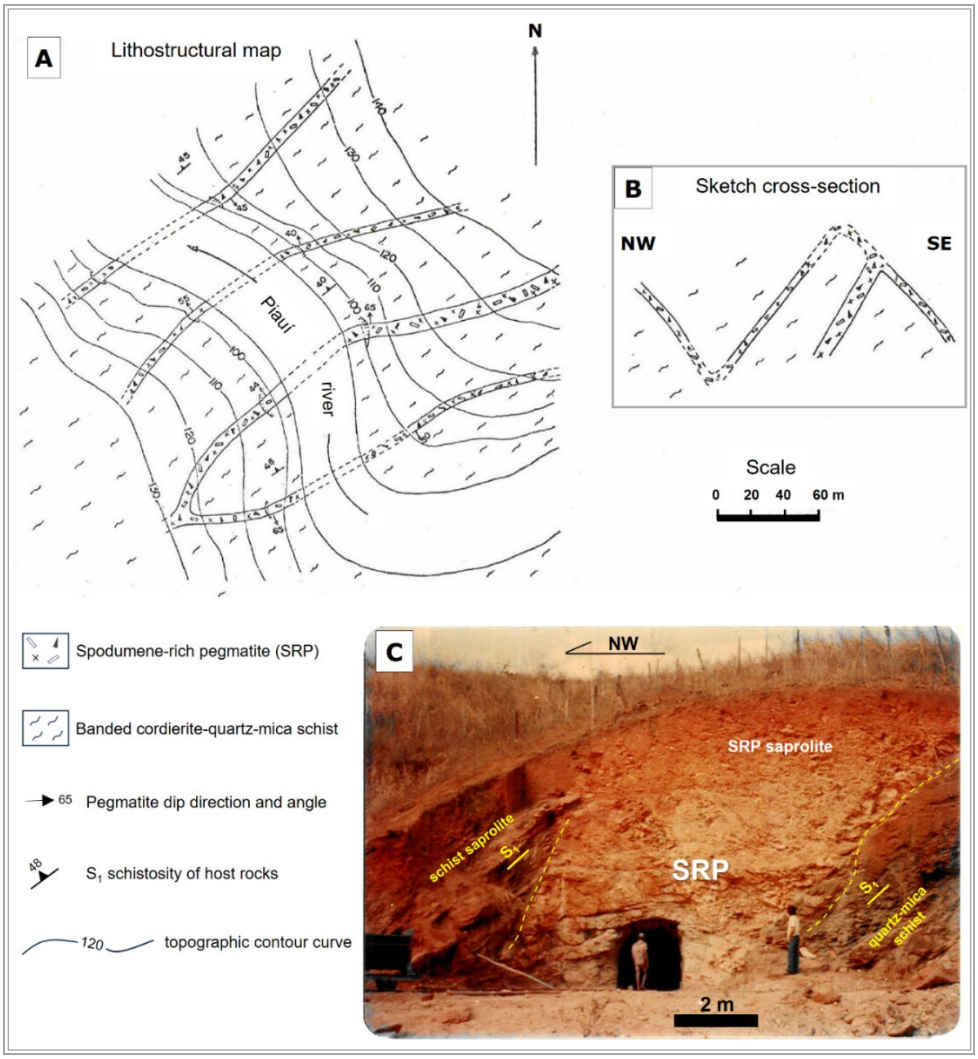


Figure 7-6: Location of the Bandeira Deposit in Relation to CBL's Cachoeira Mine and Sigma's Barreiro Deposit

The typical SRP ore bodies of the Cachoeira Pegmatite Group are non-zoned but rather inequigranular pegmatites composed of spodumene (on average 23 vol%), perthitic microcline, albite, quartz, and muscovite, generally totalling more than 95% of the whole ore body volume. Montebrasite, beryl, cassiterite, columbite-tantalite, cookeite, zabuyelite and petalite are scarce accessory minerals. The Cachoeira SRP cluster forms a pegmatite swarm characterized by a staggered (en-échelon) spatial distribution of parallel to subparallel, locally branched ore bodies showing lateral and vertical offsets

among them (Figure 7-8 and Figure 7-9). They are roughly tabular bodies with convex lens-shaped terminations, ranging from decimetres up to 30 m thick orthogonal to dip, from a few metres to many hundreds of metres long along strike, and up to many hundreds of metres down dip. The Cachoeira pegmatites were emplaced in the Salinas Formation that consists of banded cordierite-quartz-mica schist with intercalations of calcsilicate rock, recording the ideal P-T conditions (between 3.8 kbar–2.5 kbar and 550ºC–450ºC) for crystallization of large volumes of spodumene from relatively water-poor lithium-rich silicate melts (Pedrosa-Soares et al., 2025). In the Salinas Formation, the main host surfaces for pegmatites are the regional schistosity S1 and the S2 spaced cleavage, although late joints can also host SRP bodies (Figure 7-7–Figure 7-9).

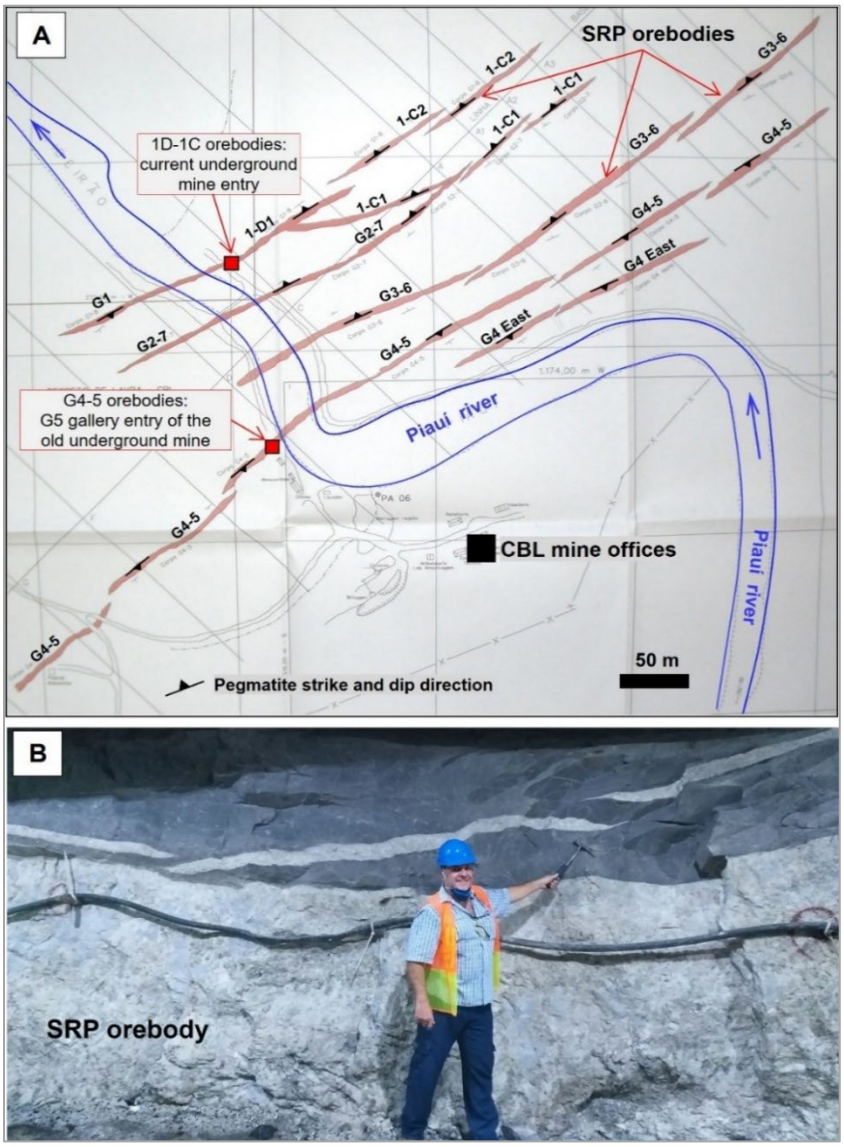


Source: Adapted from Sá (1977).

Notes: A and B: four NE-trending, parallel to sub-parallel, branched, tabular-shaped, spodumene-rich pegmatites (SRP), both concordant with the NW-dipping S1 schistosity of host rocks and discordant with S1, (i.e., emplaced in the SE-dipping S2 spaced cleavage). C: a roughly concordant, ca. 7 m-thick SRP hosted by cordierite-quartz-mica schist, with both rocks increasingly weathered (soil) towards the topographic surface.

Figure 7-7: Cachoeira Mine in the Mid-1970s

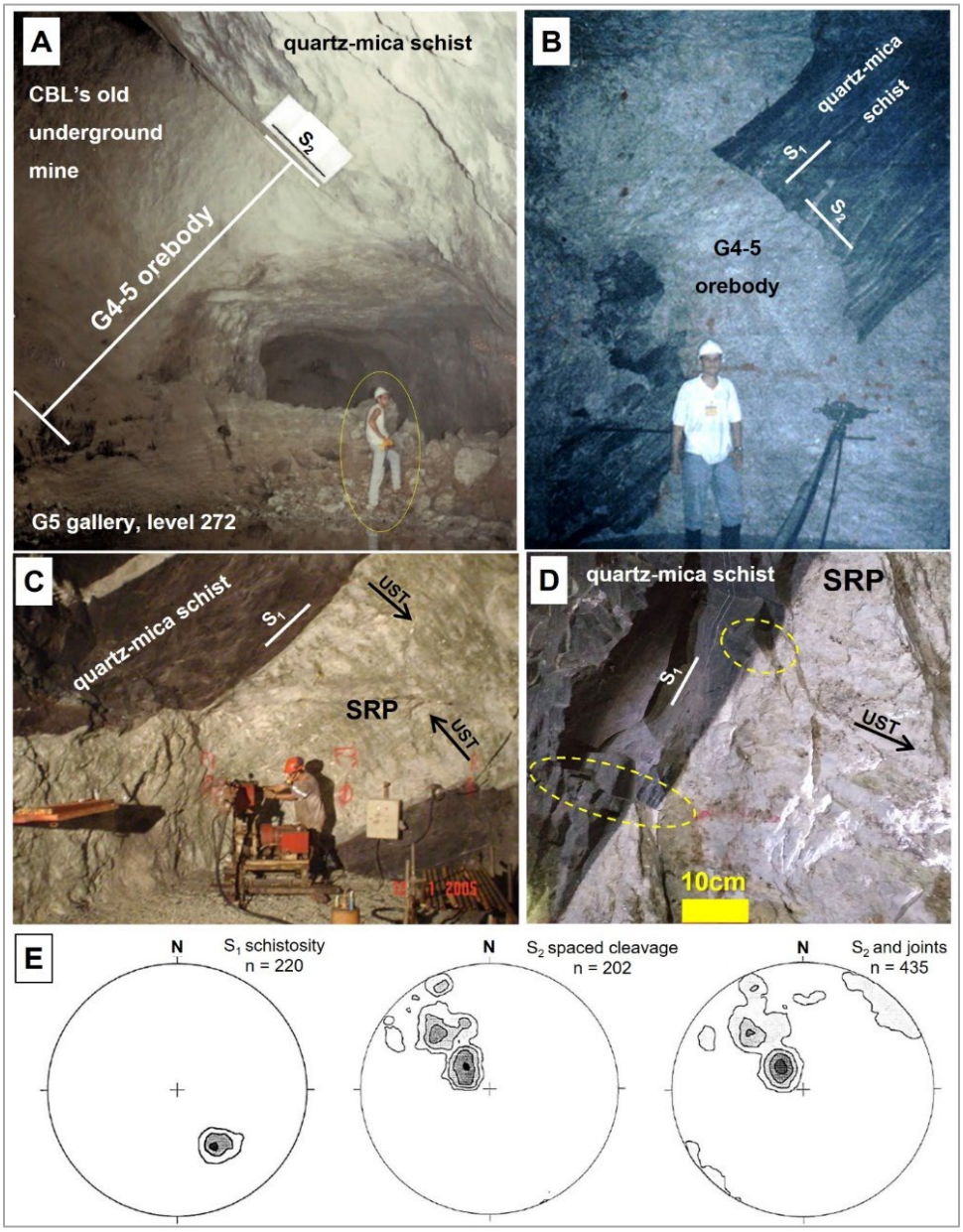
The tectonic structure of the Salinas Formation behaved passively during the intrusion of lithium-rich magmas that crystallized as spodumene-rich pegmatites, which in turn do not record any evidence of ductile or brittle deformations (Figure 7-8 and Figure 7-9), except for small faults that locally cut pegmatite contacts and may be related to the latest D2 or DG deformations (Figure 7-9; see also Section 7.2).



Source: Photo by A.C. Pedrosa Soares, August 2022.

Notes: A: map of CBL's Cachoeira pegmatite swarm (Pedrosa-Soares et al., 2025), showing the staggered (en- echelon) spatial pattern of parallel to subparallel, locally branched, NE-trending ore bodies of spodumene-rich pegmatites (SRP, in light brown) with indications of mapped strike and dip directions of the pegmatite bodies; SRP concordant bodies, emplaced along the S1 schistosity, dip to NW; SRP discordant bodies, hosted by the S2 spaced cleavage, dip to SE.
B: a fractal example of the en-échelon distribution pattern of SRP bodies shown by three smaller veins (above the main SRP ore body) in CBL's Cachoeira mine).

Figure 7-8: Cachoeira Pegmatite Swarm in CBL's Mine



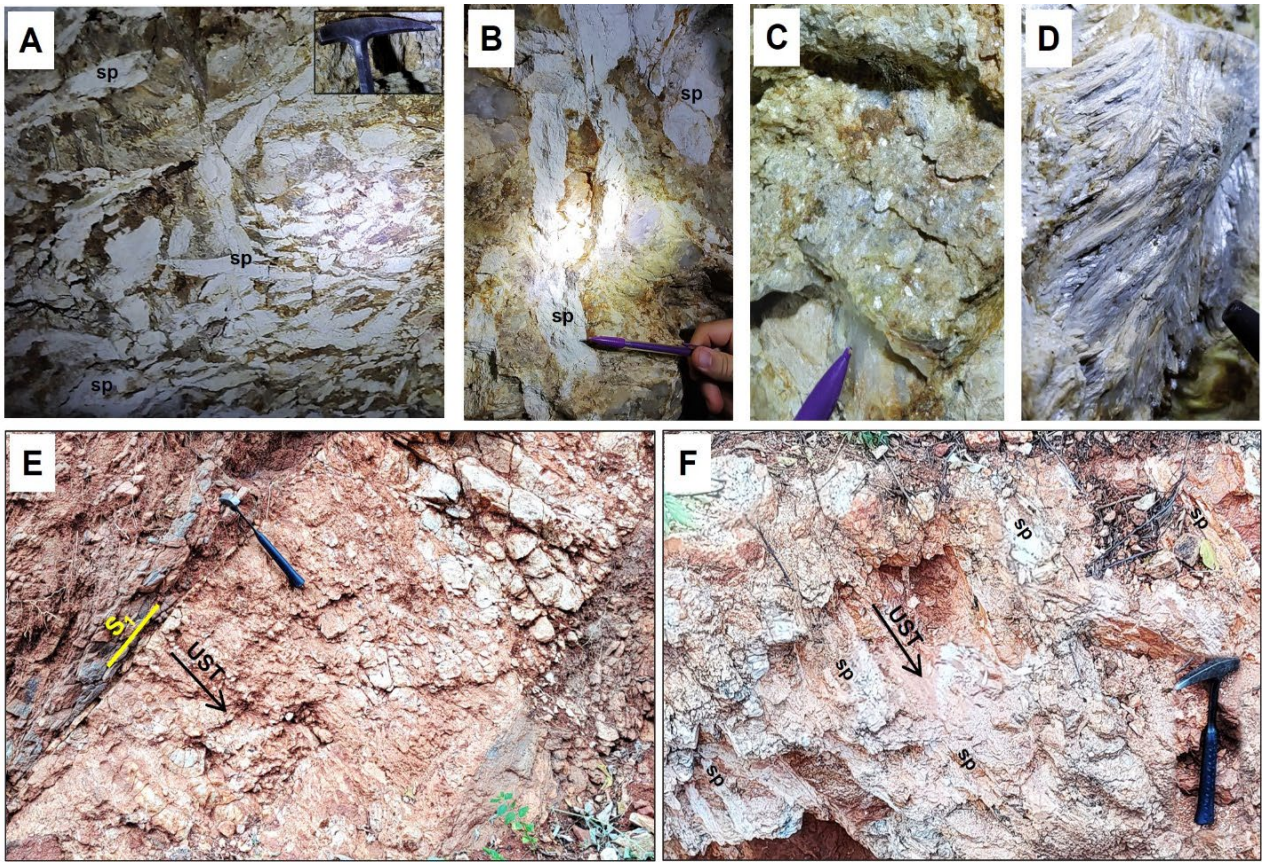
Notes: A: the G4-5 SRP in the G5 gallery, level 272, showing a discordant ore body (ca. 7 m thick) hosted by the S2 spaced cleavage (photo from Romeiro, 1998). B: a closing edge of the main G4-5 ore body, showing SRP branches cutting across the host quartz-mica schist (photo from Romeiro, 1998). C: mining front showing a concordant SRP ore body (1D/1C gallery) ranging from ca. 3 m to more than 4 m thick, hosted by the S1 foliation dipping to NW, with unidirectional solidification texture (UST, black arrows) outlined by oriented greenish spodumene crystals orthogonal to the contacts (photo from Romeiro and Pedrosa-Soares, 2005). D: sharp lithological contact, concordant with S1, between SRP and the host schist, showing small offsets along short brittle surfaces (yellow ellipses) and unidirectional solidification texture (UST, black arrow) outlined by oriented spodumene and feldspar (photo by Pedrosa-Soares, August 2025). E: stereograms (Schmidt projection, lower hemisphere) for the SRP host structures in the Cachoeira underground mine and surface outcrops showing that both S1 and S2 are NE-trending but dip in opposite directions—S1 to NW and S2 to SE (stereograms adapted from Romeiro, 1998).

Source: Pedrosa-Soares et al. (2025)

Figure 7-9: Spodumene-Rich Pegmatites (SRP) in CBL's Underground Mine

7.4 Bandeira's Mineralization Model

A soil geochemistry campaign revealed lithium anomalies roughly parallel to CBL's Cachoeira pegmatite swarm. This, together with lithological and structural data from outcrops, old diggings, and new exploration trenches (Figure 7-10), provided the basis for a very successful drilling campaign that discovered a new swarm of spodumene-rich pegmatites (SRP) extending from near surface up to 500 m deep (Figure 7-11).

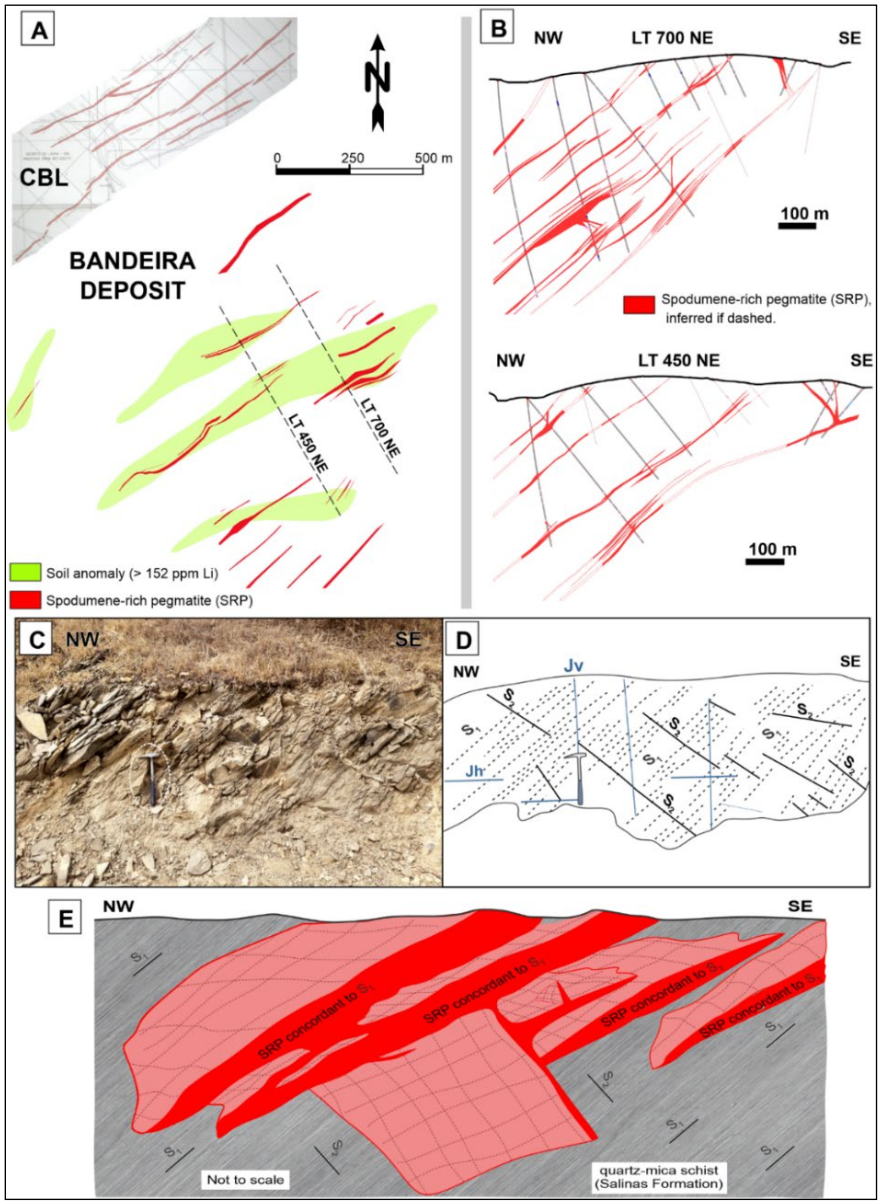


Notes: Exposures of partially weathered pegmatites very rich in pseudomorphs of spodumene (sp) replaced by white clay (A and B), with local mica-rich metasomatic bodies, small miarolitic cavities and rare lepidolite books (D) at the pegmatite top. A new trench (E) revealed another rather weathered pegmatitic body concordant with the S1 foliation of the host quartz-mica schist, showing pseudomorphs of tabular-shaped spodumene (sp) replaced by white clay (F), depicting unidirectional solidification texture (UST) orthogonal to the pegmatite/schist contact.

Figure 7-10: Old Digging for Gems (A to D) and an Exploration Trench (E and F)

Following the regional NE–SW structural trend, the Bandeira deposit comprises SRP swarms of NE-striking ore bodies mostly hosted by and concordant with the NW-dipping schistosity (S1), but also some discordant SRP bodies emplaced along the SE-dipping S2 spaced cleavage, as well as a few SRP bodies hosted by late, flat-lying joints (Figure 7-11). The Bandeira pegmatites are tabular bodies with convex lens-shaped terminations, arranged in tight and staggered (en-echellon) swarms, locally with branched connections linking ore bodies. Single SRP bodies normally reach hundreds of metres long along the strike, ranging from a few decametres to decimetres thick, with the discordant SRP bodies tending to be thicker than the concordant ones. With known down-dip width up to 800 m. The

exploration drilling work revealed two main sectors in the SRP swarm of the Bandeira deposit: i) the northern sector, with thicker, longer, and wider SRP bodies concordant with the S1 foliation of host rocks; and ii) the southern sector, with somewhat smaller SRP bodies (Figure 7-11).

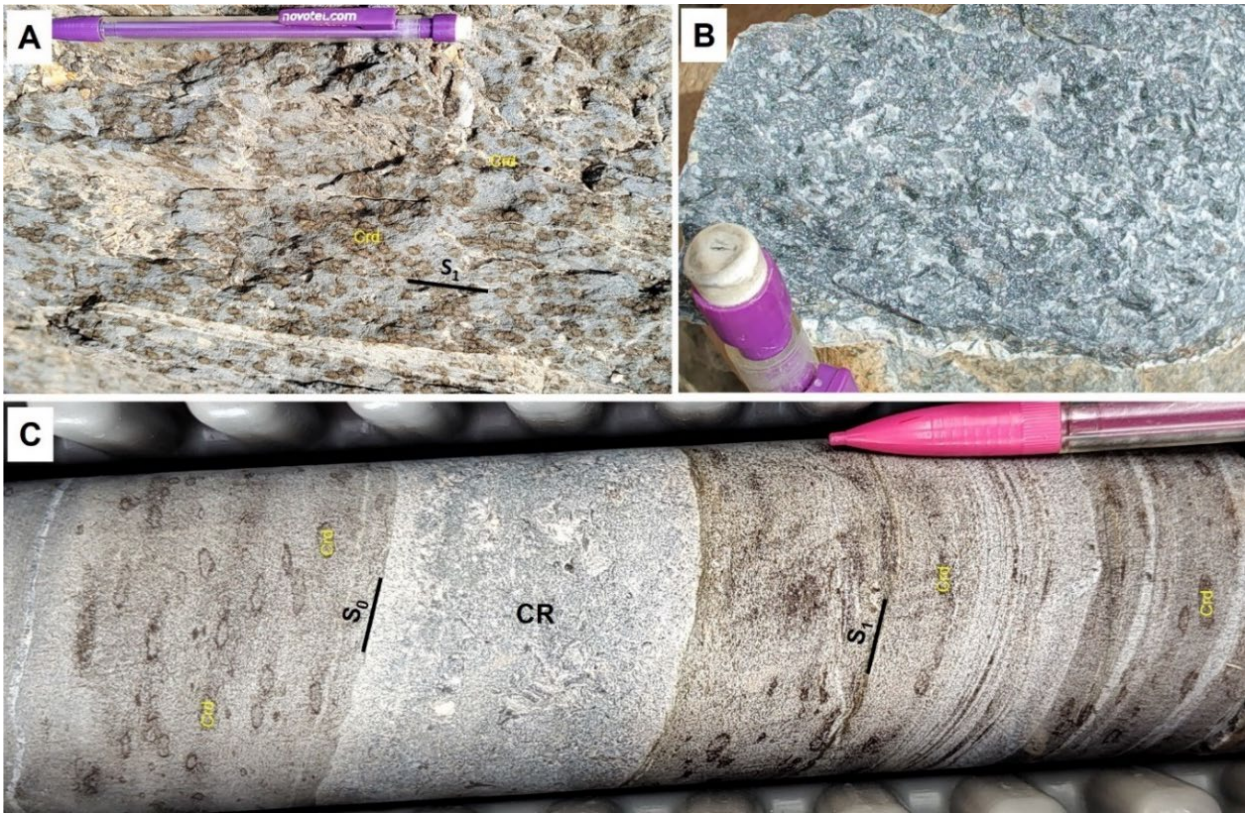


Notes: A: simplified map of the Bandeira deposit showing Li anomalies and spodumene-rich pegmatites projected to surface, and the adjacent CBL's pegmatites. B: simplified cross-sections showing the SRP swarm discovered in depth by MGLITafter exploration work. C and D: outcrop and structural sketch illustrating the tectonic surfaces of the country rocks (Salinas Formation) that host pegmatites in the Bandeira deposit—S1, regional ductile foliation (schistosity); S2, post-S1 spaced cleavage; Jh, late horizontal joints; and Jv, late vertical joints. E: cartoon illustrating a model for the spatial distribution and lateral relations of SRP ore bodies in the Bandeira deposit.

Source: A and B from MGLIT reports and CBL map from Romeiro (1998). C–E courtesy of Geologist Anderson Victoria.

Figure 7-11: Simplified Map Showing the Distributions of Lithium

The host rocks of SRP ore bodies in the Bandeira deposit are banded to laminated cordierite-quartz-mica schists, locally containing disseminated sulfide and/or graphite-rich bands, with intercalations of massive calcsilicate rocks (Figure 7-12 and Figure 7-13). Most cordierite forms ellipsoidal (egg-shaped) stretched poikiloblasts syn-kinematic to the regional S1 schistosity (Figure 7-12). The banded to laminated quartz-mica schists represent metamorphosed sand-mud sediments, and the calcsilicate rocks are metamorphosed calcium-rich carbonate-mud sediments (marls). They show sharp contacts with the SRP ore bodies that generally are concordant to the regional S1 foliation (often parallel to the compositional layering S0), but are also hosted by the S2 cleavage or foliation (Figure 7-13). The host schists may be enriched in decussate muscovite and/or biotite, black to green tourmaline, and recrystallized cordierite along narrow (cm to dm) fringes of contact metamorphism imposed by pegmatites (Figure 7-14). Although the host schists may be anomalous in lithium content close to pegmatites, they show no lithium-ore mineral.



Notes: A: partially weathered cordierite-quartz-mica schist rich in poikiloblasts (dark spots) of egg-shaped (ellipsoidal) cordierite (Crd) and/or quartz inclusions and coronated by biotite. B: calcsilicate rock with porphyroblasts of amphibole (dark green) and grossular garnet (light pink) within a massive matrix (greenish gray) mostly composed of quartz and plagioclase. C: drill core segment showing the banded to laminated cordierite-quartz-mica schist with ellipsoidal cordierite (Crd); light spots coronated by biotite), light-coloured quartz-rich laminae, and intercalation of calcsilicate rock (CR).

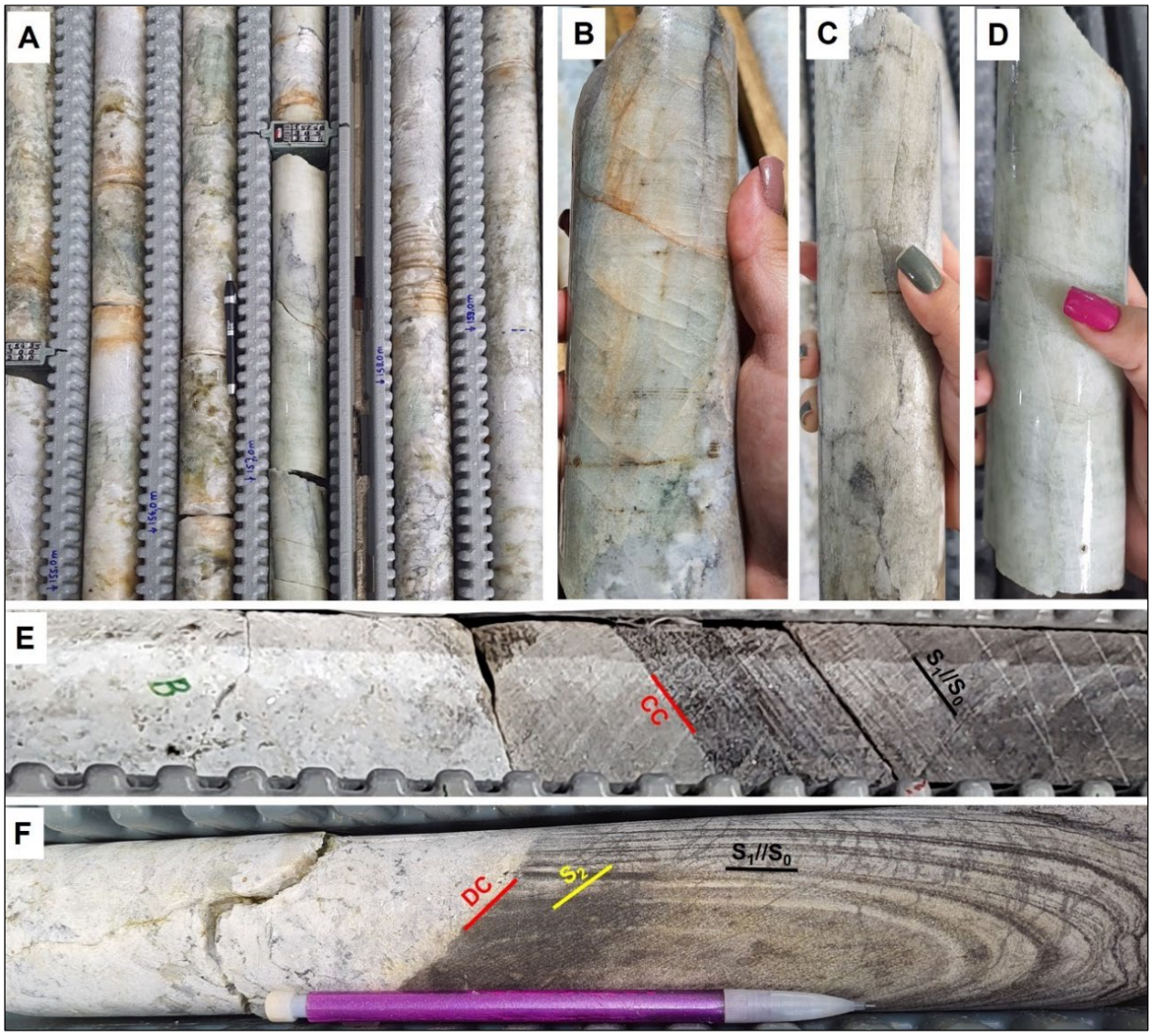
Figure 7-12: Host Rocks of Spodumene-Rich Ore bodies in the Bandeira Deposit

The Bandeira spodumene ore bodies show a rather simple mineralogical assemblage (Figure 7-13 and Figure 7-14), consisting of medium- to very coarse-grained spodumene phenocrysts, reaching up to 35 vol% on average, within a fine- to medium-grained matrix mostly composed of albite, perthitic K-feldspar (microcline), quartz, muscovite, and petalite, summing up to 95 vol% of the total matrix.

The scarce accessory minerals (mainly montebrasite, and Nb-Sn-Ta oxides) and secondary minerals (cookeite, sericite, zabuyelite, Fe-Mn oxides, clay minerals) generally comprise less than 5 vol%. In drill cores, the spodumene crystals are mostly free of hydrothermal and weathering alterations and very poor in mineral inclusions (Figure 7-13 and Figure 7-14). Conversely, surface outcrops, shallow diggings and exploration trenches cutting SRP bodies generally show weathered spodumene (Figure 7-10), forming pseudomorphs composed of white clay (kaolinite and montmorillonite). Rare spodumene-quartz intergrowth (SQUI) may be found associated with spodumene crystals (Figure 7-14). Petalite has been found in SRP's drill cores and thin sections, mostly occurring in the matrix as very fine- to fine-grained (sub-millimetre to 1 cm) crystals (Figure 7-14) and, more rarely, as coarser crystals locally found in rather restricted intervals.

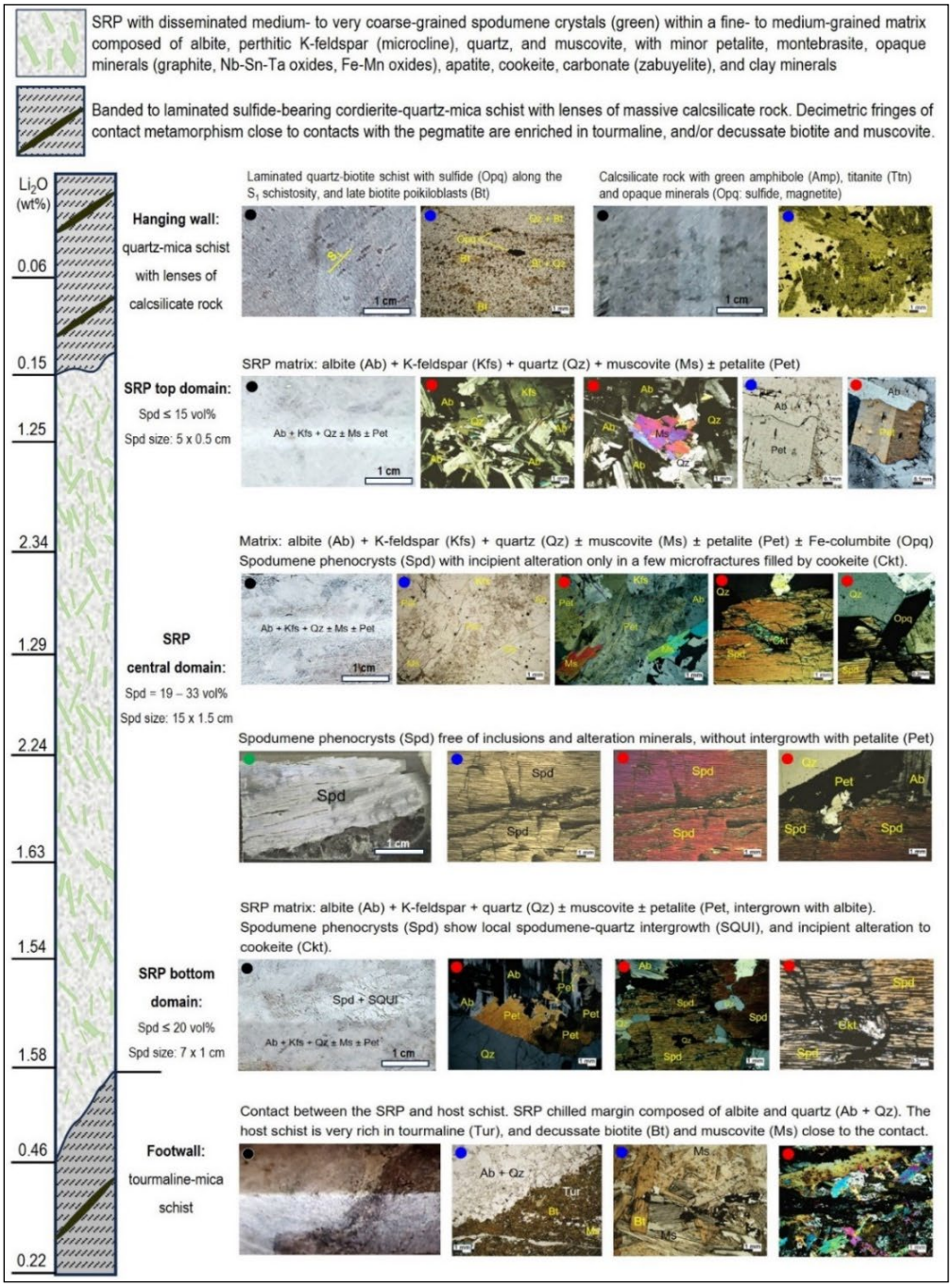
The thicker SRP bodies may show a lithium-barren and thin marginal zone rich in albite, generally rather discontinuous, followed inwards by a thick internal zone rich in disseminated spodumene (although spodumene may also be more concentrated in some domains than others along the internal zone). Owing to the upward migration of water-rich fluids, flat-lying SRP sections close to the hanging-wall contact, as well as the top termination (head) of high-angle dip bodies, may show metasomatic units with miarolitic cavities that partially replaced the primary mineral assemblage. Many SRP bodies lack the external lithium-barren zone, showing disseminated spodumene along virtually the whole ore body (Figure 7-13 and Figure 7-14). Unidirectional solidification textures outlined by tabular to telescope-shaped spodumene crystals are common in Bandeira's SRP ore bodies. Thin albite-rich pegmatites, barren to poor in lithium, are also found in the Bandeira pegmatite swarms.

In summary, the mineralization model for the Bandeira deposit consists of a dense swarm of non-zoned spodumene-rich pegmatite dikes and sparse albite-rich/spodumene-barren pegmatite dikes. The Bandeira SRP dykes show a simple mineralogy, with spodumene, albite, perthitic microcline (perthitic K-feldspar), and quartz totalling up to 95 vol%, and rather scarce accessory minerals (Al-Li mica, lithium-phosphates, petalite, zabuyelite, and others). These spodumene-rich pegmatites can generally be correlated with undeformed and non-zoned albite-spodumene pegmatites Cerný 1991, Cerný et al., 2012).



Notes: A: segment of a non-zoned SRP body with medium- to coarse-grained greenish spodumene disseminated in the quartz-albite-microcline-muscovite matrix; black minerals in spots and fracture fillings are Nb-Sn-Ta oxides and graphite. B to D: features of tabular, greenish to white spodumene crystals free of or poor in inclusions. E: concordant contact (CC) between albite-rich pegmatite border and laminated quartz-mica schist; the host surface is the regional schistosity (S1) parallel to the compositional (sedimentary) layering (S0). F: discordant contact (DC) between albite-rich pegmatite border and laminated cordierite-quartz- mica schist.

Figure 7-13: Drill Core Samples from Spodumene-Rich Ore bodies and their Host Rocks in the Bandeira Deposit



Notes: Based on intercept with 6.75 m thick and 1.99 wt% Li_2O pegmatitic textures based on average grain size: fine <2.5 cm; medium = 2.5 cm–10 cm; coarse = 1 cm–30 cm; and very coarse >30 cm. Spd size (e.g., 15 cm x 1.5 cm) based on the average length and thickness of spodumene crystals. Photo types indicated by dots: black, photo from unpolished sample; blue, photomicrography under parallel polarizers light; green, photo from polished thin section; red: photomicrography under crossed polarizers light. Drill core and thin sections described by Geologists Fabiana Guimarães and Laura Wisniowscki, respectively.

Source : Pedrosa-Soares et al. (2025).

Figure 7-14: Characterization Illustrated Summary for a Typical Spodumene-Rich Pegmatite (SRP) of the Bandeira Deposit

8 DEPOSIT TYPES

Owing to the high abundance of different types of LCT pegmatites with and without spodumene, and distinct varieties of spodumene pegmatites with quite variable amounts of spodumene in the Araçuaí Pegmatite District (cf. Pedrosa-Soares et al., 2025), the most important deposit type for lithium exploration in the region is the spodumene-rich pegmatite (SRP) found in the spodumene-rich deposits owned by CBL, Ionic Lithium, and Sigma, described in Section 7 (Figure 7-5 to Figure 7-14).

The model (Figure 8-1) for the SRP deposit type is supported by many surface and underground mine exposures, and hundreds of drill cores produced by MGLIT in the Bandeira, Baixa Grande, and Outro Lado deposits, and by the large dataset reported by other companies in the Araçuaí Pegmatite District.

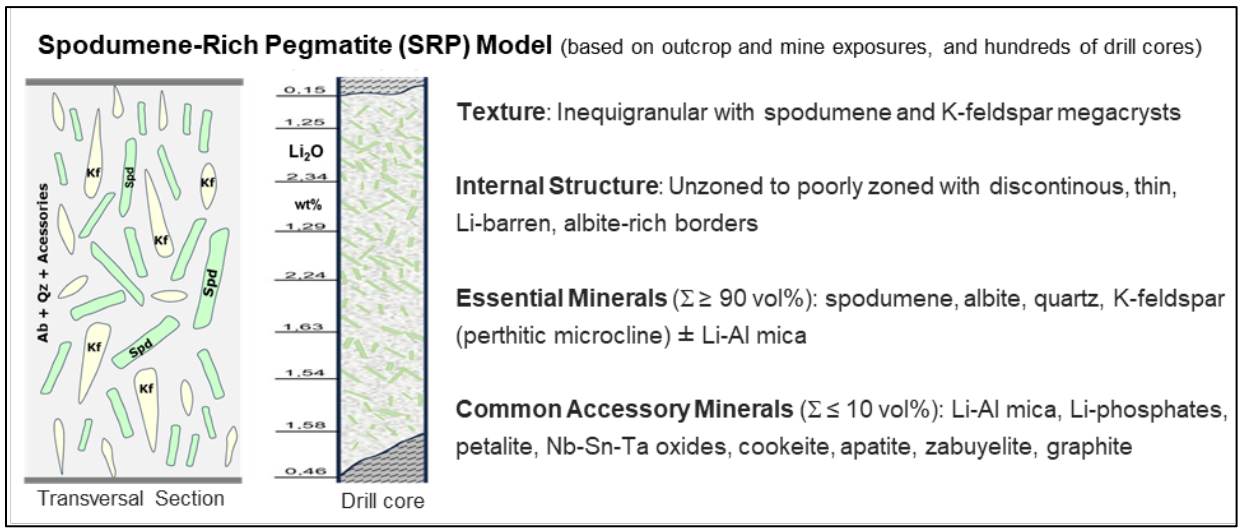


Figure 8-1: Deposit Type Model for Spodumene-Rich Pegmatite

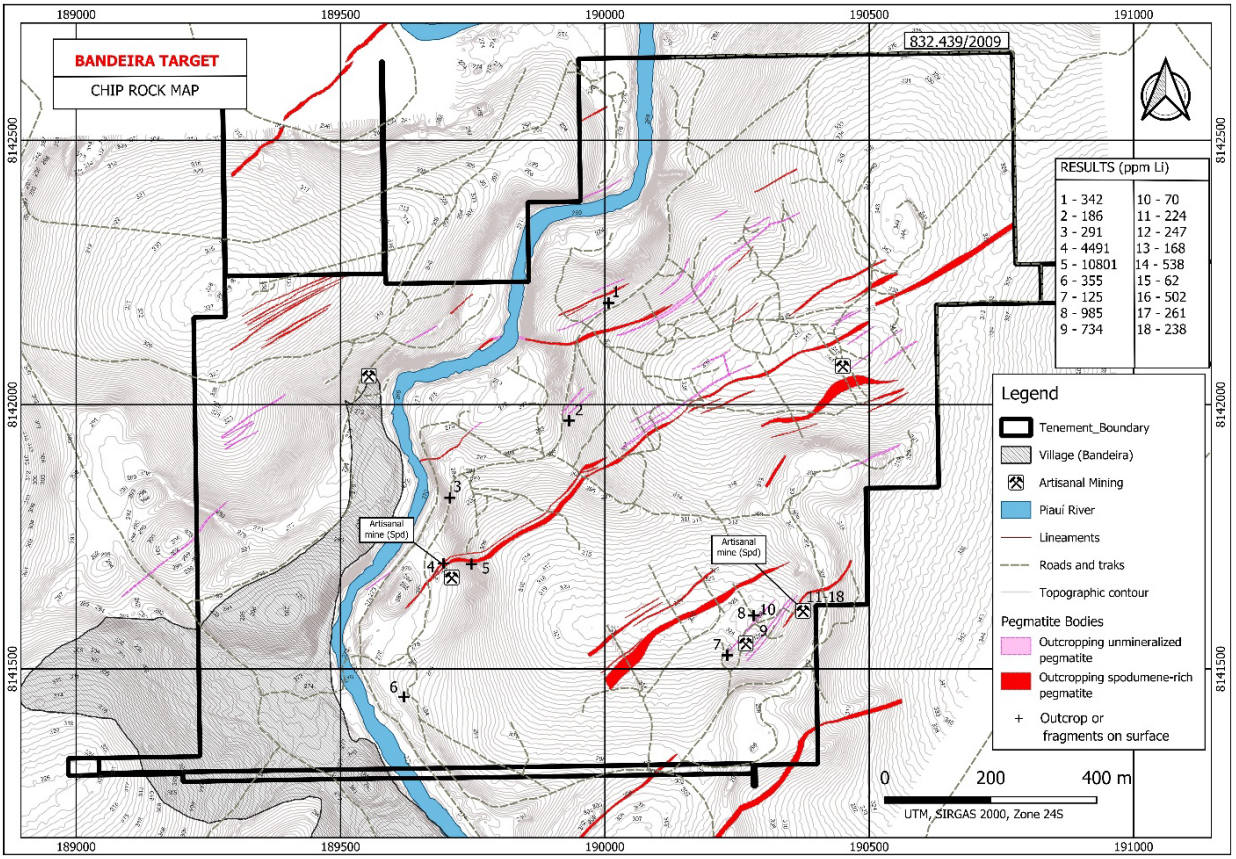
SRP deposits consist of non-zoned to poorly zoned spodumene-rich pegmatites with spodumene reaching up to 35 vol% on average, and the total modal content of spodumene, albite, K-feldspar, quartz, and white mica (muscovite and/or lithium-rich mica) summing up more than 90 vol% of the whole body. Therefore, SRP bodies are very poor in accessory minerals, which are generally represented by lithium-micas, lithium-phosphates, niobium–tin–tantalum oxides, cookeite, carbonate, and graphite. They are also poor in secondary (metasomatic) units due to their rather fluid-poor (anhydrous) nature. As a corollary, the scarcity of rare elements, except for lithium, imposes constraints on the geochemical prospecting methods to be applied in searching for spodumene-rich deposits. Conversely, the high lithium content (1.4 wt% Li_2O on average) in SRP-type magmas promotes a significant decrease in the crystallization temperature and viscosity of the silicate melt, leading to the high mobility that allows such lithium-rich magmas to crystallize as very large, but relatively narrow, SRP bodies, hundreds to thousands of metres long and wide, but only decimetres to a few decametres thick. Several SRP bodies may be correlated with the albite-spodumene pegmatite type (Cerný, 1991; Cerný et al., 2012), although significant differences have been reported in the literature (Pedrosa-Soares et al., 2025).

9 EXPLORATION

Significant fieldwork has been carried out in the Bandeira deposit, employing a comprehensive approach that included rock chip sampling, soil sampling, a trench program, and structural analysis. The drilling program is described in Section 10. These activities were instrumental in deepening understanding of the local geology and identifying potential SRPs, a crucial step in the exploration process.

9.1 Rock Chip Sampling

Despite the extensive residual soil cover, field mapping revealed pegmatites in old deactivated artisanal mines (garimpos), in situ outcrops, or fragments dispersed on the surface. Spodumene crystals were identified only in pegmatites founded in old deactivated artisanal mines and surrounding areas. Figure 9-1 shows the location of each collected sample and its lithium content (ppm), as well as the location of outcropping pegmatites, whether mineralized in spodumene or not.



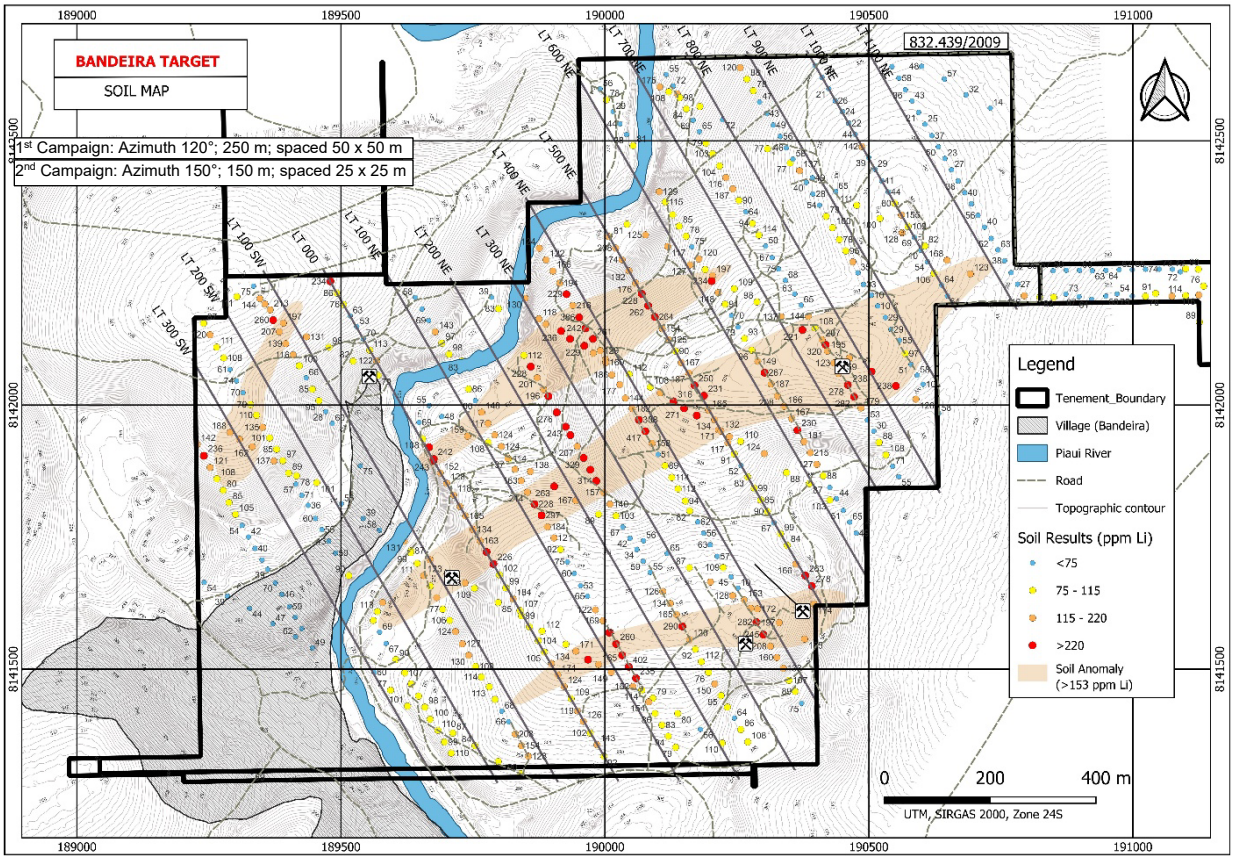
Note: Location of Each Spodumene (Spd) Sample, its Lithium Yield (ppm), and the Areas where Pegmatites are Exposed on the Surface.

Figure 9-1: Bandeira Deposit—Rock Chip Sample

9.2 Soil Sampling Program

The soil sampling program in the Bandeira area was conducted in two campaigns. In the first campaign, sample transects were spaced 250 m apart, aligned with azimuth 120°. Samples were collected every 50 m along each transect. In the second campaign, transects were 150 m apart, at azimuth 150°; samples were collected every 25 m along each transect.

In all, 537 samples were collected in the Bandeira area, and the lithium content in the soil varied from 10 ppm to 573 ppm. Calculations based on the results distribution indicated a subdivision of the lithium content as low grade (<69 ppm Li), low to moderate grade (70–107 ppm Li), moderate to high grade (108–152 ppm Li), and high grade (>153 ppm Li). Based on the distribution of the results, it was possible to identify at least five high-grade anomalous zones that represent more favourable spots to prospect SRPs (Figure 9-2). The anomalous high-grade regions are strongly oriented northeast–southwest, which is the same strike as the regional foliation and the mapped pegmatites in the Bandeira area and adjacent region.



Note: Northeast–Southwest Trend Coincides with the Direction of the SRPs.

Figure 9-2: Bandeira Deposit—Soil Geochemical

9.3 Trenching Program

Based on the soil geochemistry results, a trenching program was designed to investigate areas with anomalous lithium content. Forty-two trenches were executed, totalling 2,293 m; all were 1 m wide and up to 2.5 m deep (Table 9-1). The trenches were preferentially positioned above the soil anomalies, and most of which intercepted pegmatite (Figure 9-3). Due to the degree of weathering, the exposed pegmatites in some trenches are very decomposed, exhibiting a characteristic whitish colour distinguishing it from the horst schist in Trench ITTRE-22-006 (Figure 9-4 A and B). The decomposed pegmatites are friable, and it was possible to diagnose only quartz, kaolin, and flake muscovite. However, better-preserved pegmatites with visible spodumene centimetric crystals were observed in other trenches, for example Trench ITTRE-22-001 (Figure 9-4 C and D). As part of the procedure, to verify the lithium content in the trench independent of the conservation state, every pegmatite thicker than 30 cm was mapped. Figure 9-4 E shows an example of the pegmatite saprolite in Trench ITTRE-22-001.

In addition to confirming the presence of pegmatites and studying their mineral composition, the trenches played an important role in determining the strike and dip of the ore bodies. Their orientation provided a higher level of confidence when planning the borehole locations for the drilling campaign.

Table 9-1: Summary of Trenches Excavated in the Bandeira Deposit (X, Y, Z Coordinates—UTM Zone 24 South (Sirgas 2000)

Trench	X	Y	Z	Length (m)	Azimuth (°)	Dip (°)
ITTRE-22-001	189772	8141686	301	43	308	0
ITTRE-22-002	190395	8141705	304	67	155	0
ITTRE-22-003	190156	8142046	336	36	150	0
ITTRE-22-003B	190158	8142055	336	11	150	0
ITTRE-22-004	189960	8141898	298	64	155	0
ITTRE-22-005	190401	8142141	343	47	150	0
ITTRE-22-006	190451	8142056	342	54	150	0
ITTRE-22-007	190292	8142082	340	50	150	0
ITTRE-22-008	190055	8141994	324	80	150	0
ITTRE-22-009	189936	8142184	299	74	150	0
ITTRE-22-010	189888	8142019	279	95	150	0
ITTRE-22-011	190001	8141581	323	140	150	0
ITTRE-22-012	190077	8142201	312	51	150	0
ITTRE-22-014	190304	8141550	323	53	150	0
ITTRE-22-015	190475	8141898	308	8	150	0
ITTRE-22-016	190085	8141692	318	66	150	0
ITTRE-22-017	190319	8142037	339	109	150	0
ITTRE-22-018	190189	8141817	316	102	150	0
ITTRE-22-020	190538	8142145	341	51	150	0
ITTRE-23-021	189815	8141416	303	98	155	0
ITTRE-23-014A	190244	8141657	323	53	150	0
ITTRE-23-023	189341	8141921	315	70	150	0
ITTRE-23-013	189710	8141979	279	78	150	0
ITTRE-23-019	190173	8141685	322	100	150	0
ITTRE-23-024	189979	8142318	276	65	330	0
ITTRE-23-025	190214	8142105	336	115	150	0
ITTRE-23-022	189358	8142195	335	97	150	0

Trench	X	Y	Z	Length (m)	Azimuth (°)	Dip (°)
ITTRE-23-028	190619	8142362	341	170	147	0
ITTRE-23-030	190483	8142200	338	85	150	0
ITTRE-23-031	190454	8142178	340	70	150	0
ITTRE-24-027	190297	8142651	304	55	135	0
ITTRE-23-026	190576	8142091	337	80	140	0
ITTRE-23-029	190598	8142251	340	0	150	0
ITTRE-24-032	190562	8142012	332	88	160	0
ITTRE-24-033	190736	8142360	330	70	150	0
ITTRE-24-034	190499	8142105	345	83	150	0
ITTRE-24-035	190394	8142020	336	65	145	0
ITTRE-24-036	190848	8142268	340	72	150	0
ITTRE-24-037	190548	8142029	335	35	190	0
ITTRE-24-038	190504	8142020	338	46	150	0
ITTRE-24-039	190423	8142048	341	59	150	0
ITTRE-24-040	190189	8142021	337	0	150	0
ITTRE-24-041	189958	8141456	313	0	330	0
ITTRE-24-042	190160	8142008	335	70	150	0

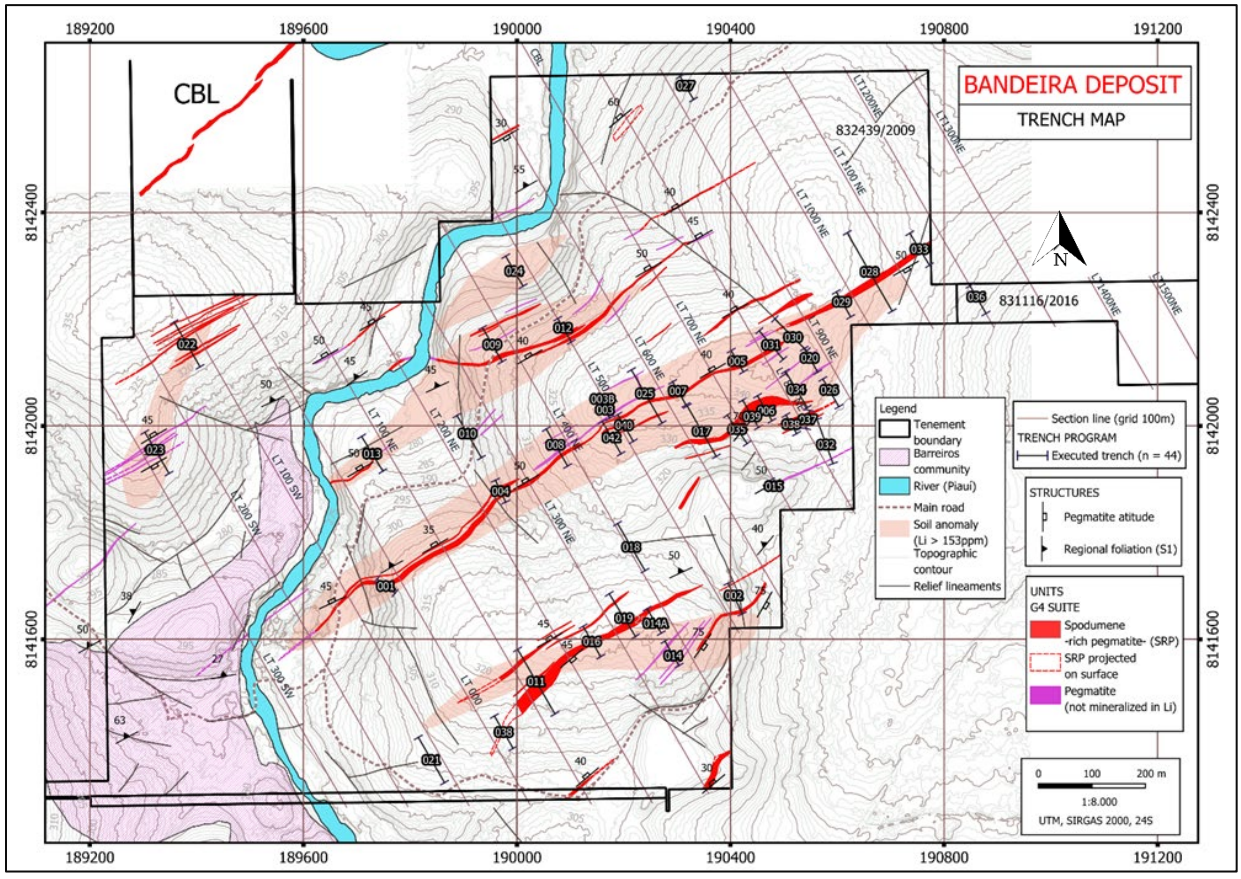
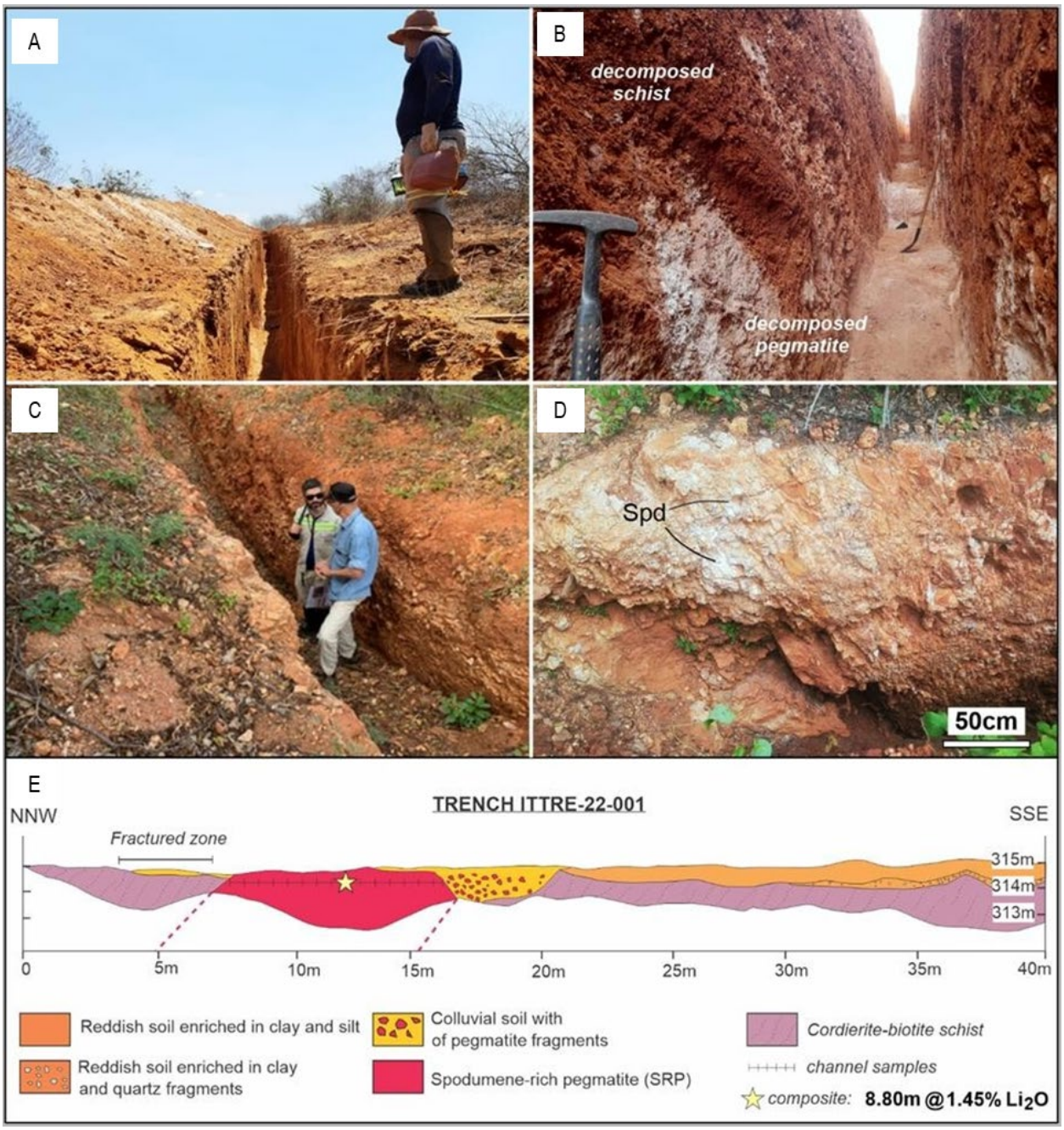


Figure 9-3: Bandeira Deposit Trench Sample Map—22 Trenches Sited Preferentially in Soil Anomalies

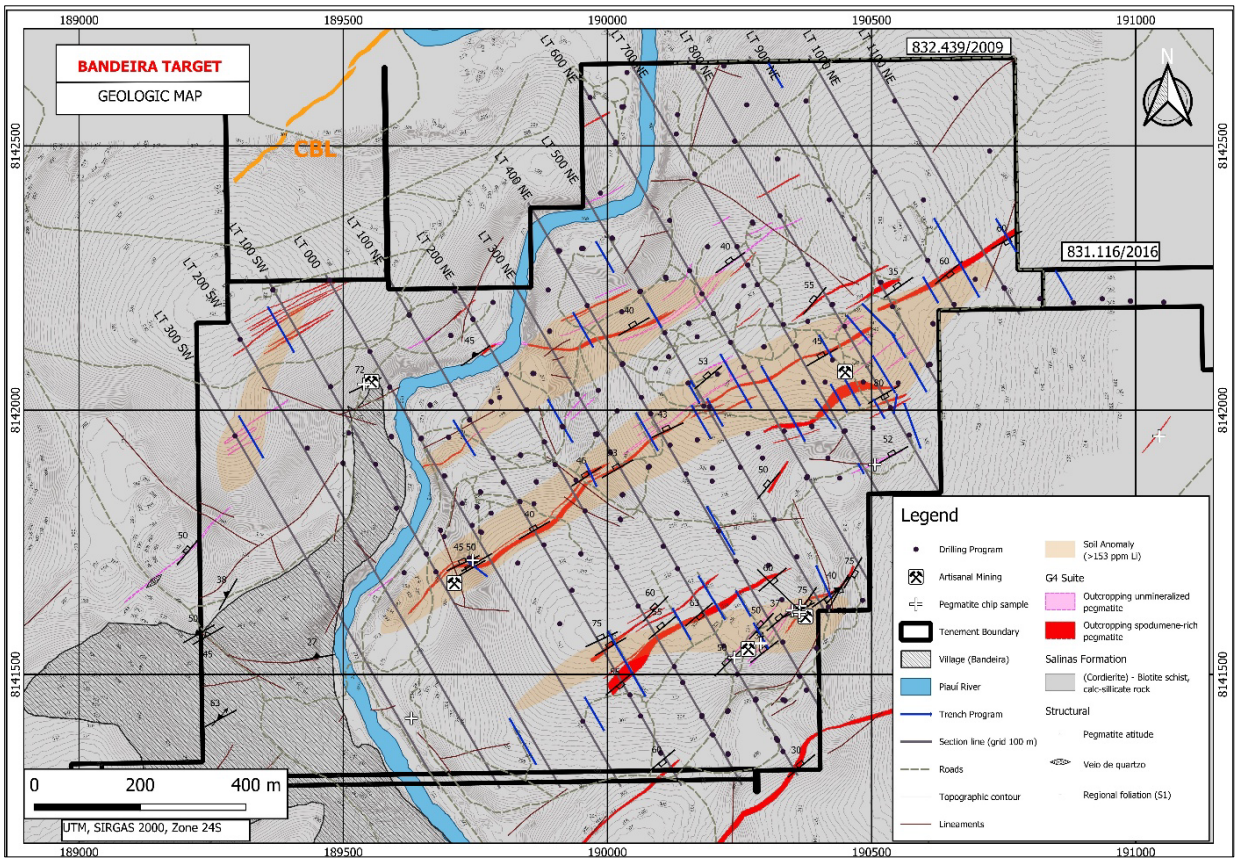


Notes: A and B: Trench ITTRE-22-006 and Detail of the Highly Decomposed Excavated Whitish Pegmatite Contrasting with the Host Reddish Decomposed Schist. C and D: General View of Trench ITTRE-22-001 and Detail of the Spodumene Crystals in the Excavated Pegmatite. E: Cross-Section of Trench ITTRE-22-001 Emphasizing the Mapped Units in the Trench and the Channel Samples Collected of Spodumene-Rich Pegmatite. Spd = Spodumene Crystals (D).

Figure 9-4: Project Sample Trenches

9.4 Structural Analysis

Although they lack outcrops of spodumene-rich pegmatites, the few outcrop exposures of mica schists from the Salinas Formation are very relevant, and helpful in understanding the Bandeira deposit structures, such as ductile and brittle. The ductile structures were produced during the progressive metamorphism related to the syn-collisional phase of the Araçuaí orogen (see Section 7). In contrast, the brittle structures are younger and are interpreted as related to the gravitational collapse of the orogen during the post-collisional phase. The structural map of the Bandeira target (Figure 9-5) shows the distribution of the structures and the projection of the non-exposed pegmatites. In that case, the attitude of each body was measured using the 3-D geological model created from the drilling information.

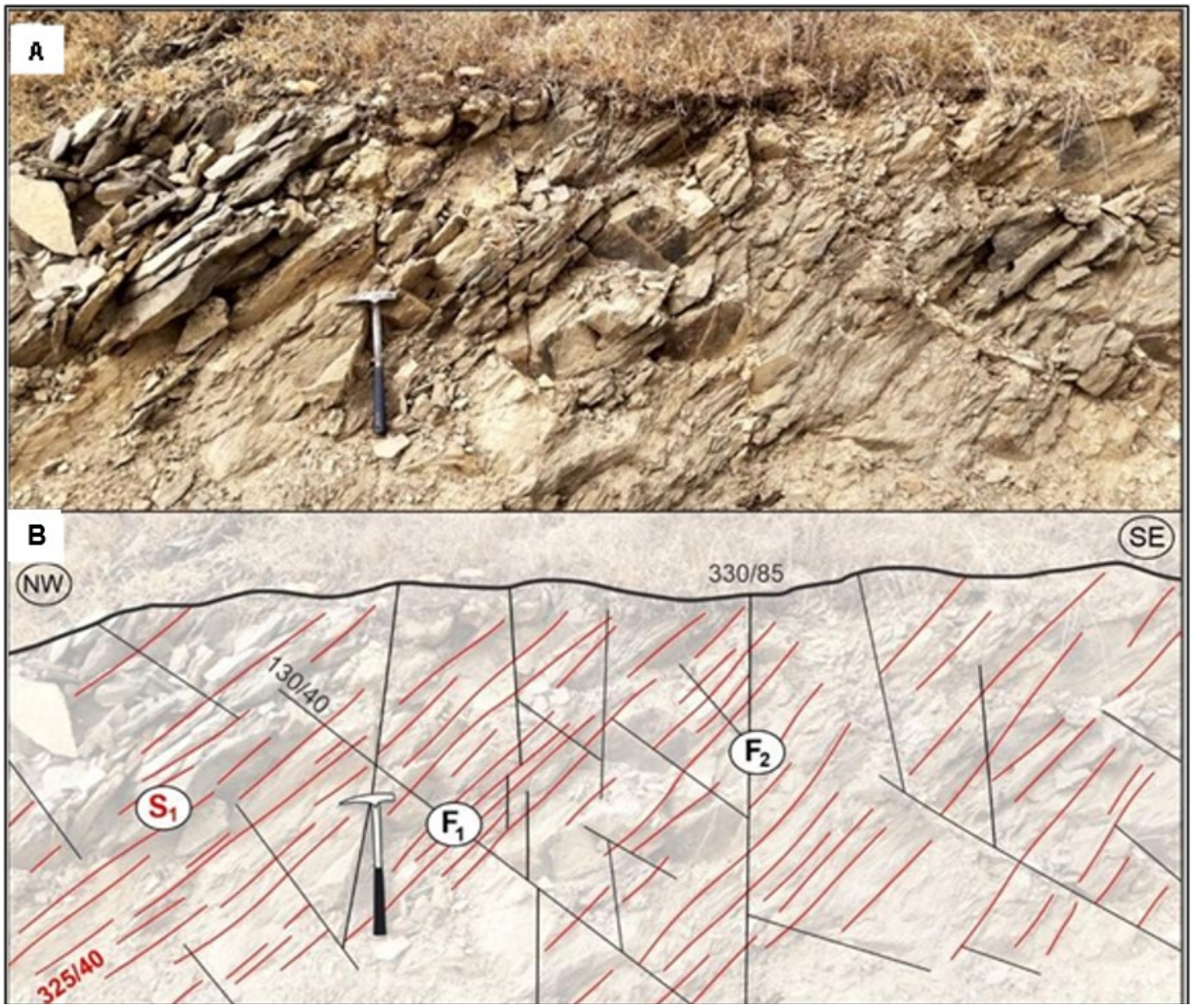


Note: The pegmatite veins are projections of the known intrusions based on the intercepts in drill holes. The attitude of each vein is based on the modelled veins.

Figure 9-5: Bandeira Target Structural Map Emphasizing the Distribution of Mapped Structures

The dominant ductile structural feature of the Bandeira deposit is the pervasive regional schistosity (S_1), which exhibits a consistent orientation in both strike and dip across the entire area (mode = N50E/45NW). The stretched lineation (Lx) complements the ductile structural framework, often manifested as elongated micas or ellipsoidal cordierite porphyroblasts crystalized along S_1. This lineation is down-dip and indicates tectonic transport along the northwest–southeast direction.

The brittle structures are represented by a series of fractures, occasionally joints, that intersect the S_1 schistosity and seem part of a conjugate system (Figure 9-6). Each structure is denoted as either F_1 (fractures with a moderate dip to the southeast) or F_2 (sub-vertical fractures), and their presence and prevalence may vary depending on the outcrop. The F_1 structure seems more pervasive in the entire region, which also allows the interpretation of these structures as related to the development of a cleavage fracture system (secondary foliation S_2). All these planar structures in the Bandeira area (S_1, F_1, and F_2) consistently display a standard orientation along the northeast–southwest strike, with variations only in their dip angles.



Notes: A) Fractured Biotite-Schist in the Bandeira Area (UTM: E-189,232, N-8,141,577). B) Schematic Cross-Section Emphasizing the Interpreted Structures in the Same Outcrop: Regional Ductile Foliation (Schistosity S_1) and Spaced Brittle Structures Possibly Related to Conjugated System, F_1, with Moderate Dip to Southeast, and F_2, Subvertical.

Figure 9-6: Fractured Biotite-Schist in the Bandeira Area and Scheme Emphasizing the Interpreted Structures in the Same Outcrop

Understanding the structural patterns in the host rocks is crucial for prospecting pegmatites, since the structures serve as the surfaces that guide the migration of the silicate magmatic residues.

Consequently, they profoundly influence the shape and continuity of the spodumene-enriched pegmatite bodies in the Bandeira area.

9.5 Geophysical Surveys

A small-scale induced polarization (IP) geophysical survey was conducted in 2022.

IP and resistivity are commonly used to delineate the resistive or conductive portions of subsurface pegmatites. The inverted data are not always helpful or productive in the very early stages of exploration; however, in MGLIT's case, there were sufficient outcrops to measure some attitude data, so the general trend of the pegmatites could be extrapolated using the subsurface IP anomalies. The Project-acquired energy-induced data were gained through the dipole–dipole arrangement. Between March and April 2022, the Project completed six lines totalling 5,150 m.

The principle for IP prospecting is based on injecting an electric current into the ground through several electrodes. Data acquired depend on the resistivity at each point, terrain geometry, and the electrode array—its geometric arrangement. For an uninterrupted current flow, the IP depends on the terrain's impedance and the current frequency. The IP can be measured in the time and frequency domains. Once processed, the raw data can be viewed in two dimensions (2-D) or, if available, in a 3-D environment. Resistivity and induced polarization data were acquired in Bandeira with the dipole–dipole arrangement (AB = MN = 25 m). Figure 9-7 shows the array's line locations and measuring stations of the chargeability and resistivity data. Some pseudo-sections of apparent chargeability and apparent resistivity 2-D models of the processed data are shown in Figure 9-7.

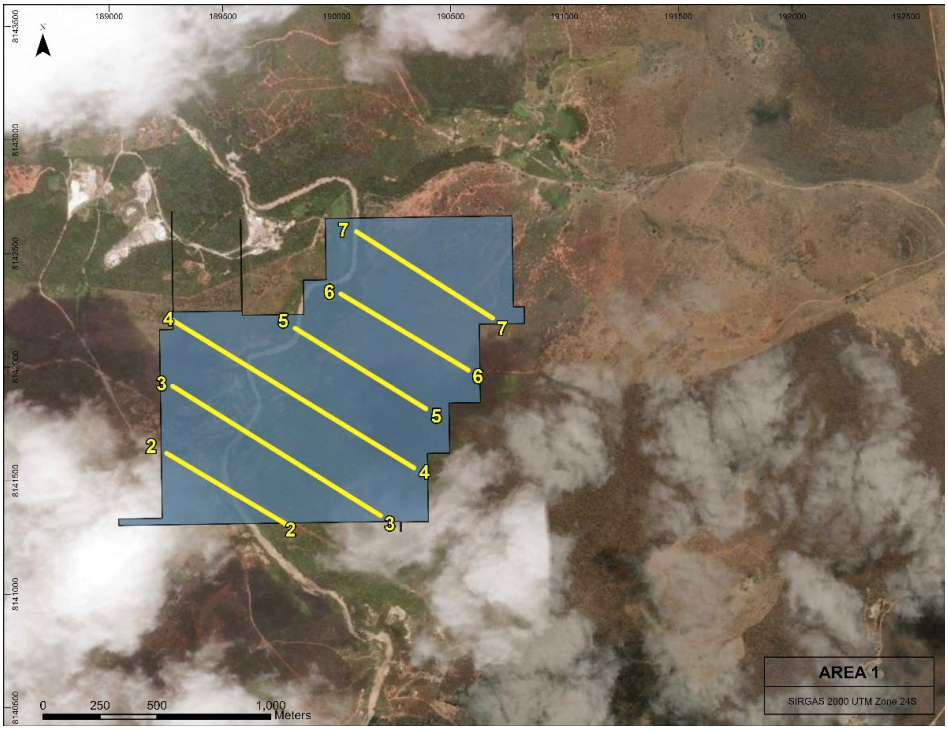
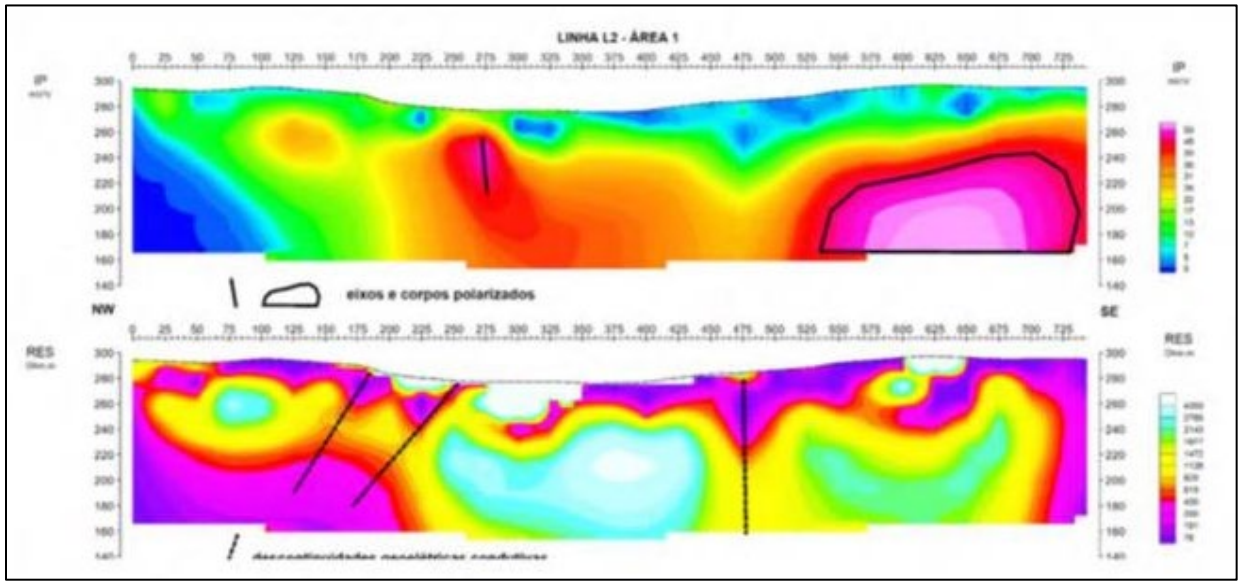


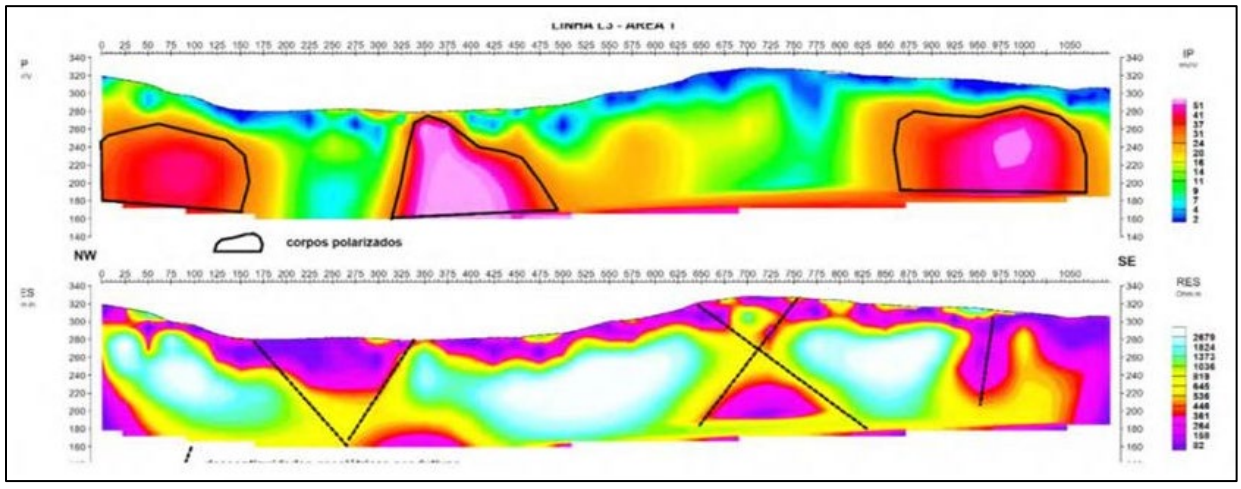
Figure 9-7: Location of the Lines and Measuring Stations of the Chargeability and Resistivity Data for Bandeira Area 1

The top panels of Figure 9-8 to Figure 9-10 show some examples of the actual chargeability sections and the lower panels the real resistivity sections of some of the lines, are shown below.



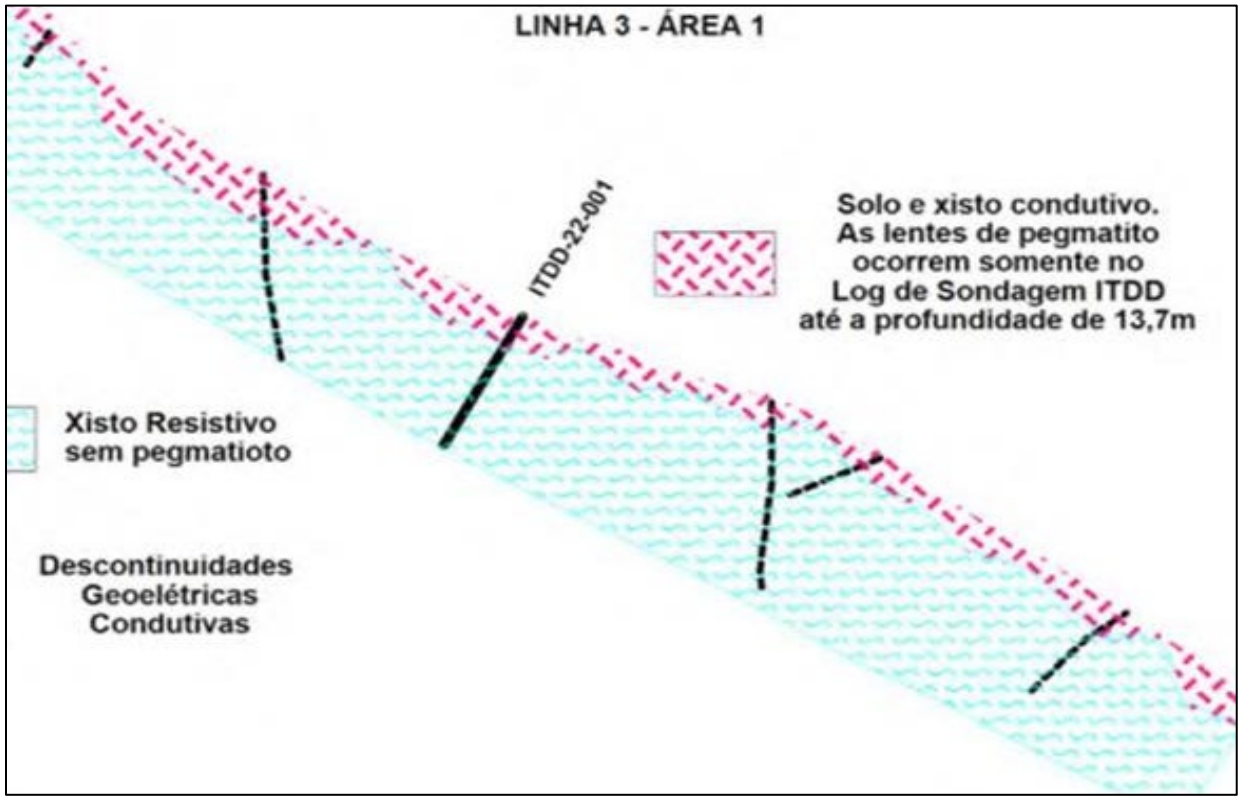
Source: Stevanato (2022).

Figure 9-8: Bandeira IP Depth Model of the Chargeability (Top) and the Actual Resistivity (Bottom) along Line 2 of Area 1 (see Figure 9-7



Source: Stevanato (2022).

Figure 9-9: Bandeira IP Depth Model of the Actual Chargeability (Top) and the Actual Resistivity (Bottom) of Line 3 of Area 1



Source: Stevanato (2022).

Figure 9-10: Conceptual Geological Model from Geophysics Data

The geophysical-geological model was designed from the resistivity data of Line 3 of Bandeira. This model was parameterized from the log data of the ITDD-22-001 rotary drilling and is composed of a unit of shales throughout the length measured by geophysics. Superimposed on this geological homogeneous unit is another consisting of soil and conductive shale that, in the probing carried out, intercepted the pegmatite lenses to a depth of 13.7 m. Other interpretations suggest the presence of conductive geoelectric discontinuities that probably correspond to fault or fracture systems.

MGLIT geoscientists reviewed the inverted data to determine some baseline information to choose a general attitude of the pegmatitic dikes and, if possible, to assist in designing some drill-hole targets.

10 DRILLING

10.1 MGLIT Drilling Campaigns

As of November 20, 2024, MGLIT has executed 297 diamond drill holes within the Bandeira deposit, (Table 101 to) (Figure 101).

All diamond drilling activities conducted within the Bandeira Property until November 20, 2024, were incorporated into the Mineral Resource estimation process, ensuring compliance with best practices and standards.

Table 10-1: Bandeira Diamond Drill-Hole Summary

Year	Drill-Hole Count	Total Length (m)
2022	49	5,570
2023	207	46,642
2024	41	8,089
Total	**297**	**60,301**

10.2 Drill Type

All drilling operations were conducted using HQ (63.5 mm diameter) and NQ (47.6 mm diameter) core sizes. This approach was chosen to ensure the retrieval of pristine and representative core samples, which are essential for accurate geological logging, adequate sample support, and to secure a material supply for future metallurgical testing purposes.

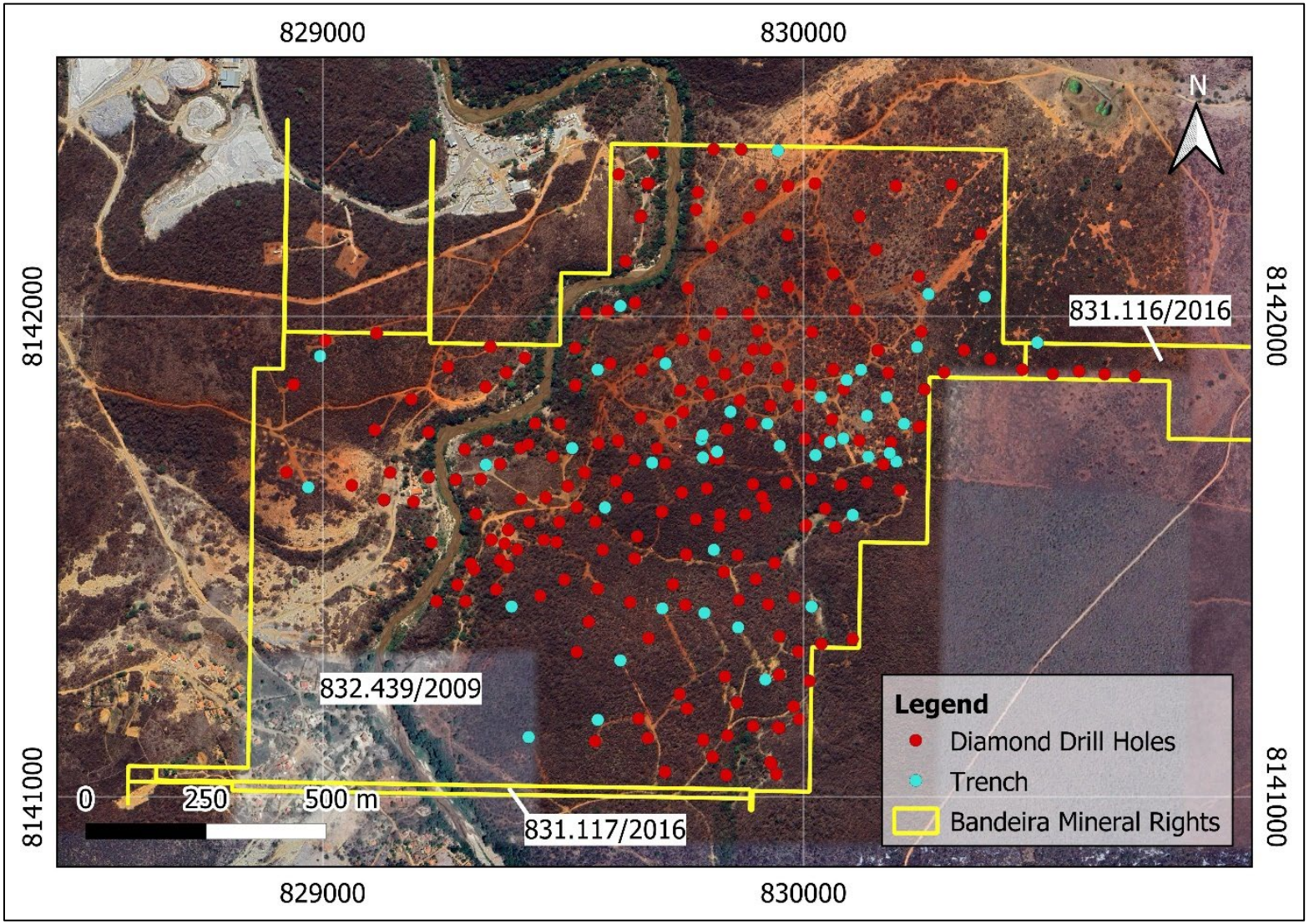
10.3 MGLIT Drilling Campaigns

The following Brazilian-based companies undertook the 2022–2024 drill program at Bandeira:

- Servdrill Perfuração e Sondagens Ltda (http://servdrill.com.br).
- Servitec Foraco Sondagem AS (https://www.foraco.com.br/).
- GEOSOL Ltda. (https://www.geosol.com.br).

10.4 Drill-Collar Monuments

All drill-collar monuments were surveyed using a differential GPS, and the driller placed the monuments once the hole had been completed.



Source: GE21 (2024).

Figure 10-1: Drill Holes and Trenches

10.5 Drill-Hole Surveying

Drill holes were drilled with a plunge between 50° and 90°. Core holes are generally oriented at azimuth 330° and 150°, perpendicular to the pegmatite intrusion orientation.

MGLIT used REFLEX GYRO SPRINT IQ EQ0394 to obtain all downhole survey data.

According to the REFLEX GYRO SPRINT IQ website, the tool can maintain high survey-accuracy. The device is connected to a cloud-based data hub with a secure chain of custody and a QA/QC application with real-time access to drilling survey data. Data transfer from field to office ensures minimum clerical errors related to processing and interpretation.

MGLIT rented the REFLEX GYRO SPRINT IQ downhole Reflex tool and completed all hole surveys in real time. MGLIT employees had quick access to results through the cloud-based data hub. The design of the high-speed survey allowed MGLIT field employees (including geologists and driller) continuous survey data from the tool's north-seeking sensors, which assisted with obtaining GPS locations.

QPs have no way to verify the accuracy of the survey method; hence, the authors will rely on the statements and information that MGLIT provided.

10.6 Core Orientation

MGLIT began implementing REFLEX ACT III to establish core orientation for drill holes within the Project after July 2023. As of the effective date, November 20, 2024, core orientation has been determined for four drill holes. MGLIT has consistently integrated core orientation into its drilling program and in the future will prioritize its application in strategically significant sections of the geological model.

The Reflex core orientation system is based on recovering the core barrel orientation after a run. The Reflex orientation tool begins the orientation process by inserting the device in the core barrel using a specially made "shoe." The tool records core-barrel orientation each minute during a core run. The Reflex sleeve that attaches to the upper drill rod measures the direction of the top-of-hole using built-in accelerometers. Upon completion of a run, the drill string is left undisturbed while the communication tool on the surface counts down the time to the next reading; after this, the barrel can be withdrawn. On the surface, the tool is inserted into the end of the barrel, and the barrel is rotated until it indicates that the barrel is in the same up–down position as it was in the hole. The core, barrel, and shoe are then marked using a level to confirm vertical upward position. After the line is split, the top-of-core line is transferred along the length of the recovered core.

The QPs could not verify the orientation method's accuracy and instead relied on and approved the statements and information that MGLIT provided.

10.7 Drill-Core Chain of Custody

The drill cores are stored in plastic or wooden boxes. The drilling companies always transport the core directly from the drilling site to the MGLIT core sheds in Araçuaí. MGLIT's employees receive all core boxes delivered.

10.8 Core-Logging Procedures

MGLIT adheres to a core-logging method carried out by MGLIT's geologists and technicians.

The following procedures are carried out:

- Preparing drilling site
- Locating drill collars
- Field-verifying and validating metreage and quality of drill cores
- Core survey drilling
- Photographing the core box
- Logging detailed petrographic and geological structural of core
- Geotechnical logging (RQD, weathering types)
- Sample geochemistry logging programming and QA/QC procedures
- Determining drill-core density for each programmed sample
- Preparing core samples for geochemistry analysis
- Sending samples to the laboratory according to logistics protocols.

Each procedure has its respective spreadsheet, which is stored in digital form within MGLIT's customized database.

Table 10-2: Project Drill Collars

HOLE-ID	Easting	Northing	Collar Elevation (m)	Length (m)	Year	HOLE-ID	Easting	Northing	Collar Elevation (m)	Length (m)	Year	HOLE-ID	Easting	Northing	Collar Elevation (m)	Length (m)	Year
ITDD-22-001	189738	8141720	296	101	2022	ITDD-22-033A	190517	8142242	339	22	2022	ITDD-23-069	190364	8141496	302	220	2023
ITDD-22-002	189760	8141770	302	96	2022	ITDD-22-034	190043	8141461	311	121	2022	ITDD-23-070	190163	8142649	280	423	2023
ITDD-22-003	190330	8141641	323	60	2022	ITDD-22-035	190326	8142368	320	205	2022	ITDD-23-071	190332	8141561	320	153	2023
ITDD-22-004	190153	8142051	336	76	2022	ITDD-22-036	190127	8141515	317	121	2022	ITDD-23-072	189691	8141876	287	140	2023
ITDD-22-004B	190153	8142051	336	40	2022	ITDD-22-037	189954	8141411	305	122	2022	ITDD-23-073	190016	8142507	275	480	2023
ITDD-22-005	190183	8142008	336	68	2022	ITDD-22-038	190379	8142276	327	150	2022	ITDD-23-074	189848	8142000	276	121	2023
ITDD-22-006	190116	8142101	331	125	2022	ITDD-22-039	190284	8142238	331	150	2022	ITDD-23-075	190395	8141550	303	169	2023
ITDD-22-007	189861	8141823	302	71	2022	ITDD-22-040	190063	8141421	306	151	2022	ITDD-23-076	190009	8142325	276	260	2023
ITDD-22-008	189744	8141782	299	75	2022	ITDD-22-041	190467	8142324	338	151	2022	ITDD-23-077	190220	8141554	322	100	2023
ITDD-22-009	190426	8142095	345	110	2022	ITDD-22-042	190606	8142283	341	110	2022	ITDD-23-078	189625	8142181	306	362	2023
ITDD-22-010	190379	8142168	341	4	2022	ITDD-22-043	190143	8141485	314	151	2022	ITDD-23-079	190483	8141640	320	171	2023
ITDD-22-011	189803	8141864	292	100	2022	ITDD-22-044	190420	8142398	334	202	2022	ITDD-23-080	190241	8142509	305	310	2023
ITDD-22-012	189901	8141897	288	100	2022	ITDD-22-045	190536	8142005	333	101	2022	ITDD-23-081	190418	8141628	304	172	2023
ITDD-22-013	189881	8141940	284	100	2022	ITDD-22-046	190179	8141423	305	120	2022	ITDD-23-082	190009	8142326	275	298	2023
ITDD-22-014	189784	8141910	285	103	2022	ITDD-22-047	190507	8142451	340	157	2022	ITDD-23-083	190017	8142506	275	420	2023
ITDD-22-015	189675	8141694	275	51	2022	ITDD-22-048	190448	8141960	326	100	2022	ITDD-23-084	189625	8142181	306	305	2023
ITDD-22-016	189980	8141955	308	103	2022	ITDD-22-050	190200	8142183	327	151	2023	ITDD-23-085	190246	8141501	315	115	2023
ITDD-22-017	189725	8141824	293	100	2022	ITDD-22-049	190179	8141421	305	109	2023	ITDD-23-086	190241	8142509	305	341	2023
ITDD-22-018	190064	8142024	326	154	2022	ITDD-23-051	190101	8141351	298	91	2023	ITDD-23-087	190322	8141375	296	90	2023
ITDD-22-019	189658	8141728	276	102	2022	ITDD-23-052	190166	8142446	294	481	2023	ITDD-23-088	190118	8142359	300	304	2023
ITDD-22-020	190082	8141993	327	91	2022	ITDD-23-053	190109	8142146	325	141	2023	ITDD-23-089	190371	8141611	317	184	2023
ITDD-22-021	190258	8142082	339	131	2022	ITDD-23-054	189739	8141981	275	145	2023	ITDD-23-090	190037	8142639	276	589	2023
ITDD-22-022	190006	8141920	311	100	2022	ITDD-23-055	190101	8141352	298	130	2023	ITDD-23-091	189367	8142228	335	544	2023
ITDD-22-023	190063	8142225	304	149	2022	ITDD-23-056	190228	8141350	299	76	2023	ITDD-23-092	189847	8142001	277	130	2023
ITDD-22-024	190156	8142264	313	180	2022	ITDD-23-058	189739	8141982	275	156	2023	ITDD-23-093	190200	8141385	302	75	2023
ITDD-22-025	190233	8142129	335	130	2022	ITDD-23-059	190229	8141349	299	57	2023	ITDD-23-094	189943	8142030	300	109	2023
ITDD-22-026	190357	8142121	342	121	2022	ITDD-23-060	190165	8142447	292	490	2023	ITDD-23-095	189746	8142172	277	250	2023
ITDD-22-027	190449	8142159	342	109	2022	ITDD-23-061	190281	8141453	297	105	2023	ITDD-23-096	189942	8142031	300	118	2023
ITDD-22-028	190333	8142162	339	112	2022	ITDD-23-062	190163	8142649	278	433	2023	ITDD-23-097	189780	8141805	299	49	2023
ITDD-22-029	189962	8142198	299	171	2022	ITDD-23-063	190281	8141452	297	121	2023	ITDD-23-098	189760	8141845	294	350	2023
ITDD-22-030	190426	8142200	337	110	2022	ITDD-23-065	190130	8142523	283	505	2023	ITDD-23-099	189836	8141914	284	79	2023
ITDD-22-031	190540	8142196	339	130	2022	ITDD-23-066	190332	8141354	297	151	2023	ITDD-23-100	189691	8141761	278	50	2023
ITDD-22-032	190245	8142309	320	163	2022	ITDD-23-067	190364	8141497	301	130	2023	ITDD-23-101	189835	8141915	284	100	2023
ITDD-22-033	190516	8142242	339	100	2022	ITDD-23-068	189692	8141876	287	136	2023	ITDD-23-102	189745	8142173	277	262	2023

Source: GE21 (2024).

Table 10-3: Project Drill Collars

HOLE-ID	Easting	Northing	Collar Elevation (m)	Length (m)	Year	HOLE-ID	Easting	Northing	Collar Elevation (m)	Length (m)	Year	HOLE-ID	Easting	Northing	Collar Elevation (m)	Length (m)	Year
ITDD-23-103	189511	8141957	273	221	2023	ITDD-23-137	189664	8142010	274	401	2023	ITDD-23-172	190274	8142355	312	392	2023
ITDD-23-104	189684	8141773	278	67	2023	ITDD-23-138	189476	8142045	298	330	2023	ITDD-23-173	189950	8141729	314	150	2023
ITDD-23-105	189907	8142302	277	421	2023	ITDD-23-140	190208	8142068	338	80	2023	ITDD-23-174	189704	8142141	284	370	2023
ITDD-23-106	189700	8141948	279	142	2023	ITDD-23-141	190297	8142120	339	61	2023	ITDD-23-175	190028	8142573	275	550	2023
ITDD-23-107	189588	8142044	273	241	2023	ITDD-23-142	190111	8142251	306	200	2023	ITDD-23-176	190018	8141999	318	255	2023
ITDD-23-108	189760	8141846	294	95	2023	ITDD-23-144	190247	8142198	331	120	2023	ITDD-23-177	189954	8142306	276	391	2023
ITDD-23-109	189780	8142016	275	316	2023	ITDD-23-139	189550	8142111	304	367	2023	ITDD-23-178	189500	8141899	273	211	2023
ITDD-23-110	189915	8141968	288	72	2023	ITDD-23-143	190190	8142309	316	439	2023	ITDD-23-179	189432	8141928	294	250	2023
ITDD-23-111	189834	8141827	299	41	2023	ITDD-23-145	189625	8142180	306	330	2023	ITDD-23-180	189987	8142411	276	509	2023
ITDD-23-113	189601	8141814	273	109	2023	ITDD-23-146	189809	8142068	274	295	2023	ITDD-23-181	189588	8142043	273	250	2023
ITDD-23-114	189916	8141968	288	92	2023	ITDD-23-147	190110	8142251	306	510	2023	ITDD-23-182	190322	8142475	322	381	2023
ITDD-23-115	189866	8141864	294	48	2023	ITDD-23-148	190310	8142199	335	350	2023	ITDD-23-183	189500	8141899	273	201	2023
ITDD-23-116	189859	8142069	276	139	2023	ITDD-23-149	189367	8142227	335	469	2023	ITDD-22-002T	189761	8141769	302	45	2023
ITDD-23-117	189891	8142149	297	220	2023	ITDD-23-150	189861	8142069	276	349	2023	ITDD-23-184	190274	8142356	313	421	2023
ITDD-23-118	189592	8141949	273	184	2023	ITDD-23-151	189474	8142246	327	442	2023	ITDD-23-185	190027	8142574	276	592	2023
ITDD-23-120	189859	8142070	277	280	2023	ITDD-23-152	190190	8142309	316	315	2023	ITDD-23-186	189305	8142134	331	421	2023
ITDD-23-112	189699	8141949	279	320	2023	ITDD-23-153	189295	8141951	322	450	2023	ITDD-23-187	189500	8141900	273	220	2023
ITDD-23-119	189779	8142016	275	139	2023	ITDD-23-154	190266	8142274	325	550	2023	ITDD-23-189	189615	8141692	277	120	2023
ITDD-23-121	189891	8142150	297	362	2023	ITDD-23-155	190110	8142252	305	241	2023	ITDD-23-191	189753	8141816	296	80	2023
ITDD-23-122	189591	8141950	273	340	2023	ITDD-23-156	190189	8142309	316	341	2023	ITDD-23-087T	190320	8141379	296	76	2023
ITDD-23-123	189712	8142030	275	351	2023	ITDD-23-157	189888	8142227	285	380	2023	ITDD-23-093T	190199	8141386	302	60	2023
ITDD-23-124	190154	8142164	327	130	2023	ITDD-23-158	189474	8142246	327	481	2023	ITDD-23-188	189967	8142591	276	664	2023
ITDD-23-125	189648	8141947	273	330	2023	ITDD-23-160	190091	8142079	329	259	2023	ITDD-23-192	189783	8142204	276	381	2023
ITDD-23-126	190154	8142165	327	170	2023	ITDD-23-161	190276	8142353	312	420	2023	ITDD-23-193	190571	8141953	323	150	2023
ITDD-23-127	190029	8142087	320	151	2023	ITDD-23-162	189367	8142228	335	487	2023	ITDD-23-194	190025	8141793	302	150	2023
ITDD-23-128	189591	8141950	273	206	2023	ITDD-23-163	190031	8142574	277	534	2023	ITDD-23-195	189983	8142037	312	106	2023
ITDD-23-129	189665	8142009	274	199	2023	ITDD-23-164	189954	8142306	275	480	2023	ITDD-23-196	190024	8141794	302	151	2023
ITDD-23-130	190154	8142164	327	300	2023	ITDD-23-165	189910	8142302	276	367	2023	ITDD-23-197	190258	8142235	330	110	2023
ITDD-23-131	190029	8142088	320	301	2023	ITDD-23-166	190132	8141805	310	121	2023	ITDD-23-198	190447	8141960	326	120	2023
ITDD-23-132	189664	8142010	274	210	2023	ITDD-23-167	189703	8142142	284	412	2023	ITDD-23-200	189910	8141596	322	100	2023
ITDD-23-133	189561	8141898	277	184	2023	ITDD-23-168	190131	8141806	310	146	2023	ITDD-23-201	190550	8142051	337	50	2023
ITDD-23-134	189648	8141947	273	165	2023	ITDD-23-169	190322	8142475	321	445	2023	ITDD-23-134T	189647	8141946	273	39	2023
ITDD-23-135	190179	8142220	321	250	2023	ITDD-23-170	189950	8141728	314	141	2023	ITDD-23-202	190028	8142086	320	281	2023
ITDD-23-136	190248	8142197	331	334	2023	ITDD-23-171	190019	8141998	317	249	2023	ITDD-23-203	190199	8141891	324	151	2023

Source: GE21 (2024).

Table 10-4: Project Drill Collars

HOLE-ID	Easting	Northing	Collar Elevation (m)	Length (m)	Year	HOLE-ID	Easting	Northing	Collar Elevation (m)	Length (m)	Year	HOLE-ID	Easting	Northing	Collar Elevation (m)	Length (m)	Year
ITDD-23-204	190029	8141840	303	40	2023	ITDD-23-233	189958	8141810	303	171	2023	ITDD-24-266	190502	8141966	329	245	2024
ITDD-23-205	190484	8142053	342	150	2023	ITDD-23-234	190243	8141714	319	199	2023	ITDD-24-267	190133	8141700	319	68	2024
ITDD-23-206	190412	8142053	341	50	2023	ITDD-23-235	190277	8141759	314	233	2023	ITDD-24-268	190211	8141771	312	260	2024
ITDD-23-207	190119	8141934	326	50	2023	ITDD-23-236	190316	8141793	309	231	2023	ITDD-24-269	190247	8142195	331	191	2024
ITDD-23-208	190371	8142053	340	50	2023	ITDD-23-159	190027	8142186	309	489	2023	ITDD-24-270	190238	8141807	315	182	2024
ITDD-23-209	190228	8141432	301	75	2023	ITDD-23-237	190376	8142585	324	100	2023	ITDD-24-271	190305	8141707	317	218	2024
ITDD-23-199	189711	8142225	293	451	2023	ITDD-23-238	190470	8142519	334	100	2023	ITDD-24-272	190170	8142139	331	226	2024
ITDD-23-211	190082	8141993	327	233	2023	ITDD-23-239	190544	8142585	332	100	2023	ITDD-24-273	190358	8141723	309	260	2024
ITDD-23-212	190149	8141879	322	150	2023	ITDD-23-240	190659	8142591	328	100	2023	ITDD-24-274	190193	8142007	336	210	2024
ITDD-23-213	190336	8141450	300	131	2023	ITDD-23-241	190723	8142490	328	100	2023	ITDD-24-275	190294	8141909	319	250	2024
ITDD-23-218	190332	8141452	299	93	2023	ITDD-23-242	190598	8142398	342	100	2023	ITDD-24-276	190386	8141970	328	211	2024
ITDD-23-214	190079	8141894	317	45	2023	ITDD-23-243	190696	8142247	333	101	2023	ITDD-24-277	190335	8141961	327	240	2024
ITDD-23-215	189981	8141954	307	233	2023	ITDD-23-244	190320	8142578	316	100	2023	ITDD-24-278	190387	8141970	328	150	2024
ITDD-23-216	189881	8141940	284	228	2023	ITDD-23-245	190264	8142578	304	100	2023	ITDD-24-279	190417	8141910	307	151	2024
ITDD-23-217	190238	8141807	315	91	2023	ITDD-23-246	190616	8142164	335	70	2023	ITDD-24-280	189951	8142306	276	250	2024
ITDD-23-219	189914	8141970	288	220	2023	ITDD-23-247	190617	8142163	335	111	2023	ITDD-24-281	190439	8141872	306	150	2024
ITDD-23-220	190106	8141742	314	99	2023	ITDD-23-248	190751	8142232	333	88	2023	ITDD-24-282	190286	8141930	323	303	2024
ITDD-23-222	189803	8141863	292	224	2023	ITDD-23-249	190752	8142230	333	150	2023	ITDD-24-283	190377	8141872	306	243	2024
ITDD-23-223	190018	8141703	315	118	2023	ITDD-24-250	190656	8142200	334	70	2024	ITDD-24-284	190266	8141956	329	90	2024
ITDD-22-023T	190061	8142224	304	49	2023	ITDD-24-251	190818	8142211	340	217	2024	ITDD-24-286	190387	8141969	328	185	2024
ITDD-22-048T	190450	8141961	326	84	2023	ITDD-24-252	190610	8142087	333	121	2024	ITDD-23-057	192600	8142101	363	300	2024
ITDD-23-221	190336	8141451	300	221	2023	ITDD-24-253	190611	8142086	333	200	2024	ITDD-23-064	192600	8141900	379	301	2024
ITDD-23-224	189835	8141827	299	193	2023	ITDD-24-254	190133	8142559	283	200	2024	ITDD-23-190	192596	8142203	353	300	2024
ITDD-23-225	189933	8141659	320	107	2023	ITDD-24-255	190220	8142651	288	182	2024	ITDD-24-285	190377	8141871	305	281	2024
ITDD-23-226	189865	8141865	294	199	2023	ITDD-24-256	190882	8142204	347	261	2024	ITDD-24-287	190387	8141970	328	150	2024
ITDD-23-227	189940	8141867	291	214	2023	ITDD-24-257	190937	8142211	353	218	2024	ITDD-24-288	190198	8141866	322	60	2024
ITDD-23-228	190377	8141470	301	153	2023	ITDD-24-258	189908	8142300	277	170	2024	ITDD-24-289	190251	8141892	323	163	2024
ITDD-23-229	189830	8141711	312	147	2023	ITDD-24-259	190936	8142211	353	200	2024	ITDD-24-290	190378	8141874	306	260	2024
ITDD-23-230	190077	8141892	317	187	2023	ITDD-24-260	190990	8142207	358	206	2024						
ITDD-22-030T	190425	8142199	337	61	2023	ITDD-24-261	189796	8142024	275	200	2024						
ITDD-23-083T	190015	8142504	276	74	2023	ITDD-24-262	190990	8142206	358	278	2024						
ITDD-23-210	190170	8141944	330	608	2023	ITDD-24-263	191053	8142204	362	350	2024						
ITDD-23-231	189880	8141745	312	157	2023	ITDD-24-264	190607	8142085	333	141	2024						
ITDD-23-232	190028	8141840	303	166	2023	ITDD-24-265	190058	8141629	322	80	2024						

Source: GE21 (2024).

10.9 Ore Drilling Intercepts

Drill spacing typically ranged from 50 m to 150 m, with narrower spacing observed in the central portion of the drill-hole array and wider spacing towards the margins. The ore intercepts vary in thickness, ranging from approximately 85% of the true width to nearly the true width of the mineralization.

The average pegmatite intersection ranges from 0.3 m to 40 m, with an average true thickness of about 5 m. In total, 760 mineralized diamond drill hole (DDH) intercepts were used for modelling the 34 mineralized solids within the Project. Each solid was assigned a numerical code in the tag column.

Table 10-5 to Table 10-7 list the mineralized intervals from Project drill holes that were incorporated into the 3-D modelling of the mineralized solids (Figure 10-2 and Figure 10-3).

Table 10-5: Mineralized Intercepts by Bandeira Drill Holes

holeid	from	to	Li2O_pct	Grade_shell
ITDD-22-001	8.50	13.70	1.53	1
ITDD-22-002	33.08	38.74	1.94	1
ITDD-22-004B	37.45	38.13	0.44	1
ITDD-22-006	54.90	57.60	2.23	1
ITDD-22-007	18.20	18.75	0.50	01A-SW
ITDD-22-007	21.62	27.58	1.33	1
ITDD-22-008	45.45	46.80	0.23	1
ITDD-22-011	53.14	59.89	1.99	1
ITDD-22-012	33.70	34.45	0.74	01A-SW
ITDD-22-012	36.23	42.03	1.69	1
ITDD-22-013	53.18	57.08	1.56	01A-SW
ITDD-22-013	62.90	65.66	1.66	1
ITDD-22-014	77.10	82.80	1.14	1
ITDD-22-015	6.16	8.74	1.04	1
ITDD-22-015	10.97	11.70	0.66	01B-SW
ITDD-22-016	39.50	45.35	1.27	1
ITDD-22-017	62.21	67.15	1.06	1
ITDD-22-018	44.96	45.96	0.52	1
ITDD-22-019	29.83	33.57	1.97	1
ITDD-22-020	17.65	19.65	0.09	1
ITDD-22-021	23.50	24.19	0.74	1
ITDD-22-021	31.90	37.33	0.76	04-NE
ITDD-22-022	14.31	18.31	0.55	1
ITDD-22-023	33.50	34.26	0.96	02-NE
ITDD-22-023	38.53	43.59	2.13	02A-NE
ITDD-22-023	114.34	115.90	1.01	1
ITDD-22-024	28.14	33.86	1.71	02-NE
ITDD-22-024	36.35	37.35	1.07	02A-NE
ITDD-22-024	117.39	118.76	0.07	1
ITDD-22-024	156.72	161.72	1.22	04-NE
ITDD-22-025	56.47	58.08	0.37	1
ITDD-22-025	67.62	71.31	2.22	04-NE
ITDD-22-027	22.78	29.09	0.43	04-NE
ITDD-22-028	34.30	35.35	2.17	04B-NE
ITDD-22-028	38.64	40.25	1.95	1
ITDD-22-028	51.39	53.39	0.67	04-NE
ITDD-22-029	41.46	42.25	1.56	02-NE
ITDD-22-029	44.28	46.93	1.29	02A-NE
ITDD-22-029	145.91	149.08	1.21	1
ITDD-22-030	46.60	53.30	1.49	04-NE
ITDD-22-032	13.18	14.33	0.29	02-NE
ITDD-22-032	18.35	19.95	1.95	02A-NE
ITDD-22-032	130.30	135.34	0.64	1
ITDD-22-032	137.40	139.20	1.58	04-NE
ITDD-22-033A	6.05	10.05	0.41	04B-NE
ITDD-22-034	17.42	18.42	1.17	SE-A
ITDD-22-035	103.27	105.17	1.04	04A-NE
ITDD-22-035	111.93	113.21	1.43	04B-NE
ITDD-22-035	128.48	129.24	0.56	1
ITDD-22-035	171.62	176.50	1.28	04-NE
ITDD-22-035	179.30	181.02	0.56	04C-NE
ITDD-22-036	39.10	45.10	0.90	SE-A
ITDD-22-038	43.26	44.66	2.43	04A-NE
ITDD-22-038	55.73	56.81	0.39	04B-NE
ITDD-22-038	67.32	71.32	1.04	1
ITDD-22-038	98.13	104.85	1.24	04-NE
ITDD-22-039	86.24	91.95	2.13	1
ITDD-22-039	94.19	95.86	1.71	04-NE
ITDD-22-040	55.90	56.90	1.36	SE-A
ITDD-22-041	37.16	37.97	0.60	04A-NE
ITDD-22-043	38.05	42.41	1.43	SE-A
ITDD-22-044	157.06	158.03	0.32	1
ITDD-22-045	21.65	24.65	0.34	10-NE
ITDD-22-045	34.94	39.78	0.36	09-NE
ITDD-22-045	40.57	44.88	1.17	09-NE
ITDD-22-046	63.00	68.00	1.17	SE-A
ITDD-22-048	57.50	60.11	0.70	10-NE
ITDD-22-048	69.39	74.20	1.08	09-NE
ITTRE-22-004	12.80	15.80	0.46	01A-SW
ITTRE-22-009	60.00	63.00	0.08	02-NE
ITTRE-22-012	33.20	37.20	0.28	02-NE
ITTRE-22-012	42.06	45.06	0.35	02A-NE
ITDD-22-050	96.60	99.31	0.81	04-NE
ITDD-22-049	64.87	67.87	0.86	SE-A
ITDD-23-051	56.98	59.68	0.64	SE-A
ITDD-23-052	99.96	100.73	0.87	02-NE
ITDD-23-052	108.25	111.94	0.63	02A-NE
ITDD-23-052	205.44	209.44	1.79	1
ITDD-23-052	223.63	225.63	2.33	04-NE
ITDD-23-052	255.36	257.46	0.89	04C-NE
ITDD-23-052	279.04	280.00	0.74	05A-NE
ITDD-23-052	308.20	312.46	0.93	05-NE
ITDD-23-052	327.28	328.28	0.92	05B-NE
ITDD-23-052	381.30	386.00	1.11	06-NE
ITDD-23-052	392.20	398.52	1.37	06A-NE
ITDD-23-052	415.48	416.48	2.07	06B-NE
ITDD-23-052	433.13	440.30	1.52	07-NE
ITDD-23-053	74.65	77.19	1.95	1
ITDD-23-054	118.00	123.00	1.66	1
ITDD-23-055	36.97	38.95	0.42	SE-A
ITDD-23-056	37.75	49.02	0.88	SE-A
ITDD-23-058	122.55	128.55	1.96	1
ITDD-23-059	28.72	32.96	1.32	SE-A
ITDD-23-060	111.44	112.13	2.00	02-NE
ITDD-23-060	170.03	174.36	0.73	02B-NE
ITDD-23-060	225.23	229.50	2.03	1
ITDD-23-060	252.75	254.57	0.04	04-NE
ITDD-23-060	283.30	284.48	2.16	04C-NE
ITDD-23-060	315.98	317.93	1.22	05A-NE
ITDD-23-060	318.40	321.20	0.72	05A-NE
ITDD-23-060	332.62	334.00	2.04	05-NE
ITDD-23-060	399.67	402.45	1.79	06-NE
ITDD-23-060	405.94	408.44	0.81	06A-NE
ITDD-23-060	444.29	449.43	1.44	07-NE
ITDD-23-061	61.50	80.19	1.32	SE-A
ITDD-23-062	104.43	124.43	1.62	03-NE
ITDD-23-062	167.88	168.86	0.74	02D-NE
ITDD-23-062	349.56	353.47	1.05	04-NE
ITDD-23-062	384.50	388.68	1.01	04C-NE
ITDD-23-063	41.67	55.24	1.73	SE-A
ITDD-23-065	159.62	164.60	1.12	02-NE
ITDD-23-065	203.93	208.16	1.53	02B-NE
ITDD-23-065	216.53	217.63	1.30	02E-NE
ITDD-23-065	271.20	277.29	2.53	1
ITDD-23-065	321.22	324.22	1.25	04-NE
ITDD-23-065	336.67	339.41	1.32	04C-NE
ITDD-23-065	354.23	378.23	1.32	05A-NE
ITDD-23-065	390.10	397.82	1.88	05-NE
ITDD-23-065	400.74	403.08	1.30	05B-NE
ITDD-23-065	431.25	434.45	0.67	06-NE
ITDD-23-065	441.88	445.37	2.04	06A-NE
ITDD-23-065	456.28	465.95	0.61	07-NE
ITDD-23-065	484.11	485.10	1.12	08-NE
ITDD-23-066	28.16	37.16	0.73	SE-A
ITDD-23-067	86.96	103.96	1.21	SE-A
ITDD-23-068	92.23	93.97	1.03	1
ITDD-23-068	112.79	114.45	0.38	01B-SW
ITDD-23-069	58.55	75.48	1.29	SE-A
ITDD-23-070	78.30	97.30	0.90	03-NE
ITDD-23-070	152.73	156.40	1.83	02D-NE
ITDD-23-070	332.74	336.36	2.15	04-NE
ITDD-23-070	339.94	343.42	1.09	04C-NE
ITDD-23-071	86.49	90.49	0.90	SE-A
ITDD-23-072	99.14	100.94	1.37	1
ITDD-23-072	113.69	117.69	1.38	01B-SW
ITDD-23-073	77.82	83.66	1.99	03-NE
ITDD-23-073	206.62	213.30	1.99	02-NE
ITDD-23-073	242.54	247.63	0.77	02B-NE
ITDD-23-073	298.08	299.08	1.06	1
ITDD-23-073	352.92	360.92	1.66	04-NE
ITDD-23-073	408.21	411.86	1.83	05A-NE
ITDD-23-073	412.04	426.35	1.11	05A-NE
ITDD-23-073	443.07	447.07	2.10	05-NE
ITDD-23-074	85.77	89.96	1.45	01A-SW
ITDD-23-074	95.31	95.91	1.98	1
ITDD-23-074	96.84	100.25	1.98	1
ITDD-23-075	109.00	113.03	1.22	SE-A
ITDD-23-075	113.57	119.43	0.74	SE-A
ITDD-23-075	130.10	141.90	1.00	08-NE
ITDD-23-076	82.64	84.05	2.03	02-NE
ITDD-23-076	85.55	86.84	2.24	02A-NE
ITDD-23-076	165.53	168.98	1.39	1
ITDD-23-078	313.14	317.90	0.89	01A-SW
ITDD-23-078	321.95	337.78	1.42	1
ITDD-23-080	63.52	65.52	0.22	02D-NE
ITDD-23-080	255.45	261.66	1.49	04-NE
ITDD-23-080	274.70	275.70	0.92	04C-NE
ITDD-23-081	120.07	129.07	1.49	08-NE
ITDD-23-081	144.40	149.12	1.50	08A-NE
ITDD-23-082	50.63	56.40	2.17	02C-NE
ITDD-23-082	99.92	102.23	1.04	02-NE
ITDD-23-082	196.20	201.00	1.48	1
ITDD-23-083	59.09	66.12	1.37	03-NE
ITDD-23-083	171.31	177.15	1.90	02-NE
ITDD-23-083	225.68	226.38	0.71	02B-NE
ITDD-23-083	230.83	231.48	1.09	02E-NE
ITDD-23-083	310.73	314.78	1.11	04-NE
ITDD-23-083	371.44	379.76	2.03	05-NE
ITDD-23-084	273.30	274.06	0.92	01A-SW
ITDD-23-084	275.42	284.87	1.31	1

Source: GE21 (2024).

Table 10-6: Mineralized Intercepts by Bandeira Drill Holes

holeid	from	to	Li2O_pct	Grade_shell
ITDD-23-085	73.40	74.47	0.67	SE-A
ITDD-23-086	69.92	72.11	1.48	02D-NE
ITDD-23-086	272.46	283.27	1.04	04-NE
ITDD-23-086	293.70	299.86	1.33	04C-NE
ITDD-23-087	53.24	69.96	1.19	SE-A
ITDD-23-088	83.32	86.32	0.96	02-NE
ITDD-23-088	199.94	210.19	1.28	04-NE
ITDD-23-088	272.46	274.62	2.21	05-NE
ITDD-23-088	287.18	287.96	0.74	05C-NE
ITDD-23-088	294.83	295.63	0.48	05B-NE
ITDD-23-089	63.26	72.02	1.37	SE-A
ITDD-23-089	155.53	161.53	1.22	08-NE
ITDD-23-090	161.74	169.95	1.03	03-NE
ITDD-23-090	253.07	263.50	0.98	02-NE
ITDD-23-090	386.98	389.98	1.62	1
ITDD-23-090	442.90	445.66	1.79	04-NE
ITDD-23-090	465.61	471.85	1.57	04C-NE
ITDD-23-090	564.45	567.45	1.56	06-NE
ITDD-23-090	580.60	581.60	0.57	07-NE
ITDD-23-091	62.26	63.07	0.95	01E-SW
ITDD-23-091	426.02	427.97	0.89	01D-SW
ITDD-23-091	479.83	489.24	1.04	1
ITDD-23-092	92.81	95.83	1.57	01A-SW
ITDD-23-092	103.81	109.42	1.23	1
ITDD-23-093	43.65	51.65	1.47	SE-A
ITDD-23-094	80.58	88.26	1.63	1
ITDD-23-095	46.35	48.48	0.70	02C-NE
ITDD-23-095	202.91	206.91	0.63	01A-SW
ITDD-23-095	216.19	223.07	1.38	1
ITDD-23-096	88.95	97.18	1.62	1
ITDD-23-097	38.70	44.12	1.48	1
ITDD-23-098	62.59	67.59	1.64	1
ITDD-23-098	194.04	196.69	1.02	05-NE
ITDD-23-099	63.04	65.04	1.91	01A-SW
ITDD-23-099	67.96	72.49	1.10	1
ITDD-23-100	27.85	28.85	0.35	1
ITDD-23-100	32.49	33.49	0.56	01B-SW
ITDD-23-101	76.74	81.74	1.55	1
ITDD-23-102	52.60	56.09	1.16	02C-NE
ITDD-23-102	202.45	204.35	0.99	01A-SW
ITDD-23-102	226.35	233.36	1.55	1
ITDD-23-103	197.00	200.00	1.33	1
ITDD-23-104	55.89	57.89	0.93	1
ITDD-23-104	58.89	59.89	1.45	01B-SW
ITDD-23-105	97.01	99.52	1.47	02C-NE
ITDD-23-105	110.73	116.40	1.49	02-NE
ITDD-23-105	214.09	215.79	0.96	01A-SW
ITDD-23-105	220.44	229.59	1.32	1
ITDD-23-105	370.38	375.38	1.24	05-NE
ITDD-23-106	133.08	135.23	0.95	01B-SW
ITDD-23-107	194.96	195.83	0.66	01A-SW
ITDD-23-107	197.74	199.94	1.37	1
ITDD-23-107	209.54	213.54	1.81	01B-SW
ITDD-23-108	75.26	81.81	1.46	1
ITDD-23-108	86.52	88.52	1.73	01B-SW
ITDD-23-109	120.09	127.08	1.28	1
ITDD-23-109	247.87	255.66	1.69	05-NE
ITDD-23-110	55.33	56.10	1.35	01A-SW
ITDD-23-110	58.58	62.84	2.15	1
ITDD-23-111	27.80	34.40	1.51	1
ITDD-23-113	97.33	99.89	1.75	1
ITDD-23-114	66.26	67.26	0.49	01A-SW
ITDD-23-114	72.40	77.06	0.97	1
ITDD-23-114	77.15	78.15	1.32	1
ITDD-23-115	34.08	41.00	1.26	1
ITDD-23-116	112.82	117.36	2.18	01A-SW
ITDD-23-116	132.12	134.17	0.91	1
ITDD-23-117	30.22	33.22	0.33	02-NE
ITDD-23-117	35.00	37.69	0.33	02A-NE
ITDD-23-117	143.90	145.00	2.81	01A-SW
ITDD-23-117	166.63	169.18	0.74	1
ITDD-23-118	155.35	156.56	1.76	01A-SW
ITDD-23-118	160.13	164.07	0.93	1
ITDD-23-120	109.66	115.92	1.24	01A-SW
ITDD-23-120	126.06	127.18	0.52	1
ITDD-23-120	253.93	259.63	1.86	05-NE
ITDD-23-112	124.79	131.18	1.74	1
ITDD-23-112	142.43	144.36	1.20	01B-SW
ITDD-23-119	118.90	119.42	0.31	01A-SW
ITDD-23-119	124.13	130.85	1.57	1
ITDD-23-121	34.85	40.85	0.57	02-NE
ITDD-23-121	44.12	46.12	0.33	02A-NE
ITDD-23-121	163.40	169.82	1.92	01A-SW
ITDD-23-121	182.04	183.59	2.59	1
ITDD-23-121	331.55	337.47	1.83	05-NE
ITDD-23-122	157.52	158.16	0.73	01A-SW
ITDD-23-122	164.11	168.11	1.49	1
ITDD-23-123	151.75	159.40	2.39	1
ITDD-23-123	285.88	286.88	1.40	05-NE
ITDD-23-124	80.04	81.04	0.99	1
ITDD-23-125	133.72	134.77	0.60	1
ITDD-23-125	144.94	147.97	1.43	01B-SW
ITDD-23-126	105.80	108.37	1.02	1
ITDD-23-127	81.91	82.66	1.11	1
ITDD-23-128	178.46	183.31	2.24	1
ITDD-23-129	153.61	155.00	0.83	01A-SW
ITDD-23-129	157.10	160.35	1.97	1
ITDD-23-130	88.49	91.08	1.15	1
ITDD-23-130	201.33	203.33	0.60	05-NE
ITDD-23-130	240.32	242.41	1.46	05B-NE
ITDD-23-131	99.48	101.48	1.98	1
ITDD-23-131	272.94	278.00	0.96	05-NE
ITDD-23-132	69.51	72.73	1.66	01C-SW
ITDD-23-132	166.14	169.88	1.36	01A-SW
ITDD-23-132	172.68	178.59	1.59	1
ITDD-23-133	150.20	154.79	1.20	1
ITDD-23-134	32.45	34.95	2.43	01C-SW
ITDD-23-134	135.63	137.16	0.50	01A-SW
ITDD-23-134	138.85	141.96	2.24	1
ITDD-23-135	111.38	112.27	0.13	1
ITDD-23-135	134.02	138.59	1.25	04-NE
ITDD-23-135	205.63	206.63	0.54	05-NE
ITDD-23-135	247.22	248.46	0.31	05B-NE
ITDD-23-136	75.02	75.76	0.43	1
ITDD-23-136	85.97	89.97	1.73	04-NE
ITDD-23-136	283.33	286.25	0.21	06-NE
ITDD-23-136	318.38	319.63	0.32	07-NE
ITDD-23-137	81.68	85.18	1.48	01C-SW
ITDD-23-137	182.18	187.28	0.98	01A-SW
ITDD-23-137	189.80	196.65	1.44	1
ITDD-23-137	207.90	208.90	1.53	01B-SW
ITDD-23-138	289.52	296.62	1.01	1
ITDD-23-140	27.30	30.62	0.84	1
ITDD-23-141	39.98	44.45	1.32	1
ITDD-23-141	47.25	51.61	0.63	04-NE
ITDD-23-142	36.36	40.36	1.37	02-NE
ITDD-23-142	40.36	41.36	1.50	02A-NE
ITDD-23-142	126.70	128.70	2.05	1
ITDD-23-144	94.46	99.42	1.85	04-NE
ITDD-23-139	304.00	315.16	1.63	1
ITDD-23-143	48.05	49.46	1.18	02-NE
ITDD-23-143	49.87	52.40	2.21	02A-NE
ITDD-23-143	156.45	158.76	0.71	1
ITDD-23-143	164.12	169.75	1.09	04-NE
ITDD-23-143	187.65	191.02	0.58	04C-NE
ITDD-23-143	231.53	233.40	0.64	05-NE
ITDD-23-143	251.16	251.77	0.94	05C-NE
ITDD-23-143	341.86	344.37	1.52	06-NE
ITDD-23-143	347.82	349.48	0.73	06A-NE
ITDD-23-143	359.64	361.75	0.42	06B-NE
ITDD-23-143	383.35	388.72	1.72	07-NE
ITDD-23-143	398.90	400.75	2.40	07A-NE
ITDD-23-145	290.15	302.05	1.39	1
ITDD-23-146	132.78	134.82	0.34	01A-SW
ITDD-23-146	142.88	147.88	1.29	1
ITDD-23-146	267.31	276.18	1.57	05-NE
ITDD-23-147	41.30	44.43	1.96	02-NE
ITDD-23-147	45.04	47.62	1.35	02A-NE
ITDD-23-147	138.02	140.27	1.11	1
ITDD-23-147	268.30	271.03	1.63	05-NE
ITDD-23-147	285.15	287.81	1.57	05C-NE
ITDD-23-147	307.66	310.36	2.16	05B-NE
ITDD-23-147	391.75	401.23	0.65	07-NE
ITDD-23-147	404.20	409.13	0.77	07A-NE
ITDD-23-147	430.72	436.67	2.01	08-NE
ITDD-23-147	448.24	449.52	1.54	08C-NE
ITDD-23-147	479.02	486.52	1.20	08A-NE
ITDD-23-148	60.55	61.40	1.07	04B-NE
ITDD-23-148	62.30	64.65	0.50	1
ITDD-23-148	73.61	77.87	1.17	04-NE
ITDD-23-148	257.50	260.54	3.18	06-NE
ITDD-23-148	262.83	266.60	1.39	06A-NE
ITDD-23-148	317.40	320.17	2.11	07-NE
ITDD-23-148	326.16	328.99	1.44	07A-NE
ITDD-23-149	46.51	48.45	1.52	01E-SW
ITDD-23-149	434.80	440.56	1.66	1
ITDD-23-150	123.60	129.60	1.74	01A-SW
ITDD-23-150	142.44	146.34	2.15	1
ITDD-23-150	293.11	301.75	1.45	05-NE
ITDD-23-151	8.66	10.35	0.68	01E-SW
ITDD-23-151	348.98	351.05	1.17	01D-SW
ITDD-23-151	411.87	421.66	1.84	1
ITDD-23-152	53.19	55.35	0.44	02-NE

Source: GE21 (2024).

Table 10-7: Bandeira 2022–2024 Diamond Drill Holes

holeid	from	to	Li2O_pct	Grade_shell
ITDD-23-085	73.40	74.47	0.67	SE-A
ITDD-23-086	69.92	72.11	1.48	02D-NE
ITDD-23-086	272.46	283.27	1.04	04-NE
ITDD-23-086	293.70	299.86	1.33	04C-NE
ITDD-23-087	53.24	69.96	1.19	SE-A
ITDD-23-088	83.32	86.32	0.96	02-NE
ITDD-23-088	199.94	210.19	1.28	04-NE
ITDD-23-088	272.46	274.62	2.21	05-NE
ITDD-23-088	287.18	287.96	0.74	05C-NE
ITDD-23-088	294.83	295.63	0.48	05B-NE
ITDD-23-089	63.26	72.02	1.37	SE-A
ITDD-23-089	155.53	161.53	1.22	08-NE
ITDD-23-090	161.74	169.95	1.03	03-NE
ITDD-23-090	253.07	263.50	0.98	02-NE
ITDD-23-090	386.98	389.98	1.62	1
ITDD-23-090	442.90	445.66	1.79	04-NE
ITDD-23-090	465.61	471.85	1.57	04C-NE
ITDD-23-090	564.45	567.45	1.56	06-NE
ITDD-23-090	580.60	581.60	0.57	07-NE
ITDD-23-091	62.26	63.07	0.95	01E-SW
ITDD-23-091	426.02	427.97	0.89	01D-SW
ITDD-23-091	479.83	489.24	1.04	1
ITDD-23-092	92.81	95.83	1.57	01A-SW
ITDD-23-092	103.81	109.42	1.23	1
ITDD-23-093	43.65	51.65	1.47	SE-A
ITDD-23-094	80.58	88.26	1.63	1
ITDD-23-095	46.35	48.48	0.70	02C-NE
ITDD-23-095	202.91	206.91	0.63	01A-SW
ITDD-23-095	216.19	223.07	1.38	1
ITDD-23-096	88.95	97.18	1.62	1
ITDD-23-097	38.70	44.12	1.48	1
ITDD-23-098	62.59	67.59	1.64	1
ITDD-23-098	194.04	196.69	1.02	05-NE
ITDD-23-099	63.04	65.04	1.91	01A-SW
ITDD-23-099	67.96	72.49	1.10	1
ITDD-23-100	27.85	28.85	0.35	1
ITDD-23-100	32.49	33.49	0.56	01B-SW
ITDD-23-101	76.74	81.74	1.55	1
ITDD-23-102	52.60	56.09	1.16	02C-NE
ITDD-23-102	202.45	204.35	0.99	01A-SW
ITDD-23-102	226.35	233.36	1.55	1
ITDD-23-103	197.00	200.00	1.33	1
ITDD-23-104	55.89	57.89	0.93	1
ITDD-23-104	58.89	59.89	1.45	01B-SW
ITDD-23-105	97.01	99.52	1.47	02C-NE
ITDD-23-105	110.73	116.40	1.49	02-NE
ITDD-23-105	214.09	215.79	0.96	01A-SW
ITDD-23-105	220.44	229.59	1.32	1
ITDD-23-105	370.38	375.38	1.24	05-NE
ITDD-23-106	133.08	135.23	0.95	01B-SW
ITDD-23-107	194.96	195.83	0.66	01A-SW
ITDD-23-107	197.74	199.94	1.37	1
ITDD-23-107	209.54	213.54	1.81	01B-SW
ITDD-23-108	75.26	81.81	1.46	1
ITDD-23-108	86.52	88.52	1.73	01B-SW
ITDD-23-109	120.09	127.08	1.28	1
ITDD-23-109	247.87	255.66	1.69	05-NE
ITDD-23-110	55.33	56.10	1.35	01A-SW
ITDD-23-110	58.58	62.84	2.15	1
ITDD-23-111	27.80	34.40	1.51	1
ITDD-23-113	97.33	99.89	1.75	1
ITDD-23-114	66.26	67.26	0.49	01A-SW
ITDD-23-114	72.40	77.06	0.97	1
ITDD-23-114	77.15	78.15	1.32	1
ITDD-23-115	34.08	41.00	1.26	1
ITDD-23-116	112.82	117.36	2.18	01A-SW
ITDD-23-116	132.12	134.17	0.91	1
ITDD-23-117	30.22	33.22	0.33	02-NE
ITDD-23-117	35.00	37.69	0.33	02A-NE
ITDD-23-117	143.90	145.00	2.81	01A-SW
ITDD-23-117	166.63	169.18	0.74	1
ITDD-23-118	155.35	156.56	1.76	01A-SW
ITDD-23-118	160.13	164.07	0.93	1
ITDD-23-120	109.66	115.92	1.24	01A-SW
ITDD-23-120	126.06	127.18	0.52	1
ITDD-23-120	253.93	259.63	1.86	05-NE
ITDD-23-112	124.79	131.18	1.74	1
ITDD-23-112	142.43	144.36	1.20	01B-SW
ITDD-23-119	118.90	119.42	0.31	01A-SW
ITDD-23-119	124.13	130.85	1.57	1
ITDD-23-121	34.85	40.85	0.57	02-NE
ITDD-23-121	44.12	46.12	0.33	02A-NE
ITDD-23-121	163.40	169.82	1.92	01A-SW
ITDD-23-121	182.04	183.59	2.59	1
ITDD-23-121	331.55	337.47	1.83	05-NE
ITDD-23-122	157.52	158.16	0.73	01A-SW
ITDD-23-122	164.11	168.11	1.49	1
ITDD-23-123	151.75	159.40	2.39	1
ITDD-23-123	285.88	286.88	1.40	05-NE
ITDD-23-124	80.04	81.04	0.99	1
ITDD-23-125	133.72	134.77	0.60	1
ITDD-23-125	144.94	147.97	1.43	01B-SW
ITDD-23-126	105.80	108.37	1.02	1
ITDD-23-127	81.91	82.66	1.11	1
ITDD-23-128	178.46	183.31	2.24	1
ITDD-23-129	153.61	155.00	0.83	01A-SW
ITDD-23-129	157.10	160.35	1.97	1
ITDD-23-130	88.49	91.08	1.15	1
ITDD-23-130	201.33	203.33	0.60	05-NE
ITDD-23-130	240.32	242.41	1.46	05B-NE
ITDD-23-131	99.48	101.48	1.98	1
ITDD-23-131	272.94	278.00	0.96	05-NE
ITDD-23-132	69.51	72.73	1.66	01C-SW
ITDD-23-132	166.14	169.88	1.36	01A-SW
ITDD-23-132	172.68	178.59	1.59	1
ITDD-23-133	150.20	154.79	1.20	1
ITDD-23-134	32.45	34.95	2.43	01C-SW
ITDD-23-134	135.63	137.16	0.50	01A-SW
ITDD-23-134	138.85	141.96	2.24	1
ITDD-23-135	111.38	112.27	0.13	1
ITDD-23-135	134.02	138.59	1.25	04-NE
ITDD-23-135	205.63	206.63	0.54	05-NE
ITDD-23-135	247.22	248.46	0.31	05B-NE
ITDD-23-136	75.02	75.76	0.43	1
ITDD-23-136	85.97	89.97	1.73	04-NE
ITDD-23-136	283.33	286.25	0.21	06-NE
ITDD-23-136	318.38	319.63	0.32	07-NE
ITDD-23-137	81.68	85.18	1.48	01C-SW
ITDD-23-137	182.18	187.28	0.98	01A-SW
ITDD-23-137	189.80	196.65	1.44	1
ITDD-23-137	207.90	208.90	1.53	01B-SW
ITDD-23-138	289.52	296.62	1.01	1
ITDD-23-140	27.30	30.62	0.84	1
ITDD-23-141	39.98	44.45	1.32	1
ITDD-23-141	47.25	51.61	0.63	04-NE
ITDD-23-142	36.36	40.36	1.37	02-NE
ITDD-23-142	40.36	41.36	1.50	02A-NE
ITDD-23-142	126.70	128.70	2.05	1
ITDD-23-144	94.46	99.42	1.85	04-NE
ITDD-23-139	304.00	315.16	1.63	1
ITDD-23-143	48.05	49.46	1.18	02-NE
ITDD-23-143	49.87	52.40	2.21	02A-NE
ITDD-23-143	156.45	158.76	0.71	1
ITDD-23-143	164.12	169.75	1.09	04-NE
ITDD-23-143	187.65	191.02	0.58	04C-NE
ITDD-23-143	231.53	233.40	0.64	05-NE
ITDD-23-143	251.16	251.77	0.94	05C-NE
ITDD-23-143	341.86	344.37	1.52	06-NE
ITDD-23-143	347.82	349.48	0.73	06A-NE
ITDD-23-143	359.64	361.75	0.42	06B-NE
ITDD-23-143	383.35	388.72	1.72	07-NE
ITDD-23-143	398.90	400.75	2.40	07A-NE
ITDD-23-145	290.15	302.05	1.39	1
ITDD-23-146	132.78	134.82	0.34	01A-SW
ITDD-23-146	142.88	147.88	1.29	1
ITDD-23-146	267.31	276.18	1.57	05-NE
ITDD-23-147	41.30	44.43	1.96	02-NE
ITDD-23-147	45.04	47.62	1.35	02A-NE
ITDD-23-147	138.02	140.27	1.11	1
ITDD-23-147	268.30	271.03	1.63	05-NE
ITDD-23-147	285.15	287.81	1.57	05C-NE
ITDD-23-147	307.66	310.36	2.16	05B-NE
ITDD-23-147	391.75	401.23	0.65	07-NE
ITDD-23-147	404.20	409.13	0.77	07A-NE
ITDD-23-147	430.72	436.67	2.01	08-NE
ITDD-23-147	448.24	449.52	1.54	08C-NE
ITDD-23-147	479.02	486.52	1.20	08A-NE
ITDD-23-148	60.55	61.40	1.07	04B-NE
ITDD-23-148	62.30	64.65	0.50	1
ITDD-23-148	73.61	77.87	1.17	04-NE
ITDD-23-148	257.50	260.54	3.18	06-NE
ITDD-23-148	262.83	266.60	1.39	06A-NE
ITDD-23-148	317.40	320.17	2.11	07-NE
ITDD-23-148	326.16	328.99	1.44	07A-NE
ITDD-23-149	46.51	48.45	1.52	01E-SW
ITDD-23-149	434.80	440.56	1.66	1
ITDD-23-150	123.60	129.60	1.74	01A-SW
ITDD-23-150	142.44	146.34	2.15	1
ITDD-23-150	293.11	301.75	1.45	05-NE
ITDD-23-151	8.66	10.35	0.68	01E-SW
ITDD-23-151	348.98	351.05	1.17	01D-SW
ITDD-23-151	411.87	421.66	1.84	1
ITDD-23-152	53.19	55.35	0.44	02-NE

Source: GE21 (2024).

Table 10-8: Mineralized Intercepts by Bandeira Drill Holes

holeid	from	to	Legth	Li2O %	Domain
ITDD-23-142	126.70	128.70	2.00	2.05	1
ITDD-23-144	82.50	82.98	0.48	2.34	1
ITDD-23-144	94.46	99.42	4.96	1.85	04-NE
ITDD-23-139	304.00	315.16	11.16	1.63	1
ITDD-23-143	48.05	49.46	1.41	1.18	02-NE
ITDD-23-143	49.87	52.40	2.53	2.21	02A-NE
ITDD-23-143	156.45	158.76	2.31	0.71	1
ITDD-23-143	164.12	167.19	3.07	1.34	04-NE
ITDD-23-143	168.75	169.75	1.00	1.43	04-NE
ITDD-23-143	187.65	188.03	0.38	2.99	04C-NE
ITDD-23-143	189.75	190.05	0.30	0.32	04C-NE
ITDD-23-143	190.45	191.02	0.57	0.65	04C-NE
ITDD-23-143	231.53	233.40	1.87	0.64	05-NE
ITDD-23-143	251.16	251.77	0.61	0.94	05C-NE
ITDD-23-143	341.86	344.37	2.51	1.52	06-NE
ITDD-23-143	347.82	349.48	1.66	0.73	06A-NE
ITDD-23-143	359.64	361.75	2.11	0.42	06B-NE
ITDD-23-143	383.35	384.95	1.60	1.79	07-NE
ITDD-23-143	385.37	388.72	3.35	1.89	07-NE
ITDD-23-143	398.90	400.75	1.85	2.40	07A-NE
ITDD-23-145	283.58	284.05	0.47	1.70	01A-SW
ITDD-23-145	290.15	290.59	0.44	2.33	1
ITDD-23-145	290.95	302.05	11.10	1.38	1
ITDD-23-146	132.78	134.82	2.04	0.34	01A-SW
ITDD-23-146	142.88	147.88	5.00	1.29	1
ITDD-23-146	267.31	276.18	8.87	1.57	05-NE
ITDD-23-147	41.30	44.43	3.13	1.96	02-NE
ITDD-23-147	45.04	47.62	2.58	1.35	02A-NE
ITDD-23-147	138.02	140.27	2.25	1.11	1
ITDD-23-147	268.30	271.03	2.73	1.63	05-NE
ITDD-23-147	285.15	287.81	2.66	1.57	05C-NE
ITDD-23-147	307.66	310.36	2.70	2.16	05B-NE
ITDD-23-147	391.75	392.34	0.59	1.87	07-NE
ITDD-23-147	393.84	395.03	1.19	0.75	07-NE
ITDD-23-147	395.79	396.24	0.45	0.47	07-NE
ITDD-23-147	396.66	398.68	2.02	1.30	07-NE
ITDD-23-147	399.92	401.23	1.31	0.63	07-NE
ITDD-23-147	404.20	405.27	1.07	1.00	07A-NE
ITDD-23-147	406.79	409.13	2.34	1.12	07A-NE
ITDD-23-147	430.72	436.67	5.95	2.01	08-NE
ITDD-23-147	479.02	480.29	1.27	1.25	08A-NE
ITDD-23-147	481.53	481.90	0.37	0.95	08A-NE
ITDD-23-147	483.52	486.52	3.00	2.13	08A-NE
ITDD-23-147	488.57	489.06	0.49	2.05	08B-NE
ITDD-23-148	60.55	61.40	0.85	1.07	04B-NE
ITDD-23-148	62.30	64.65	2.35	0.50	1
ITDD-23-148	73.61	77.87	4.26	1.17	04-NE
ITDD-23-148	257.50	260.54	3.04	3.18	06-NE
ITDD-23-148	262.83	266.60	3.77	1.39	06A-NE
ITDD-23-148	317.40	320.17	2.77	2.11	07-NE
ITDD-23-148	326.16	328.99	2.83	1.44	07A-NE
ITDD-23-149	46.51	48.45	1.94	1.52	01E-SW
ITDD-23-149	434.80	438.60	3.80	1.94	1
ITDD-23-149	439.41	440.56	1.15	1.61	1
ITDD-23-150	123.60	129.60	6.00	1.74	01A-SW
ITDD-23-150	142.44	146.34	3.90	2.15	1
ITDD-23-150	293.11	301.75	8.64	1.45	05-NE
ITDD-23-151	8.66	10.35	1.69	0.68	01E-SW
ITDD-23-151	348.98	351.05	2.07	1.17	01D-SW
ITDD-23-151	411.87	421.66	9.79	1.84	1
ITDD-23-152	53.19	55.35	2.16	0.44	02-NE
ITDD-23-152	56.15	58.31	2.16	1.29	02A-NE
ITDD-23-152	165.09	166.09	1.00	0.42	1
ITDD-23-152	183.78	185.86	2.08	0.30	04-NE
ITDD-23-152	250.73	252.51	1.78	0.92	05A-NE
ITDD-23-152	272.95	274.60	1.65	1.52	05-NE
ITDD-23-152	291.98	295.53	3.55	2.02	05B-NE
ITDD-23-154	108.52	113.42	4.90	1.57	1
ITDD-23-154	116.50	118.26	1.76	0.56	04-NE
ITDD-23-154	119.76	121.15	1.39	1.46	04-NE
ITDD-23-154	296.12	298.14	2.02	1.58	06-NE
ITDD-23-154	302.70	303.78	1.08	2.80	06A-NE
ITDD-23-154	305.07	306.29	1.22	2.38	06A-NE
ITDD-23-154	308.01	308.78	0.77	1.09	06A-NE
ITDD-23-154	310.17	310.99	0.82	0.77	06A-NE
ITDD-23-154	332.07	335.08	3.01	1.80	06B-NE
ITDD-23-154	336.32	337.38	1.06	0.68	06B-NE
ITDD-23-154	337.82	338.28	0.46	0.90	06B-NE
ITDD-23-154	359.89	361.12	1.23	2.19	07-NE
ITDD-23-154	361.50	363.56	2.06	1.89	07-NE
ITDD-23-154	369.23	370.37	1.14	1.24	07A-NE
ITDD-23-155	44.50	49.50	5.00	1.71	02-NE
ITDD-23-155	49.50	50.49	0.99	1.71	02A-NE
ITDD-23-155	149.36	151.36	2.00	1.67	1
ITDD-23-156	63.03	67.36	4.33	1.30	02A-NE
ITDD-23-156	209.37	211.94	2.57	0.90	04-NE
ITDD-23-156	213.86	218.63	4.77	2.02	04-NE
ITDD-23-156	290.10	292.08	1.98	0.94	05A-NE
ITDD-23-156	299.55	301.20	1.65	1.11	05-NE
ITDD-23-156	301.70	302.52	0.82	1.30	05-NE
ITDD-23-156	305.01	306.31	1.30	1.41	05-NE
ITDD-23-156	313.78	317.61	3.83	1.78	05B-NE
ITDD-23-157	78.37	79.17	0.80	0.77	02-NE
ITDD-23-157	87.20	89.20	2.00	0.93	02A-NE
ITDD-23-157	190.25	194.07	3.82	0.61	01A-SW
ITDD-23-157	203.54	205.60	2.06	1.78	1
ITDD-23-157	354.35	359.35	5.00	1.53	05-NE
ITDD-23-158	13.30	14.55	1.25	1.44	01E-SW
ITDD-23-158	393.02	396.02	3.00	1.09	01D-SW
ITDD-23-158	444.60	445.03	0.43	1.22	01A-SW
ITDD-23-158	445.93	446.80	0.87	0.86	01A-SW
ITDD-23-158	453.28	453.59	0.31	0.39	1
ITDD-23-158	453.97	455.14	1.17	2.92	1
ITDD-23-158	456.50	468.92	12.42	2.02	1
ITDD-23-160	66.94	67.50	0.56	0.50	1
ITDD-23-160	230.18	230.77	0.59	1.50	05-NE
ITDD-23-160	234.27	237.37	3.10	1.18	05-NE
ITDD-23-161	13.66	14.34	0.68	1.77	02-NE
ITDD-23-161	25.12	25.77	0.65	1.41	02A-NE
ITDD-23-161	129.12	133.12	4.00	1.27	1
ITDD-23-161	174.56	177.56	3.00	2.57	04C-NE
ITDD-23-161	313.74	315.43	1.69	2.10	06-NE
ITDD-23-161	322.93	324.22	1.29	0.95	06A-NE
ITDD-23-161	326.51	327.94	1.43	1.10	06A-NE
ITDD-23-161	351.41	354.37	2.96	1.16	06B-NE
ITDD-23-161	377.01	378.76	1.75	0.15	07-NE
ITDD-23-162	53.69	56.49	2.80	1.10	01E-SW
ITDD-23-162	395.57	398.57	3.00	1.56	01D-SW
ITDD-23-162	458.62	462.24	3.62	1.22	1
ITDD-23-163	204.32	206.32	2.00	0.87	02-NE
ITDD-23-163	245.30	245.81	0.51	0.20	02B-NE
ITDD-23-163	256.24	257.48	1.24	1.78	02E-NE
ITDD-23-163	298.22	299.76	1.54	0.66	1
ITDD-23-163	301.28	302.28	1.00	0.21	1
ITDD-23-163	348.35	349.35	1.00	0.14	04-NE
ITDD-23-163	354.35	359.42	5.07	0.72	04C-NE
ITDD-23-163	382.72	385.73	3.01	1.03	05A-NE
ITDD-23-163	387.92	389.09	1.17	1.51	05A-NE
ITDD-23-163	392.27	394.69	2.42	1.26	05A-NE
ITDD-23-163	395.05	397.65	2.60	0.96	05A-NE
ITDD-23-163	404.30	410.30	6.00	0.75	05-NE
ITDD-23-163	425.03	434.90	9.87	2.11	05B-NE
ITDD-23-163	469.10	473.67	4.57	1.75	06-NE
ITDD-23-163	474.65	477.57	2.92	1.79	06A-NE
ITDD-23-163	511.31	517.88	6.57	1.62	07-NE
ITDD-23-164	64.12	65.36	1.24	1.46	02C-NE
ITDD-23-164	80.29	83.39	3.10	1.22	02-NE
ITDD-23-164	87.48	100.06	12.58	1.50	02A-NE
ITDD-23-164	170.49	173.30	2.81	1.73	1
ITDD-23-164	325.78	326.42	0.64	1.82	05-NE
ITDD-23-164	328.68	333.75	5.07	0.74	05-NE
ITDD-23-164	415.18	417.35	2.17	0.86	07-NE
ITDD-23-164	418.75	419.65	0.90	0.54	07-NE
ITDD-23-164	424.78	427.02	2.24	0.84	07A-NE
ITDD-23-164	434.58	437.39	2.81	0.78	08-NE
ITDD-23-164	438.59	443.52	4.93	2.06	08-NE
ITDD-23-165	79.48	80.70	1.22	0.20	02C-NE
ITDD-23-165	100.21	101.21	1.00	0.35	02-NE
ITDD-23-165	195.00	202.00	7.00	2.08	1
ITDD-23-165	202.64	202.99	0.35	0.72	1
ITDD-23-165	338.94	342.77	3.83	1.42	05-NE
ITDD-23-166	89.68	90.72	1.04	1.58	05D-NE
ITDD-23-166	97.55	99.71	2.16	2.03	05-NE
ITDD-23-167	65.42	67.10	1.68	0.12	02C-NE
ITDD-23-167	228.46	229.56	1.10	0.81	01A-SW
ITDD-23-167	230.45	238.50	8.05	1.93	1
ITDD-23-167	345.55	351.27	5.72	1.86	05-NE
ITDD-23-168	88.20	88.79	0.59	1.07	05D-NE
ITDD-23-168	116.69	120.59	3.90	0.88	05-NE
ITDD-23-169	32.29	33.27	0.98	1.71	02D-NE
ITDD-23-169	199.77	200.44	0.67	0.43	04B-NE
ITDD-23-169	214.79	215.79	1.00	0.53	1
ITDD-23-169	241.60	243.89	2.29	1.27	04-NE
ITDD-23-169	359.01	360.46	1.45	2.26	06-NE
ITDD-23-170	101.62	106.04	4.42	1.46	05-NE
ITDD-23-171	51.37	52.05	0.68	1.22	1
ITDD-23-171	52.69	54.96	2.27	0.64	1
ITDD-23-171	208.35	208.77	0.42	1.74	05D-NE
ITDD-23-171	222.89	228.56	5.67	1.95	05-NE
ITDD-23-172	15.84	16.93	1.09	1.89	02-NE
ITDD-23-172	26.83	27.74	0.91	1.11	02A-NE
ITDD-23-172	136.38	140.13	3.75	1.78	1
ITDD-23-172	180.94	185.33	4.39	1.58	04C-NE
ITDD-23-172	317.72	320.13	2.41	2.05	06-NE
ITDD-23-172	331.69	332.79	1.10	2.92	06A-NE
ITDD-23-172	350.08	352.13	2.05	0.52	06B-NE
ITDD-23-172	353.90	354.98	1.08	2.17	06B-NE
ITDD-23-172	368.65	368.95	0.30	1.89	07-NE
ITDD-23-172	369.88	371.88	2.00	1.84	07-NE
ITDD-23-173	122.48	129.13	6.65	1.50	05-NE
ITDD-23-174	55.70	57.78	2.08	0.74	02C-NE
ITDD-23-174	211.36	212.40	1.04	0.72	01A-SW
ITDD-23-174	213.11	214.99	1.88	2.09	1
ITDD-23-174	216.09	221.72	5.63	1.58	1
ITDD-23-174	342.54	346.82	4.28	1.65	05-NE

Source: GE21 (2024).

Table 10-9: Mineralized Intercepts by Bandeira Drill Holes

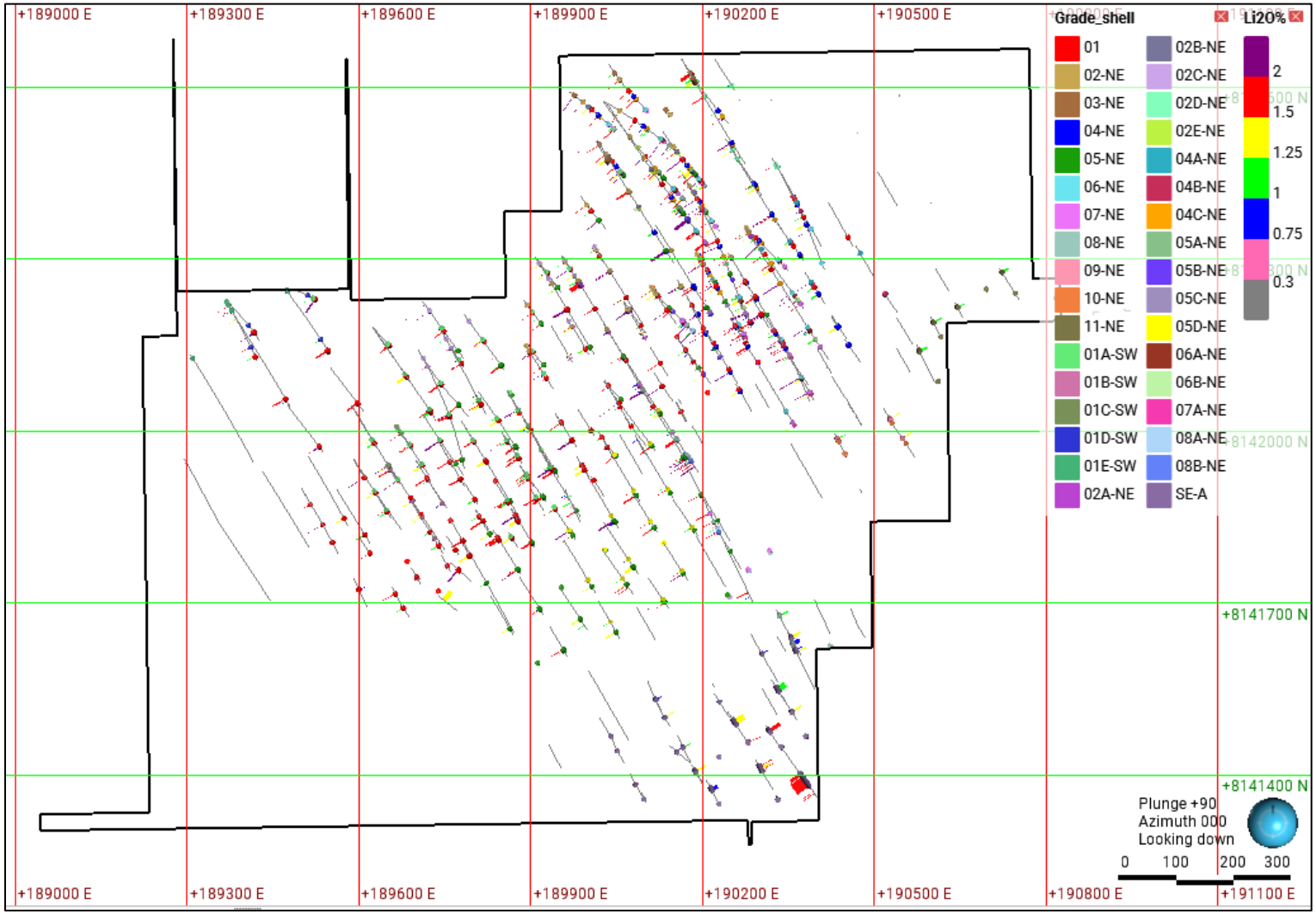
holeid	from	to	Li2O_pct	Grade_shell
ITDD-23-152	56.15	58.31	1.29	02A-NE
ITDD-23-152	165.09	166.09	0.77	1
ITDD-23-152	183.78	186.86	0.65	04-NE
ITDD-23-152	250.73	252.51	0.92	05A-NE
ITDD-23-152	272.95	274.60	1.52	05-NE
ITDD-23-152	291.98	295.53	2.02	05B-NE
ITDD-23-154	108.52	113.42	1.57	1
ITDD-23-154	116.50	121.15	0.71	04-NE
ITDD-23-154	296.12	298.14	1.58	06-NE
ITDD-23-154	302.70	310.99	0.97	06A-NE
ITDD-23-154	332.07	338.28	1.13	06B-NE
ITDD-23-154	359.89	363.56	1.82	07-NE
ITDD-23-154	369.23	370.37	1.24	07A-NE
ITDD-23-155	44.50	49.50	1.65	02-NE
ITDD-23-155	49.50	50.49	2.03	02A-NE
ITDD-23-155	149.36	151.36	1.67	1
ITDD-23-156	61.03	62.03	0.11	02-NE
ITDD-23-156	63.03	67.36	1.30	02A-NE
ITDD-23-156	209.37	218.63	1.36	04-NE
ITDD-23-156	290.10	292.08	0.94	05A-NE
ITDD-23-156	299.55	306.31	0.76	05-NE
ITDD-23-156	313.78	317.61	1.78	05B-NE
ITDD-23-157	78.37	79.17	0.77	02-NE
ITDD-23-157	87.20	89.20	0.93	02A-NE
ITDD-23-157	190.25	194.07	0.61	01A-SW
ITDD-23-157	203.54	205.60	1.78	1
ITDD-23-157	354.35	359.35	1.53	05-NE
ITDD-23-158	393.02	396.02	1.09	01D-SW
ITDD-23-158	444.60	446.80	0.68	01A-SW
ITDD-23-158	453.28	468.92	1.87	1
ITDD-23-160	66.94	67.50	0.50	1
ITDD-23-160	230.18	237.37	0.72	05-NE
ITDD-23-161	13.66	14.34	1.77	02-NE
ITDD-23-161	25.12	25.77	1.41	02A-NE
ITDD-23-161	129.12	133.12	1.27	1
ITDD-23-161	174.56	177.56	2.57	04C-NE
ITDD-23-161	313.74	315.43	2.10	06-NE
ITDD-23-161	322.93	327.94	0.61	06A-NE
ITDD-23-161	351.41	354.37	1.16	06B-NE
ITDD-23-161	377.01	378.76	0.16	07-NE
ITDD-23-162	53.69	56.49	1.10	01E-SW
ITDD-23-162	395.57	398.57	1.56	01D-SW
ITDD-23-162	458.62	462.24	1.22	1
ITDD-23-163	204.32	206.32	0.87	02-NE
ITDD-23-163	244.30	247.81	0.26	02B-NE
ITDD-23-163	256.24	257.48	1.78	02E-NE
ITDD-23-163	298.22	302.28	0.53	1
ITDD-23-163	348.35	349.35	0.54	04-NE
ITDD-23-163	354.35	359.42	0.72	04C-NE
ITDD-23-163	382.72	397.65	0.78	05A-NE
ITDD-23-163	404.30	410.30	0.75	05-NE
ITDD-23-163	425.03	434.90	2.11	05B-NE
ITDD-23-163	469.10	473.67	1.75	06-NE
ITDD-23-163	474.65	477.57	1.79	06A-NE
ITDD-23-163	511.31	517.88	1.62	07-NE
ITDD-23-164	64.12	65.36	2.61	02C-NE
ITDD-23-164	80.29	83.39	1.22	02-NE
ITDD-23-164	87.48	100.06	1.50	02A-NE
ITDD-23-164	170.48	173.30	1.73	1
ITDD-23-164	325.78	333.75	0.67	05-NE
ITDD-23-164	415.18	419.65	0.76	07-NE
ITDD-23-164	424.78	427.02	0.84	07A-NE
ITDD-23-164	434.58	443.52	1.40	08-NE
ITDD-23-165	79.48	80.70	0.20	02C-NE
ITDD-23-165	100.21	101.21	1.48	02-NE
ITDD-23-165	195.00	202.99	1.88	1
ITDD-23-165	338.94	342.77	1.42	05-NE
ITDD-23-166	89.68	90.72	1.58	05D-NE
ITDD-23-166	97.55	99.71	2.03	05-NE
ITDD-23-167	65.42	67.10	0.12	02C-NE
ITDD-23-167	228.46	229.56	0.81	01A-SW
ITDD-23-167	230.45	238.50	1.93	1
ITDD-23-167	345.55	351.27	1.86	05-NE
ITDD-23-168	88.20	88.79	1.07	05D-NE
ITDD-23-168	116.69	120.59	0.88	05-NE
ITDD-23-169	32.29	33.27	1.71	02D-NE
ITDD-23-169	199.77	200.44	0.43	04B-NE
ITDD-23-169	214.79	215.79	0.87	1
ITDD-23-169	241.60	243.89	1.27	04-NE
ITDD-23-169	359.01	360.46	2.26	06-NE
ITDD-23-170	101.62	106.04	1.46	05-NE
ITDD-23-171	51.37	54.96	0.77	1
ITDD-23-171	222.83	228.56	1.95	05-NE
ITDD-23-172	15.84	16.93	1.89	02-NE
ITDD-23-172	26.83	27.74	1.11	02A-NE
ITDD-23-172	136.38	140.13	1.78	1
ITDD-23-172	180.94	185.33	1.58	04C-NE
ITDD-23-172	317.72	320.13	2.05	06-NE
ITDD-23-172	331.69	332.79	2.92	06A-NE
ITDD-23-172	350.08	354.98	0.79	06B-NE
ITDD-23-172	368.65	371.88	1.43	07-NE
ITDD-23-173	122.48	129.13	1.50	05-NE
ITDD-23-174	55.70	57.78	0.74	02C-NE
ITDD-23-174	211.36	212.40	0.72	01A-SW
ITDD-23-174	213.11	221.72	1.55	1
ITDD-23-174	342.54	346.82	1.65	05-NE
ITDD-23-175	214.57	216.50	0.58	02-NE
ITDD-23-175	275.37	276.40	0.48	02E-NE
ITDD-23-175	323.64	325.56	1.85	1
ITDD-23-175	383.34	385.19	1.02	04C-NE
ITDD-23-175	398.59	407.49	1.34	05A-NE
ITDD-23-175	479.11	480.55	0.60	06-NE
ITDD-23-175	484.82	492.19	1.80	06A-NE
ITDD-23-175	502.82	503.65	1.52	07-NE
ITDD-23-175	524.36	529.94	1.11	08-NE
ITDD-23-176	56.11	61.88	1.00	1
ITDD-23-176	221.74	223.08	0.91	05D-NE
ITDD-23-176	230.14	235.14	1.57	05-NE
ITDD-23-177	77.86	80.86	0.20	02C-NE
ITDD-23-177	110.89	113.89	1.12	02-NE
ITDD-23-177	199.14	200.30	1.03	01A-SW
ITDD-23-177	204.16	209.98	2.18	1
ITDD-23-177	354.96	363.55	1.02	05-NE
ITDD-23-178	171.00	173.18	0.67	1
ITDD-23-180	171.59	177.38	1.78	02-NE
ITDD-23-180	264.35	269.85	1.15	1
ITDD-23-180	390.61	401.35	1.85	05-NE
ITDD-23-181	203.14	205.32	1.26	01A-SW
ITDD-23-181	223.00	229.00	1.02	1
ITDD-23-182	30.47	31.47	0.40	02D-NE
ITDD-23-182	151.73	152.75	0.47	04A-NE
ITDD-23-182	181.36	182.40	0.77	04B-NE
ITDD-23-182	201.09	202.74	1.21	1
ITDD-23-182	226.06	231.25	1.32	04-NE
ITDD-23-182	358.81	359.69	0.35	06-NE
ITDD-23-183	177.37	178.64	3.40	1
ITDD-23-184	21.01	22.05	0.56	02-NE
ITDD-23-184	156.12	159.73	1.03	1
ITDD-23-184	188.74	189.51	0.87	04-NE
ITDD-23-184	201.67	210.57	1.28	04C-NE
ITDD-23-184	337.76	341.69	1.20	06-NE
ITDD-23-184	348.01	349.42	1.94	06A-NE
ITDD-23-184	384.79	387.52	0.75	07-NE
ITDD-23-185	240.77	244.06	1.84	02-NE
ITDD-23-185	360.36	365.03	1.54	1
ITDD-23-185	417.41	420.23	0.98	04-NE
ITDD-23-185	434.34	437.34	1.22	04C-NE
ITDD-23-185	443.78	447.25	1.10	05A-NE
ITDD-23-185	520.91	521.41	0.04	06-NE
ITDD-23-185	529.52	531.92	3.57	06A-NE
ITDD-23-185	539.78	540.32	0.59	07-NE
ITDD-23-185	567.15	569.57	2.00	08-NE
ITDD-23-186	16.90	17.95	0.32	01E-SW
ITDD-23-187	196.58	198.86	1.85	1
ITDD-23-189	70.07	72.93	0.97	1
ITDD-23-191	53.51	58.65	1.71	1
ITDD-23-188	130.48	139.59	2.45	03-NE
ITDD-23-188	272.46	275.86	2.07	02-NE
ITDD-23-188	347.55	356.50	1.30	02B-NE
ITDD-23-188	391.25	394.86	0.77	1
ITDD-23-188	461.28	471.60	1.17	04-NE
ITDD-23-188	483.13	485.78	0.39	04C-NE
ITDD-23-188	581.89	584.23	0.17	06-NE
ITDD-23-188	631.34	643.24	1.61	08-NE
ITDD-23-192	49.72	50.72	0.29	02C-NE
ITDD-23-192	196.40	202.91	1.40	01A-SW
ITDD-23-192	210.10	210.75	1.46	1
ITDD-23-192	346.48	355.84	1.50	05-NE
ITDD-23-193	48.07	49.34	0.47	10-NE
ITDD-23-193	65.08	68.85	1.39	09-NE
ITDD-23-194	96.22	96.94	1.02	05D-NE
ITDD-23-194	114.65	119.50	1.15	05-NE
ITDD-23-195	80.91	86.51	0.86	1
ITDD-23-196	110.73	113.82	0.93	05D-NE
ITDD-23-196	137.13	146.05	1.42	05-NE
ITDD-23-197	94.36	95.84	0.57	1
ITDD-23-197	97.91	102.40	1.76	04-NE
ITDD-23-198	67.98	71.67	0.91	10-NE
ITDD-23-198	93.91	99.94	1.26	06-NE
ITDD-23-200	69.11	72.49	1.06	05-NE
ITDD-23-202	85.10	87.62	1.78	1
ITDD-23-202	252.08	253.19	1.20	05D-NE
ITDD-23-202	258.82	262.81	1.83	05-NE
ITDD-23-209	41.61	51.61	1.21	SE-A
ITDD-23-199	127.38	129.42	2.03	02C-NE

Source: GE21 (2024).

Table 10-10: Mineralized Intercepts by Bandeira Drill Holes

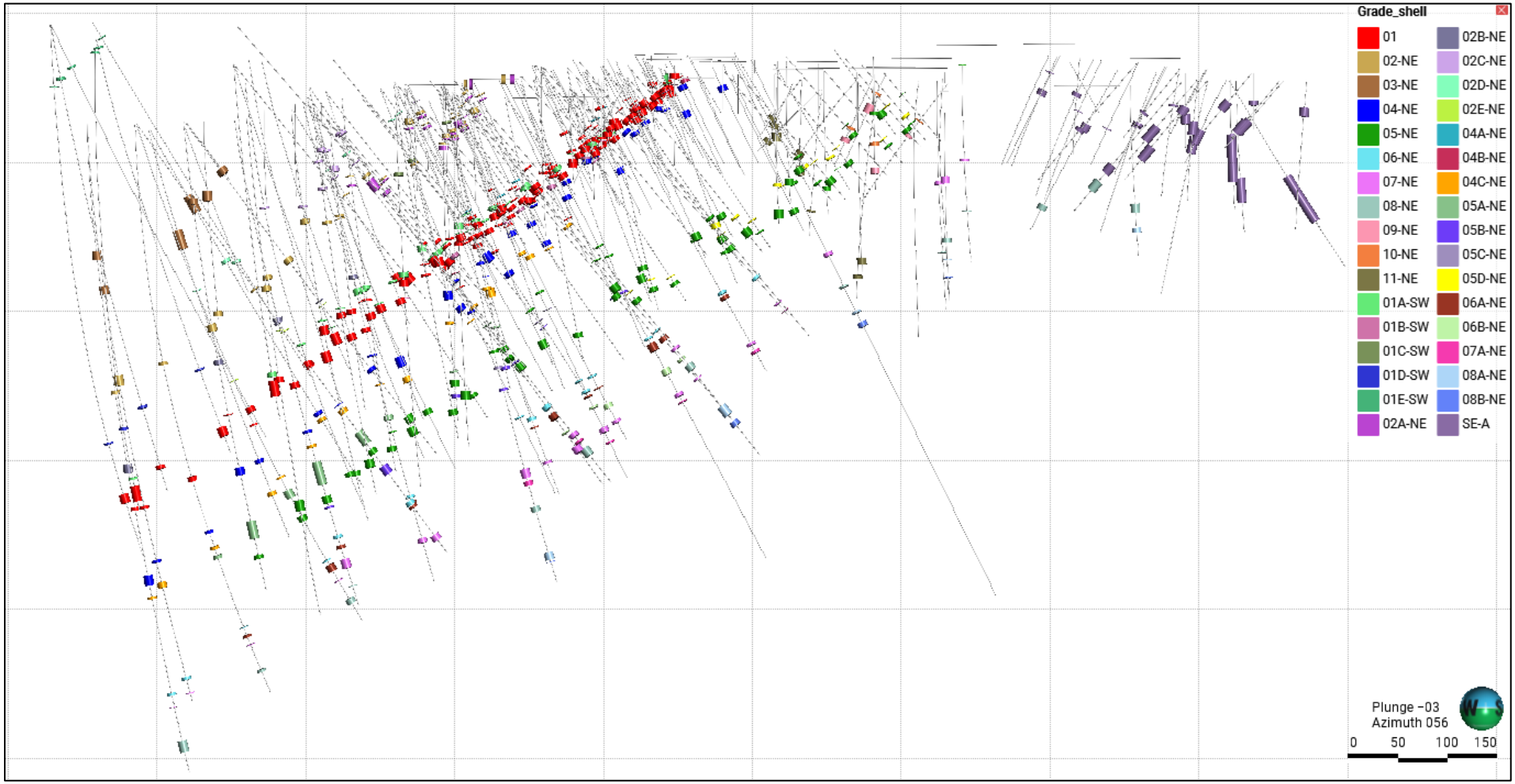
holeid	from	to	Li2O_pct	Grade_shell
ITDD-23-199	270.33	272.10	0.93	01A-SW
ITDD-23-199	288.91	294.47	1.59	1
ITDD-23-199	408.52	413.16	0.74	05-NE
ITDD-23-211	16.51	18.46	0.77	1
ITDD-23-211	197.53	198.63	1.54	05D-NE
ITDD-23-211	211.54	212.82	0.40	05-NE
ITDD-23-212	110.38	112.78	1.21	05D-NE
ITDD-23-212	124.48	124.98	0.71	05-NE
ITDD-23-213	54.87	103.98	1.26	SE-A
ITDD-23-218	56.17	72.40	1.65	SE-A
ITDD-23-215	37.48	43.52	1.36	1
ITDD-23-215	187.71	189.90	0.40	05D-NE
ITDD-23-215	203.86	212.54	1.78	05-NE
ITDD-23-216	55.24	60.12	1.54	01A-SW
ITDD-23-216	65.36	70.42	1.13	1
ITDD-23-216	197.59	206.18	1.59	05-NE
ITDD-23-219	56.49	62.54	0.85	01A-SW
ITDD-23-219	67.05	69.31	0.53	1
ITDD-23-219	197.86	200.53	1.62	05-NE
ITDD-23-220	66.48	69.48	0.70	05D-NE
ITDD-23-220	76.92	78.00	1.60	05-NE
ITDD-23-222	57.30	63.57	1.22	1
ITDD-23-222	197.78	202.62	1.45	05-NE
ITDD-23-223	64.00	64.70	1.20	05D-NE
ITDD-23-223	94.04	98.19	1.49	05-NE
ITDD-23-221	113.37	163.37	1.72	SE-A
ITDD-23-221	163.37	167.10	1.79	SE-A
ITDD-23-224	28.43	34.32	1.96	1
ITDD-23-224	166.46	172.45	1.73	05-NE
ITDD-23-225	78.99	85.97	0.85	05-NE
ITDD-23-226	35.27	42.50	2.12	1
ITDD-23-226	171.61	179.57	1.53	05-NE
ITDD-23-227	9.76	14.82	1.24	1
ITDD-23-227	149.37	154.62	2.19	05D-NE
ITDD-23-227	179.03	181.93	1.67	05-NE
ITDD-23-228	98.34	122.94	1.29	SE-A
ITDD-23-229	122.55	124.72	1.30	05-NE
ITDD-23-230	136.25	137.06	1.63	05D-NE
ITDD-23-230	161.98	167.49	1.65	05-NE
ITDD-23-210	139.91	142.91	1.79	05-NE
ITDD-23-210	219.57	223.51	1.98	07-NE
ITDD-23-210	256.99	259.01	1.75	08-NE
ITDD-23-210	276.43	278.98	0.65	08C-NE
ITDD-23-210	285.60	287.94	1.22	08A-NE
ITDD-23-210	298.00	302.98	0.83	08B-NE
ITDD-23-231	129.79	136.35	1.12	05-NE
ITDD-23-232	116.40	116.98	0.86	05D-NE
ITDD-23-232	138.70	145.95	1.35	05-NE
ITDD-23-233	125.59	129.17	0.58	05D-NE
ITDD-23-233	146.75	148.90	1.27	05-NE
ITDD-23-234	95.12	97.53	1.44	07-NE
ITDD-23-234	147.34	148.34	0.74	08-NE
ITDD-23-235	104.46	111.29	1.20	07-NE
ITDD-23-235	167.04	171.04	1.29	08-NE
ITDD-23-235	188.10	189.10	0.73	08A-NE
ITDD-23-235	206.29	207.29	0.32	08B-NE
ITDD-23-236	101.89	104.89	1.39	07-NE
ITDD-23-236	173.04	174.04	1.15	08-NE
ITDD-23-159	16.50	18.75	0.43	02-NE
ITDD-23-159	23.36	25.16	0.77	02A-NE
ITDD-23-159	115.78	117.32	0.42	1
ITDD-23-159	278.40	279.00	1.24	05D-NE
ITDD-23-159	287.50	292.65	0.98	05-NE
ITDD-23-159	350.16	353.08	0.89	07-NE
ITDD-23-159	372.21	379.28	1.78	08-NE
ITDD-23-159	413.39	415.32	0.46	08C-NE
ITDD-23-159	425.97	437.60	1.40	08A-NE
ITDD-23-159	445.38	450.94	1.52	08B-NE
ITDD-23-243	45.06	54.06	1.52	11-NE
ITDD-23-246	45.70	50.70	1.17	11-NE
ITDD-23-247	86.62	96.77	0.95	11-NE
ITDD-23-248	71.41	76.41	1.02	11-NE
ITDD-23-249	122.10	124.10	0.56	11-NE
ITDD-24-250	43.42	49.42	1.09	11-NE
ITDD-24-251	193.16	197.00	1.28	11-NE
ITDD-24-252	94.07	101.07	1.14	11-NE
ITDD-24-253	181.75	188.30	1.01	11-NE
ITDD-24-254	90.69	98.50	0.71	03-NE
ITDD-24-254	125.73	132.87	1.33	02D-NE
ITDD-24-254	190.25	191.25	0.15	02-NE
ITDD-24-255	143.39	143.93	0.86	02D-NE
ITDD-24-256	177.72	209.30	1.51	11-NE
ITDD-24-257	189.17	207.78	2.03	11-NE
ITDD-24-258	105.66	108.66	1.53	02C-NE
ITDD-24-258	116.44	122.44	1.34	02-NE
ITDD-24-259	146.95	178.95	1.26	11-NE
ITDD-24-261	148.31	158.33	1.38	1
ITDD-24-262	220.00	267.48	1.16	11-NE
ITDD-24-264	114.40	116.17	1.95	11-NE
ITDD-24-265	54.27	56.65	1.59	05-NE
ITDD-24-266	46.22	53.22	1.25	10-NE
ITDD-24-266	53.22	59.28	0.95	09-NE
ITDD-24-266	118.28	129.00	1.19	06-NE
ITDD-24-266	189.55	190.75	0.51	07-NE
ITDD-24-266	215.41	217.41	0.49	07A-NE
ITDD-24-267	35.48	39.00	0.97	05D-NE
ITDD-24-267	46.19	47.14	0.56	05-NE
ITDD-24-268	83.74	90.63	1.37	16-SW
ITDD-24-268	94.87	103.34	1.81	15-SW
ITDD-24-268	124.62	126.57	2.37	07-NE
ITDD-24-268	176.52	179.57	0.73	08-NE
ITDD-24-269	76.25	76.98	1.11	1
ITDD-24-269	88.72	93.47	2.28	04-NE
ITDD-24-270	70.65	77.32	2.11	16-SW
ITDD-24-270	110.03	122.03	1.09	15-SW
ITDD-24-270	142.75	146.48	2.01	07-NE
ITDD-24-271	70.38	73.38	0.89	07-NE
ITDD-24-272	67.38	70.00	1.62	1
ITDD-24-272	214.26	215.99	0.45	05B-NE
ITDD-24-273	51.58	52.80	0.66	07-NE
ITDD-24-273	141.71	143.52	0.60	08-NE
ITDD-24-274	169.03	170.03	1.10	05-NE
ITDD-24-274	185.82	189.61	0.59	05B-NE
ITDD-24-275	156.38	159.55	0.74	07-NE
ITDD-24-275	206.21	210.09	1.07	08-NE
ITDD-24-275	213.70	215.17	2.49	08C-NE
ITDD-24-276	35.00	85.00	1.37	09-NE
ITDD-24-276	85.00	99.70	1.49	09-NE
ITDD-24-276	182.00	183.00	2.23	07-NE
ITDD-24-276	189.38	192.03	0.37	07A-NE
ITDD-24-277	26.73	33.73	0.83	09-NE
ITDD-24-277	206.04	211.57	0.99	07-NE
ITDD-24-278	101.24	104.96	1.83	09A-NE
ITDD-24-279	94.92	99.46	0.81	09-NE
ITDD-24-279	133.82	135.45	0.46	09A-NE
ITDD-24-280	137.41	153.41	1.77	02-NE
ITDD-24-282	85.72	89.24	1.60	05-NE
ITDD-24-282	131.78	153.05	1.02	15-SW
ITDD-24-282	200.75	208.57	1.51	07-NE
ITDD-24-282	210.46	211.82	1.69	07A-NE
ITDD-24-282	250.50	252.56	0.50	08-NE
ITDD-24-282	264.64	269.20	1.79	08C-NE
ITDD-24-282	283.28	286.21	0.98	08A-NE
ITDD-24-283	105.10	119.94	1.72	09-NE
ITDD-24-283	146.03	149.28	1.35	07-NE
ITDD-24-283	193.34	200.02	0.62	08-NE
ITDD-24-283	218.85	221.33	1.08	08C-NE
ITDD-24-286	24.25	31.25	1.01	09-NE
ITDD-24-286	113.12	114.12	0.36	09A-NE
ITDD-24-285	115.78	119.50	0.81	07-NE
ITDD-24-285	157.87	171.87	1.54	08-NE
ITDD-24-289	77.14	81.80	0.93	05-NE
ITDD-24-289	148.13	152.61	0.57	15-SW
ITDD-24-290	108.26	110.26	0.96	07-NE
ITDD-24-290	159.87	160.85	0.35	08-NE
ITDD-24-290	176.45	183.45	1.72	08C-NE

Source: GE21 (2024).



Source: GE21 (2024).

Figure 10-2: Horizontal Projection of Bandeira Drill Holes with Mineralized Intercepts (Scale in Metres)



Source: GE21 (2024).

Figure 10-3: Oblique View of Drill Holes with Mineralized Intercepts (Scale in Metres)

10.10 Qualified Person's Comments

No significant drilling, sampling, or recovery factors would affect the outcome of the drilling results and the Mineral Resource estimate (Section 14).

In the QP's opinion, based on a review of all possible information, the drilling procedures put in place by MGLIT meet acceptable industry standards. The data can be and have been used for geological and resource modelling.

11 SAMPLE PREPARATION, ANALYSIS, AND SECURITY

11.1 Sampling

Samples are prepared from HQ (63.5 mm) and NQ (47.6 mm) diameter drill cores. The sampling procedures described in this section reflect MGLIT's current Standard Operating Procedures (SOP).

Sample intervals in the mineralized zones are defined based on one metre. Mineralized samples must have a minimum length of 1.00 m and a maximum length of 1.50 m. In some situations, samples shorter than 1.00 m can be selected; the SOP describes these situations in detail.

Outside the mineralized domains, the sampling definition is 1.50 m, and samples can range from 1.00 m to 3.00 m.

The visual indicators for sample interval definition include lithological contacts, mineral structures, and mineralization.

MGLIT's sample collection and sample definition procedures are:

- The drilling contractor team transports drill core from the drill rig to a drill-logging and sampling area one or more times per shift.
- The disposition and orientation of boxes are checked, and the depths are marked.
- Groups of three core boxes are photographed and logged.
- Sample intervals are marked on the core box.
- A line is drawn along the drill core at high angles to the foliation, to orient the saw cut before sampling. The right half of the core is selected as a sample, and the other half is retained for future reference.
- Sample tags are attached to the core box at the end of each sample.
- Sample bags are numbered before sampling.
- Sample tags are inserted in the bags only after samples are bagged.
- After the samples are tagged and bagged, they are weighed.
- The core is cut lengthwise along the core axis. A geologist defines the position of the cut, and a geology technician performs the cutting.
- For weathered material, a spatula or a machete is used to split the sample into two subsamples along the drilling direction.
- Fresh-rock cores are cut in half using a diamond saw and flushed with water between cuts.

After bagging, the samples are weighed, and the weight is registered; sample batches are assembled and sent to the laboratory. The standard batch size is 35 samples, consisting of 29 core samples and six QC samples.

11.2 Sample Preparation, Control, and Custody

A sample is selected and marked with a tag. After logging, it is inserted into the Project database. Cores are split in half using a diamond saw. Half of the core is left in the core box, while the other half is stored in plastic bags, accompanied by a printed sample tag, and sent to the lab.

SGS Geosol (SGS), an independent commercial laboratory, prepares and analyzes drill-core samples. The SGS facility has ISO 9001, ISO 14001, and ISO 17025 certifications. A parcel transport company delivers the sample shipment to the SGS facility in Vespasiano, Minas Gerais. Samples are in the custody and control of the transportation company representatives at all times until delivery to the laboratory, where samples are held in a secure enclosure until processing. Upon delivery, SGS sends a confirmation email with details of samples received. The chain of custody of each batch is carefully maintained from collection at the drill rig to delivery at the laboratory to prevent accidental contamination or mixing of samples, and to render active tampering as difficult as possible.

All samples received at SGS are inventoried and weighed before processing. Samples are dried at 105°C, crushed to 75% passing (P_{75}) a 3 mm sieve, homogenized, split (jones riffle splitter), and 250 g to 300 g of sample are pulverized in a steel mill to P_{95} 150 mesh.

11.3 Density Measurements

The density SOP “MGLIT” states that density measurements should be taken for every geochemical sample generated. When the drill-core quality does not allow for the density assay, this should be registered in the density sampling plan with a specified tag.

Density assay in the unsampled half-cores generally does not include drying or sample sealing.

For heterogeneous samples, three density assays were taken: one at the top, one in the middle, and one at the base of the sample. Homogenous samples were generated in only one density assay. All density data are stored in a database.

This list summarizes the procedures described in the density SOP:

- Sample selection and registration in the density plan
- Density samples must have a minimum length of 10 cm and a maximum of 25 cm
- Weighing the sample (PA)
- Weighing the sample submerged (PB)
- Density values are acquired from the formula D = PA / (PA – PB), where
  - D = density
  - PA = sample weight (in the air)
  - PB = sample weight (submerged in water).

11.4 Sample Preparation

All samples are inventoried and weighed before processing them. Samples are dried at 105°C, crushed to P_{75} <3 mm sieve, homogenized, split (Jones Riffle splitter), and pulverized (250 g to 300 g of sample) in a steel mill to P_{95} 150 mesh.

11.5 Sample Analysis

The chemical assays were performed using the ICP90A method, a multi-element analysis involving fusion with sodium peroxide (Na_2O_2) and inductively coupled plasma–optical emission spectroscopy (ICP-OES). If the lithium results exceeded 15,000 ppm, the samples were reanalyzed using the ICP90Q_Li method, which has higher detection limits.

All chemical analyses conducted by SGS are reported to MGLIT on PDF certificates, accompanied by an MS Excel digital file.

11.6 Quality Assurance and Quality Control

The implementation of the QA/QC program was proposed by the independent company, GE21. The sample batch composition includes six QC samples for every 29 regular samples. The QC composition of the batches comprises:

- Coarse (preparation) and fine (analytical) blanks: 5.7% of the batch or two blanks per batch—one of each type
- Standards: 5.7% of the batch or two standards per batch
- Crushed duplicates: 2.8% of the batch, or one sample per batch
- Pulverized duplicates: 2.8% of the batch, or one sample per batch.

Additionally, one sample is selected for the check assay procedure for every sample batch, representing 3% of the batch. Check samples are chosen from the pulverized material of a regular sample reserved by the primary laboratory. These samples are sent to a secondary laboratory, ALS Vancouver, British Columbia, Canada, monthly. ALS Vancouver is ISO 17025 accredited.

The same control-sample proportion criteria was respected on check assay batches: two standards, two blanks, and two duplicates. Particle-size analysis (PSA) is also performed on the check-assay samples. Figure 11-1 presents the batch-composition scheme for batches with mineralized samples or zones, and unmineralized batches. Figure 11-1 and Table 11-1 show the proportion of QC samples in the MGLIT geochemical database.

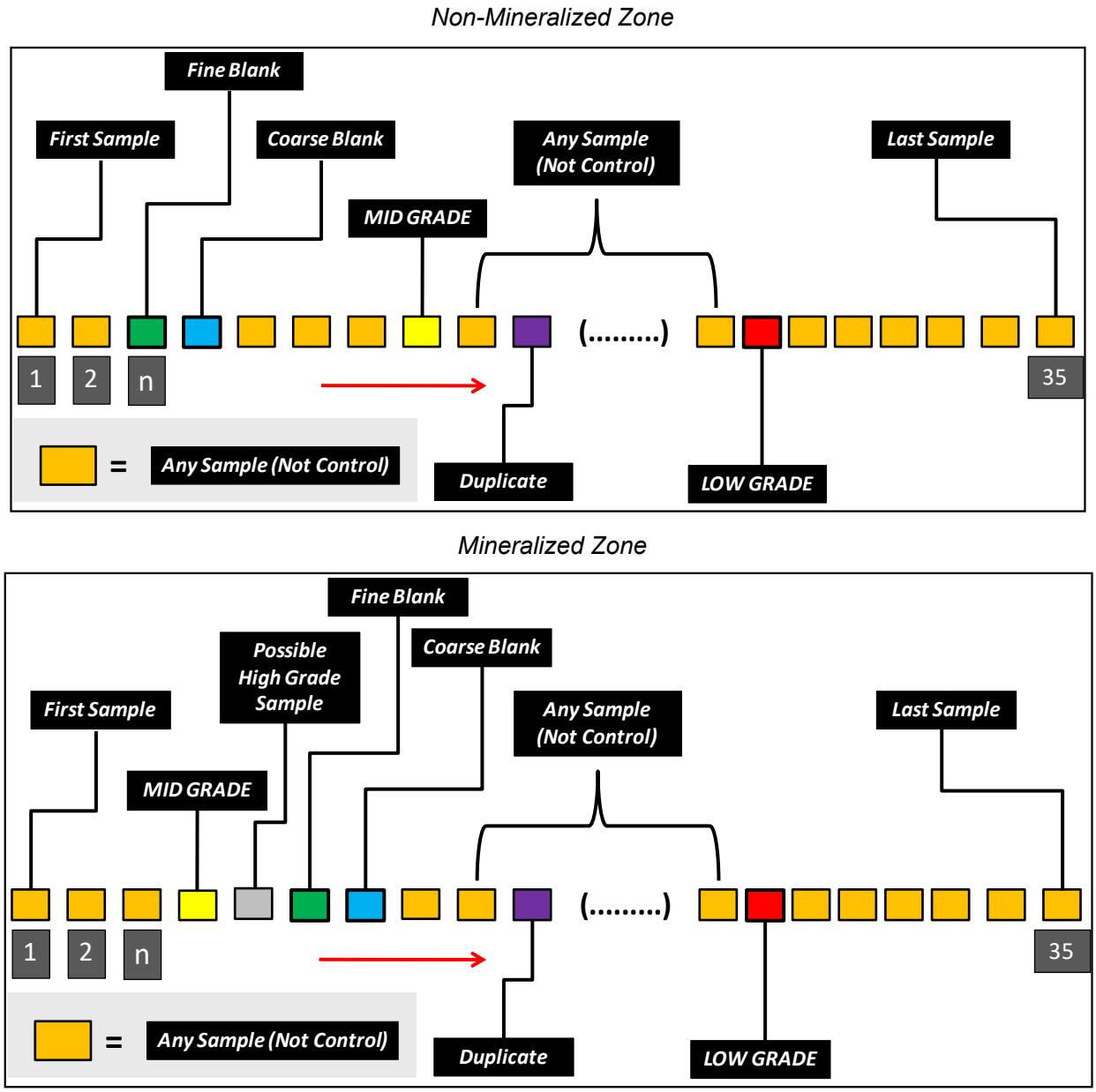


Figure 11-1: QA/QC Program

Table 11-1: QA/QC Program Summary

CRM/SRM	Crushed Duplicates	Pulverized Duplicates	Preparation Blanks	Analytical Blanks	Check Assay	Total QA/QC Samples	Total Database
649	321	319	326	326	72	1,941	12,385
5.2%	2.6%	2.6%	2.6%	2.6%	0.6%	15.7%	100%

Notes: CRM = certified reference material; SRM = standardized reference material.

11.6.1 Preparation Blank—Coarse Blank

Preparation blank samples are inserted in the sample batch before the physical preparation of the samples. This measure helps to track any contamination problems that might occur in the granulometric-reduction or sample-splitting process. Blank samples are inserted at the beginning of the possibly mineralized intervals, following the sequence:

- Mineralized sample
- Analytical/fine blank
- Preparation/coarse blank.

If an unmineralized batch is assembled, blank samples must be inserted at the beginning of the batch.

MGLIT uses a commercial blank, ITAK-QG-01, as its coarse blank material. More than 95% of the coarse blank samples are below the 5x detection limit threshold, indicating no major contamination. Figure 11-2 presents the preparation blank control chart for lithium.

Type of control	Blank
Reference	ITAK QG-01
Variable	Li ppm
Number of analysis	326

Blank code	ITAK-QG-01
Limit of Detection (LOD)	10.0
Upper limit (5 x LOD)	50.0
Reference Value (REF)	5.0
Standard deviation	11.642

Minimum	10.0
Maximum	129.0
Average	14.8
Median	10.0

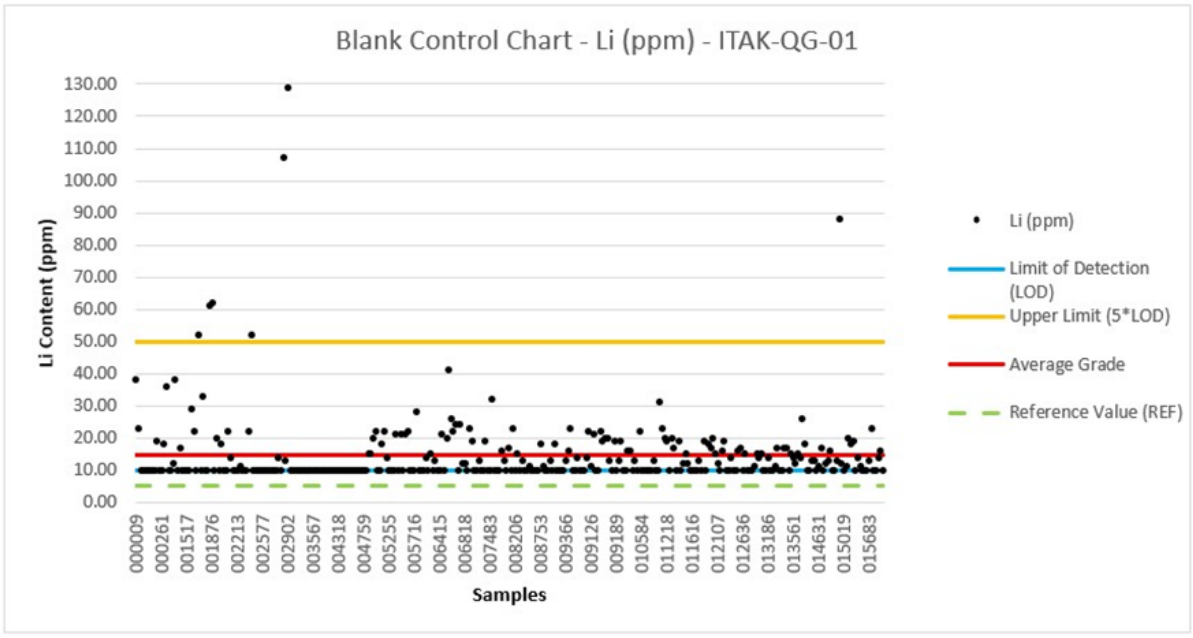


Figure 11-2: Blank Control Chart—ITAK QG-01

11.6.2 Analytical Blank—Fine Blank

Analytical or fine blank samples were inserted in the analytical batches after the samples' physical preparation. This control was used to assess potential contamination issues that might have occurred during the sample digestion or fusion processes and to evaluate any miscalibrations of the analytical equipment. Blank samples are inserted at the beginning of the possibly mineralized intervals, following the sequence:

1. Mineralized sample
2. Analytical/fine blank
3. Preparation/coarse blank.

If an unmineralized batch was assembled, blank samples must be inserted at the beginning of the batch.

MGLIT used three types of commercial Fine Blank controls: ITAK-QF-15, ITAK-QF-16 and ITAK-QF-18. No systematic contamination or calibration problems were indicated in the final stage of the geochemical analysis. Figure 11-3 to Figure 11-5 present the analytical blanks control charts for lithium.

Type of control	Blank
Reference	ITAK QF-15
Variable	Li ppm
Number of analysis	38

Blank code	ITAK-QF-15
Limit of Detection (LOD)	10.0
Upper limit (3 x LOD)	30.0
Reference Value (REF)	18.7
Standard deviation	13.096

Minimum	10.0
Maximum	62.0
Average	17.7
Median	12.0

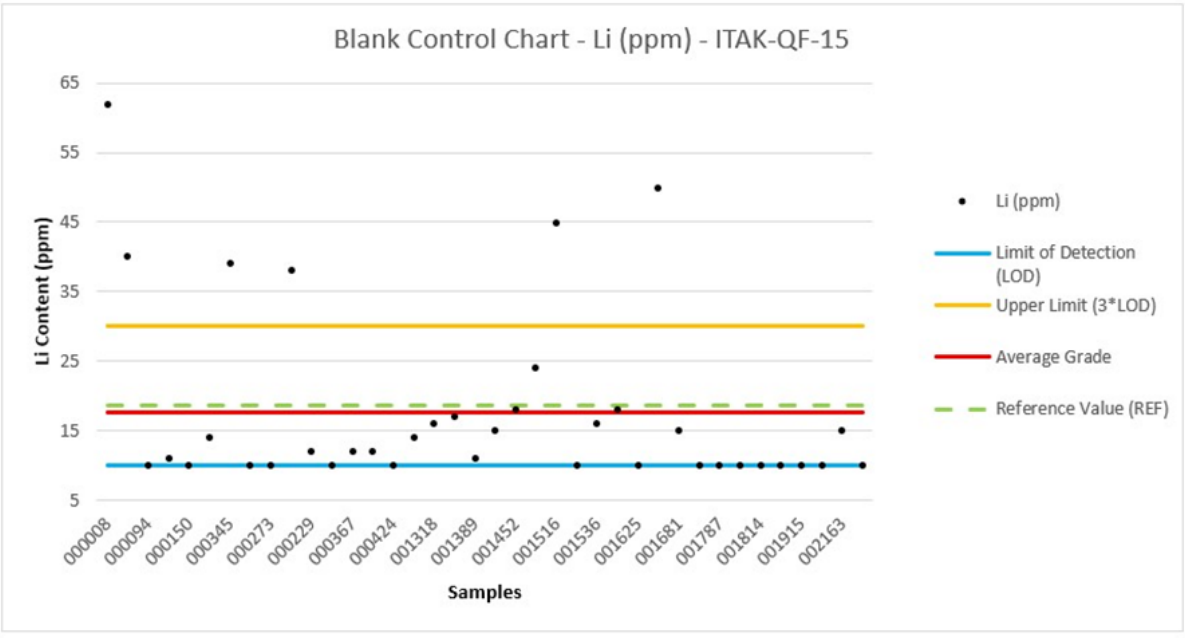


Figure 11-3: Blank Control Chart—ITAK QF-15

Type of control	Blank
Reference	ITAK QF-16
Variable	Li ppm
Number of analysis	229

Blank Code	ITAK-QF-16
Limit of Detection (LOD)	10.0
Upper limit (3 x LOD)	30.0
Reference Value (REF)	36.6
Standard deviation	5.889

Minimum	10.0
Maximum	74.0
Average	13.8
Median	12.0

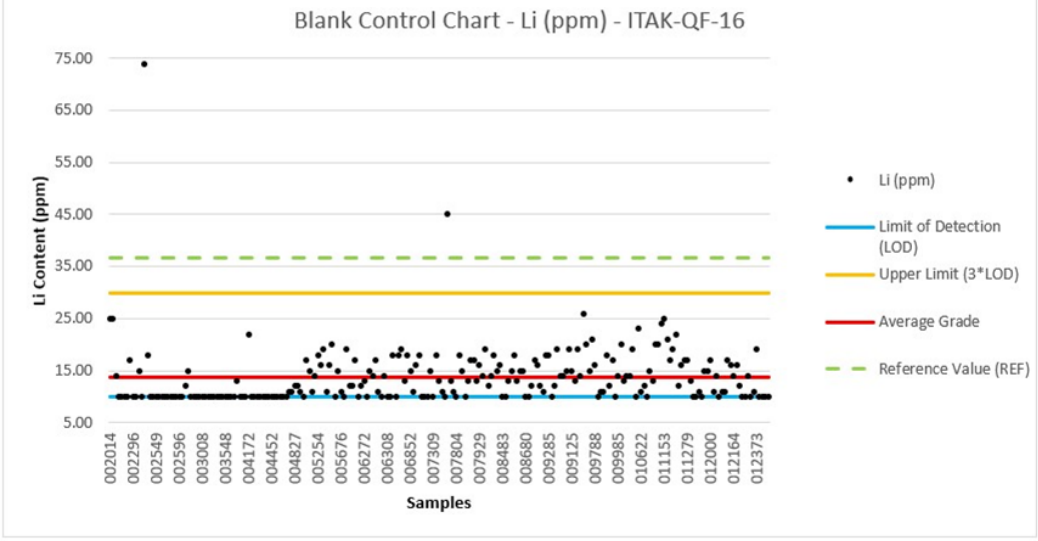


Figure 11-4: Blank Control Chart—ITAK QF-16

Type of control	Blank
Reference	ITAK QF-18
Variable	Li ppm
Number of analysis	59

Blank code	ITAK-QF-18
Limit of Detection (LOD)	10.0
Upper limit (3 x LOD)	30.0
Reference Value (REF)	18.3
Standard deviation	3.303

Minimum	10.0
Maximum	22.0
Average	12.1
Median	10.0

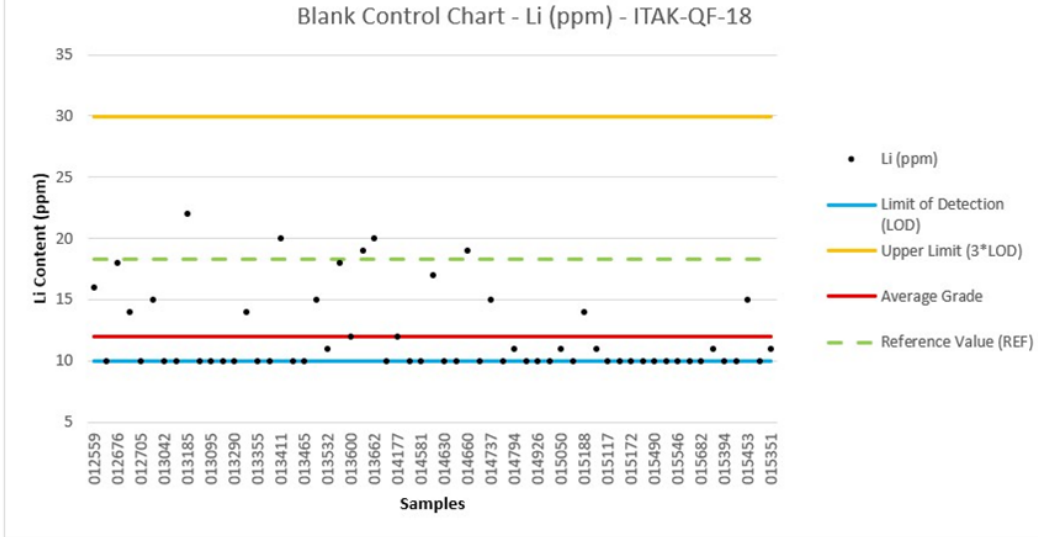


Figure 11-5: Blank Control Chart—ITAK QF-18

11.6.3 Certified or Standard Reference Material—CRM/SRM

Certified reference materials (CRM) or standard reference materials (SRM) are materials for which one or more parameters have been certified by a technically valid and recognized procedure. A certifying body has issued a certificate or other accurate documentation. These materials are used as QC samples to evaluate the accuracy of the analytical methods and procedures.

MGLIT uses four CRMs or SRMs: ITAK 1100, ITAK 1101, OREAS 750, and OREAS 752.

These reference materials evaluate high-, medium-, and low-grade assay results.

Medium-grade or high-grade reference materials are inserted at the beginning of the possible mineralized zones. The insertion can occur immediately or a few samples before the mineralized zone. The low-grade materials are inserted at the end of the zone where the geologist interprets mineralization. The insertion can be immediately after or a few samples after the mineralized zone. The order of the reference materials can be changed based on geological features or mineralization characteristics.

Figure 11-6 to Figure 11-9 present Lithium's CRM/SRM control charts. More than 80% of the samples are constrained within the two standard deviation limits.

Type of Control	CRM
Reference	ITAK-1100
Variable	Li (%)
Number of analysis	228

Code	ITAK-1100
Certificate Value	0.243
Standard Deviation	0.004
Upper limit (+2SD)	0.250
Lower limit (-2SD)	0.236

Minimum	0.226
Maximum	0.270
Average	0.248
Median	0.248
Bias	1.98%

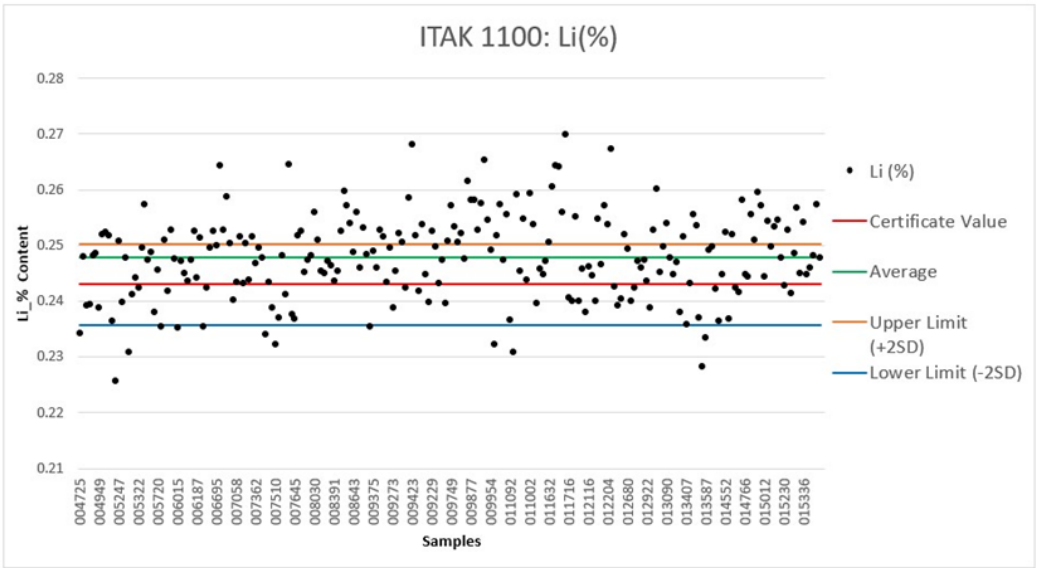


Figure 11-6: Standard Reference Material Chart—ITAK 1100

Type of Control	CRM
Reference	ITAK-1101
Variable	Li (%)
Number of analysis	223

Code	ITAK-1101
Certificate Value	0.671
Standard desviation	0.010
Upper limit (+2SD)	0.691
Lower limit (-2SD)	0.651

Minimum	0.644
Maximum	0.720
Average	0.685
Median	0.685
Bias	2.042%

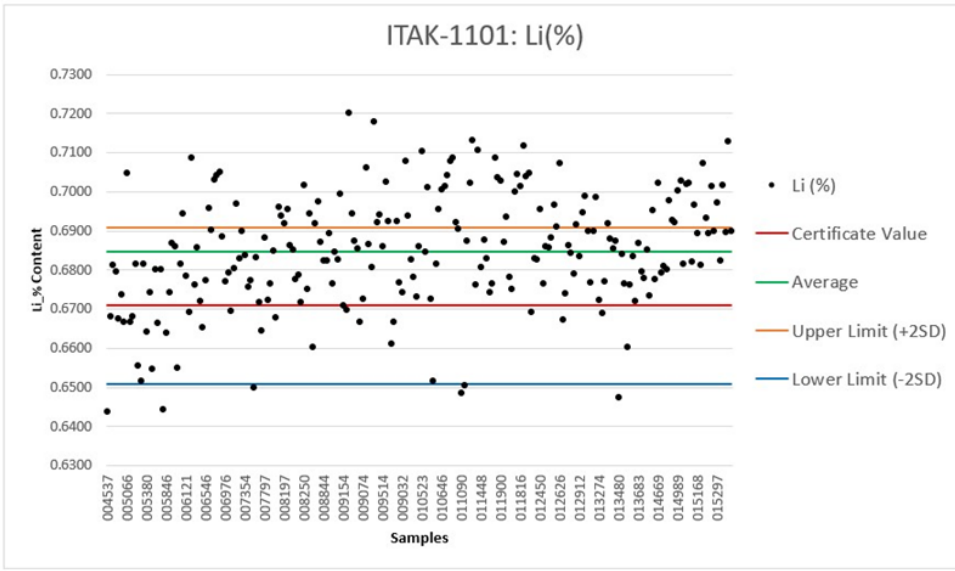


Figure 11-7: Standard Reference Material Chart—ITAK 1101

Type of Control	CRM
Reference	OREAS-750
Variable	Li (%)
Number of analysis	97

Code	OREAS-750
Certificate Value	0.230
Standard desviation	0.010
Upper limit (+2SD)	0.250
Lower limit (-2SD)	0.210

Minimum	0.209
Maximum	0.252
Average	0.228
Median	0.230
Bias	-0.674%

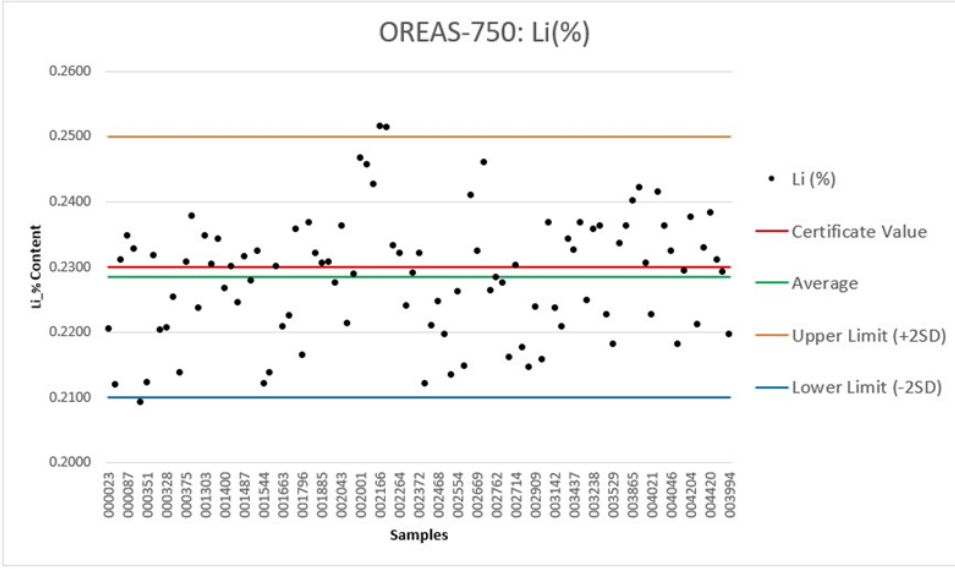


Figure 11-8: Standard Reference Material Chart—OREAS 750

Type of Control	CRM
Reference	OREAS-752
Variable	Li (%)
Number of analysis	101

Code	OREAS-752
Certificate Value	0.707
Standard desviation	0.010
Upper limit (+2SD)	0.727
Lower limit (-2SD)	0.687

Minimum	0.635
Maximum	0.739
Average	0.701
Median	0.702
Bias	-0.780%

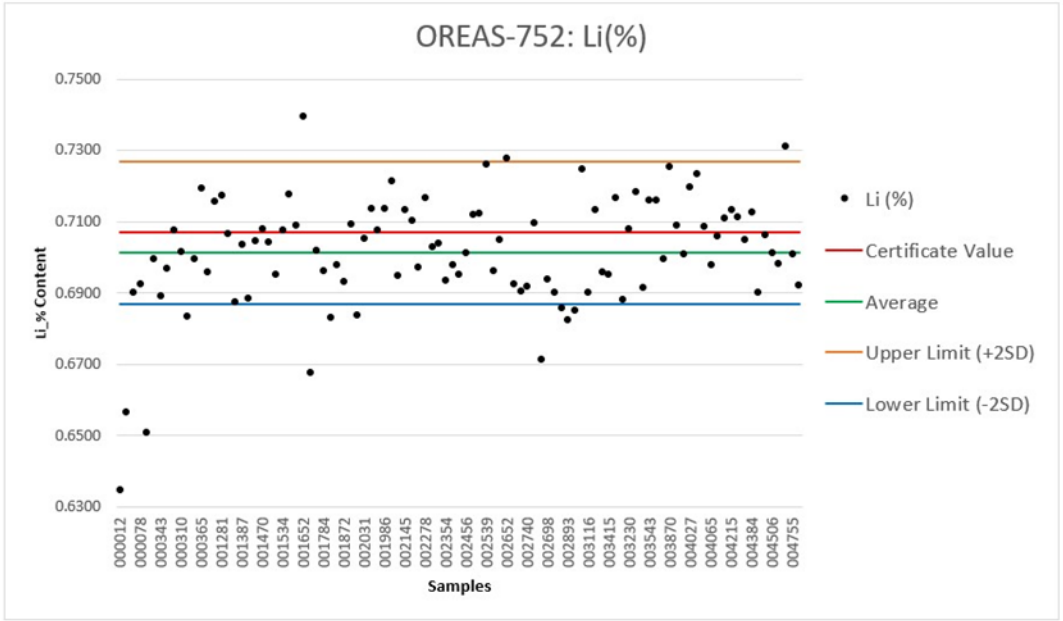


Figure 11-9: Standard Reference Material Chart—OREAS 752

11.6.4 Crushed Duplicates

Duplicates are used in the QC program to evaluate the precision of geochemical analysis. Insertion of blind duplicates of crushed material is used to test the laboratory's reproducibility and determine if the crushing process generates bias or imprecision in the results.

In all, 321 crushed duplicates were evaluated. Control charts for this control type show high correlations and good reproducibility, with over 90% of the samples falling below the 20% hard limit (Figure 11-10).

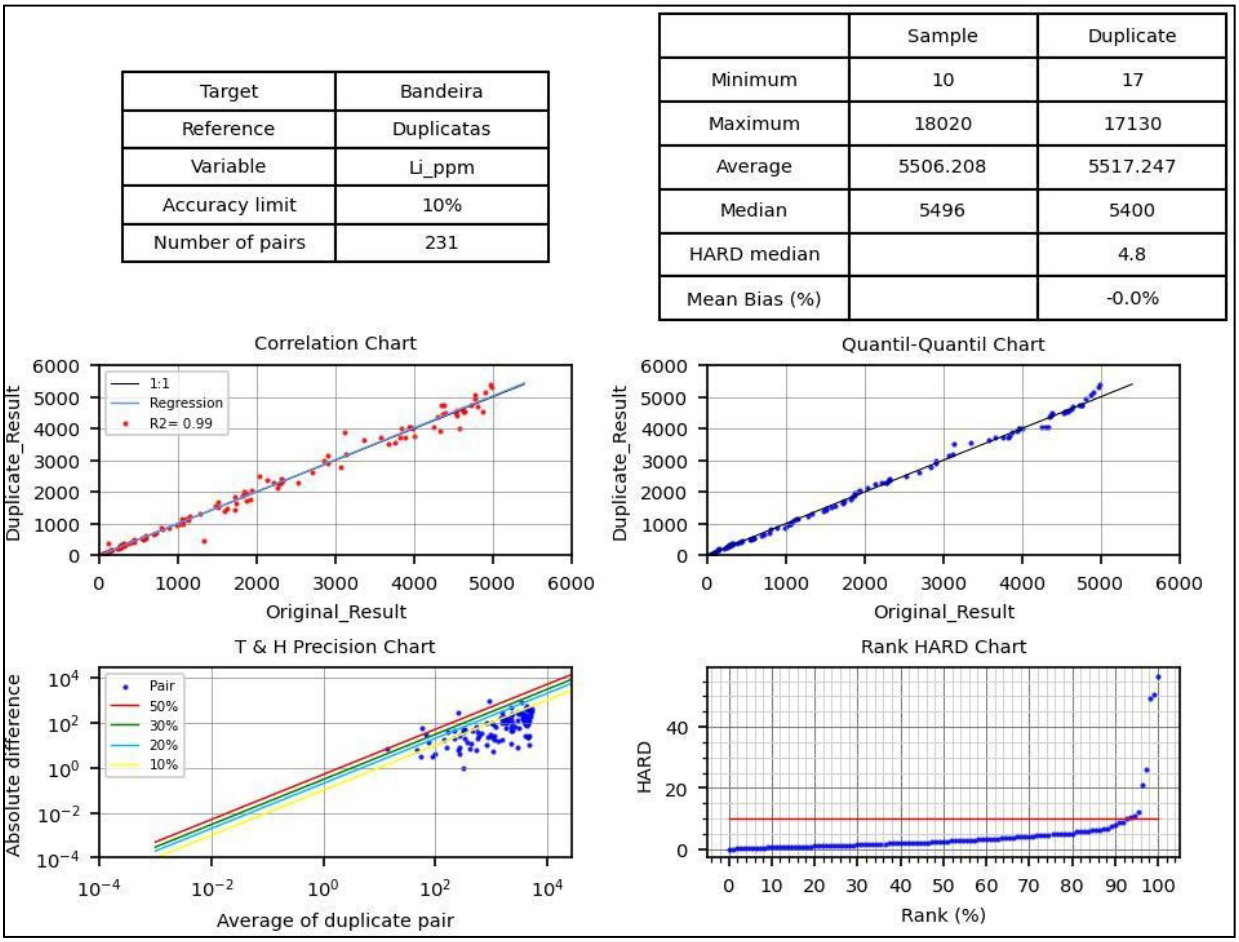


Figure 11-10: Crushed Duplicates Control

11.6.5 Pulverized Duplicates

Duplicates are used in the quality control program to evaluate the precision of the geochemical analysis. The insertion of blind duplicates of pulverized material is used to test the laboratory's reproducibility and determine if the milling process is not generating bias or imprecision in the results.

A total of 319 pulverized duplicates were evaluated. Control charts for this control type show high correlations and good reproducibility, with approximately 91% of the samples falling below the 5% HARD limit (Figure 11-11).

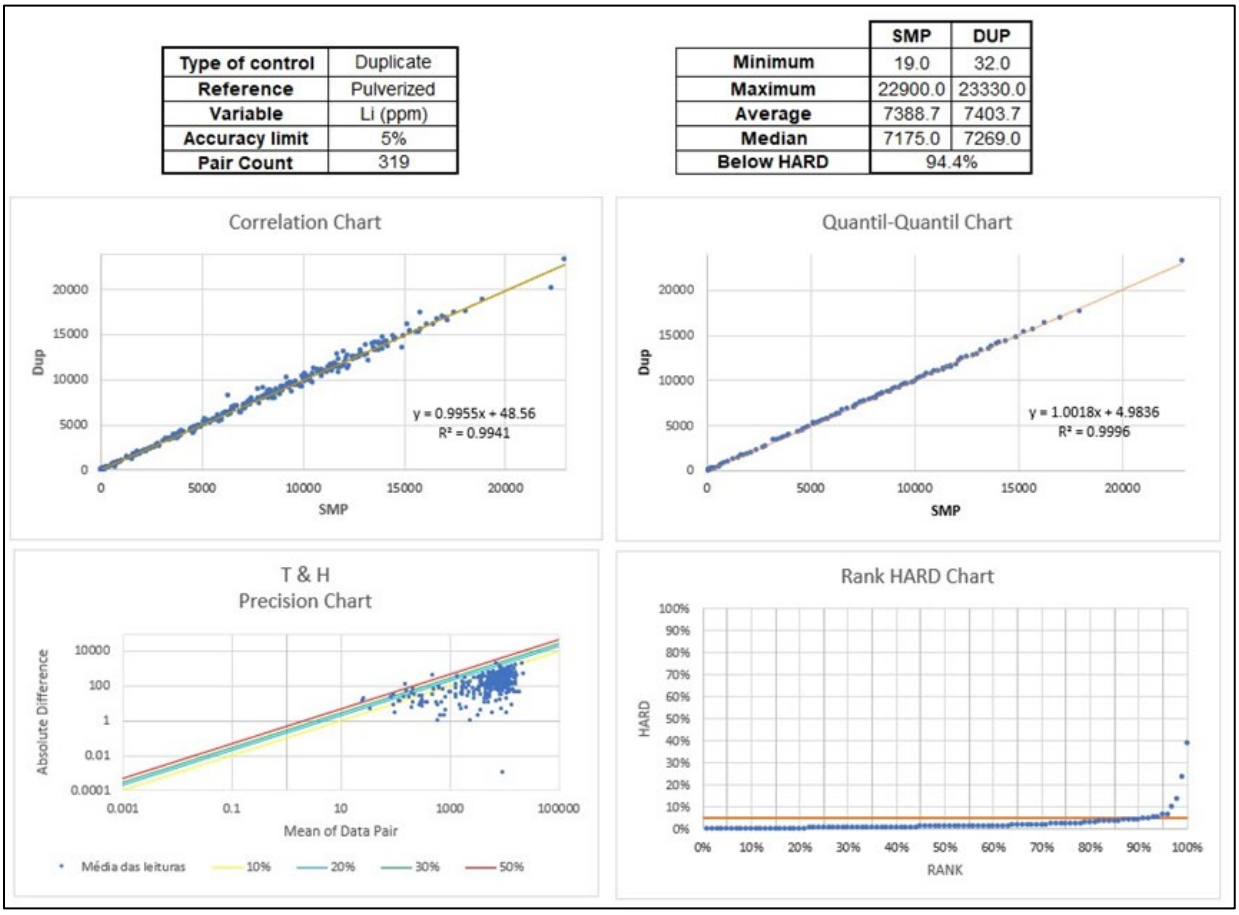
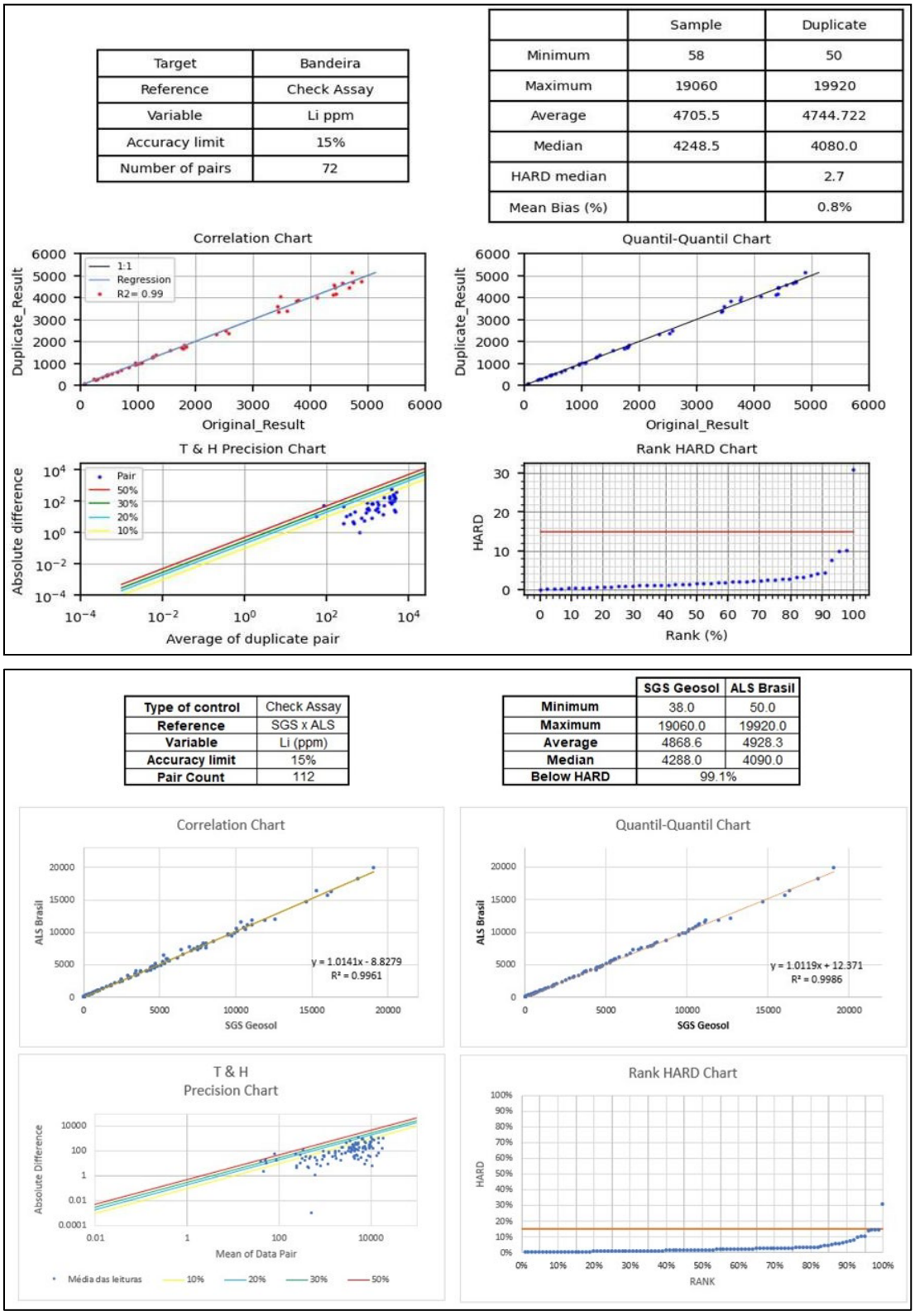


Figure 11-11: Pulverized Duplicates Control Chart

11.6.6 Check Assay

MGLIT has submitted check assay batches for analysis at the ALS Laboratory in Vancouver. This procedure is used to verify the reliability of the primary laboratory results by crosschecking them with a secondary reference laboratory. Check assay results are presented in Figure 11-12. Only one sample of 112 has returned a pair above the 15% HARD limit, representing 1.4% of the total check assays.



Target	Bandeira
Reference	Check Assay
Variable	Li ppm
Accuracy limit	15%
Number of pairs	72

	Sample	Duplicate
Minimum	58	50
Maximum	19060	19920
Average	4705.5	4744.722
Median	4248.5	4080.0
HARD median		2.7
Mean Bias (%)		0.8%

Type of control	Check Assay
Reference	SGS x ALS
Variable	Li (ppm)
Accuracy limit	15%
Pair Count	112

	SGS Geosol	ALS Brasil
Minimum	38.0	50.0
Maximum	19060.0	19920.0
Average	4868.6	4928.3
Median	4288.0	4090.0
Below HARD	99.1%	

Figure 11-12: Check the Assay Control Chart

11.7 Qualified Person's Opinion

The QP believes that the sampling, sample preparation, security, and analysis performed by MGLIT and hired companies are suitable for estimating Mineral Resources as part of the feasibility study. QA procedures follow industry best practices, and QC results are within industry standards, attesting to the quality of the database information.

12 DATA VERIFICATION

12.1 Qualified Person's Verification

GE21 independent QPs Mr. Carlos José Evangelista Silva and Mr. Leonardo Silva Santos Rocha have visited the Project in Araçuaí since 2023 to evaluate MGLIT's infrastructure, operational procedures, and the results of activities performed by MGLIT employees. Both QPs specialize in geological exploration and Mineral Resource estimation.

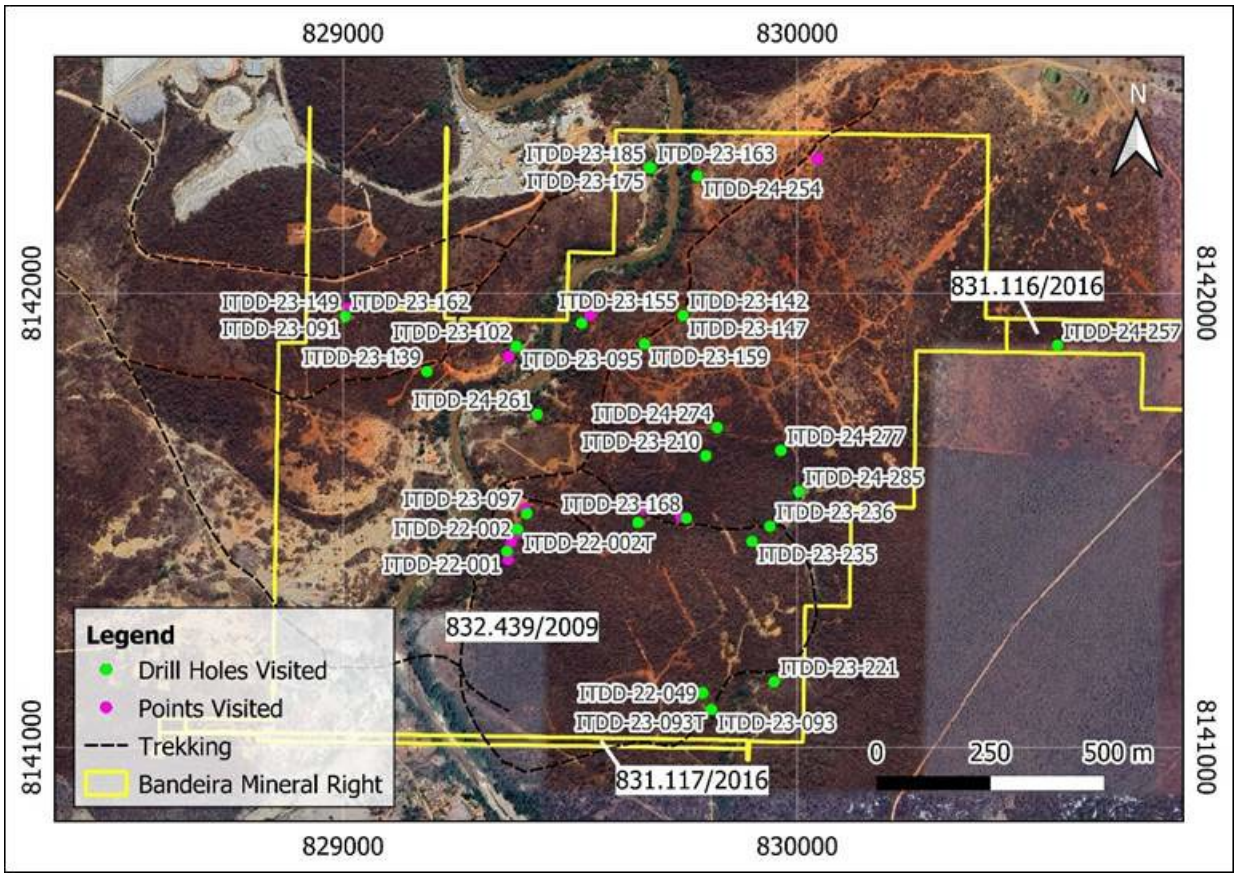
Mr. Silva conducted site visits on September 13 and 14, 2023; December 12, 2023; and November 26 and 27, 2024. Mr. Rocha visited the Project on April 11, 2024 (Figure 12-1).

The QPs' inspections focused on the following:

- Trenches (Figure 12-2)
- Collar landmarks (Figure 12-3 and Figure 12-4)
- Drilling rigs (Figure 12-5)
- Office and drill-core sheds (1, 2, and 3) (Figure 12-5 to Figure 12-10)
- Installations and overall core-shed procedures flowchart
- Core-box archive and drill-hole landmark checking
- Drill-core saw and drill-core sample bags
- Batches of sample bags
- Pulverized and crushed samples returned from labs
- Density test procedures using water-displacement method
- Physical file storage for drill-hole logs and bulletins
- Mineralization style and sampling procedures.

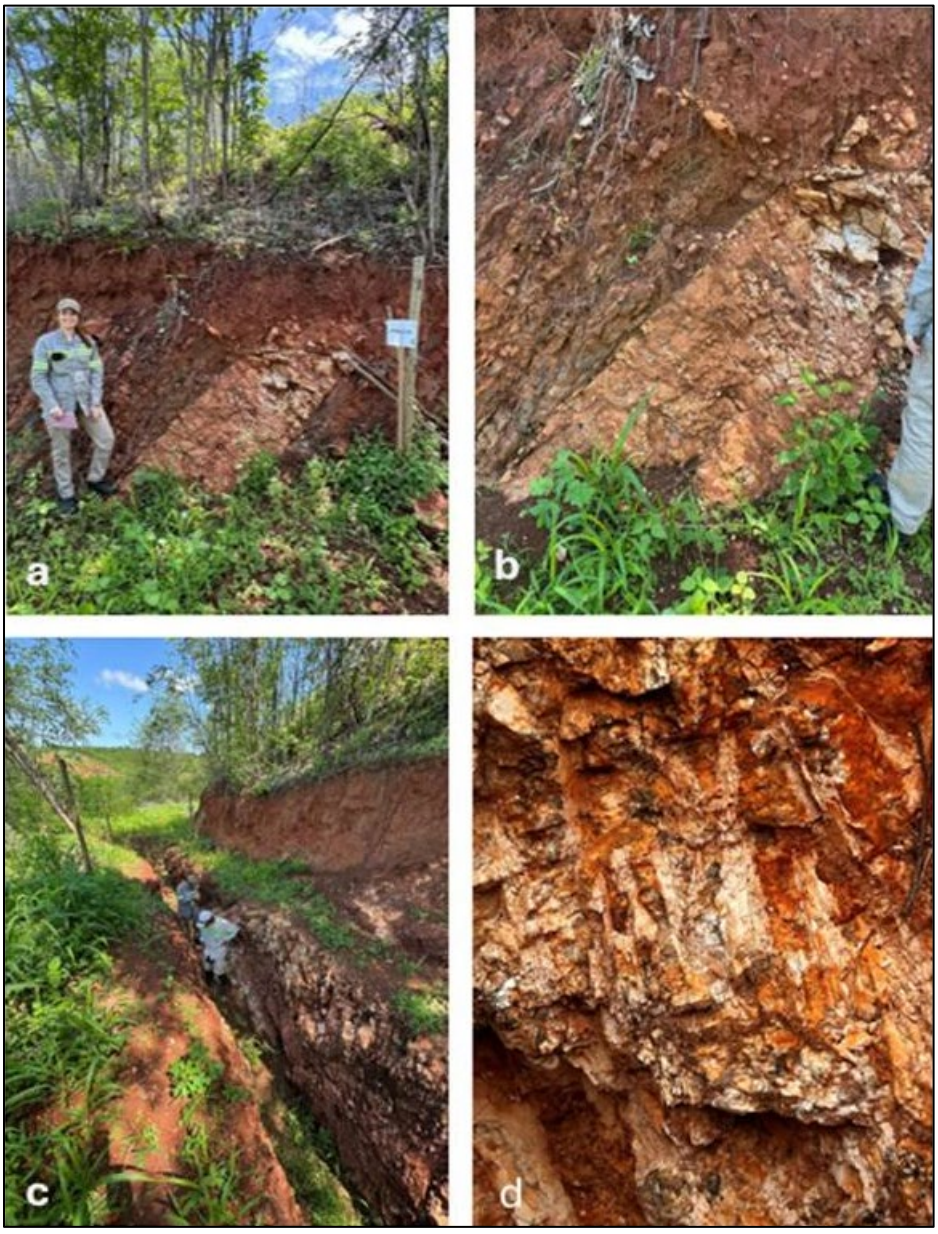
The assay data were cross-checked within the drill sample database. Digital assay records were randomly selected and scrutinized against the available laboratory assay certificate reports.

A comprehensive review of the assay database was conducted to identify errors, including overlaps, interval gaps, and typographical errors in assay values. The database was found to exhibit high accuracy, instilling confidence in the reliability of the data.



Source: GE21 (2024).

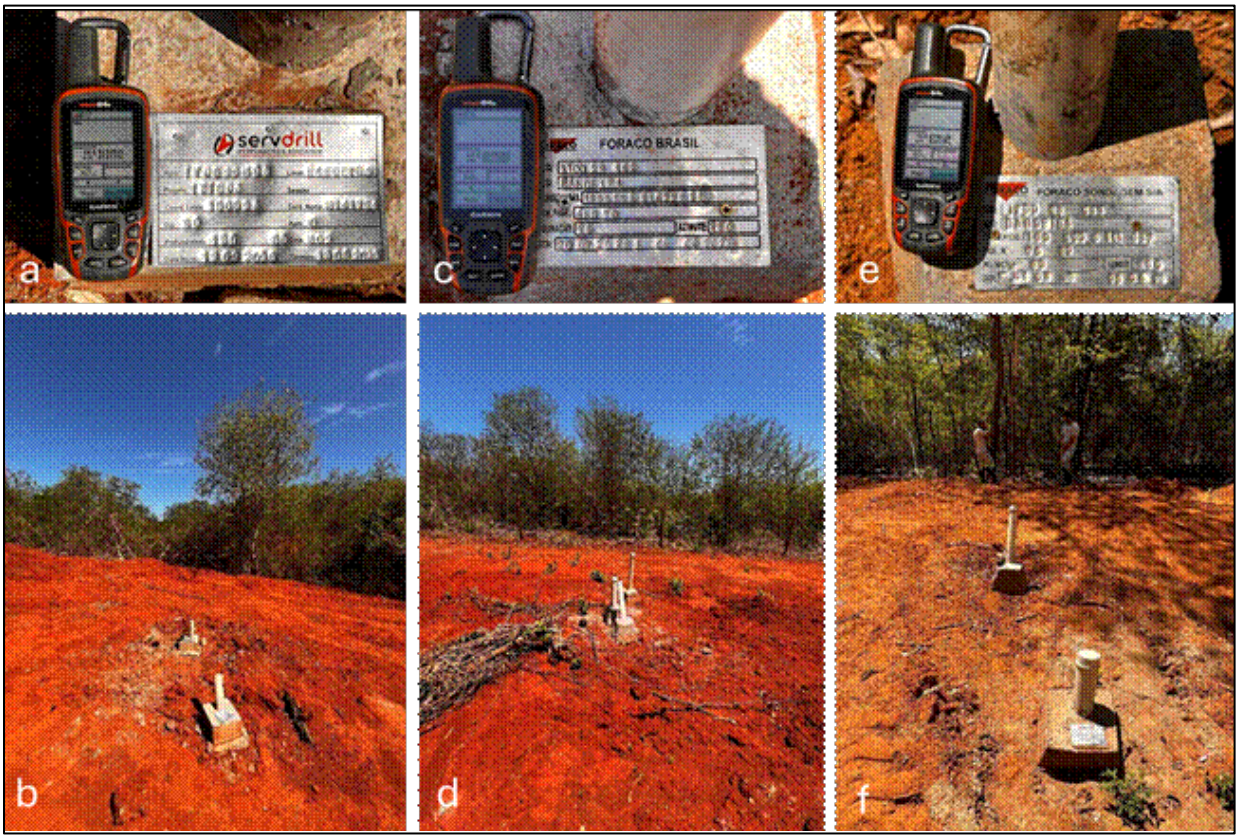
Figure 12-1: Field Points During the Site Visit on September 13 and 14, 2023



Notes: a) Pegmatite Vein with Spodumene Outcrop; b) Pegmatite Vein with Spodumene Outcrop; c) Trench ITTRE-22-001—Pegmatite Vein with Spodumene Outcrop; d) Trech ITTRE-22-001—Spodumene Pegmatite Vein Outcrop

Source: GE21 (2024).

Figure 12-2: Spodumene Pegmatites Outcrop and Trench on MGLIT Bandeira Property Site Visit November 25, 2024



Notes: a and b) Collar Landmarks—Drilling Site ITDD-23-196; c) and d) Collar Landmarks—Drilling Site ITDD-23-162; e and f) Collar Landmarks—Drilling Site ITDD-23-093

Source: GE21 (2024).

Figure 12-3: Collar Landmarks, September 2023 Site Visit



Notes: a and b) Collar Landmarks—Drilling Site ITDD-24-254; c and d) Collar Landmarks—Drilling Site ITDD-24-257; e and f) Collar Landmarks—Drilling Site ITDD-24-285.

Source: GE21 (2024).

Figure 12-4: Collar Landmarks, November 2024 Site Visit



Notes: a) Drill Rig on Site of Bandeira Drilling on 13/09/2023 at DDH ITDD-23-192—Azimuth 140°, dip ~70°; b) Drill Rig on Site of Bandeira Drilling on 13/09/2023 at DDH ITDD-23-192—Spodumene in Pegmatite Vein Cores Recovered from Drilling, depth 355 m; c) Drill Rig on Site of Bandeira Drilling on 13/09/2023 at DDH ITDD-23-192—Technicians Recovering the Cores and using the REFLEX ACT III for Core Orientation; d) Drill Rig on Site of Bandeira Drilling on 13/09/2023 at DDH ITDD-23-192—MGLIT employees using REFLEX GYRO IQ to Perform the Survey Measurement

Source: GE21 (2024).

Figure 12-5: Drilling Rig and Survey Equipment on MGLIT Bandeira Property, September 13, 2023, Site Visit



Notes: a) Office and Core Shed 1—External View; b) Office and Core Shed 1—Internal View; c) Shed 1 —Team Present at QP's Visit; d) Core Shed 2—External View; e) Core Shed 2—Internal View; f) Shed 2—Core Box Storage; g) Core Shed 3—External View; h) Core Shed 3—Internal View; i) Shed 3—Core Box Storage.

Source: GE21 (2024).

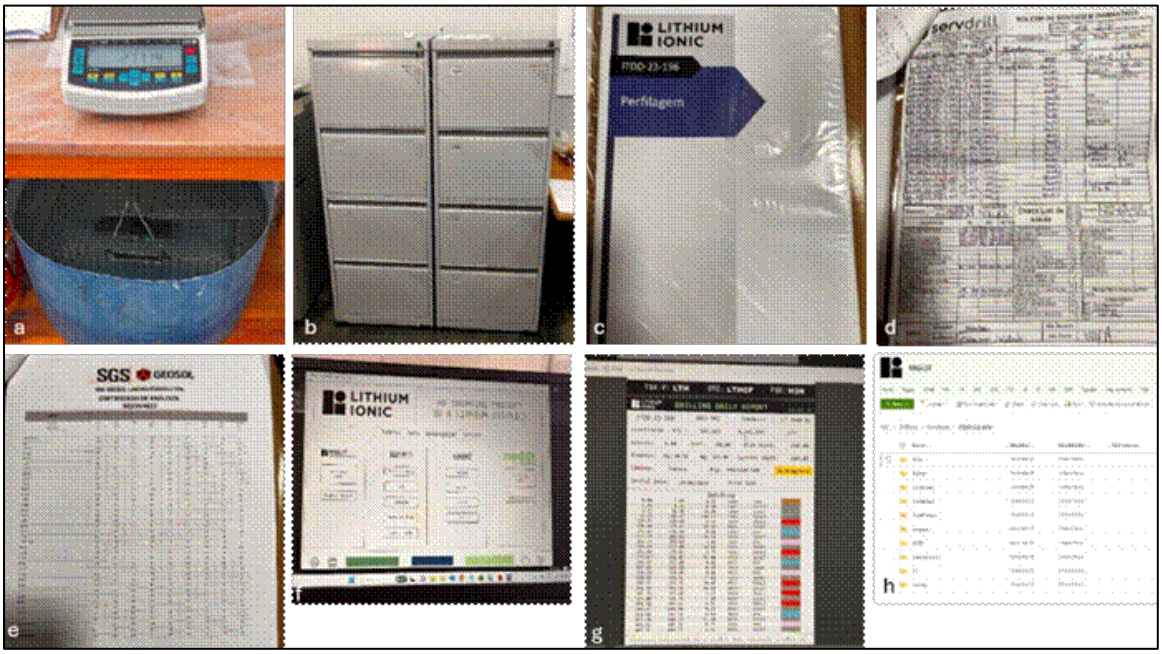
Figure 12-6: MGLIT Core Shed Storage in Araçuaí



Notes: a) Marking for Sawing; b) Core saw; c) Cores after Sampling with Assays Identified; d) Identified Samples to Send to Lab; e) QA/QC—Standard to Insert in Batch; f) Batch to Send to Lab; g and h) Storage of Pulverized Samples and Crushed Samples after Return from Labs, Custody Chair.

Source: GE21 (2024).

Figure 12-7: Workflow, Sampling, QA/QC, and Chain of Custody



Notes: a) Density Measurement—Core Weighed Under Water; b) Physical Drill-Hole File Storage; c) DDH ITDD-23-196 Folder with Drill-Hole Documents; d) DDH ITDD-23-196 Folder—Daily Drilling Bulletin; e) DDH ITDD-23-196 Folder—Assay Results, Certificates; f) MGLIT Customized Database Management System for Mineral Research; g) Customized Database Management System—Registration of the Drilling Daily Report; h) MGLIT Cloud Data Center MGLIT.

Source: GE21 (2024).

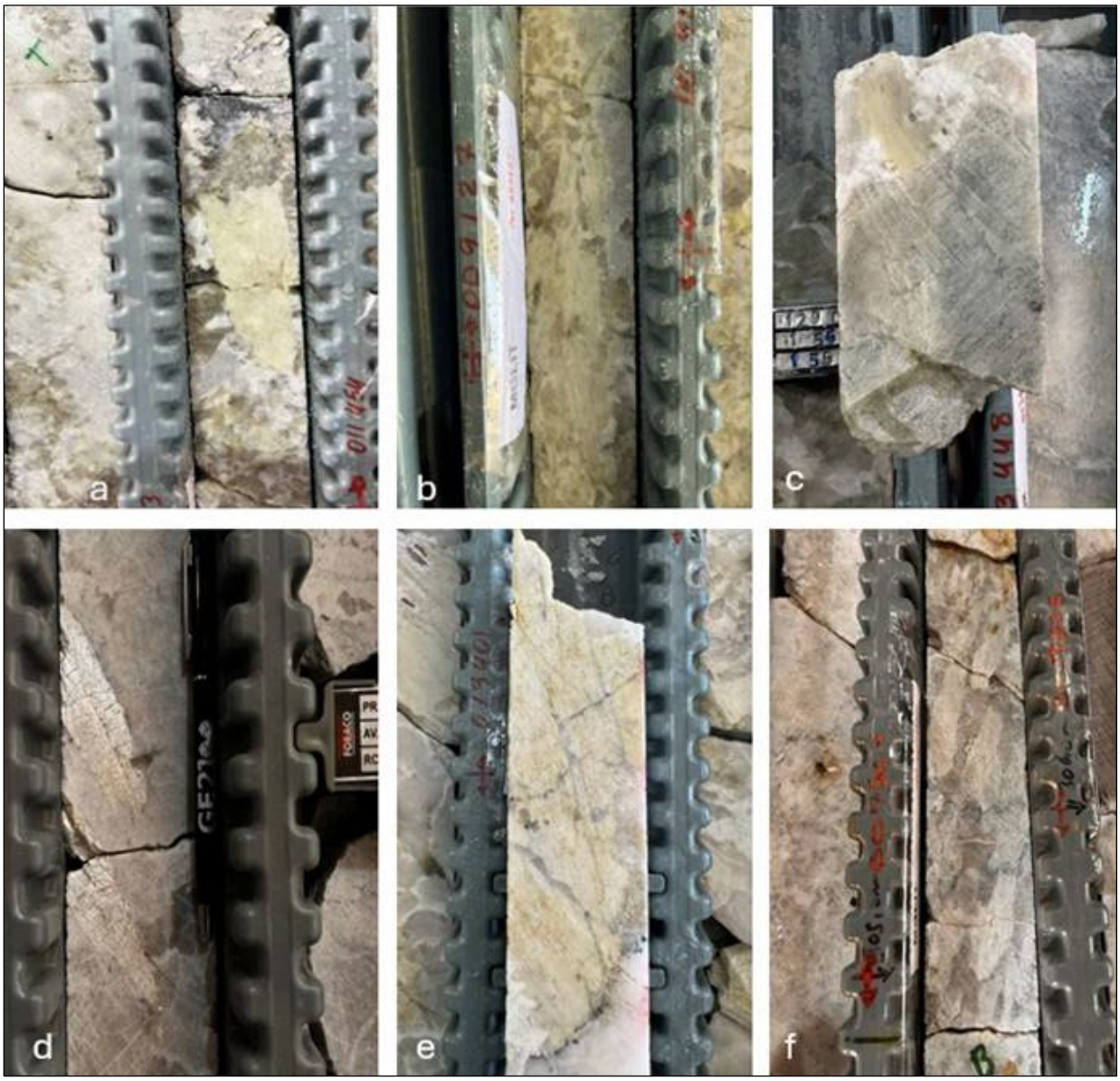
Figure 12-8: Density Measurement and Physical and Digital File Storage



Notes: a) ITDD-23-091—479 m to 489 m; b) ITDD-23-120—109 m to 115 m.

Source: GE21 (2024).

Figure 12-9: Core Boxes of the Interval Mineralized Spodumene Pegmatite



Notes: a) ITDD-23-163—146 m; b) ITDD-23-162—460.5 m; c) ITDD-24-254—129 m; d) ITDD-23-120—111 m; e) ITDD-24-257—1,197 m; f) ITDD-23-139—305 m

Source: GE21 (2024).

Figure 12-10: Bandeira Spodumene Pegmatite Intercept Core Boxes of the Modelled Mineralized Spodumene Zone—Detail of the Spodumene Crystal

12.2 Qualified Person's Opinion

No significant issues were identified with the database. The QPs believe that the practices and procedures used to generate the MGLIT database are sufficient to support Mineral Resource estimation. Some observations that were recorded during visits as they relate to the generation, collection, control, and storage of exploration data on-site at Araçuaí are:

- Reviewing the QA/QC
- Field checking core shed
- Drilling in progress
- Reviewing density procedures
- Discussions of the current geological interpretations with MGLIT geologists.
- Drill-hole collars have a physical identification marker comprising a concrete pad with a metal plate designating the drilling contractor, drill-hole number, drilling area, orientation, map coordinates, start and end date drilled, and total depth. A PVC pipe protruding from the marker provides a physical record of the drill-hole orientation.
- All core boxes were labelled and adequately stored in a core shed. Sample tags were present in the boxes, and it was possible to validate sample numbers and confirm the presence of mineralization in the witness half-core samples from the mineralized zone.
- The QPs considered the drill-hole logging standard industry practice logging procedures, which MGLIT has standardized. They reviewed logging procedures for randomly selected drill cores and verified the completeness of the logs.
- MGLIT has its own database software. Data storage procedures at MGLIT are industry standard practice. As part of the validation process, 12 holes were verified. Database validation was conducted with the MGLIT employees according to standard validation procedures, including a review of collar locations, drill-hole deviations, and database check-assay review. The QPs found no inconsistencies in the database.
- An extensive database of humidity density information was collected during the exploration phase. Assessing the impact of density samples' moisture and porosity on bulk density measurements is strongly recommended.

The QPs checked the MGLIT procedures for sampling management, storage, logging, sample preparation, and assay. They considered it within acceptance limits and in compliance with mineral-industry practices.

Rock-type descriptions fit with the checked mineralization style. MGLIT has demonstrated that it understands the geology of the area.

13 MINERAL PROCESSING AND METALLURGICAL TESTING

The Bandeira ore is SRP-type spodumene-rich pegmatite, characterized by non-zoned to poorly zoned pegmatites, rich in spodumene crystals (average size 5 cm to 30 cm) disseminated in a matrix composed of albite, quartz, perthitic microcline (i.e., potassium feldspar with exsolved albite lamellae), muscovite, and montebrasite, totalling over 90% volume, with subordinate amounts (up to 10% volume) of accessory and alteration minerals, such as lithium minerals (cookeite, petalite, triphylite, and zabuyelite), apatite, niobium–tin–tantalum and iron–manganese oxides, graphite, and clay minerals (kaolinite and montmorillonite).

Mineral processing and metallurgical testing programs are comprehensive, encompassing chemical and mineralogical analyses, physical tests for hardness, particle-size distribution in crushing assays, abrasiveness, and spodumene concentration tests. These tests are specifically designed to understand spodumene's behaviour when subjected to simulations of the industrial process of ore mineral concentration. This information is indispensable for devising an efficient and cost-effective processing method.

13.1 Ore Mineralogical Characterization

Table 13-1 presents the lithium-bearing minerals along with their chemical composition, specific gravity, and Li_2O content.

Table 13-1: Lithium Minerals Characteristics

Mineral	Formula	Specific Density (g/cm³)	Mohs Hardness	Li_2O (% weight)	Li_2O[1] (% weight)
Montebrasite	$LiAl(PO_4)(OH)$	3.0–3.1	5.5–6.0	10.21	9.0
Cookeite	$(Al, Li)_3Al_2(Si, Al)_4O10(OH)_8$	2.6–2.7	2.5 –3.5	2.86	2.5
Elbaíte	$Na(Li,Al)_3Al_6(BO_3)_3Si_6O_{18}(OH)_4$	2.9–3.1	7.5	4.07	4.0
Spodumene	$LiAlSi_2O_6$	3.1–3.2	6.5–7.0	8.03	7.4
Spodumene Partially Altered	-	<3.1	<6.5	-	<7.4
Lepidolite (Polilitionite–Trilitionite)	$KLi_2Al(Si_4O_{10})(F, OH_2)$ $K(Li_{1.5}Al_{1.5})(AlSi_3O_{10})(F,OH_2)$	2.8–2.9	2.5–3.5	6.46–7.70	7.1
Litiofilite–Trifilite	$LiMn(PO_4)$–$LiFe(PO_4)$	3.4–3.6	4	9.53–9.47	9.0
Petalite (Cristal)	$LiAlSi_4O_{10}$	2.4	6.5	4.90	4.7
Petalite Altered (Mass)	-	<2.4	<6.5	<4.90	3.0
Zabuyelite	Li_2CO_3	2.09	3	40.44	40.0

Note: [1] Actual lithium oxide grade is usually determined.
Source: www.mindat.org; Pöllmann & König (2021).

The lithium-bearing minerals in the Bandeira deposit pegmatites were systematically characterized through detailed visual logging of drill cores and the selection of representative core intervals. Following macroscopic identification, selected samples were analyzed in greater detail by means of polished thin sections examined under an optical microscope. Both macroscopic and microscopic observations were supported by modal estimations (in vol%) of spodumene relative to the other

mineral constituents of the matrix, particularly those that may significantly affect processing plant performance.

Spodumene is the dominant lithium mineral and represents the primary economic interest in the Project. It accounts for approximately 75%–80% of the total lithium content in the ore, followed by montebrasite, which contributes about 15%–20%, and a minor proportion of petalite, around 5%. In certain drill holes, zabuyelite and trace amounts of lepidolite were also identified.

The principal gangue minerals observed in the ore include albite, quartz, perthitic potassium feldspar, and muscovite. Accessory minerals, generally present in amounts below 1 vol%, comprise apatite, beryl, cassiterite, columbite-tantalite, and graphite.

The average mineralogical analysis using XRD, Rietveld Method, for seven drill holes used in the variability study Phase I, is presented in Table 13-2.

Table 13-2: Average Mineralogical Composition for Seven Metallurgical Drill Holes (XRD, Rietveld Method)

Mineral	%Weight
Albite	31.70
Quartz	26.50
Microcline	15.00
Spodumene	14.30
Moscovite	6.10
Montebrasite	3.30
Petalite	1.10
Others (Polilitionite, Elbaíte, Cookeite, and Pyrite)	2.00

13.2 Ore Chemical Analysis

The average chemical analyses for the Bandeira deposit, considering samples from drill holes used for metallurgical tests and the mean values from the geological exploration database (7,516 chemical analysis, cut-off grade of Li_2O >0.5%), are presented in Table 13-3.

Table 13-3: Average Chemical Composition for Metallurgical Drill Holes

Metal Oxides	Metallurgical Drill Holes	Geological Database
Li_2O (% weight)	1.24	1.37
Fe_2O_3 (% weight)	1.71	1.11
Al_2O_3 (% weight)	15.08	14.40
K_2O (% weight)	2.47	2.58
P_2O_5 (% weight)	0.79	0.85
CaO (% weight)	1.34	0.45
SnO_2 (ppm)	301.00	280.00
Ta_2O_5 (ppm)	79.00	80.00
Nb_2O_5 (ppm)	145.00	130.00

13.3 Metallurgical Testing

SGS Geosol conducted preliminary metallurgical tests using heavy liquid separation (HLS). TOMRA carried out ore-sorting tests in Germany, and Steinert in Brazil. Ore variability testwork campaigns were developed at research centers and laboratories such as SGS Geosol, SGS Chile, Centro de Tecnologia Mineral (CETEM), Metso Outotec, and Delkor. These tests were aimed at understanding the behaviour of the ore under different processing conditions, which is crucial for optimizing the processing method and ensuring the production of high-quality lithium concentrate.

Several series of metallurgical tests were carried out at reputable and well-known laboratories over a period of three years. The type of test, date performed, and drill holes used to sample source are summarized in Table 13-4.

Table 13-4: Metallurgical Tests Performed

Testwork	Date Performed		Supplier/Vendor	Drill Holes for Sample
	Month	Year		
HLS Series 1	December	2022	SGS Geosol	ITDD-22-001
				ITDD-22-002
				ITDD-22-007
Flotation Open Circuit	January	2023	SGS Geosol	ITDD-22-002
				ITDD-22-023
				ITDD-22-030
				ITDD-22-048
				ITDD-23-083
				ITDD-23-087
				ITDD-23-093
Ore Sorter Undiluted samples	October	2023	TOMRA	ITDD-22-013
				ITDD-22-015
				ITDD-22-029
				ITDD-22-032
				ITDD-22-035
				ITDD-22-036
HLS Variability 1	November	2023	SGS Geosol	ITDD-22-002
				ITDD-22-023
				ITDD-22-030
				ITDD-22-048
				ITDD-23-083
				ITDD-23-087
				ITDD-23-093

Testwork	Date Performed		Supplier/Vendor	Drill Holes for Sample
	Month	Year		
Thickener	November	2023	Ecolution	ITDD-22-002
				ITDD-22-023
				ITDD-22-030
				ITDD-22-048
				ITDD-23-083
				ITDD-23-087
				ITDD-23-093
Ore Sorter Diluted Samples	December	2023	TOMRA	ITDD-23-054
				ITDD-23-098
Bond Work Index	January	2024	SGS Chile	ITDD-23-134
Spirals/Tables	January	2024	Mineral Technologies	ITDD-22-002
				ITDD-22-023
				ITDD-22-030
				ITDD-22-048
				ITDD-23-083
				ITDD-23-087
				ITDD-23-093
Ore Sorter Pilot Diluted Samples	March	2024	Steinert	ITDD-22-002
				ITDD-22-023
				ITDD-22-030
				ITDD-22-048
				ITDD-23-083
				ITDD-23-087
				ITDD-23-093
Crushability	March	2024	Metso	ITDD-22-023
				ITDD-22-030
				ITDD-22-048
				ITDD-23-083
				ITDD-23-087
				ITDD-23-093
Thickener/Filtration	March	2024	Delkor	ITDD-22-002
				ITDD-22-023
				ITDD-22-030
				ITDD-22-048
				ITDD-23-083
				ITDD-23-087
				ITDD-23-093

Testwork	Date Performed		Supplier/Vendor	Drill Holes for Sample
	Month	Year		
HLS Variability 2	April	2024	SGS Geosol	ITDD-22-039
				ITDD-23-065
				ITDD-23-073
				ITDD-23-105
				ITDD-23-123
				ITDD-23-131
				ITDD-23-145
				ITDD-23-146
				ITDD-23-226
				ITDD-23-232
				ITDD-23-247
Mineralogical Characterization	April	2024	CETEM	ITDD-22-002
				ITDD-22-023
				ITDD-22-030
				ITDD-22-048
				ITDD-23-083
				ITDD-23-087
				ITDD-23-093
Ore Sorter Diluted Samples	April	2024	Steinert	ITDD-22-039
				ITDD-23-065
				ITDD-23-073
				ITDD-23-105
				ITDD-23-123
				ITDD-23-131
				ITDD-23-145
				ITDD-23-146
				ITDD-23-226
				ITDD-23-232
				ITDD-23-247
DMS Pilot (Post ore sorter pilot plant)	May	2024	SGS Geosol	ITDD-22-002
				ITDD-22-023
				ITDD-22-030
				ITDD-22-048
				ITDD-23-083
				ITDD-23-087
				ITDD-23-093

Testwork	Date Performed		Supplier/Vendor	Drill Holes for Sample
	Month	Year		
HLS Test Circuit comparison Hatch recommendation	January	2025	SGS Geosol	ITDD-22-023
				ITDD-22-030
				ITDD-22-048
				ITDD-23-083
				ITDD-23-087
				ITDD-23-093
HLS Phase 3	June	2025	SGS Geosol	ITDD-23-063
				ITDD-23-141
				ITDD-23-209
				ITDD-23-215
Mag Sep	July	2025	Steinert	ITDD-23-063
				ITDD-23-141
				ITDD-23-209
				ITDD-23-215
Thickener/Filtration	July	2025	Delkor	ITDD-23-063
				ITDD-23-141
				ITDD-23-209
				ITDD-23-215
Flotation Locked Cycle Test	August	2025	SGS Geosol	ITDD-23-063
				ITDD-23-141
				ITDD-23-209
				ITDD-23-215

The location of drill holes that provided samples for each test are shown in Figure 13-1.

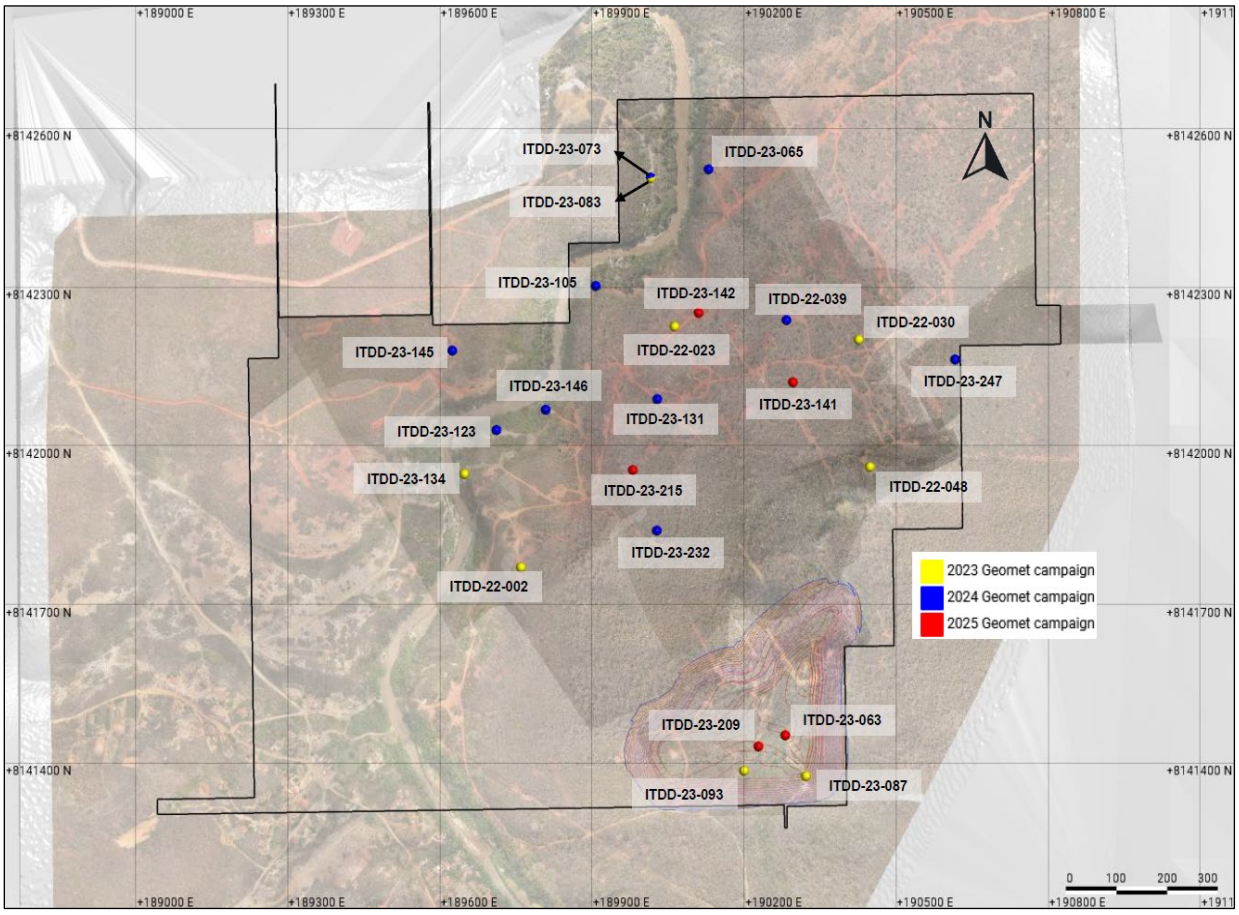


Figure 13-1: Drill-Hole Locations

13.3.1 Preliminary Heavy Liquid Separation Tests at SGS Geosol—HLS Series 1, December 2022

Samples from drill holes ITDD-22-001, -002, and -007 were combined to generate a composite, and sent to SGS Geosol. Before the HLS test, the composite sample was prepared according to the procedure shown in Figure 13-2, to proceed with the HLS test. This test aims to evaluate the performance of dense-media separation in obtaining lithium concentrate for the Project, according to market specifications, by varying the dense media's particle-size distribution and density.

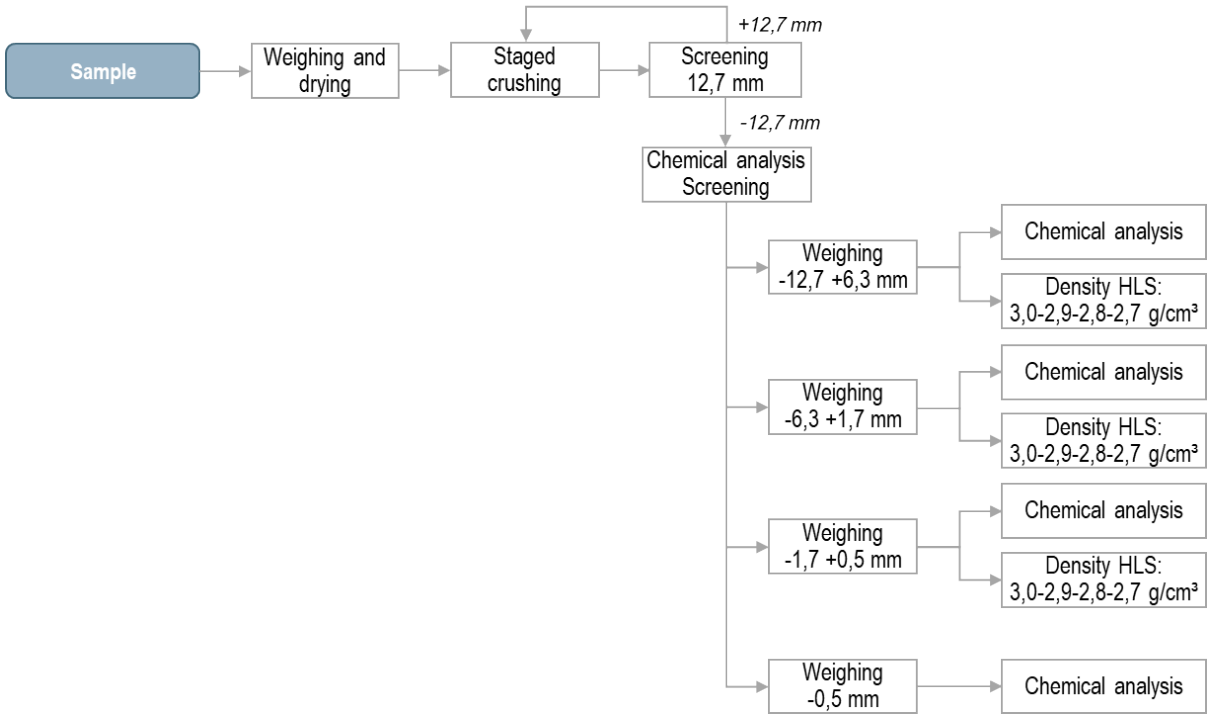
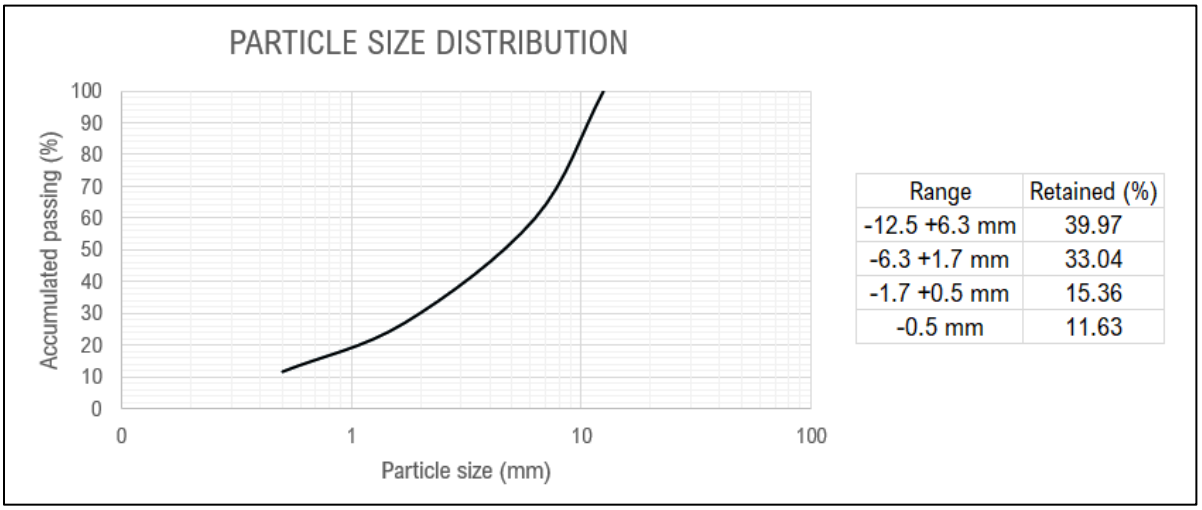


Figure 13-2: Bandeira Composite Sample Preparation Procedure

A 20 kg sample was dried and crushed in a jaw crusher with openings of 31.5 mm, 25.4 mm, and 12.7 mm to obtain material with 100% passing (P_{100}) 12.7 mm. After this, particle-size analysis was conducted using a sequence of 12.7 mm, 6.3 mm, 1.7 mm, and 0.5 mm sieves. For each size fraction, a representative sample was collected for chemical analysis. HLS tests were conducted at 3.0, 2.9, 2.8, and 2.7 g/cm³ densities for the size fractions −12.7+6.3, −6.3+1.7, and −1.7+0.5 mm.

The particle-size distribution of the P_{100} 12.7 mm material is presented in Figure 13-3. Approximately 12% of the mass does not have a suitable particle size for the dense-media separation stage, meaning it is smaller than 0.5 mm. However, the Project sees this as an opportunity for future study and potential improvement—that is, concentrating the −0.5 mm fraction using gravity equipment or flotation.

Chemical analysis identified the predominance of aluminum oxide (17.10%), potassium oxide (2.39%), and lithium oxide (1.63%) (Figure 13-4). The presence of aluminum can be mainly attributed to albite, K-feldspar, and spodumene. Potassium is predominant in K-feldspar, while lithium is predominant in spodumene. With respect to iron oxide, which is the primary contaminant for market specifications, the concentration in the ore is 0.23%. The mineral origin of iron is mainly schists (biotite). In addition to the presence of iron, there is concern regarding schist density, which can vary between 2.40 g/cm^3 and 3.05 g/cm³, similar to the cut-off density used for dense-media separation commonly employed for spodumene concentration, considering the density of the mineral of interest varies between 3.15 g/cm^3 and 3.20 g/cm³ (Peixoto et al., 2016).



Range	Retained (%)
-12.5 +6.3 mm	39.97
-6.3 +1.7 mm	33.04
-1.7 +0.5 mm	15.36
-0.5 mm	11.63

Figure 13-3: Product Size Distribution After Crushing to P_{100} 12.7 mm

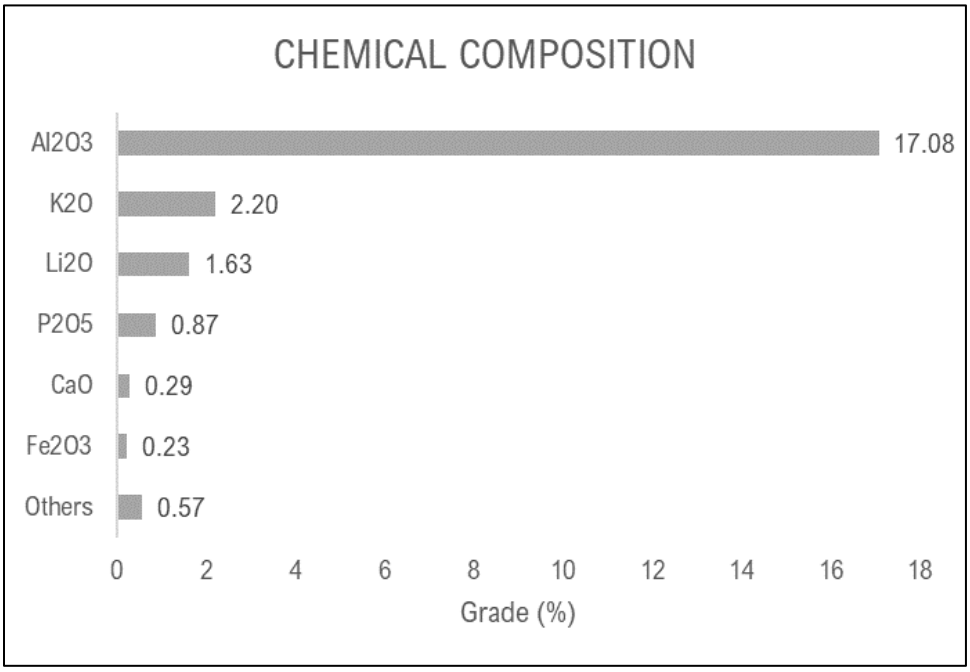


Figure 13-4: Bandeira Composite Sample Chemical Analysis

The heavy liquid separation tests were conducted for each particle-size fraction: −12.7 mm +6.3 mm, −6.3 mm +1.7 mm, and −1.7 mm +0.5 mm—using organic liquid to evaluate the optimal density to achieve the market specification of lithium concentrate (i.e., a minimum of 5.5% Li_2O and a maximum of 1% Fe_2O_3). The densities evaluated were 2.7, 2.8, 2.9, and 3.0 g/cm³, for which solutions with different proportions of methylene iodide (3.29 g/cm³) and acetone (0.79 g/cm³) were prepared.

The tests for the particle-size fractions of −12.7 mm +6.3 mm and −6.3 mm +1.7 mm were conducted in beakers, while the test for the finer particle-size fraction (−1.7 mm +0.5 mm) was carried out using a separating funnel. The test involves mixing the ore and the dense-media solution in the reactor

(beaker or separating funnel) and waiting for separation. Afterward, the sunken material, the dense media, and the floated material are collected separately. Densities were evaluated sequentially as shown in Figure 13-5, and for each stage, chemical composition and mass partition were assessed.

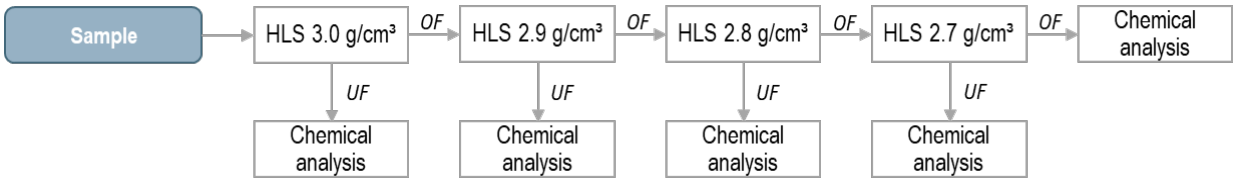


Figure 13-5: HLS Test Flowsheet

Figure 13-6 presents the cumulative content of lithium oxide and ferric oxide for each density of the three particle-size fractions evaluated. The content was calculated based on the individual content of each sample and the mass partition.

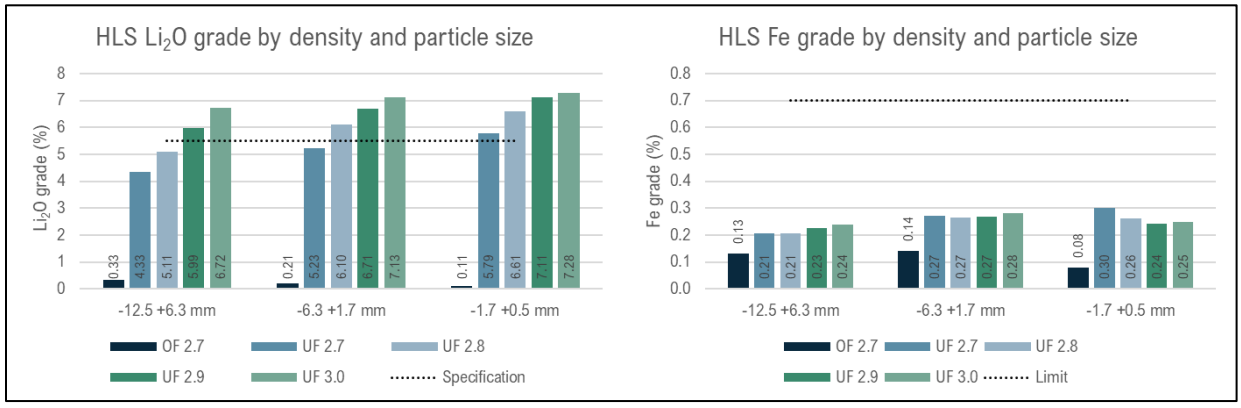


Figure 13-6: Li_2O and Fe Chemical Analysis Results for each HLS Step

It can be noted that the cut-off density increases with particle size. For finer particles, obtaining a concentrate meeting the specification is possible using a cut-off density of 2.7 g/cm^3. However, for the intermediate particle-size range, the cut-off should be performed at 2.8 g/cm^3, and for the coarser material, at 2.9 g/cm^3.

The lithium oxide content in the floated material for the coarser particles is approximately three times higher than that in the floated material for the finer particles. This indicates lower liberation of spodumene in the coarser particle-size range.

Regarding iron oxide, it was found that all concentrates remained below the target content limit of 1.0%.

The recovery results by particle-size range and the overall recovery of the HLS are presented in Figure 13-7, along with the lithium oxide content in the concentrate. For the particle-size range −12.7 mm +6.3 mm, the cut density was 2.84 g/cm³, representing a recovery of 70.5%. These values were obtained by interpolation. The density of the −6.3 mm +0.5 mm range was 2.71 g/cm³, and the recovery was 90.1%. However, the HLS recovery was 74.8% considering the loss of fines (i.e., fractions smaller than 0.5 mm) representing 12% of the mass and 11% of the lithium.

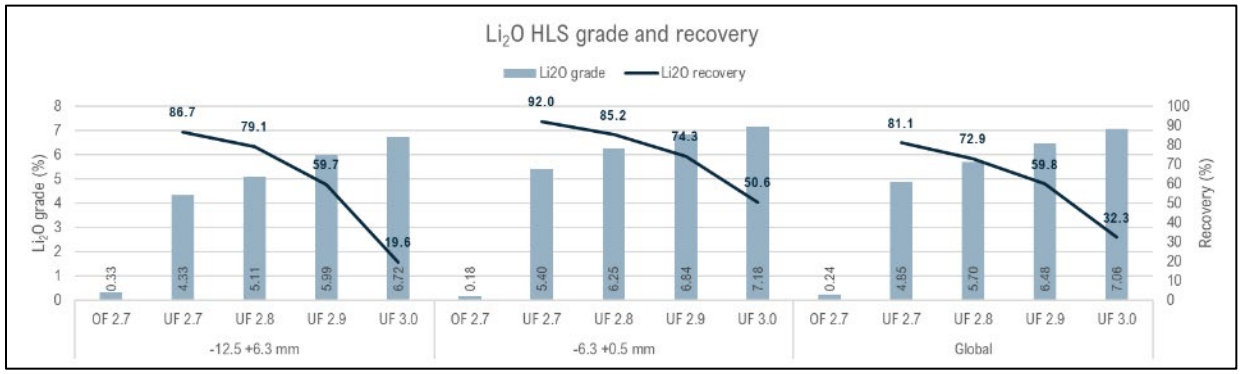


Figure 13-7: Li_2O Recovery and Grade per HLS Step

These initial HLS tests demonstrated that concentrate grades of between 5.2% and 5.5% Li_2O could be achieved at acceptable lithium recoveries. This was confirmed in subsequent variability testing in in November 2023 and April 2024.

13.3.2 New Set of HLS Tests—June 2025

New PQ holes were drilled in Bandeira area to detail the behaviour of the ore in the HLS test, using a modified test procedure that was designed to mimic actual plant operation. The sample preparation is shown in Figure 13-8. First the drill core was separated into the pegmatite and schist portion, then crushed to the top size of 15.9 mm and mixed in the proportion of 18% of schist and 82% of pegmatite. After removing the fines (−0.6 mm) the sample was sent to HLS sequential tests and the HLS to simulate the proposal flowsheet (see Diluted Variability Samples—HLS Tests in Section 13.3.3).

The sequential HLS test was performed from the lowest density to the highest, refeeding the sinks from the previous density into the next density (Figure 13-9). The objective is to define the cut point of the first DMS step.

The average results from the sequential HLS are shown in Figure 13-10. A slight difference is observed between the top size of 15.9 mm and 12.7 mm. To minimize fines generation, the top size of 15.9 mm was selected. Regarding the density cut point, the density of 2.65 g/cm³ was selected for the first DMS, as with this density, it is possible to increase the grade and achieve higher lithium recovery.

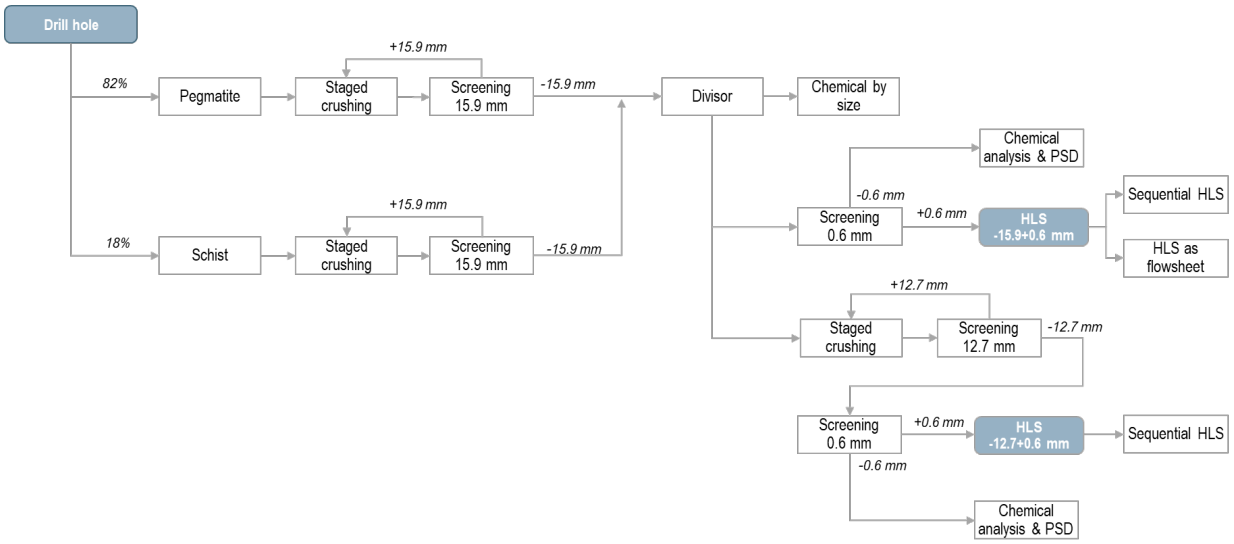


Figure 13-8: Sample Preparation for HLS Test

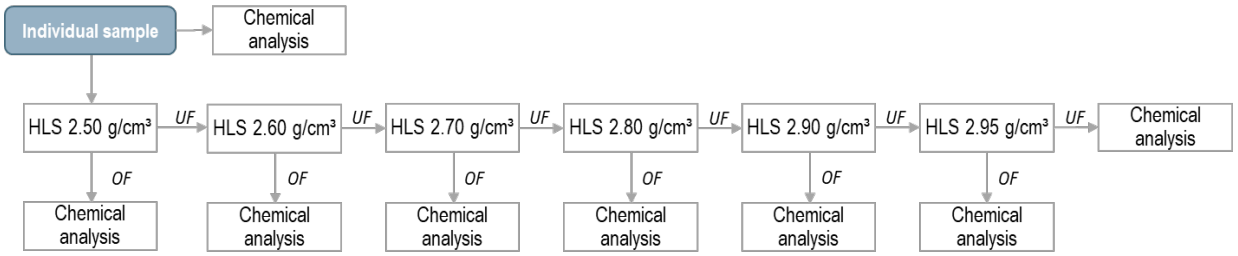


Figure 13-9: Sequential HLS Test Flowsheet

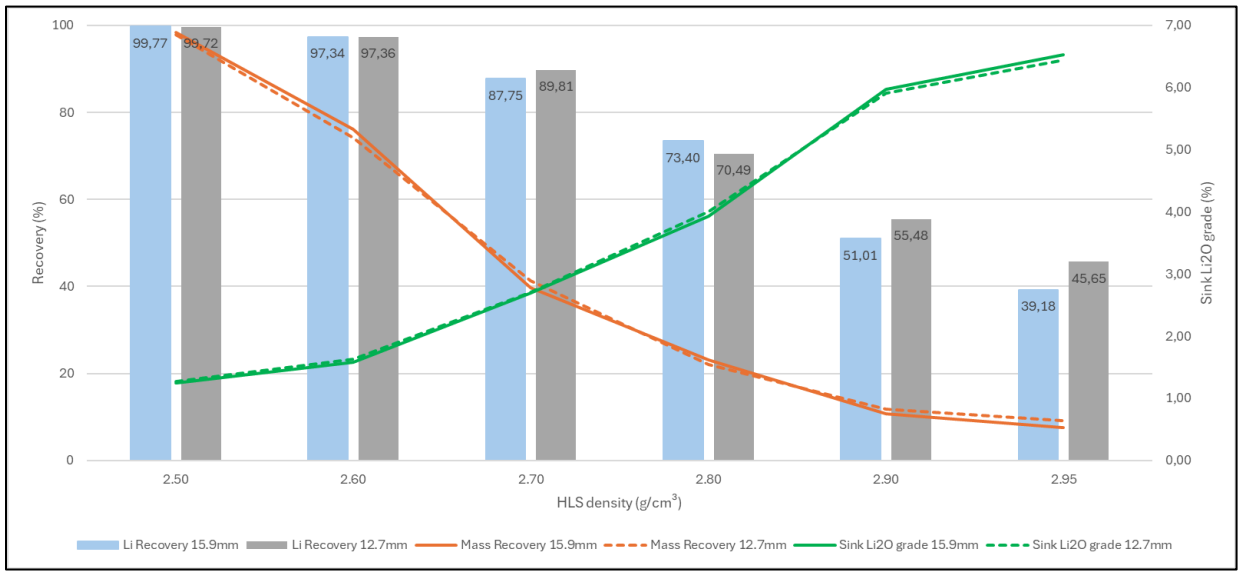


Figure 13-10: Sequential HLS Test Results

Figure 13-11 shows the photos of the products generated in the HLS with the top size of 15.9 mm. In the lower densities, the products are white, which may be albite, quartz, or feldspar. By increasing the density to between 2.8 and 2.9, the schists are concentrated. Then, at the higher density of 2.95 g/cm^3 it is possible to see the spodumene.

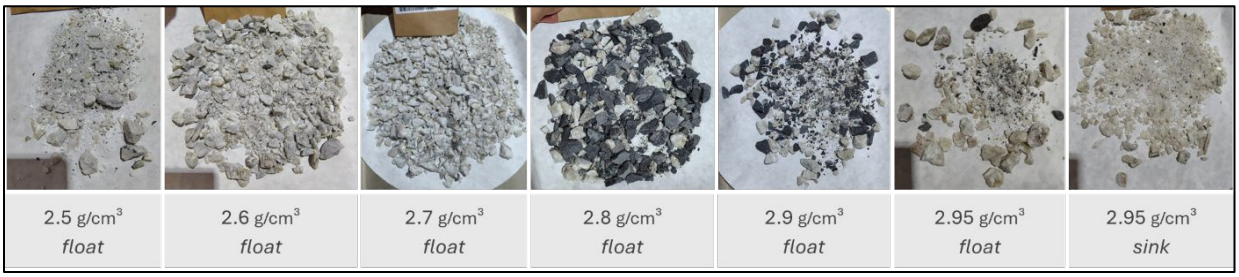


Figure 13-11: Sequential HLS Products

This HLS testing again confirmed that acceptable concentrate grades and recoveries could be achieved using dense medium separation. The detailed analysis and determination of overall recovery is presented in Section 17.

A pilot-scale DMS test was conducted, discussed in Section 13.4.2.

13.3.3 Ore Variability

A comprehensive study was conducted to analyze the geological and metallurgical variability of the ore. First, seven PQ drill holes without schists were selected for use in evaluating the HLS performance for different samples, and one for determining crushability work index (Phase 1). Then, 15 new samples from 11 HQ drill holes were selected to evaluate the ore sorter and HLS performance in other areas and depths with schist dilution (Phase 2). In addition, six new samples from five PQ drill holes were selected to perform HLS tests to validate the top size and the DMS circuit (Phase 3).

Chemical and Mineralogical Characterization

The seven metallurgical drill holes were prepared for chemical and mineralogical analysis (Table 13-5 and Table 13-6). In addition, two composite samples were prepared to evaluate the combined behaviour of the samples.

Table 13-5: Chemical Analysis for the Seven Drill Holes and Two Composites (Phase 1)

	Al (%)	Be (ppm)	Ca (%)	Cr (ppm)	Fe_2O_3 (%)	K_2O (%)	Li_2O (%)	Nb (ppm)	P (%)	Sn (ppm)	Ta (ppm)
ITDD-22-048T	8.1	170	0.18	864	0.83	2.34	1.14	175	0.28	275	99
ITDD-23-093T	8.58	155	0.22	102	0.57	2.02	1.12	84	0.24	348	45
ITDD-23-087T	7.86	188	0.12	37	0.70	1.98	1.78	90	0.25	353	61
ITDD-22-023T	8.09	142	0.23	31	0.56	2.34	1.59	106	0.39	174	46
ITDD-22-002T	8.04	193	0.9	1008	0.76	2.82	1.21	127	0.49	299	72
ITDD-23-083T	8.7	138	0.3	144	0.56	2.39	1.62	110	0.37	293	112
ITDD-22-030T	7.95	297	<0.1	19	0.74	2.37	1.46	109	0.63	644	49
COMPOSITE1	7.89	175	0.32	14	0.83	2.18	1.26	92	0.38	365	54
COMPOSITE2	8.23	148	0.38	18	0.84	2.16	1.58	99	0.47	268	44

Table 13-6: Mineralogical Analysis by XRD (Rietveld) for the Seven Drill Holes (Wt%) (Phase 1)

	Albite	Chlorite	Elbaite	Microcline	Montebrasite	Muscovite	Petalite	Polylithionite	Pyrite	Quartz	Spodumene
ITDD-22-002	32.5	0.3	1.1	20.8	5.1	4.0	1.2	0.2	0.1	23.3	11.4
ITDD-22-023	32.1	0.3	0.9	16.1	1.9	4.2	1.2	0.4	0.0	25.6	17.2
ITDD-22-030	25.2	1.1	1.3	15.7	3.1	7.0	1.1	0.4	0.0	34.3	10.7
ITDD-22-048	32.8	0.3	0.3	12.8	3.3	8.4	1.3	0.6	0.1	27.8	12.2
ITDD-23-083	35.6	0.4	0.7	16.1	3.6	3.7	1.6	1.8	0.1	19.3	17.2
ITDD-23-087	28.9	0.4	0.4	12.4	2.2	6.4	0.7	0.4	0.0	28.2	20.0
ITDD-23-093	34.5	0.6	0.7	11.4	3.8	9.2	0.9	0.4	0.1	26.8	11.6

The chemical analysis of the fifteen samples from the variability study Phase 2 is shown in Table 13-7 and the chemical analysis of the samples from Phase 3 is shown in Table 13-8.

Table 13-7: Chemical Analysis for the Fifteen Samples (Phase 2)

	Al (%)	Be (ppm)	Ca (%)	Cr (ppm)	Fe_2O_3 (%)	K_2O (%)	Li_2O (%)	Nb (ppm)	P (%)	Sn (ppm)	Ta (ppm)
Sample 1	8.06	122	0.19	17	1.49	1.70	1.85	102	0.24	146	40
Sample 2	7.14	77	1.59	31	2.29	2.25	1.05	70	0.13	85	32
Sample 3	7.62	149	3.93	41	2.27	2.05	0.34	114	0.21	151	66
Sample 4	7.93	245	1.5	42	2.63	1.29	1.46	160	0.35	605	175
Sample 5	8.14	78	0.76	25	1.96	3.60	1.38	58	0.38	79	23
Sample 6	7.92	92	0.59	42	3.17	3.34	0.83	79	0.22	50	57
Sample 7	8.72	87	0.56	34	3.35	2.08	2.09	67	0.28	88	32
Sample 8	7.85	147	0.24	36	1.63	2.64	1.32	77	0.29	127	68
Sample 9	7.93	251	1.44	15	1.47	2.98	1.32	142	0.73	154	71
Sample 10	7.05	110	5.85	48	2.53	1.73	1.27	100	0.61	160	68
Sample 11	7.79	126	0.42	53	2.57	3.20	0.42	101	0.18	67	29
Sample 12	7.25	90	2.89	25	2.19	2.16	1.04	113	0.44	279	88
Sample 13	7.22	118	0.26	34	1.89	2.37	1.13	107	0.17	50	49
Sample 14	7.55	179	0.24	27	1.66	3.35	1.09	62	0.20	286	40
Sample 15	7.58	172	1.01	71	4.32	2.94	0.64	140	0.16	151	91

Table 13-8: Chemical Analysis for the Samples (Phase 3)

	Al (%)	Be (ppm)	Ca (%)	Cr (ppm)	Fe_2O_3 (%)	K_2O (%)	Li_2O (%)	Nb (ppm)	P (%)	Sn (ppm)	Ta (ppm)
ITDD-23-063	8.18	133	0.48	58	1.46	3.00	1.09	78	0.25	192	59
ITDD-23-141 a	9.13	116	0.74	51	1.72	3.47	0.90	113	0.69	435	100
ITDD-23-209	8.25	116	0.38	51	1.64	2.42	1.31	62	0.22	195	54
ITDD-23-215	8.66	199	1.02	77	1.18	1.93	1.50	104	0.38	310	77
ITDD-23-141 b	-	-	-	-	-	-	-	-	-	-	-
ITDD-23-142	-	-	-	-	-	-	-	-	-	-	-

Undiluted Samples—Heavy Liquid Separation Tests

Figure 13-12 shows the location of the selected eight drill holes, those with a maximum 100 m depth and minimum 5 m interception, except ITDD-23-134T, which was used only for the Bond Low-Energy Impact Test. A total of 906 kg was sent to SGS Geosol to be prepared, which includes crushing, screening, and sampling. The HLS was performed in duplicate at two particle-size ranges, −12.7 +6.3 mm and −6.3 +0.85 mm for three densities 2.8, 2.7, and 2.4 g/cm³, simulating a rougher–scavenger circuit and a polishing step for petalite recovery.

HLS rougher–scavenger results are presented in Table 13-9 and Table 13-10 for each particle-size range. The 2.4 g/cm³ step did not present significative mass for all samples, which indicates a minor presence of petalite. In general, rougher concentrate presented a lithium oxide grade above 5.5% with an average global recovery of 84% for the coarse and 89% for the fine fraction.

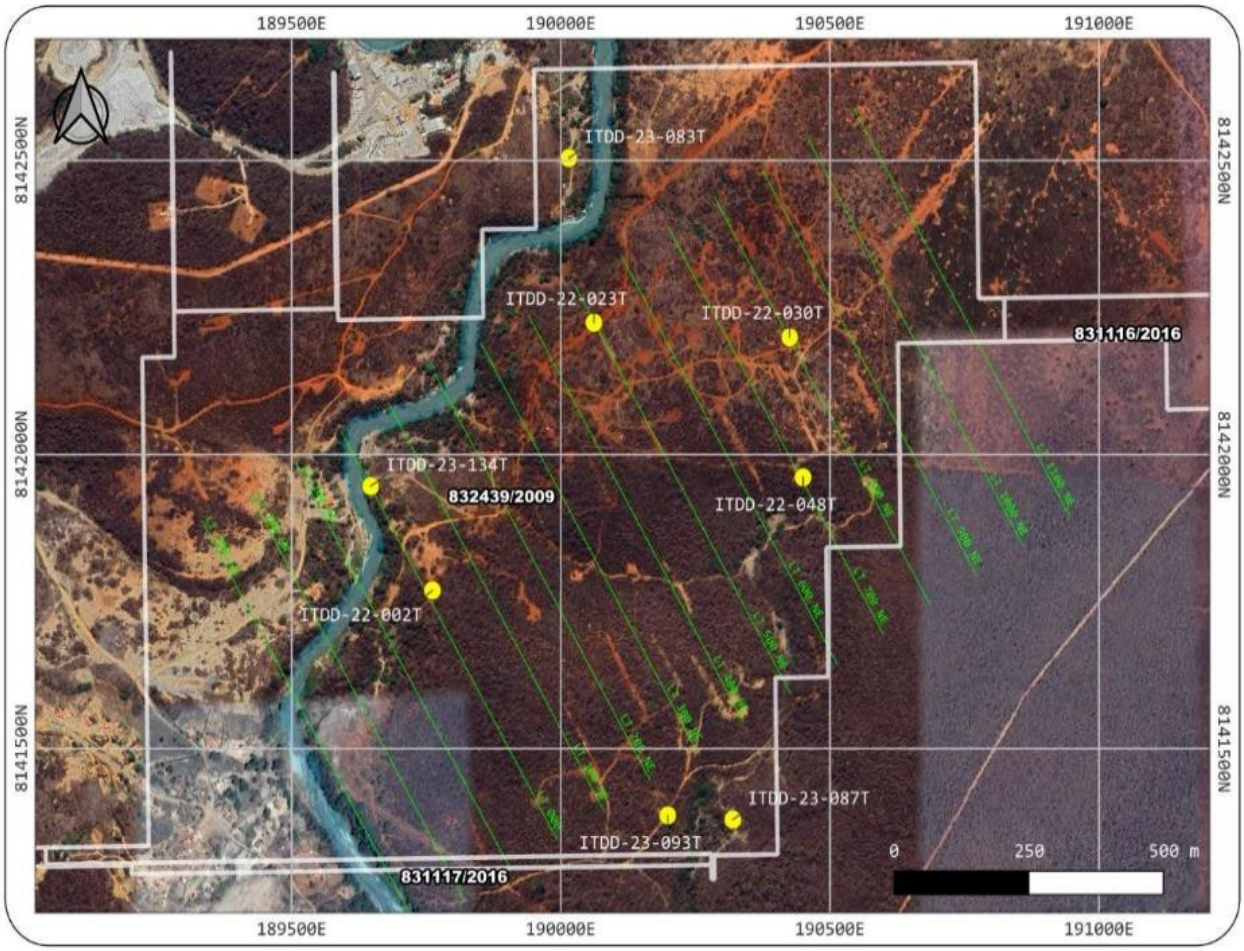


Figure 13-12: Variability Study Drill Holes for Phase 1 HLS Testwork

Table 13-9: HLS Results for Coarse Fraction (−12.7 +6.35 mm)

Drill Hole	Li_2O Feed Grade (%)			Li_2O Float Grade (%)			Li_2O Sink Grade (%)			Li_2O HLS Recovery (%)		
	T1	T2	$\bar{x}$	T1	T2	$\bar{x}$	T1	T2	$\bar{x}$	T1	T2	$\bar{x}$
ITDD-22-002T	1.10	1.40	1.25	0.33	0.26	0.29	4.18	3.95	4.06	76.80	88.18	82.50
ITDD-22-023T	1.60	1.48	1.54	0.22	0.23	0.23	5.82	5.55	5.68	89.90	89.30	89.61
ITDD-22-030T	0.83	1.63	1.23	0.38	0.35	0.36	7.13	7.65	7.39	60.40	84.49	72.42
ITDD-22-048T	1.26	0.95	1.10	0.26	0.28	0.27	5.40	5.43	5.41	86.20	78.00	82.08
ITDD-23-083T	1.61	2.14	1.88	0.10	0.14	0.12	6.76	6.33	6.55	95.30	95.93	95.61
ITDD-23-087T	1.53	2.12	1.83	0.38	0.21	0.30	4.96	5.57	5.27	83.20	94.43	88.81
ITDD-23-093T	0.60	0.59	0.60	0.19	0.13	0.16	6.75	6.15	6.45	72.30	81.80	77.06
Composite 1	1.40	-	-	0.27	-	-	4.52	-	-	87.20	-	-
Composite 2	1.33	-	-	0.29	-	-	5.50	-	-	84.40	-	-

Table 13-10: HLS Results for Fine Fraction (−6.35 +0.85 mm)

Drill Hole	Li_2O Feed Grade (%)			Li_2O Float Grade(%)			Li_2O Sink Grade(%)			Li_2O HLS Recovery (%)		
	T1	T2	$\bar{x}$	T1	T2	$\bar{x}$	T1	T2	$\bar{x}$	T1	T2	$\bar{x}$
ITDD-22-002T	1.14	1.07	1.10	0.17	0.17	0.17	5.59	4.98	5.29	88.32	87.71	88.01
ITDD-22-023T	1.59	1.33	1.46	0.22	0.17	0.19	6.75	6.01	6.38	89.57	90.25	89.91
ITDD-22-030T	1.44	1.36	1.40	0.31	0.27	0.29	7.37	6.56	6.96	82.64	84.37	83.51
ITDD-22-048T	0.96	1.00	0.98	0.18	0.13	0.16	6.25	6.83	6.54	85.33	89.91	87.62
ITDD-23-083T	1.45	1.48	1.46	0.12	0.12	0.12	7.15	7.25	7.20	93.48	93.89	93.69
ITDD-23-087T	1.51	1.58	1.54	0.19	0.21	0.20	6.55	6.37	6.46	91.25	90.26	90.76
ITDD-23-093T	1.04	1.19	1.12	0.16	0.15	0.15	6.99	6.74	6.87	87.67	90.48	89.08
Composite 1	1.34	-	-	0.19	-	-	6.74	-	-	89.1	-	-
Composite 2	1.42	-	-	0.18	-	-	6.54	-	-	90.8	-	-

Composite samples were tested to evaluate the combined behaviour of seven drill holes. The composite results fit the polynomial adjustment (Figure 13-13 and Figure 13-14).

The metallurgical recovery polynomial adjustment adherence with the composite results is shown in Figure 13-15, with an $R^2 = 0.89$.

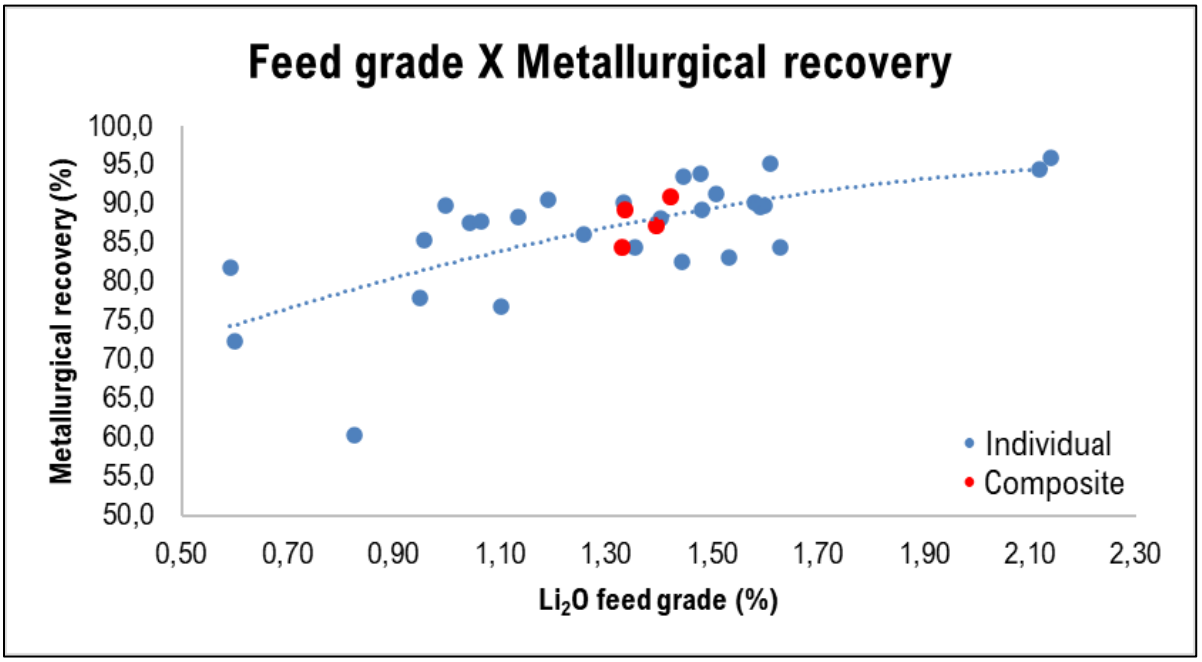


Figure 13-13: HLS Metallurgical Recovery as a Function of Feed Grade

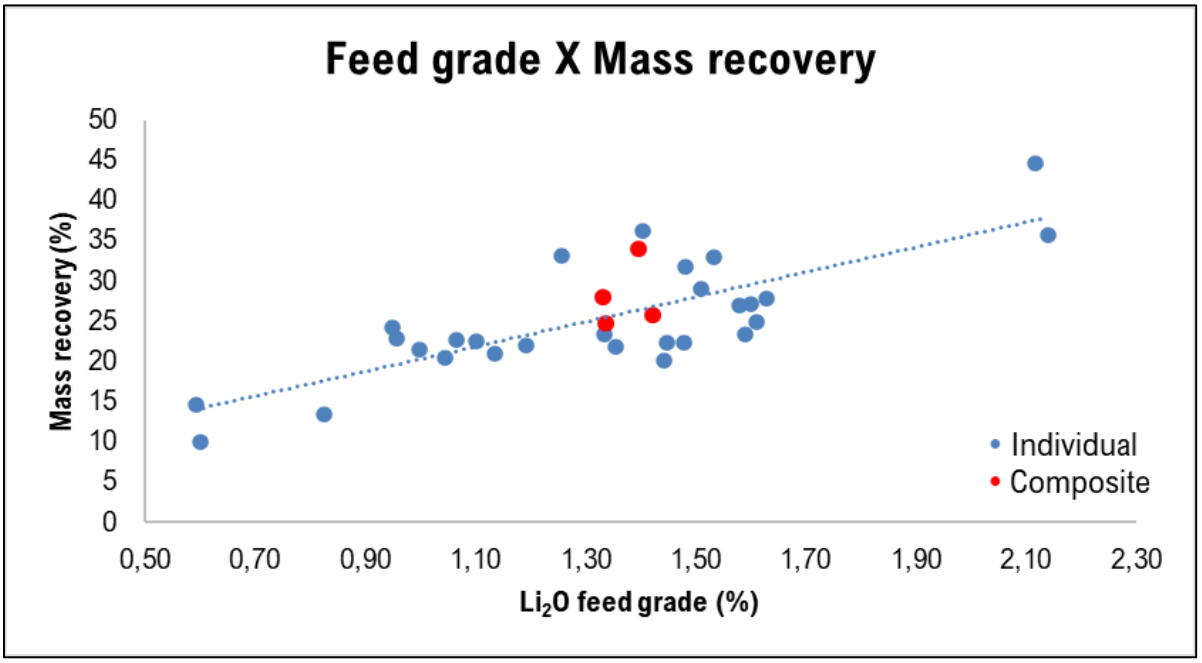


Figure 13-14: HLS Mass Recovery as a Function of Feed Grade

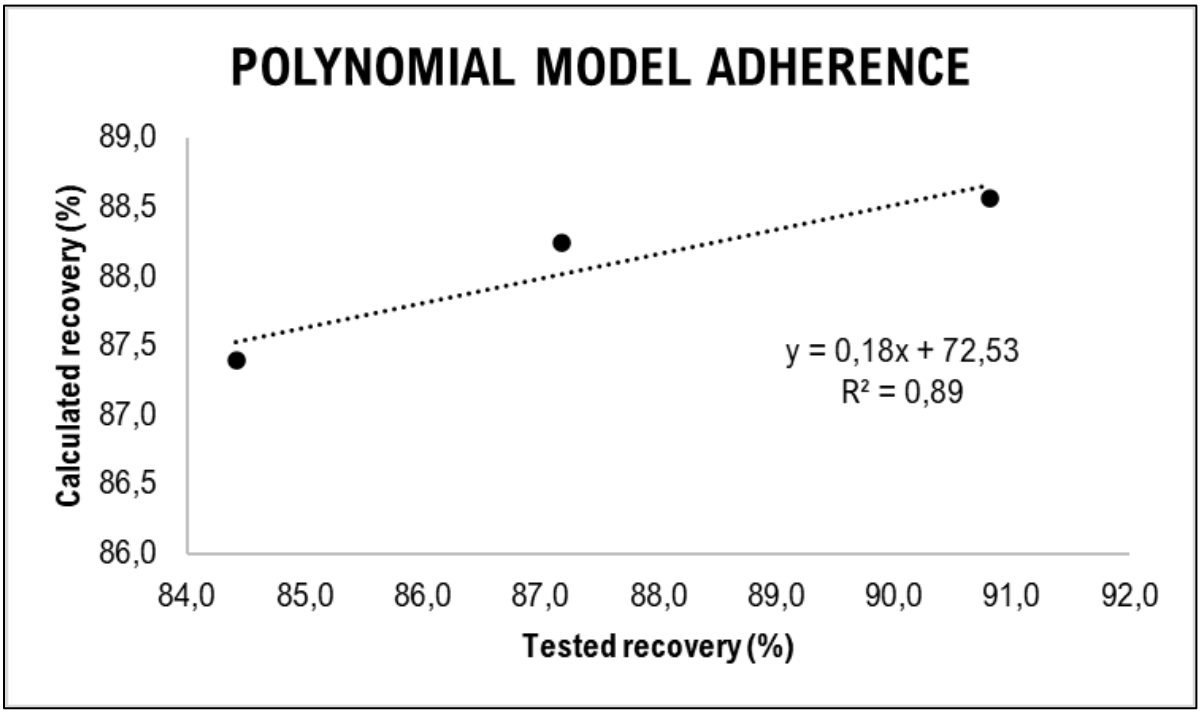


Figure 13-15: Metallurgical Polynomial Model Adherence

All HLS samples were analyzed using XRD to understand the mineralogical behaviour of HLS. The main lithium-bearing minerals found were spodumene, montebrasite, petalite, and elbaite. As shown in Figure 13-16 and Figure 13-17, spodumene is mainly in the concentrate for both particle-size distributions. Montebrasite distribution is presented in Figure 13-18 and Figure 13-19, reported mainly in the tailings fraction. The same behaviour applies to petalite distribution (Figure 13-20 and Figure 13-21). Elbaite distribution has no concentration preference following the mass distribution (Figure 13-22 and Figure 13-23).

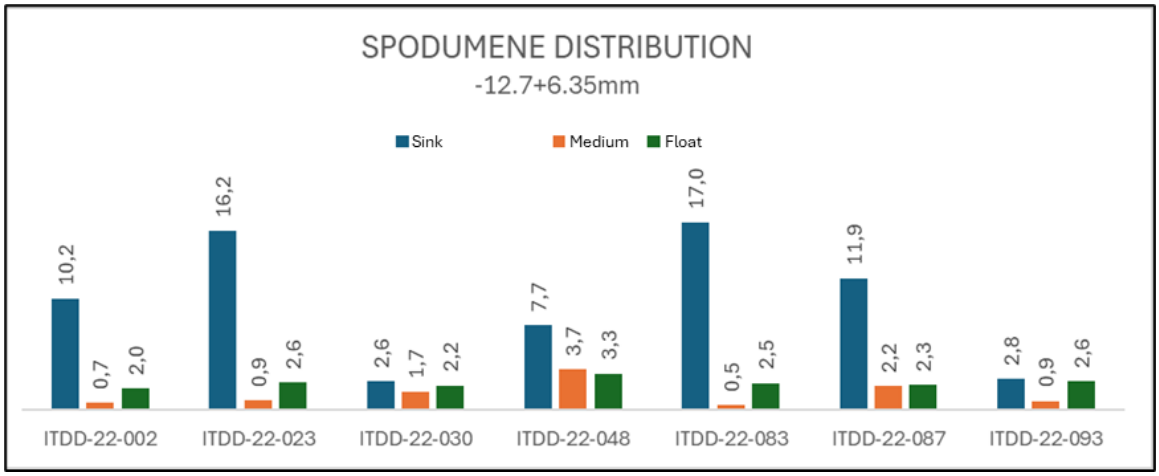


Figure 13-16: Spodumene Mass Distribution in HLS Test for Coarse Material (−12.7 +6.35 mm)

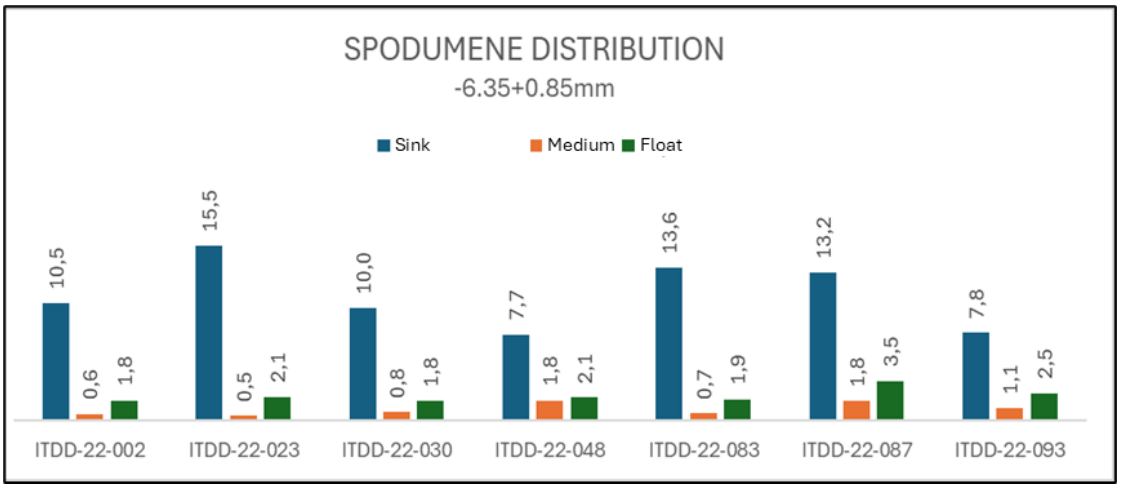


Figure 13-17: Spodumene Mass Distribution in HLS Test for Fine Material (−6.35 +0.85 mm)

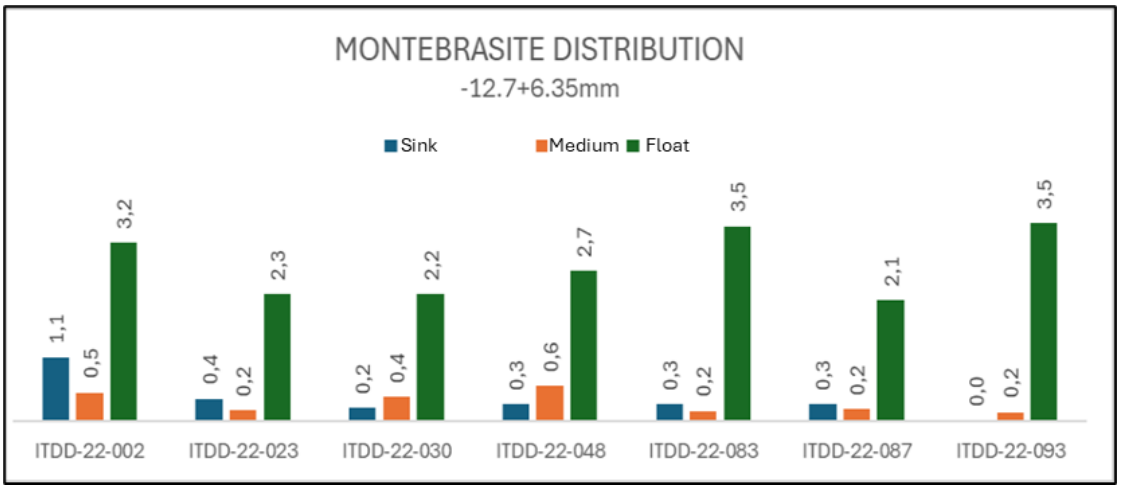


Figure 13-18: Montebrasite Mass Distribution in HLS Test for Coarse Material (−12.7 +6.35 mm)

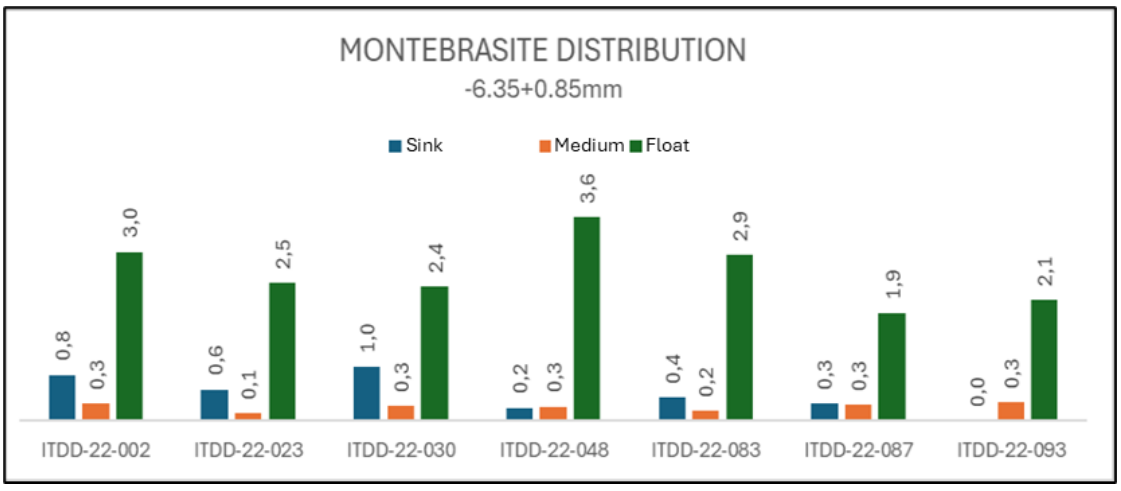


Figure 13-19: Montebrasite Mass Distribution in HLS Test for Fine Material (−6.35 +0.85 mm)

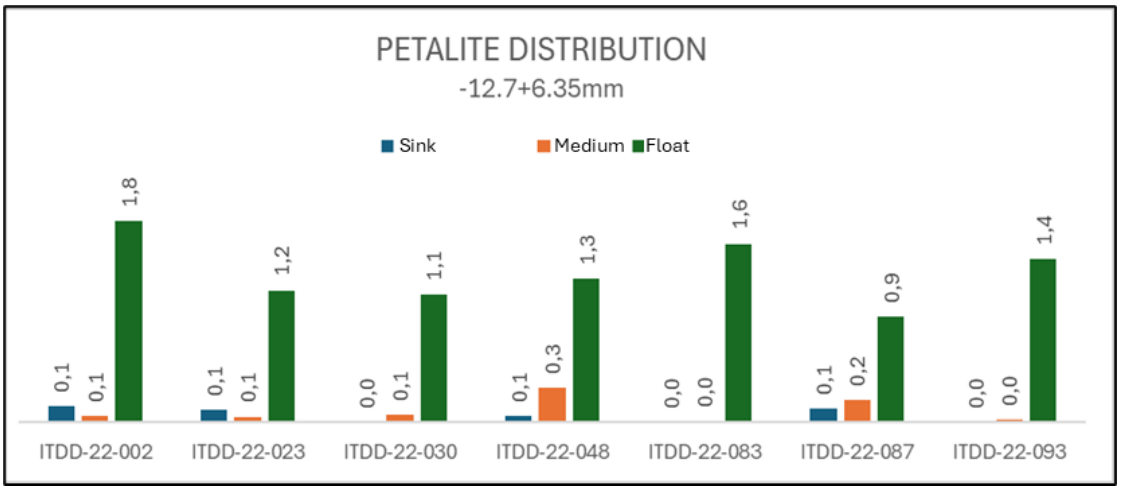


Figure 13-20: Petalite Mass Distribution in HLS Test for Coarse Material (−12.7 +6.35 mm)

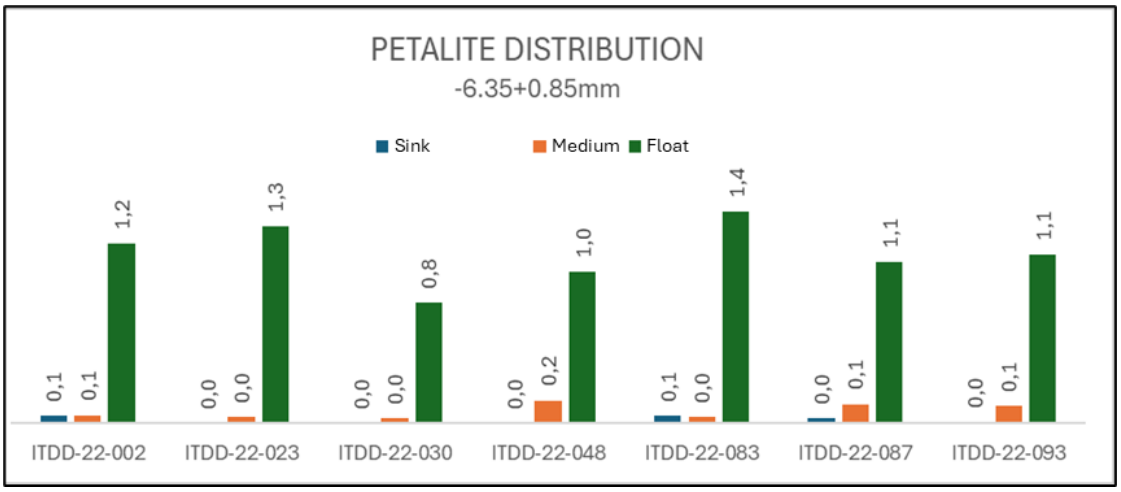


Figure 13-21: Petalite Mass Distribution in HLS Test for Fine Material (−6.35 +0.85 mm)

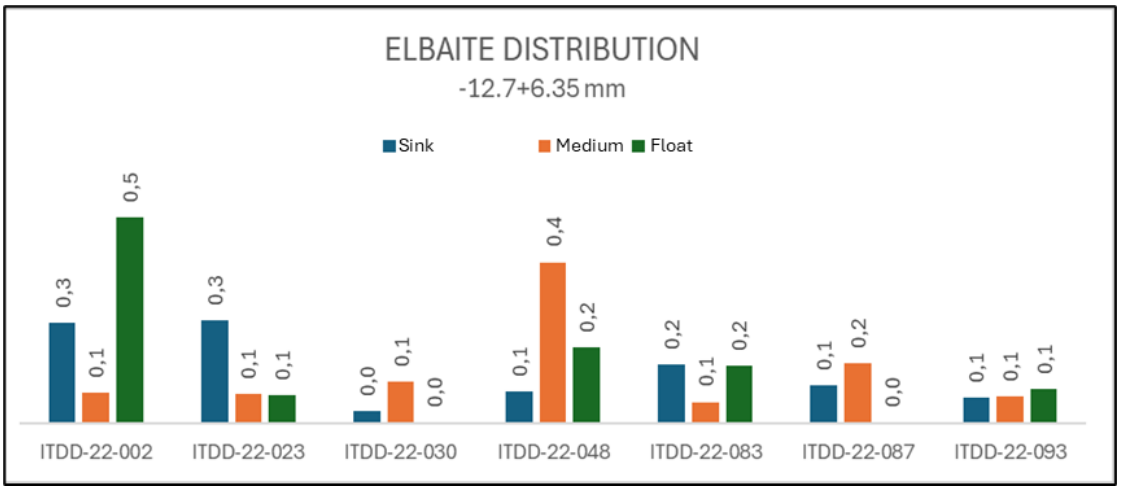


Figure 13-22: Elbaite Mass Distribution in HLS Test for Coarse Material (−12.7 +6.35 mm)

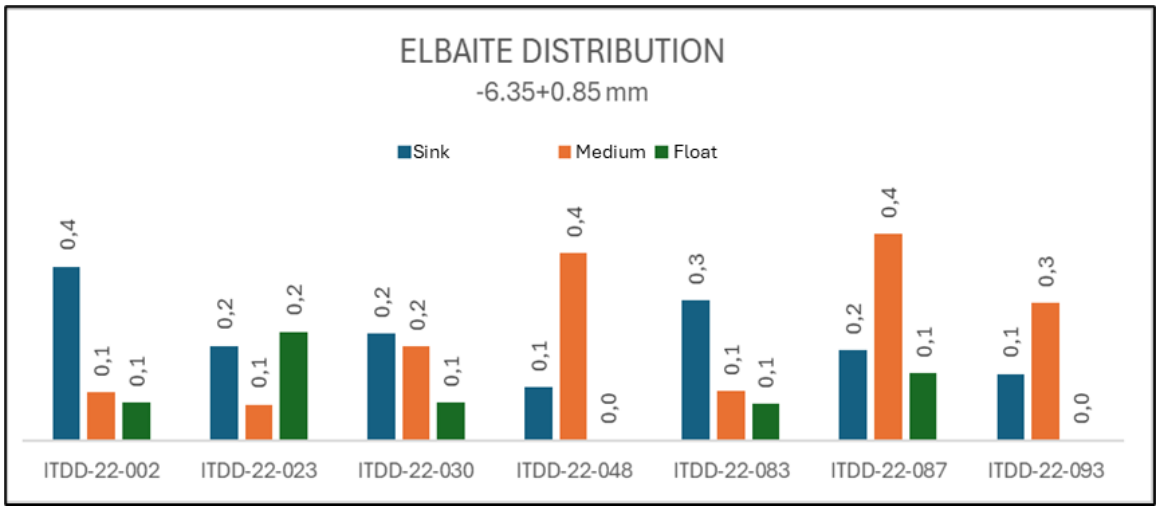


Figure 13-23: Elbaite Mass Distribution in HLS Test for Fine Material (−6.35 +0.85 mm)

Diluted Variability Samples—Ore Sorter and HLS Tests

Figure 13-24 shows the location of the 11 new drill holes (Phase 2 in blue). From among those 11, two (ITDD-23-065 and ITDD-23-073) were sampled at three different depths to evaluate the metallurgical response over the life-of-mine (LOM). Ore sorter tests and HLS were performed for the 15 samples.

Ore sorter tests were done in two particle-size ranges: 31.5 +19.1 mm and 19.1 +7.5 mm. Then, both composites were combined with a size fraction below 7.5 mm that did not pass through the ore sorter concentration. These composite samples were used to perform HLS tests in two particle-size ranges, −12.7 +6.35 mm and −6.35 +0.5 mm; and in three densities, 2.8 g/cm³, 2.7 g/cm³, and 2.45 g/cm³. Ore sorter results are presented in Figure 13-25. Lithium average recovery for the coarse and fine fractions was 93.6% and 92.6%, respectively.

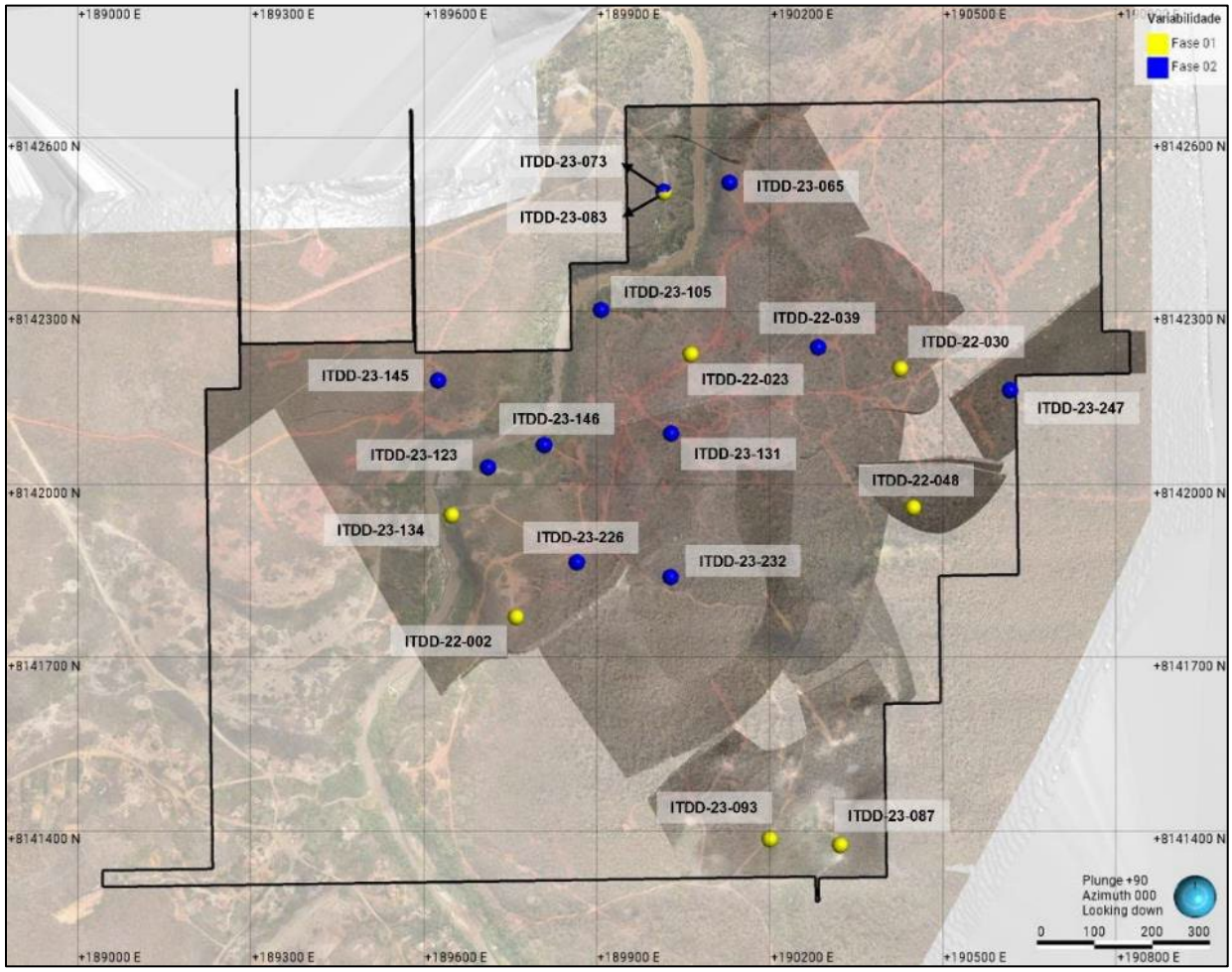


Figure 13-24: Variability Additional Drill-Hole Locations (Phase 2 in Blue)

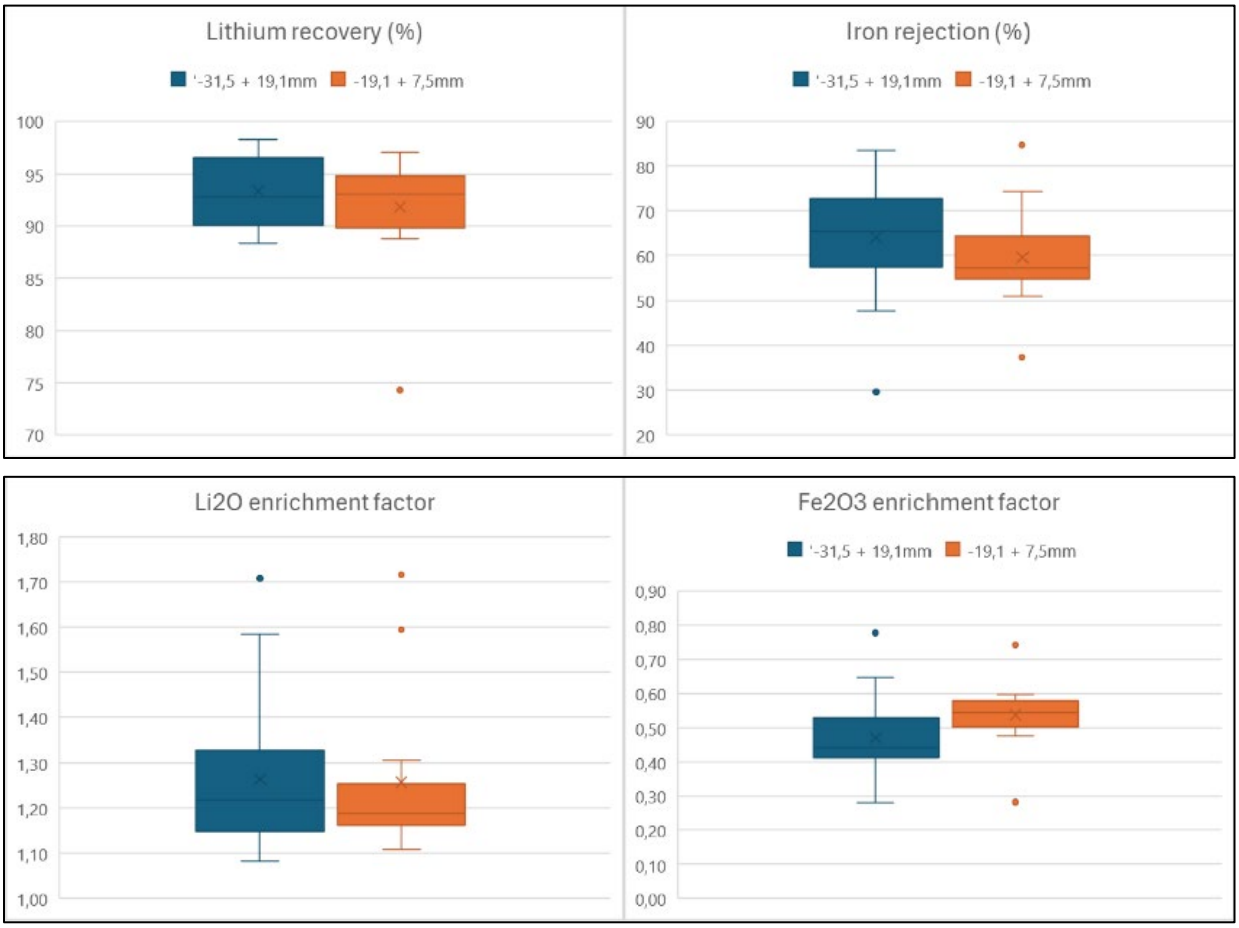


Figure 13-25: Ore Sorter Results for Lithium and Iron

Coarse and fine ore sorter concentrate was combined with the −7.5 + 0.5 mm fine fraction to perform HLS tests. The particle sizes used in HLS were −12.7 +6.35 mm and −6.35 +0.5 mm. A 3-stage circuit was simulated by the HLS test using 2.80, 2.70, and 2.45 g/cm³ fluid density targets. Table 13-11, Table 13-12, and Table 13-13 present the HLS results. Rougher average metallurgical recovery was 77.8%, with 22.1% mass recovery. The scavenger step increases the metallurgical recovery to 86.1%, with 34.0% mass recovery. The polishing step using 2.45 g/cm³ increases average metallurgical recovery to 88.2% and average mass recovery to 34.7%. Figure 13-26 indicates the polishing effect.

Table 13-11: HLS Rougher Step Results

Sample	Size (mm)	Cut-Point (g/cm^3)	Mass Recovery (%)	Met. Recovery (%)	Li_2O Feed (%)	Li_2O Conc. (%)	Li_2O Tailings (%)
ITDD-23-065 270.2 to 277.97	−6.35 +0.5	2.80	28.7	85.1	2.22	6.57	0.46
ITDD-23-065 351.23 to 380.7	−6.35 +0.5	2.80	8.7	47.4	0.97	5.27	0.56
ITDD-23-065 455.28 to 462.88	−6.35 +0.5	2.80	12.4	81.0	0.7	4.59	0.15
ITDD-23-073 76.82 to 84.66	−6.35 +0.5	2.80	25.1	90.0	1.83	6.55	0.24
ITDD-23-073 205.62 to 214.3	−6.35 +0.5	2.80	24.4	88.2	2.01	7.25	0.31
ITDD-23-073 406.21 to 428.35	−6.35 +0.5	2.80	15.0	71.9	1.17	5.60	0.39
ITDD-23-146 266.31 to 277.18	−6.35 +0.5	2.80	19.1	81.7	1.53	6.56	0.35
ITDD-23-145 289.82 to 303.05	−6.35 +0.5	2.80	19.1	82.0	1.59	6.84	0.35
ITDD-23-226 170.61 to 180.57	−6.35 +0.5	2.80	16.4	73.1	1.53	6.83	0.49
ITDD-22-039 85.24 to 96.86	−6.35 +0.5	2.80	25.7	85.4	1.59	5.29	0.31
ITDD-23-247 84.62 to 99.58	−6.35 +0.5	2.80	12.0	79.1	0.81	5.36	0.19
ITDD-23-232 137.7 to 146.95	−6.35 +0.5	2.80	20.6	80.6	1.53	6.00	0.38
ITDD-23-105 219.44 to 230.59	−6.35 +0.5	2.80	14.3	80.4	1.16	6.54	0.27
ITDD-23-123 148.16 to 160.4	−6.35 +0.5	2.80	14.2	81.2	1.08	6.19	0.24
ITDD-23-131 97.48 to 103.88	−6.35 +0.5	2.80	25.4	88.9	1.36	4.76	0.20
ITDD-23-065 270.2 to 277.97	−12.7 +6.35	2.80	44.6	89.7	3.30	6.63	0.61
ITDD-23-065 351.23 to 380.7	−12.7 +6.35	2.80	7.8	37.0	1.07	5.04	0.73
ITDD-23-065 455.28 to 462.88	−12.7 +6.35	2.80	23.5	74.7	0.90	2.85	0.30
ITDD-23-073 76.82 to 84.66	−12.7 +6.35	2.80	30.3	82.9	2.10	5.75	0.51
ITDD-23-073 205.62 to 214.3	−12.7 +6.35	2.80	31.0	85.7	2.25	6.23	0.47
ITDD-23-073 406.21 to 428.35	−12.7 +6.35	2.80	25.2	68.6	1.99	5.41	0.84
ITDD-23-146 266.31 to 277.18	−12.7 +6.35	2.80	29.4	83.9	2.19	6.27	0.50
ITDD-23-145 289.82 to 303.05	−12.7 +6.35	2.80	34.2	83.7	2.03	4.95	0.50
ITDD-23-226 170.61 to 180.57	−12.7 +6.35	2.80	25.1	69.3	2.08	5.73	0.85
ITDD-22-039 85.24 to 96.86	−12.7 +6.35	2.80	31.5	84.7	2.14	5.74	0.48
ITDD-23-247 84.62 to 99.58	−12.7 +6.35	2.80	13.0	64.9	0.87	4.32	0.35
ITDD-23-232 137.7 to 146.95	−12.7 +6.35	2.80	25.8	71.6	1.59	4.42	0.61
ITDD-23-105 219.44 to 230.59	−12.7 +6.35	2.80	14.0	71.0	1.25	6.33	0.42
ITDD-23-123 148.16 to 160.4	−12.7 +6.35	2.80	20.3	84.8	1.65	6.90	0.32
ITDD-23-131 97.48 to 103.88	−12.7 +6.35	2.80	27.2	86.4	1.60	5.07	0.30

Table 13-12: HLS Scavenger Step Results

Sample	Size (mm)	Cut-Point (g/cm³)	Mass Recovery (%)	Met. Recovery (%)	Li_2O Feed (%)	Li_2O Conc. (%)	Li_2O Tailings (%)
ITDD-23-065 270.2 to 277.97	6.35 +0.5	2.70	13.4	32.7	0.46	1.13	0.36
ITDD-23-065 351.23 to 380.7	6.35 +0.5	2.70	5.6	6.2	0.56	0.62	0.55
ITDD-23-065 455.28 to 462.88	6.35 +0.5	2.70	10.9	38.4	0.15	0.53	0.11
ITDD-23-073 76.82 to 84.66	6.35 +0.5	2.70	13.8	44.9	0.24	0.79	0.16
ITDD-23-073 205.62 to 214.3	6.35 +0.5	2.70	8.2	23.5	0.31	0.89	0.26
ITDD-23-073 406.21 to 428.35	6.35 +0.5	2.70	15.5	25.8	0.39	0.64	0.34
ITDD-23-146 266.31 to 277.18	6.35 +0.5	2.70	9.2	25.9	0.35	0.98	0.28
ITDD-23-145 289.82 to 303.05	6.35 +0.5	2.70	15.1	46.5	0.35	1.09	0.22
ITDD-23-226 170.61 to 180.57	6.35 +0.5	2.70	6.5	24.9	0.49	1.89	0.40
ITDD-22-039 85.24 to 96.86	6.35 +0.5	2.70	12.2	48.4	0.31	1.24	0.18
ITDD-23-247 84.62 to 99.58	6.35 +0.5	2.70	9.5	47.7	0.19	0.97	0.11
ITDD-23-232 137.7 to 146.95	6.35 +0.5	2.70	14.7	62.8	0.38	1.60	0.16
ITDD-23-105 219.44 to 230.59	6.35 +0.5	2.70	14.6	47.7	0.27	0.87	0.16
ITDD-23-123 148.16 to 160.4	6.35 +0.5	2.70	13.5	43.9	0.24	0.77	0.15
ITDD-23-131 97.48 to 103.88	6.35 +0.5	2.70	38.7	75.3	0.20	0.39	0.08
ITDD-23-065 270.2 to 277.97	−12.7 +6.35	2.70	18.1	50.7	0.61	1.72	0.37
ITDD-23-065 351.23 to 380.7	−12.7 +6.35	2.70	6.4	12.4	0.73	1.41	0.68
ITDD-23-065 455.28 to 462.88	−12.7 +6.35	2.70	20.9	71.9	0.30	1.02	0.11
ITDD-23-073 76.82 to 84.66	−12.7 +6.35	2.70	11.4	18.4	0.51	0.83	0.47
ITDD-23-073 205.62 to 214.3	−12.7 +6.35	2.70	8.7	27.9	0.47	1.49	0.37
ITDD-23-073 406.21 to 428.35	−12.7 +6.35	2.70	28.9	45.2	0.84	1.31	0.65
ITDD-23-146 266.31 to 277.18	−12.7 +6.35	2.70	13.7	45.2	0.50	1.64	0.32
ITDD-23-145 289.82 to 303.05	−12.7 +6.35	2.70	17.4	36.8	0.50	1.06	0.38
ITDD-23-226 170.61 to 180.57	−12.7 +6.35	2.70	13.5	49.5	0.85	3.12	0.50
ITDD-22-039 85.24 to 96.86	−12.7 +6.35	2.70	10.4	46.9	0.48	2.17	0.28
ITDD-23-247 84.62 to 99.58	−12.7 +6.35	2.70	11.3	52.8	0.35	1.64	0.19
ITDD-23-232 137.7 to 146.95	−12.7 +6.35	2.70	19.7	57.8	0.61	1.79	0.32
ITDD-23-105 219.44 to 230.59	−12.7 +6.35	2.70	19.1	46.9	0.42	1.04	0.28
ITDD-23-123 148.16 to 160.4	−12.7 +6.35	2.70	19.8	29.5	0.32	0.47	0.28
ITDD-23-131 97.48 to 103.88	−12.7 +6.35	2.70	45.9	12.7	0.30	0.08	0.48

Table 13-13: Polishing HLS Results

Sample	Size (mm)	Cut-Point (g/cm³)	Mass Recovery (%)	Met. Recovery (%)	Li_2O Feed (%)	Li_2O Conc. (%)	Li_2O Tailings (%)
ITDD-23-065 270.2 to 277.97	−6.35 +0.5	2.45	2.3	27.4	0.36	4.22	0.27
ITDD-23-065 351.23 to 380.7	−6.35 +0.5	2.45	5.7	48.8	0.55	4.72	0.30
ITDD-23-073 205.62 to 214.3	−6.35 +0.5	2.45	0.8	6.6	0.26	2.05	0.24
ITDD-23-073 406.21 to 428.35	−6.35 +0.5	2.45	1.0	13.5	0.34	4.84	0.30
ITDD-23-065 351.23 to 380.7	−12.7 +6.35	2.45	8.9	49.4	0.68	3.79	0.38
ITDD-23-073 205.62 to 214.3	−12.7 +6.35	2.45	2.2	6.2	0.37	1.06	0.36
ITDD-23-073 406.21 to 428.35	−12.7 +6.35	2.45	4.5	30.7	0.65	4.45	0.47

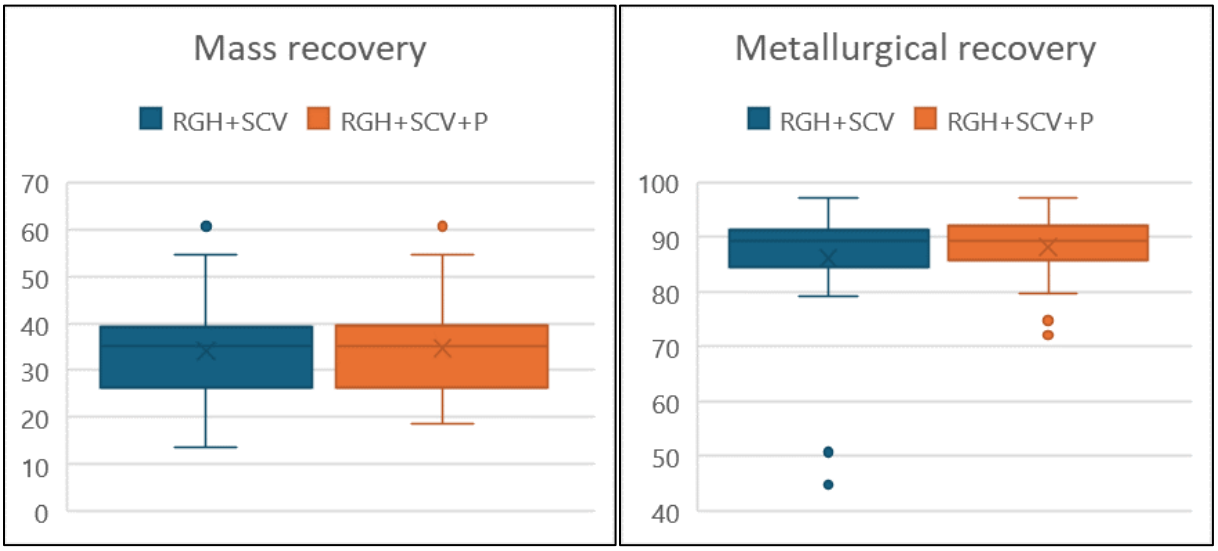


Figure 13-26: Comparative Recovery for 2-Stage and 3-Stage Circuits (−12.7 mm +0.5 mm)

Diluted Variability Samples—HLS Tests

After the sample preparation procedure presented in Figure 13-8 the sample was submitted to HLS test to simulate the flowsheet, as shown in Figure 13-27. The first HLS step was at 2.65 g/cm³, then the concentrate was screened in 6.4 and 0.6 mm. The fractions −15.9 +6.4 and −6.4 +0.6 mm, were sent to HLS test at 2.85 g/cm³. The floats from the coarse fraction were recrushed at a 6.4 mm top size and screened in 0.6 mm, before being sent to HLS at 2.90 g/cm³.

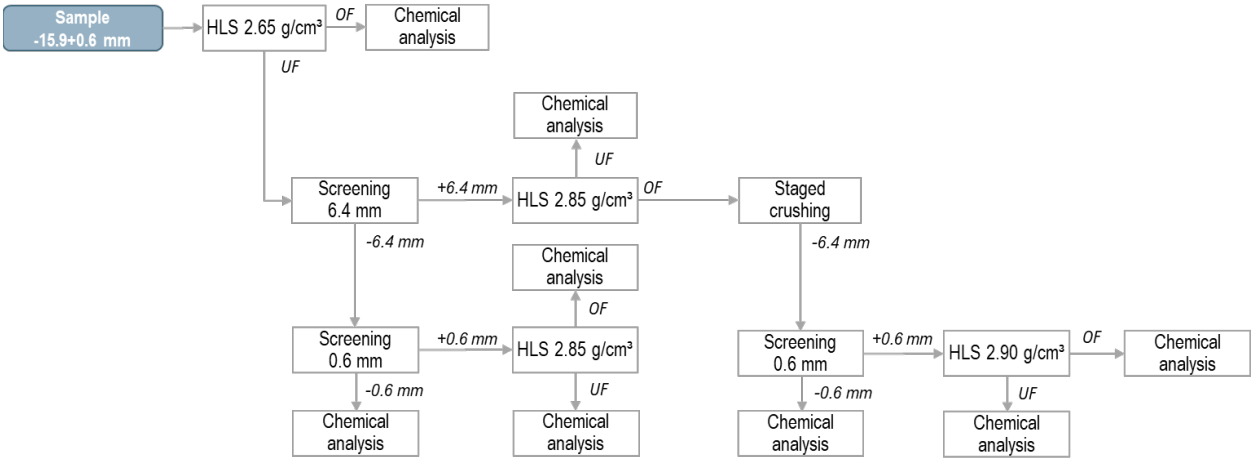


Figure 13-27: HLS Test to Simulate the Flowsheet DMS Operations

Table 13-14 presents the results of the HLS test conducted to simulate the Bandeira DMS plant, using samples from four drill holes. Fines generation during sample preparation ranged from 10% to 12%; however, this figure is expected to be slightly higher, around 18%, in the plant's crushing circuit. Lithium oxide losses in the HLS tests averaged 30% (Table 13-14), while plant operations are expected to achieve lower Li_2O losses of 20% (Table 13-14) inside of the DMS circuit. The lithium oxide grade of the HLS concentrate was higher than anticipated, particularly in the secondary and

recrush stages, with values exceeding 6.0%. However, iron oxide levels in all products were outside of specification.

Based on these results, a decision was made to perform an additional HLS test using a single 5 kg composite sample composed of 25% mass from each drill hole. The cut density for the HLS secondary fines was reduced from 2.85 to 2.80 g/cm³, and the density for the recrush HLS was also reduced, from 2.90 g/cm³ to 2.80 g/cm³. However, this additional test presented concentrate grade below specification.

Table 13-14: HLS Results Simulating the Process Flowsheet

Average	Mass Distribution (%)	Li_2O Content (%)	Li_2O Distribution (%)	Fe_2O_3 Content (%)	Fe_2O_3 Distribution (%)
Test Feed	100.00	1.20	100.00	1.50	100.00
Sample Prep-Fines (-0.60 mm)	10.38	1.00	8.67	1.99	13.72
HLS Feed	89.62	1.22	91.33	1.44	86.28
Sinks (SPO Conc.)	14.24	5.35	63.35	2.12	19.49
HLS Coarse	8.12	4.66	31.51	2.58	14.18
HLS Fines	4.52	6.31	23.59	1.52	3.97
HLS Recrush	1.60	6.13	8.24	1.47	1.34
Floats (HLS Tailings)	72.23	0.39	23.78	1.21	57.22
HLS Primary	49.83	0.17	7.31	0.20	7.04
HLS Fines	7.92	1.08	6.93	3.72	20.25
HLS Recrush	14.48	0.78	9.55	3.29	29.92
Fines Generation	3.18	1.45	4.20	4.50	9.57
Recrush	2.97	1.49	4.04	4.51	8.95
Screen	0.22	0.82	0.17	4.34	0.62
Reconciliation	100	-	100	0	100
Global Concentrate	14.24	5.35	63.35	2.12	19.49

Note: SPO = spodumene

Figure 13-28 shows the sinks of the HLS at 2.85 g/cm³ for each drill hole. In general, the schists were not concentrated at 2.85 g/cm³ for both size fractions, except for drill hole ITDD-23-141.



Figure 13-28: Flowsheet HLS Products (left to right: ITDD-23-063, ITDD-23-141, ITDD-23-209, ITDD-23-215)

13.3.4 Flotation Testing

Early in the test campaign, flotation was investigated as a possible alternative to gravity separation or as an addition to the gravity plant to process gravity waste-streams. Preliminary flotation tests were done in 2023 on lower-grade samples from the Bandeira deposit.

After grinding to 150 µm, whereas good recoveries were achieved, the concentrate grades were low; as a result, the focus of the flowsheet development was centred on gravity DMS.

Indicative flotation results are shown in Table 13-15.

Table 13-15: Indicative Flotation Results

	Head % Li_2O	Concentrate % Li_2O	Tailings % Li_2O	Recovery % Li_2O
Bandeira	1.56	4.69	0.58	90.3

At the end of the test campaign, further flotation tests were done in August 2025 to demonstrate whether flotation was viable as an add-on process to recover lithium from DMS waste streams and fines generated in crushing.

The 0.6 mm fines were chosen for the tests; they were ground to 150 µm and tested in a locked-cycle configuration. Encouraging results were obtained, as summarized in Table 13-16.

Table 13-16: Flotation Locked Cycle Test Results—Eight Cycles

	Li_2O (%)	Fe_2O_3 (%)	Nb (ppm)	Sn (ppm)	Ta (ppm)
Feed	1.02	0.60	200	404	126
Concentrate	5.94	2.56	1,890	1,673	1,109
Tailings	0.45	0.37	4.73	257	12.1
Met. Rec. (%)	60.6	44	98	43	91

Of interest is the recovery of potentially economic values of tantalum, niobium, and tin. Flotation recovery remains as a future opportunity to further enhance the designed performance of the Project concentrator.

The proposed flowsheet includes floats and rejects within the DMS circuit that contain recoverable lithium oxide grades and should be stored separately from the primary floats. These materials—comprising fines floats, recrush floats, and recrush fines—can be combined with fines smaller than 0.6 mm and processed in a flotation plant to produce additional spodumene concentrate.

13.3.5 Vendor Tests

Testwork conducted by vendors comprises:

- Ore sorting
- Bond crushing (impact) work index (CWi)
- Crushing equipment to determine Bond ball mill work index (BWi), ore abrasiveness, and equipment working capacity
- Sedimentation tests for thickening
- Filtration tests for fines filtration
- Upgrading fines by spirals.

Ore Sorter at TOMRA

A composite sample from six drill holes (ITDD-22-013, -015, -029, -032, -035, and 036) with lithium oxide content ranging from 1.31% to 1.52% was sent to TOMRA in Germany to evaluate the applicability of the ore sorter in the pre-concentration stage. The material was crushed to achieve P_{100} 31.5 mm and separated into three particle-size ranges (−31.5 +19.1 mm, −19.1 +9.5 mm, and −9.5 mm). Tests were conducted on two particle-size ranges −31.5 +19.1 mm and −19.1 +9.5 mm, while the −9.5 mm material was weighed, and its content determined to complete the mass and metal content balance of the test. A preliminary sample analysis indicated the use of an X-ray transmission (XRT) sensor for conducting the test.

The ore sorter tests were conducted using the principle of cascade classification (Figure 13-29).

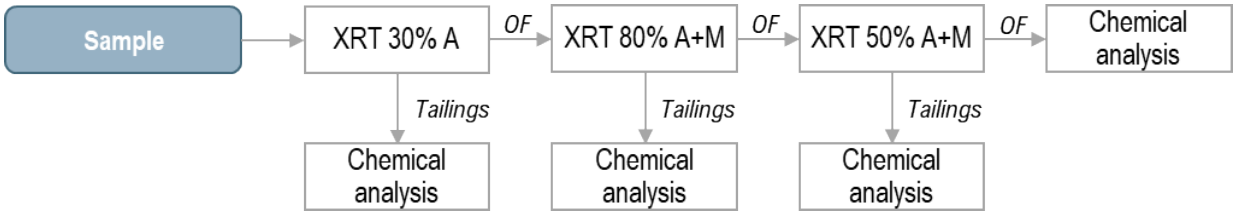


Figure 13-29: Ore Sorter Test Procedure Using XRT Sensor

The results obtained for the particle-size ranges of −31.5 +19.1 mm and −19.1 +9.5 mm are presented in Table 13-17 and Table 13-18, respectively. The −9.5 mm fraction accounted for 16.9% of the mass, which will be sent to the dense-medium concentration stage. From the results, it is possible to see that with a decrease in the ore-sorter's average atomic density cut-off, the concentrate grade increases,

and the metallurgical recovery decreases for both particle-size ranges. Therefore, Configuration 2 was selected as the most promising, as it could enrich the feed grade by 25% to 26%, recovering 91% to 94% of the lithium.

Table 13-17: Ore Sorter Results for the −31.5 +19.1 mm Size Fraction

Configuration	Mass Reduction (%)	Conc. Li_2O Grade (%)	Reject Li_2O Grade (%)	Li_2O Recovery (%)	Enrichment (%)
1	17.15	1.46	0.23	96.85	17
2	24.81	1.56	0.30	93.97	25
3	48.43	1.74	0.73	71.69	39

Table 13-18: Ore Sorter Results for the −19.1 + 9.5 mm Size Fraction

Configuration	Mass Reduction (%)	Conc. Li_2O Grade (%)	Reject Li_2O Grade (%)	Li_2O Recovery (%)	Enrichment (%)
1	16.49	1.52	0.29	96.37	16
2	26.86	1.65	0.43	91.26	26
3	55.01	1.95	0.80	66.51	50

Subsequently, tests were conducted at TOMRA to evaluate the effect of dilution with shale on the equipment's performance. For this purpose, two drill holes were selected, ITDD-22-054 and ITDD-22-098, with 10% dilution at the intersection with the pegmatite. The samples were crushed to achieve P_{100} 31.5 mm and separated into four particle-size ranges (−31.5 +19.1 mm, −19.1 +9.5 mm, −9.5 mm +0.85 mm, and −0.85 mm). Tests were conducted for two particle-size ranges, −31.5 +19.1 mm and −19.1 +9.5 mm, while the material from the other size ranges was weighed, and its content was determined to complete the metallurgical balance.

The tests used the same cascade classification principle previously applied (Figure 13-29). Table 13-19 and Table 13-20 present the results of the ore-sorter test for the particle-size range −19.1 +9.5 mm for the two drill holes. It is possible to observe that the results obtained for both samples were similar and indicate that Configuration 1 is the most suitable. This is because, in this set-up, enrichment between 19% and 20% was achieved with 94% to 96% recovery.

Table 13-19: Ore Sorter Results for the −19.1 +9.5 mm Size Fraction (ITDD-22-054)

Configuration	Mass Reduction (%)	Conc. Li_2O Grade (%)	Reject Li_2O Grade (%)	Li_2O Recovery (%)	Enrichment (%)
1	20.81	1.77	0.43	94.00	19
2	27.15	1.83	0.56	89.83	23
3	50.68	2.29	0.70	76.09	54

Table 13-20: Ore Sorter Results for the Size Fraction of −19.1 +9.5 mm (ITDD-22-098)

Configuration	Mass Reduction (%)	Conc. Li_2O Grade (%)	Reject Li_2O Grade (%)	Li_2O Recovery (%)	Enrichment (%)
1	19.90	1.61	0.26	96.19	20
2	30.89	1.72	0.48	88.94	29
3	54.45	1.98	0.80	67.28	48

The results for the particle-size range −31.5 +19.1 mm are presented in Table 13-21 and

Table 13-22 for drill holes ITDD-22-054 and ITDD-22-098, respectively. There were discrepancies in the results between the two samples for the coarse particle-size range despite the difference in lithium oxide content in the test feed being less than 5% (1.31% for ITDD-22-054 and 1.26% for ITDD-22-098). Since a) no significant variation was observed in the results of the tests with and without dilution for the particle-size range of −19.1 +9.5 mm, and b) no relevant effect of particle size on the undiluted test was observed, the result of drill-hole ITDD-22-054 for coarse particle size was not considered in the ore sorter application analysis, as it differs from the other results obtained. Therefore, the second configuration is the most interesting, as it recovered almost 93% of lithium, with an enrichment of 17%.

Table 13-21: Ore Sorter Results for the −31.5 +19.1 mm Size Fraction (ITDD-22-054)

Configuration	Mass Reduction (%)	Conc. Li_2O Grade (%)	Reject Li_2O Grade (%)	Li_2O Recovery (%)	Enrichment (%)
1	21.35	1.47	0.74	87.97	12
2	30.63	1.62	0.62	85.54	23
3	48.03	1.93	0.65	76.32	47

Table 13-22: Ore Sorter Results for the −31.5 +19 mm Size Fraction (ITDD-22-098)

Configuration	Mass Reduction (%)	Conc. Li_2O Grade (%)	Reject Li_2O Grade (%)	Li_2O Recovery (%)	Enrichment (%)
1	14.90	1.39	0.49	94.17	11
2	20.71	1.47	0.43	92.84	17
3	42.17	1.70	0.65	78.24	35

Steinert Ore Sorting

Further to the ore sorting work at TOMRA, further testing was done at Steinert, where a pilot-scale test was conducted. The details and results of this test are discussed in Section 13.4.1.

SGS Chile—Crushability Work Index

The Bond low-energy impact test was conducted at SGS Chile to determine the CWi, a factor indicating the power required for crushing. For the assay, 20 pieces cut to a thickness of 51 mm were sent. Each specimen was subjected to the impact of two hammers mounted on a pendulum. The test was repeated, increasing the pendulum angle and, therefore, increasing the impact until the sample

fractured. CWi results vary from 4.1 kWh/t to 10.2 kWh/t. The average result was 7.0 kWh/t, characterizing a medium CWi. Table 13-23 and

Table 13-24 give the results obtained for this test.

Table 13-23: Average CWi Results for the Bond Low-Energy Impact Tests

Specimen No.	Impact Energy (Joules)	Work Index (kWh/t)
1	14.9	5.9
2	10.4	4.1
3	14.9	5.9
4	10.4	4.1
5	14.9	5.9
6	26	10.2
7	26	10.2
8	20.1	7.9
9	10.4	4.1
10	26	10.2
11	10.4	4.1
12	14.9	5.9
13	26	10.2
14	26	10.2
15	20.1	7.9
16	14.9	5.9
17	14.9	5.9
18	20.1	7.9
19	20.1	7.9
20	14.9	5.9

Table 13-24: Bond Low-Energy Impact Testwork Statistics

Parameter	kWh/t
Maximum Impact Work Index	10.2
Minimum Impact Work Index	4.1
Average Impact Work Index	7
Standard Deviation	2.3

The specific gravity of the specimens was 2.68 g/cm^3.

Metso Outotec Crushability Tests

Metso Outotec performed crushability tests to define crushing size with three composite samples of a minimum of 50 kg. The material was classified as abrasive and very easy to crush (Table 13-25). In general, the results did not vary between the composite samples.

Table 13-25: Crushability Tests Results

	Composite 1	Composite 2	Composite 3
Samples	ITDD-22-023T/030T and ITDD-23-083T	ITDD-22-048T	ITDD-23-093T/087T
Abrasion Index (Bond)	Average (0.295 g)	Average (0.300 g)	Average (0.212 g)
Abrasion Index (Macon)	Abrasive (1,698 g/t)	Abrasive (1,602 g/t)	Abrasive (1,600 g/t)
Crushability (Macon)	69.0 % (very easy)	68.8% (very easy)	79.0 % (very easy)
Work index (Bond)	Average (12.25 kWh/st)	Average (11.35 kWh/st)	Average (10.50 kWh/st)
Bulk Density	1.56 t/m³	1.61 t/m³	1.60 t/m³
Specific Gravity	2.66 t/m³	2.71 t/m³	2.70 t/m³
Jaw CrusherCrushability	Crusher 75 x 50 mm—Smooth Jaw Plates. CSS=4.5 mm—Load Cell on Toggle	Crusher 75 x 50 mm—Smooth Jaw Plates. CSS=4.5 mm—Load Cell on Toggle	Crusher 75 x 5 0 mm—Smooth Jaw Plates. CSS=4.5 mm—Load Cell on Toggle
Volumetric Capacity Index	Standard methods (107.84%)	Standard methods (107.40%)	Maximum value (116.47%)
Strength Index	Smallest leaflet setting (96.21%)	Smallest leaflet setting (106.96%)	Minimum setting reduced 20% (88.57%)
Product FlakinessIndex	Cubical material (13.29 %)	Cubical material (5.45%)	Cubical material (4.91%)

Steinert Magnetic Separation at Concentrate

A spodumene HLS concentrate, produced by simulating the DMS process flowsheet (Figure 13-27), was blended to generate a composite sample. This composite reported a lithium oxide grade of 5.40% and an iron oxide grade of 2.06%. The sample was sent to Steinert in Germany for High Gradient Magnetic Separation (HGMS) testing, with the objective of removing biotite schists and reducing the iron oxide content to below 1.0%, in line with market specifications. Figure 13-30 presents the mass balance for the test, along with images of the magnetic and non-magnetic fractions. The results clearly indicate that the equipment is significantly more effective for processing fine fractions below 3.4 mm.

Magnetic Separation at Steinert - Cologne, Germany		
Equipment: HGS - Magnetic Separator of High Gradient		
Magnetic Field: 14.000 Gauss		
	Mass, Kg	Dist., %
Coarse Fraction: 15.9 + 3.4mm	1.43	100.00
Magnetic material	0.11	7.69
Non Magnetic material	1.32	92.31
Fines Fraction: 3.4 + 0.6mm	0.61	100.00
Magnetic material	0.07	11.48
Non Magnetic material	0.54	88.52
Blended Coarse + Fines: 15.9 + 0.6mm	2.03	100.00
Magnetic material	0.12	5.91
Non Magnetic material	1.91	94.09



Figure 13-30: HGS Steinert Magnetic Separation Results

Magnetic and non-magnetic fractions of the blended (coarse and fine) sample presented the following chemical analysis (Table 13-26).

Table 13-26: HGS Magnetic Separation Chemical Results for the Blended Sample

Products	Mass (%)	Li_2O (%)	Li_2O Distr. (%)	Fe_2O_3 (%)	Fe_2O_3 Distr. (%)
Feed Analyzed	100	5.41	100	1.96	100
Non-Magnetic	94.09	5.73	99.20	0.70	53.46
Magnetic	5.91	0.74	0.80	9.70	46.54
Calculated	-	5.44	-	1.23	-
Li_2O Enrichment Factor	-	1.05	-	-	-

Magnetic separation presents a good result, removing 46.54% of iron oxide from the HLS concentrate producing a non-magnetic concentrate with 5.73% Li_2O and 0.70% Fe_2O_3 and metallurgical recovery of 99.20%. Lithium losses on the magnetic fraction are a contamination associated with the biotite–schists.

Steinert recommends using this equipment for size fractions from 0.2 mm to 10 mm and moisture content up to 5%. The results of the four HLS tests showed concentrate grades with lithium oxide slightly above the specification of 5.2% and iron oxide below the limit of 1.0%. However, magnetic separation demonstrated the capability to remove more than half of the iron oxide content, thereby bringing the iron oxide grade within specification. The lithium oxide grade was also increased by approximately 5% due to the removal of certain material fractions.

Delkor Thickening and Filtration Tests

Several thickening and filtration tests were done throughout the test series, but only the latest, done in July 2025, is reported here. This test was done after the crush size of 15.9 mm and bottom cut-off size of 0.6 mm were decided on.

Delkor conducted the tests using fines (<0.6 mm) generated during sample preparation of the four PQ core samples for Phase 3 HLS tests.

Sedimentation Test for Thickening

Sedimentation test conditions and results were:

- Ore top size: 0.6 mm
- Slurry solids content: 6.5% CwS
- pH: 8.8
- Underflow solids content: 55% to 60%
- Residence time (minutes): 30
- Overflow turbidity (NTU): <200
- Floculant: SNF Flonex 920SHR at 0.25 g/L
- Recommended dosage rate: 10 g/t
- Coagulant: not required
- Thickener technology: Ultra Sep

- Sedimentation rate: >20 m/h
- Rise Rate Internal: 8.56 m/h
- Thickener diameter calculated: 12 m for 62.62 t/h of solids.

Filtration

Filtration test conditions and results were:

- Filter element: Sefar ML05-C045
- Cake thickness: 20–30 mm
- Cake formation time: 2–10 sec
- Drying factor: 1.0
- Drying time: 30–50 sec
- Total cycle: 0.6–0.9 min
- Cake moisture: 15%
- Total Unfiltered Fraction (TUF): 2,350 kg/h.m^2
- Project feed rate: 62.62 t/h
- Required filtration area (m^2): 26.35 m^2
- Solids in the filtrate (%): <1.0%
- Selected filter model/available filtration area (m^2): Horizontal Belt Filter Model 24B/04-30V (27m^2).

13.3.6 Upgrading Fines by Gravity

In December 2024, Mineral Technologies performed a preliminary investigation into upgrading fines using spirals. The objective was to produce a concentrate grade of 3% Li_2O at a recovery of 60%.

The feed material had a particle-size distribution of nominally −0.85 mm (100% −2 mm and 80% −0.75 mm.) and a head grade of 1.05% Li_2O.

The spirals were run in a rougher/cleaner configuration. Results obtained are shown in Table 13-27.

Table 13-27: Spirals Results for Fines Concentration

Test	Mass Recovery (%)	Concentrate Grade (% Li_2O)	Lithium Recovery (%)
1	30.2	1.81	52.2
2	57.8	1.40	80.7
3	12.7	2.14	31.9
4	31.4	1.89	61.4

These results are consistent with other testwork the QPs are familiar with. Generally, spodumene does not upgrade very well on spirals.

The recovery of other potentially commercial metals like tantalum, niobium, and tin were not considered, and in view of the results obtained in flotation tests, the mineral recovery represents an opportunity.

13.4 Pilot Plant—Ore Sorter (Steinert) and Dense Media Separation (SGS Geosol)

After completing the variability study of samples from seven drill holes, a bulk reserve of the composite was tested using ore sorter equipment and the SGS Geosol DMS pilot plant (Figure 13-31). An additional composite sample was used to perform HLS tests by size to evaluate spodumene liberation.

13.4.1 Ore Sorter Pilot Plant and HLS

Ore sorter tests were performed using the flowsheet shown in Figure 13-31. For the coarse material (−25.4 +6.35 mm), each sample had a mass of around 7 kg. Two samples were tested individually, and the other five samples were compiled into one bulk sample to improve test representativeness. The −12.7 +6.35 mm material was tested individually.

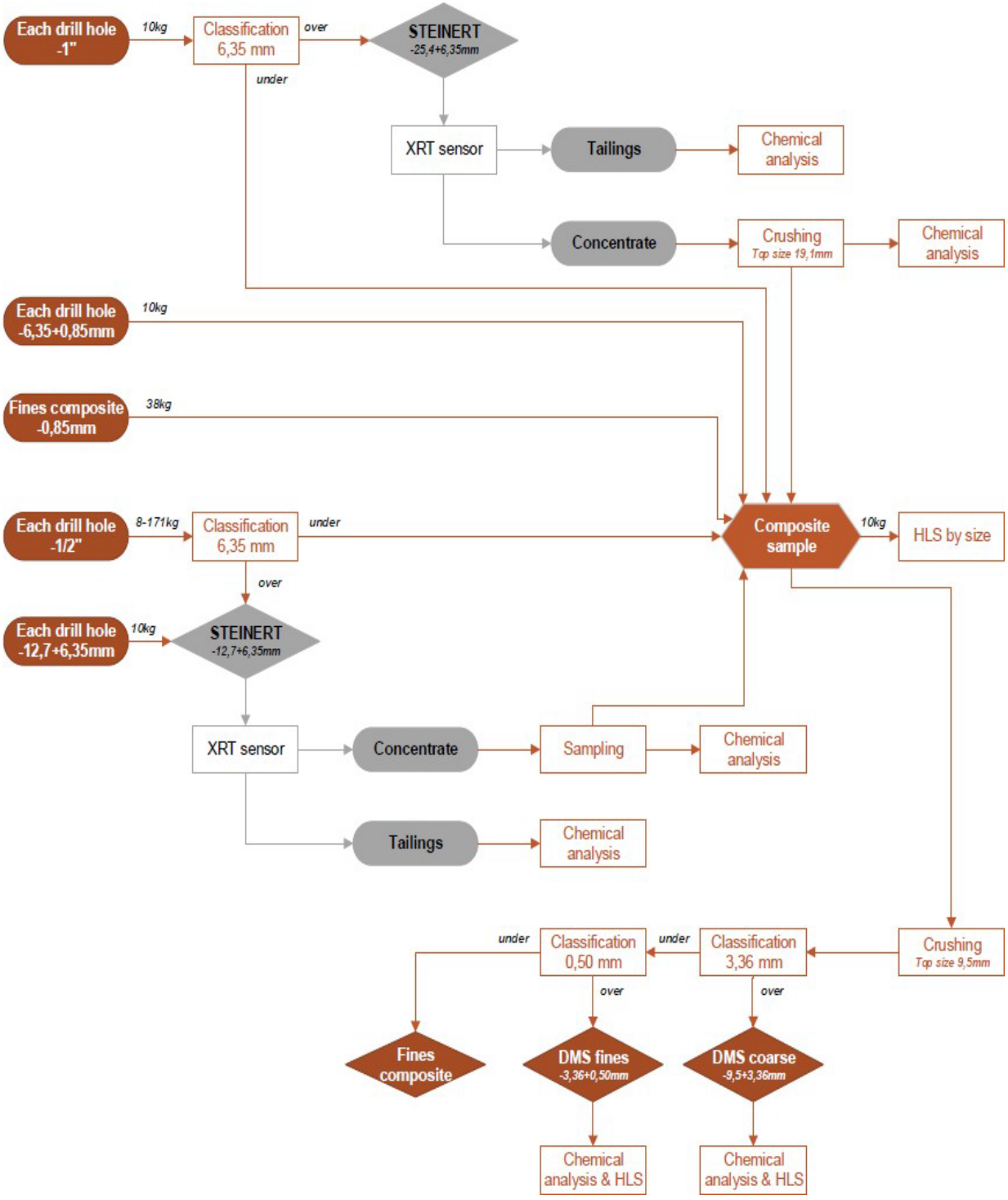


Figure 13-31: Pilot Plant Flowsheet

The degree of liberation was evaluated by performing an HLS test on seven particle-size ranges, from a top size of 19.1 mm down to 0.5 mm. To avoid sampling error, all the mass retained in a 15.9 mm sieve was used in the coarser HLS test. For the HLS test with a particle size between 1.7 mm and 15.9 mm, 500 g was sampled from the total mass retained in each sieve, and for the finer samples, 150 g was used. SGS Geosol recommends this procedure as best practice.

The tests used two densities, 2.8 and 2.7 g/cm³, simulating rougher and scavenger stages. The results for each particle-size range are shown in Table 13-29. The results generally indicated that the recovery decreases as the particle-size increases. Similarly, the lithium oxide grade decreases as the particle-size increases.

Table 13-30 presents the grade and recovery results accumulated by mass distribution. Figure 13-32 shows the ore sorter pilot plant. Figure 13-33 shows the results of each HLS particle-size range.



Figure 13-32: Ore Sorter Pilot Plant

Table 13-28: Ore Sorter Pilot Plant Results

Sample	Particle Size	Feed			Concentrate			Tailing			Recovery			
		Li_2O (%)	Fe (%)	K (%)	Li_2O (%)	Fe (%)	K (%)	Li_2O (%)	Fe (%)	K (%)	Mass (%)	Li_2O (%)	Fe (%)	K (%)
ITDD-23-087T	−25.4 +6.35 mm	1.36	0.51	1.62	1.43	0.45	1.37	0.61	1.08	4.19	91.3	96.1	81.3	77.4
ITTD-22-002T	−25.4 +6.35 mm	0.96	0.68	1.90	1.07	0.48	1.47	0.53	1.51	3.74	80.9	89.5	57.4	62.4
Composite	−25.4 +6.35 mm	1.21	0.54	1.74	1.29	0.51	1.27	0.46	0.75	5.77	89.5	96.0	85.3	65.3
ITTD-22-048T	−12.7 +6.35 mm	1.03	0.73	1.83	1.11	0.67	1.34	0.67	1.01	4.00	81.6	88.1	74.6	59.8
ITDD-23-087T	−12.7 +6.35 mm	1.59	0.65	1.79	1.76	0.63	1.29	0.82	0.72	4.03	81.6	90.5	79.6	58.7
ITTD-23-083T	−12.7 +6.35 mm	1.80	0.48	1.84	2.02	0.48	1.15	0.90	0.47	4.60	79.9	89.9	80.3	49.9
ITTD-22-002T	−12.7 +6.35 mm	1.23	0.88	2.16	1.59	0.53	1.56	0.31	1.79	3.71	72.1	93.0	43.3	52.1
ITTD-23-093T	−12.7 +6.35 mm	0.66	0.51	1.82	0.72	0.54	1.37	0.35	0.36	3.82	81.7	90.2	87.0	61.5
ITTD-22-030T	−12.7 +6.35 mm	1.19	0.46	1.83	1.33	0.50	1.14	0.63	0.32	4.56	79.8	89.3	86.0	49.6
ITTD-22-023T	−12.7 +6.35 mm	1.53	0.40	2.07	1.72	0.39	1.42	0.73	0.42	4.79	80.8	90.8	79.6	55.5

Table 13-29: HLS Results for Each Particle-size Range for Spodumene Liberation (Li_2O Dist. %)

	−19.1 +15.9 mm		−15.9 +12.7 mm		−12.7 +9.5 mm		−9.5 +6.3 mm		−6.3 +3.4 mm		−3.4 +1.7 mm		−1.7 +0.5 mm	
	Li_2O Assay (%)	Li_2O Dist. (%)	Li_2O Assay (%)	Li_2O Dist. (%)	Li_2O Assay (%)	Li_2O Dist. (%)	Li_2O Assay (%)	Li_2O Dist. (%)	Li_2O Assay (%)	Li_2O Dist. (%)	Li_2O Assay (%)	Li_2O Dist. (%)	Li_2O Assay (%)	Li_2O Dist. (%)
Feed	1.25	100.0	1.36	100.0	1.54	100.0	1.51	100.0	1.40	100.0	1.34	100.0	1.30	100.0
Sink 2.8 (g/cm³)	4.13	59.0	4.97	77.9	5.32	74.1	5.87	75.4	6.02	82.3	6.75	84.2	6.48	89.4
Sink 2.7 (g/cm³)	1.76	25.1	2.48	10.9	2.09	11.7	1.83	16.2	1.43	8.5	1.22	7.3	0.80	3.2
Float 2.7 (g/cm³)	0.31	15.9	0.21	11.1	0.31	14.1	0.19	8.4	0.18	9.2	0.15	8.6	0.13	7.4

Table 13-30: Accumulated HLS Results by Particle Size

	−19.1 +15.9 mm	−15.9 +12.7 mm	−12.7 +9.5 mm	−9.5 +6.3 mm	−6.3 +3.4 mm	−3.4 +1.7 mm	−1.7 +0.5 mm
Mass Retained (%)	1.53	7.96	12.03	12.72	15.58	12.05	13.28
Li_2O Grade by Size (%)	4.13	4.97	5.32	5.87	6.02	6.75	6.48
Li_2O Recovery by Size (%)	84.1	88.9	85.9	91.6	90.8	91.4	92.6

	−19.1 +0.5 mm	−15.9 +0.5 mm	−12.7 +0.5 mm	−9.5 +0.5 mm	−6.3 +0.5 mm	−3.4 +0.5 mm	−1.7 +0.5 mm
Li_2O Grade Accumulated (%)	5.93	5.97	6.09	6.26	6.39	6.61	6.48
Li_2O Recovery Accumulated (%)	90.2	90.3	90.5	91.6	91.6	92.0	92.6

−19.1 +15.9 mm



−15.9 +12.7 mm



−12.7 +9.5 mm



−9.5 +6.3 mm



−6.3 +3.3 mm



−3.3 +1.7 mm



−1.7 +0.5 mm



Figure 13-33: HLS Separation for Rougher Stage

13.4.2 DMS Pilot Plant (SGS Geosol) Results

DMS Pilot Plant Samples

The tests at the DMS pilot plant were conducted using composite samples from the seven drill holes of the variability tests. These samples underwent testing in an ore sorter at Steinert to remove schist and feldspar, followed by particle-size adjustment to meet the specification of the DMS pilot plant. The DMS tests were conducted in two size fractions. The coarser fraction was prepared at 9.5 +3.55 mm, and the finer fraction was prepared at −3.55 +0.5 mm. Following is a list of drill holes from which the samples were composed:

- ITDD-22-048T
- ITDD-23-093T
- ITDD-23-087T
- ITDD-22-023T
- ITDD-22-002T
- ITDD-23-083T
- ITDD-23-030T.

Dense Media Separation Pilot Plant Overview

Figure 13-34 presents a flowchart reproducing the unit operations in the SGS Geosol DMS pilot plant. Twenty-five DMS pilot plant tests were performed (21 rougher and 4 scavenger) to obtain supporting information for the Project process development. Figure 13-35 to Figure 13-37 show the DMS pilot plant flowsheet and equipment.

The circuit includes a manually fed ore hopper connected to a vibrating feeder responsible for feeding ore into the static mixer. The solid, dense media (iron silicon) is fed directly into the agitated tank. This dense media undergoes dilution and subsequent pulp-density adjustment by injecting water into the tank or the first section of the screen's chute.

The prepared media of appropriate density feeds by gravity into the chute of the first section of the screen. From this point, the dense media is pumped through a demagnetizing coil and a flow divider with manual valves. The flow divider directs part of the dense media to the screen, and the rest recirculates to the agitated tank. The screen's function is to protect the system and retain undesirable or inadequately sized materials. The screen underflow feeds the static mixer positioned just above the DMS cyclone. This static mixer promotes mixing of the ore from the vibrating feeder with the dense media from the screen underflow. The gravity feed of the DMS cyclone establishes a cyclone feed-pressure based on the height of the liquid column relative to the vertical distance between the DMS cyclone feed flange and the pulp level in the static mixer.

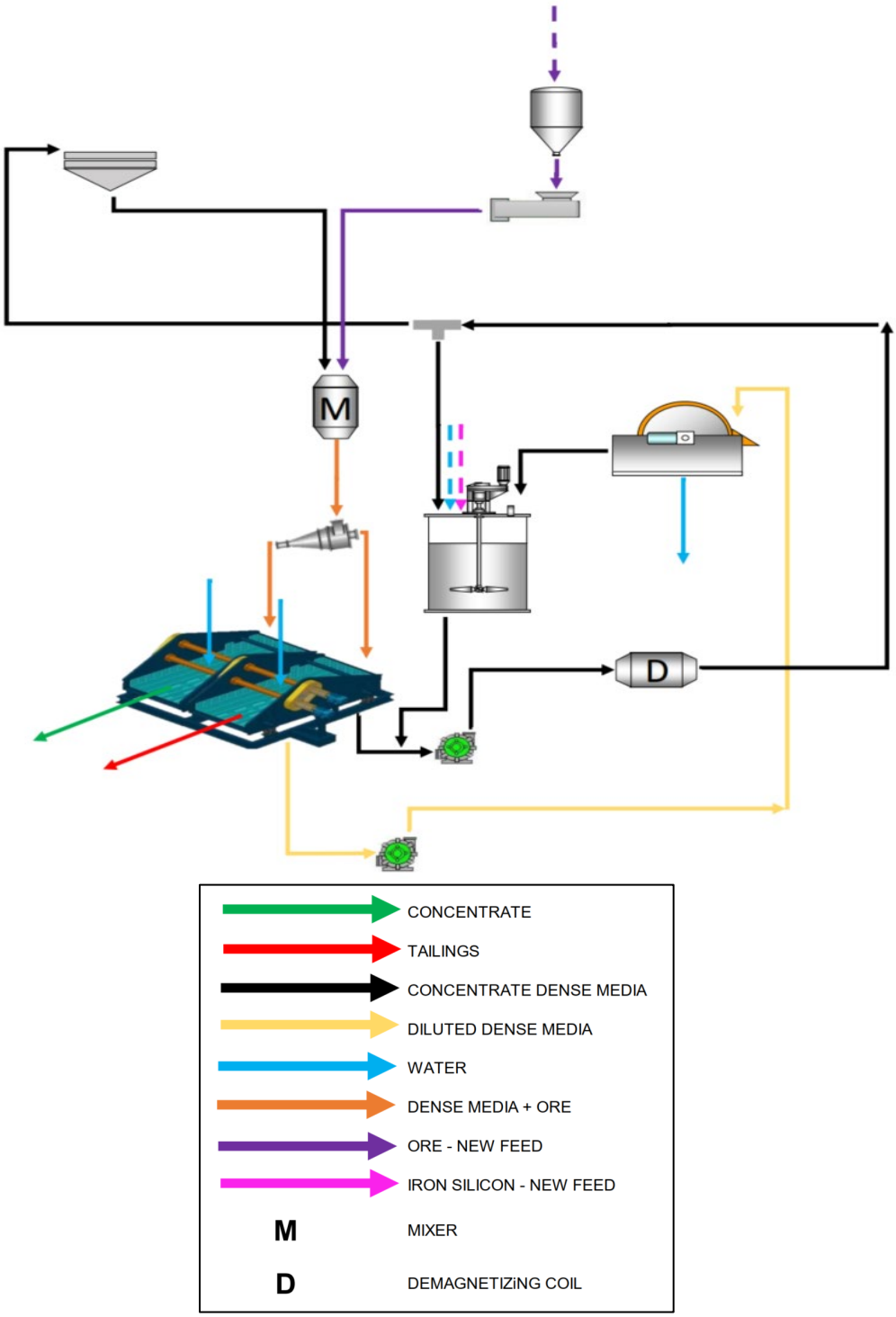


Figure 13-34: DMS Pilot Plant Flowchart



Figure 13-35: DMS Pilot Plant Second Floor 1/2



Figure 13-36: DMS Pilot Plant First Floor 2/2

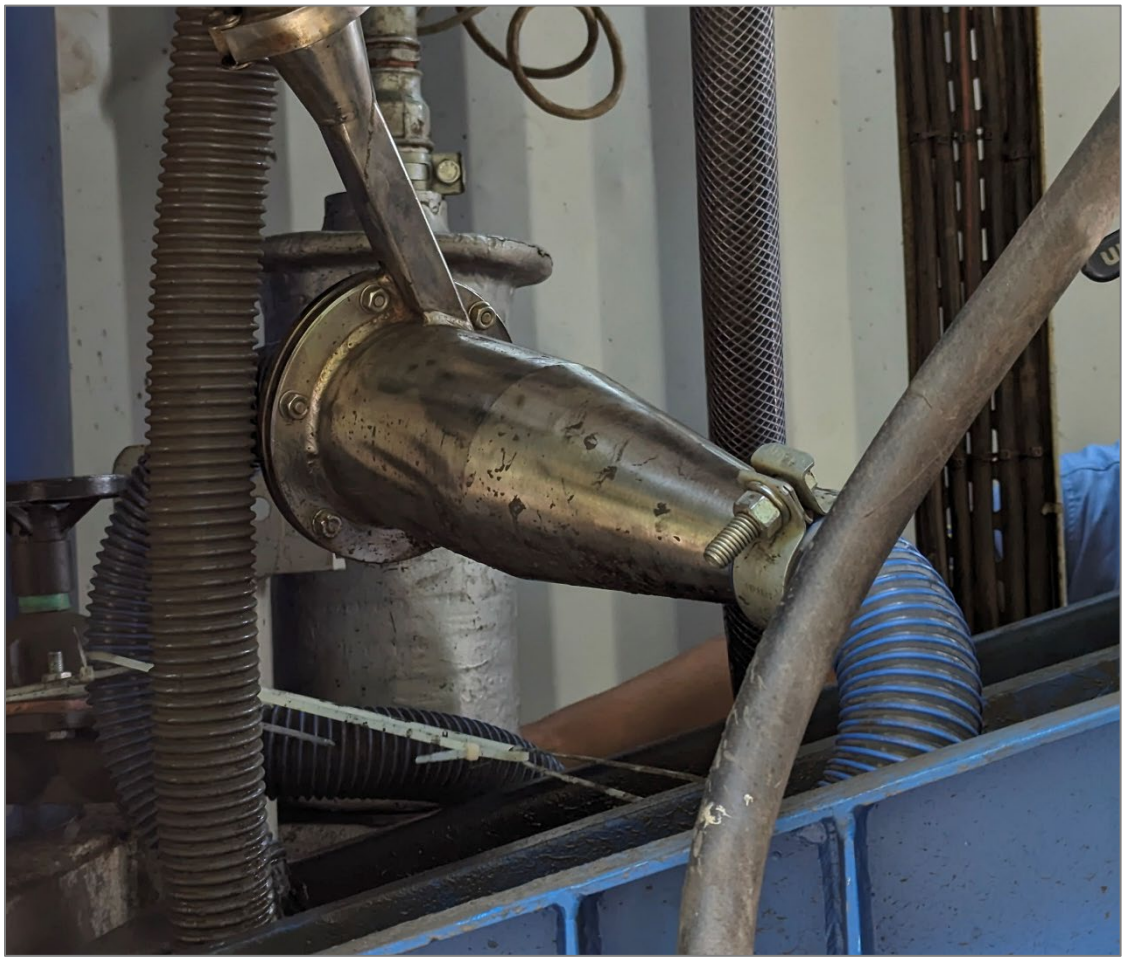


Figure 13-37: DMS Cyclone

The DMS cyclone, positioned at a 20° incline relative to its centreline, separates the mixture by density, partitioning it into sink (underflow) and float (overflow). In this process, the concentrate is directed to the sink flow, and the reject is directed to the float flow. The dewatering screen is partitioned into two parallel sections and two underflow chutes. Each chute receives drainage from half of the parallel sections' area. The cyclone sink is directed to the first section of the screen, and the float is directed to the second section. In the first screen chute, the dense-media concentrate is drained. From the second chute, wash water is injected to remove residual dense media and drain the diluted flow. The diluted dense media is then pumped to the magnetic separator, which retains ferrosilicon particles and removes excess water, concentrating the dense-media mixture. The concentrated dense media is then recirculated to the agitated tank while the water is discarded. The DMS concentrate is equivalent to the oversize from the first section of the dewatering screen, and the DMS reject is equivalent to the oversize from the second section of the screen.

The scavenger stage test is repeated by refeeding the reject obtained in the rougher stage.

DMS Pilot Plant Rougher Stage Results

The results of the pilot tests were presented graphically to define trend lines and points of coherence for a comprehensive analysis.

The initial rougher tests for the coarse fraction were discarded, as they were part of the pilot plant's calibration period. The results of the tests considered for the rougher stage indicated the trend curve for the −9.5 +3.35 mm fraction shown in Figure 13-38.

The analysis of these data converges to achieve a metallurgical recovery of about 64.0% to obtain a concentrate with a lithium oxide grade of 5.50% in the −9.5 +3.35 mm fraction.

The initial rougher tests for the fine fraction were discarded, as they were part of the pilot plant's calibration period. The results of the tests considered for the rougher stage indicated the trend curve for the −3.35 +0.5 mm fraction shown in Figure 13-39.

Although this trend line does not fit the points as well as in that for the coarse fraction, the analysis of these data converges to achieve a metallurgical recovery of 80.5%, obtaining a concentrate with a lithium oxide grade of 5.50% in the −3.35 +0.5 mm fraction.

The combination of the most coherent result points obtained in the two fractions, −9.5 +3.35 mm and −3.35 +0.5 mm, presented the trend curve shown in Figure 13-40.

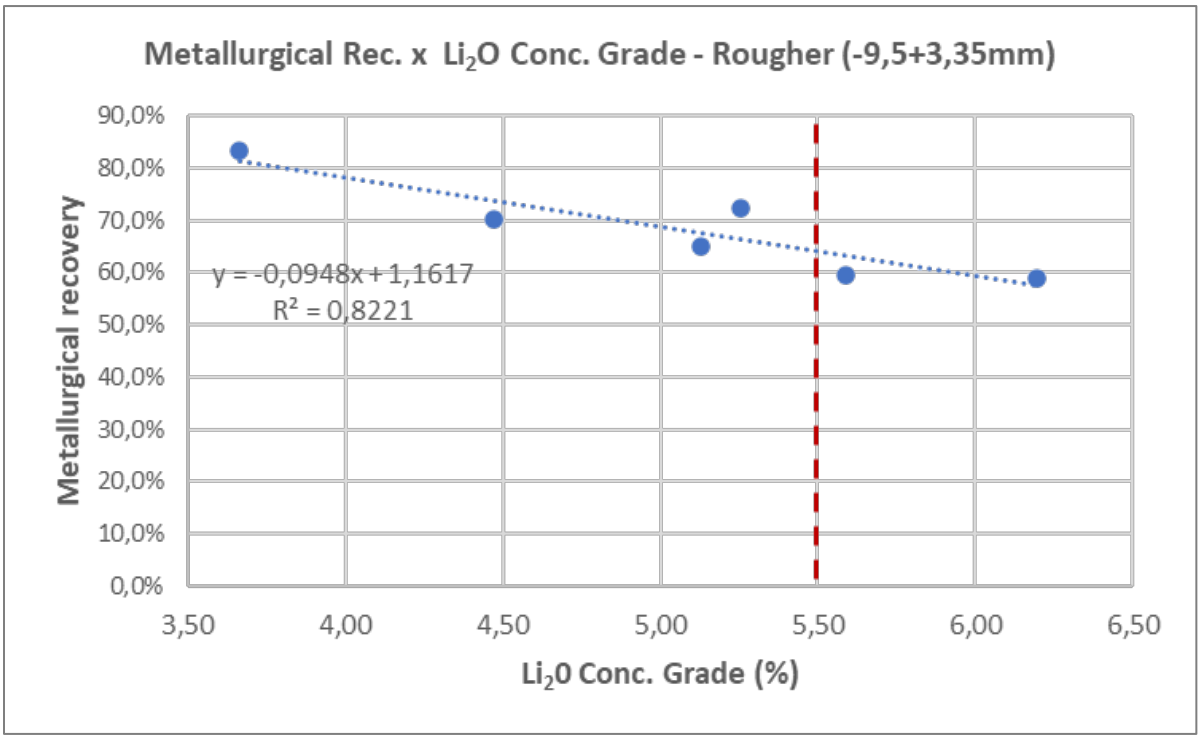


Figure 13-38: Rougher Coarse Metallurgical Recovery x Li_2O Grade in Concentrate

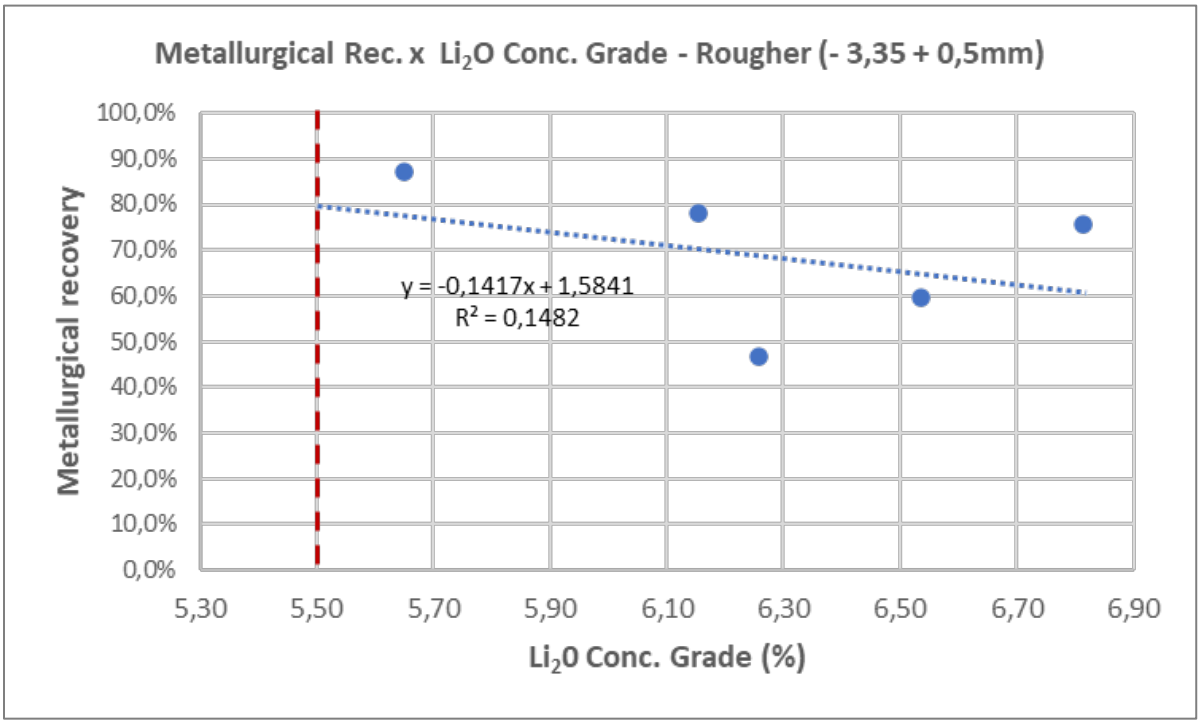


Figure 13-39: Rougher Fine Metallurgical Recovery x Li_2O Grade in Concentrate

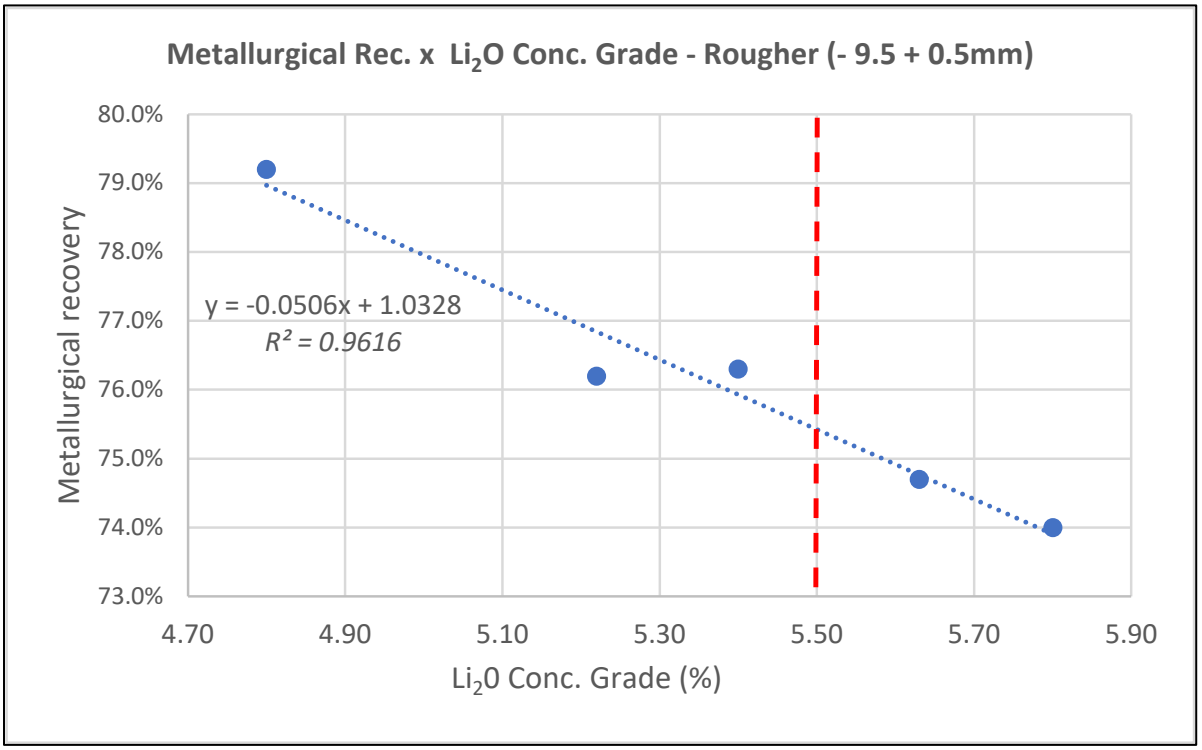


Figure 13-40: Rougher Composite Metallurgical Recovery x Li_2O Grade in Concentrate

The analysis of these data converges to achieve a metallurgical recovery of 75.42%, to obtain a concentrate with a lithium oxide grade of 5.50% in the rougher stage, considering the combination of the two tested size-fractions. To achieve this metallurgical recovery, the results of Tests 16 and 17 were adopted as references. Since both produced concentrates with lithium oxide grades higher than 5.50%, it was necessary to recalculate the metallurgical recoveries. Table 13-31 presents the results of Tests 16 and 17, as well as the adjusted metallurgical recoveries to obtain a 5.50% concentrate and an overall rougher stage metallurgical recovery of 75.42%.

Table 13-31: Rougher Testwork Results and Metallurgical Recovery

Testwork No.	Li_2O Grade Conc. (%)	Metall. Rec. (%)
Test 16	5.65	87.06
Test 17	5.59	59.48
Rougher Mass Balance		
−9.5 +3.35 mm	5.50	60.41
−3.35 +0.5 mm	5.50	88.42
−9.5 +0.5 mm	5.50	75.42

Therefore, the rougher stage of the DMS plant was assumed to achieve the following recoveries:

- Coarse fraction DMS rougher metallurgical recovery: 60.41%
- Fine fraction DMS rougher metallurgical recovery: 88.42%
- Composite DMS rougher metallurgical recovery: 75.42%.

13.5 Conclusions

A detailed work program for the development of the lithium ore concentration process for the Project has been completed. The ore predominantly contains spodumene as the lithium-bearing mineral. The liberation size, considering concentration via DMS, is 15.9 mm. Bench-scale tests showed fines generation (particles smaller than 0.6 mm) ranging from 10% to 12%.

The ore preparation stage consists of three crushing stages (jaw and cone crushers), with an ore-sorting stage to remove part of the dilution material from the mine, followed by a three-stage DMS circuit (primary, secondary, and recrush). The spodumene concentrate will undergo magnetic separation to adjust the product's iron content. The final chemical specification for the spodumene concentrate is expected to be between 5.2% and 5.5% Li_2O, with iron oxide below 1.0%.

The average metallurgical recovery for the HLS tests was 66.24% (not considering drill hole ITDD23-141). The core drill ITDD23-141 presented lower grade of 0.90% Li_2O generating lower mass and metallurgical recoveries.

A potential upside for the Project lies in the beneficiation, through flotation and spirals, of the fine fraction (below 0.6 mm), combined with the fine rejects from the DMS and the fines from the recrushing stage, which contains 27% of the total lithium from run of mine (ROM based on HLS test results. This opportunity presents low capital and operating costs and potentially increases the concentrate production by around 40,000 t/a.

14 MINERAL RESOURCE ESTIMATES

GE21 conducted comprehensive three-dimensional (3-D) geological modelling, statistical and geostatistical studies, as well as grade estimation for the MGLIT Bandeira Property. This estimation considered various factors, such as the quantity and distribution of available data, interpreted controls on mineralization, mineralization style, and the quality of the sampling data.

The geological modelling and estimation processes were executed using Leapfrog Edge 2024.1.3 software. The UTM Projection—Zone 23 South (SIRGAS 2000) was adopted as the reference coordinate system for the Project database.

This section has been updated to reflect new exploration data from November 13, 2023, through the effective date of November 20, 2024. This updated resource estimate supersedes the previous effective report date of April 2024.

14.1 Drilling Database

The drilling database underwent a comprehensive visual validation, considering the interrelation of tables, identifying gaps and overlaps, and ensuring the inclusion of crucial information. Using Leapfrog Edge 2024.1.3 software, GE21 also conducted validation checks on the collar, survey, assay, and lithology tables. This stage of the work revealed no significant inconsistencies, as these had already been verified during data verification.

Mineral Resource estimation was based on drill-hole and trench databases, incorporating lithology logs and assay results from HQ-drill core samples. The topographic surface bounds the extent of these estimates. Figure 14-1 illustrates the spatial distribution of the drill holes used in the estimates.

The original data set MGLIT provided encompassed data from 297 surface diamond drill holes (60,301 m) and 44 trench channels (2,923 m) that MGLIT had executed. This data set reflects work from 2022 until November 20, 2024.

The Bandeira database contains 10,298 assay intervals, comprising 247 assays from trenches and 10,051 assay intervals from drill holes.

The assay table includes data for Li_2O (%) and various elements, including Li (ppm), Al (%), As (ppm), B (%), Ba (ppm), Be (ppm), Ca (%), Cd (ppm), Co (ppm), Cr (ppm), Cu (ppm), Fe (%), K (%), La (ppm), Mg (%), Mn (ppm), Mo (ppm), Nb (ppm), Ni (ppm), P (%), Pb (ppm), Sb (ppm), Sc (ppm), Sn (ppm), Sr (ppm), Ta (ppm), Ti (%), V (ppm), W (ppm), Y (ppm), and Zn (ppm). Following a thorough review of the database, the Li_2O (%) data was extracted explicitly for subsequent statistical analysis, block modelling, and Mineral Resource estimates.

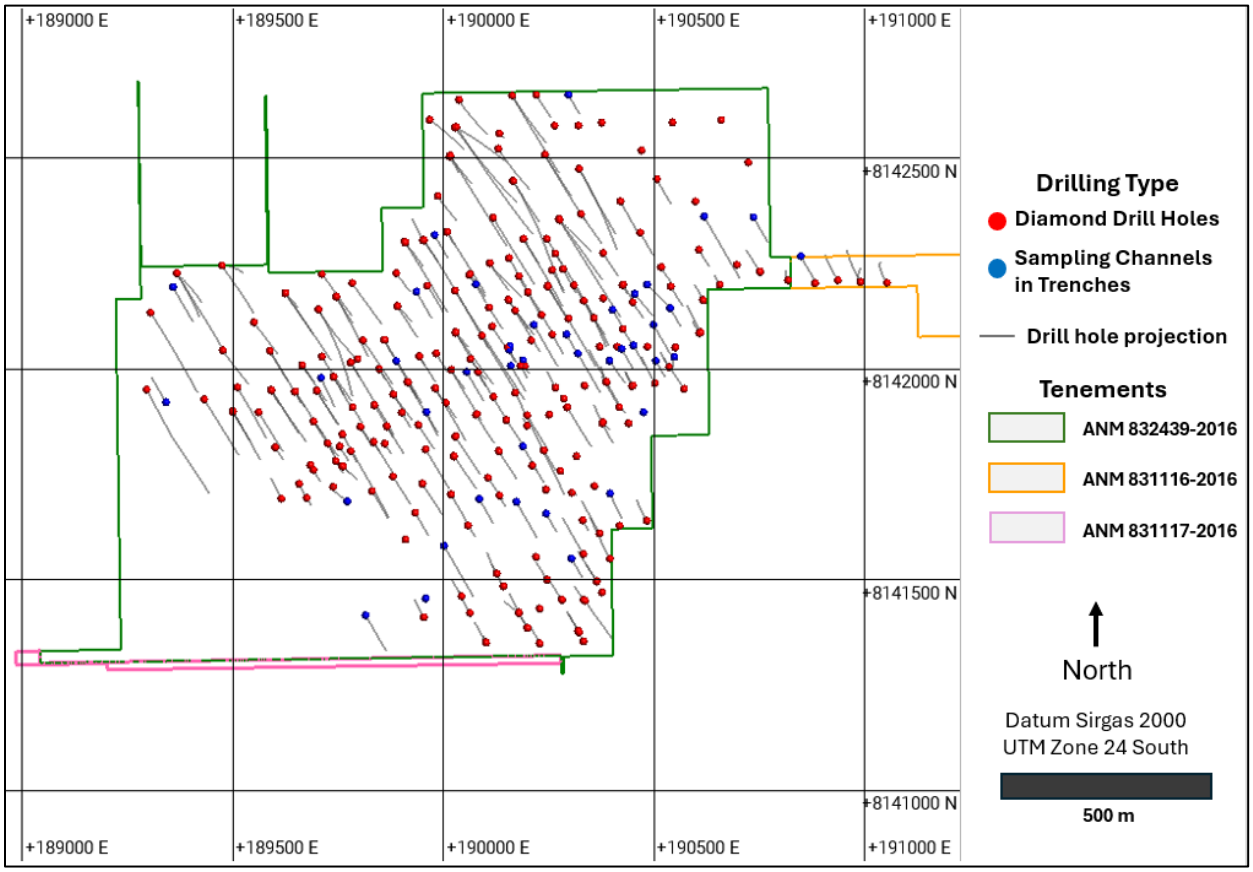


Figure 14-1: Drill-Hole Location

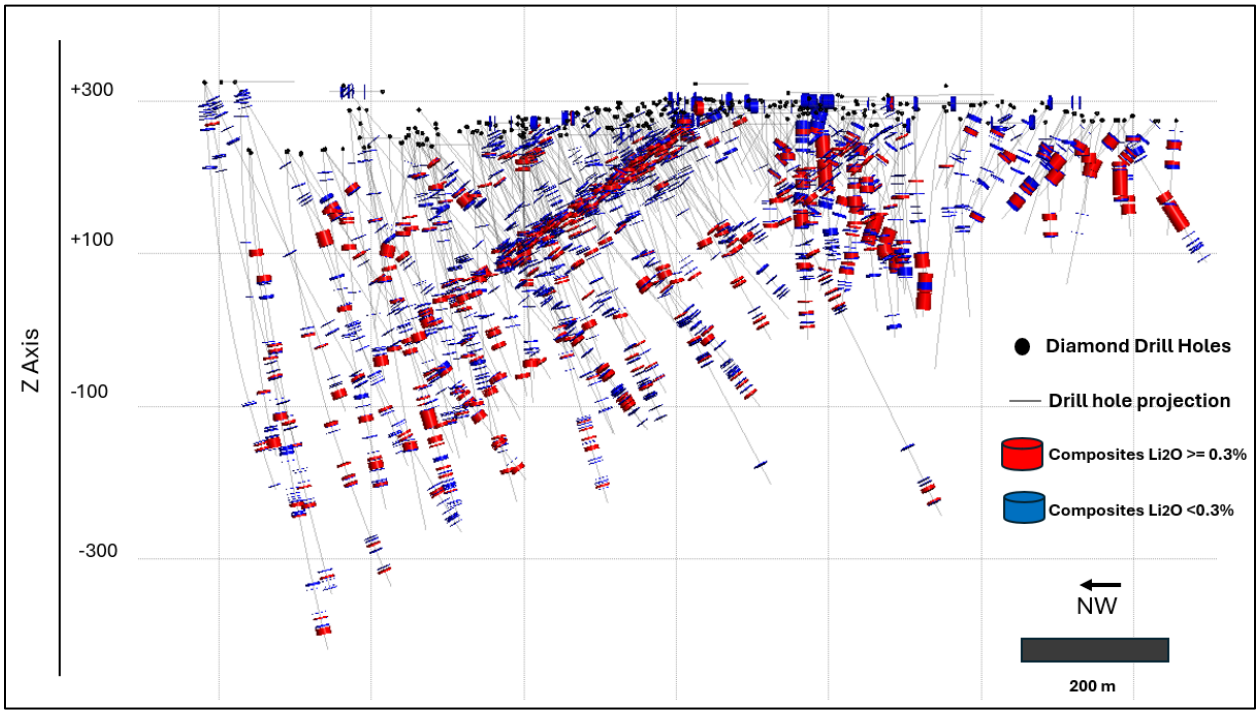
14.2 Geological Modelling

MGLIT undertook a geological interpretation encompassing all documented pegmatite intervals within the Bandeira deposit. Initially, cross-sectional interpretations were crafted using traditional manual techniques and advanced cartographic software platforms such as QGIS, ArcGIS, and Leapfrog. These initial steps laid the groundwork for a robust modelling process.

The MGLIT team interpreted a set of grade shell sections, with an envelope delimiting a zone with a cut-off grade of 0.3% Li_2O (%) (Figure 14-2 and Figure 14-3). The resulting interpretations were developed into a series of implicit 3-D models aligned with two prevailing strike directions: 235° and 140° (Figure 14-4 and Figure 14-5).

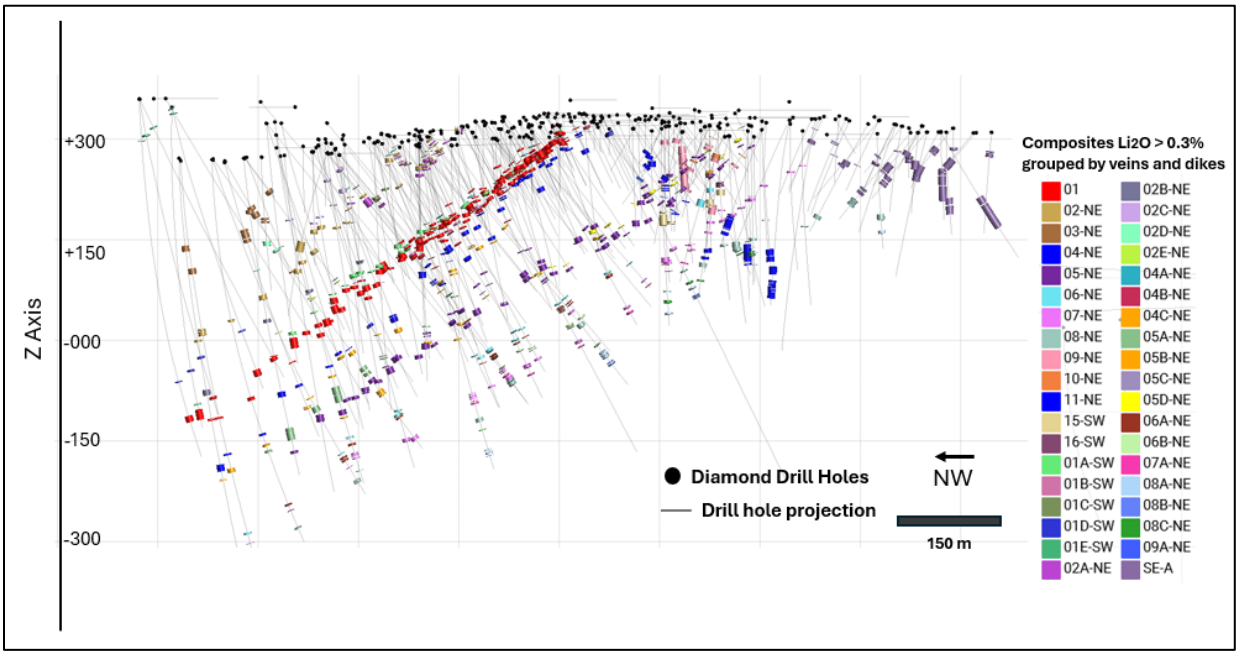
MGLIT also conducted weathering modelling, basing the analysis on the descriptions provided in the logs (Figure 14-6).

The QP considers that the geological interpretations and modelling are suited to an estimation of the Mineral Resource. The quality assurance procedures follow industry best practices, and the model honours the mineralized pegmatite intervals and has adequate continuity of the modelled bodies.



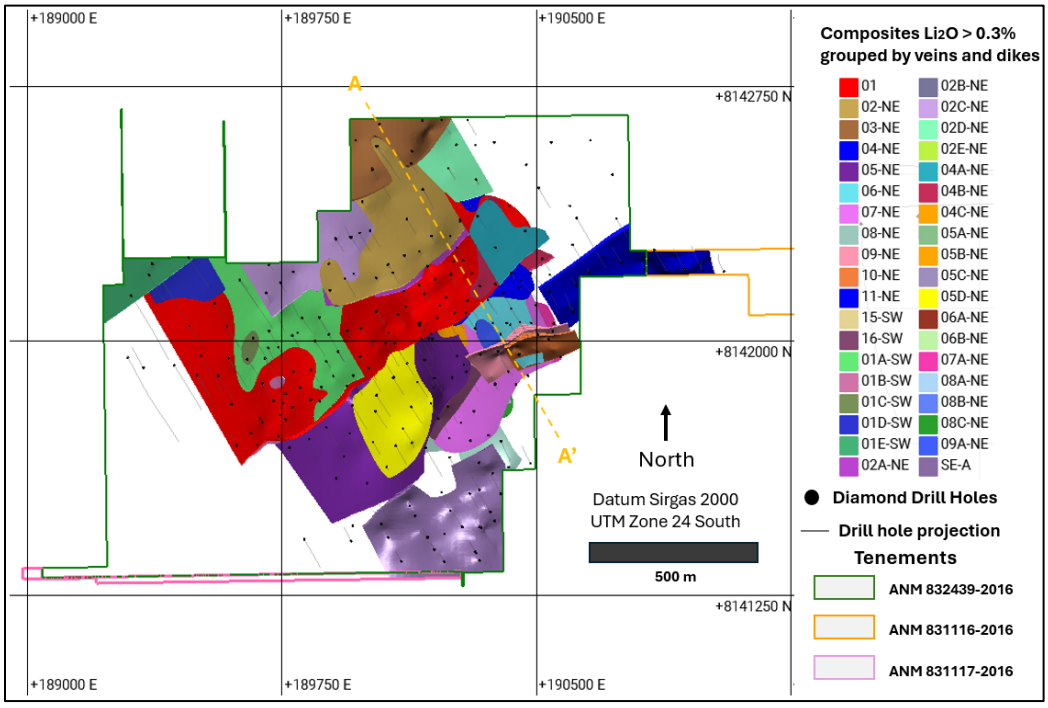
Source: GE21 (2025).

Figure 14-2: Assay Composites Classified by Li_2O >0.3% Grade Limit in Pegmatites Veins (Oblique View NW–SE)



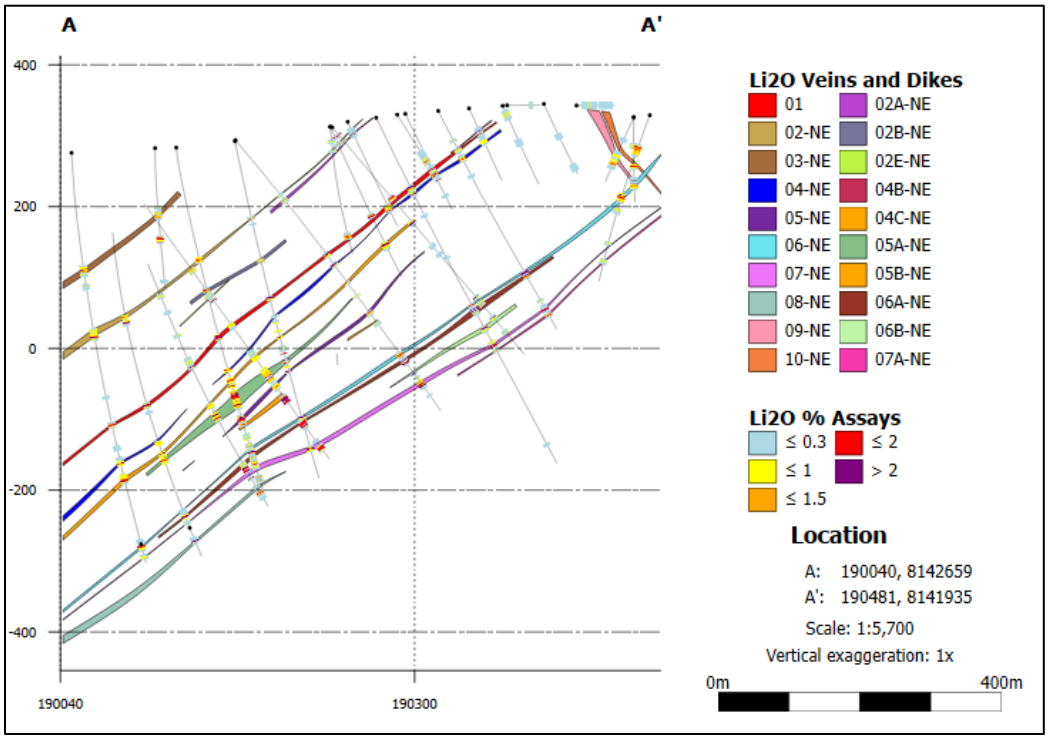
Source: GE21 (2025).

Figure 14-3: Assay Composites Within the Li_2O >0.3% Limit in Pegmatite Veins Grouped by Separated Lenses and Dykes



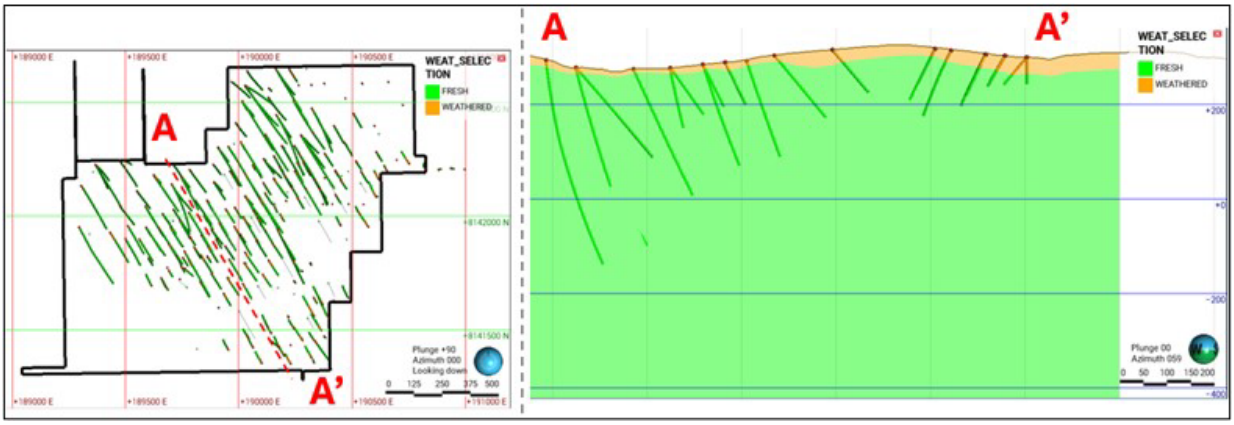
Source: GE21 (2025).

Figure 14-4: Spodumene Grade Shells Modelled with Assay Composites Li_2O >0.3% (Plan View)



Source: GE21 (2025).

Figure 14-5: Spodumene Grade Shell Model—Assay Composites Li_2O >0.3% (Cross-Section)



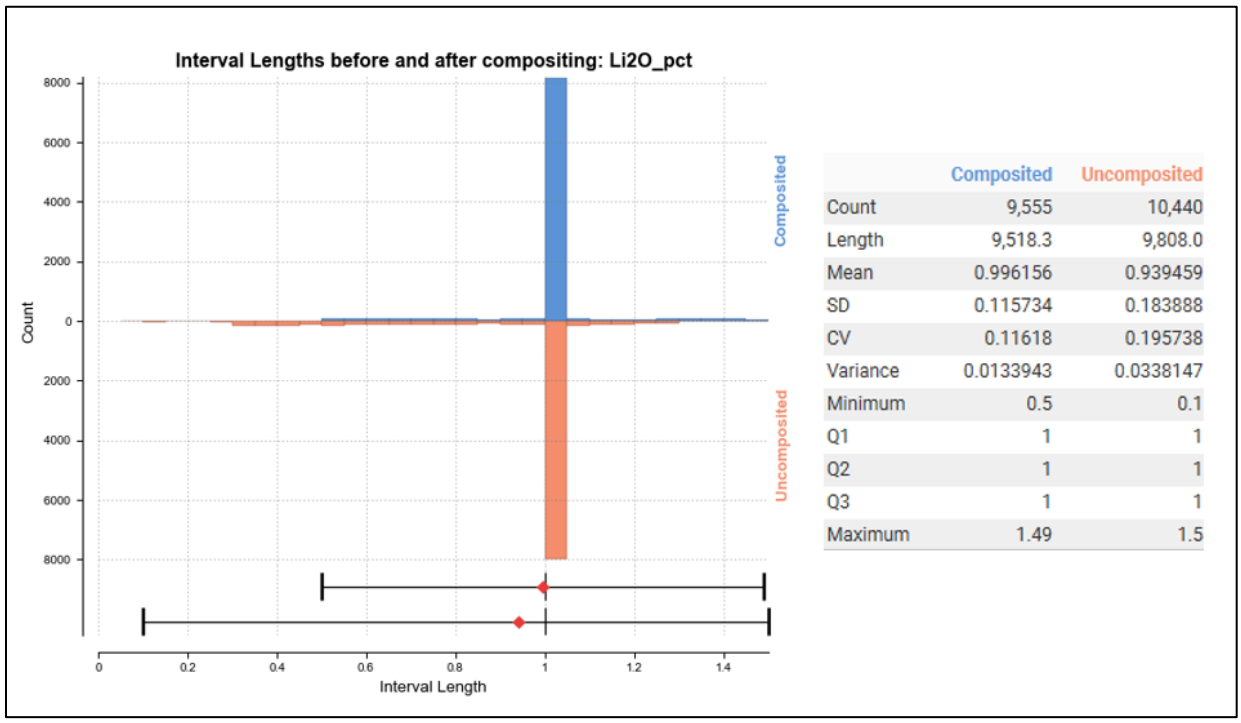
Source: GE21 (2025).

Figure 14-6: Weathering Zone Model (Left, Plan View; Right, Cross-Section View)

14.3 Geostatistical Structural Analysis

14.3.1 Sample Regularization

The analysis of the sample support showed that over 95% of the drilling samples are greater than 1 m long. GE21 regularly analyzed 1 m samples for complementary studies of statistics and geostatistics (Figure 14-7).



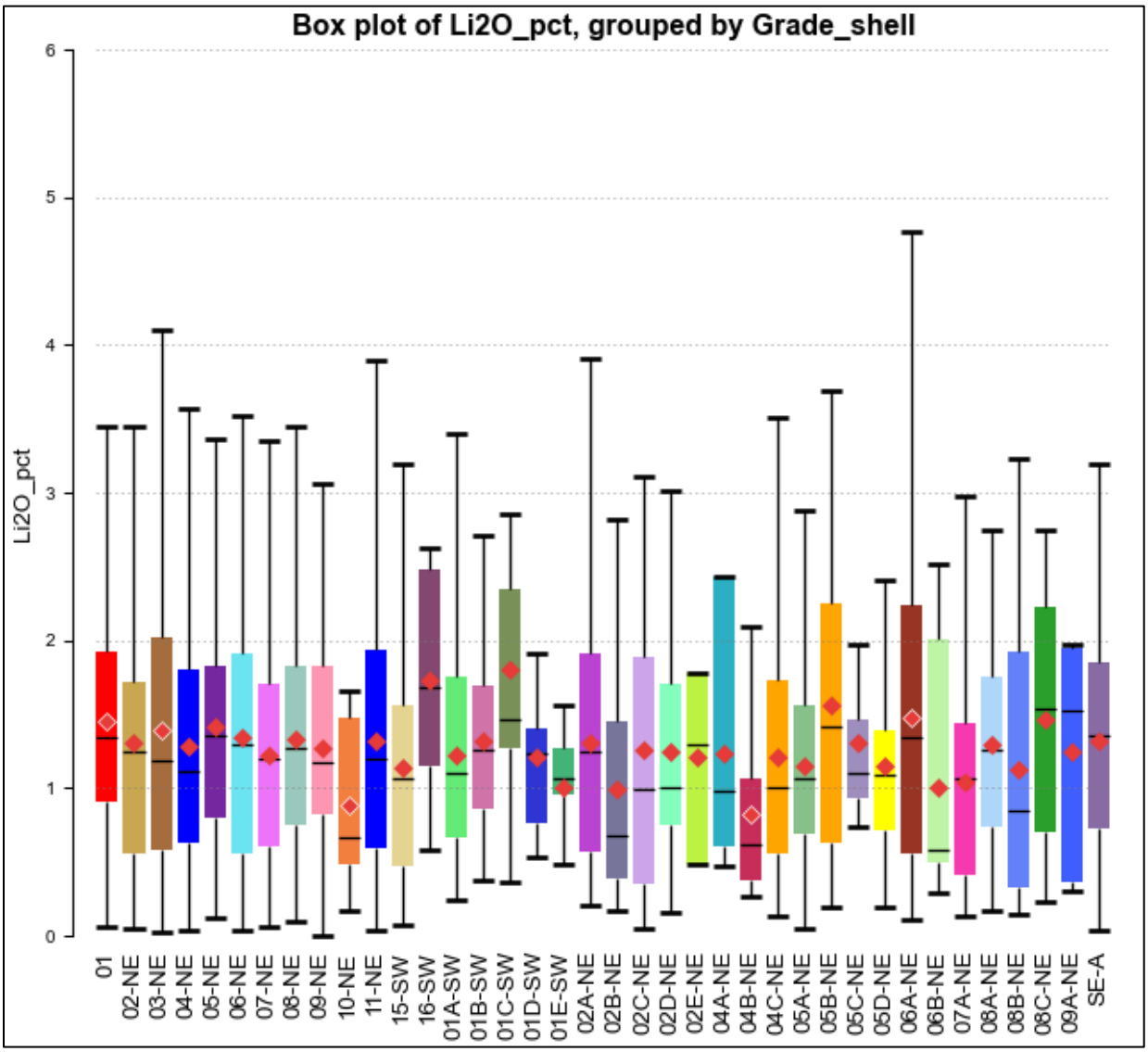
	Composited	Uncomposited
Count	9,555	10,440
Length	9,518.3	9,808.0
Mean	0.996156	0.939459
SD	0.115734	0.183888
CV	0.11618	0.195738
Variance	0.0133943	0.0338147
Minimum	0.5	0.1
Q1	1	1
Q2	1	1
Q3	1	1
Maximum	1.49	1.5

Source: GE21 (2025).

Figure 14-7: Bandeira Assay Interval Length Statistics

14.3.2 Exploratory Data Analysis

Statistical analysis on composited drilling samples was performed for the Li_2O% variable inside each modelled typology. Figure 14-8 and Table 14-1 show the statistics for pegmatite veins.



Source: GE21 (2025).

Figure 14-8: Li_2O (%) Box Plots of the Spodumene Pegmatite Vein Model Statistics

Table 14-1: Li_2O (%) Spodumene Pegmatite Vein Model Statistics

Domain	Count	Length	Mean	Standard Deviation	Coefficient of Variation	Variance	Minimum	Lower Quartile	Median	Upper Quartile	Maximum
1	644	632	1.46	0.77	0.53	0.60	0.07	0.91	1.34	1.93	5.99
02-NE	135	135	1.30	0.86	0.66	0.74	0.05	0.56	1.24	1.72	4.56
03-NE	77	77	1.39	1.01	0.72	1.01	0.02	0.58	1.18	2.02	4.10
04-NE	181	180	1.28	0.81	0.63	0.65	0.04	0.63	1.11	1.80	4.05
05-NE	321	317	1.41	0.75	0.53	0.57	0.12	0.80	1.36	1.83	3.58
06-NE	61	60	1.34	0.85	0.63	0.73	0.04	0.56	1.29	1.92	3.52
07-NE	123	122	1.22	0.71	0.59	0.51	0.06	0.60	1.19	1.71	3.74
09-NE	123	122	1.27	0.63	0.50	0.40	0.01	0.82	1.17	1.82	3.06
01A-SW	107	104	1.22	0.71	0.58	0.50	0.24	0.66	1.10	1.76	3.54
01B-SW	23	22	1.31	0.64	0.49	0.41	0.38	0.86	1.26	1.70	2.71
01C-SW	10	9	1.80	0.73	0.41	0.54	0.37	1.27	1.47	2.34	2.86
01D-SW	10	10	1.21	0.46	0.38	0.21	0.53	0.77	1.23	1.40	1.91
01E-SW	9	8	1.00	0.45	0.45	0.20	0.32	0.95	1.06	1.27	1.56
02A-NE	57	55	1.31	0.84	0.64	0.70	0.21	0.57	1.24	1.91	3.91
02B-NE	27	27	0.99	0.75	0.76	0.57	0.18	0.39	0.68	1.45	2.82
02C-NE	29	29	1.25	0.94	0.75	0.89	0.05	0.35	0.99	1.89	3.10
04A-NE	5	5	1.24	0.86	0.69	0.74	0.47	0.60	0.98	2.43	2.43
04B-NE	10	10	0.82	0.62	0.76	0.39	0.27	0.38	0.62	1.07	2.17
04C-NE	60	61	1.21	0.80	0.66	0.64	0.14	0.56	1.00	1.73	4.15
05A-NE	79	79	1.15	0.66	0.57	0.43	0.05	0.69	1.06	1.56	3.31
05B-NE	34	33	1.56	1.02	0.65	1.04	0.20	0.62	1.42	2.25	3.69
05C-NE	5	4	1.31	0.51	0.39	0.26	0.74	0.94	1.10	1.47	1.97
06A-NE	45	46	1.48	1.07	0.72	1.14	0.10	0.55	1.34	2.24	5.23
06B-NE	17	17	1.01	0.80	0.80	0.64	0.29	0.49	0.58	2.01	2.51
07A-NE	19	19	1.05	0.78	0.75	0.61	0.14	0.42	1.07	1.44	3.52
SE-A	319	318	1.32	0.71	0.54	0.50	0.03	0.73	1.35	1.85	3.19
02D-NE	19	19	1.25	0.81	0.65	0.65	0.15	0.74	1.00	1.71	3.01
08-NE	111	110	1.32	0.74	0.56	0.54	0.09	0.75	1.27	1.82	3.65

Domain	Count	Length	Mean	Standard Deviation	Coefficient of Variation	Variance	Minimum	Lower Quartile	Median	Upper Quartile	Maximum
10-NE	18	18	0.88	0.51	0.58	0.26	0.17	0.48	0.66	1.48	1.66
02E-NE	4	4	1.21	0.57	0.47	0.33	0.48	0.48	1.30	1.78	1.78
05D-NE	33	32	1.15	0.72	0.63	0.52	0.19	0.71	1.09	1.39	3.47
11-NE	187	186	1.32	0.89	0.68	0.80	0.04	0.59	1.20	1.94	3.89
08A-NE	31	30	1.29	0.71	0.55	0.51	0.17	0.73	1.25	1.76	2.75
08B-NE	12	12	1.12	0.96	0.85	0.91	0.15	0.32	0.85	1.92	3.23
08C-NE	21	21	1.46	0.85	0.58	0.73	0.23	0.71	1.54	2.22	2.75
15-SW	45	46	1.14	0.74	0.65	0.54	0.07	0.47	1.06	1.56	3.47
16-SW	14	14	1.74	0.79	0.45	0.62	0.58	1.14	1.68	2.48	2.63
09A-NE	7	6	1.25	0.77	0.62	0.59	0.31	0.36	1.52	1.95	1.97
Total	3,032	2,999	1.26								

Source: GE21 (2025).

14.3.3 Variographic Analysis

The structural analysis of the domains was conducted to determine the variographic parameters, which are essential for determining the spatial continuity model of the grade variables and for the grade estimate.

Variograms were generated explicitly for Li_2O% within the spodumene vein suite. This approach considered the geological similarity among them, enhancing the robustness of the variograms. Two distinct sets of veins were considered:

- NW Vein Suite
- SE Vein Suite.

The variographic analysis was executed using Leapfrog software. Figure 14-9 to Figure 14-12 show the variograms for the Li_2O% variable for each set of vein domains. Additionally, Table 14-2 presents the variographic parameters obtained from all analyses. These parameters were applied in the grade estimation process.

Table 14-2: Variographic Parameters

Variogram Name	Variance	Nugget	Normalized Nugget	Structures	Sill	Normalized Sill	Structure	Major	Semi-Major	Minor	Dip (°)	Dip Azi. (°)	Pitch (°)
NW	0.63	0.14	0.22	Structure 1	0.23	0.36	Spherical	53	12	1.6	35	330	0
				Structure 2	0.26	0.41	Spherical	107	65	2.5	35	330	0
SE	0.56	0.08	0.15	Structure 1	0.23	0.40	Spherical	50	24	1.8	46	155	0
				Structure 2	0.25	0.45	Spherical	81	60	6	46	155	0

Source: GE21 (2025).

14.4 Block Model

A block model was built to carry out the grade estimation. The model's dimensions (12 m x 12 m x 4 m) were defined based on the minimum spacing of the drilling grid. The sub-block model was set at 1.5 m x 1.5 m x 2 m to ensure the geometric adherence of the modelled bodies. The dimensions of the block models and the attributes are shown in Table 14-3 and Table 14-4.

Table 14-3: Block Model Dimensions

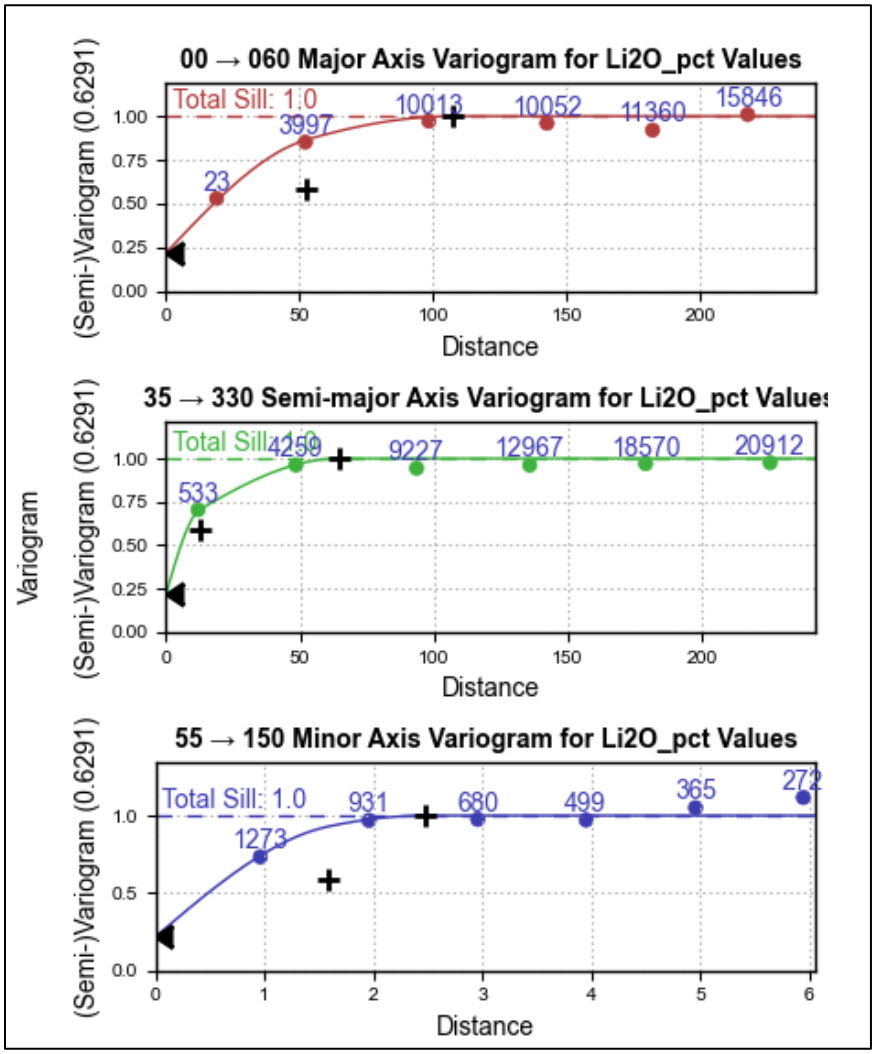
Attribute	X	Y	Z
Minimum Coordinates (Center) (m)	189,006	8,141,106	-510
Maximum Coordinates (Center) (m)	193,002	8,142,798	458
Minimum Coordinates (Corner) (m)	189,000	8,141,100	-512
Maximum Coordinates (Corner) (m)	193,008	8,142,804	460
Number of Nodes	334	142	243
Block Size (m)	12	12	4
Sub-Block	1.5	1.5	2

Source: GE21 (2025).
Notes: Azimuth: 0 Degrees (rotate clockwise around the Z-axis when looking down)
Dip: 0 Degrees (then turn around the X-axis down from the horizontal plane)
Pitch: 0 Degrees (then rotate clockwise around the Z-axis when looking down.

Table 14-4: Block Model Variables Summary

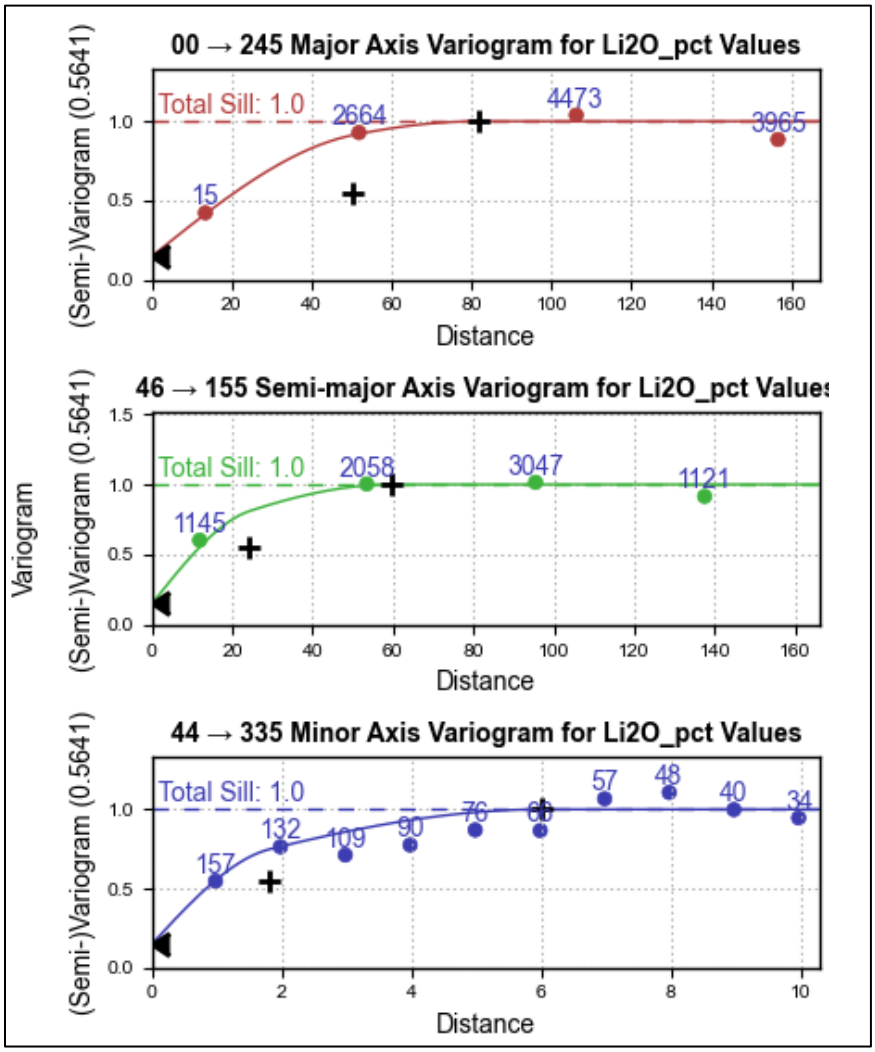
Attribute Name	Type	Deals	Background	Description
GM_weat	Character	-		Weathering model
GM_ grad	Character	-		Spodumene veins model
Class	Character	-		Mineral classification
Density	Real	4	−99	Density values
GM_miner	Character	-		Bandeira mineral right
Li_2O_ok	Real	4	−99	Li_2O OK estimation

Source: GE21 (2025).



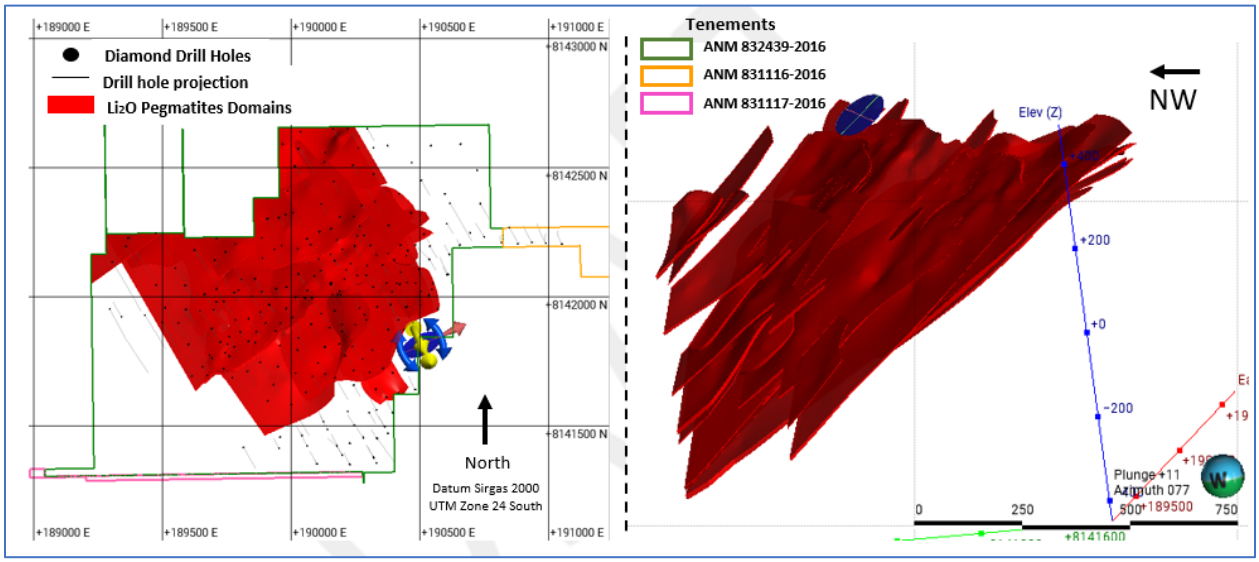
Source: GE21 (2025).

Figure 14-9: Variographic Model—Domains Set NW



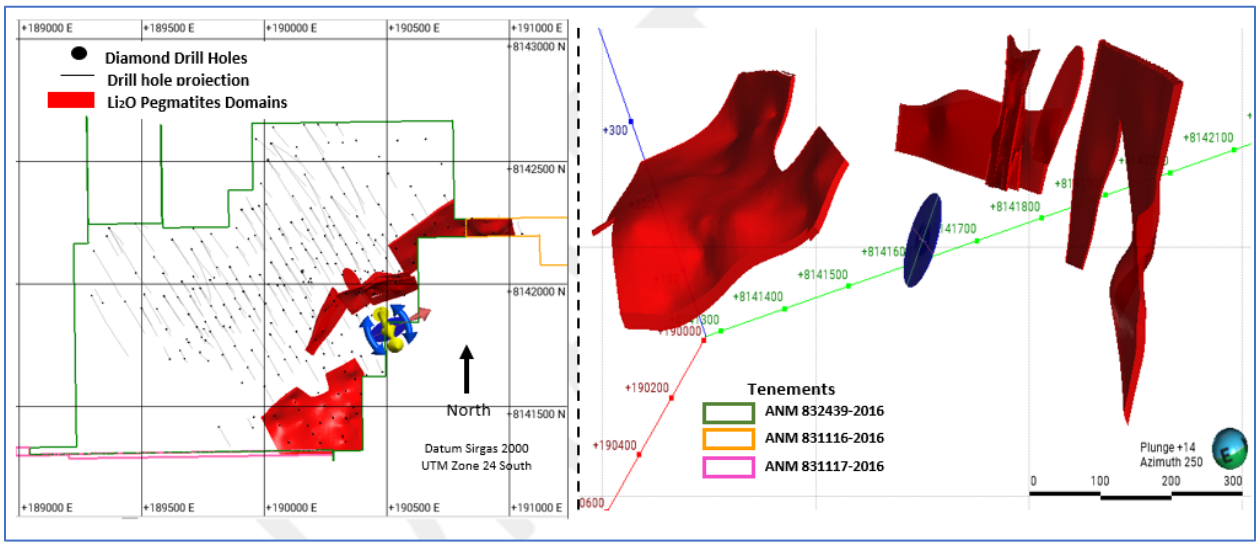
Source: GE21 (2025).

Figure 14-10: Variographic Model—Domains Set SE



Source: GE21 (2025).

Figure 14-11: Variographic Ellipsoid—Domains Set NW



Source: GE21 (2025).

Figure 14-12: Variographic Ellipsoid—Domains Set SE

14.5 Grade Estimation

Ordinary kriging (OK) was carried out using the Leapfrog Edge 2024.1.3 software to estimate the Li_2O (%) variable based on the structural analysis results described in this Technical Report.

Each mineralized vein was estimated independently, using a hard-boundary strategy to ensure that samples from one domain did not influence neighbouring domains. The variograms were initially modelled considering the structural continuity across the entire set of domains, followed by an

adjustment for honouring the specific behaviour for each domain. Table 14-5 shows the main parameters of the OK strategy applied in the grade estimation.

Table 14-5: OK Parameters

Type	Steps	Ellipsoid Ranges			Number of Samples	
		Maximum	Intermediate	Minimum	Minimum	Maximum
Li_2O	Step 1	50	50	4	6	16
	Step 2	100	100	8	6	16
	Step 3	150	150	16	4	16
	Step 4	1,500	1,500	1,600	4	16

Notes: Dynamic variable orientation for estimation was applied to each domain in Leapfrog software.
Moving the neighbourhood from the ellipsoid. Dip = 37° Dip Azimuth = 323° Pitch = 00° (NW Veins).
Moving the neighbourhood from the ellipsoid. Dip = 20° Dip Azimuth = 128° Pitch = 28° (SE Veins).
Maximum number of samples per drill = 2.
Source: GE21 (2025).

14.6 Estimation Validation

The QP validated the estimate through visual inspection (Figure 14-13 and Figure 14-14), as well as global and local bias analysis. For these bias checks, the nearest neighbour (NN) method was used as the comparison estimate, supported by NN-check plots. Figure 14-15 and Figure 14-16 present the results of the global bias analysis of the estimated Li_2O% and density variables. The analysis confirmed the expected estimation smoothing by OK within the acceptance limits. The comparison showed that OK globally preserved the average grades, and the resulting global bias is within the industry-accepted tolerance range.

The local bias assessment using the swath plot method aims to evaluate potential deviations by comparing average grades from the OK and NN estimates within swath plot intervals along the X, Y, and Z axes. Figure 14-17 and Figure 14-18 present the validation results for the Li_2O% and density swath plots.

The results from the OK grade estimate validation show that the smoothing effect, or local and global bias, are inside acceptance limits for Mineral Resource estimation.

14.7 Density

The density (g/cm³) in the spodumene pegmatites was estimated using inverse distance weighting (IDW). An exponent of 2, a minimum of 1 sample, and a maximum of 28 samples were used as parameters.

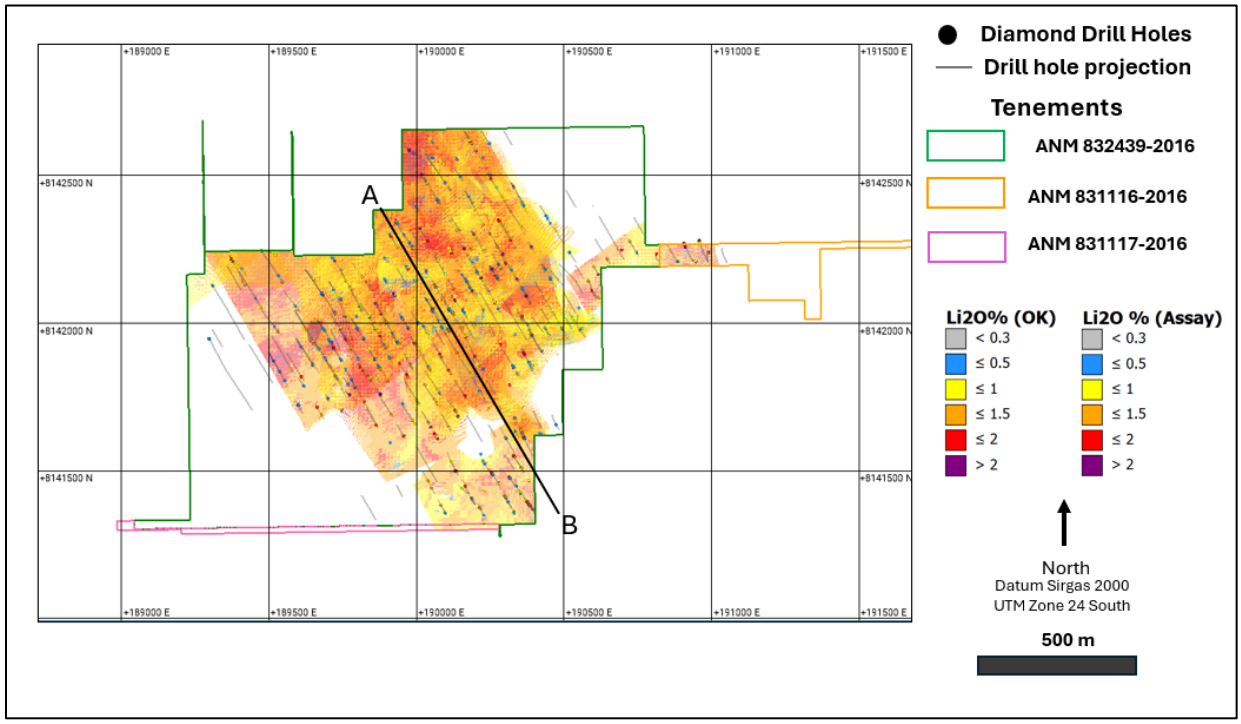
The schist density was defined as the mean of the 8,660 samples from the MGLIT database. The weathered zone does not have measurements, and GE21 has adopted the value 1.8 g/cm³ for this domain, a common value used by other companies in the Jequitinhonha Valley region. GE21 recommends carrying out additional density tests in weathered zones.

Table 14-6 shows the average IDW densities of each estimated pegmatite domain and the adopted densities of the host rocks.

Table 14-6: Density Values

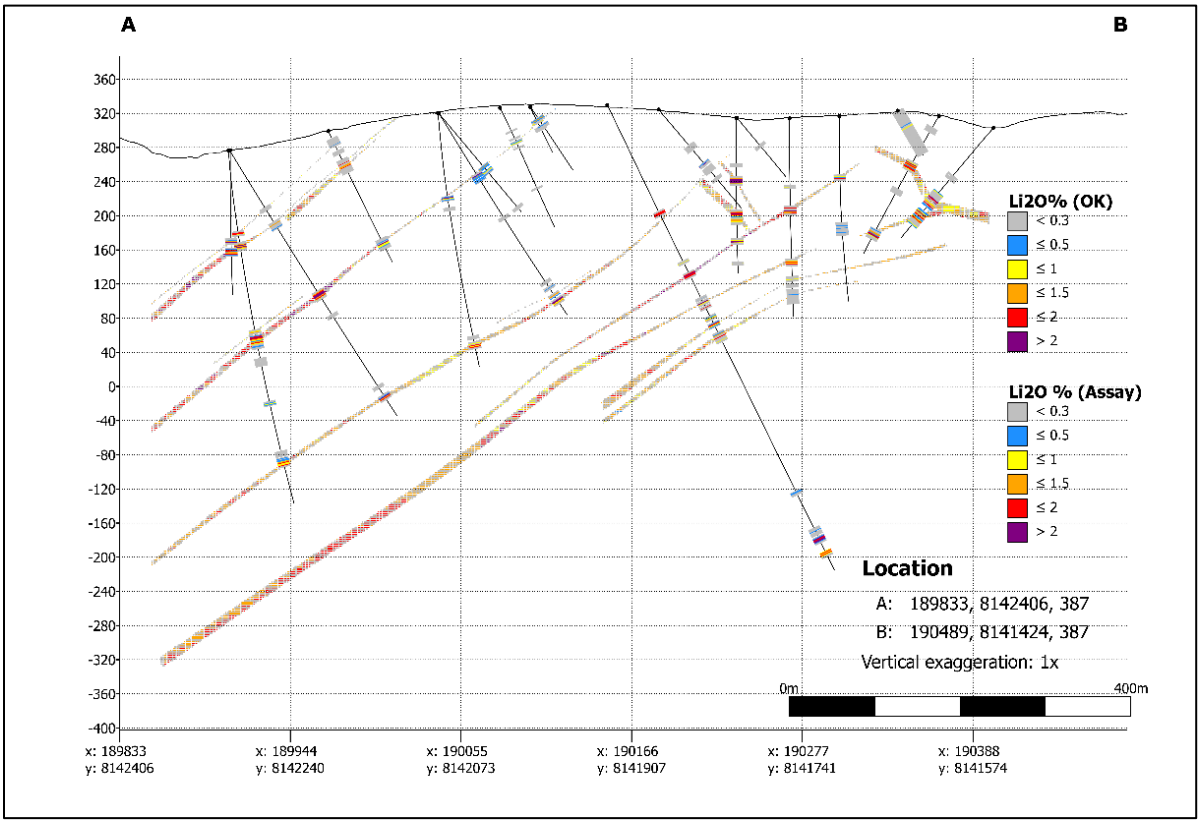
Spodumene Domains	Density Mean (g/cm³)	Spodumene Domains	Density Mean (g/cm³)	Spodumene Domains	Density Mean (g/cm³)
1	2.68	01B-SW	2.68	05C-NE	2.69
02-NE	2.66	01C-SW	2.67	05D-NE	2.66
03-NE	2.70	01D-SW	2.71	06A-NE	2.70
04-NE	2.66	01E-SW	2.34	06B-NE	2.69
05-NE	2.69	02A-NE	2.60	07A-NE	2.71
06-NE	2.69	02B-NE	2.71	08A-NE	2.74
07-NE	2.71	02C-NE	2.64	08B-NE	2.73
08-NE	2.71	02D-NE	2.65	09A-NE	2.71
09-NE	2.46	02E-NE	2.71	SE-A	2.62
10-NE	2.32	04A-NE	2.53		
11-NE	2.56	04B-NE	2.49	Domains	Density Mean g/cm³
15-SW	2.69	04C-NE	2.68		
16-SW	2.70	05A-NE	2.66	Shists Rocks	2.8
01A-SW	2.70	05B-NE	2.70	Weathered Zone	1.8

Source: GE21 (2025).



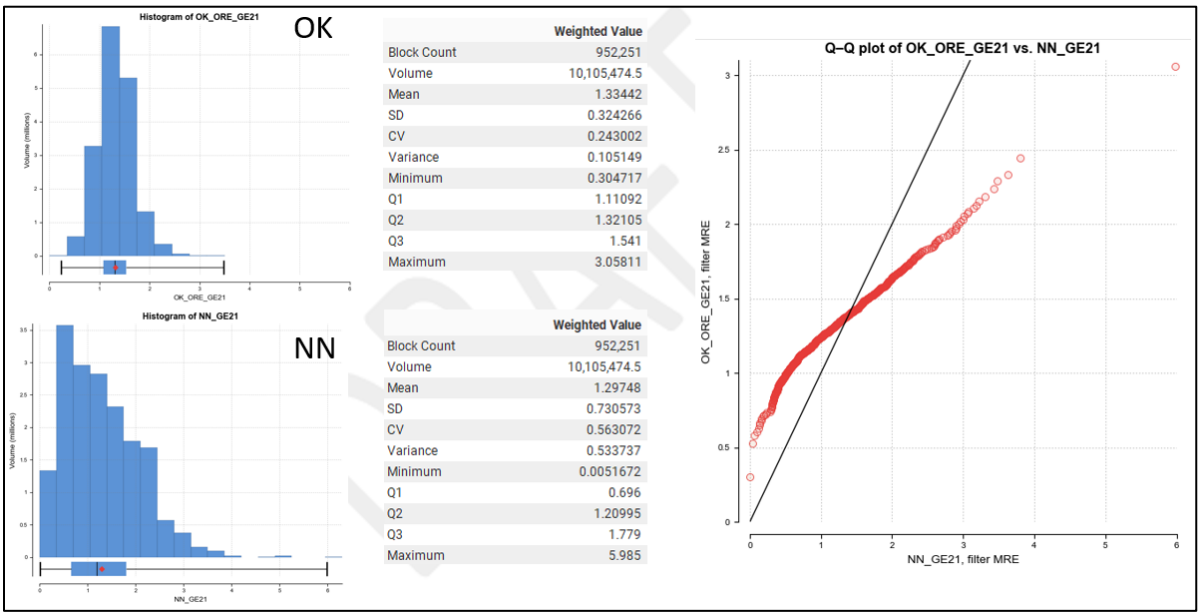
Source: GE21 (2025).

Figure 14-13: Project Li_2O % Grades Estimation (Plan View)



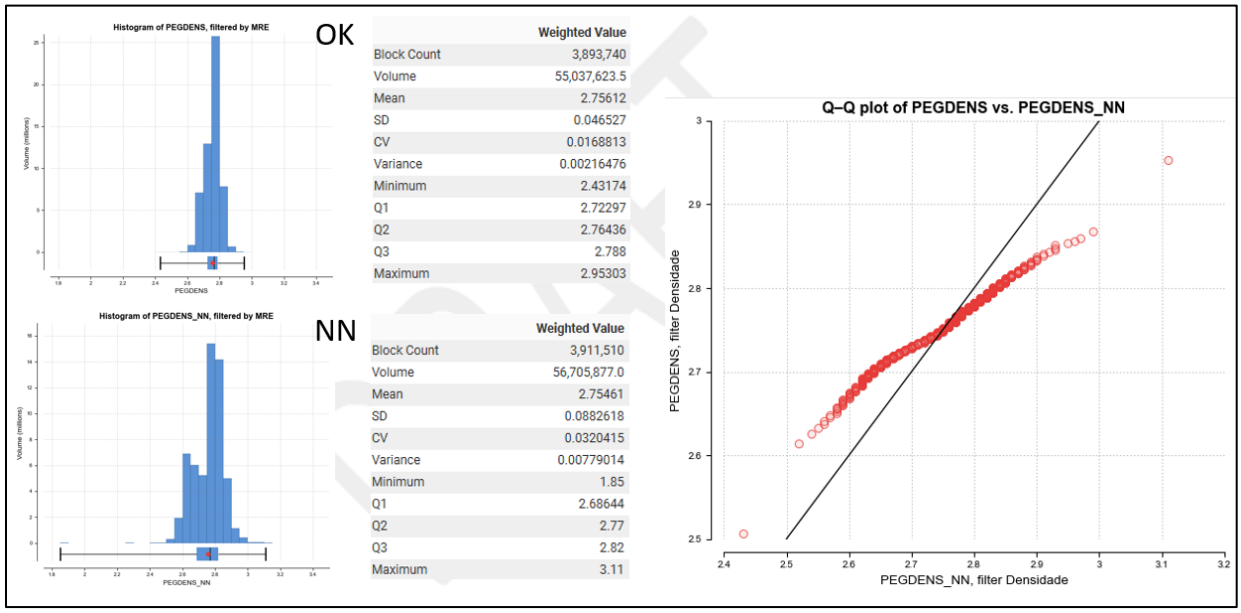
Source: GE21 (2025).

Figure 14-14: Project Li_2O % Grades Estimation (Cross-Section)



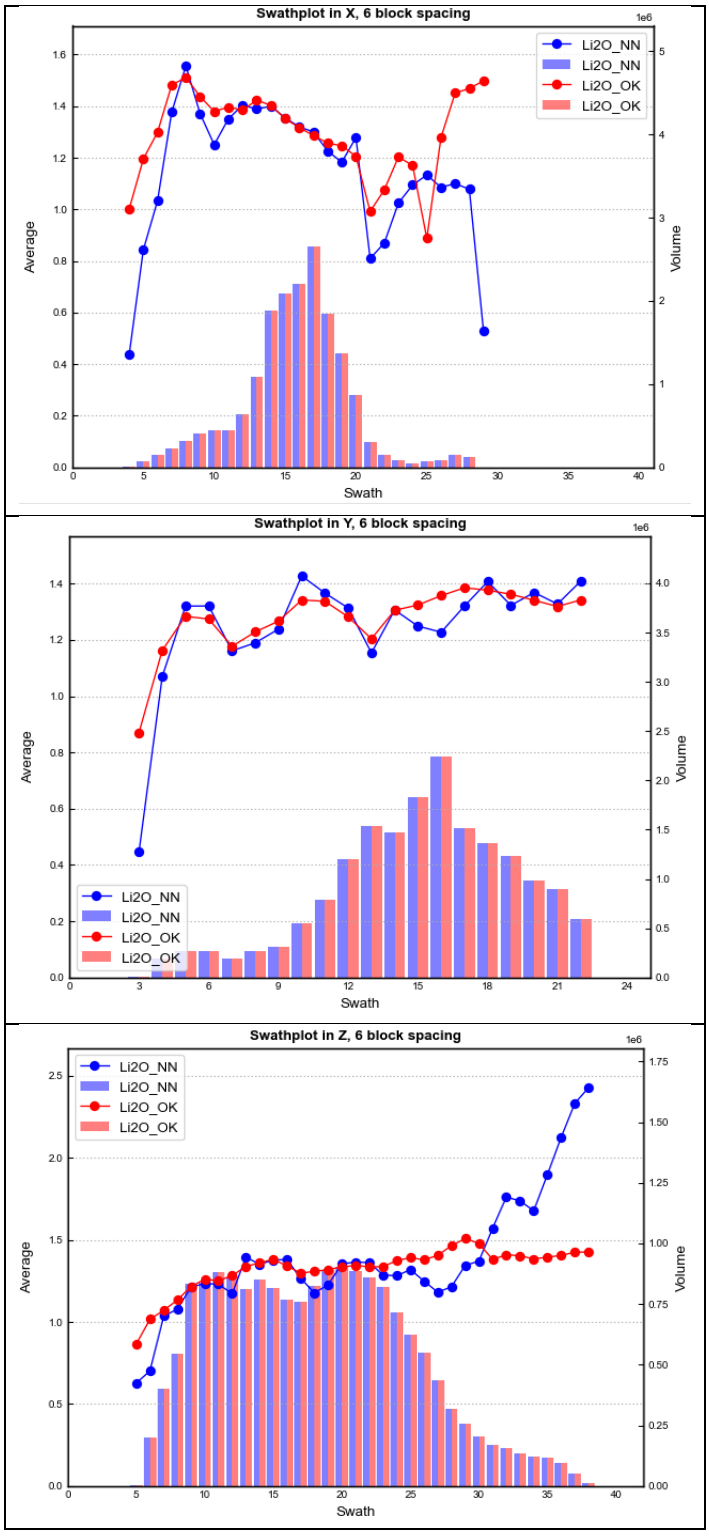
Source: GE21 (2025).

Figure 14-15: Estimation Validation—NN-Check of Li_2O



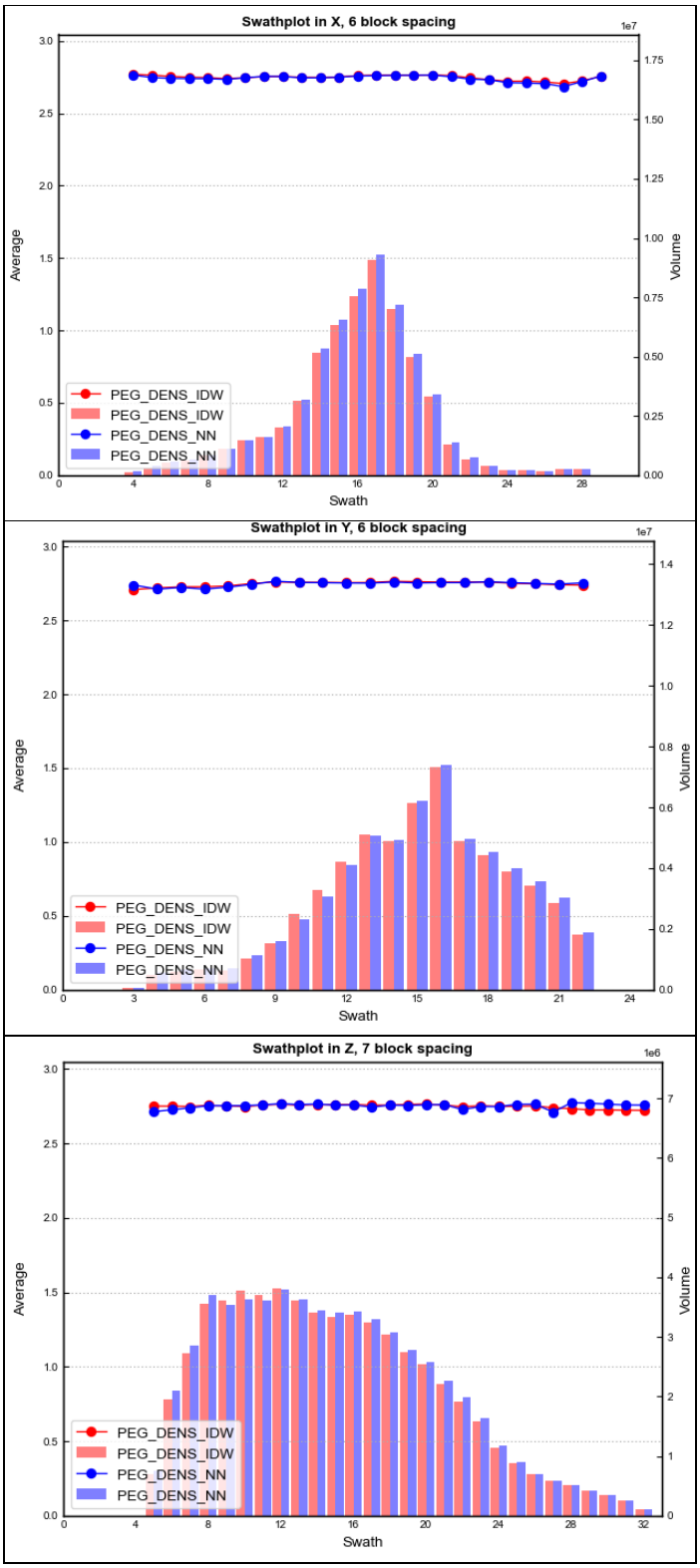
Source: GE21 (2025).

Figure 14-16: Estimation Validation—NN-Check of Density



Source: GE21 (2025).

Figure 14-17: Estimation Validation—Swath Plot on the X, Y, and Z Axes for Li_2O Grades



Source: GE21 (2025).

Figure 14-18: Estimation Validation—Swath Plot on the X, Y, and Z Axes for Density

14.8 Classification of Mineral Resources

The Mineral Resource was classified per CIM Definition Standards and *CIM Standards for Mineral Resources & Mineral Reserves* (CIM 2014), using geostatistical and classical methods and economically and mining-appropriate parameters relevant to the deposit type.

The classification boundaries made by GE21 for the Measured, Indicated, and Inferred categories were established through an approach that considered a comprehensive set of factors.

These factors included the sampling procedure analysis, sample grid spacing, survey methodology, and quality of assay data.

Additionally, drilling spacing and the progressive expansion of the search radius during grade estimation stages were also considered, as well as the average anisotropic distance of the samples and the continuity of pegmatite mineralization.

This multi-faceted approach ensured the robustness and accuracy of the classification process.

- The Measured Mineral Resource classification referenced the 50 m of the average Euclidean distance to sample (AvgD) used in OK estimation, with a minimum of six composites in at least three different drill holes.
- The Indicated Mineral Resource classification referenced the 100 m of the AvgD used in OK, with a minimum of six composites in at least three different drill holes.
- The Inferred Mineral Resource classification is all remaining estimated blocks.
- The total Mineral Resources were limited to the boundaries of the mining rights.
- The total Mineral Resources were constrained by the boundaries of the Mining Rights and the Reasonable Prospect for Eventual Economic Extraction (RPEEE) process for underground mining.

The resource classification was supported by a grade shell representing the underground mining appliance (Reasonable Prospect for Eventual Economic Extraction—RPEE), performed through a restricted wireframe based on a grade shell elaborated considering a cut-off of 0.5% Li_2O.

The calculations for the applied cut-off for the resource were based on the project's economic factors. That is, the values of the main costs were considered, including the extraction and processing costs of the ore, as well as other costs related to the production chain, taxes, and transportation expenses.

The long-term selling price value is based on the average of the projected curve values for the sale of 5.5% spodumene concentrate at Shanghai Port in China.

The calculation details are presented in Table 14-7 to Table 14-10.

The cut-off calculation resulted in 0.31%. However, a more conservative cut-off of 0.5% Li_2O was chosen for the RPEEE.

Table 14-7: Financial Assumptions

COG Inputs	Unit	Value
Selling Price SPO 5.5%	$/t concentrate	1,877.88
Selling Cost (CIF China)	$/t concentrate	112.47
TFRM	R$/t concentrate	2.11
CFEM	%	2.00
Royalties	%	1.00
Selling Price SPO 5.5%-Net	$/t concentrate	1,864.40
FLX	BRL/USD	5.07

Notes: COG = cut-off grade; CIF = cost, insurance, and freight; SPO = spodumene.

Table 14-8: Expected Costs

Costs	Unit	Value
Mine Cost	$/t	36.73
Pre-Operation Mine Cost	$/t	0.48
G&A	$/t	3.00
Plant Cost	$/t	24.63
SIB Cost	$/t	4.89

Table 14-9: Operational Parameters

Metallurgical Recovery SC5.5 (%)	69
Mass Recovery SC5.5 (%)	14.5
SPO Concentrate Grade 5.5	5.5

Table 14-10: Cut-Off Grade

Calculated Cut-Off	Li_2O
Cut-Off Grade %	0.31

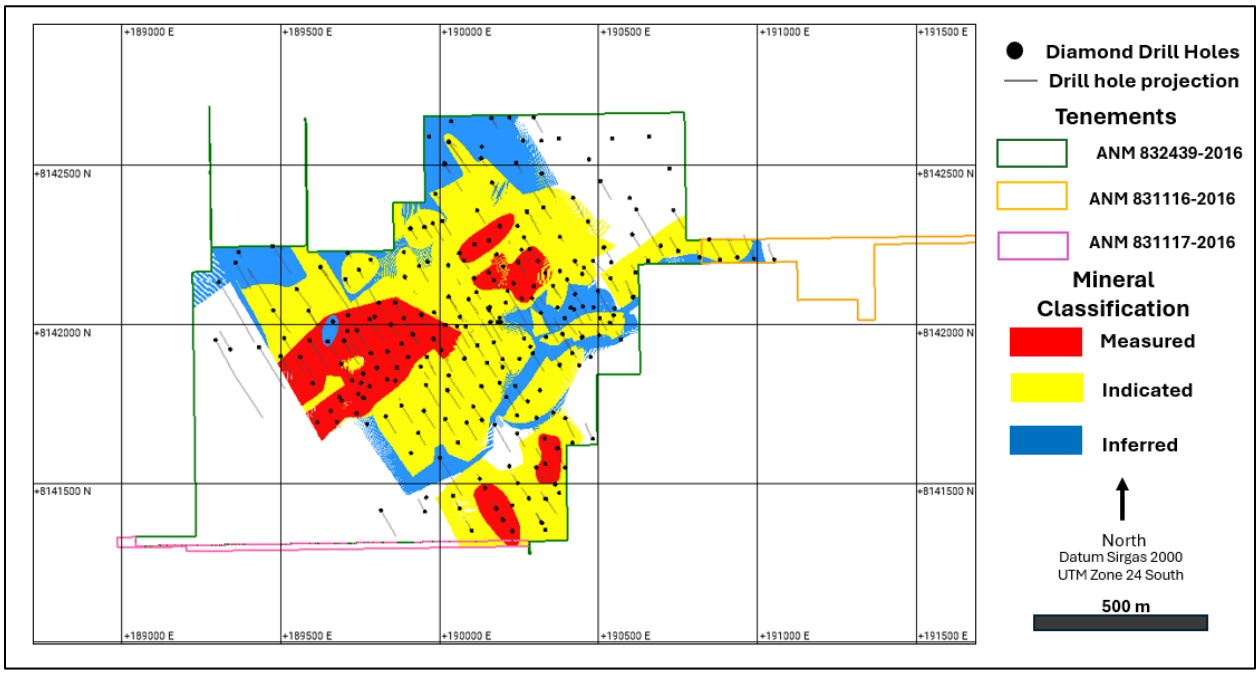
The Bandeira Mineral Resources estimate results are shown in Table 14-11, Figure 14-19, and Figure 14-20.

Table 14-11: Bandeira Mineral Resource Estimates (Base-Case Cut-Off Grade of 0.5% Li_2O)

Deposit/Cut-Off Grade	Category	Resource (Mt)	Grade % Li_2O	Contained LCE (kt)
Bandeira (0.5% cut-off)	Measured	3.36	1.38	115
	Indicated	23.91	1.33	786
	Measured + Indicated	27.27	1.34	901
	Inferred	18.55	1.34	615

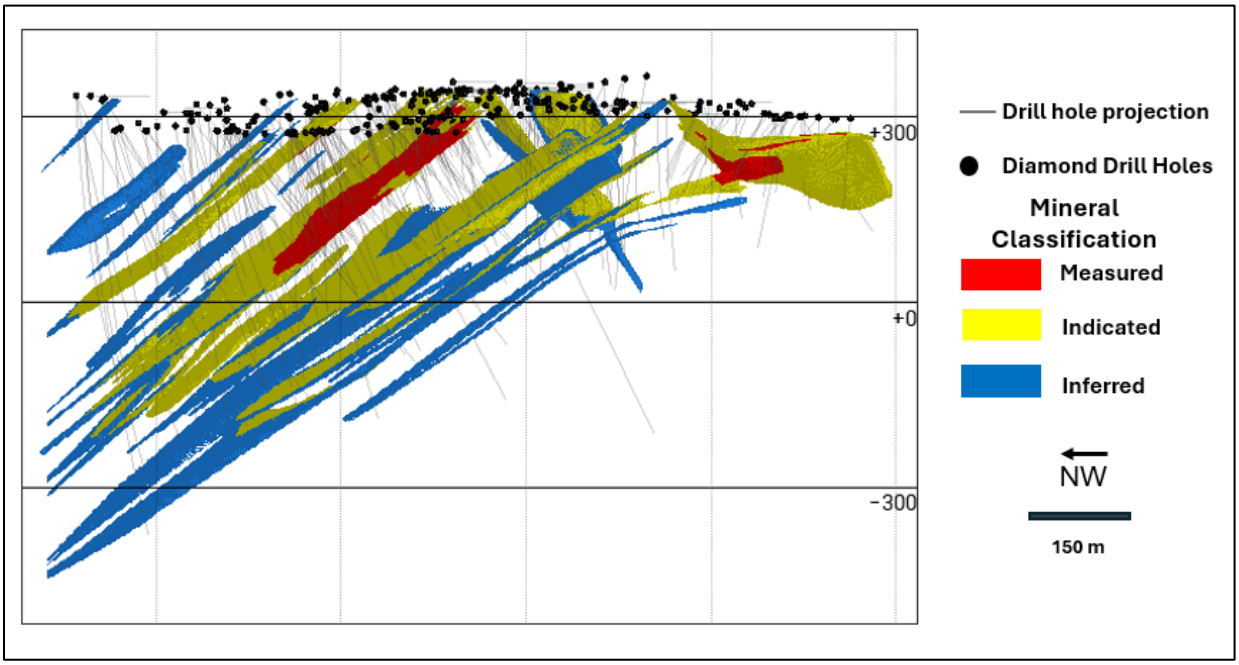
Source: GE21, 2025.
Notes:

- The Mineral Resource estimates effective date is November 20, 2024.
- Carlos J. E. Silva (MAIG #7868) prepared the Mineral Resource estimate using CIM (2014).
- The report meets the Canadian Securities Administrators' NI 43-101 requirements.
- Mineral Resources are not Mineral Reserves and have no economic viability. There is no certainty that any portion of the Mineral Resource will be converted into a Mineral Reserve.
- Figures are rounded to appropriate levels of precision, and discrepancies may occur due to rounding.
- The spodumene pegmatite domains were modelled using composites with Li_2O grades exceeding 0.3%.
- Grade estimation was conducted using OK within Leapfrog Edge 2024.1.3 software.
- The Mineral Resource estimate is confined to the MGLIT Bandeira mining rights (ANM) and includes only fresh rock domains.
- The Mineral Resource estimate was restricted by interpreting suitable-grade shells using a 0.5% Li_2O cut-off for underground resources.
- Inferred Mineral Resources are conceptual in nature and can only form the basis for economic analyses with further drilling and evaluation.
- The Mineral Resource estimate may be materially affected by environmental, legal, tax, sociopolitical, permitting, title, marketing, and other relevant factors.



Source: GE21 (2025).

Figure 14-19: Resource Classification with RPEEE (Plan View)



Source: GE21 (2025).

Figure 14-20: Resource Classification with RPEEE (Cross-Section)

15 MINERAL RESERVE ESTIMATES

GE21 prepared the Mineral Reserve estimates in this Technical Report based on the Mineral Resources estimate with the effective date of November 20, 2024 (Horta de Cerqueira Viana, et al., 2025, June 6). Mineral Reserves are classified as either Probable or Proven, and are based on Indicated and Measured Mineral Resources only, in accordance with the CIM Definition Standards.

The Mineral Reserve estimates were made using metal prices and foreign exchange rates in accordance with the US Securities and Exchange Commission Industry Guide 7, which requires the use of prices that reflect current economic conditions at the time of Mineral Reserve determination. The assumptions used in this Mineral Reserve estimate based on the Mineral Resource with an effective date of November 20, 2024, are a selling price of $1,157.20/t of concentrate at 5.2% Li_2O and an exchange rate of R$5.85:$1.00.

There is no known mining, metallurgical, infrastructure, permitting, or other relevant factors that could materially affect the Mineral Reserve estimates (Table 15-1).

Table 15-1: Project Mineral Reserves

Ore Reserve Class	Volume (Mm^3)	Mass (Mt	Grade (Li_2O %)	Contained LCE (kt)
Proven				
Underground	0.85	2.29	1.12	63.8
Open Pit	0.11	0.28	1.10	7.5
Subtotal Proven	0.95	2.57	1.12	71.4
Probable				
Underground	7.29	19.80	1.09	534.2
Open Pit	0.31	0.82	1.13	22.9
Subtotal Probable	7.59	20.63	1.09	557.1
Total Proven & Probable	8.54	23.20	1.10	628.5

Notes: dmt = dry metric tons

- CIM (2014) was followed for Mineral Reserves estimates.
- Conventional sublevel stoping and open-pit mining methods have been proposed.
- The Mineral Reserves were calculated considering a cut-off grade of 0.5% Li_2O for underground and 0.3% for open pit.
- For the sublevel stoping mining method, Mineral Reserves volumes and tonnages assume 90% of mine recovery, 21% of planned dilution, and 0% of operational dilution the stopes are being cabled.
- Minimum stope width: 2.5 m.
- For the ore from development to work, Mineral Reserve volumes and tonnages assume 100% of mine recovery, 31% of planned dilution, and 10% of operational dilution due to overbreaking.
- For the open pit, Mineral Reserves assume 100% of mine recovery and 10% of dilution.
- The processing plant is expected to produce at a maximum feed rate of 1.3 Mt/a (dry basis) with a process recovery of 65.3%.
- Figures are rounded to appropriate levels of precision, and discrepancies may occur due to rounding.

15.1 Cut-Off Grade

Cut-off grades are estimated on a fully costed basis for underground mining and on an incremental basis for open pit. The calculations for the cut-off grades are presented in Table 15-2 and Table 15-3,

corresponding to open-pit and underground mining, respectively. The cut-off grade was calculated based on $1,157.20/t Li_2O price and R$5.85:$1.00 exchange rate.

Table 15-2: Open Pit Cut-off Grade Calculation

COG Inputs	Unit	Value
Selling Price	$/t concentrate	1,157.2
Selling Cost (CIF China)	$/t concentrate	122.8
TFRM	R$/t ore	2.2
CFEM	%	0.02
Royalties	%	0.01
Appian Royalty	%	0.02
Selling Price SPO 5.2%—NET	$/t concentrate	973.6
FLX	BRL/USD	5.85
Mine Cost	$/t	2.2
Strip Cost	$/t	27.2
G&A	$/t	2.7
Plant Cost	$/t	13.3
Metallurgical Recovery SC 5.2%	%	65.3
SPO Concentrate Grade 5.5	%	5.2
Calculated Cut-Off	**Unit**	**Li_2O**
Full-Grade Ore	%	0.3

Table 15-3: Underground Cut-off Grade Calculation

COG Inputs	Unit	Value
Selling Price SPO 5.2%	$/t concentrate	1,157.2
Selling Cost (CIF China)	$/t concentrate	122.8
TFRM	R$/t concentrate	2.2
CFEM	%	2.0
Royalties	%	1.0
Appian Royalty	%	2.3
Selling Price SPO 5.2%—NET	$/t concentrate	973.6
FLX	BRL/USD	5.85
Stoping Mine	$/t	23.1
Cost Raise Borer	$/t	0.8
Cost Dev Lateral	$/t	12.3
Cost G&A	$/t	2.7
Cost Pant	$/t	13.3
Cost SIB	$/t	8.2
Cost Haulage DVP	$/t	2.5
Metallurgical Recovery SC 5.2 (%)	%	65.3
SPO concentrate Grade 5.5	%	5.2
Calculated Cut-Off	**Unit**	**Li_2O**
Full-Grade Ore	%	0.5

15.2 Pit Shell Selection

The optimization of the open pit for the Mineral Reserves was conducted using NPV Scheduler software (Version 3.0.373.0). The chosen pit shells for the final design were determined based on $1,145.63/t Li_2O price with a revenue factor (RF) of 0.99. The ultimate pit was selected to maximize the net present value as shown in Table 15-4.

Table 15-4: Pit Optimization Results

Phase	Factor	Profit	Profit Per Unit Mass	NPV	Worst Case NPV	Rock	Total Ore	Strip Ratio	Total Waste
60	90	113,416,745	8.96	109,701,544	108,502,856	12,658,810	1,190,588	9.63	11,468,222
61	91	113,417,412	8.96	109,702,164	108,503,089	12,661,433	1,190,648	9.63	11,470,785
62	96	113,418,352	8.95	109,703,037	108,503,133	12,668,855	1,190,807	9.64	11,478,048
63	97	113,419,440	8.95	109,704,048	108,504,125	12,678,419	1,191,122	9.64	11,487,297
64	98	113,419,828	8.94	109,704,409	108,504,048	12,684,212	1,191,231	9.65	11,492,981
65	99	113,419,906	8.94	109,704,481	108,504,031	12,685,792	1,191,256	9.65	11,494,536
66	102	113,418,223	8.92	109,702,915	108,499,603	12,720,356	1,192,323	9.67	11,528,033
67	104	113,417,128	8.91	109,701,898	108,497,141	12,733,627	1,192,564	9.68	11,541,063
68	106	113,416,922	8.91	109,701,706	108,496,745	12,735,218	1,192,600	9.68	11,542,618
69	107	113,416,644	8.90	109,701,447	108,496,319	12,736,820	1,192,649	9.68	11,544,171
70	108	113,416,104	8.90	109,700,946	108,495,245	12,739,957	1,192,721	9.68	11,547,236
71	110	113,414,975	8.90	109,699,896	108,492,978	12,744,636	1,192,877	9.68	11,551,758
72	111	113,414,288	8.90	109,699,258	108,491,770	12,747,278	1,192,950	9.69	11,554,328
73	112	113,413,454	8.89	109,698,484	108,490,901	12,750,425	1,193,024	9.69	11,557,402
74	113	113,413,027	8.89	109,698,086	108,490,412	12,752,033	1,193,048	9.69	11,558,985
75	114	113,411,782	8.89	109,696,929	108,488,753	12,756,221	1,193,133	9.69	11,563,088
76	116	113,411,257	8.89	109,696,441	108,488,134	12,757,799	1,193,157	9.69	11,564,642
77	120	113,409,379	8.89	109,694,697	108,485,732	12,762,416	1,193,229	9.70	11,569,187

15.3 Underground Mineral Reserve Estimates

The underground Mineral Reserves are being estimated by the stope optimization, which defines the portions of the Mineral Resource that can be mined safely, technically, and economically. This process incorporates economic parameters, development and mining costs, metallurgical recovery, dilution, mining losses, and geotechnical criteria such as minimum stope dimensions and pillar requirements.

Based on these parameters, specialized Datamine MSO software (Version 3.4.304.0) automatically delineates the mineable stopes using a cut-off grade of 0.50 % Li_2O, which are then refined to reflect operational conditions. Following this step, all required accesses are designed, including ramps, crosscuts, ventilation raises, and supporting infrastructure, ensuring technical and operational feasibility.

With stopes and accesses defined, a full economic assessment of the Project is carried out, integrating capital and operating costs, development schedule, and cash-flow analysis. The outcome is an optimized mine plan that ensures efficient resource utilization and the long-term economic sustainability of the underground operation.

16 MINING METHODS

This section summarizes the Project underground mine and open-pit studies. Selecting the mine method took into consideration economic and geological factors, such as sale, price, costs, and dip and orientation of the ore body veins as other features. The primary ore bodies represent approximately 22.1 Mt of the Bandeira deposit. These will be extracted in an underground mine using top-down, longhole, sublevel stoping; the secondary, southeast ore body, comprising approximately 1.09 Mt, will be mined from an open pit.

The target production of run-of-mine (ROM) ore is scheduled to be 1.3 Mt/a; the mining strategy will be:

- Year −2: develop the first decline beginning once the mine entrance is completed.
- Year −1: a key Project year. The second mine entrance is completed, and the focus remains on advancing underground development. To increase efficiency and improve development rates in both main declines, the multi-blast technique is applied. To bring ore into the process earlier, open-pit operations are planned to start.
- Year 1: As underground development advances, ore production from underground operations increases as part of the mine ramp-up phase. Open-pit ore is depleted, and the processing plant continues operating using ore from underground production, complemented by stockpiled ore.
- Year 2: The underground mine reaches full production capacity, achieving output of 1.3 Mt/a.

The underground mine will operate three 6-hour shifts a day for 365 days a year (6,552 hours per year of planned production). A two-hour interval between shifts will allow mine ventilation to dissipate blasting gases, during which the crew will have their meal. The open pit will operate two 10.5-hour shifts on weekdays and one shift on weekends, with a 1.5-hour meal break per shift, for 365 days a year (5,616 hours per year of planned production). The administrative operating schedule will be one 9-hour shift per weekday, including one hour for lunch (2,080 hours per year).

16.1 Geotechnical Appraisal

16.1.1 Domaining and Geotechnical Characterization

The domaining and geotechnical characterization is based on detailed geotechnical core logging combined with laboratory testing, enabling the systematic classification of geotechnical domains. This approach defines the mechanical and structural properties of the two principal lithological units comprising the Project rock mass: the banded quartz-mica to mica-quartz schists (schists); and the metasedimentary host rock and magmatic ore body (pegmatites).

London (2008), Pedrosa-Soares et al. (2025), and MGLIT previous reports (2024) confirm that the pegmatites postdate the schists, with pegmatites forming sharp, undeformed contacts with thin chilled margins, and the schists forming local thermal metamorphism and metasomatism recrystallization aureoles. The two lithologies display contrasting fabrics: schists exhibit a tectonic framework with ductile structure (e.g., S1 schistosity) and brittle structure (S2 spaced cleavage, late joints), while pegmatites crystallized in an undeformed setting as dykes and lenses.

Pegmatite fabrics reflect magmatic processes, including mineral alignment parallel to contacts, unidirectional solidification textures (e.g., spodumene laths perpendicular to contacts), and grain-size coarsening toward the core. Cooling fractures are common and oriented parallel to contact, but increasingly chaotic in thicker bodies (>10 m). Unlike schists, pegmatites lack regional foliation, cleavage, and jointing though minor fractures and small faults occasionally occur near contacts.

To date, 31,524.20 m of core have been logged, with a focus on characterizing the rock mass and defining its geotechnical domains (Figure 16-1) guided by the vertical zoning of the Bandeira deposit, which is driven by weathering processes associated with meteoric water infiltration. These processes result in varying degrees of rock alteration, and consequently different geotechnical qualities within the rock mass. In general, the Project area presents a shallow weathering profile, with the thickness of the residual soil and saprolite rarely exceeding 12 m. Geotechnical properties were defined based on the degree of weathering and rock quality designation (RQD), correlated with laboratory test results. This integrated approach enabled defining representative strength ranges for the horizons of soil, saprolite, sap rock, weathered rock, and fresh rock in both schists and pegmatites (Figure 16-2).

Analysis of discontinuities and anisotropies in the drill cores indicates that the rock mass is structurally homogeneous, arranged homoclinally. The pegmatitic intrusions occur as dykes consistently hosted within the main regional metamorphic foliation (S1 schistosity), a ductile planar structure representing the most penetrative anisotropy of the country-rock mass. Within the fresh-rock domain, at least two sets of discontinuities were identified in the host rocks, typically characterized by small apertures and no infilling material.

The Project structural analysis is based on data from 41 oriented drill holes, with 643 structural features logged. These were classified into five main categories: Bottom Contact, Fracture, S1 Foliation (schistosity), S2 Foliation (spaced cleavage), and Top Contact (Figure 16-3). The S1 foliation is highly penetrative, well-developed, and exhibits a regional NE–SW orientation that represents the primary anisotropy of the country rock mass. The S1 foliation controls the geometry of concordant pegmatite intrusions and is observed exclusively within the schist domain. Table 16-1 presents the average orientation of each discontinuity type.

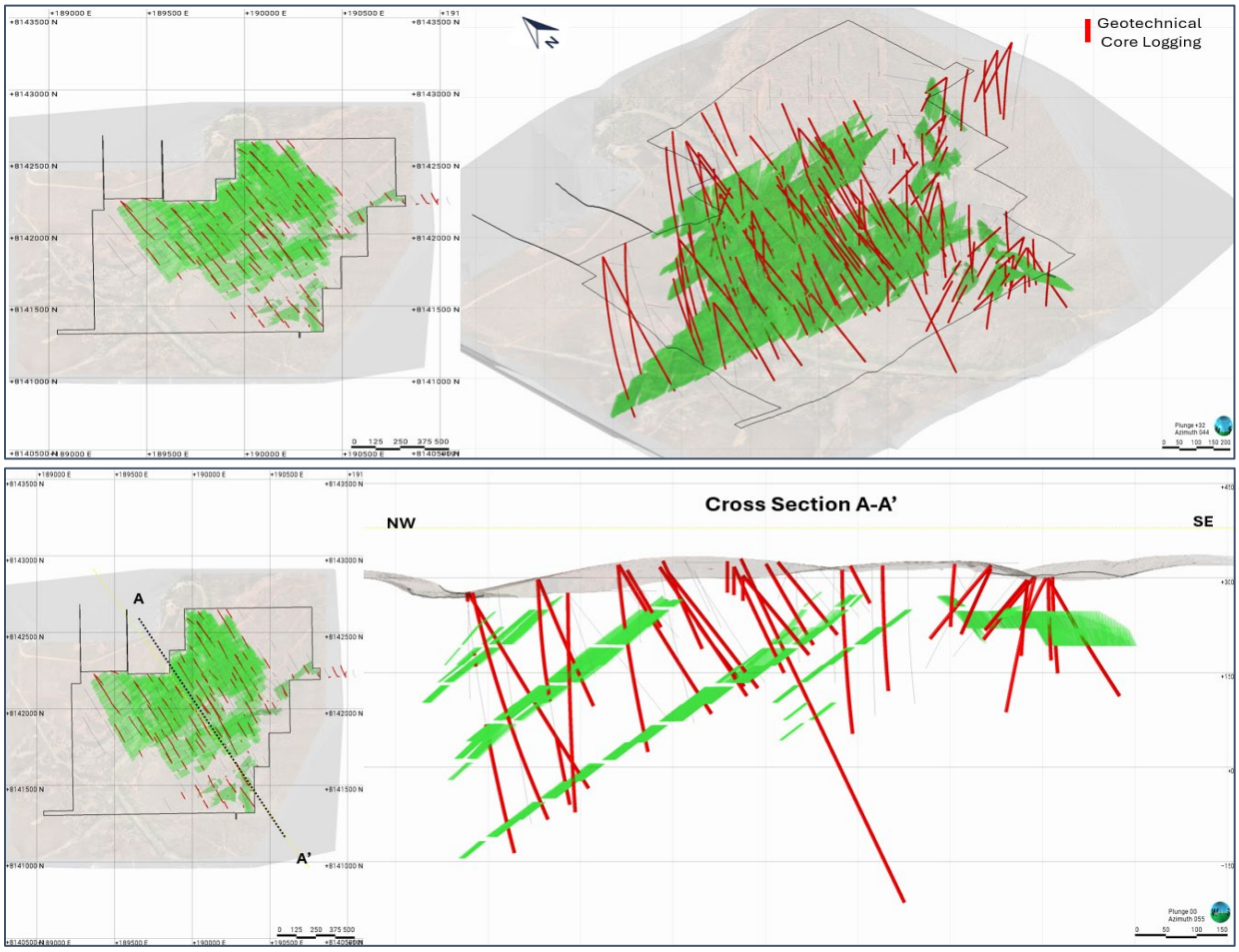


Figure 16-1: Spatial Distribution of Drill Core Geotechnical Logging at the Bandeira's Project—Top Left, Plan; Top Right, Oblique View of Geotechnical Core Logging Holes at the Project Stopes; Bottom Left, Section A–A´ in Plan; Bottom Right, Cross-Section A–A´ (Ore body, Green; Drill Holes, Red)

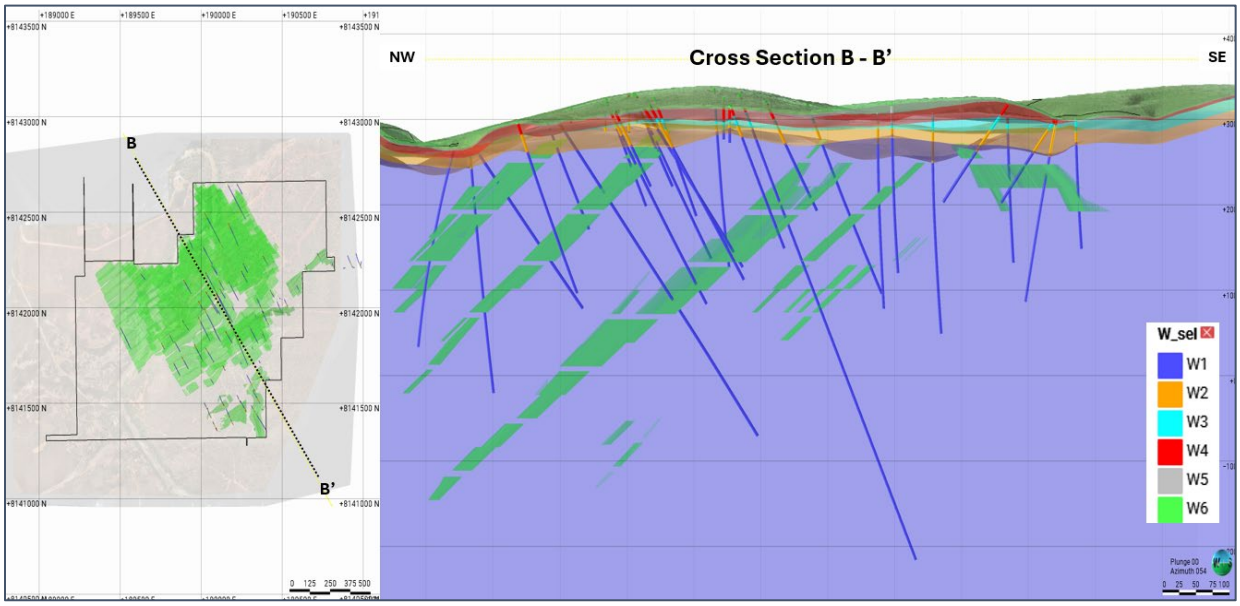


Figure 16-2: Left, Underground Mine Plan Showing Stopes Plan and Section B–B'; Right, Cross-Section B–B´ Project Weathering Profile Model (Ore body, Green; Drill Holes, Red) (Drill Holes Vary in Colour According to the Weathering Profile Classification)

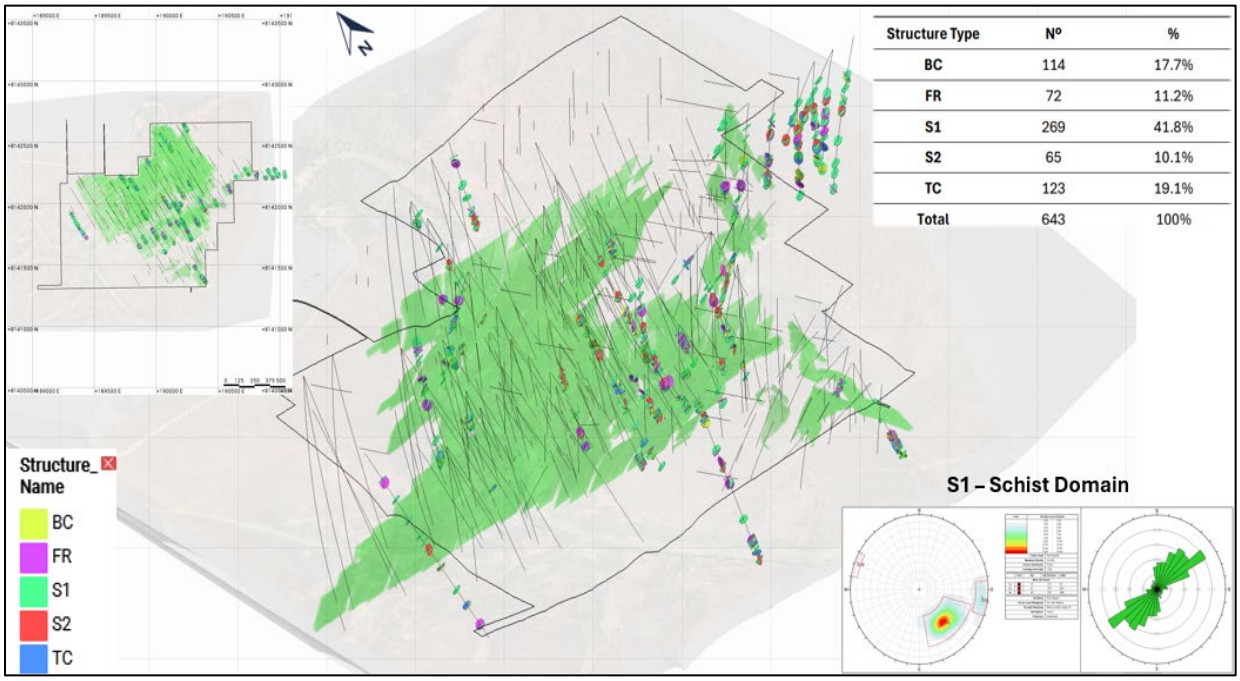


Figure 16-3: Plan (Inset), and Oblique View of Spatial Distribution and Statistical Data Relating to the Project Structural Analysis

Table 16-1: Average Orientation of Project Structures

Structure	Structure Type	Dip (°)	Dip Direction (°)
S1	Foliation	46	316
S2	Spaced Cleavage	72	275
FR1	Fracture dipping to NW	36	302
FR2	Fracture dipping to SE	21	141
Contact	Ore contacts in pegmatite	31	315

An extensive geotechnical program was conducted, including 999 m of mixed drilling, and new soil and rock tests to improve the understanding of geotechnical domains. This effort significantly expanded the database, reaching 31,524.20 m of geotechnical descriptions. A new technical logging campaign is underway to further refine the understanding of rock mass behaviour through detailed characterization of the crown pillar and the entire mine area, complemented by laboratory tests and a borehole televiewer survey campaign (Figure 16-4).

The results will enable a more accurate definition of geomechanical domains and a robust characterization of strength parameters, allowing for continuous improvement and optimization of design parameters. Although additional testing is planned, the current data are considered sufficient for the feasibility-level design.

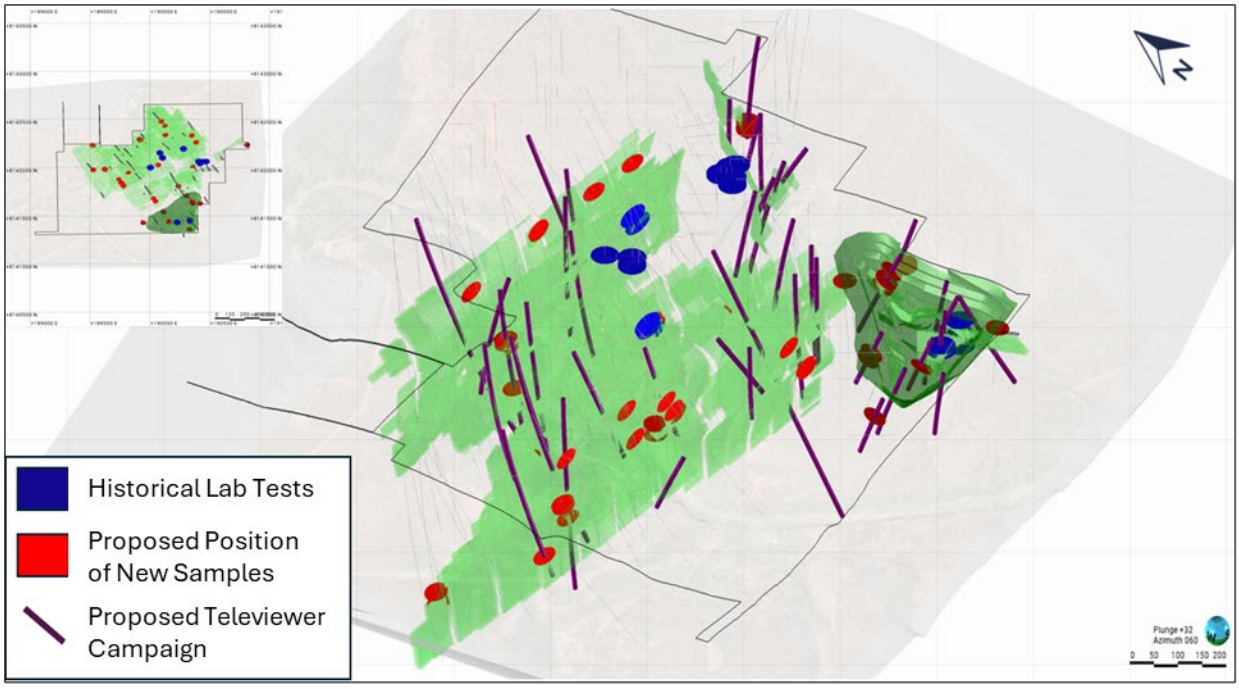


Figure 16-4: Plan (Inset) and Oblique View of Spatial Distribution of Historical Laboratory Tests and Newly Proposed Additional Sampling Positions for Testing as well as the Planned Drill Hole Televiewer Campaign

Subject to scale limitations, the data obtained from drill-core geotechnical logging are considered adequate for the current stage of geomechanical and soil characterization. They provide a sound basis

for preliminary definition of strength parameters and geotechnical indices that support mine planning and development of the Project.

The geomechanical domains were based on the analysis of the drill-core data, enabling the identification of fracture patterns, RQD, weathering profiles, and discontinuity characteristics. The classification of the Project rock mass is based on industry-recognized rock-mass classification systems, Bieniawski's (1973) rock mass rating (RMR) and Barton's (1974) Q-index.

Rock Mass Rating

The RMR classification assesses quality on a scale of 0 to 100 (Table 16-2). The system evaluates:

- RQD
- Intact rock strength
- Discontinuity spacing
- Discontinuity conditions
- Groundwater conditions
- Discontinuity orientation.

Table 16-2: Rock Mass Rating Ranges

Rock Mass Rating	Range
Very Good	81–100
Good	61–80
Fair	41–60
Poor	21–40
Very Poor	<20

Q-System

The Q-System (Barton et al., 1974) estimates rock mass quality (*Q*) based on the equation:

$$Q = \frac{RQD}{J_n} \times \frac{J_a}{J_r} \times \frac{J_w}{SRF}$$

where *RQD* is the rock quality designation,
J_n is the joint set number,
J_r is the joint roughness number,
J_a is the joint alteration number,
Jw is the joint water-reduction factor, and
SRF is the stress reduction factor.

The Q-system range is presented in Table 16-3.

Table 16-3: Q-System Rock Mass Quality Range

Rock Mass Quality	Range
Very Good	≥40
Good	10.0–40.0
Fair	4.0–0.0
Poor	1.0–0
Very Poor	0.1–1.0
Exceptionally Poor	<0.1

The combined use of RMR and Q-System provides a more comprehensive assessment of rock mass conditions. This dual approach directly supports engineering design and the dimensioning of underground excavations, underground openings, and ground-support strategies, thereby contributing to successful Project implementation.

16.1.2 Residual Soil and Saprolite Domain

To classify the soil and saprolite domains, the International Society for Rock Mechanics and Rock Engineering (ISRM) weathering classification system (Brown, 1981) was used and is described in more detail in Table 16-4. The saprolite layer extends approximately 12 m below the surface and is characterized by intense weathering, corresponding predominantly to ISRM's weathering alteration grades W5/W6. From a rock mechanics perspective, this material exhibits very low strength, typically corresponding to rock strength classes R0/R1. The near-surface location of the W5/W6 weathered material zone is shown in Figure 16-5.

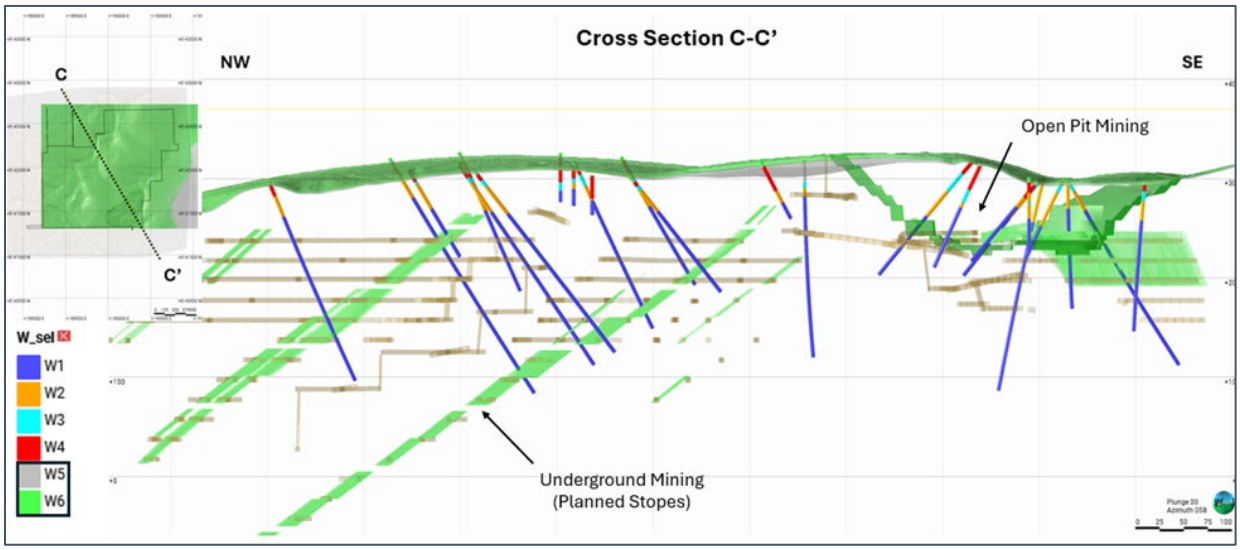


Figure 16-5: Plan (Inset) Showing Section C–C' and Cross-Section C–C' of the Soil and Saprolite Domains in the Open Pit (Arrow) and Underground Mine Excavations (Light Green) (Drill Holes Coloured According to Degree of Weathering Alteration Grades W1 through W5)

Due to its nature, this highly weathered material—comprising residual soil and saprolite—is not suitable for conventional rock mass classification systems such as RMR or Q. Instead, this horizon is described

using integrated soil classification methods, and geotechnical core logging, complemented by a dedicated soil investigation program to determine his features. This combined program drilled 1,000 m and included mixed drilling methods, with borehole depths ranging from 11 m to 46 m, and included the following tests:

- Standard penetration tests (SPT) in soil layers
- Infiltration tests to assess soil permeability
- Direct shear and triaxial tests on soil material
- Lugeon (Packer) tests to evaluate permeability in the fractured rock mass
- Uniaxial compressive strength (UCS) tests on core samples with varying degrees of consistency and cohesion.

The mixed drilling program was designed to characterize the geomechanical behaviour of the soil and weathered rock mass. For this purpose, technical criteria were adopted based on the evaluation of the following parameters:

- Degree of weathering (W)
- Degree of coherence (C1 to C5)
- Degree of fracturing (F1 to F5).

Table 16-4 and Table 16-5 present the criteria applied in the classification of the parameters analyzed for the weathering horizon.

Table 16-4: Degree of Weathering of the Rock Mass

Degree	Geotechnical Classification	Features
W1	Fresh or Intact Rock	No mineralogical alteration. Minerals retain original luster, colour, and cleavage. Occasional discolouration along discontinuities. Foliation visible and sealed. Rock strength unaffected.
W2	Slightly Weathered Rock	Perceptible mineralogical alteration, with faded colours and loss of luster. Slight discolouration and oxidation in the matrix and along discontinuities. Foliation visible and sealed. Joints closed, walls slightly altered. Original rock strength partially affected by alteration.
W3	Moderately Weathered Rock	The matrix is discoloured, with evidence of oxidation. Open joints (<1.0 mm) and oxidized, with more weathered material possibly occurring along discontinuities. Foliation enhanced by weathering. Strength affected by weathering.
W4	Highly Weathered Rock (Sap Rock transition)	Very intense mineralogical alteration, with some minerals partially decomposed into clay minerals. Matrix completely oxidized and colours strongly modified. Open

Degree	Geotechnical Classification	Features
		fractures (2–5 mm), oxidized and filled with altered materials. Foliation enhanced by weathering. Delamination along foliation. Strength strongly affected by alteration.
W5	Completely Weathered Rock (Saprolite)	All material completely weathered to structured soil. Extremely discoloured, resistant minerals broken down and others transformed into clay minerals. Foliation preserved. Joints not discernible. Disintegrates in water after a period of immersion.
W6	Soil (Residual Soil)	Original rock fabric destroyed. Material consists entirely of soil derived from in situ weathering.

Note: Adapted from Brown (1981).

Table 16-5: Consistency According to ISRM Standards

Degree of Coherence	Label	Features	Brown (R)	UCS (MPa)
C5	Extremely weak	Scratched with fingernail	R0	0.25–1
	Very weak	Crumbles under impact of geologist's hammer; can be scraped with a pocket knife	R1	1.0–5.0
C4	Weak	Can be scraped with a pocket knife with difficulty; marked by a firm blow with the tip of a geologist's hammer	R2	5.0–25.0
C3	Moderately strong	Cannot be scratched with a pocket knife; samples can be fractured with a single blow from a geologist's hammer	R3	25.0–50.0
C2	Strong	Samples require more than one blow with a hammer to fracture	R4	50.0–100.0
C1	Very strong	Samples require many blows with a hammer to fracture	R5	100.0–250.0
	Extremely strong	Samples can only be chipped with a geologist's hammer	R6	>250

Source: Associação Brasileira de Geologia de Engenharia e Ambiental—ABGE (1983), and according to ISRM.

Summary of soils and saprolite classification are as follows:

- Surface cover (W6, R0): a clayey-silty-sandy soil with a thickness of 2.5 to 6.0 m. SPT values range from 2 to 10 blows/30 cm; average permeability is 3.2×10^{-5} cm/s.
- Underlying saprolite (W5, R1): corresponds to weathered quartz-biotite schist, with a thickness of 1 m to 7 m, sandy-silty grain size, and low clay content. SPT values range from 20 to 30 blows/30 cm, with an average hydraulic conductivity of 2.9×10^{-5} cm/s.

Figure 16-6 provides examples of the residual soil and saprolite materials forming this domain, as observed within the drilled-core samples. These cores display varying degrees of weathering; therefore, different geotechnical qualities can be identified within a single core interval (e.g., W5 and W6 in Drill Hole ITDD-22-009: 0.0 m–6.4 m). This domain represents an unconfined granular aquifer with low hydraulic conductivity, formed by weathering of surface rocks and acting as a medium for groundwater storage and flow.



Figure 16-6: An Example of a Soil and Saprolite Domain within which Different Weathering Profiles can be Identified

Figure 16-7 presents the geological–geotechnical profile of the longitudinal section along the Portal 1 axis, planned to provide access to the underground mine. The profile summarizes results from investigations aimed at the detailed characterization of soils and weathered rocks, focusing on the geotechnical behaviour of residual soil and mica-schist saprolite.

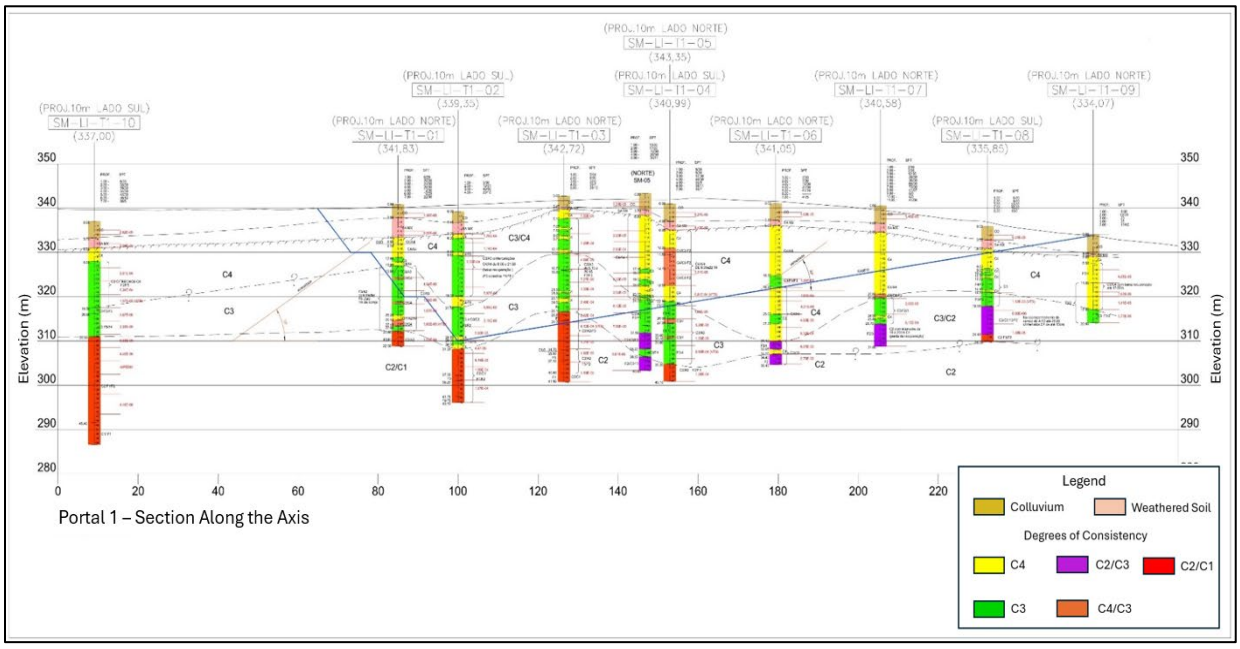


Figure 16-7: Longitudinal Section Along the Axis of Portal 1

Shear strength parameters, defined using the Mohr–Coulomb criterion, are:

- Residual soil (W6):
  - γ = 17 kN/m³; c' = 20 kPa; φ' = 35°
- Saprolite (W5):
  - γ = 18 kN/m³; c' = 15 kPa; φ' = 38°

where y = unit weight,
C' = cohesion, and
φ' = friction angle.

The Mohr–Coulomb criterion was applied, as it is appropriate for soil materials. Based on SPT results, core logging, laboratory testing, and field observations, these parameters support the definition of geotechnical domains and the characterization of the near-surface zone, which is critical for assessing slope stability, foundation performance, and the hydrogeological response of the upper layers of the Bandeira deposit.

16.1.3 Sap Rock and Weathered Rock Domain

The sap rock and weathered rock domain extends to approximately 35 m below the surface, and is characterized by moderate weathering, which results in a predominant alteration grade of W3/W4. This domain exhibits low mechanical-strength parameters, in rock strength classes R2/R3 (Figure 16-8).

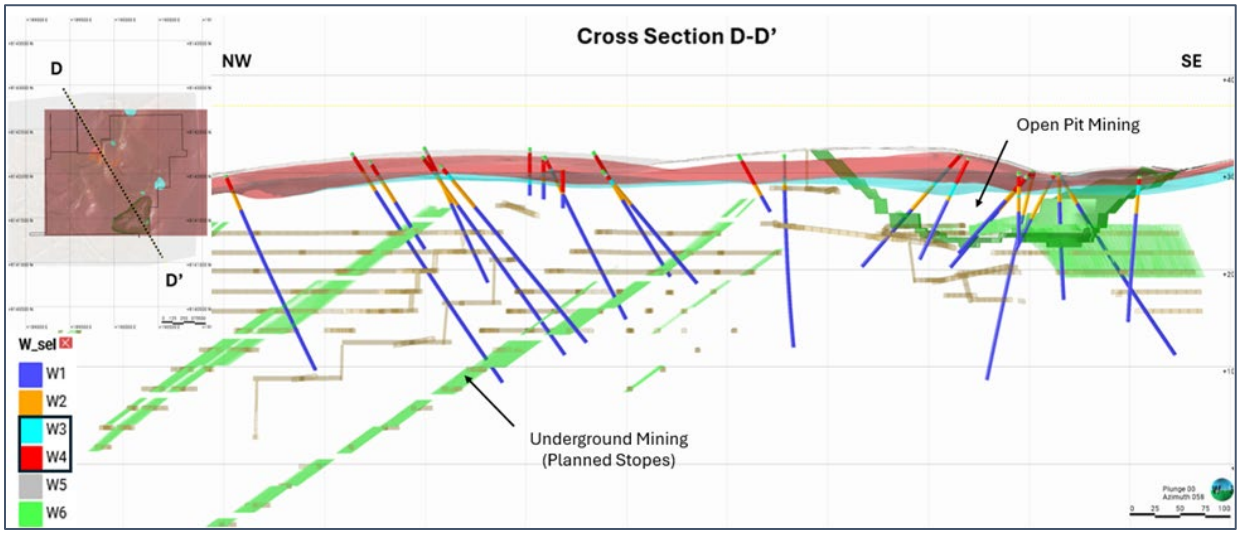


Figure 16-8: Plan (Inset) Showing Section D–D' and Cross-Section D–D' of the Sap Rock and Weathered Rock Domain (W4/W3 Open Pit (Arrow) and Underground Mine Excavations (Light Green and Brown) (Drill Holes Coloured According to Degree of Weathering Alteration Grades W1 through W5)

According to the geotechnical investigation campaign focused on soils and weathered rock, the sap rock consists of friable and weathered rock (C3/A3 and C4/A4), extending from 13 m to 35 m below surface. Permeability varies from 6.8×10^{-4} to 1.4×10^{-5} cm/s.

The rock mass exhibits low to moderate fracturing (F2/F3), with fractures aligned with the schist foliation, both dipping northwest at 30° and 50°. These fractures are typically smooth and oxidized, often indistinguishable from mechanically opened foliation planes. Water-pressure tests indicate hydraulic conductivity values ranging between 1 x 10^{-4} cm/s and 1 x 10^{-5} cm/s, with localized zones reaching up to 1 x 10^{-3} cm/s in fractured sections. Water is frequently observed along these fractured planes.

Based on the current characterizations and tests conducted, the following criteria were established to classify the weakly and moderately weathered rock domains and their corresponding material properties.

- Weakly weathered rock (C4, W4):
  - Hoek–Brown parameters
    - GSI = 25; mi = 12; σci = 35 MPa; s = 1; D = 0.5.
  - Equivalent Mohr–Coulomb parameters:
    - c′ = 50 kPa and φ′ = 36° were adopted, reduced to c′ = 30 kPa and φ′ = 35° along the dominant schistosity.
    - An anisotropic strength function was applied within a 5° range to account for directional variability.
- Moderately weathered rock (C3, W3):
  - Hoek–Brown parameters:
    - GSI = 35; mi = 12; σci = 35 MPa; s = 1; D = 0.7.
  - Equivalent Mohr–Coulomb parameters:
    - c′ = 100 kPa and φ′ = 40° were adopted, reduced to c′ = 50 kPa and φ′ = 35° along the schistosity
    - Anisotropic strength function within a 5° range.

where GSI = geological strength index (Hoek–Brown),
mi = material constant for the intact rock,
σci = unconfined compressive strength,
D = disturbance factor, and
c′ = cohesion.

From a rock mechanics perspective, this domain—immediately below the soil and saprolite domain—exhibits highly variable thickness. In the schist (W3/W4), this horizon is particularly well characterized by RQD values ranging from 5% to 50%, with most around 40%. The subdomain displays a predominantly F3/F4 fracturing pattern and a moderate degree of alteration, with the presence of at least three families of discontinuities.

Figure 16-9 presents an example of the sap rock and the weathered rock domain, characterized by varying degrees of weathering and, consequently, different geotechnical qualities alternating within the same interval (e.g., Drill Hole ITDD-23-197: 13.2 m–23 m). Between 13.20 m and 16.50 m, sap rock (W4) is characterized with poor mechanical quality characterized (strength class R0/R1), fracturing degree F3/F4, RQD of 32.36%, and three predominant joint sets. Below this interval, weathered rock (W3) predominates, also with poor mechanical quality (strength class R3/R4, fracturing degree F3/F4, RQD of 29.60%, and three predominant joint sets) and hard discontinuity walls—rough to irregular.

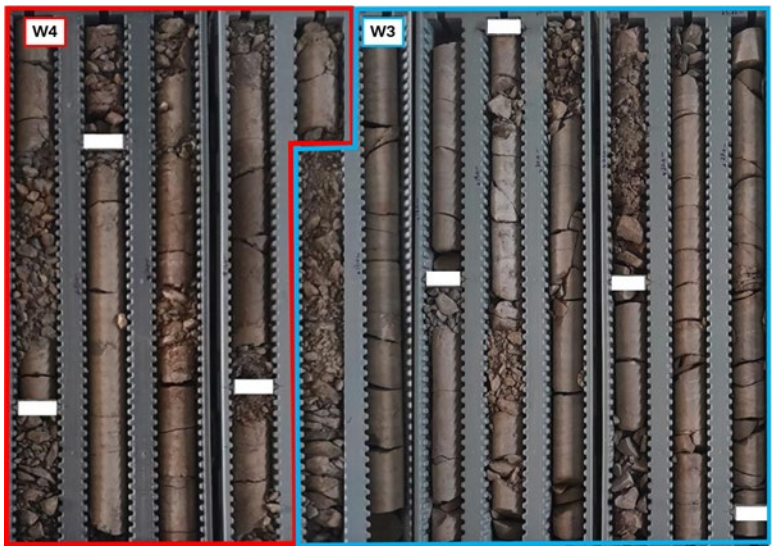


Figure 16-9: Example of a Sap Rock and Weathered Rock Domain (W3/W4) where Different Weathering Profiles can be Identified

For the sap rock and weathered rock domain, it is necessary to further refine the strength parameters, since the values currently adopted were obtained only from the basic design of the underground mine portals, and therefore do not represent the entire strike of the ore body. The planned testing campaign includes a dedicated sampling program for the W3 horizon, which corresponds to the upper portion of the crown pillar.

The underground mining activities planned for the Project will be carried out exclusively below the altered rock geotechnical domain. Only the main decline will be constructed within the upper portion of the rock mass, for which a robust and long-term ground-support strategy is planned. Only the portals for access to the underground mine will be excavated within the residual soil/saprolite and sap rock/altered rock domains (Figure 16-10).

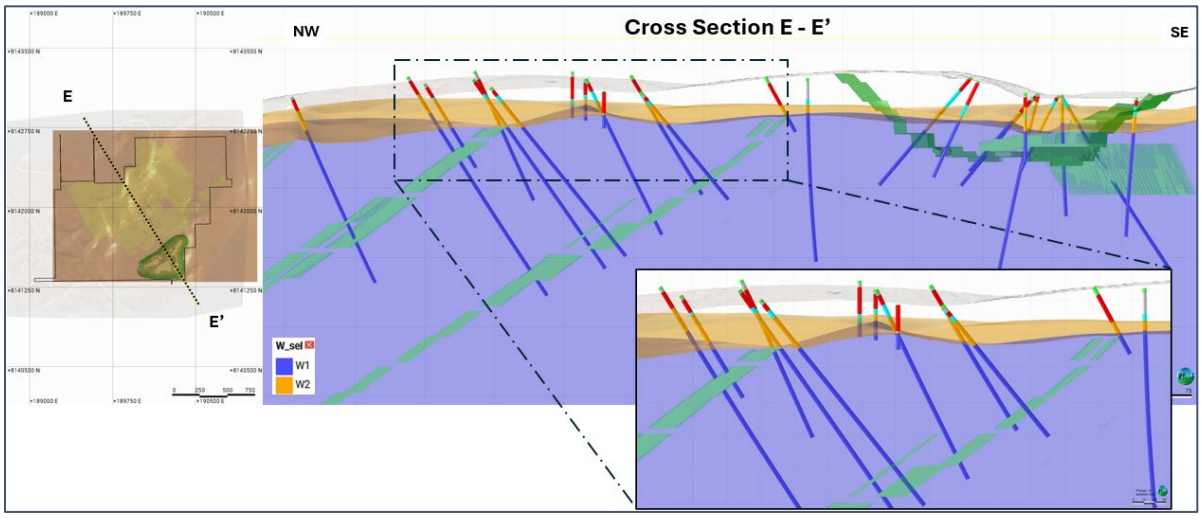


Figure 16-10: Plan (Inset) Showing Section E–E' and Cross-Section E–E' Showing the Planned Underground Mining Excavations, Mostly Within the Competent Rock Mass (W1 and W2)

16.1.4 Slightly Altered and Fresh Rock Domain

The slightly altered and fresh rock domain occurs beyond 35 m below the surface and is characterized by incipient or low alteration, with W1/W2 the predominant alteration grade. Compared to the upper layers, it exhibits higher mechanical strength, typically associated with rock strength class R5 (Figure 16-11).

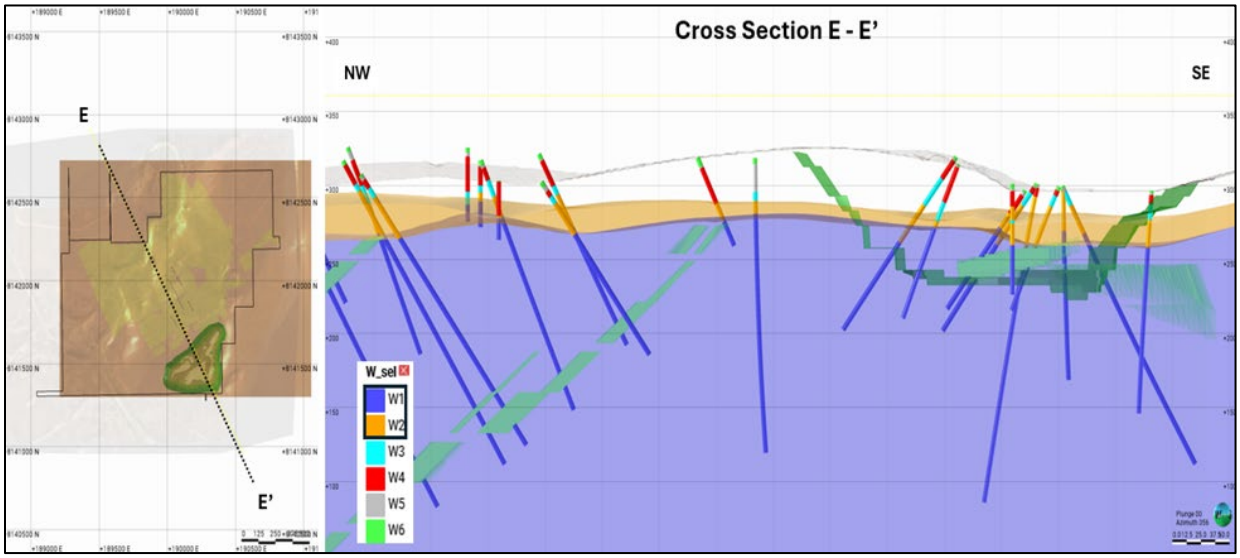


Figure 16-11: Plan (Inset) Showing Section E–E' and Cross-Section E–E' of the Slightly Altered and Fresh Rock Domain (W1 Purple and W2 Orange)

In general, the geomechanical domain corresponding to the transition between slightly altered and fresh rock can be characterized by RQD values ranging from 65% to 95%, most around 85%. The prevailing lithology in this domain consists essentially of schist, the host rock. Based on the structural analysis, at least two families of discontinuities have been identified in the schist. In contrast the pegmatite bodies exhibit discontinuities associated with igneous processes, such as cooling fractures and fractures resulting from stress imbalances caused by the uplift of these intrusions within the crust, unrelated to the deformational history of the host rock.

Figure 16-12 presents a cross-section that represents the domain of slightly altered and fresh rock, defined based on RQD values (>50%) and alteration grades described in the drill-hole logs. This domain contains two fresh rock subdomains corresponding to the schist (host rock) and pegmatite (mineralized body) are detailed below.

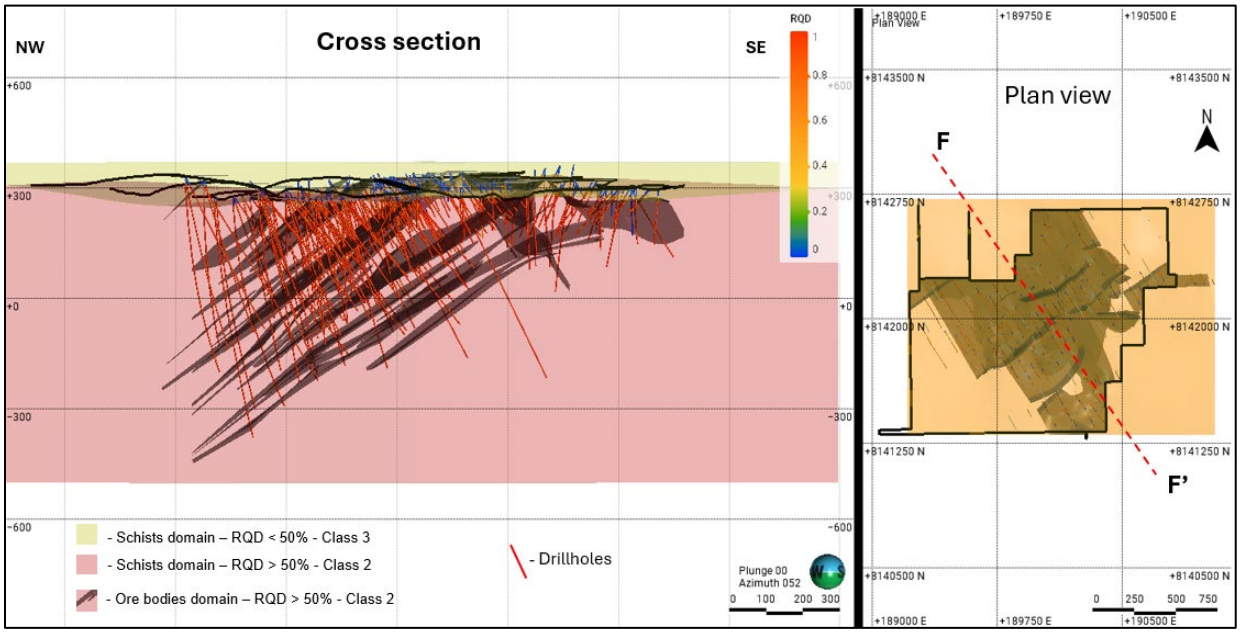


Figure 16-12: Project Geotechnical Domains—Left, Cross-Section NW to SE of Ore bodies based on RQD Classification; Right, Plan View of Section F–F'

16.2 Fresh Rock Domains

16.2.1 Schist Domain (Salinas Formation)

The Salinas Formation schist domain is the most representative of the Project, as it encompasses the hanging wall and footwall of the stopes, as well as the rock excavated in all declines and primary developments. It is characterized by the absence of weathering and no evidence of water flow. From a hydrogeotechnical perspective, it exhibits very low transmissivity and storage capacity, resulting in an almost impermeable rock mass.

The fracturing degree is low, with up to two predominant families of discontinuities (F1/F2 pattern), F1 being the most common. RQD values range from 85% to 95%, often exceeding 90%. Fractures are generally rough, planar, unweathered, and show no signs of water seepage.

Figure 16-13 shows a representative interval (Drill Hole ITDD-23-197: 43.48 m–54.99 m), starting at a depth where the typical characteristics of this domain prevail—localized oxidation in the rock matrix, gradually transitioning to unweathered conditions, low fracturing degree, and high intact-rock strength. These conditions confer excellent geomechanical quality to the domain, with high strength and notable self-supporting behaviour, favouring the excavation of underground openings and slopes with steep face angles.

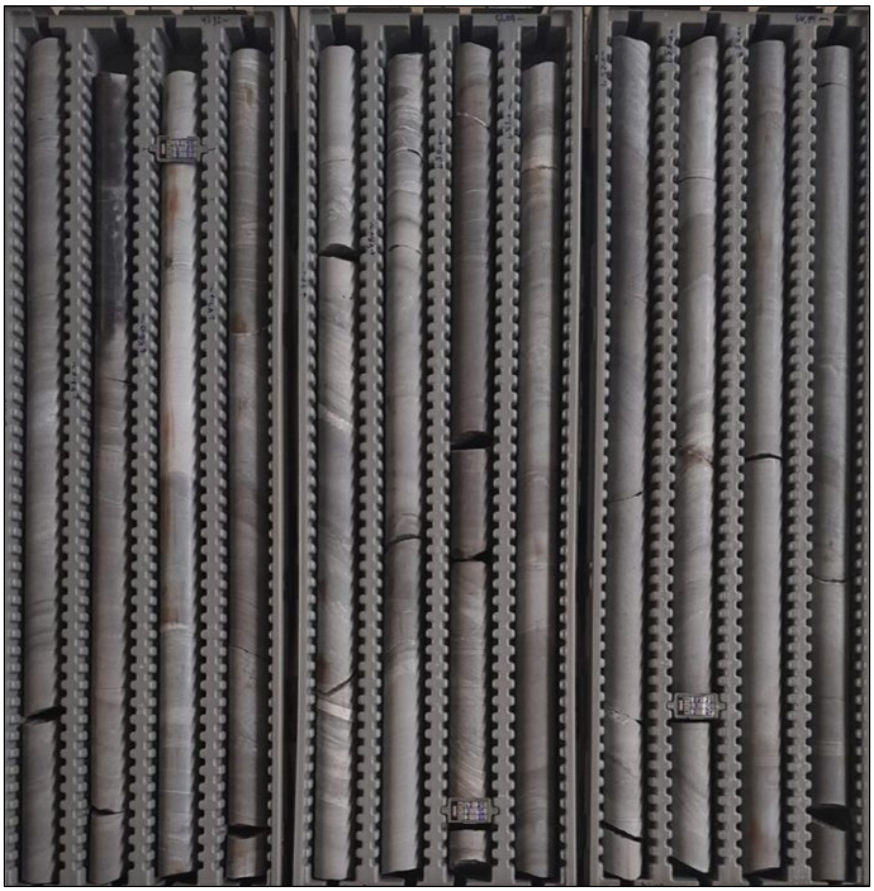


Figure 16-13: Example of Slightly Altered to Fresh Rock Schist Domain (W1/W2)

When analyzing the tests conducted exclusively for the slightly altered rock and fresh rock domains, regardless of depth (i.e., W1 or W2)—UCS values ranged from 9.8 MPa to 309.86 MPa, with an average of 98.57 MPa. This variability is partly explained by the occurrence of failures along weakness planes. Excluding the anomalous uniaxial UCS values of 209.76 MPa and 309.86 MPa, both obtained at a depth of 96 m, a linear correlation between depth and strength is observed (Figure 16-14). From depths >50 m, two distinct populations emerge, characterized by the predominance of strengths close to or above 100 MPa (Figure 16-14).

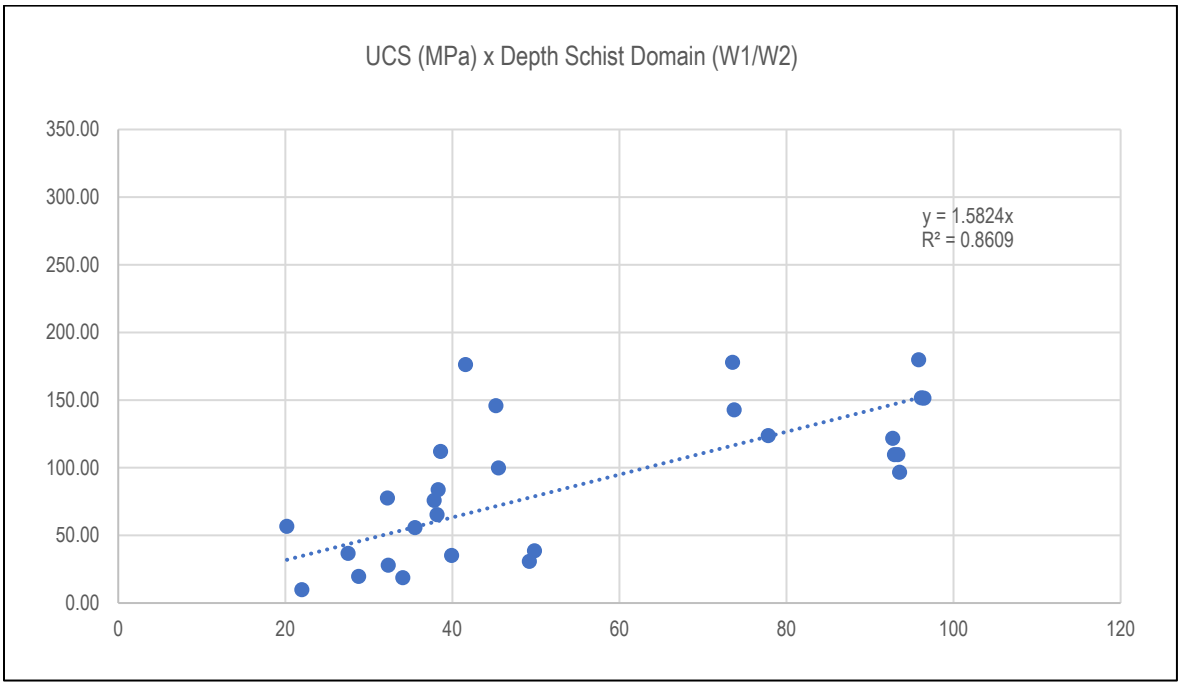


Figure 16-14: UCS Results of the Schist Domain—Classified as W1 and W2

To better understand the relationship between depth and strength, the tests results were grouped according to the geotechnical core logging, distinguishing samples from depths shallower and deeper than 50 m below surface. Figure 16-15 presents the distribution of UCS with depth, based on all raw test values. Notably, samples collected at depths >50 m were classified W1.

The strength results obtained for the schist domain, organized by depth, are still preliminary and will be better interpreted upon completion of the new testing campaign currently underway. For greater consistency, an outlier analysis was conducted using the interquartile range statistical criterion, establishing an upper limit for the removal of anomalous values. Tests with results exceeding this limit were discarded as outliers, thus ensuring a more conservative analysis.

Following these changes to the data set, average strengths for schist material considering W1/W2 classes were determined; 56.78 MPa at depths <50 m, and 142.25 MPa for material domain W1 at depths >50 m (Figure 16-16).

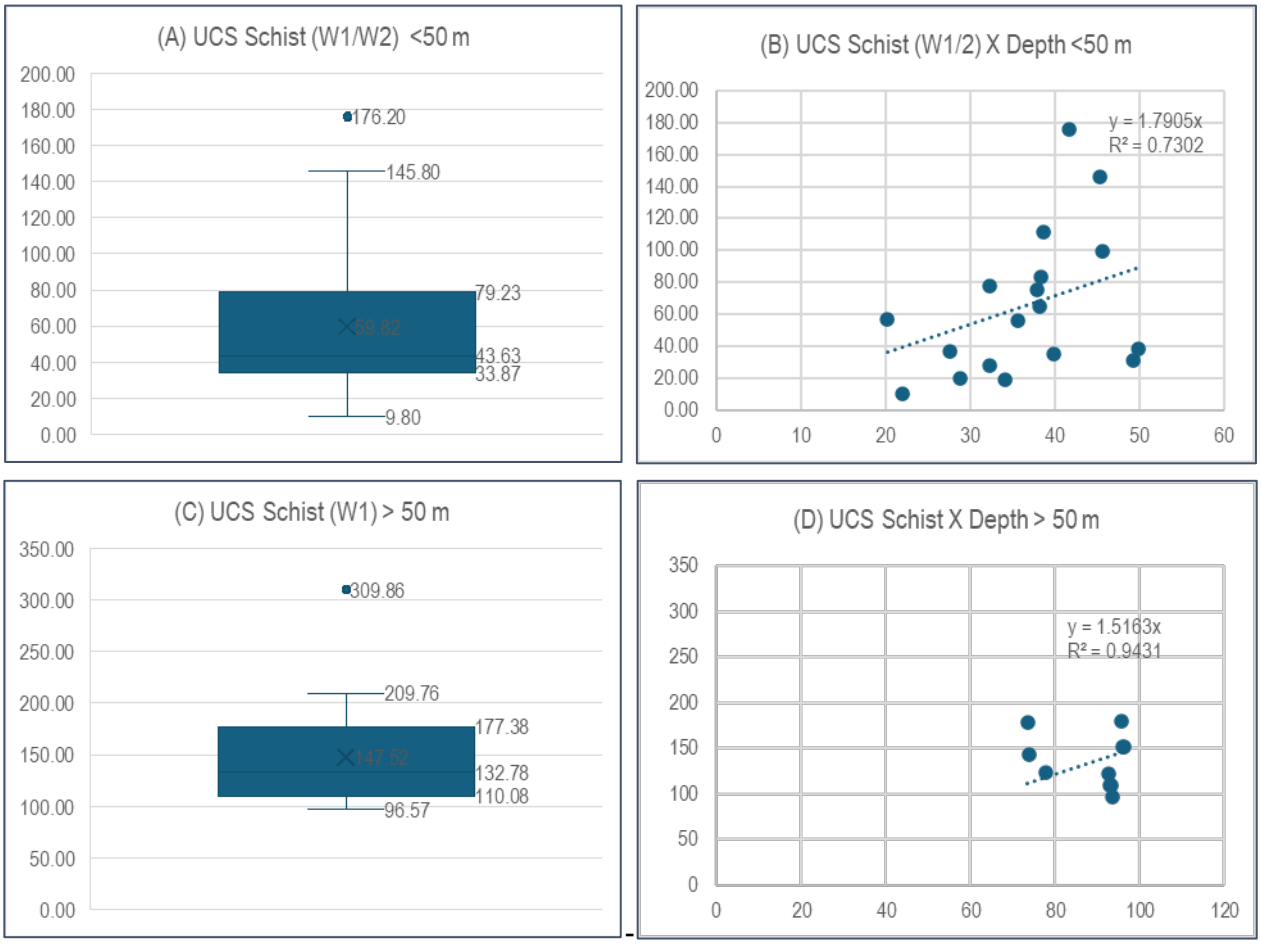


Figure 16-15: ***A) UCS Tests Performed on Schist Classified as W1 and W2 at Depths <50 m Below Surface; B) UCS Test Results at Depths <50 m Below Surface; C) UCS Tests Performed on Schist Classified as W1 at Depths >50 m Below Surface; D) UCS Test Results at Depths >50 m Below Surface (X-Axis Scales in Metres)***

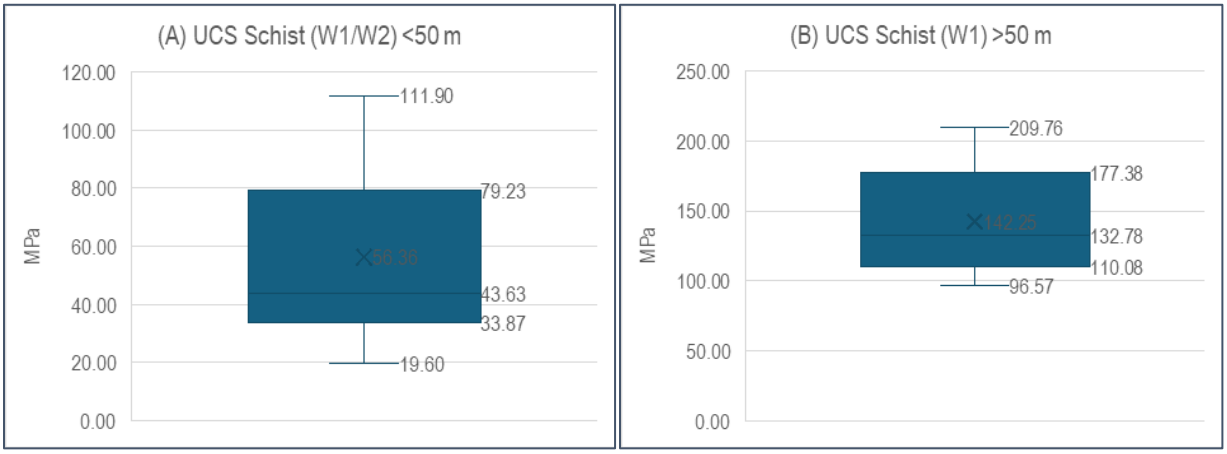


Figure 16-16: ***A) UCS for Domain W1/W2 at Depths <50 m (Outliers Removed); B) UCS for the Fresh W1 Domain at Depths >50 m (Outliers Removed)***

16.2.2 Pegmatite Domain (Ore)

The pegmatite domain is characterized by a nearly intact rock mass, with original strength parameters preserved and predominantly classified as R5 (very strong rock). Its geometry comprises a series of tabular pegmatite intrusions forming a dense swarm of parallel to subparallel dykes concordant with the S1 schistosity. In addition, less frequent, but thicker, discordant dykes are present, intruded along the S2 spaced cleavage or filling sub-horizontal joints (Jh) (Figure 16-17).

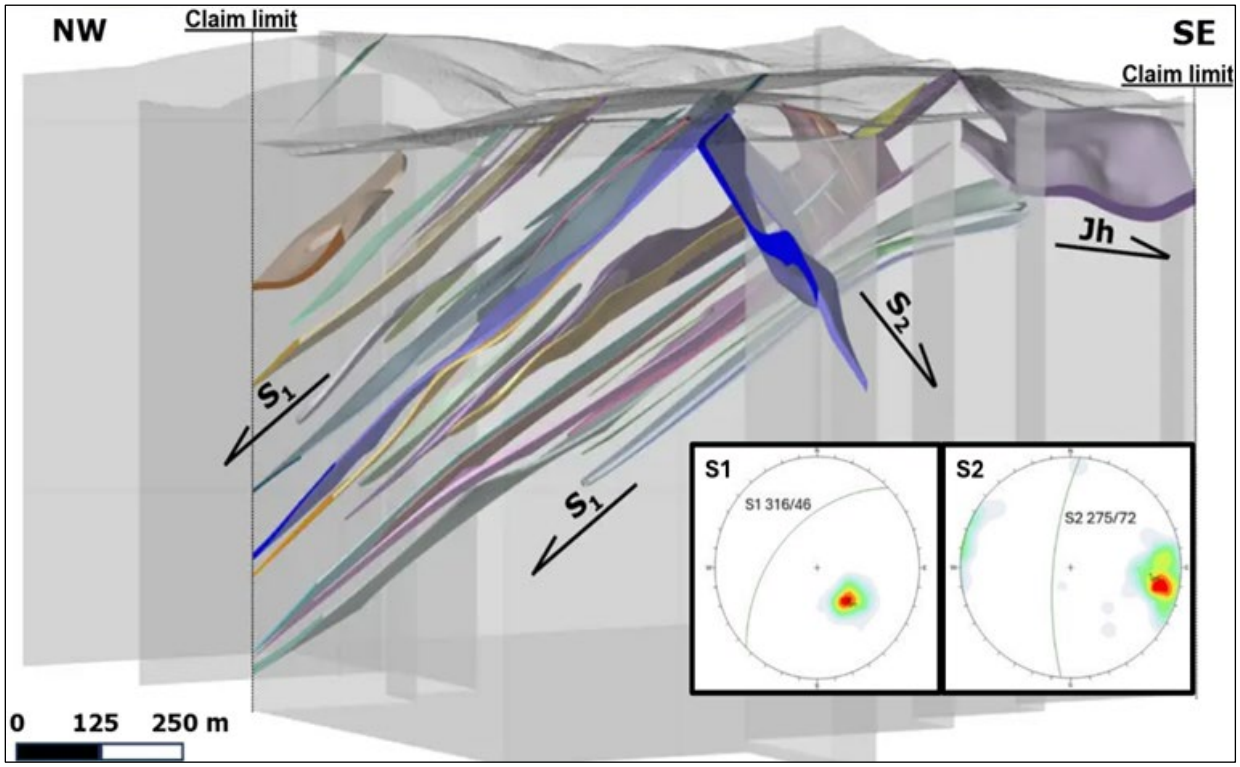


Figure 16-17: Oblique View of the Project's 3-D Resource Model

Concordant dykes predominate, with principal strike directions ranging from N32° to N37°E and dips between 31° and 53° toward the northwest. Discordant bodies, although less frequent, display the same strike directions and dip ranges but dip toward the southeast. In both cases, the inclinations are suitable for a sublevel stoping method.

In the SW portion is a discordant pegmatite intrusion structurally controlled by a sub-horizontal fracture. Due to its inclination, the initial plan was to mine it using the room-and-pillar method; however, considering cost and recovery, an open-pit method was chosen (Figure 16-18).

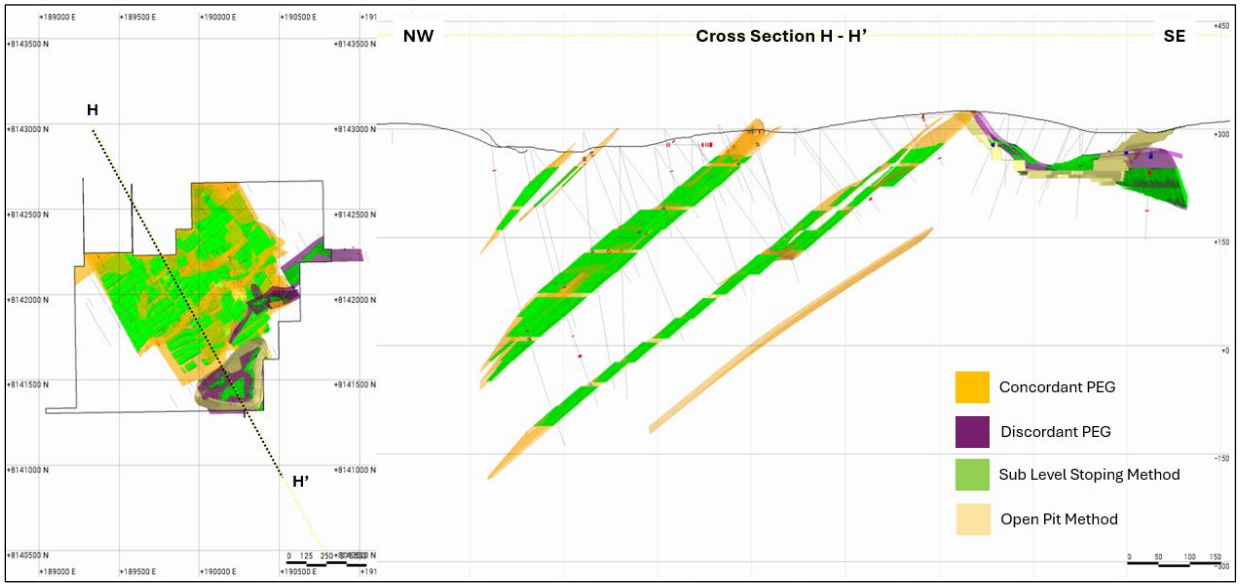


Figure 16-18: Plan and Section H–H' (Inset), and Cross-Section H–H' Illustrating the Different Pegmatite Intrusions and their Respective Mining Methods

At least two fracture sets were identified in the pegmatite domain, following an F1/F2 fracturing pattern, with the former being the most frequent. The RQD ranges from 65% to 90%, most around 85%. The fractures generally exhibit rough and irregular surfaces, with localized oxidations showing little to no evidence of alteration, indicating the absence of water flow. Figure 16-19 illustrates a representative interval (Drill Hole ITDD-23-213: 77.93 m–89.22 m), starting at a depth where the characteristics of this domain predominate.

It is important to note that the discontinuities in pegmatites are associated with natural cooling fractures, resulting from the solidification and thermal contraction process, as well as the unloading caused by the reduction of lithostatic pressure due to isostatic uplift. Originally formed under high lithostatic pressure, isostacy exposes the crystallized bodies to environments with significantly lower pressures.

The pegmatite sub-domain shows continuity at depth and varies in strength. Based on 32 UCS tests performed on specimens of this lithology collected at relatively shallow depths and in a predominantly fresh condition (W1), the strength values ranged from 59.23 MPa to 125.36 MPa, with an average of 90.36 MPa (Figure 16-20). It must be noted that these values represent the raw strength results without any statistical alterations, and for this stage of the Project these results are considered adequate for the design of stable spans, sill pillars, and rib pillars.

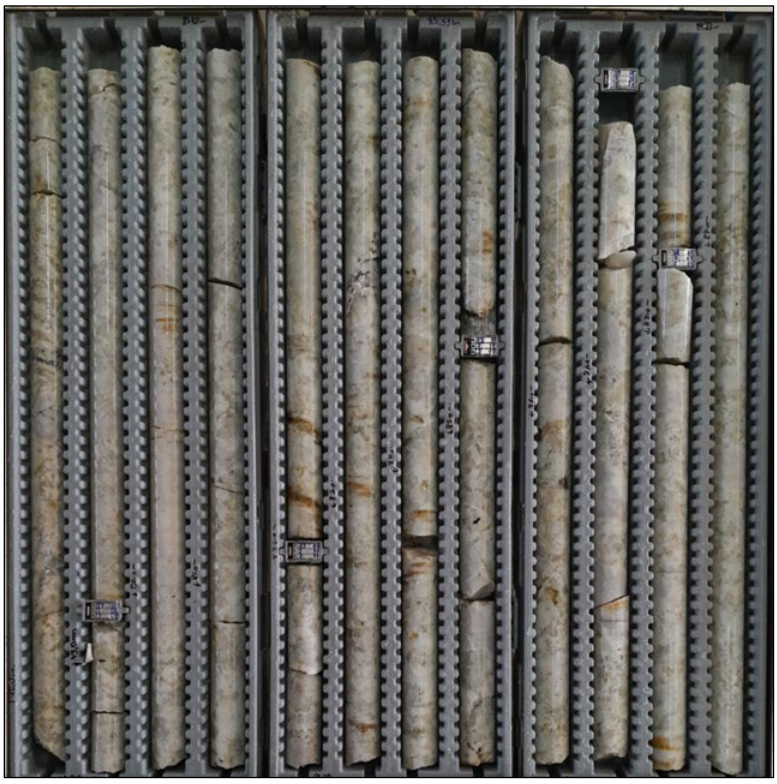


Figure 16-19: Example of Slightly Altered to Fresh Rock Pegmatite (W1/W2)

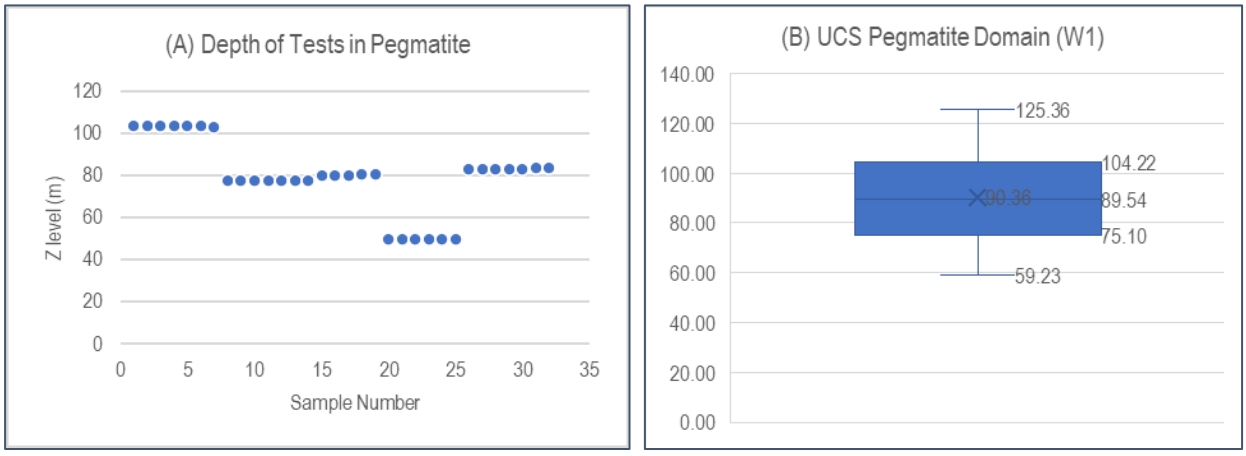


Figure 16-20: A) UCS Test Results for the Pegmatite Domain Classified as W1 Related to Depth (X-Axis in Metres); B) Box-and-Whisker Plot for the Range of Pegmatite UCS Strengths N

16.3 Mining Method

There is an area where the ore body exhibits a tabular geometry, steep dip, and extensive continuity at depth, with the host-rock mass characterized by high mechanical strength and good geomechanically quality. For this area, the recommended mining method is sublevel open stoping, ensuring selectivity and operational stability.

In the sector where the ore body shows a gentle dip, horizontal continuity, and shallow depth, associated with a host-rock mass presenting favourable geomechanical parameters, open-pit mining is indicated. This method allows for greater volumetric recovery, optimization of pit-slope angles, and maximization of productivity, while ensuring structural stability and operational safety throughout the production cycle.

The Project initially involves developing access to reach and expose the ore in the subsurface through underground excavations without immediate ore recovery. In parallel, open-pit excavations are planned to commence with the same objective of removing waste and exposing the ore. Both work fronts involve drilling, blasting, excavation, ore loading, and waste hauling.

This initial phase is designed to exploit the upper portion of the Bandeira deposit, optimizing capital costs (CAPEX) and operating costs (OPEX) while ensuring the rapid start of ore supply to the processing plant. The operation will be supported by essential infrastructure, including access roads, drainage systems, waste-rock piles, and ore stockpiles.

In the subsequent phase, a combined operation of underground and open-pit mining methods is planned, contributing to the production ramp-up while ensuring operational stability and synergy between the mine and the processing plant.

As open-pit mining approaches its economic limit, underground development will be sufficiently advanced to allow production rates to be achieved via sublevel stoping panels. This approach ensures a smooth transition to underground mining without production impacts, maintaining a continuous supply to the lithium processing plant.

16.3.1 Open-Pit Geotechnical Design Parameters

In the Project's southeast portion is a discordant pegmatite intrusion forming a shallow, low-dip mineralized body. Initially, this body was planned to be mined using the room-and-pillar method. However, considering cost, recovery, and the time frame for ore release, the mining plan was changed to an open pit.

In this context, the development of a small-scale starter open pit is planned, with a maximum vertical depth of 95 m and an estimated LOM of 13 months. Slope stability analyses were carried out to determine the factors of safety (FOS) for the individual bench face angles and overall pit-slope angles. The process considered the different material types, potential failure mechanisms, and the geometric and hydrogeological conditions. The acceptance criteria adopted followed the recommendations of Read and Stacey (2009), as presented in Table 16-6.

The proposed pit geometry was defined by the mine planning department, focusing on the economic and operational components of the open pit, with the aim of maximizing ore recovery and minimizing the costs associated with waste removal and mining operations. This approach initially resulted in optimistic geometric parameters based solely on economic criteria.

Table 16-6: Typical FOS Acceptance Criteria Values

Slope Scale	Consequences of Failure	Acceptance Criteria FOS (min) (static)
Bench	Low–High	1.1
Inter ramp	Low	1.15–1.2
	Medium	1.2
	High	1.2–1.3
Overall	Low	1.2–1.3
	Medium	1.3
	High	1.3–1.5

Source: Read & Stacey (2009).

After evaluation in light of empirical criteria and the experience of the geotechnical team, the parameters were redefined, resulting in an integrated approach that balances economic feasibility with geotechnical criteria. In this way, a preliminary design was established, serving as the basis for the numerical assessment using the limit equilibrium method presented in this Technical Report.

The evaluation aims to validate the preliminary geometry against the acceptance criteria established by Brazilian standards and international guidelines, ensuring both Project operational safety and economic feasibility. Listed below are the recommendations for the preliminary geometry of the pit slopes:

- Residual soil and saprolite domain:
  - Maximum bench height soil—20 m
  - Minimum berm width soil—5.0 m
  - Maximum slope face angle soil—50°.

  - Sap rock and weathered rock domain:
  - Maximum bench height—20 m
  - Minimum berm width—5.0 m
  - Maximum slope face angle—50°.
- Slightly weathered and fresh rock domain:
  - Maximum bench height—15.0 m
  - Minimum berm width—5.0 m
  - Slope face angle—85°.

The analysis of the proposed final pit geometry was based on the field geotechnical data collection program (Section 16.1), conducted for the design of the Project's surface and underground geotechnical structures. The geotechnical domains were simplified as follows: residual soil and saprolite as soil; saprock and weathered rock with RQD <50%; and slightly weathered and fresh rock with RQD ≥50%.

In the open-pit area, stability analysis sections were structured, and geotechnical domains were defined according to RQD and weathering grade. RQD values increase with depth, with the lowest values

observed in the near-surface portions of the schist rock mass, indicating a reduction in fracturing with depth and suggesting improved geomechanical conditions at greater depth (Figure 16-21).

Figure 16-22 shows that the designed pit slopes fully intersect the weathering profile, being most representative within the intervals from slightly weathered to fresh rock. The upper layer, composed of residual soil and saprolite, exhibits a high degree of weathering (W5/W6) and low mechanical strength. For the present analysis, this horizon was treated as a single unit, with the parameters of residual soil applied, as it presents the lowest stability values, resulting in a conservative approach.

The intermediate, transitional horizon is less prominent, with an average thickness of 12 m, a moderate degree of weathering (W3/W4), low mechanical strength, and an average RQD of approximately 40%, characterizing a material of low geotechnical quality. In the basal portion, the schist subdomain predominates, characterized by high RQD values, the presence of two discontinuity sets, and classified as a rock mass of excellent quality, presenting, according to the database, high strength (average UCS of 112 MPa), although strongly influenced by structural anisotropy. Based on this definition, four distinct geomechanical domains were established for the analyzed sections: soil, schist with RQD <50%, schist with RQD >50%, and pegmatite.

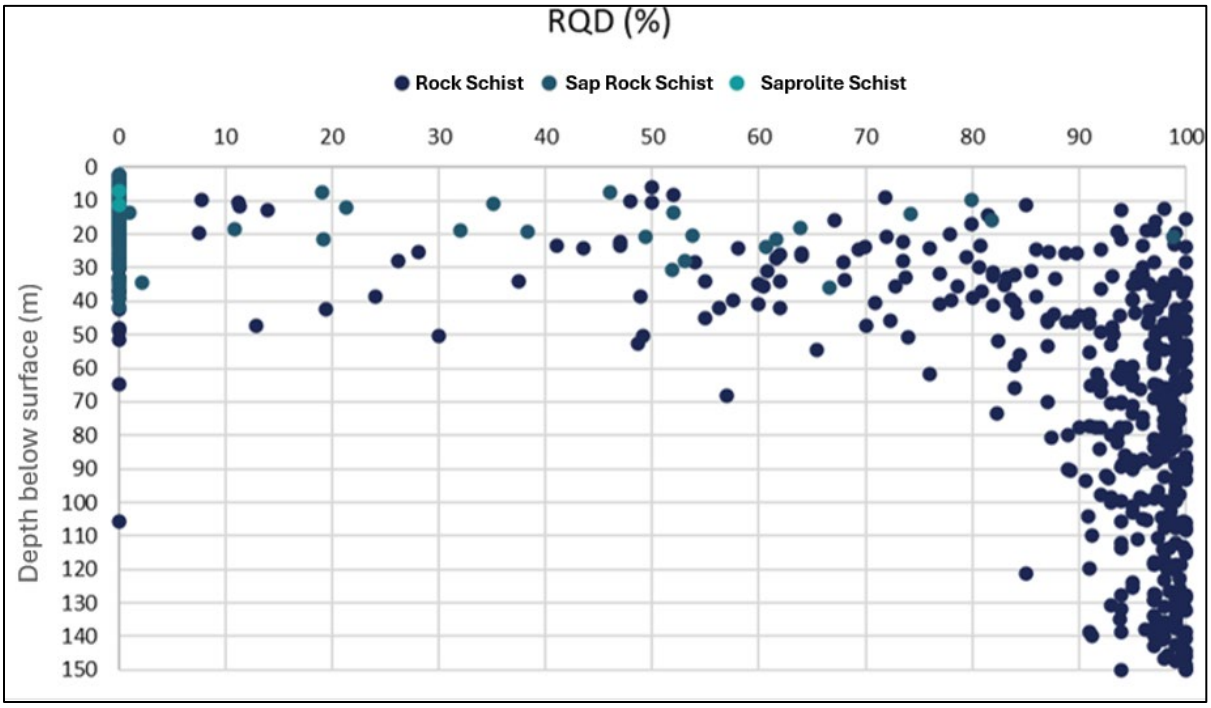


Figure 16-21: Association Graph of the RQD in Relation to Depth, Evaluated in the Database

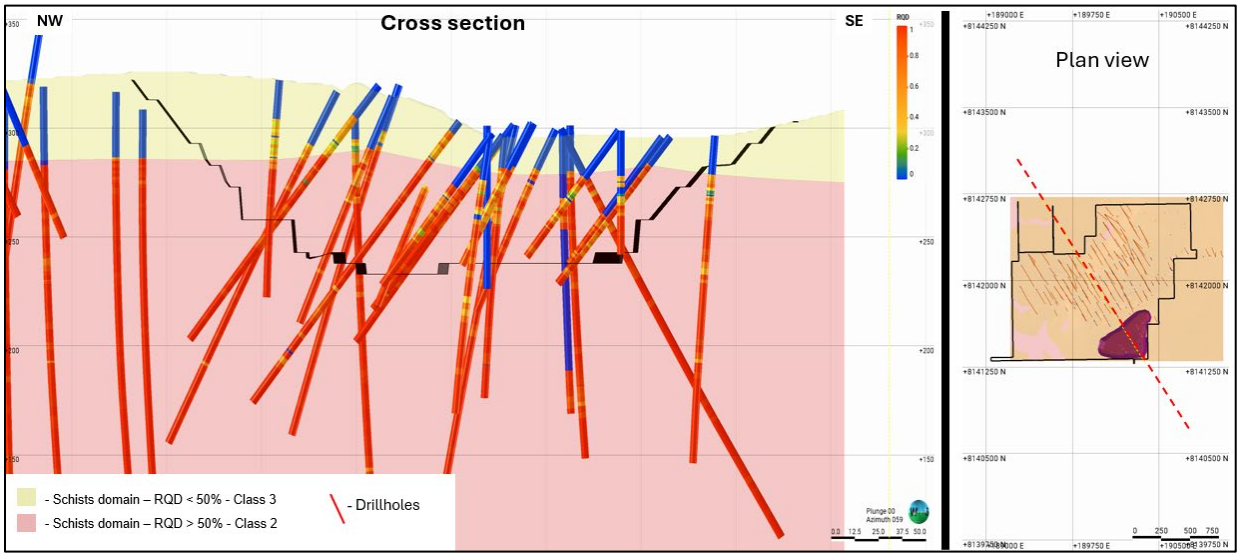
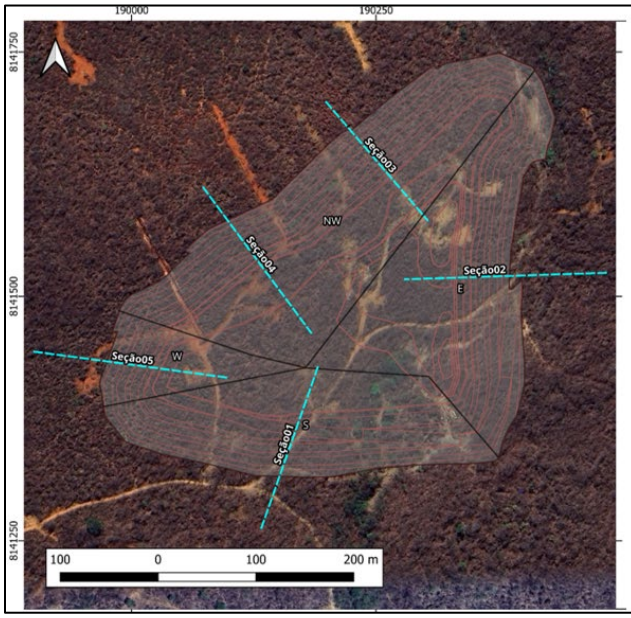


Figure 16-22: Left, Geological NW–SE Cross-Section (Left) in the Project Property; Right, Plan of NW–SE Section Showing Section Line and Open Pit (Dark Red) in Southeast

Thus, the proposed slope angles for the different domains intersected by the pit are defined by the hydrogeological conditions, the strength and anisotropy of the rock mass, and the orientation of the pit walls in relation to the discontinuities. Based on these variables, cross-sections were established in the representative sectors of the pit, considering the predominant material in each of them, as well as the deepest sectors of the pit. Figure 16-23 presents these sections and indicates the average orientations of each sector.



Design Sector	Section	Geomechanical Domain	Slope Face Angle (°)	Slope Orientation Dip Direction (°)	Overall Angle (°)	Pit Depth (m)
S	1	Soil	50	10°	40	58
		Sap Rock and Weathered Rock	50			
		Slightly Altered and Fresh Rock	85			
E	2	Soil	50	270°	51	74
		Sap Rock and Weathered Rock	50			
		Slightly Altered and Fresh Rock	85			
NW	3	Soil	50	145°	38	95
		Sap Rock and Weathered Rock	50			
		Slightly Altered and Fresh Rock	85			
	4	Soil	50		40	70
		Sap Rock and Weathered Rock	50			
		Slightly Altered and Fresh Rock	85			
W	5	Soil	50	145°	44	67
		Sap Rock and Weathered Rock	50			
		Slightly Altered and Fresh Rock	85			

Figure 16-23: Left, Plan Showing Open Pit Design Sectors and Sections; Right, Sector and Section Pit-Slope Angle, Dip, Overall Angle, and Depth

Assuming that residual soil (W6) and saprolite (W5) can be treated as homogeneous and isotropic, typically exhibiting matrix-controlled failures with approximately circular shapes, while the intact rock mass is considered anisotropic with strength governed by discontinuities; it becomes necessary to adopt distinct approaches to validate the proposed slope angles for the different sectors and pit domains.

These approaches include limit equilibrium analyses performed using Rocscience Slide2 (Version 9.040), which calculates the FOSs for different slope heights, angles, and saturation conditions. The strength of fresh rock was defined based on laboratory tests and the Hoek–Brown failure criterion, whereas weathered materials were assessed using the Mohr–Coulomb criterion.

Additionally, kinematic analyses were conducted, based on the geometric relationships between the orientation of rock mass discontinuities and the slope faces, through stereographic projections using Rocscience Dips 6.0 (Version 8.029) and RocSlope2 (Version 1.007). These analyses allowed the identification of the most likely failure mechanisms within the anisotropic domains.

16.3.2 Soil Domain—Bench-Scale Analysis

The stability analysis for defining the optimal bench-face angle was carried out using the limit equilibrium method, with the Mohr–Coulomb failure criterion and the Morgenstern-Price methodology, among others. The phreatic surface was defined based on the diagrams proposed by Hoek and Bray (1981), allowing the simulation of different groundwater conditions, ranging from fully drained to fully saturated, with the aim of evaluating the effects of pore pressure on the horizon geometry.

Figure 16-24 presents the five saturation conditions assessed, highlighting the scenarios of fully drained and fully saturated slopes, the latter representing the most critical stability condition. For face angles of 50° and heights of 10 m all scenarios exhibit FOS greater than 1.1, meeting the acceptance criteria.

When applying the same strength parameters and face angle to benches 20 m high, Diagrams 4 and 5 in Figure 16-24 do not meet the required minimum FOS, with FOS of 1.0 and 0.84, respectively, indicating a potential risk of instability under these conditions.

For 10 m-high slopes, the analysis of groundwater level (blue line in Figure 16-25), influence showed that, even under the critical scenario (Diagram 5 in Figure 16-24), the FOS remained above the minimum recommended value. For 20 m-high slopes, the acceptance factors are not met starting from Diagram 4 in Figure 16-24 (surface water = 4 × slope height).

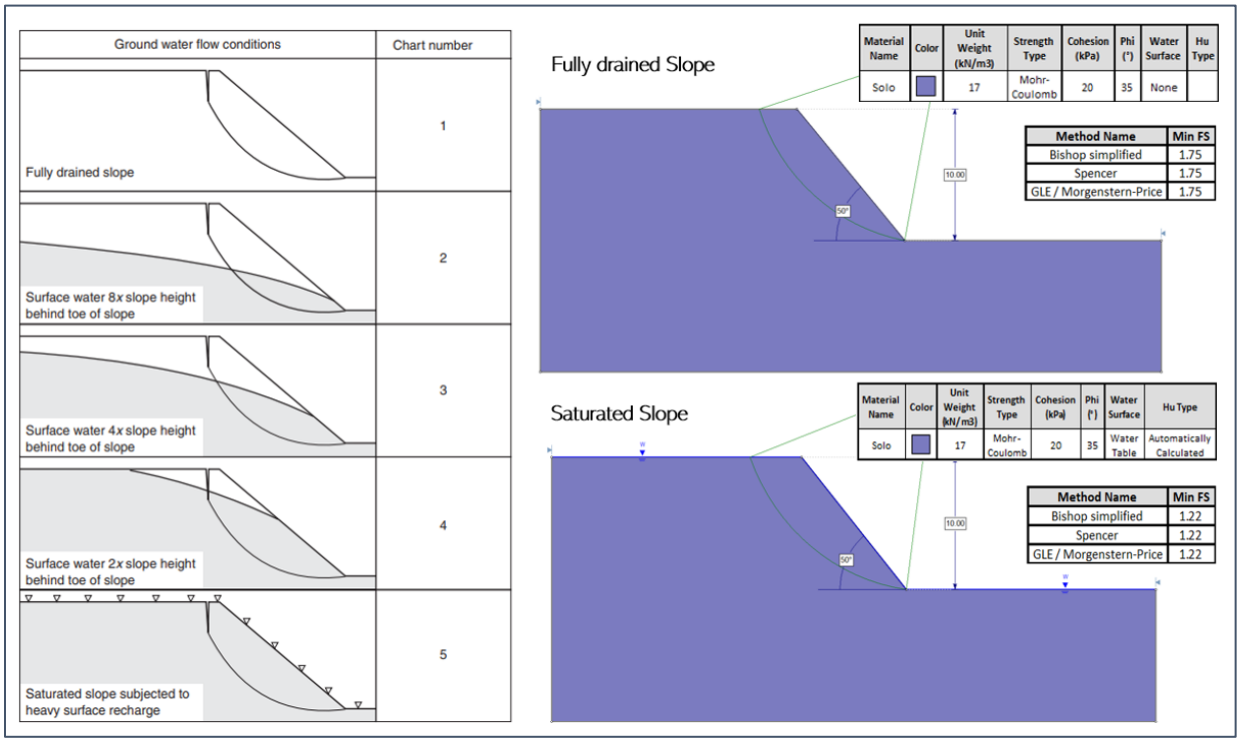


Figure 16-24: Groundwater Flow Models Applied in Circular Failure Analyses for the Soil Domain, Considering Slopes with a Face Angle of 50° and a Height of 10 m proposed by Hoek and Bray (1981) (GLE = General Limit Equilibrium)

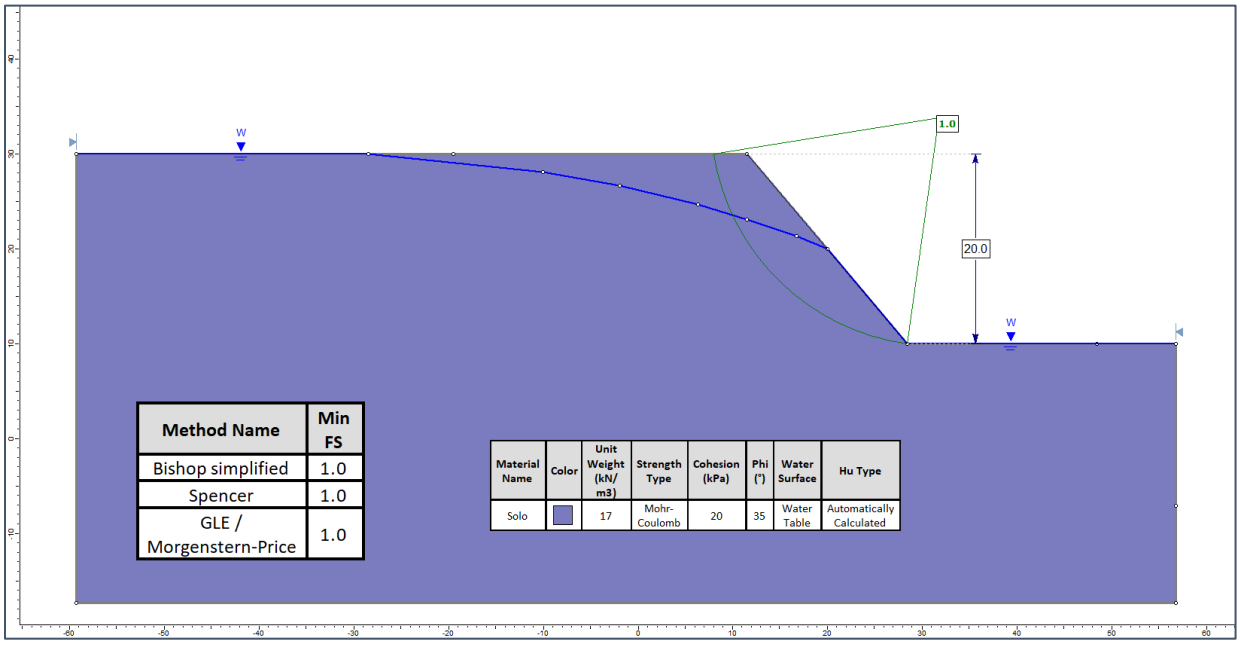


Figure 16-25: Evaluation of Slope FOS in Diagram 4 in Figure 16-24: Scenario Proposed by Hoek and Bray (1981) Considering Slopes with a Face Angle of 50° and a Height of 20 m (GLE =General Limit Equilibrium; Blue Line is Groundwater Level)

Although these saturation scenarios are conservative, given that drill-hole investigations indicated predominantly dry conditions, the absence of piezometers or water-level gauges in the pit area justifies adopting saturation Diagram 4 (Figure 16-24) as representative, an approach aimed at operational safety during rainy periods.

Based on the adopted parameters and established acceptance criteria, 20 m slopes are not recommended at this time for the soil domain. However, there is potential for optimizing the geometry validated for 10 m-high slopes, considering that the design and operation of equipment should be coordinated with the proposed geometry to ensure safe access and maintenance of the slopes and berms.

Thus, based on the preliminary 2-D limit-equilibrium method analyses, for the soil domain, a 10 m-high bench with face angles of up to 50° is recommended. This geometry is considered stable and representative, assuming a homogeneous and isotropic slope under the influence of hydrostatic pressure associated with groundwater flow (Table 16-7).

Table 16-7: Summary of Bench-Scale Stability Analysis for All Design Sectors

Design Sector	Geomechanical Domain	Bench Angle (°)	Groundwater Flow Conditions	Chart Number[1]	Bench Height (m)	Minimum FOS		
						Bishop Simplified	Spencer	Morgenstern–Price
All	Soil	50	Fully drained slope	1	10	1.75	1.75	1.75
All	Soil	50	Surface water 8x slope height	2	10	1.66	1.65	1.66
All	Soil	50	Surface water 4x slope height	3	10	1.53	1.52	1.53
All	Soil	50	Surface water 2x slope height	4	10	1.40	1.40	1.39
All	Soil	50	Saturated Slope	5	10	1.22	1.22	1.22
All	Soil	50	Fully drained slope	1	20	1.3	1.3	1.3
All	Soil	50	Surface water 8x slope height	2	20	1.1	1.1	1.1
All	Soil	50	Surface water 4x slope height	3	20	1.1	1.1	1.1
All	Soil	50	Surface water 2x slope height	4	20	1.0	1.0	1.0
All	Soil	50	Saturated Slope	5	20	0.84	0.85	0.84

Note: [1] Refers to Figure 16-24.

Finally, it is assumed that natural drawdown will be sufficient to provide the required depressurization of the slopes. Since the hydrogeological model is still under development, in future works these analyses will be revisited considering a higher level of detail, given the influence of groundwater conditions on slope stability, particularly in weathered materials.

Furthermore, it is essential that the surface drainage system be adequately designed to prevent runoff over the crest of the planned pit. This measure is of particular importance given the high susceptibility of weathered materials to erosion.

16.3.3 Schist Domain—Bench-Scale Analysis

In the schist domain, it is assumed that the rock mass strength is governed by discontinuities. The bench design, including face angle, height, and berm width, is initially defined based on kinematic analyses, aimed at assessing the potential for planar, wedge, and toppling failures across the different geometric sectors of the pit.

The assumptions adopted for the analyses, carried out using Dips 6.0 (Version 8.029), were as follows:

- Application of the Markland Test to define the types of failure at the bench scale
- Consideration of a friction angle (φ) of 25° in the analyses, a preliminary value used solely for identifying failure types and defining the preliminary face angles
- Use of a ±30° kinematic window (difference between the slope direction and discontinuity orientation) to evaluate the feasibility of planar and toppling failures.

Figure 16-26 illustrates the kinematic analyses performed for the northwest geometric sector, considering all structures present in the previously described structural database.

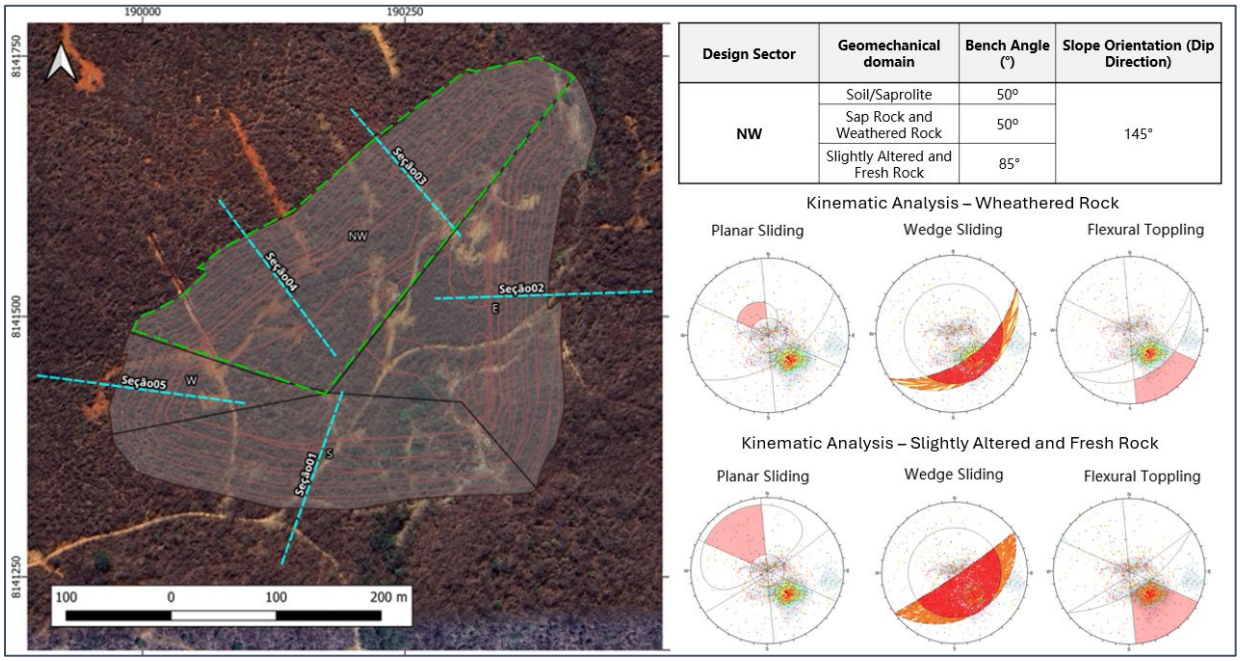


Figure 16-26: Left, Plan of Project Property showing Four Sectors and Five Sections; Righ,t Example of a Kinematic Analysis Conducted for the Northwest Sector (Dashed Green Outline on Plan), Considering Face Angles of 50° and 85°

The application of the Markland Test evaluates the relative orientation of all structure poles in the database with respect to the instability zone; overall, the test indicated a low susceptibility to planar, wedge, and toppling failures. Table 16-8 summarizes the probabilities of failure for each sector, by slope angle and type of failure.

Table 16-8: Probability of Failure for the Pit Design Sectors—Markland Test

Design Sector	Slope Dip Direction (°)	Bench Angle (º)	Failure Mode	Probability of Failure (%)
W	145	50	Planar	1.85
			Wedge	1.77
			Toppling	3.95
		85	Planar	4.71
			Wedge	5.97
			Toppling	41.26
E	270	50	Planar	7.9
			Wedge	15.38
			Toppling	1.85
		85	Planar	15.38
			Wedge	31.34
			Toppling	5.04
S	10	50	Planar	9.41
			Wedge	20.84
			Toppling	1.09
		85	Planar	13.45
			Wedge	33.03
			Toppling	2.35
NW	155	50	Planar	1.34
			Wedge	1.72
			Toppling	3.7
		85	Planar	3.7
			Wedge	6.36
			Toppling	37.65

The main foliation (S1) is the predominant structure controlling the failure mechanisms in the analyzed sectors. Its orientation relative to the slopes explains flexural toppling failures in the Sectors W and NW, planar failures in Sectors E and S, and wedge failures in Sectors S and E. The continuity and orientation of the foliation directly influence pit-slope stability, defining potential sliding surfaces. It is recommended that the foliation be thoroughly characterized and subjected to direct-shear testing to obtain representative geomechanical parameters, enabling more accurate stability analyses.

However, it should be noted that stereographic analyses do not account for the physical conditions of the discontinuities, being limited to a geometric assessment of the sectors where each failure mode may occur.

Therefore, considering the potential geometric conditions, highest observed probabilities should be evaluated using another method. They correspond to direct and flexural toppling at face angles of 85° in Sectors W and NW, respectively. In Sector E, wedge failures show the highest geometric potential also at a face angle of 85°, while in Sector E a higher probability of wedge failure was identified for both analyzed face angles.

Additionally, the safety factor was evaluated using Rocscience RocSlope2 software, applying the limit equilibrium method for potential failure mechanisms, including wedge, planar, and flexural toppling failures. Since each sector has slopes with the same orientation, but different face angles within the same sector, the decision was made to evaluate the steepest slopes of each sector, corresponding to the bottom pit slopes at 85°, as the kinematic analysis indicated that the probability of failure is higher for slopes with this inclination.

The analyses were carried out using the Barton-Bandis criterion, with the following input parameters:

- Unit weight: 26 kN/m³
- Face angle: 85°
- Slope direction: variable for each sector
- Height: 15 m
- Slope length: default length
- Upper face dip: 0°
- Berm width: the smallest present in each design sector
- Overall base inclination (for flexural toppling): 65°
- Dip and Dip direction of the discontinuities: according to Figure 16-1 presented in the geotechnical characterization section
- JRC: 10 (estimated value) for all discontinuities
- JCS: 88.3 kPa (75% of the UCS value measured for the schist) for all discontinuities
- Discontinuity cohesion: 0
- Discontinuity friction angle: 25° (estimated value)
- Tensile strength: 6.18 kPa
- Waviness: 20°
- Discontinuity spacing: S1—0.5 m; S2—2 m; Contacts—10 m; Fractures for NW—2 m; Fractures for SE—2 m.
- Absence of water in the discontinuities (assumption adopted based on the evaluation of boreholes, which were predominantly dry).

Table 16-9 presents the safety factors obtained from the stability analyses corresponding to the highest probabilities of failure occurrence identified in the Markland tests. It should be noted that, in the sectors where a specific failure mechanism is not represented, this is because, kinematically, no unstable blocks susceptible to that type of failure were formed.

Table 16-9: Stability Analysis Results for the Highest Probabilities of Failure in the Pit Design Sectors

Design Sector	Slope Dip Direction (°)	Bench Angle (º)	Failure Mode	Probability of Failure (%)	FOS
W	145	85	Toppling	41.26	1.5
E	270	85	Wedge	31.34	1.1
S	10	85	Wedge	33.03	2.3
NW	155	85	Toppling	37.65	1.5

Based on the stability analyses carried out for the different sectors of the pit, the safety factors varied according to the evaluated failure mechanism (wedge, planar, and flexural toppling). The results indicate that the slopes meet the established acceptance criteria and can be considered stable. Only the slopes in the east sector showed bench safety factors below the minimum recommended value for planar failures (Figure 16-27).

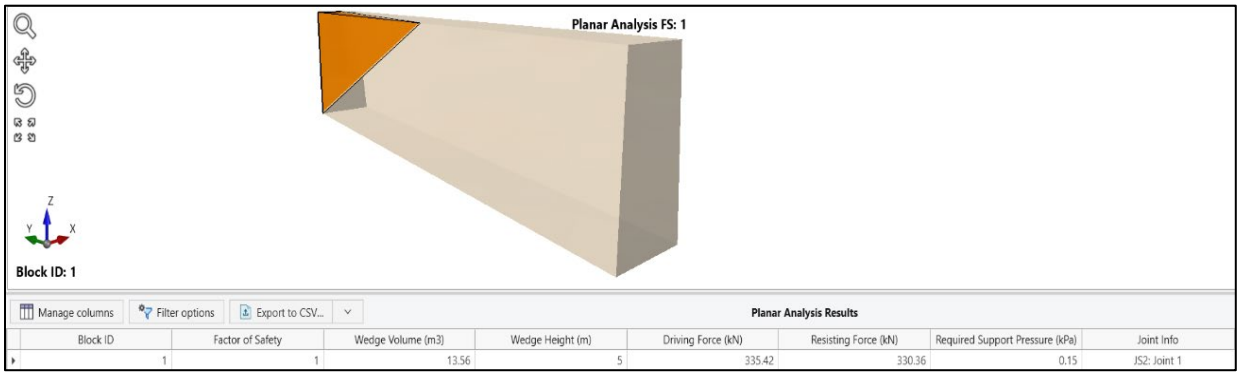


Figure 16-27: Stability Analysis of South Pit Sector E (FOS = 1.0 for Planar Failures); the Main Foliation is the Structure Associated with this FOS in Sector E

Based on the result shown in Figure 16-27, geometric alternatives were studied for Sector E, and it was found that adopting a maximum slope angle of 75° for the rock slopes allows achieving the minimum safety factor required for operation (Figure 16-28).

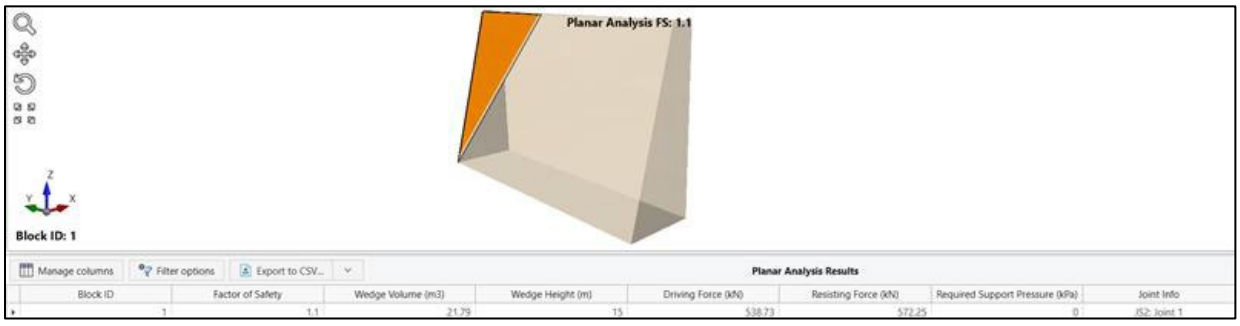


Figure 16-28: Stability Analysis of South Pit Sector E (FOS = 1.1 for Planar Failures in 75° Bench Angle Slopes)

This condition was specifically observed in final the pit bottom, in the schist domain with RQD >50%, where the slopes are steeper and have a 2 m bench (Figure 16-29). Although the risk of damage is low, since there will be no operations beneath these slopes, a minimum bench width of 5 m is recommended to ensure safe access to the benches, and operational safety.

Summing up, the analyzed sectors present satisfactory stability, and the implementation of blast-control measures and a continuous-monitoring program is recommended to ensure operational safety throughout the pit's life cycle.

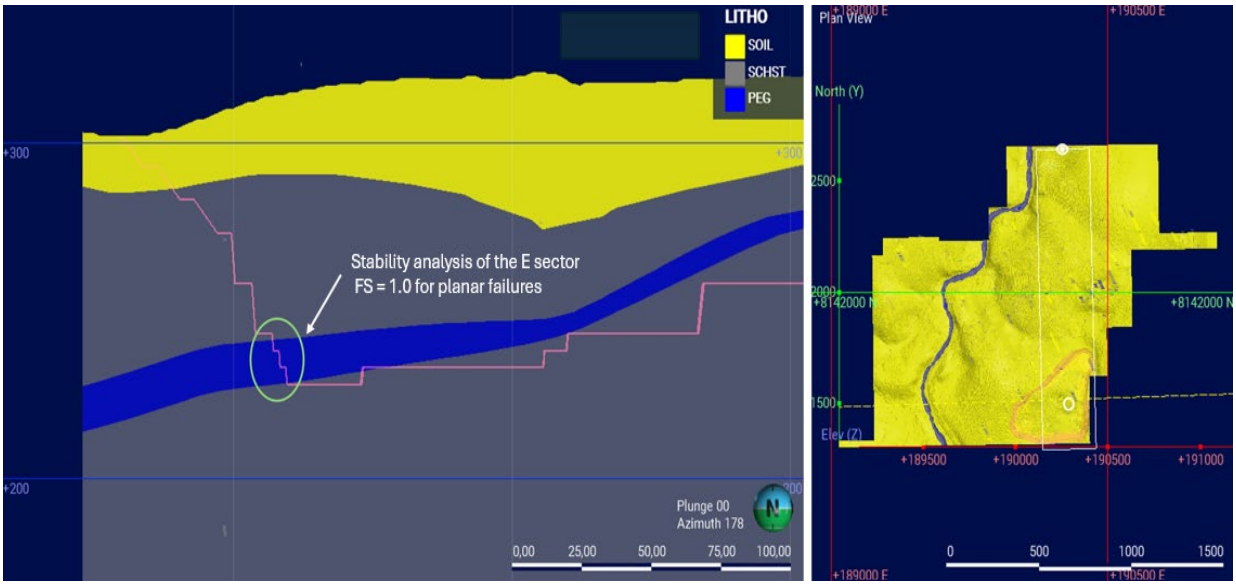


Figure 16-29: Left, South Pit Sector E Cross-Section Highlighting the Critical Area of the Section (FOS = 1.0 for Planar Failures, with a Face Angle of 85° and a 2 m Bench), Right, Project Property Plan Showing Pit (Pink Outline)

16.3.4 2-D Limit Equilibrium Analyses—Interramp and Overall Slope Scale

Stability analyses, at both interramp and global scales, were performed using Rocscience Slide2 software with the limit equilibrium method, considering the following assumptions:

- Materials considered isotropic and homogeneous
- Safety factors evaluated using GLE/Morgenstern–Price, Spencer, and Janbu Simplified methods
- Analysis of optimized non-circular surfaces
- Material strength characterized by the Mohr–Coulomb criterion for soils and the generalized Hoek–Brown criterion for other materials.

Table 16-10 presents the parameters adopted for each material, in accordance with the previously described values.

Table 16-10: Parameters Adopted in the 2-D Analyses

Material Name	Colour	Unit Weight (kN/m³)	Strength Type	Cohesion (kPa)	Phi (°)	UCS (Intact) (kPa)	Parameters Vary with Depth	GSI	mi	D	Water Surface	Ru Value	Tensile Strength (kPa)
Soil		17	Mohr–Coulomb	20	35	-	-	-	-	-	None	0	-
Schist RQD <50		26	Generalized Hoek-Brown	-	-	25,000	No	35	12	1	None	0	6.18
Pegmatite		27	Generalized Hoek-Brown	-	-	90,360	No	55	15	1	None	0	5.47
Schist RQD >50		26	Generalized Hoek-Brown	-	-	112,450	No	55	12	1	None	0	6.18

Notes: D = disturbance factor ; GSI = geological strength index, mi = material constant for the intact rock.

In general, the proposed pit presents two distinct geometric configurations, defined by depth and the material intercepted. In the first four, shallower benches, the bench faces have a slope of 50°, with heights ranging from 10 m to 20 m and 5 m-wide berms, resulting in average inter ramp angle of 50°.

In the deeper benches, face angles of 85° were adopted, with a height of 15 m and 5 m-wide berms, corresponding to an inter ramp angle of 60°. Considering the overall configuration, the pit reaches a maximum height of 95 m in Sector NW, with an average overall slope angle of approximately 43°, reaching a maximum value of 51° in Section 2, corresponding to Sector E.

It should be noted that in different sectors and sections of the pit, local variations occur that may locally modify the geometry. These variations were incorporated into the global-scale stability analyses and are summarized as ranges (Figure 16-30).

Material	Bench Angle (°)	Maximum Bench Height (m)	Minimum Berm Width (m)	Interramp Angle (°)	Range Overall Slope Angle (°)	Range Pit Depth (m)
Soil	50	20	5	39	38–51	57–95
Schist RQD <50	50	20	5	60		
Schist RQD >50	50	15	5			

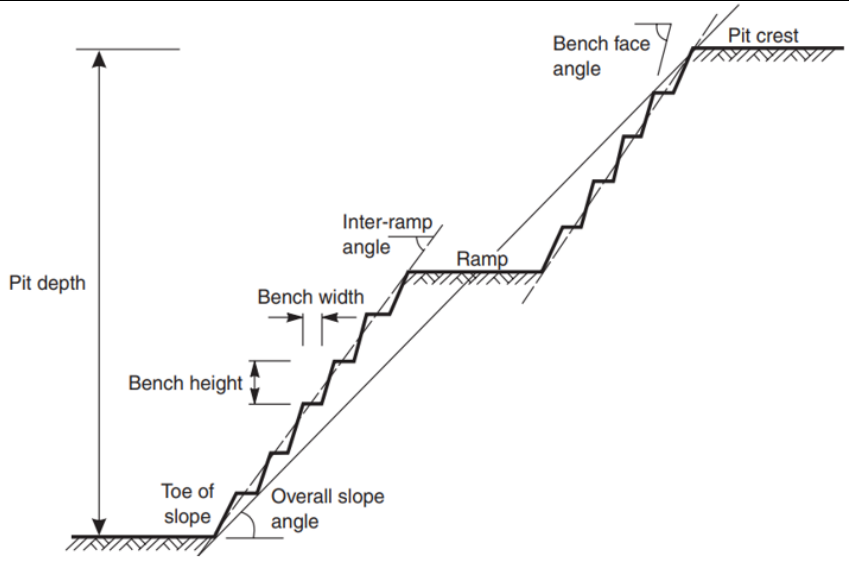


Figure 16-30: Geometric Parameters Used in the Stability Assessment

The evaluations conducted, together with the proposed geometry, considered different scenarios to assess the influence of the groundwater table on the pit-slope safety factors. Critical groundwater level scenarios were defined for all sections, in a manner consistent with the bench-scale analyses in soil materials.

Initially, a conservative assumption was adopted, with the groundwater table positioned at the pit bottom and slopes considered fully drained. In the critical scenario, the water level within the slopes was raised to full saturation, enabling a conservative assessment of the impact of groundwater on slope stability.

Figure 16-31 and Figure 16-32 show the results of the analysis for the representative section in Sector NW.

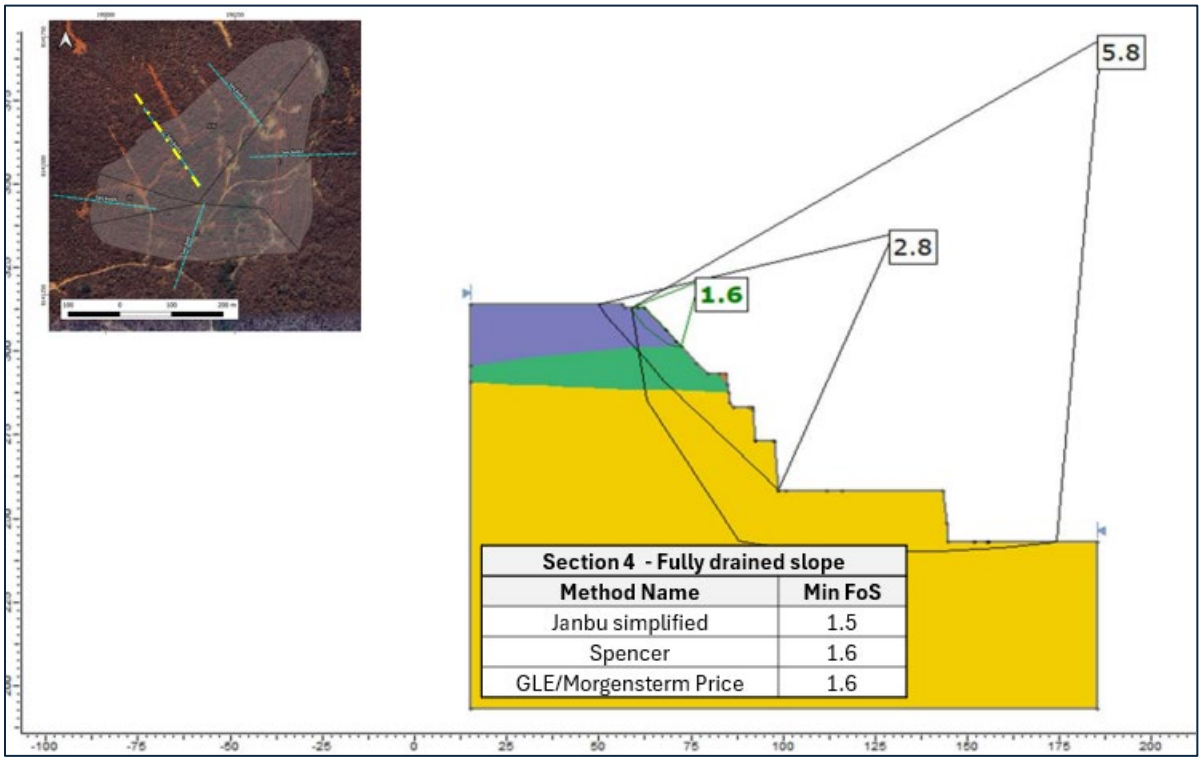


Figure 16-31: Plan of Pit Sectors and Sections (Inset) and Pit Southern Sector Section 4, Stability Analysis Considering the Fully Drained Slope Scenario

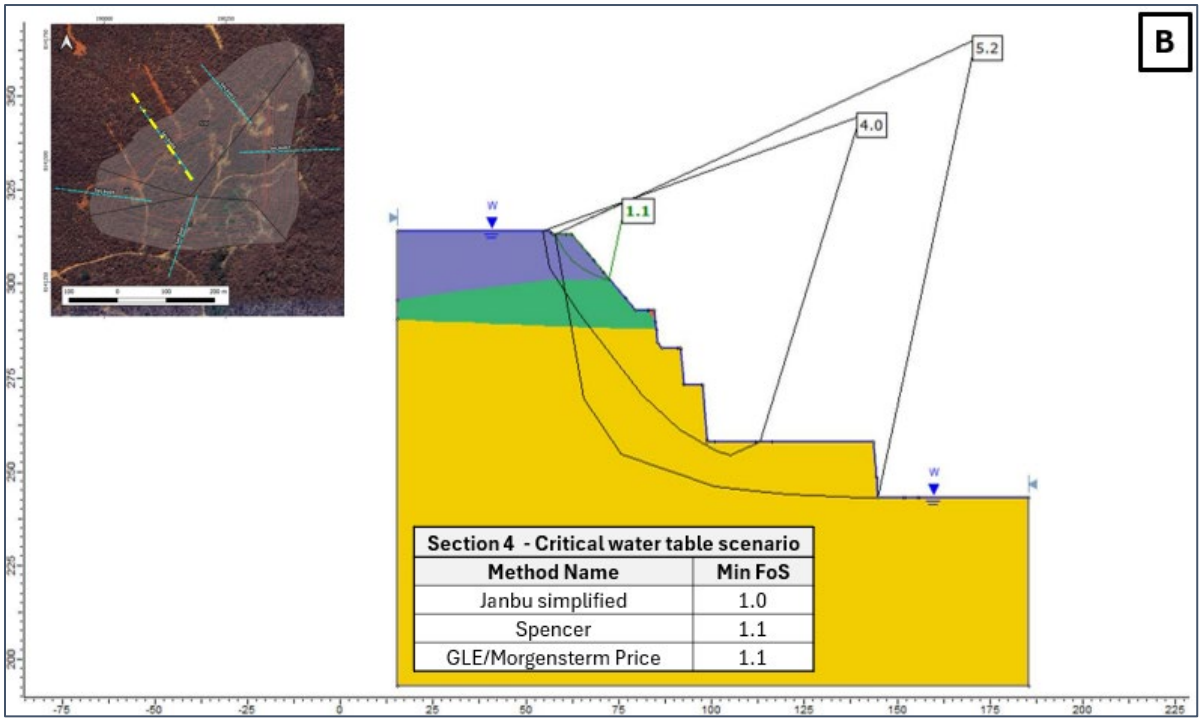


Figure 16-32: Plan of Pit Sectors and Sections (Inset) and Pit Southern Sector Section 4, Stability Analysis of Critical Water Table Scenario

In general, the five analyzed sections of the South pit present global FOS greater than 1.5, while interramp and bench FOS values remain above 1.2, meeting the minimum limits Read & Stacey (2009) recommend for final pit slopes. Considering groundwater level variations between Scenarios 1 and 4, the results proved satisfactory, and consistently above the reference values.

However, under the Groundwater Level Scenario 5 proposed by Hoek—regarded as a very conservative and unlikely scenario—Sections 2, 3, and 5 did not meet the defined acceptability criteria. The lowest FOS values were observed in soil domains and schist, with RQD <50 at the bench or interramp scales.

Table 16-11 presents the minimum safety factors obtained for global analysis in each section, considering the proposed groundwater level scenarios.

Table 16-11: Min FOS for Open Pit Global-Scale Analysis

Pit Design Sector	Pit Section	Overall Angle (°)	Pit Depth (m)	Groundwater Flow Conditions	Diagram Number	Min FOS		
						Jambu	Spencer	Morgenstern–Price
S	1	40	58	Fully drained slope	1	2.0	2.2	2.1
				Surface water 8x slope height	2	2.0	2.2	2.1
				Surface water 4x slope height	3	1.9	2.2	2.1
				Surface water 2x slope height	4	1.9	2.2	2.1
				Saturated slope	5	1.3	1.5	1.5
E	2	51	74	Fully drained slope	1	1.7	1.8	1.8
				Surface water 8x slope height	2	1.7	1.8	1.8
				Surface water 4x slope height	3	1.7	1.8	1.8
				Surface water 2x slope height	4	1.7	1.8	1.8
				Saturated slope	5	1.0	1.2	1.1
NW	3	38	95	Fully drained slope	1	1.2	1.3	1.2
				Surface water 8x slope height	2	1.2	1.3	1.2
				Surface water 4x slope height	3	1.2	1.3	1.2
				Surface water 2x slope height	4	1.0	1.2	1.2
				Saturated slope	5	0.7	0.8	0.7
	4	40	70	Fully drained slope	1	1.5	1.6	1.6
				Surface water 8x slope height	2	1.5	1.6	1.6
				Surface water 4x slope height	3	1.5	1.6	1.6
				Surface water 2x slope height	4	1.5	1.6	1.6
				Saturated slope	5	1.0	1.1	1.1
W	5	44	67	Fully drained slope	1	1.3	1.4	1.4
				Surface water 8x slope height	2	1.3	1.4	1.4
				Surface water 4x slope height	3	1.3	1.4	1.4
				Surface water 2x slope height	4	1.3	1.4	1.4
				Saturated slope	5	0.8	0.9	0.9

Following the detailed analysis of failures with FOS values below 1, as well as those that did not meet the established acceptance criteria, it was found that their occurrence is restricted to the soil horizon. These failures are shallow, involve at most two benches, exhibit a circular shape, and occur under the critical saturation scenario (saturated slope).

Table 16-12 summarizes the minimum FOS<1.5 values obtained for each scale of analysis, based on the global results of the five geotechnical sections evaluated.

It is observed that the instabilities (FOS <1), as well as the factors that do not meet the acceptance criteria in Sections 2, 3, and 5, are concentrated in the soil horizon, under fully saturated conditions, and at heights exceeding 10 m (Figure 16-33 to Figure 16-35). Therefore, the global-scale analyses corroborate the results of circular failure analyses carried out at the bench scale, indicating that 20 m-high soil slopes, when fully saturated, are unstable.

Table 16-12: FOS by Scale for the Open Pit Sections that Present a Minimum FOS <1.5

Pit Design Sector	Pit Section	Groundwater Flow Conditions Diagram Number	Scale of Analysis	Min FOS (Morgenstern–Price)
E	2	5	Bench	1.1[1]
			Interramp	3.9
			Global	3.6
NW	3	1	Bench	1.5
			Interramp	3.4
			Global	4.2
		2	Bench	1.4
			Interramp	3.4
			Global	3.6
		3	Bench	1.3
			Interramp	3.6
			Global	4
		4	Bench	1.5
			Interramp	3.5
			Global	5
		5	Bench	1.0[2]
			Interramp	3.1
			Global	3.1
	4	5	Bench	1.1
			Interramp	4
			Global	5.2
W	5	1	Bench	1.4
			Interramp	1.4
			Global	4.1
		2	Bench	1.4
			Interramp	1.4
			Global	4.6
		3	Bench	1.4
			Interramp	1.4
			Global	4.8
		4	Bench	1.4
			Interramp	1.4
			Global	3.8
		5	Bench	0.9[2]
			Interramp	0.9[2]
			Global	4.6

Notes: [1] FOS at the limit of acceptability for Morgenstern–Price and below the acceptable level for Janbu Simplified (FOS 1.0).
[2] FOS below the acceptability criterion proposed by Read & Stacey (2009).

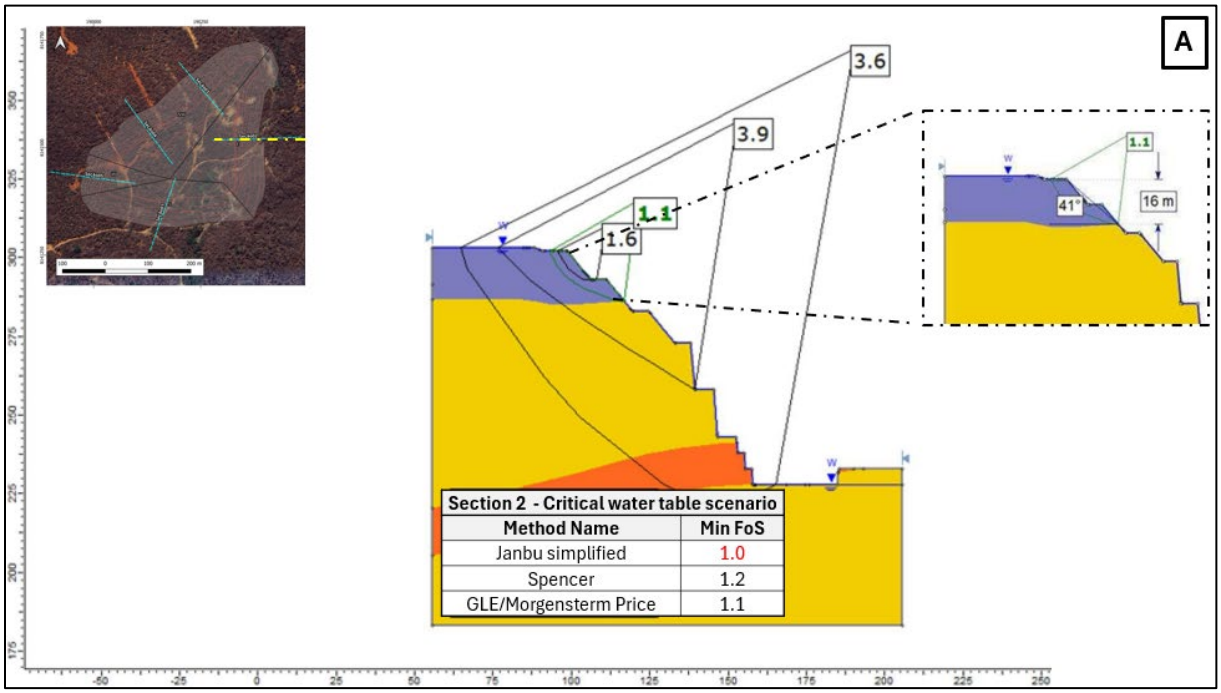


Figure 16-33: Plan of Pit Sectors and Sections (Inset) and Pit Southern Sector Section 2 Stability Analysis Considering the Critical Water Level and Highlighting the Lowest FOS in the Shallowest Pit Horizon

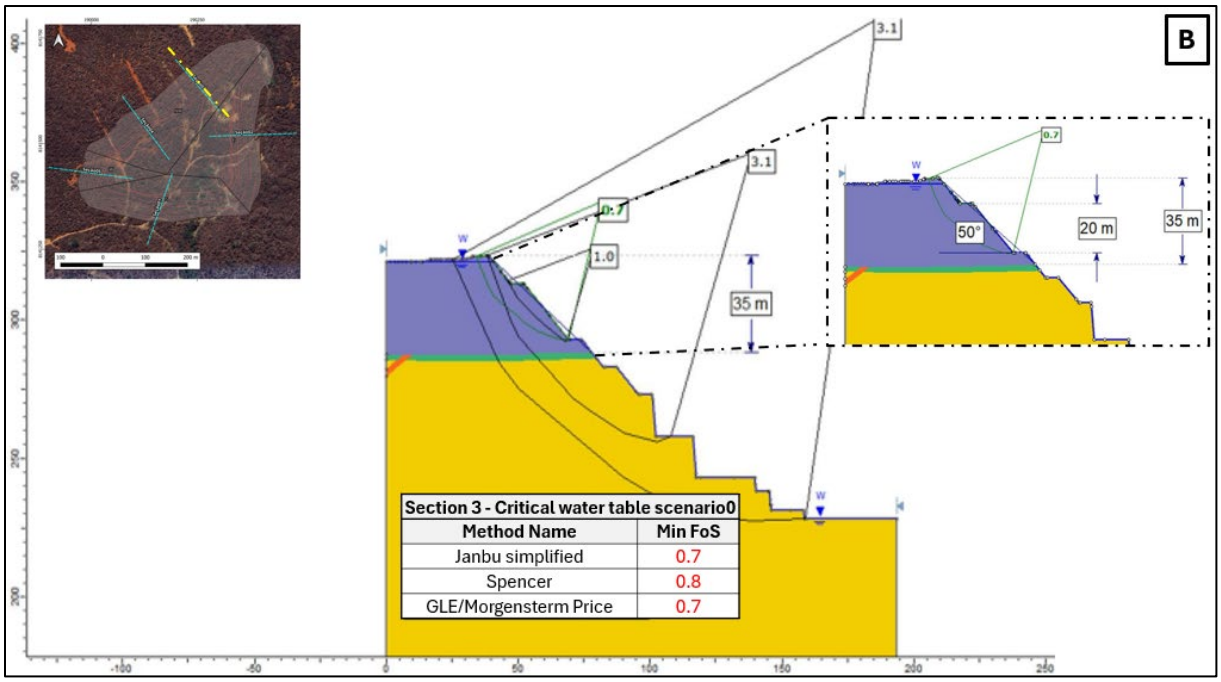


Figure 16-34: Plan of Pit Sectors and Sections (Inset) and Pit Southern Sector Section 3 Stability Analysis Considering the Critical Water Level and Highlighting the Lowest FOS in the Shallowest Pit Horizon

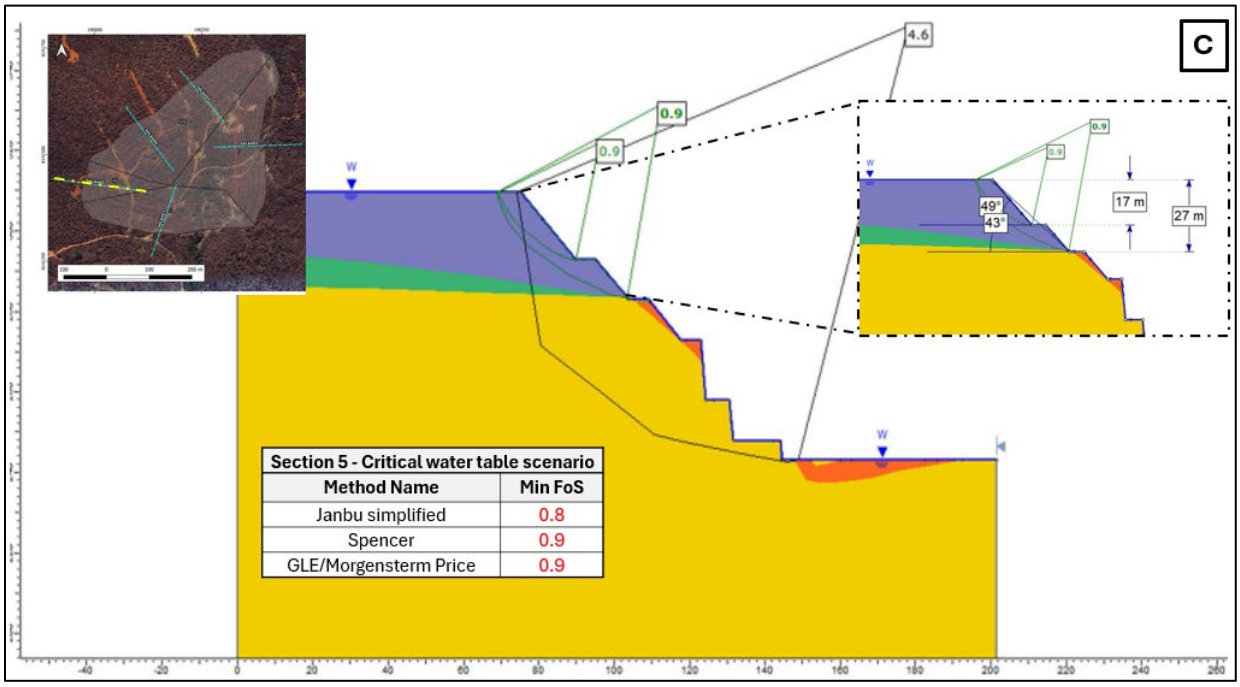


Figure 16-35: Plan of Pit Sectors and Sections (Inset) and Pit Southern Sector Section 5 Stability Analysis Considering the Critical Water Level and Highlighting the Lowest FOS in the Shallowest Pit Horizon

Given the absence of a hydrogeological monitoring network capable of confirming groundwater level variations, groundwater flow models associated with circular failure analyses were adopted as an evaluation criterion. Although these analyses indicate localized instabilities exclusively under fully saturated conditions, such scenarios are considered conservative.

During the geotechnical investigation campaigns, most boreholes indicated dry groundwater levels. Furthermore, the Araçuaí region, presents a semi-arid climate (BSh), typical of northern Minas Gerais, characterized by relatively low rainfall.

The hydrological data in the Project area derive from the historical series of the rain gauge station 1642028, in Araçuaí, spanning October 2003 to March 2023. On average, the multi-year average precipitation was around 651.2 mm. It is observed that the rainiest month in the region is December (164.7 mm), while the driest month is July (1.2 mm). These climatic conditions significantly reduce the likelihood of widespread soil saturation, limiting its influence on slope stability and reinforcing the interpretation that the identified instabilities do not represent critical conditions for the Project.

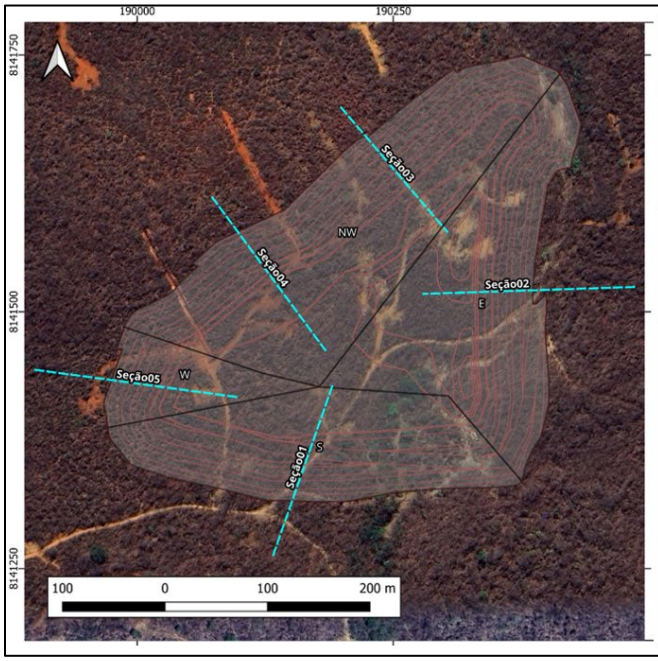
Therefore, even though the fully saturated scenarios are deemed unrepresentative for the Project region, it is recommended, in the absence of a hydrogeological monitoring network, to limit the height of soil benches to 10 m, thus fully satisfying the acceptance criteria under different groundwater flow conditions.

For rock materials, it is further recommended to reduce the face angle to 75° only in Design Sector E. These measures aim to minimize localized failure mechanisms, reduce the overall slope angle, and

ensure a more conservative geometric configuration, consistent with best practices in geotechnical engineering.

Based on the analyses conducted for the initially proposed geometry, at different observation scales, no critical failures were identified in the pit layout. The recommendations presented consist only of minor adjustments, intended to mitigate risks related to groundwater fluctuations, pore pressure, and the use of estimated parameters in some stability analyses.

Figure 16-36 presents the validated geometries for the different design sectors of the pit:



Design Sector	Section	Geomechanical Domain	Maximum Bench Height (m)	Bench Angle (°)	Minimum Berm Width (m)	Overall Angle (°)	Pit Depth (m)
S	1	Soil	10	50	5	40	58
		RQD <50%	10	50			
		RQD>50%	15	85			
E	2	Soil	10	50	5	46	74
		RQD <50%	10	50			
		RQD>50%	15	75			
NW	3	Soil	10	50	5	40	95
		RQD <50%	10	50			
		RQD>50%	15	85			
	4	Soil	10	50		34	70
		RQD <50%	10	50			
		RQD>50%	15	85			
W	5	Soil	10	50	5	44	67
		RQD <50%	10	50			
		RQD>50%	15	85			

Figure 16-36: Left, Plan Showing Open Pit Design Sectors and Sections; Right, Proposed Geometry for the Respective Design Sectors

Based on the above, and with the aim of increasing the Project's level of maturity, the following actions are recommended for pre-ops and operational phase:

- Implement a field investigation program and laboratory testing, with the objective of complementing the geotechnical characterization and consolidating the parameters of the materials composing the slope faces. Additionally, obtain direct shear–strength data for the main discontinuities, with emphasis on foliations S1 and S2—previously estimated and presented herein—as they represent the primary kinematic controls identified. These data will support the optimization of slope angles for the operational pit.
- Characterize the detailed local hydrogeology and implement a continuous groundwater monitoring network, covering both pre-operational and operational phases. Effective groundwater drawdown and maintaining unsaturated conditions along the pit slopes are considered critical elements for ensuring geotechnical stability.
- Verify the saturation conditions assumed in the current stability analyses, through development of a computational hydrogeological model encompassing all materials forming

the pit slopes. This model should also account for the effects of groundwater drawdown due to mining operations. Based on the model outcomes, the stability analyses presented in this study should be re-evaluated.

- Develop and implement a slope stability monitoring and control plan, including routine visual inspections, geotechnical instrumentation readings, and systematic compilation of collected data. The early identification of unanticipated conditions, followed by the prompt implementation of corrective actions, may prevent the development of larger-scale instabilities.
- Evaluate the influence of adjacent structures in the pit stability, also do future assessments considering the influence of blasting activities on nearby structures during the pre-ops or operation phase. To this end, carry out seismic data collection from blasting operations to obtain representative acceleration values, enabling a more accurate assessment of their potential impact on surrounding structures.

16.3.5 Underground Mine

Sublevel Open-Stope Mining

For the empirical stability analysis, Villaescusa's (2014) stability graph method was used. This approach accounts for the effects of stress and is based on a larger database of historical studies collected in Canadian and Australian mines, along with revised factors used for estimating the stability number. Figure 16-37 presents the proposed stope design currently being used, together with the proposed dimensions for the rib and sill pillars.

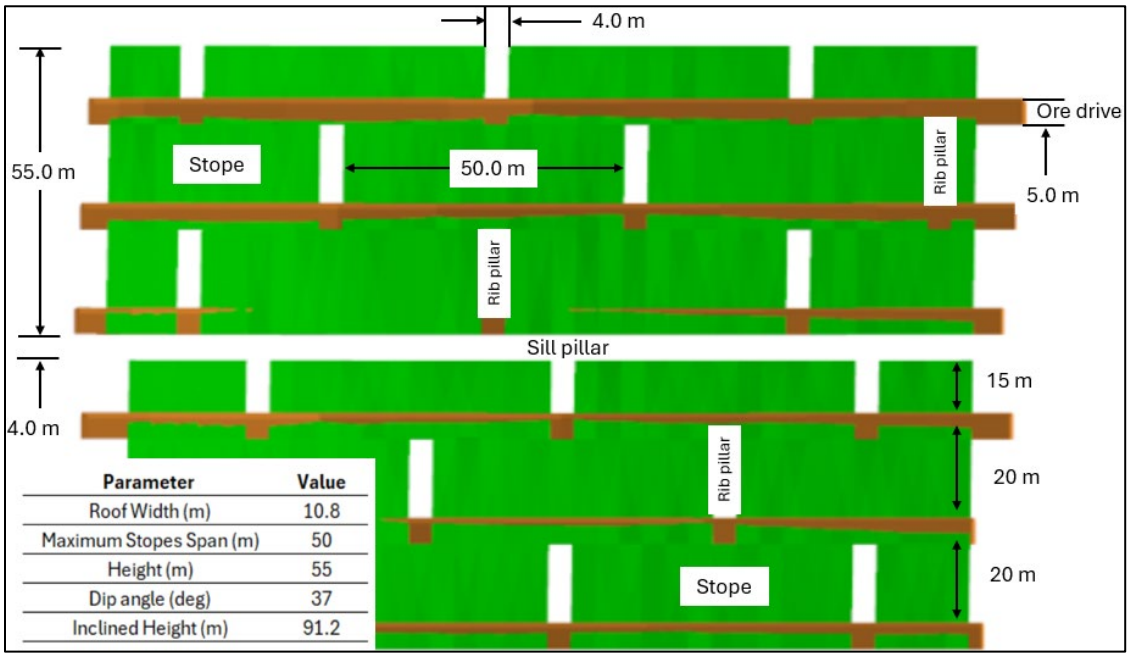


Figure 16-37: Open Stope Mine Design and Stope Dimensions

The empirical design used the results from the geomechanical characterization of the host rock, classified as the slightly altered and fresh rock schist domain (W1/W2), which comprises the hanging wall, footwall, and partially the crown stopes.

The stability number (*N'*) was calculated using the following equation:

$$N' = Q' \times A \times B \times C$$

Where *Q'* is the modified Barton's Q, or Q-prime, which represents an adaptation of the original Q-system proposed by Barton et al. (1974) for rock mass classification,
A denotes the strength-to-stress ratio,
B indicates the structural influence on stope wall conditions, and
C represents the impact of gravity on the excavation.

Thus, the empirical stability analyses were performed for the slightly altered and fresh rock schist domain classified as W1 and W2, with variations only applied to A, the strength-to-stress ratio in the equation above, corresponding to different planned depths of the stopes. The adjustments reflect the increase in in situ stress as the depth increases.

Due to the absence of confirmed pre-mining stress data and based on empirical assessments, the estimated in situ stress field for a range of representative depths was calculated using published crustal tectonic stress tensors (Handley, 2013). It is acknowledged that the stress state may not be representative for mining areas in Brazil; however, the increase in horizontal stress at shallower depths provides a conservative stress estimate for the LOM.

The primitive stress state through the use of Heims rule can be calculated using the following equation for the virgin vertical stress:

$$\sigma_v = \rho \, . \, g . \, h$$

where σ_v is the virgin vertical stress, representing the pressure exerted by the weight of the overlying rock column at the considered point,
ρ is the material density generally expressed in kg/m³,
g is acceleration due to gravity, and
h is the depth of the point of interest relative to the surface.

Through the use of the crustal data Handley (2013) presents, and the use of σ_v, it is possible to determine the relationship between the vertical stress and the horizontal-to-vertical stress ratio (k) (Figure 16-38). This method suggests that the principal stress is predominantly horizontal, while the minimum stress is vertical. The magnitudes of the k-ratio are considered realistic, considering the highest horizontal principal stress and the lowest vertical principal stress, as well as the vertical stress component.

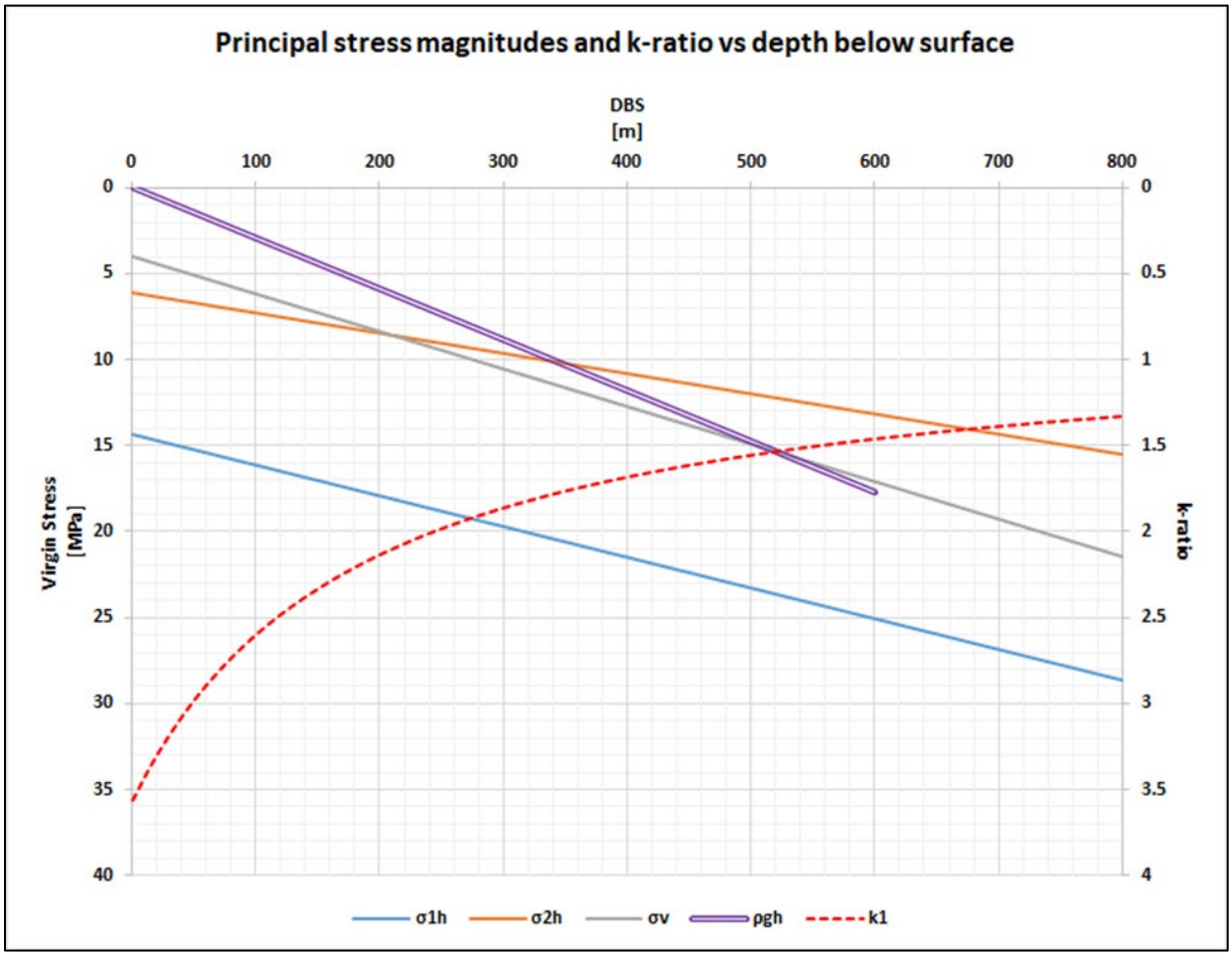
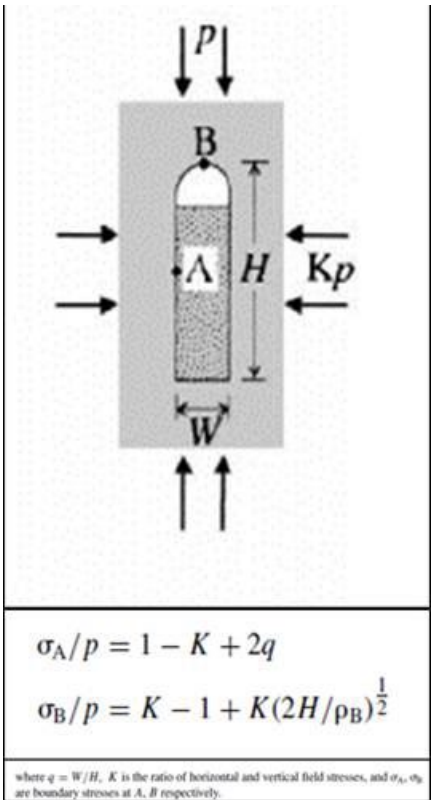


Figure 16-38: Pre-Mining Stress Magnitudes and k-ratio vs. Depth Below Surface

However, it must be noted that the change in stress direction is not yet known for this study therefore the k-ratio per depth range is assumed to apply to both the XX and YY stress direction. Notably once excavations are created, the induced stress affecting excavation stability needs to be assessed and is required for the determination of the strength-to-stress ratio (Factor A, above). To achieve this, the induced stresses can be calculated using Brady and Brown's (1985) method, where the stress is calculated on the periphery of an excavation (Figure 16-39).

In the following sections, the procedure adopted for calculating Factors A, B, and C, as well as the parameters Q' (Q-prime) and N', representing the stability number, is described.



Source: Brady and Brown (1985).

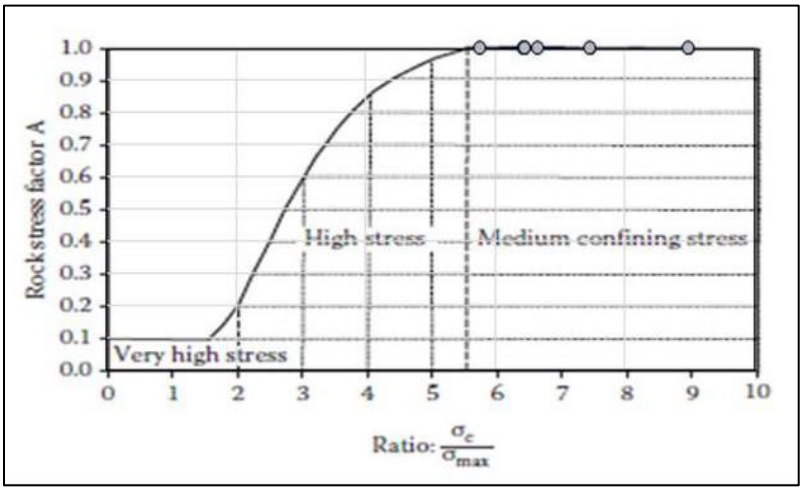
Figure 16-39: Estimation of Crown and Hanging-Wall Stress for an Open Excavation

Factor A

Factor A is defined as the ratio between the UCS of the intact rock and the compressive stress induced tangential to the surface of the stope walls. To access depth range, was adopted from 50 m to 600 m below surface, sufficient to cover the mine footprint, and considered a UCS of 147.52 MPa for the slightly altered and fresh rock schist (W1/W2), which is predominately within the hanging wall. The calculated stress-to-strength ratings can be found in Table 16-13 and Figure 16-40, plotted on the A-parameter graph (Villaescusa, 2014).

Table 16-13: Calculated Hanging-Wall Induced Stresses and Rock Stress Factor A

Depth (m)	Virgin Stress @ A (MPa)	Width (m)	Height (m)	q	k-ratio	Induced Stress @ A (MPa)	Rock Strength (MPa)	$\sigma_{strength}/\sigma_{stress}$ at A	Factor A
50	2.28	10	55	0.182	2.97	15.81	142.25	9.00	1.00
100	3.75	10	55	0.182	2.59	18.99	142.25	7.49	1.00
200	6.69	10	55	0.182	2.13	21.30	142.25	6.68	1.00
300	9.64	10	55	0.182	1.86	21.94	142.25	6.48	1.00
400	12.58	10	55	0.182	1.68	22.06	142.25	6.45	1.00
500	15.52	10	55	0.182	1.55	21.98	142.25	6.47	1.00
666	20.41	10	55	0.182	1.46	24.54	142.25	5.8	1.00



Source: adapted from Villaescusa (2014, p. 203), *Geotechnical Design for Sublevel Open Stoping.*

Figure 16-40: Rock Stress Factor A and Resultant Strength-To-Stress Ratios for Depths Ranging from 50 m below Surface to 666 m Below Surface

Factor B

Factor B is a weighting parameter based on the orientation of the discontinuity set considered most likely to compromise the stability of a given stope wall (Potvin, 1988). Its determination requires calculating the true angle between a stope wall and the most critical discontinuity. The most critical structure affecting the Project's planned stope walls is associated with the S1 foliation, which is subparallel to the surfaces of the planned stopes in concordant ore bodies and orthogonal to the surfaces of the planned stopes in discordant ore bodies. Under these conditions, no correction factor was applied.

For the concordant ore bodies with the inclination of the hanging wall ranging from 25° to 90°, the average value of 37° was adopted, while the average dip of the foliation is 47°, resulting in Factor B being 0.25. In the discordant ore bodies, the dip of the hanging wall shows greater variability, ranging from 36° to 74°. Considering the lower inclination values of the hanging wall, the Factor B for the discordant ore bodies is estimated to be 0.9.

Factor C

Potvin (1988) introduced Factor C to incorporate the effect of gravity in assessing stope stability, based on the premise that, under gravitational influence, compared to horizontal backs, vertical walls exhibit greater stability.

This Technical Report assumes that, since most of the planned stopes have an average inclination of approximately 37°, the predominant failure mechanism is gravitational in nature. Under these conditions, Factor C is 4.7 for both ore bodies, which results in a lower stability number (N′) and, consequently, in the determination of more restrictive maximum admissible spans.

Table 16-14 shows the depths considered in the stability analyses, as well as the results of the stability number and Q′ values obtained from the rock-mass characterization for the domain.

Table 16-14: Calculated Modified Stability Number for All Depth Ranges

Ore-Body Type	Depth Below Surface (m)	Geotechnical Domain	Domain	Factor A	Stress State	Factor B	Factor C	Q'	N'
Concordant	50–666	Schist	W1/W2	1	Low	0.25	4.7	40.46	47.54
Discordant	50–666	Schist	W1/W2	1	Low	0.9	4.7	40.46	171.14

Based on the stability numbers (*N'*) determined for the various ore body hanging walls using Villaescusa's (2014) stability chart, the estimated hydraulic radius is 14.4 for the concordant ore bodies and 21 for the discordant ore bodies (Figure 16-41). This corresponds to maximum strike lengths of approximately 60 m for the concordant ore bodies and 170 m for the discordant ore bodies.

However, due to uncertainties in some of the geotechnical parameters, the limited characterization of the hanging wall, and following SRK's (2025, May 29) review, the stope spans have been conservatively limited to a maximum strike length of 50 m across all depth ranges.

It should be noted that further geotechnical studies are ongoing to increase confidence in the material properties and strength parameters, which will in turn allow for refinement and validation of the stope design criteria.

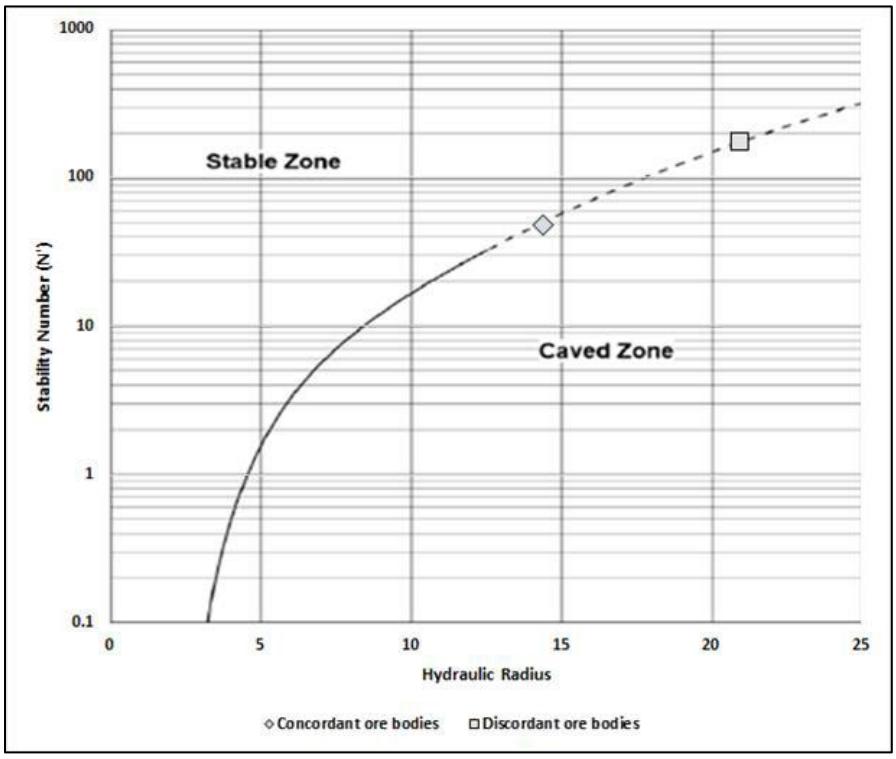


Figure 16-41: Estimated Hydraulic Radius Using Calculated N' Numbers for the Concordant and Discordant Ore-Body Hanging Wall

Considering general good stability conditions for the hanging wall, for concordant and discordant ore bodies, cable bolting was designed for safe access to ore drives during production, and to avoid dilution. MGLIT's technical team estimated a 0.5 m-thick layer as dilution at the hanging wall. For 55 m-high stopes, dipping 37°, Figure 16-42 gives a schematic view of dilution.

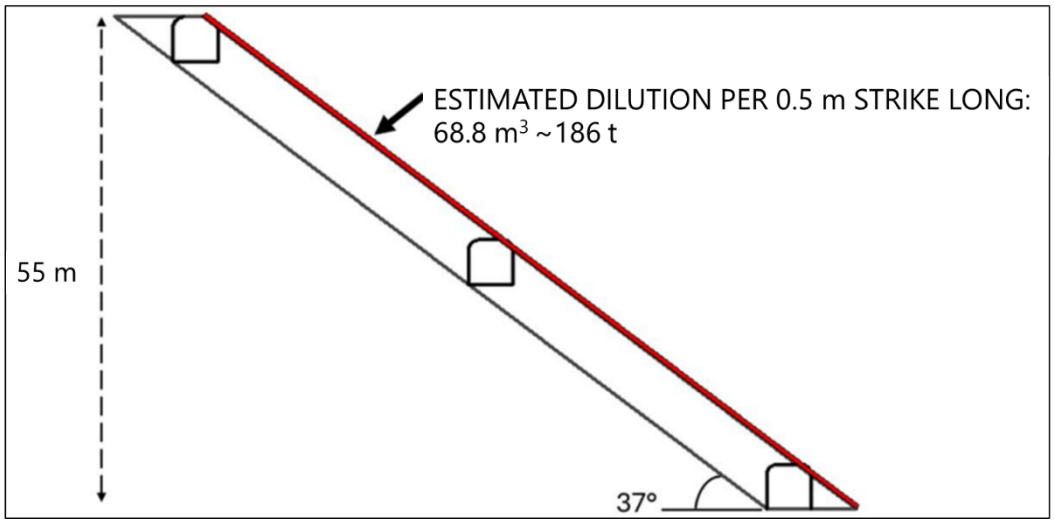


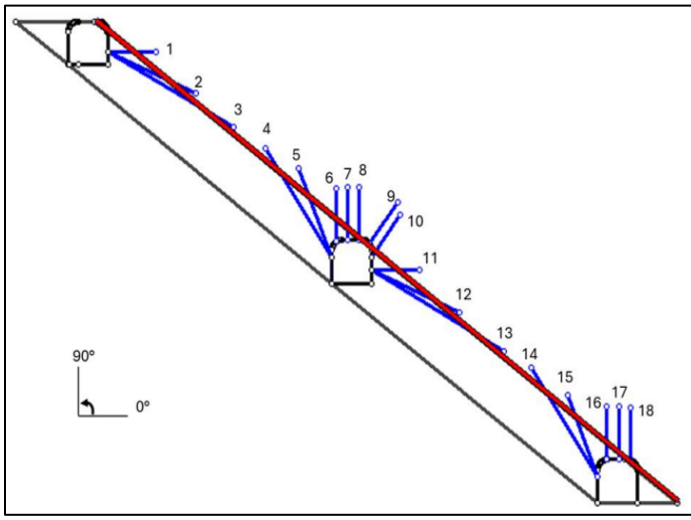
Figure 16-42: Dilution Estimation and Schematic Section for Sublevel

As the hanging wall is stable, dilution is considered to originate due to being loosened by blasting damage. Thus, gravity and vertical movement are the dominant issues in cable design. Vertical cables should work at a maximum axial load capacity (25 tonnes for common cable bolts in the Brazilian mining market). Inclined cable bolts should work at 10%–30% of their capacity, 2.5 tonnes to 7.5 tonnes, respectively.

A conceptual cable-bolt design was made to decrease spans without support and reinforce the ore-drive supports to allow safe access during operation. The design considers installing cable bolts at least 1.5 m above ground. All cable bolts are to be installed at least 2 m beyond the dilution layer. The distance between sections is 1.5 m, following the strike direction. Figure 16-43 shows the cable bolt design, cable bolts position, inclination, length, and load considered.

The results presented in Figure 16-42 indicate a total load capacity of 210 tonnes for each 1.5 m-strike advance. Considering this is a limit equilibrium analysis, the comparison with the estimated dilution load of 186 tonnes requirement for the same advance (Figure 16-43) results in an FOS of 1.13 (210/186). This value is considered acceptable in the context of dilution assessment, particularly given the stope geometry, which imposes constraints on cable-bolt positioning.

It is important to mention that the cable bolts were designed not only to control dilution but also to ensure the safety of the ore drives, complementing the support previously installed during development excavations. The use of cable bolts represents a safety enhancement, avoiding the need to reposition support (rehabilitation) during stope production, and increasing the efficiency of the ground support system, particularly to prevent brow instabilities.



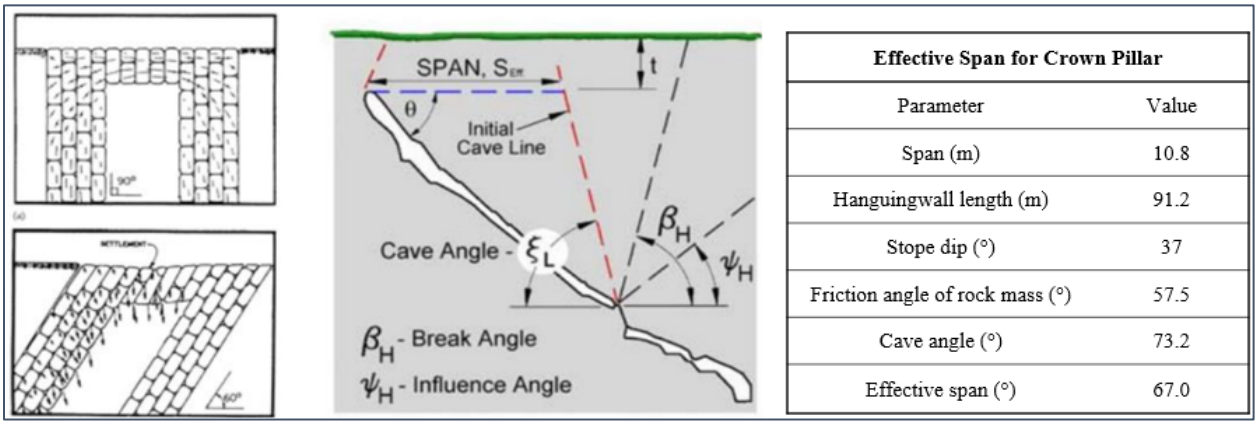
Cablebolt ID#	Instalation position	Inclination (°)	Efficiency (%)	Load (t)	Length (m)
1	1.5m above ground	0	30	7.5	6
2	1.5m above ground	-23	10	2.5	12
3	1.5m above ground	-29	10	2.5	18
4	3.0m above ground	123	10	2.5	15
5	3.0m above ground	112	30	7.5	11
6	Roof	90	100	25	6
7	1.5m away C6	90	100	25	6
8	1.5m away C7	90	100	25	6
9	1.5m away C8	51	30	7.5	6
10	3.0 above ground	51	30	7.5	6
11	1.5m above ground	0	30	7.5	6
12	1.5m above ground	-24	10	2.5	12
13	1.5m above ground	-29	10	2.5	19
14	3.0 above ground	123	10	2.5	15
15	3.0 above ground	111	30	7.5	10
16	Roof	90	100	25	6
17	1.5m away C16	90	100	25	6
18	1.5m away C17	90	100	25	6
			TOTAL	210	172

Figure 16-43: Cable Bolt Design and Cable Bolting Information for Each 1.5 m Strike Long Section

Crown Pillar Assessment

The stability of the crown pillar was assessed using Carter's (2014) method, which identifies five main failure mechanisms depending on the exposure conditions of the pillar. This methodology is typically applied to stopes with steeper dips; therefore, stopes with low dip angles (<40°) are considered challenging for direct application of the method. To address this limitation, Carter's empirical approach (2014) was adopted, incorporating an adjustment to the effective span for low-dipping stopes.

Based on these considerations, a conceptual model was developed using the Rocscience CPillar software to simulate the vertical loading conditions imposed by the 30 m of residual soil and saprolite column. The effective span was calculated considering the average dip of the Project stopes, following the relationship shown in Figure 16-44.



Effective Span for Crown Pillar	
Parameter	Value
Span (m)	10.8
Hanguingwall length (m)	91.2
Stope dip (°)	37
Friction angle of rock mass (°)	57.5
Cave angle (°)	73.2
Effective span (°)	67.0

Source: adapted from Carter (2014, p.15).

Figure 16-44: Span Dipping for Shallow Effective Stopes based on Zone of Influence and Cave and Break Angles

Considering the simulated failure mechanism (plug failure), a horizontal stress-state equivalent to the vertical stress (Kh = 1.0) represents the most critical scenario for the crown pillar. To estimate the

minimum pillar height required to ensure stability (FOS ≥1.50) for a semi-temporary pillar located away from sensitive mine infrastructure, a sensitivity analysis was conducted (Table 16-15).

Table 16-15: Sensitivity Analysis for Crown Pillar Height

Pillar Height (m) Schist Domain (W1/W2)	FOS (Plug Failure) Kh = 1.0 (Hydrostatic)
15	0.68
20	0.91
22	0.99
23	1.04
24	1.08
25	1.13
30	1.34
33	1.47
34	1.51
35	1.55

The results indicate that a minimum rock thickness of 34 m, measured downward from the W3 top contact, is required to ensure crown pillar stability. It should be noted that this value does not consider the effects of blasting, and also depends on the local stress state. Therefore, even when adopting a conservative approach, a more detailed assessment is recommended to adjust the design to the site-specific conditions.

Ground-Support Requirements

In general, the support system for the Project underground excavations was evaluated using an analytical approach (limit equilibrium), considering ore bodies and types of access separately—both permanent and temporary. Given the relatively shallow depths (<700 m), the absence of evidence of high stresses, and the high UCS values (>100 MPa) for excavations in fresh rock, it is estimated that the main instability issues are associated with rock mass discontinuities.

As stated in the paragraph above, a wedge formation can impose significant loads on the support system. Therefore, the ground-support study focused on potential wedge patterns controlled by the discontinuities in the rock mass, as well as the possibility of block-fall resulting from the unloading of these discontinuities.

The analysis was carried out using Rocscience Unwedge (Version 5.021) to evaluate wedges in underground excavations and estimate support requirements. The following parameters were adopted: FOS of 1.3 as a reference, and the number of wedges with FOS values below the design threshold, which will require additional treatment to reach the desired stability level, normally achieved by closing the support mesh.

The limit equilibrium assessment of the main wedge patterns considered the discontinuity sets S1, S2, FR1, and FR2 for the schist domain, and FR1, FR2, TC, and BC for the pegmatite. The latter were treated as a single structure (contact), as they have similar dip and dip direction values. The friction

properties (JRC, JCS, and ϕr), shown in Table 16-16, were estimated based on the technical team's prior experience with similar materials in other underground mines.

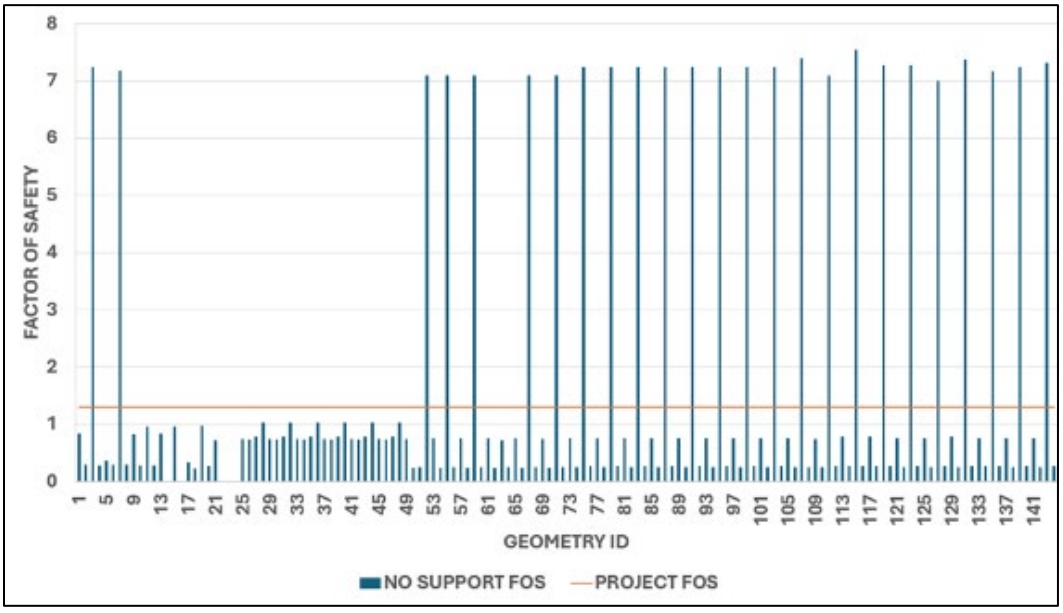
Table 16-16: Structural Data and Strength Parameters for Discontinuities

ID	Description	Dip Direction (°)	Dip (°)	JRC	JCS (MPa)	Ø r (°)
S1	Main foliation	316	46	4	40	25
S2	Secondary foliation	275	72			
FR1	Fractures dipping to NW	302	36			
FR2	Fractures dipping to SE	141	21			
Contact	Ore contacts in pegmatite	315	31			

Notes: JRC = joint roughness coefficient; JCS = compressive strength of the joint wall; ϕr = residual friction angle.

The planned geometry for primary and secondary development included the ramp inclination, intersections, lateral development, loading point, drilling location, raiseborer, crosscuts, and mucking bay. For each geometry, three orientations relative to the main foliation were evaluated: parallel, perpendicular, and oblique.

Additionally, the possibility of inclined development was considered alongside horizontal development. In total, 144 simulations were evaluated, encompassing different directions and inclinations of the underground excavations (Figure 16-45).



Source: Geotech Geotechnical Recommendation Bandeira Lithium Project Minas Gerais, Brazil. Geotech (2024, December)

Figure 16-45: Safety Factor Results for the Schist's Wedge-Limit Equilibrium Assessment in the Underground Development Excavations

Safety factors below the acceptance criteria indicate that the geometry should be evaluated for support requirements. To incorporate support into the wedge simulations, two types of helical bolts were

assessed: 2.4 m-long 19 mm x 22 mm and 22 mm x 25 mm, applied in a 1.5 m x 1.5 m anchoring mesh. The properties of the bolts used in the simulations are detailed in Table 16-17.

Table 16-17: Rebar Properties Considered in Wedge Limit Equilibrium Assessment

Rebar Section (mm)	Tensile Capacity (MN)	Plate Capacity (MN)	Bond Strength (MN/m)	Shear Strength[1] (MN)
19 x 22	0.18	0.007	0.14	0.05
22 x 25	0.25	0.007	0.25	0.75

Notes: MN = mega-newton = 10^6 N.
[1] Considered as 30% of Tensile Capacity.

In summary, the support recommendation for schist development consists of 2.4 m-long 22 mm x 25 mm bolts, installed 1.5 m above the floor in a 1.5 m x 1.5 m mesh, except at intersections, where a staggered pattern is recommended, combining two configurations: 2.4 m-long, 22 mm x 25 mm bolts in a 1.5 m x 1.5 m mesh and 3.3 m-long, 22 mm x 25 mm bolts in a 1.5 m x 1.5 m mesh. Additionally, the use of welded wire-mesh on the main ramps will ensure greater safety and operational efficiency in permanent excavations.

For the pegmatite assessment, involving FR1, FR2, and the Contact, 36 geometries were simulated due to the presence of only three discontinuity sets in the pegmatite. The contact was considered the primary joint set for comparison with the development orientation. Based on the results, a conservative recommendation is to adopt 2.4 m long, 22 mm x 25 mm bolts in a 1.5 m x 1.5-m mesh.

All results refer to fresh rock conditions. Blasting effects were not considered, which is one of the reasons for selecting an FOS of 1.3. Once development begins, this work should be reviewed and updated using attenuation curve data to further refine and optimize support recommendations.

Future assessments will be conducted for weathered rock, including the design of shotcrete or other shear-strength surface supports, as well as support for the mine portal, specifically for this domain. A summary of the results is presented in Table 16-18.

Table 16-18: Project Ground-Support Recommendation

Rock Mass	Development Geometry	Rebar 22 x 25 (mm)		Sidewall Support (Grade Line 1.5 m Above	Surface Mesh
		Mesh (m x m)	Length (m)		
Schist	Decline, lateral development, drilling site, raiseborer, load point, mucking bay, and passing bay	1.5 x 1.5	2.4	Yes	Yes
	Other lateral development: cross cuts, mucking bays, load points, ventilation drives, and waste connections	1.5 x 1.5	2.4	Yes	No
	Decline intersection and tunnel intersection	1.0 x 1.0	2.4 intercalated with 3.3 Figure 5-52)	Yes	Yes
Pegmatite	Lateral development, drilling site, raiseborer, load point, mucking bay, passing bay, decline intersection, and tunnel intersection	1.5 x 1.5	2.4	No	No

Hydrological Characterization

The Project hydrological data come from the historical series of the rain-gauge station 1642028, in Araçuaí, spanning October 2003 to March 2023. On average, the multi-year average precipitation was around 651.2 mm. It is observed that the rainiest month in the region is December (164.7 mm), while the driest month is July (1.2 mm).

The spring inventory conducted during the dry season helps identify the lowest-elevation springs, which in turn indicate downstream areas where surface-water flow remains continuous throughout the year (perennial drainage). In the absence of water points during this period, it can be assumed that water occurrences in the drainages are only occasional, associated with the rainy season or occasional precipitation.

Sixty-three points were registered over the dry period:

- 2 springs
- 41 dry drainages
- 20 control points.

Geologically, it is believed that this saturated zone is a package of silty-sandy material with much organic material, which overlies the Salinas Formation. It is recharged by rainwater and, due to its low permeability and hydraulic conductivity, remains moist for almost the entire year.

Geophysical studies of electrical resistivity and spontaneous potential indicated that there is a higher presence of regions with lower resistivities, mainly in the western and eastern portions of the Project area, except for the massif in the extreme western portion, whose location limits the saturated zone, with unsaturation evident from the beginning.

It is possible to observe three important locations with lower saturation compared to others in the central portion of the target area. Zones of high saturation were identified even at lower elevations in the area, and these anomalies could indicate possible associations with geological structures.

16.3.6 Regional Hydrogeological Context

The Project is in the Jequitinhonha Valley, in the middle sector of the Jequitinhonha River basin, and it is characterized by a semi-arid climate. The prevailing conditions make the use of underground water resources the main alternative for suppling water. However, the predominance of fissure aquifers and reports of high salinity in the water impose restrictions on any use of groundwater in the region (Menegasse et al., 2003).

According to previous investigations, lithologies in the region can be classified into four aquifer units:

Unit 1: These comprise rare alluvial covers found in some portions of the Jequitinhonha River, Araçuaí River, and Piauí River, all three with very small dimensions. They may be locally important: properties along these rivers do not face water-scarcity issues as they are perennial.

Unit 2: Aquifers in this unit are granular and consist of thick packages of coarsely stratified sediments from the São Domingos Formation, which can exceed 100 m thick in the Virgem da Lapa region. This unit also includes other eluvial–colluvial covers that overlay tertiary planation surfaces.

Unit 3: This unit, the largest in the area, comprises lithologies from the Macaúbas Group, especially the Salinas Formation. The hydrogeological characteristics of the Salinas Formation are primarily fractured aquifers with a small contribution in its altered portion of granular material where it has considerable thickness. The Salinas Formation is widespread, supporting a relief dominated by gentle to moderately undulating and polyconvex hills, predominantly composed of schist, representing dissected areas with altitudes generally up to 500 m. It has an alteration layer of variable thickness, averaging 10 m, with a dense drainage network clearly dictated by the regional structural pattern (schistosity, fracturing, faulting), facilitating surface runoff at the expense of infiltration. When composed of quartzite, the Salinas Formation occupies higher altimetric positions, supporting plateaus and cliffs.

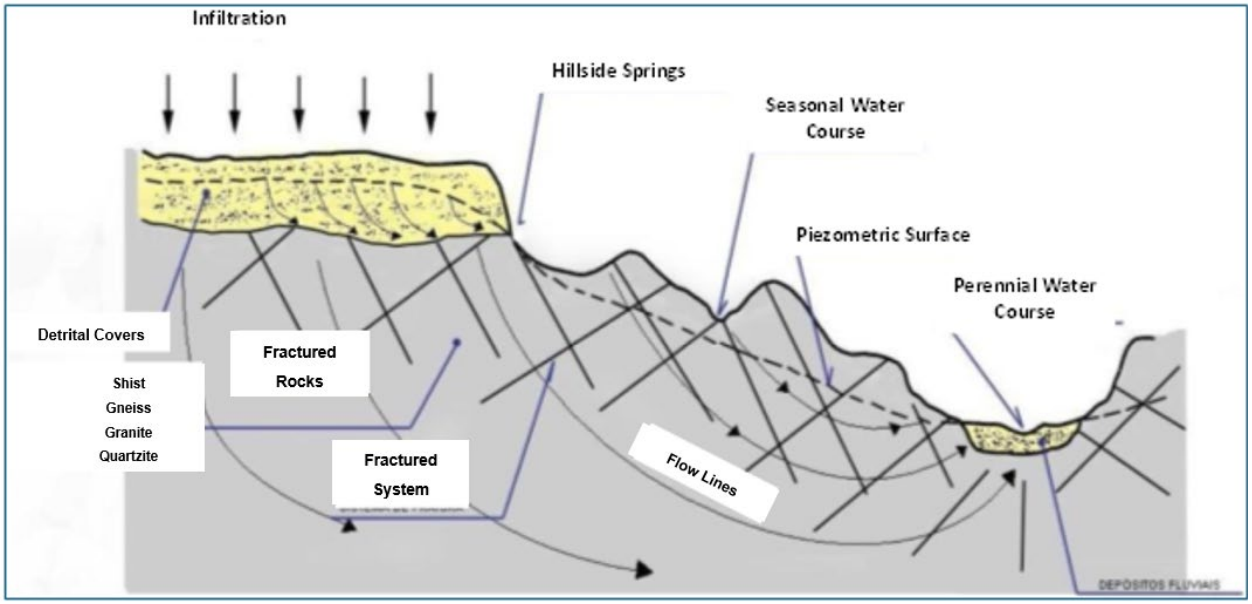
Portions of the Salinas Formation, predominantly composed of schist, have the possibility of constituting reasonably significant aquifers, by regional standards, when the following conditions coexist:

- Patterns of metamorphic–structural discontinuity
- Thick alteration levels
- Gentle relief
- Overlap with the São Domingos Formation.

Unit 4: This unit encompasses intrusive granitic rocks and is highly significant. The granitoids in the region are little altered or unaltered, not forming an expressive alteration layer (soil + weathered layer), as occurs in humid tropics where the weathering layer can reach tens of metres, giving rise to extensive aquifers. Granite terrains occupy elevated topographic portions, with morphologies resembling “sugarloafs,” cliffs, and ridges. They have drainage networks in radial and dendritic patterns, especially in larger bodies. Fractures represent the most important means by which local granitic rocks can conduct and store water.

Figure 16-46 presents a conceptual model of regional groundwater circulation. In this condition, primary permeability is very low, with fractured aquifers predominating. Recharge occurs through the fracture system, which also controls surface drainage. This structural control of drainage is less pronounced compared to areas where schist and quarzitic rocks of the Macaúbas Group and Espinhaço Supergroup occur, respectively. Discharge from these fractured aquifers occurs predominantly in valley bottoms.

Therefore, it can be said that the watercourses present in the Project area are represented by perennial drainage, where alluvial deposits or coverings prove to be very important in water supply.



Source: MDGEO (2025).

Figure 16-46: Conceptual Model of Regional Groundwater Circulation

The exception is Piauí Creek, which exhibits incipient drainage, almost dry, for at least two months of the year (September and October). The significance of these alluvial ridges on the riverbanks becomes evident during the dry period when they release water stored during the rainy season, contributing to surface flow.

Short and medium-term underground flows originate from the hydrogeological cover units and possibly from the alluvial ridges deposited by rivers. Drainage in the fractured aquifer is represented by longer-term flows that are logically dependent on the degree of rock fracturing.

16.3.7 Conceptual Hydrogeological Model

The conceptual hydrogeological model aims to define the hydrogeological units within the study area, their hydrodynamic characteristics, and groundwater circulation conditions (recharge, flow, and discharge). This model serves as the basis for the numerical model.

Based on field data collected during the spring inventory and compilation of hydrogeological data, the conceptual hydrogeological model for the MGLIT area.

An aquifer is any geological formation that allows water to circulate through pores and fractures, enabling its exploitation in economically viable quantities. Aquifers are classified by porosity (primary/granular, secondary/fissural, and karstic) and by confinement (confined, semi-confined, unconfined).

The conceptual model boundaries were defined considering the limits of local micro-watersheds that feed the Jequitinhonha River via the Piauí River, which crosses the Bandeira target. The model area extends beyond the immediate Bandeira deposit to include the drainage basins (Figure 16-47).

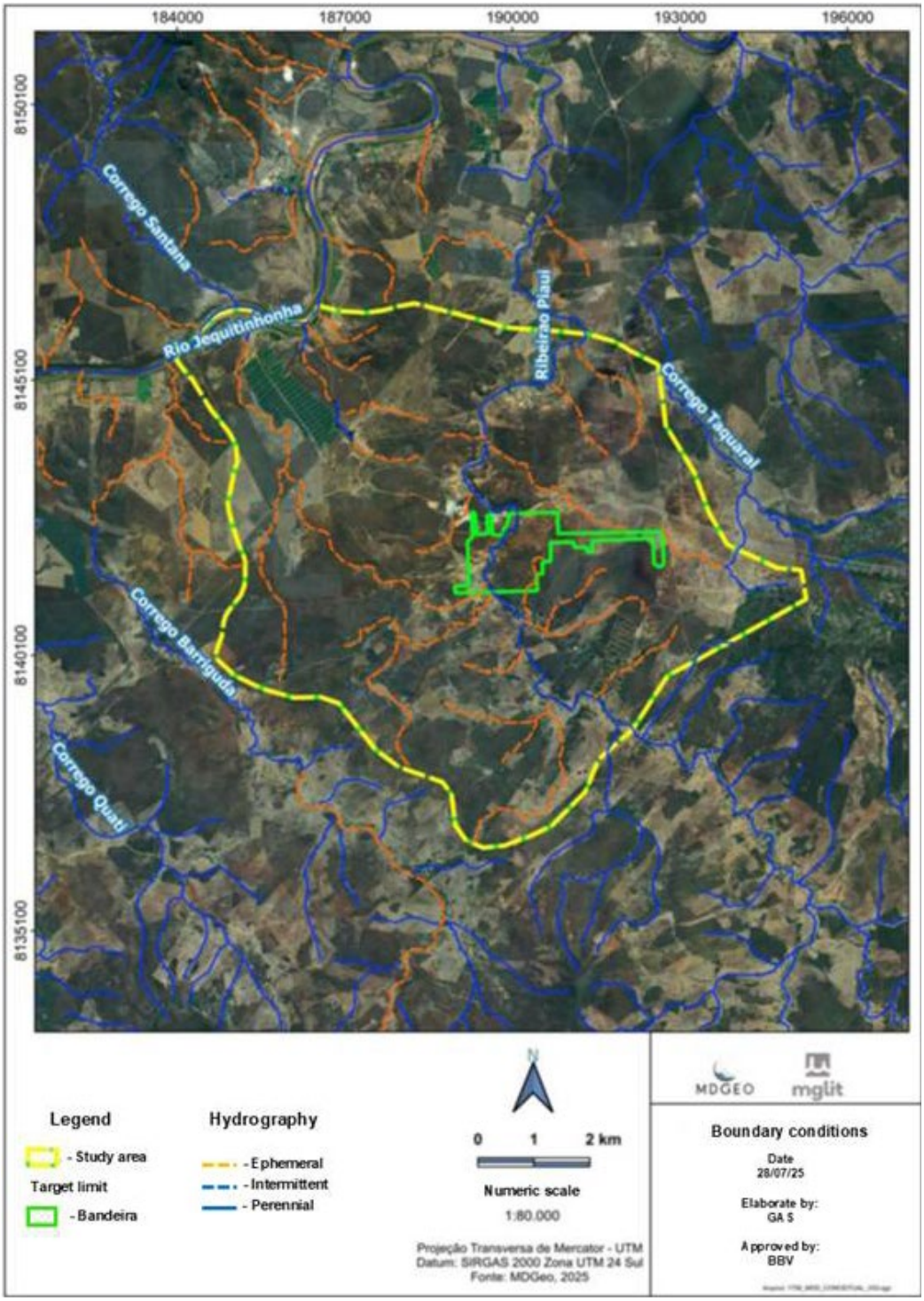
The hydrogeological behaviour is directly linked to lithological units:

- Residual soil and alluvial cover: storage and circulation through intergranular porosity, transmissivity defined from literature (10^{-8} m/s to 10^{-2} m/s depending on texture).
- Pegmatite: fissural aquifer, moderate conductivity (1.3E-6 cm/s to 3.6E-5 cm/s).
- Schist: fissural aquifer, heterogeneous, influenced by structural anisotropy (8.8E-7 cm/s to 1.3E-3 cm/s).
- Aquicludes: low-porosity units, acting as hydraulic barriers (e.g., massive rocks with low weathering).

Results from Lugeon (Packer) tests were compiled (Table 16-19). Values were grouped by lithology, showing the range of hydraulic conductivity for schist and pegmatite. For residual soil and alluvial cover, values were based on established literature.

Table 16-19: Packer Tests Results

Lithology	Hydraulic Conductivity (cm/s)	Source
Schist	8.8E-07 to 1.3E-03	Packer Test
Pegmatite	1.3E-06 to 3.6E-05	Packer Test
Residual Soil	1E-08 to 1E-05 (clayey); 1E-06 to 1E-04 (sandy)	Literature
Alluvium	1E-05 to 1E-02 (depending on grain size)	Literature

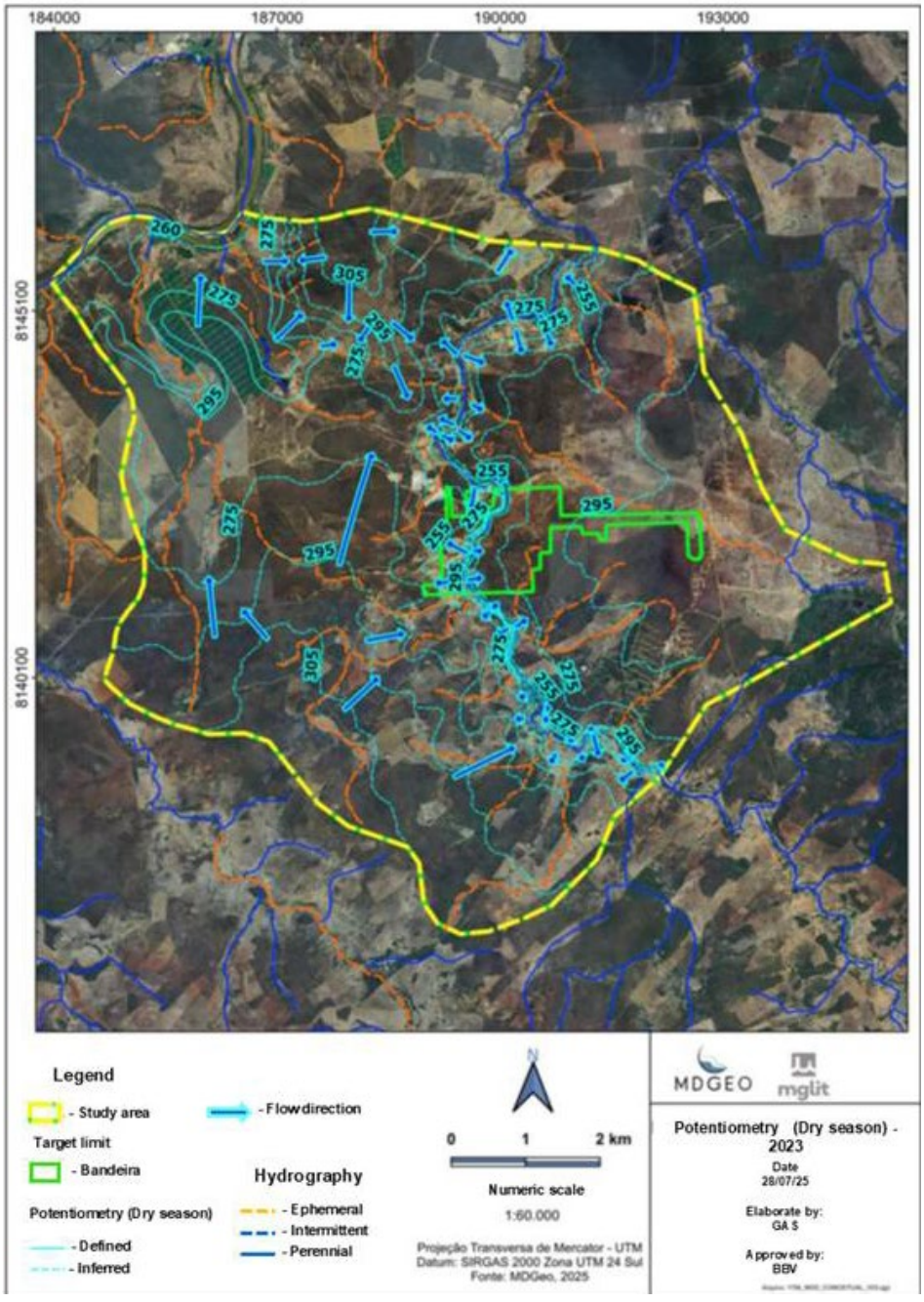


Source: MDGEO (2025).

Figure 16-47: Boundary Conditions

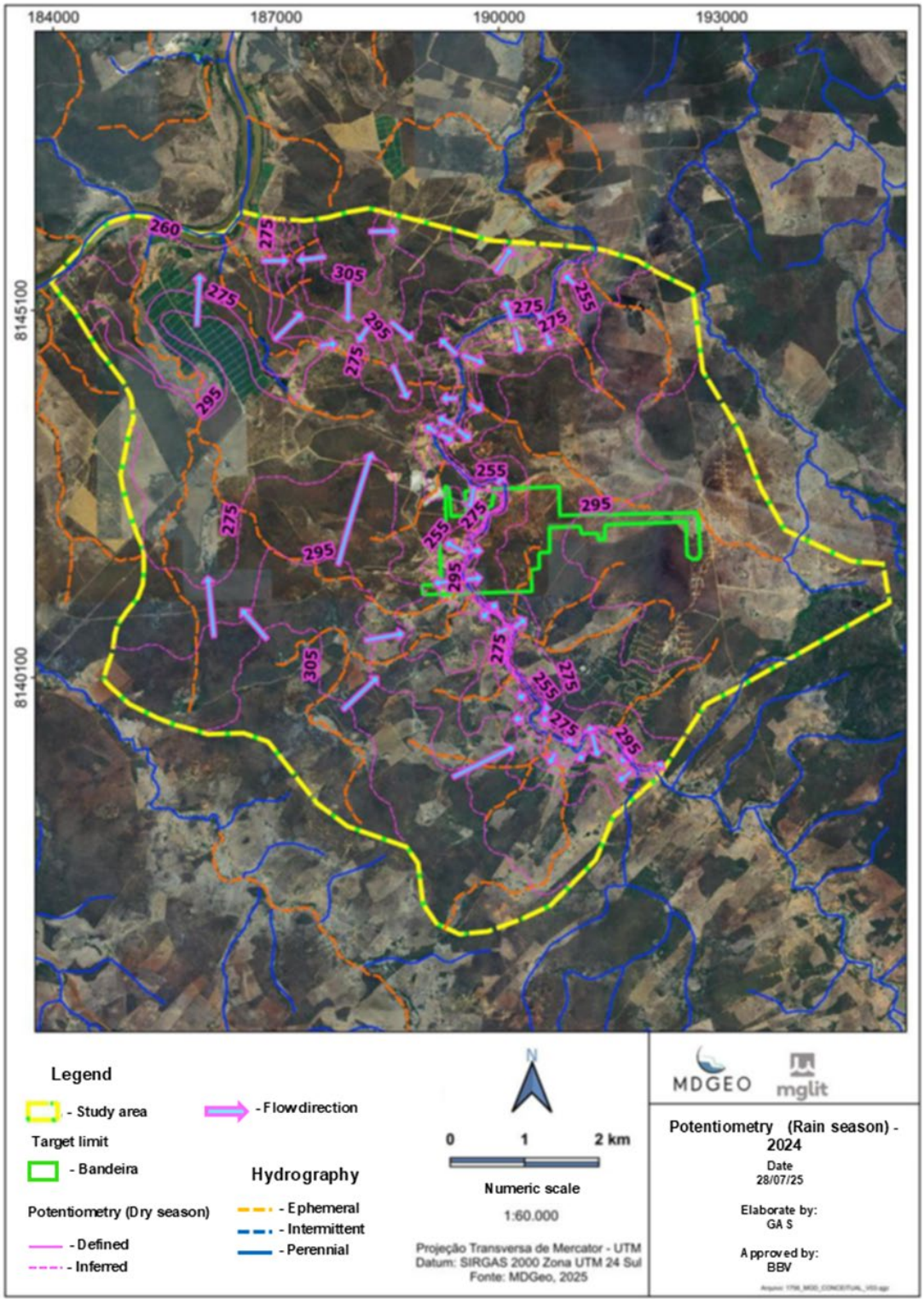
16.3.8 Conditions of Groundwater Flow

Flow conditions are represented by potentiometric maps (Figure 16-48 and Figure 16-49). In the fractured aquifer, equipotential lines are closely spaced, reflecting low transmissivity and strong dependence on structural controls. Groundwater flow direction is predominantly towards the Jequitinhonha River.



Source: MDGEO (2025)

Figure 16-48: Potentiometric Map—Dry—Conceptual Hydrogeological Model Report (July 2025)



Source: MDGEO (2025)

Figure 16-49: Potentiometric Map—Rainy Season Conceptual Hydrogeological Model Report (July 2025)

16.4 Mine Planning and Design

16.4.1 Open-Pit Mining

The open-pit mining operation will be developed as a short-term project with an expected mine life of approximately one year, serving as a strategic solution to supply ore to the processing plant during ramp-up while underground development advances toward long-term production. The operation will be fully mechanized, conducted by a contractor using a fleet of drills, loaders, bucket, and haul trucks.

The mining cycle will follow conventional open-pit methods, including drilling, blasting, loading, hauling, and dumping. Production drilling will be performed using a Sandvik DX800, ensuring proper fragmentation according to rock mass characteristics. Blasted material will be loaded by Volvo EC700 excavators (5.16 m³ bucket) and transported by Volvo FMX500 trucks (22 m³ capacity) either to the primary crusher or to nearby waste piles to minimize haul distances and optimize cycle times.

Under the mine plan that the Project's engineering team developed, the contractor will execute all operations—drilling, blasting, loading, hauling, and infrastructure maintenance. Mine infrastructure, including maintenance and fuel facilities, drainage systems, and haul roads, will support safe and efficient operations.

The process involves removing layers of overburden (waste material) to access the ore body beneath. The mine is developed in a series of benches or steps to ensure slope stability and safe working conditions. Open-pit mining allows for the efficient recovery of large volumes of ore and is often used when the mineral deposit is near the surface and spread over a wide area.

The final pit design was established using pit optimization, considering product price, operating costs, geotechnical slope parameters, and environmental constraints. The design incorporates safety berms, haul roads of sufficient width to accommodate the truck fleet, and slope angles compatible with rock-mass geomechanics (Figure 16-50).

Given the short mine life, the open-pit operation will prioritize efficiency, safety, and environmental responsibility. After ore extraction, the pit will be progressively backfilled with waste rock to support rehabilitation and reduce the environmental footprint, ensuring early revenue generation and a smooth transition to sustainable underground mining. The results are shown in Table 16-20.

Table 16-20: Open-Pit Designed Results, Including Waste and Mineral Resources

Category	Tonnage (Mt)	Grade (% Li_2O)
Proven	0.26	1.21
Probable	0.83	1.23
Proven and Probable	1.09	1.22
Waste	12.84	0.00

Note: Grade estimated before dilution.

Design Sector	Section	Geomechanical Domain	Maximum Bench Height (m)	Bench Angle (°)	Minimum Berm Width (m)	Overall Angle (°)	Pit Depth (m)
S	1	Soil	10	50	5	40	58
		RQD <50%	10	50			
		RQD>50%	15	85			
E	2	Soil	10	50	5	46	74
		RQD <50%	10	50			
		RQD>50%	15	75			
NW	3	Soil	10	50	5	40	95
		RQD <50%	10	50			
		RQD>50%	15	85			
	4	Soil	10	50		34	70
		RQD <50%	10	50			
		RQD>50%	15	85			
W	5	Soil	10	50	5	44	67
		RQD <50%	10	50			
		RQD>50%	15	85			

Figure 16-50: Geotechnical Parameters for Open Pit

Figure 16-51 and Figure 16-52 shows a plane and vertical section of the designed pit.

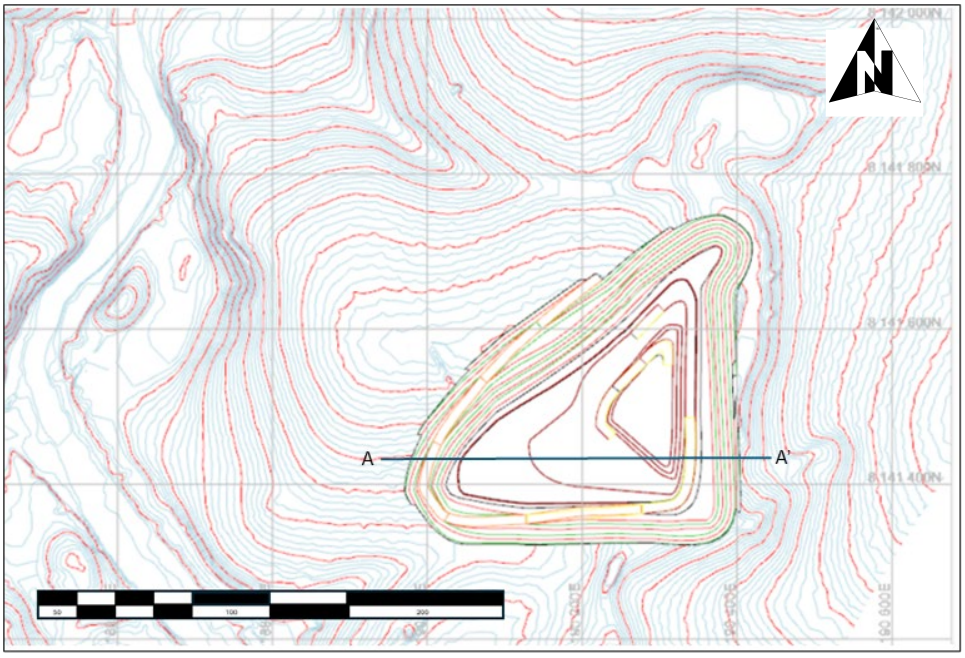


Figure 16-51: Open-Pit Layout. Section A–A' is Shown in Cross-Section in Figure 16-52

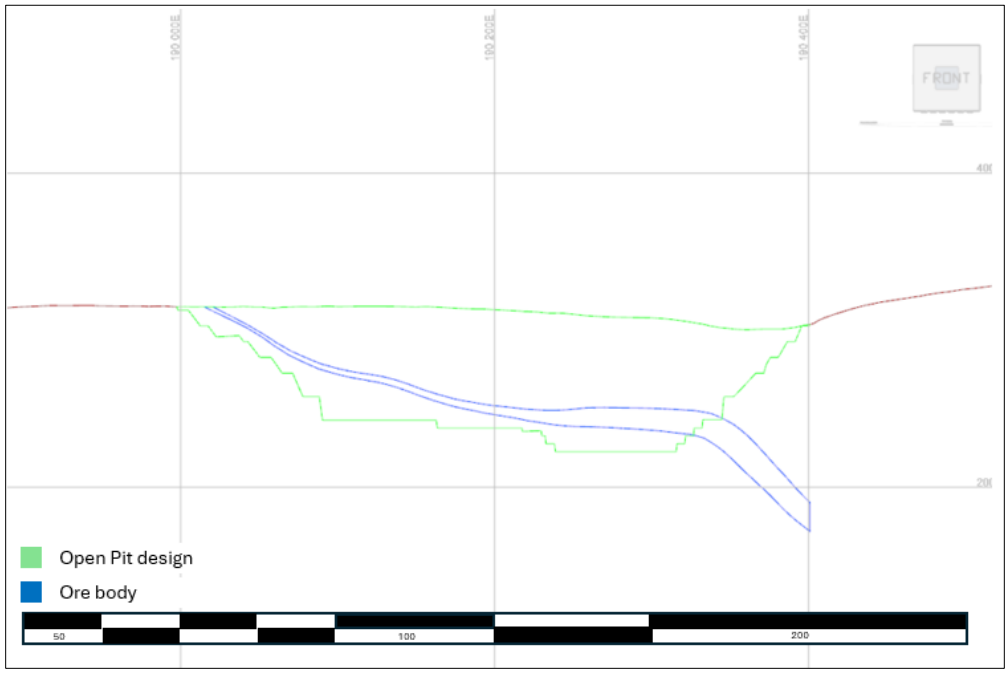


Figure 16-52: Cross-Section A-A' (See Figure 16-51), Showing the Open-Pit Layout (Green Line = Pit Outline; Blue Line = Mineralized Ore body; Brown Line =Topography)

Figure 16-53 illustrates how changes in product price and key cost components affect the variations in product price, and mine, processing plant, and total Project costs, highlighting the relative impact of each parameter on overall economic.

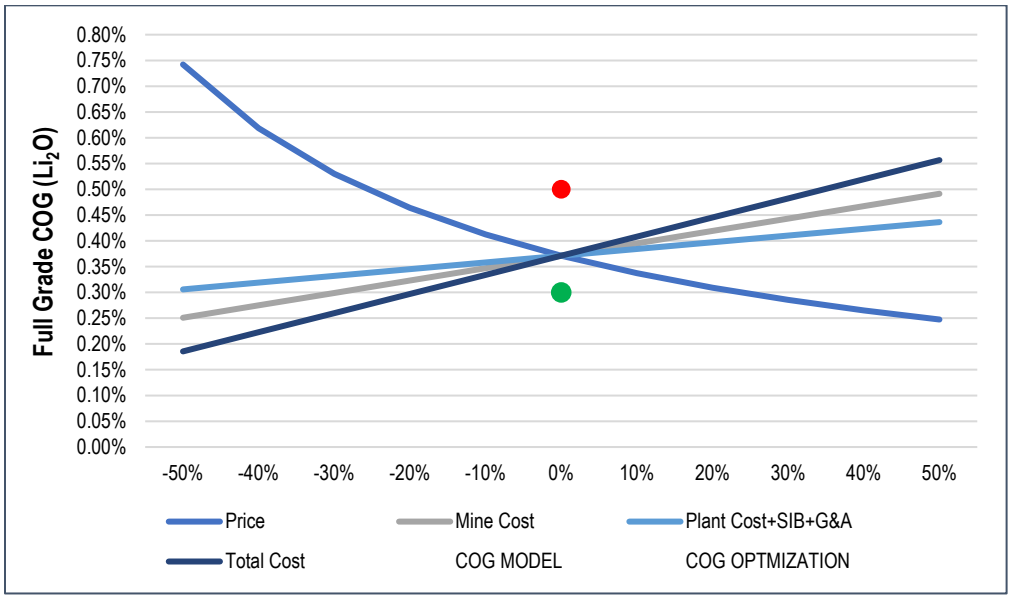


Figure 16-53: Open Pit Cut-Off Grade Sensitivity Analysis

16.4.2 Underground Mine

The underground mine project will be accessed by two ramp portals (declines) in the footwall of the ore body to expose the tunnel section. Both ramps have slopes designed to be 50°, with 10 m-high, 5 m-wide berms (catch bench) (Figure 16-54). The two portals will be constructed using the New Austrian Tunneling Method (NATM).

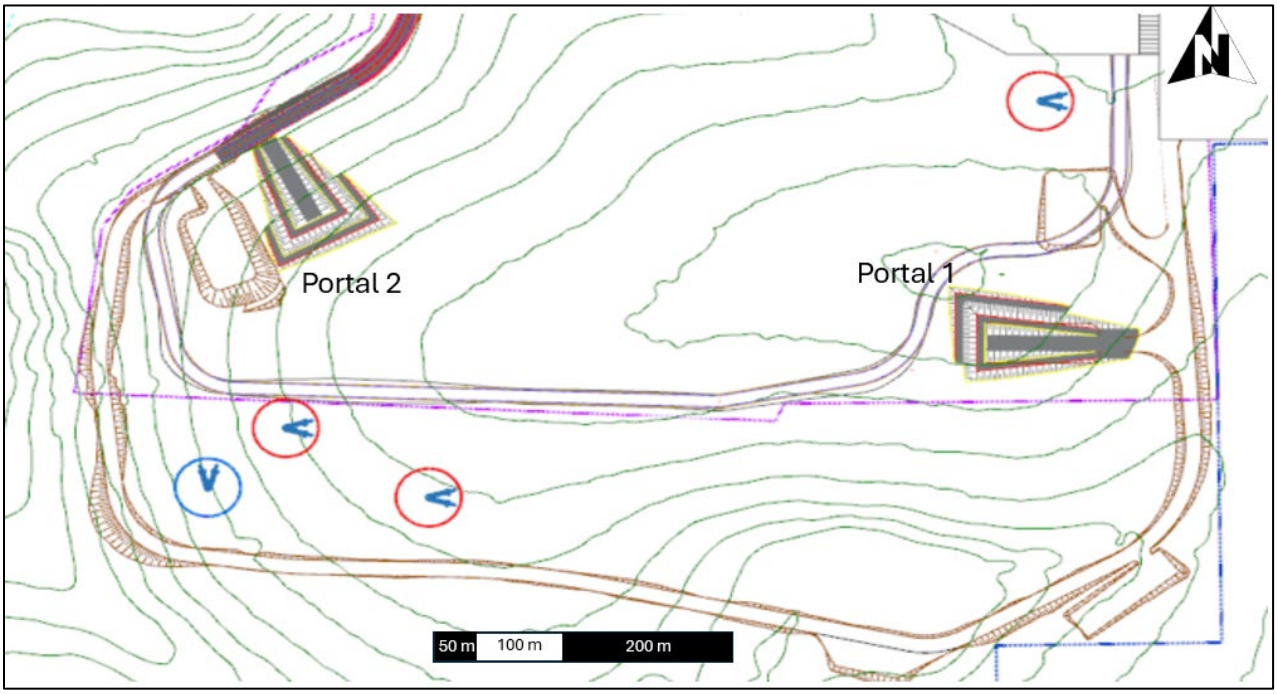


Figure 16-54: Underground Mine Portal

The portals will be reinforced with shotcrete to preserve the slopes, prevent erosion, and facilitate safe transportation of ore, waste rock, equipment, and personnel inside the mine.

The ramp will be designed in a figure eight format and will be repeated until the last panel of the mine. This configuration allows for optimized entry into all mineralized ore bodies.

The excavation profile will be arched on the roof for better stability. The gallery will be 5.5 m high by 5.3 m wide, adequate to accommodate 40-tonne-capacity trucks, ventilation, service ducts, and equipment access (Figure 16-55).

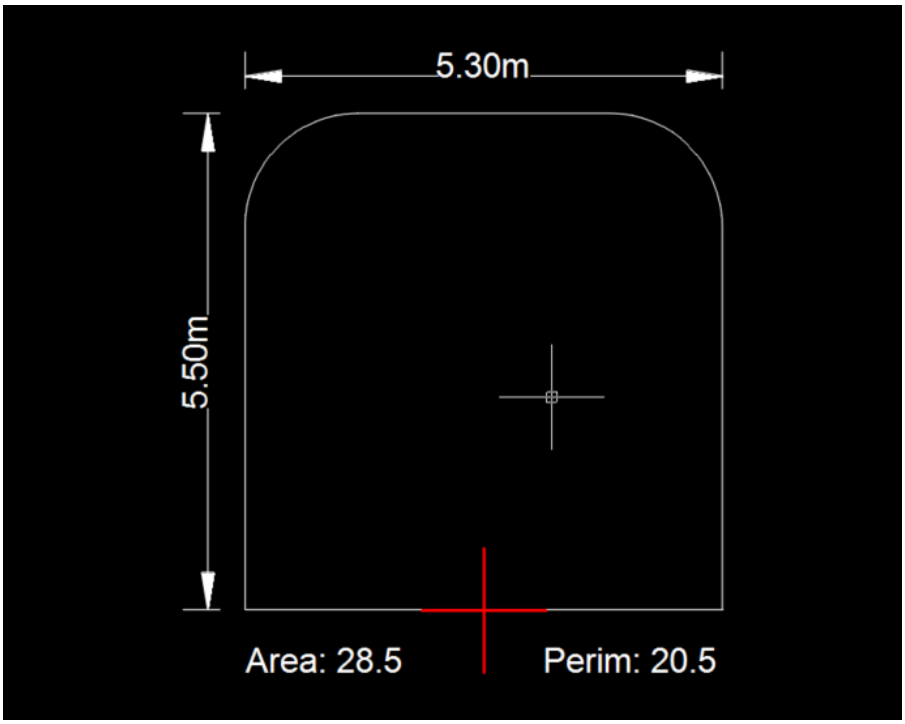


Figure 16-55: Typical Section of the Decline

The ramps, as part of the main ventilation system, serve as a source of fresh air, allowing clean air from the surface to flow through the mine and ventilate the working faces within the panels. Secondary fans are installed at the entrances of each level to collect this air and force it inside the working faces.

The ramps will be designed with a maximum inclination of 15%, with pullouts or mucking bays every 100 m to improve vehicle traffic and facilitate the drifting process.

Each level or mine panel will be accessed from the ramps developed close to the ore bodies.

At each sublevel, crosscuts will be developed to access the ore bodies, generally in transverse to the mineralized bodies, which must be at least 20 m from the ramp, respecting the pillar between the ramp and the mineralized zones.

Once the mining area is accessed, development must occur parallel to the ore body's strike. For this Project, all ore drives are planned to follow the operational design after completion of the infill-drilling model. The ore drives are intended for longhole blast drilling (ring drilling) and mineral extraction. Loading points will be opened every 100 m, measuring 16 m wide and 5 m high. The first 3 m will be post-excavated with 7 m height to allow the low-bed underground wheel loader (load-haul-dump [LHD]) to tip inside the truck. Figure 16-56 shows the positioned drives.

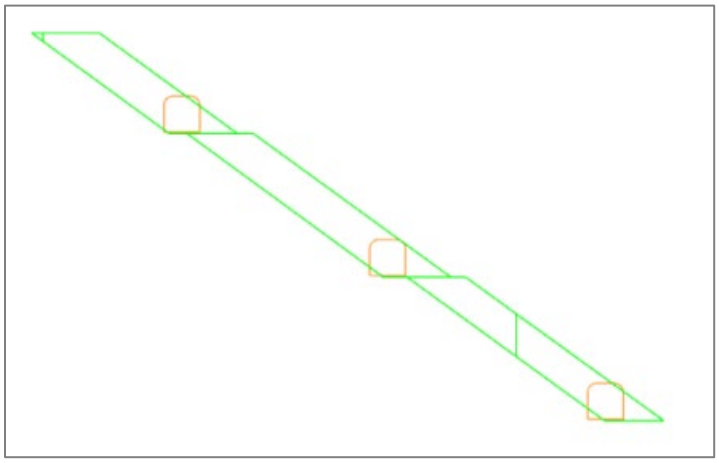


Figure 16-56: Schematic Arrangement of the Gallery Position for Top-Down Stope Mining (Drives in Brown within the Projected Stopes in Green)

In each panel, a gallery will be excavated to accommodate facilities such as the electrical substation, pumping station, water tank, bathrooms, and refuge chamber. Additionally, ventilation drives will be excavated to receive the return air, connecting the working faces to the main exhaust system. Exploration bays will also be established at each panel for grade-control drilling, commencing at the ramp. The mucking bays, which will be opened every 100 m, can later be used as sites for grade-control drilling.

Mine vertical development will incorporate a network of ventilation raises to facilitate air intake and exhaust between the surface and underground areas. The intake ventilation raises will be equipped with escape ladders. These raises will be excavated using a raiseborer. The intake risers will have diameters of 4.1 m or sections of 4.0 m x 4.0 m, while the return risers will have diameters of 4.1 m or sections of 5.0 m x 5.0 m.

16.4.3 Mine Design Parameters

Ore reserve grades are diluted along lithological boundaries and assume a selective mining operation.

For sublevel stoping, ore reserve volumes and tonnages assume 90% mine recovery and 21% dilution, since the stope stability is being reinforced by cable bolts installed in the hanging wall or in any required area.

For the ore from development works, ore reserve volumes and tonnages assume 100% mine recovery, 31% planned dilution, and 10% operational dilution.

For the open pit, ore reserve volumes and tonnages assume 100% mine recovery, and 10% operational dilution.

A technical cut-off grade of 0.5% Li_2O was applied for underground operations and 0.3% Li_2O for open-pit operations. These cut-off grades were incorporated into the block model to classify material as ore or waste.

The geotechnical parameters adopted for the mine planning design of sublevel stoping are given in Table 16-21.

Table 16-21: Sublevel Stoping Geotechnical Parameters

Parameter	Value
Crown Pillar	Variable top W3
Panel Height (m)	55
Maximum Stopes Span (m)	50
Pillar Between Main Ramp and Ore body in Footwall (m)	22
Pillar Between Main Ramp and Ore body in Hanging Wall (m)	40
Inclination of Main Ramp (%)	±15%
Minimum Radius of Curvature (m)	25
Inclination of Secondary Ramp (%)	±15%
Minimum Pillar Between Ore body and Raiseborer (Hanging Wall) (m)	10
Minimum Pillar Between Ore body and Raiseborer (Footwall) (m)	10
Minimum Inclination to Drill a Raise	45°
Sill Pillar (m)	4
Rib Pillar (m)	4
Minimum Mining Width (m)	2
Minimum Stope Inclination Angle (°)	37
Minimum Pillar Between Stopes (m)	4
Main Ramp Section (m)	5.3 x 5.5; arch 1.25
Ore Development Section (m)	5.0 x 5.0; arch 1.25
Mucking Bay Section (m)	5.0 x 5.0; arch 1.25
Drill Area Section (m)	5.0 x 5.0; arch 1.25
Cross-Cut Section (m)	5.0 x 5.0; arch 1.25
Infrastructure Section (m)	5.0 x 5.0; arch 1.25
Slot Raise (m)	4.0 x 4.0
Diameter of Raiseborer (Sublevel Stoping) (m)	4.1

The panels will be up to 55 m high, with three sublevels, the first two from the bottom measure 20 m high, and the topmost 15 m. Figure 16-57 shows a typical mine panel schematically, with a representation of the sill pillar, rib pillar, development galleries, and the mining sequence numbered 1 and 2.



Figure 16-57: Schematic Typical Panel of the Project Underground Mine (Green = Main Decline; Blue = Crosscuts; Orange = Developments; Grey = Rib and Sill Pillars; Red = Exhaust Ventilation System; Light Blue = Intake Ventilation System)

16.4.4 Stope Optimization

The stope design optimization was conducted using Datamine's mineable stope optimization (MSO) software, allowing for the creation of stopes based on pre-set dimensions and achieving cut-off values selected based on economic parameters. This software was used to determine the economic division of the mineral deposit.

The MSO algorithms consider economic parameters, geological and geotechnical factors, and operational constraints for the optimal design of stopes throughout the ore body, encompassing elevations from 260 m to −420 m. Due to the complexity of the ore bodies along the azimuth, and the number of veins present, a method of creating multiple frameworks was adopted for stope optimization. Each vein was optimized in a configuration that best respected the dip angle of the material and its irregular behaviour along the azimuth.

The stopes were optimized following operational and technical parameters, resulting in an estimated mine life of 18 years. In the sublevel stoping method, the scenarios were configured to result in solids divided into 55 m-high panels, a minimum 2 m thick, and a minimum dip of 37°. The software ensured compliance with the minimum cut-off grade, and dilution was set free to maximize mine recovery, with no dilution skin considered. During the optimization rounds, all mineral resource categories were ore, and inferred stopes was excluded later during the stope feasibility evaluation.

Table 16-22 presents the parameters used for optimization.

Table 16-22: Optimization Parameters

Item	Unit	Value
Economic Parameters		
Selling Price Spodumene Concentrate 5.2%	$/t	1,157.15
Transportation Cost (CIF China)	$/t concentrate	122.75
TFRM	R$/t concentrate	2.21
CFEM	%	0.020
Royalties	%	0.010
Appian Royalty	%	0.023
Selling Price Spodumene Concentrate 5.2%—NET	$/t	973.65
Foreign Exchange	BRL/USD	5.85
Physical Parameters		
Optimized Variable		Li_2O
Cut-Off Full Grade	%	0.50
Minimum Mining Width	m	2
Sublevel Panel Height	m	55
Sublevel Stope Height	m	(15 and 20)
Sublevel Stope Width	m	10
Sill Pillar	m	4
Dip	°	Minimum 37
Azimuth	°	By lens

Figure 16-58 shows the cut-off grade sensitivity analysis for underground mining.

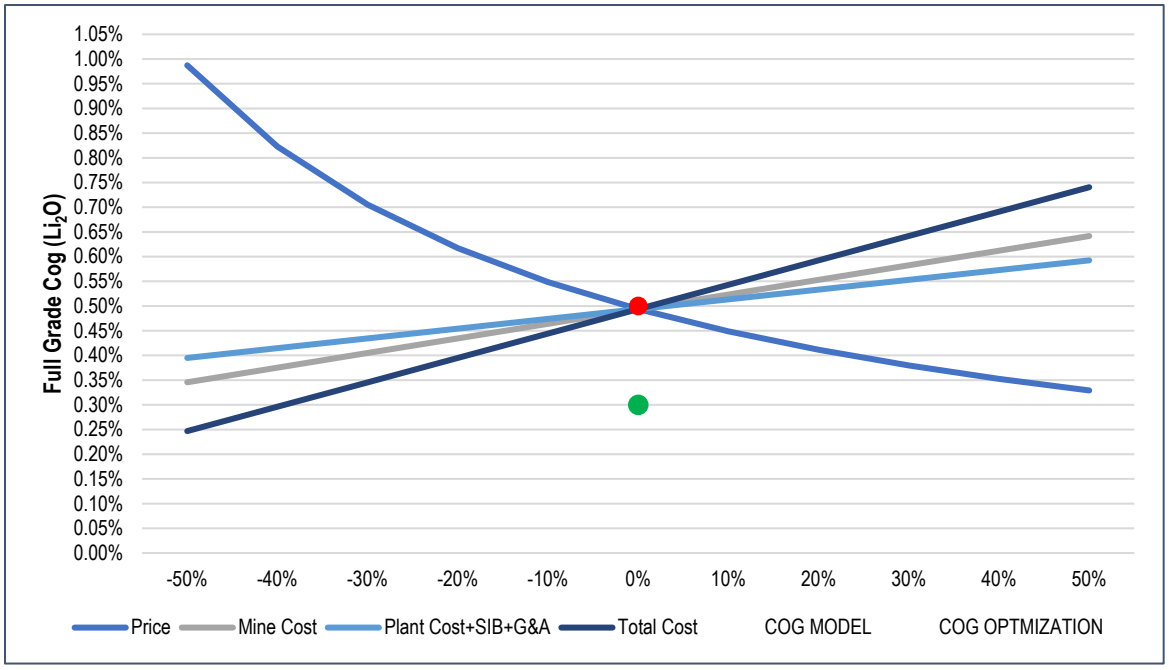


Figure 16-58: Cut-Off Grade Sensitivity Analysis for Underground Mining

The optimization results are presented in Figure 16-59.

Stope access structures were created, including crosscuts, ore drives, declines, waste connections, mucking bays, and ventilation drives. The declines are 5.30 m wide and 5.50 m high; primary and secondary development drifts are 5.0 m x 5.0 m, with an arch radius of 1.25 m. Ventilation raise diameter will be 4.1 m for the sublevel stoping mine.

Figure 16-60 shows the mine development structures and Figure 16-61 show how these structures connect with the stopes for sublevel stoping methods.

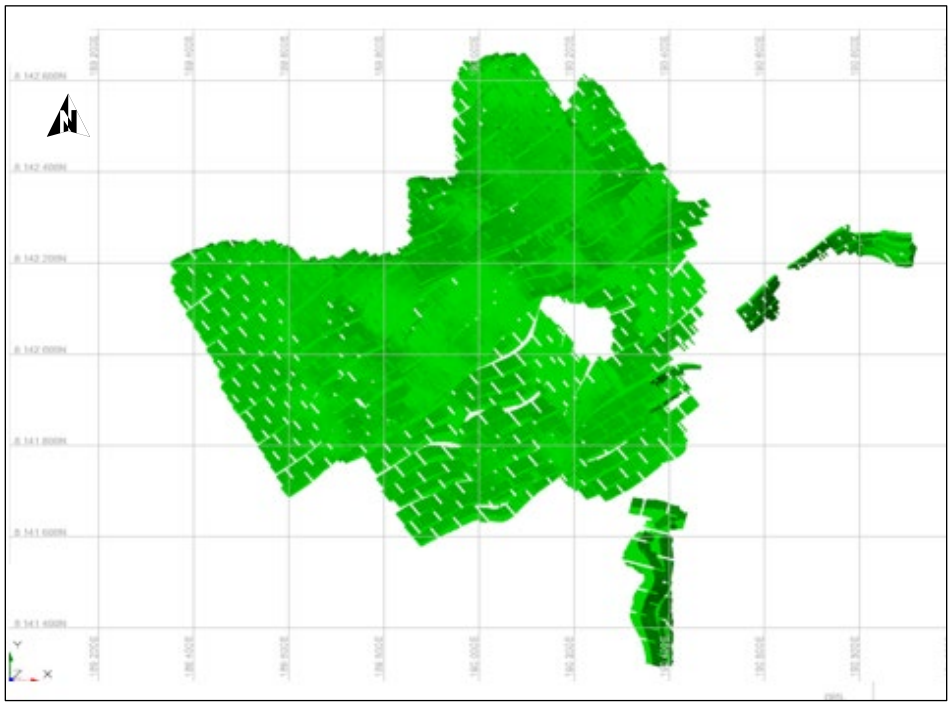


Figure 16-59: Wireframe Plan Viewer

Total mineable mass of 24.5 Mt at 1.14% Li2O for sublevel stoppage is shown in detail in Table 16-23.

Table 16-23: Underground Mineable Stopes

Mineral Resource Category	Tonnage (Mt)	Grade (% Li_2O)
Measured	2.59	1.16
Indicated	21.91	1.14
Total	24.50	1.14

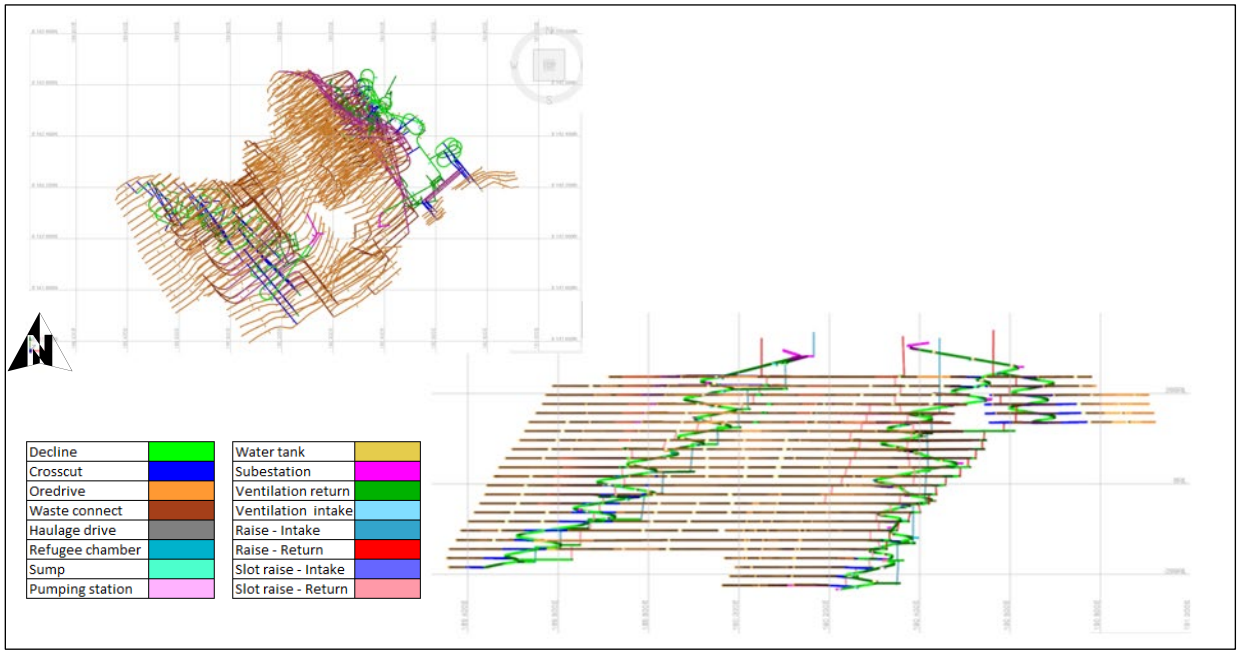


Figure 16-60: Left, Plan View of Mine Development; Right, Cross-Section of Mine Development

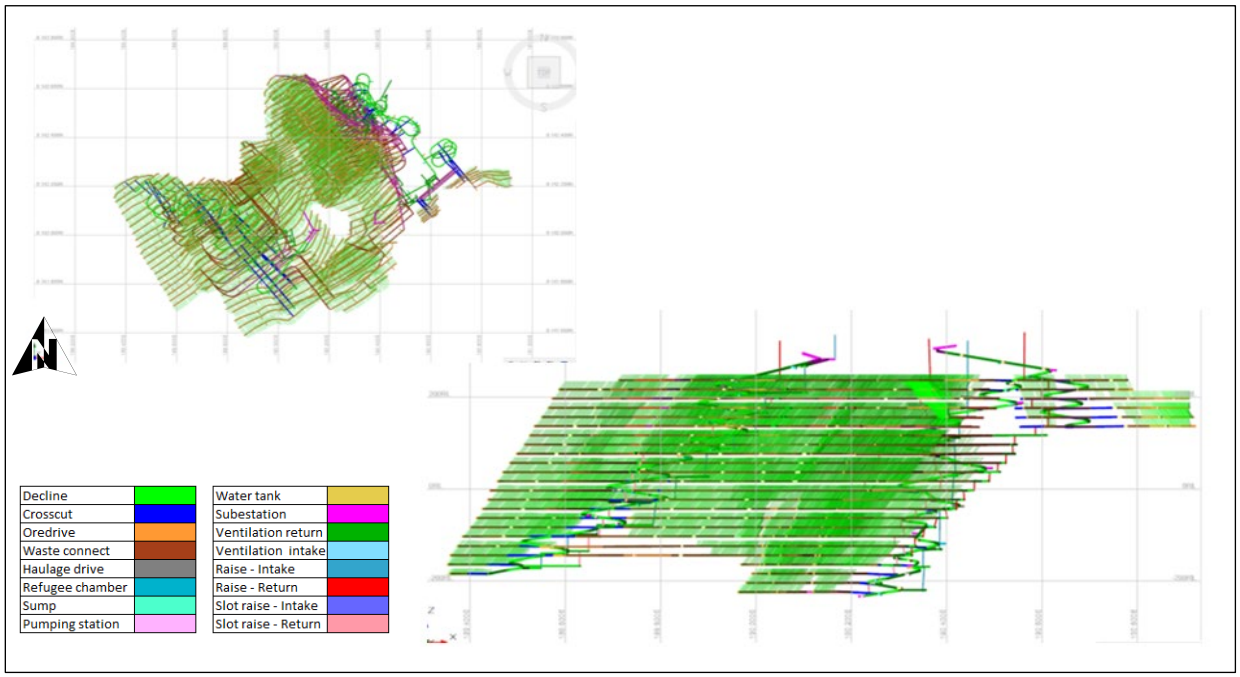


Figure 16-61: Left, Plan View of Mine Development and Sublevel Stopes; Right, Cross-Section of Mine Development and Sublevel Stopes

To calculate the reserves, a new resource category called “RESCAT” was established, based on the largest amount of metal within a resource category inside the mine solids (stopes). This was necessary to exclude all Inferred Mineral Resource stopes from the calculations. Additionally, all Inferred material

present in the Mineral Reserve stopes was considered to be waste, and treated as dilution material. Results are in Table 16-24.

Table 16-24: Underground Stope Optimization Results

Category	Resource (Mt)	Grade (% Li_2O)
Proven	2.29	1.12
Probable	19.80	1.09
Total	22.09	1.10

The ore will be transported directly to the crusher yard, ensuring a steady feed to the processing plant. Waste material will be hauled to designated waste piles.

After all development was designed, a stope feasibility analysis was conducted, including all main mine costs such as stoping, mineral process, development, raises, and G&A. Additionally, CFEM, TRFM, and royalties were subtracted from the long-term lithium price used in this evaluation. Table 16-25 presents the first-pass parameters used in the mine economic evaluation.

Table 16-25: First-Pass Parameters in the Stope Optimization

	Unit	Total
Net Concentrate Selling Price 5.2% Li_2O	$/t	1,157.15
Process Cost	$/t	13.52
G&A	$/t	2.65
Mine Cost—Sublevel	$/t	23.5
Development Cost	$/m	2,352.70
Raiseborer Cost	$/m	6,130.80
Metallurgical Recovery	%	65.30
Concentrate Grade	Li_2O %	5.20

An average ROM metallurgical recovery of 65.3% and the mining dilution were already included. The dilution varies from stope to stope, with an average value of 21%. As a result, the ore reserves are, from underground, 22.09 Mt at 1.10% Li_2O; from open pit, 1.09 Mt at 1.12%Li_2O, dilution average 10%; for a total of 23.3 Mt at 1.10% Li_2O.

After additional tests have been completed, a revised average metallurgical recovery of 65.3% was assumed to produce the 5.2% Li_2O concentrate, Table 16-26 summarizes the Project production profile with the new changes.

Table 16-26: Total Production Profile

	Unit	Total
Total Project Life (LOM)	a	18.5
Total LOM Production (Ore Mined)	Mt	23.2
Nominal Plant Capacity	Mt/a	1.5
Average Plant Throughput	Mt/a	1.3
ROM Li_2O Grade (Diluted)	%	1.1
ROM Underground Mine Dilution	%	21
Average Waste Generation	kt/a	308.4
Spodumene Concentrate Annual Production @ 5.2% Li_2O	kt/a	177
Spodumene Concentrate 5.2% Li_2O Metallurgical Recovery	%	65.3
Spodumene Concentrate 5.2% Li_2O Mass Recovery	%	13.8

16.4.5 Mining Development

Two main declines were developed for the underground mine. The east decline starts at Elevation 310 and ends at Elevation −218. The west decline begins at Elevation 293 and ends at Elevation −217. Both have a 15% gradient, a minimum radius of 25 m, and footwall access. Safety measures include minimum 20 m pillars between the stopes on mineralized walls and 4 m pillars between galleries.

Sumps developed in crosscuts are 12 m long, with the first 3 m having 0% gradient, and the remaining 9 m having a −15% gradient. Sumps developed in the declines have the first 3 m with 0% gradient, and the next 12 m with −15% gradient. Sumps are created every 360 m of decline development.

The extraction configuration was designed for top-down, sublevel stoping. Each level includes three sublevels, with accesses excavated at the lower level of the stopes. This setup allows drilling of upward holes from the lower sublevel to the upper level, enabling the extraction of the entire 55 m panel.

All crosscuts are at least 20 m long, starting from the decline, with a gradient of approximately 1%, which helps prevent water accumulation and provides connection between the declines and the ore drives. The ore drives are developed from the crosscuts along the stopes.

Connections between ore bodies, known as waste connections, were designed in sublevels where multiple stopes occur in different veins, allowing simultaneous stoping in multiple areas. The ore drives include 15 m mucking bays positioned every 100 m to meet equipment maneuvering requirements.

Ventilation raises extend from the surface level down to the lowest elevation of the declines. They are connected to the mine through ventilation galleries, with the same development configuration as the crosscuts and ore drives and subsequently connecting to the ventilation raises.

These raises have a minimum incline of 45%, with both intake and return air shafts measuring 4.1 m and 3.6 m in diameter. They are separated from nearby excavations by a minimum 7 m pillar. The raises from the surface will be excavated using a raiseboring machine. From within the mine, vertical developments will be drilled using fandrill equipment. The blast firing design will be similar to that of a slot raise, and the resulting excavations—known as slot raises—will have a square cross-section

measuring approximately 4 m. Regarding development, the advancement for each structure is shown in Table 16-27.

The development cycle begins with front drilling. At the end of the shift, the blasting team charges the face. After the explosive gases have dissipated, the LHD loads the broken material into haulage trucks, which transport it to its destination. Depending on the material, the trucks either discharge directly into the crusher, the crusher yard if it is ore, or into a void stope or waste pile if it is waste. Once all material from the face has been mucked out, the scaler removes any loose rock, the rock bolter installs the required roof supports, and a small backhoe cleans up the material generated during scaling. After these activities, production drilling for the next mining cycle can begin. To achieve the required development rates, several faces are operated simultaneously.

Table 16-27: Length of Underground Development Structures (m/a)

	Year−2	Year −1	Year 1	Year 2	Year 3	Year 4	Year 5	Year 6	Year 7	Year 8	Year 9	Year 10	Year 11	Year 12	Year 13	Year 14	Year 15	Year 16	Year 17	Year 18
Develop Primary (m)	194	2,547	2,331	2,139	2,269	2,305	1,662	1,271	1,326	871	1,103	1,085	980	1,064	1,138	860	1,101	855	648	0
Develop Secondary (m)	0	2,788	8,186	8,909	8,200	7,542	7,267	7,538	7,482	7,605	7,467	6,488	6,191	4,940	4,632	3,466	2,641	2,672	1,796	155
Develop Lat Total (m)	194	5,335	10,517	11,048	10,469	9,847	8,929	8,809	8,808	8,476	8,570	7,573	7,171	6,004	5,770	4,326	3,742	3,527	2,444	155
Develop Decline (m)	194	1,618	678	767	705	728	396	377	371	90	312	390	238	317	197	198	311	250	272	0
Develop Xcut (m)	0	477	644	727	756	964	490	399	281	293	442	334	507	266	421	275	282	300	201	0
Develop Mckbay(m)	0	334	595	734	685	588	660	575	714	631	620	530	456	449	315	261	285	230	120	15
Develop Ore Drive (m)	0	899	5,009	6,099	5,139	4,619	4,734	4,575	4,910	4,530	5,012	3,916	4,182	2,802	3,452	2,635	1,817	1,678	804	140
Develop Waste Con (m)	0	390	1,476	1,143	1,464	923	1,094	1,265	1,248	1,246	1,132	948	755	871	592	152	199	330	342	0
Develop Vent Drive (m)	0	452	1,009	645	808	613	776	495	674	488	349	361	235	481	520	387	508	305	175	0
Develop Pump (m)	0	30	0	15	35	0	15	15	15	0	15	0	15	15	0	0	0	15	15	0
Develop Sump	0	135	45	0	30	65	15	30	15	15	30	15	15	15	0	15	15	0	30	0
Develop Toilet	0	75	0	15	45	0	15	15	0	0	30	0	0	0	15	0	0	0	15	0
Develop Refuge Chamber	0	45	0	30	0	0	15	0	15	0	0	0	15	0	15	0	0	0	15	0
Develop Subset	0	60	0	15	10	15	15	0	15	15	0	15	0	15	0	0	15	0	15	0
Develop Haulage Drift (m)	0	820	1,061	858	792	1,332	704	1,063	550	1,168	628	1,064	753	773	243	403	310	419	440	0
Develop Vertical	0	218	652	636	598	342	474	246	481	322	280	347	342	273	224	172	354	222	186	0
Develop Raise (m)	0	0	61	119	63	81	120	104	76	161	140	125	97	79	60	44	39	42	41	0
Develop Raise 3.1 (m)	0	109	265	199	226	80	117	19	164	0	0	49	74	58	42	42	128	69	52	0
Develop Raise (m)	0	109	326	318	309	181	237	123	241	161	140	173	171	136	122	86	187	111	93	0

16.4.6 Stoping Activities

For the sublevel operation, the cycle time starts after completing the ore drive development with the roof support reinforcement. Cable bolts (steel strand wires grouted into boreholes) ranging from 6 m to 18 m long will be installed in the hanging wall to control dilution, and to protect the stoping brow area.

Then, the fandrill begins drilling the blast rings upward according to the blast plan. To open the slot free-face, the fandrill follows the firing design plan, typically drilling 10 blast holes and 6 void holes of 6½ inches in diameter for each slot position. Once the drilling activities are completed and the stope area has been scaled, the blast crew charges the free-face rings and performs the blast.

As the free face develops, production ring blasting commences with a limited number of rings. Progressive blasting enlarges the void space, permitting larger blast rounds and the simultaneous firing of additional rings.

Between blasts, the LHD loads the fragmented ore, usually stockpiling it at the loading point to optimize the loading cycle, while mine trucks haul the ore to surface. These activities of ring blasting, loading, and hauling continue until the stope is completely depleted. After that, the void space will be filled with rock fill.

16.4.7 Mining Schedule

Mining scheduling was performed using Mine EPS (Version 3.1.144). The software was set up to respect the mine direction and restrictions to deliver a long-term mine plan that offers good predictability. Sublevel mining activities occur in retreat at the end of each level's ore drive-development. Targets are set for decline development, lateral gallery development, and mass movement.

Total monthly targets are defined for both decline developments, ranging from 50 m per month for the first three months, increasing at a varied rhythm from 90 m to 160 m per month. By the start of Year −1, the decline development drops to an average of 80 m per month per decline, and in Year 1 it decreases to 70 m per month until the end of mine life.

The Project mining schedule aims to achieve an average processing plant feed of 1.3 Mt of ROM. The parameters used in the EPS software can be seen in Table 16-28.

Table 16-34 and Figure 16-62 to Figure 16-66 present the mining scheduling results.

Table 16-28: Mine Scheduling—Development Rates

Location	Unit	Scheduled
Ramp (First Access)	m/month	80
Ramp (W6-W3)	m/month	40
Ramp (W2-W1)—1°Year (Multi-Blast)	m/month	80
Ramp (W2-W1)	m/month	65
Ore drive	m/month	50
Production Drive	m/month	40
Cross Cut	m/month	40
Raise	m/month	50

To determine the number of active stopes required to achieve the planned mine production capacity, a simulation was performed assuming an available ore mass of 30,000 tonnes extracted from a single stope. In this case, the term stope refers to an ore block with a strike length of 50 m developed within one sublevel (between two rib pillars), where all stoping cycle activities must be completed before ore cleaning can begin.

Based on the total ore mass, the required development lengths were calculated for the derived activities, which include cable bolting, ring drilling, and slot drilling. Once these quantities were defined, the duration of each activity was estimated using the operational rates, including loading and hauling times. The total estimated time to complete the extraction of this stope was 88 days.

With these data, it was possible to calculate the average daily production rate for a single stope, which is 341 t/d. According to the mine plan for the steady-state production years—targeting 1.3 Mt/a of ROM ore—the stopes are expected to contribute an annual average of 1.075 Mt. This means that 2,945 t/d must be extracted from the stopes.

Based on these figures, it can be concluded that at least nine stopes must be active simultaneously at different stages of the mining cycle, with five of them in the loading and hauling phase, to meet the mine production plan proposed by MGLIT.

The stoping cycle simulation was conducted considering the main activities of the mining cycle, which were represented in the EPS software as derived activities. This means that all the time required for the tasks preceding the load and haul operations is included in the total stope duration time. The specific values MGLIT assumed are presented in Table 16-29 to Table 16-33.

Table 16-29: Stoping Activities Specific Values Based on Tonnes per Day

Derived Activity	Unit	Value
Support Drilling—Fandrill	ROM t/m	6.26
Production Drilling—Fandrill (SLOT)	ROM t/m	581
Production Drilling—Fandrill (RINGS)	ROM t/m	5.7

Table 16-30: Quantities Required for Derived Activities in Drilled Metres

Derived Activity	Unit	Value
Cable Bolting	m	4,796
Slot Drilling	m	52
Ring Drilling	m	5,263

Table 16-31: Daily Production Rates

Derived Activity	Unit	Value
Production Drilling—Fandrill	m/d	255
Production Drilling—Fandrill (SLOT)	m/d	15
Support Drilling—Cable Bolter	m/d	250
Load and Hauling	ROM t/d	700

Table 16-32: Time Duration of Each Activity

Derived Activity	Unit	Value
Ring Drilling	d	21
Slot Drilling	d	4
Cable Bolting	d	20
Load and Hauling	d	43
Total Time	d	88

Table 16-33: Stope Requirement

Item	Unit	Value
Daily Requirement—ROM	t/d	2945
Stope Average Rate—ROM	t/d	341
Total Stopes in Activity		9
Stopes in Load and Haul Activity		5

Note: Ore sourced from development works in addition to this table.

Table 16-34: Mine Scheduling—Production Plan

	Year −2	Year −1	Year 1	Year 2	Year 3	Year 4	Year 5	Year 6	Year 7	Year 8	Year 9	Year 10	Year 11	Year 12	Year 13	Year 14	Year 15	Year 16	Year 17	Year 18
Production																				
Feed Mass (t)	0	610,520	1,224,167	1,300,000	1,300,000	1,300,000	1,300,000	1,300,000	1,300,000	1,300,000	1,300,000	1,300,000	1,300,000	1,300,000	1,300,000	1,300,000	1,300,000	1,300,000	1,171,889	700,741
Li_2O (%)	0	1.12	1.02	0.96	0.99	1.08	1.09	1.05	1.10	1.09	1.08	1.13	1.10	1.13	1.16	1.19	1.19	1.19	1.07	1.10
Metallurgical Recovery 5.2 (%)	0	0.65	0.65	0.65	0.65	0.65	0.65	0.65	0.65	0.65	0.65	0.65	0.65	0.65	0.65	0.65	0.65	0.65	0.65	0.65
Mass Recovery 5.2 (%)	0	0.14	0.13	0.12	0.12	0.14	0.14	0.13	0.14	0.14	0.14	0.14	0.14	0.14	0.15	0.15	0.15	0.15	0.13	0.14
Total Concentrate Mass 5.2% (t)	0	86,174	156,040	156,484	162,059	177,076	178,194	172,045	180,074	178,582	176,814	183,914	178,851	184,191	189,525	194,438	194,030	194,360	158,011	96,666
Fines (−0.6 mm) (t)	0	129,736	260,135	276,250	276,250	276,250	276,250	276,250	276,250	276,250	276,250	276,250	276,250	276,250	276,250	276,250	276,250	276,250	249,027	148,907
Rich DMS Tailings	0	97,866	196,234	208,390	208,390	208,390	208,390	208,390	208,390	208,390	208,390	208,390	208,390	208,390	208,390	208,390	208,390	208,390	187,854	112,329
Tailings Mass (t)	0	296,744	611,757	658,876	653,301	638,284	637,166	643,315	635,286	636,778	638,546	631,446	636,509	631,169	625,835	620,922	621,330	621,000	576,998	342,839
Stockpile Balance																				
Stockpile Mass (t) Period Start	0	0	203,625	39,167	53,332	30,916	27,212	26,947	48,357	73,758	99,489	103,918	106,744	120,610	123,970	142,920	133,753	122,372	122,483	0
Stockpile Grade (%) Period Start	0	0.00	1.12	1.02	0.96	0.99	1.14	1.14	1.10	1.10	1.10	1.10	1.10	1.10	1.10	1.11	1.20	1.20	1.20	0.00
Stockpile Mass (t) In	0	814,145	1,059,709	1,314,165	1,277,584	1,296,296	1,299,735	1,321,410	1,325,401	1,325,731	1,304,429	1,302,826	1,313,866	1,303,360	1,318,950	1,290,833	1,288,619	1,300,111	1,049,406	700,741
Stockpile Grade (%) In	0	1.12	0.99	0.96	0.99	1.09	1.09	1.05	1.10	1.09	1.08	1.13	1.10	1.13	1.16	1.20	1.19	1.19	1.06	1.10
Stockpile Mass (t) Out	0	610,520	1,224,167	1,300,000	1,300,000	1,300,000	1,300,000	1,300,000	1,300,000	1,300,000	1,300,000	1,300,000	1,300,000	1,300,000	1,300,000	1,300,000	1,300,000	1,300,000	1,171,889	700,741
Stockpile Grade (%) Out	0	1.12	1.02	0.96	0.99	1.08	1.09	1.05	1.10	1.09	1.08	1.13	1.10	1.13	1.16	1.19	1.19	1.19	1.07	1.10
Stockpile Mass (t) Closure	0	203,625	39,167	53,332	30,916	27,212	26,947	48,357	73,758	99,489	103,918	106,744	120,610	123,970	142,920	133,753	122,372	122,483	0	0
Stockpile Grade (%) Closure	0	1.12	1.02	0.96	0.99	1.14	1.14	1.10	1.10	1.10	1.10	1.10	1.10	1.10	1.11	1.20	1.20	1.20	0.00	0.00
Detailed Production																				
Total ROM Mass (t)	0	814,145	1,059,709	1,314,165	1,277,584	1,296,296	1,299,735	1,321,410	1,325,401	1,325,731	1,304,429	1,302,826	1,313,866	1,303,360	1,318,950	1,290,833	1,288,619	1,300,111	1,049,406	700,741
Total Li_2O (%) ROM	0	1.12	0.99	0.96	0.99	1.09	1.09	1.05	1.10	1.09	1.08	1.13	1.10	1.13	1.16	1.20	1.19	1.19	1.06	1.10
Open-Pit Mass (t)	0	794,687	304,221	0	0	0	0	0	0	0	0	0	0	0	0	0	0	0	0	0
Li_2O Open-Pit (%)	0	1.12	1.11	0,00	0,00	0,00	0,00	0,00	0,00	0,00	0,00	0,00	0,00	0,00	0,00	0,00	0,00	0,00	0,00	0,00
ROM Mass Sublevel (t)	0	512	503,585	1,059,101	1,031,668	1,036,874	1,006,791	1,055,037	1,023,501	1,034,819	985,263	1,045,703	1,042,949	1,114,610	1,090,511	1,156,075	1,218,347	1,221,167	1,002,287	673,425
Li_2O Sublevel (%)	0	0.78	1.02	0.98	1.03	1.13	1.13	1.07	1.16	1.14	1.11	1.17	1.11	1.15	1.18	1.22	1.20	1.21	1.06	1.10
ROM Mass Develop (t)	0	18,946	251,903	255,064	245,916	259,422	292,944	266,373	301,900	290,912	319,166	257,123	270,917	188,750	228,439	134,758	70,272	78,944	47,119	27,316
Li_2O Develop (%)	0	0.84	0.86	0.85	0.86	0.92	0.96	0.99	0.91	0.93	1.00	0.95	1.04	1.00	1.07	1.04	0.99	0.89	1.06	0.99
Dev Primary (m)	194	2,547	2,331	2,139	2,269	2,305	1,662	1,271	1,326	871	1,103	1,085	980	1,064	1,138	860	1,101	855	648	0
Dev Secondary (m)	***0***	***2,788***	***8,186***	***8,909***	***8,200***	***7,542***	***7,267***	***7,538***	***7,482***	***7,605***	***7,467***	***6,488***	***6,191***	***4,940***	***4,632***	***3,466***	***2,641***	***2,672***	***1,796***	***155***
Develop Lateral Total (m)	194	5,335	10,517	11,048	10,469	9,847	8,929	8,809	8,808	8,476	8,570	7,573	7,171	6,004	5,770	4,326	3,742	3,527	2,444	155
Develop Decline (m)	194	1,618	678	767	705	728	396	377	371	90	312	390	238	317	197	198	311	250	272	0
Develop Crosscut (m)	***0***	***477***	***644***	***727***	***756***	***964***	***490***	***399***	***281***	***293***	***442***	***334***	***507***	***266***	***421***	***275***	***282***	***300***	***201***	***0***
Develop Muckbay (m)	0	334	595	734	685	588	660	575	714	631	620	530	456	449	315	261	285	230	120	15
Develop Ore Drive (m)	0	899	5,009	6,099	5,139	4,619	4,734	4,575	4,910	4,530	5,012	3,916	4,182	2,802	3,452	2,635	1,817	1,678	804	140
Develop Waste Connection (m)	0	390	1,476	1,143	1,464	923	1,094	1,265	1,248	1,246	1,132	948	755	871	592	152	199	330	342	0
Develop Vent Drive (m)	0	452	1,009	645	808	613	776	495	674	488	349	361	235	481	520	387	508	305	175	0
Develop Pump (m)	0	30	0	15	35	0	15	15	15	0	15	0	15	15	0	0	0	15	15	0
Develop Sump	0	135	45	0	30	65	15	30	15	15	30	15	15	15	0	15	15	0	30	0
Develop Toilet	0	75	0	15	45	0	15	15	0	0	30	0	0	0	15	0	0	0	15	0
Develop Refuge chamber	0	45	0	30	0	0	15	0	15	0	0	0	15	0	15	0	0	0	15	0

	Year −2	Year −1	Year 1	Year 2	Year 3	Year 4	Year 5	Year 6	Year 7	Year 8	Year 9	Year 10	Year 11	Year 12	Year 13	Year 14	Year 15	Year 16	Year 17	Year 18
Develop Substation	0	60	0	15	10	15	15	0	15	15	0	15	0	15	0	0	15	0	15	0
Dev Haulage Drift (m)	0	820	1,061	858	792	1,332	704	1,063	550	1,168	628	1,064	753	773	243	403	310	419	440	0
Dev Vertical	0	218	652	636	598	342	474	246	481	322	280	347	342	273	224	172	354	222	186	0
Dev Raise (m)	0	0	61	119	63	81	120	104	76	161	140	125	97	79	60	44	39	42	41	0
Dev Raise 3.1 (m)	0	109	265	199	226	80	117	19	164	0	0	49	74	58	42	42	128	69	52	0
Dev Raise (m)	0	109	326	318	309	181	237	123	241	161	140	173	171	136	122	86	187	111	93	0
Return Raise Decline 1 — Ø= = 4.10 M	0	0	0	0	0	0	0	0	0	0	0	0	0	0	0	0	0	0	0	0
Intake Raise Decline 2 — Ø= = 4.10 M	0	0	0	0	0	0	0	0	0	0	0	0	0	0	0	0	0	0	0	0
Additional Return Raises — Ø= = 4.10 M	0	0	0	0	0	0	0	0	0	0	0	0	0	0	0	0	0	0	0	0
Dev Raise (m)	0	0	0	0	0	0	0	0	0	0	0	0	0	0	0	0	0	0	0	0
Waste																				
Waste Mass (t) Open Pit	0	10,565,237	2,273,083	0	0	0	0	0	0	0	0	0	0	0	0	0	0	0	0	0
Waste Mass (t) Underground	***13,712***	***391,424***	***542,206***	***581,116***	***547,692***	***490,504***	***383,893***	***395,244***	***364,823***	***343,334***	***323,554***	***314,079***	***267,609***	***264,297***	***203,074***	***190,969***	***217,429***	***189,876***	***141,016***	***3,039***
Waste Mass (t) Total	13,712	10,956,661	2,815,289	581,116	547,692	490,504	383,893	395,244	364,823	343,334	323,554	314,079	267,609	264,297	203,074	190,969	217,429	189,876	141,016	3,039
Back Fill Mass (t)	0	0	135,431	241,611	270,977	182,819	165,310	819,324	494,124	602,896	327,361	710,364	502,980	546,615	346,686	996,668	570,522	654,955	825,814	2,252,990
Tonnage (dmt)																				
Ore to Stockpile	0.54	0.99	1.44	1.59	1.64	1.98	2.18	2.55	2.83	2.87	2.78	3.27	3.34	3.56	3.44	3.80	3.83	4.09	4.43	4.63
Ore to Stope	***0.64***	***0.64***	***1.37***	***1.35***	***1.53***	***1.56***	***1.64***	***2.13***	***2.38***	***2.74***	***2.49***	***2.67***	***2.82***	***3.41***	***3.29***	***3.63***	***3.93***	***4.19***	***4.53***	***4.73***
Ore to Dev	0.64	1.09	1.54	1.69	1.74	2.08	2.28	2.65	2.93	2.97	2.88	3.37	3.44	3.66	3.54	3.90	4.08	4.32	4.48	4.46
Ore to Stockpile to Plant	0.50	0.50	0.50	0.50	0.50	0.50	0.50	0.50	0.50	0.50	0.50	0.50	0.50	0.50	0.50	0.50	0.50	0.50	0.50	0.50
Waste to Rockfill	1.20	1.20	1.20	1.20	1.20	1.20	1.20	1.20	1.20	1.20	1.20	1.20	1.20	1.20	1.20	1.20	1.20	1.20	1.20	1.20
Waste to Dump	1.04	1.48	1.61	2.64	2.83	3.14	3.26	3.68	3.79	3.93	3.89	4.35	4.25	4.47	4.32	4.70	4.72	5.14	5.13	1.85

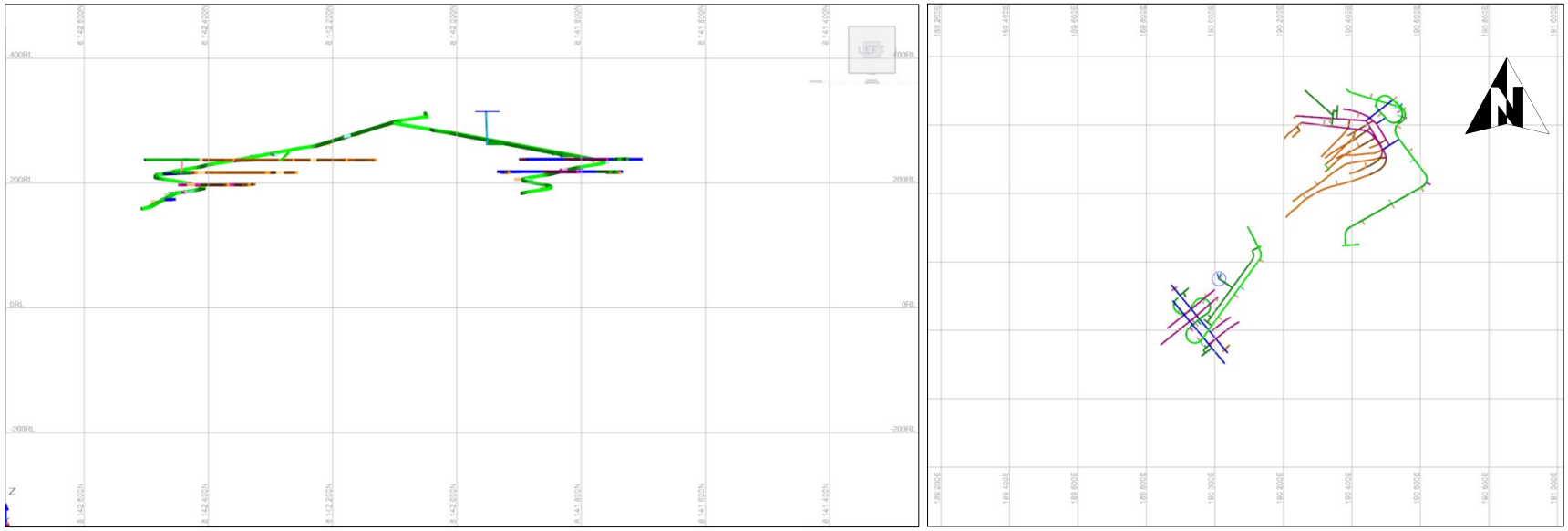


Figure 16-62: Year −2 Mine Sequencing

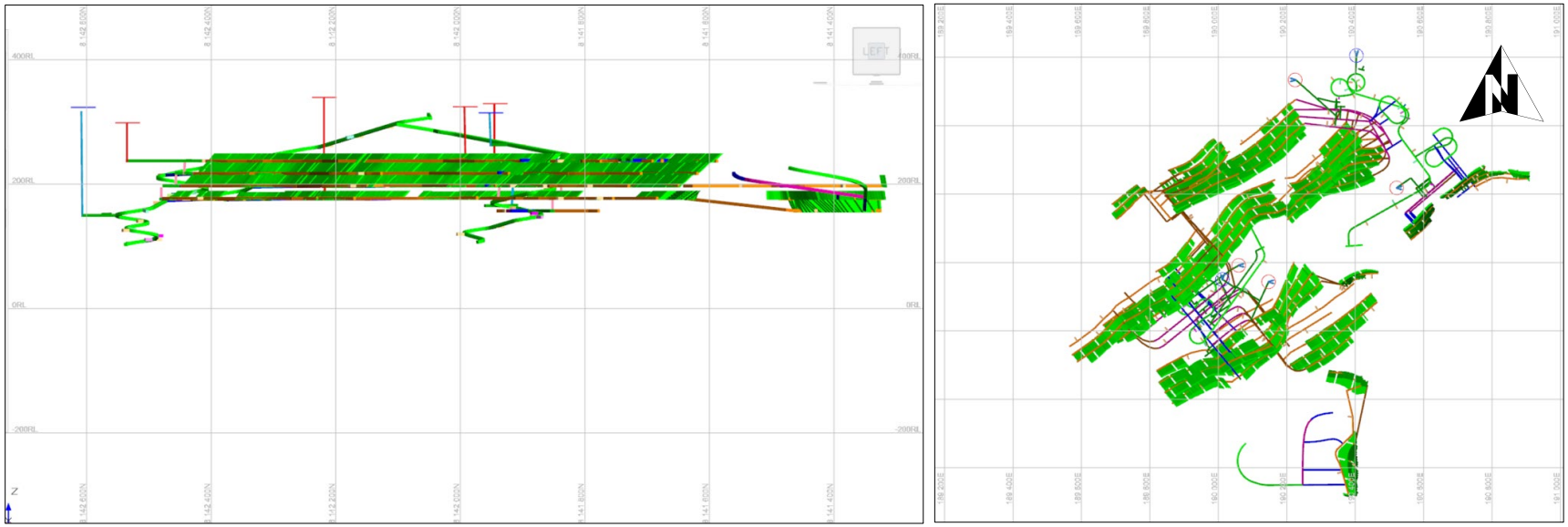


Figure 16-63: Year 5 Mine Sequencing

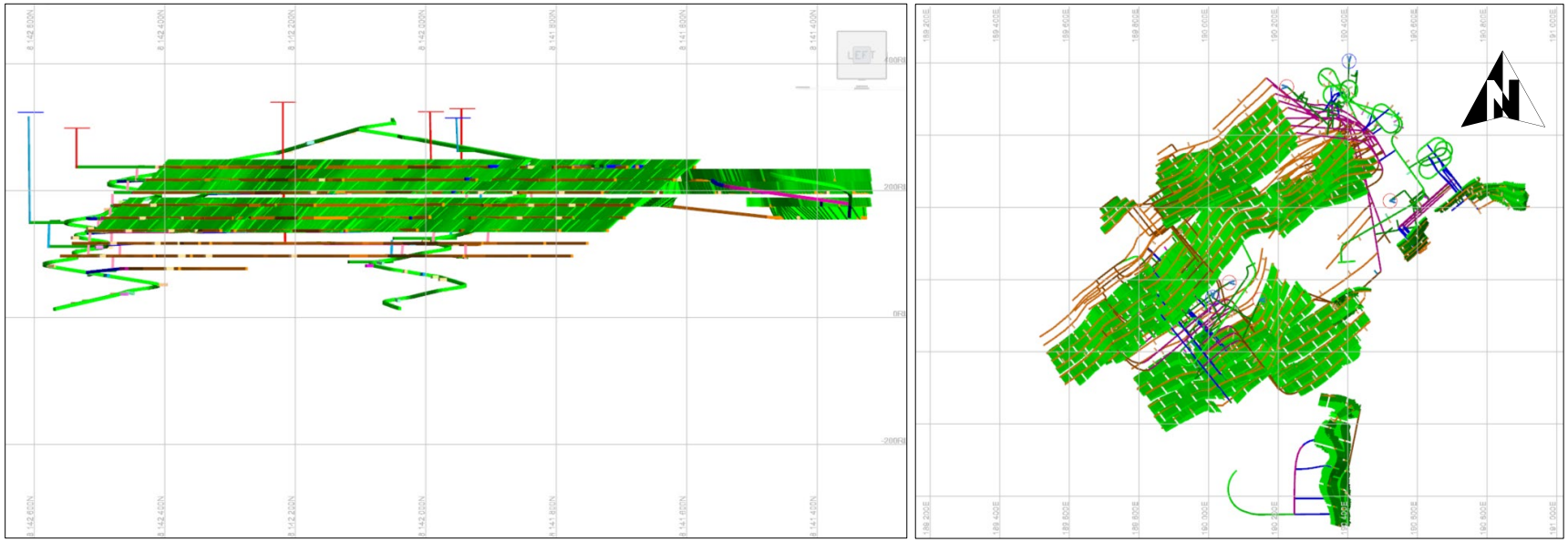


Figure 16-64: Year 8 Mine Sequencing

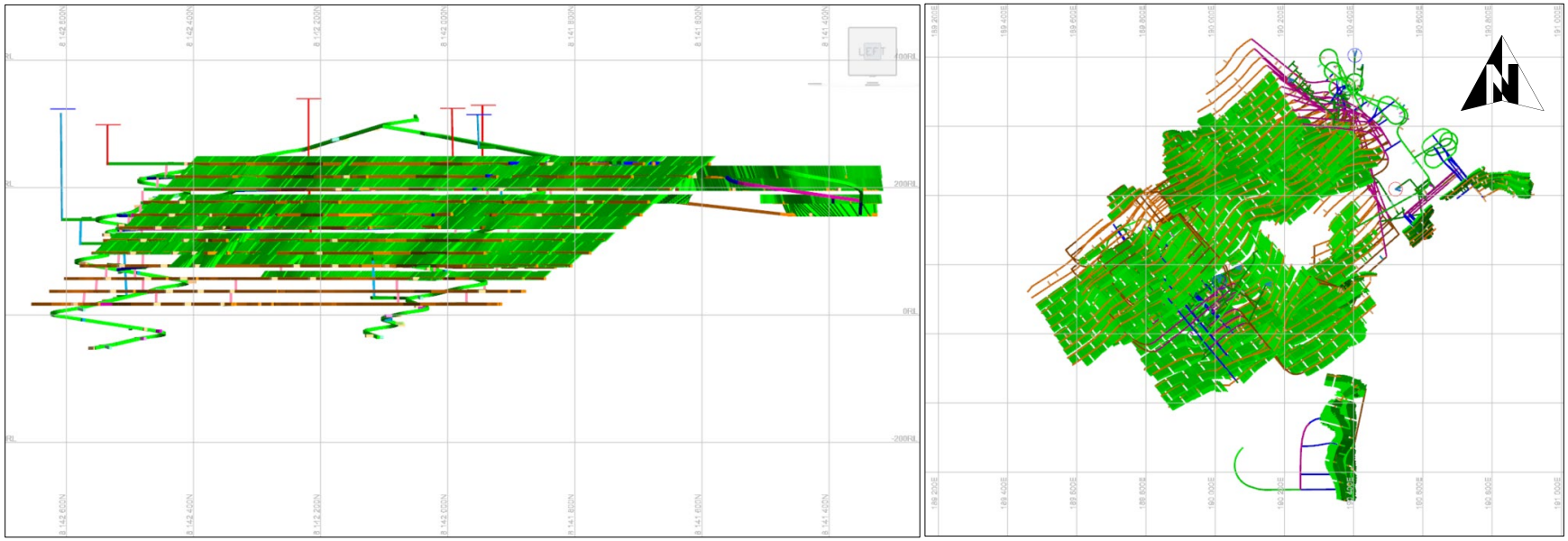


Figure 16-65: Year 11 Mine Sequencing

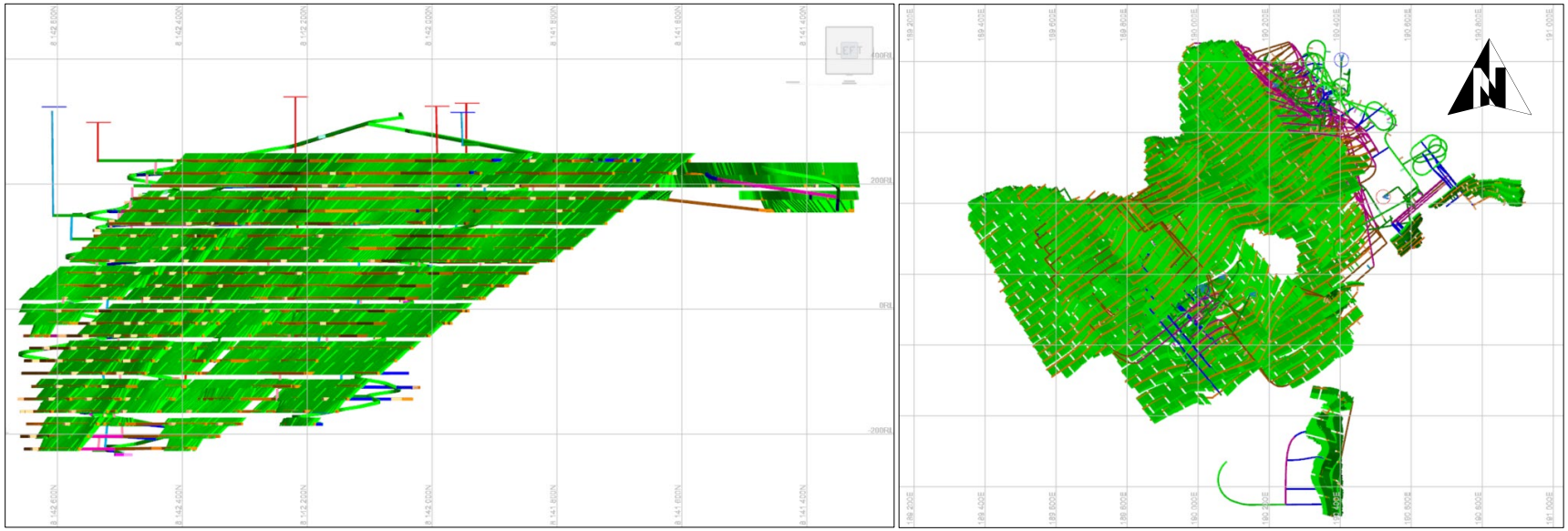


Figure 16-66: Year 18 End of Mine Life

16.5 Waste-Rock Dump and Dry-Tailings Management

16.5.1 Waste-Rock Dump Sequencing

During Years −1 to 1, waste rock generated from the open-pit operation will be hauled to designated waste-rock piles near the pit. Once open-pit mining is completed, the pit will be backfilled with waste rock and tailings produced from the concentration process. The waste rock will be deposited following a bottom-up sequence, and the dumping schedule will match the progress of the mining phases, ensuring continuous and safe disposal.

Waste generated from the underground mine will also be disposed of on the surface; however, the quantities are expected to be significantly smaller compared to those from the open pit or the tailings facility. There are two main reasons for this: first, the expected strip ratio of the underground mine is 0.3; second, most of this waste will be used as backfill in depleted stopes.

Waste deposition activities are designed with controlled lift heights and slope angles to ensure geotechnical stability throughout the mine life. Progressive rehabilitation measures, such as surface contouring and drainage control, will be implemented as early as possible to minimize erosion and facilitate future reclamation.

Given the short life of the open pit—with full depletion expected within one year of operation, the external dump sequencing has been planned to accommodate the total waste-volume generated. This approach minimizes land disturbance and allows for progressive backfilling of mined-out areas as they become available, restoring portions of the landscape throughout the Project life.

16.5.2 Dry-Tailings Deposition

Tailings generated from processing plant will be transported by truck and placed together with the waste in the planned waste piles. Dry stacking was selected due to its significant environmental and operational advantages, including reduced water consumption, higher water recovery for plant recirculation, elimination of the need for large tailings dams, and improved long-term geotechnical stability.

The dry-tailings facility will be developed in coordinated stages, aligned with both the mine schedule and the waste-rock dump sequencing. Co-disposal opportunities, where filtered tailings are placed in conjunction with waste rock, will be evaluated to optimize space utilization and reduce the overall disturbed area. Final closure of the dry-tailings storage will include surface contouring and revegetation, ensuring a stable landform that blends into the surrounding environment.

16.5.3 Integration of Waste and Tailings Management

The integrated approach between waste-rock sequencing and dry-tailings deposition ensures efficient land use, a reduced environmental footprint, and early implementation of reclamation practices. This strategy also provides flexibility in adapting to changes in ore-to-waste ratios and tailings generation rates, ensuring compliance with environmental standards and alignment with the overall mine closure plan. Figure 16-67 shows the plan view of waste and tailings piles.

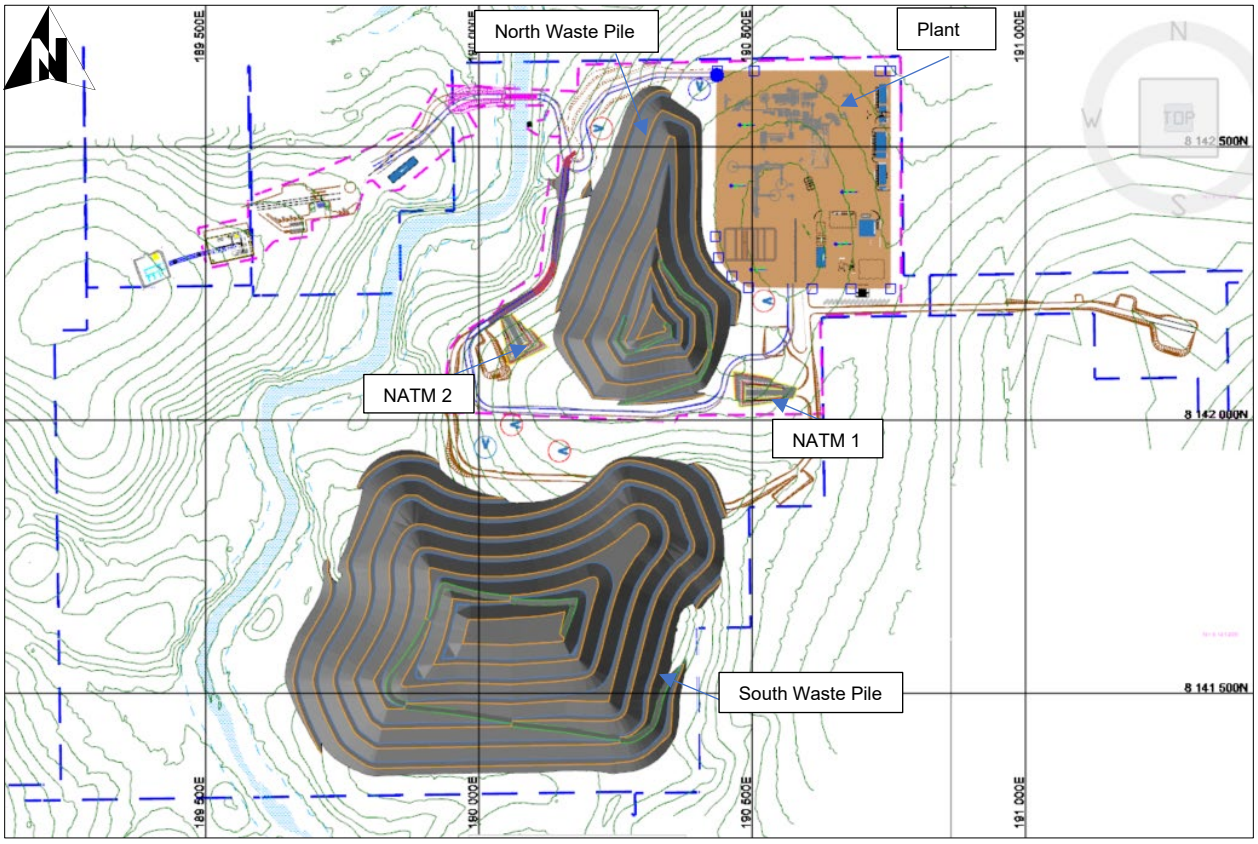


Figure 16-67: Plan View of Waste-Rock Dumps (Dashed Blue Line is the Mining Right Boundary; Dashed Pink Line is the Directly affected area =ADA Area; NATM 1 and 2 are the Portals that Access the Underground Mine

In Table 16-35 backfill capacity refers to the void volume within the stopes after ore extraction; rockfill represents the amount of waste material used as fill within the underground mine. Waste dump corresponds to the quantity of waste rock generated from underground operations that will be deposited in surface waste piles. Reject is the material processed through the plant that has no economic value. Valuable tailings are the tailings produced after processing that still contain recoverable value. They will be stored separately and managed under controlled conditions, to be reprocessed in the future once the flotation circuit becomes available.

Table 16-35: Waste and Tailings Schedule (Tonnes per Year)

	Year −2	Year −1	Year 1	Year 2	Year 3	Year 4	Year 5	Year 6	Year 7	Year 8	Year 9	Year 10	Year 11	Year 12	Year 13	Year 14	Year 15	Year 16	Year 17	Year 18
Backfill Capacity	0	287	282,385	593,891	578,508	581,427	564,558	591,612	573,928	580,275	552,486	586,378	584,834	625,018	611,504	648,269	683,188	684,769	562,032	377,623
Rockfill	0	0	282,385	464,893	438,154	392,403	307,114	316,195	291,858	274,667	258,843	251,263	214,087	211,438	162,459	152,775	173,943	151,901	112,813	2,431
Waste Dump	13,712	10,956,661	2,532,904	116,223	109,538	98,101	76,779	79,049	72,965	68,667	64,711	62,816	53,522	52,859	40,615	38,194	43,486	37,975	28,203	608
Reject Pile	0	296,744	611,757	658,876	653,301	638,284	637,166	643,315	635,286	636,778	638,546	631,446	636,509	631,169	625,835	620,922	621,330	621,000	576,998	342,839
Valuable tailings	0	227,602	456,369	484,640	484,640	484,640	484,640	484,640	484,640	484,640	484,640	484,640	484,640	484,640	484,640	484,640	484,640	484,640	436,880	261,236
Schedule																				
Waste Pile	13,712	391,424	259,821	116,223	109,538	98,101	76,779	79,049	72,965	68,667	64,711	62,816	53,522	52,859	40,615	38,194	43,486	37,975	28,203	608
Reject Pile	0	296,744	611,757	658,876	653,301	638,284	637,166	643,315	635,286	636,778	638,546	631,446	636,509	631,169	625,835	620,922	621,330	621,000	576,998	342,839
% Waste	1.00	0.57	0.30	0.15	0.14	0.13	0.11	0.11	0.10	0.10	0.09	0.09	0.08	0.08	0.06	0.06	0.07	0.06	0.05	0.00
% Reject	0.00	0.43	0.70	0.85	0.86	0.87	0.89	0.89	0.90	0.90	0.91	0.91	0.92	0.92	0.94	0.94	0.93	0.94	0.95	1.00

16.6 Mine Equipment

16.6.1 Mine Production Equipment

Table 16-36 lists the production equipment selected for the Project underground mine operation.

Table 16-36: Mine Production Equipment

Equipment	Basic Specification	Reference Model
Truck	45-tonne	FMX500
Jumbo 2 Boom	22 tonnes	Sandvik DD321
LHD	15-tonne	Sandvik LH515i
Wheel Loader	5.0 m³	CAT 966
Longhole Drill	Top hammer 76 mm	Sandvik DL421
Slot Raiseborer	ITH Long hole 165mm	Sandvik DU412i
Cable Bolter	25-tonnes	Sandvik DS421
Rock Bolter	18-tonnes op. Weight	Sandvik DS312

16.6.2 Drilling Equipment

The equipment used for drilling ore in the stopes will be a hydraulic top hammer longhole fandrill capable of drilling vertical and inclined fans and single or parallel longholes up to 54 m deep.

Ore drilling and blasting will be carried out from inside the galleries in the active stope. Blasting is planned to occur after all drilling is completed and all cables installed. The blasted material will be removed from the lower gallery.

The equipment used for drilling the ramps, galleries, and other horizontal openings will be a compact two-boom jumbo with an operational weight of 22 tonnes. The jumbo is capable of face drilling, crosscut drilling, and bolt-hole drilling. The boom provides coverage of 49 m², which is more than enough to cover the required area of 29 m². The equipment is also capable of drilling based on electronic blast-fire plan, which achieves higher productivity. Additionally, the operator's safety cabin is equipped with rollover protective-structures and falling-object protective structures.

For roof reinforcement, the Project includes a specialized machine capable of installing cable bolts grouted with cement to be used inside the stoping area and for underground openings that require this kind of support. The cable bolter has an operational weight of 25 tonnes and can drill and install bolts up to 25 m long.

The articulated mobile raiseborer is fully mechanized and self-contained. It is specially designed for slot raising in drifts measuring at least 4.7 m x 4.7 m, and will perform void-hole drilling in stoping blasts. Capable of drilling upward or downward, it handles vertical and inclined raises ranging from 660 mm to 1,420 mm in diameter.

Table 16-37 and Table 16-38 summarize the productivity estimates for the fandrill and the cable bolter, respectively.

Table 16-37: Fandrill Productivity Parameters and Annual Unit Production

Fandrill Productivity	Unit	Production
Slots	m/d	195
	t/m	2.15
	Mt/a	0.15
Rings	m/d	195
	t/m	4.5
	Mt/a	0.32

Table 16-38: Cable Bolter Productivity Parameters and Annual Unit Production

Parameters	Unit	Production
Bolt Length	m	10
Cable Bolter Productivity	bolts/d	150
	t/bolt	25
	Mt/a	1.35

The productivity of the jumbo and the slot raiseborer are shown in Table 16-39 and Table 16-40, respectively.

Table 16-39: Jumbo Productivity

Decline	Development (m/month)
Multiblast (Years −2 and −1)	90
Single Blast	60
Drives and Infrastructure	50
Jumbo Productivity (m/month)	180

Table 16-40: Slot Raiseborer Productivity Parameters and Annual Unit Production

	Unit	Production
Raiseborer Productivity (Slots)	m/d	15
	m/a	5,400

16.6.3 Loading and Haulage Equipment

Remote-controlled LHDs with a 15-tonne capacity will load both the blasted ore and the mine-development waste onto 45-tonne underground mine trucks. Table 16-41 and Table 16-42 show the parameters considered for estimating LHD productivity and truck fleet sizing, respectively.

Table 16-41: LHD Productivity Parameters

LHD	Unit	Productivity
Scheduled Time	h/a	6,552
Availability	%	80
Utilization	%	65
Worked Hours	h/a	3407
Efficiency Factor	%	83
Effective Time	h/a	2828
Cycles per Hour	h	25
Bucket Capacity	m^3	6.3
Bucket Capacity	t	13.12
Fill Factor	%	90
Productivity	Mt/a	0.57

A rehandle of 50% of the ore and waste materials has been added to the LHD production requirements.

Table 16-42: Truck Productivity Parameters

Truck	Unit	Productivity
Scheduled Time	h/a	6,552
Availability	%	80
Utilization	%	65
Worked Hours	h	3,407
Efficiency Factor	%	83
Effective Time	h/a	2,828
Capacity	m^3	20
Average Load	t	40

16.6.4 Auxiliary Equipment

Table 16-43 presents a list of planned auxiliary equipment, including their basic specifications and reference models.

An average availability of 75% was applied to all auxiliary equipment. Utilizations were calculated based on the estimated hours worked by the fleet and the number of units required.

Table 16-43: Mining Auxiliary Equipment

Equipment	Basic Specification	Reference Model
Scaler	8.5 m Vertical boom reach	Normet Scamec 2000 S
Explosive Truck	45t Emulsion carrying capacity	Contractor
Scissor Lift	3-tonne, 3.5 m	Normet Utilift SF 330
Shotcrete Spray Truck	Up to 27 m³/h (electric operation)	JCB
Jackleg Drill	34 kg	Tornibras TB303AM+TB300
Stope Drill	40 kg	Tornibras TB303S
Air Compressor	Mobile, diesel, 286 cfm, 10 bar	Atlas Copco XATS 300 Pd
Grader	10-tonne operating weight	Paus PG 10HA
Ventilation Fax	110 kW	Howden 4800-VAX-2700 FB 15TG
Exhauster	800 kW	Howden MVC2293.00.15 SOV4T ARR8
Dewatering Pump	Submersible, 170 m³/h, 73 m maximum height	Atlas Copco WEDA D80H
Diesel Generator	70 kVA	Atlas Copco QAS 70 Pd
Utility Vehicle	1-tonne, flat deck	Toyota Hilux

16.6.5 Fleet Sizing

Table 16-44 shows the fleet requirements for the Project mining operation.

Table 16-44: Mining Equipment Fleet Sizing

Year	−2	−1	1	2	3	4	5	6	7	8	9	10	11	12	13	14	15	16	17	18
TRK	2	4	6	8	10	10	10	12	12	12	13	13	13	13	13	13	12	12	10	10
JUMBO	3	4	4	5	5	5	5	5	5	5	5	5	4	4	4	3	0	0	0	0
LHD	0	2	3	5	5	5	5	5	5	5	5	5	5	5	5	5	5	5	5	5
Wheel loader	2	2	2	0	0	0	0	0	0	0	0	0	0	0	0	0	0	0	0	0
Fandrill	0	2	3	6	6	6	6	6	6	6	6	6	6	6	6	6	6	6	6	6
Slot Raiseborer	0	0	1	1	1	1	1	1	1	1	1	1	1	1	1	1	1	1	1	0
Cable Bolter	0	1	1	1	1	1	1	1	1	1	1	1	1	1	1	1	1	1	1	1
Rock Bolter	0	1	2	3	3	3	3	3	3	3	3	3	3	3	3	3	3	3	3	3
Scaler	1	2	3	3	3	3	3	3	3	3	3	3	3	3	3	3	3	3	3	3
Scissor Lift	1	1	1	1	1	1	1	1	1	1	1	1	1	1	1	1	1	1	1	1
JCB 540-170	1	2	3	4	4	4	4	4	4	4	4	4	4	4	4	4	4	4	4	4
Fuel & Lube Truck	1	1	2	2	2	2	2	2	2	2	2	2	2	2	2	2	2	2	2	2
Personnel Carrier	1	1	2	2	2	2	2	2	2	2	2	2	2	2	2	2	2	2	2	2
Maintenance Truck	1	1	2	2	2	2	2	2	2	2	2	2	2	2	2	2	2	2	2	2
Jackleg Drill	1	2	4	4	4	4	4	4	4	4	4	4	4	4	4	4	4	4	4	4
Stoper Drill	1	1	2	2	2	2	2	2	2	2	2	2	2	2	2	2	2	2	2	2
Air Compressor	1	1	2	2	2	2	2	2	2	2	2	2	2	2	2	2	2	2	2	2
Grader	1	1	2	2	2	2	2	2	2	2	2	2	2	2	2	2	2	2	2	2
Ventilation Fan	2	9	11	11	11	11	11	11	11	11	11	11	11	11	11	11	11	11	11	11
Exhauster	2	4	4	4	4	4	4	4	4	4	4	4	4	4	4	4	4	4	4	4
Dewatering Pump	2	4	6	6	6	6	6	6	6	6	6	6	6	6	6	6	6	6	6	6
Diesel Generator	1	2	3	3	3	3	3	3	3	3	3	3	3	3	3	3	3	3	3	3
Utility Vehicle	4	8	10	10	10	10	10	10	10	10	10	10	10	10	10	10	10	10	10	10
Total	**28**	**56**	**79**	**87**	**89**	**89**	**89**	**91**	**91**	**91**	**92**	**92**	**91**	**91**	**91**	**90**	**86**	**86**	**84**	**83**

16.7 Drilling and Blasting Plan

16.7.1 Longhole Drilling and Blasting

The drilling and blasting plan for longhole drilling is shown in Table 16-45 and Figure 16-68.

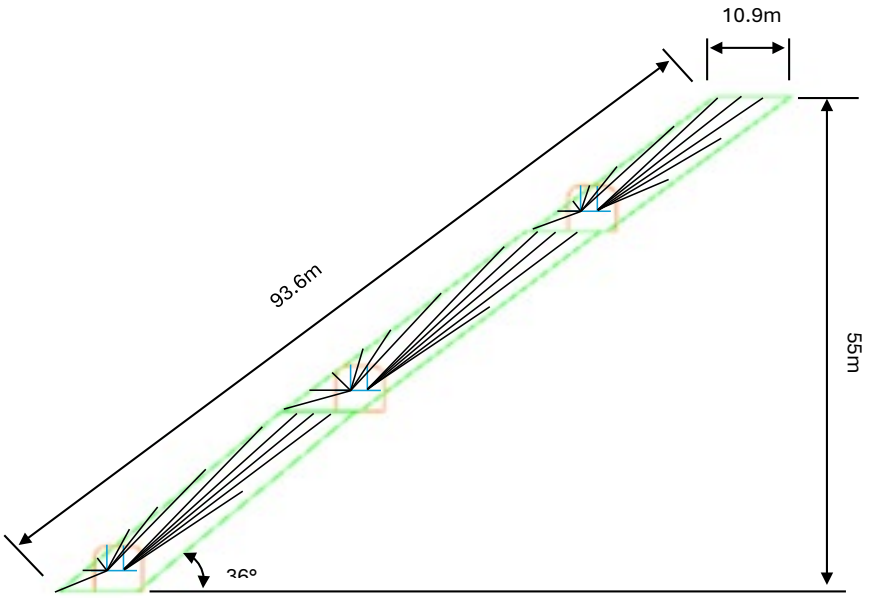


Figure 16-68: Longhole Drilling

Table 16-45: Longhole Drilling and Blasting Plan

Longhole	Unit	Plan
Drill Holes	No.	29
Total Length	m	462
Average Drill-Hole Length	m	15.93
Solid Volume	m^3	1,953
Ore Density	m^3/t	2.7
Solid Mass	t	5,273
Mining Recovery	%	90
Spacing	m	2
Fan Mass	t	1,318
Specific Drilling	t/m	5.71
Charge Ratio	kg/m	4.76

16.7.2 Slot-Raise Drilling and Blasting

Table 16-46 presents the slot-raise drilling and blasting plan designed for the Project sublevel stoping operation.

Table 16-46: Slot-Raise Drilling and Blasting Plan

Slot-Raise	Unit	Parameters
Total Drill Holes		**16**
Enlarged 6"		6
Loaded Drill Holes		10
Average Drill-Hole Length	m	38
Enlarged Total Length	m	460
Loaded Total Length	m	383.33
Total Length	m	843.33
Average Dip	°	37
Solid Volume	m³	44.14
Ore Density	m³/t	2.7
Slot Mass	t	119
Specific Drilling	t/m	0.14
Plug	m	0.675
Drill-Hole Diameter	mm	89
Drill-Hole Volume	cm³	2,343
Explosives Density	(g/cm³)	1.5
Drill-Hole Mass	g	3,514
Drill-Hole Mass	kg	3.51
Booster	g	450
Total Booster Mass	g	4,500
Total Emulsion	kg	35.14
Total Booster Mass	kg	4.5
Slot Total Mass	kg	39.64
Charge Ratio	g/t	333

Development

The design of the drilling and blasting plans for the ramp and drives is summarized in Table 16-47 and illustrated in Figure 16-69 and Figure 16-70.

Table 16-47: Development Drilling and Blasting Plan

Description	Unit	Plan
Section Area	m²	28.50
Section Width	m	5.30
Total Holes Drilled		51.00
Drill Length	m	3.70
Blast Yield	%	90.00
Blast Advance	m	3.33
Total Drilled	m	188.70
Specific Drill	t/m	1.55
Drill Plan Index	m/m³	1.81
Drill Blast Round Index	m/m	57

Description	Unit	Plan
Productivity	t/h	125.47
Drilled Metres Productivity	m/h	81.00
Productivity	drills/h	21.89
Overbreak	%	10.00

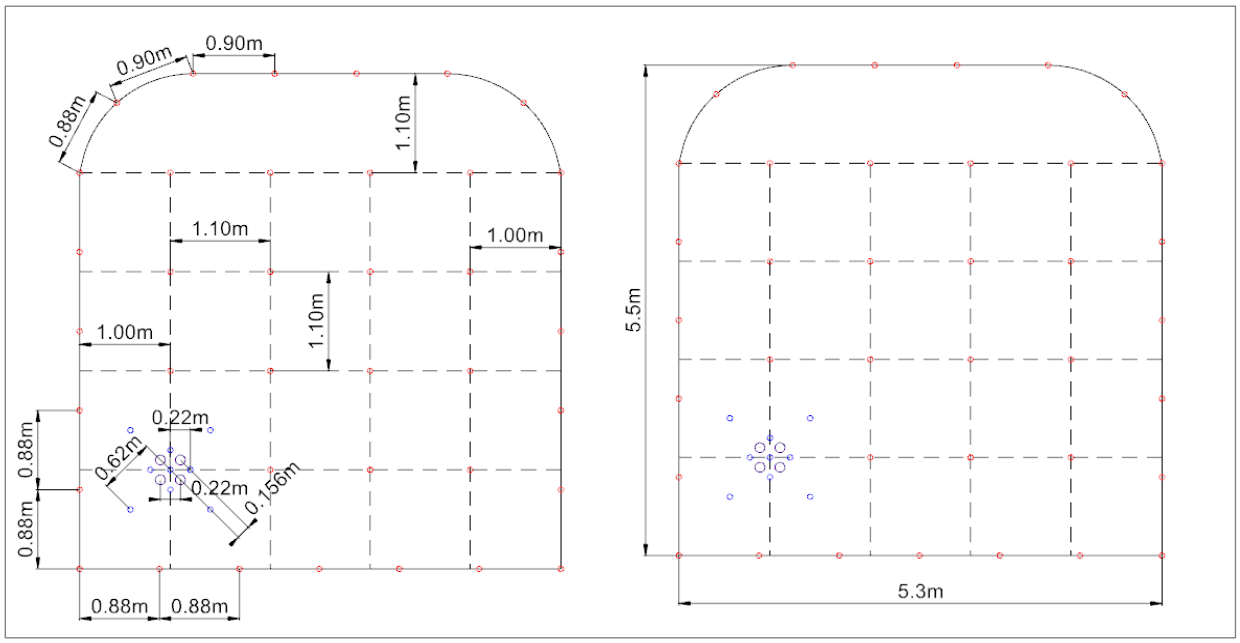


Figure 16-69: Drilling and Blasting Plan for the Ramps (Red Circles = Charged Holes; Blue = Burn Cut Holes)

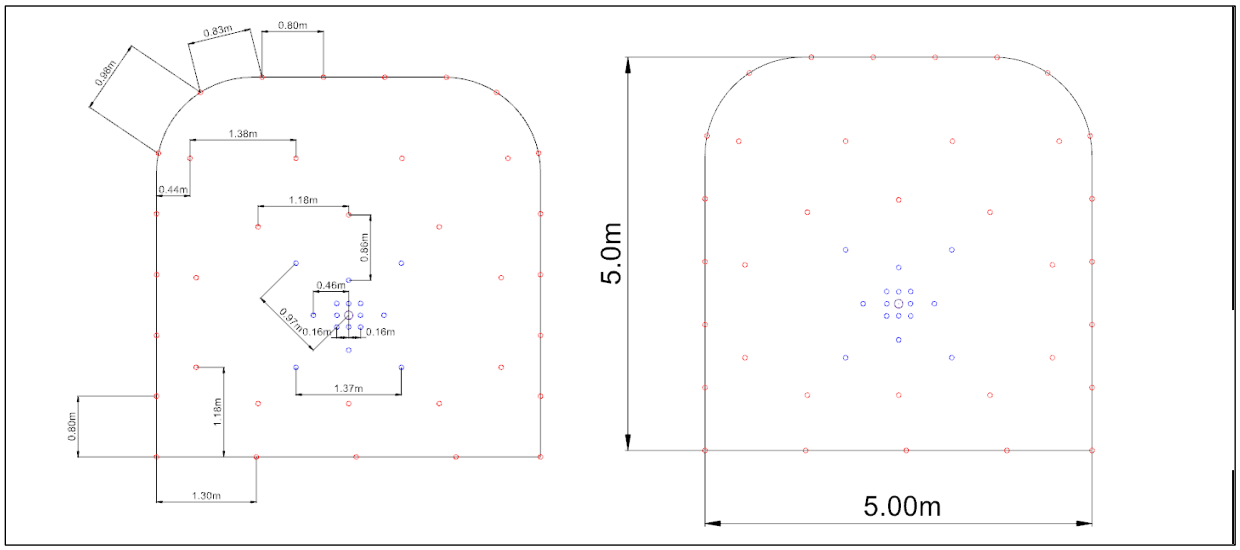


Figure 16-70: Drilling and Blasting Plan for the Drives (Red Circles = Charged Holes; Blue = Burn Cut Holes)

16.8 Roof Support

16.8.1 Sublevel Stopes

The design parameters of the roof-support cable bolting of sublevel stopes are listed in Table 16-48.

Table 16-48: Design Parameters of the Roof Support Bolting for the Sublevel Stopes

Description	Unit	Value
Average Length of Stopes	m	4
Number of Galleries per Stope	unit	1 or 2
Typical Stope with Galleries Area	m^2	25.5
Cabled Area	%	100
Typical Stope Mass	t	2,003
Cabling Burden	m	1.5
Cabling Spacing	m	1.5
Number of Cables per Line		4
Number of Lines		3
Number of Cables per 5.5 m Line		2
Number of Cables per 8.0 m Line		3
Total Number of Cables per 5.5 m Solid		5
Total Number of Cables per 8.0 m Solid		5
Hanging Wall/Footwall Cable Length	m	8.0
Brown Cable Length (middle of Gallery)	m	5.5
Total 8.0 m Cabled Length	m	43
Total 5.5 m Cabled Length	m	29
Specific Drilling per 8.0 m Cable	t/m	47
Specific Drilling per 5.5 m	t/m	68
Specific Drilling per Total Cable	t/m	17
Grout Consumption per 10 m Cable	kg	45
Volume of a 10 m Drill Hole	L	20.43
Cement Density	t/m^3	2.20
Volume of an 8 m Drill Hole	l	16.34
Grout Consumption per mm Cable	kg	36.00
Grout Consumption	kg/m	4.50
Total Grout Mass per Stope Solid	kg	192.00
Tonnes per Grout Mass	t	10.43
Volume of a 5.50 m Drill Hole	L	11.24
Grout Consumption per 5.5 m Cable	kg	24.75
Grout Consumption	kg/m	4.50
Total Grout Mass per Stope Solid	kg	132.00
Tonnes per Grout Mass	t	15.17

16.8.2 Development

Roof support drilling and blasting parameters for the Project underground mine operation development works are shown in Table 16-49 and Table 16-50.

Table 16-49: Development and Auxiliary Roof-Support Drilling

Description	Unit	Value
Development Roof-Support Drilling		
Roof Support Drill Pattern	m^2	2.3
Supported Area	m^2	19.4
Number of Bolts		9.0
Bolt Length	m	3.0
Bolt Length per Blast Round	m	27.0
Bolt Length per Blast Metre	m	8.1
Auxiliary Drilling		
Infrastructure Holes per Blast		6
Hole Length	m	0.8
Total Drilled per Blast Round	m	4.8
Drilled Infrastructure per Blast Metre	m	1.44

Table 16-50: Mesh Installation Design Parameters for Decline

Description	Unit	Value
Ramp Roof Support		
Length	m	3.05
Width	m	2.13
Grid Dimensions	m	100 x 100
Number of Overlapping Squares		3
Overlapping Squares Distance	m	0.3
Effective Width	m	1.8
Area	m^2	5.58
Steel Mesh Area		
Length	m	3.05
Width	m	12.7
Area	m^2	38.58
Number of Meshes		7
Bolt Drilling		
Burden	m	1.2
Spacing	m	1.2
Area	m^2	1.44
Bolt Length	m	0.91
Number of Drill Holes		27
Rework Factor	%	0
Estimated Number of Drill Holes		26.8
Estimated Drilling	m	24.4
Number of Clips per Mesh		4
Total Number of Clips		28

16.9 Backfilling

Due to the limited surface area available for waste disposal at the Project, it has been determined that approximately 80% of the waste material generated during mine development will be reused as rock backfill, provided that open stopes are available to receive the material.

When stopes are exposed, a dedicated unloading point will be established to allow trucks to discharge waste material directly for backfilling purposes. To comply with underground height restrictions and ensure safe and controlled dumping operations, ejector buckets will be used. These systems enable material discharge without raising the truck body, thereby reducing the risk of overhead collisions, enhancing operator safety, and ensuring precise placement of the backfill within the stope.

Rockfill backfilling does not provide effective confinement of the hanging wall, serving mainly to offset the Project's limited surface disposal capacity while reducing transport and disposal costs. Its use is therefore focused on operational and environmental efficiency rather than structural reinforcement.

16.10 Mine Services

16.10.1 Ventilation

The ventilation plan for the underground mine establishes that fresh air will enter through the two portals and two intake shafts. Air will be exhausted through four large return-air drives.

Production haulage will be carried out via two declines. Fresh air will enter through mine entries and converge in the production areas along the ore body. From there, a spiral ramp extends to the end of the deposit. Exhaust airways connect all production zones to the return-air drive.

Based on the ventilation manufacturer's modelled peak airflow requirement of 443 m³/s, this arrangement allows the system to operate across a wide performance envelope, where fan speed control alone may be insufficient. Fans can therefore be switched on or off at different ventilation milestones to maintain efficiency.

The main ventilation system will rely on mechanical ventilation, consisting of intake and exhaust fans. Its operating principle is to force clean air into the mine while exhausting contaminated air to the surface, ensuring continuous air exchange and renewal of the underground atmosphere.

16.10.2 Airflow Requirement

Global Airflow Requirements

The ventilation system was designed to accomplish the local regulation NR22 airflow requirement. To determine whether diesel equipment plus personnel or total mine tonnage comprise the higher requirement at any point in the LOM, a comparison between these requirements is given in Figure 16-71.

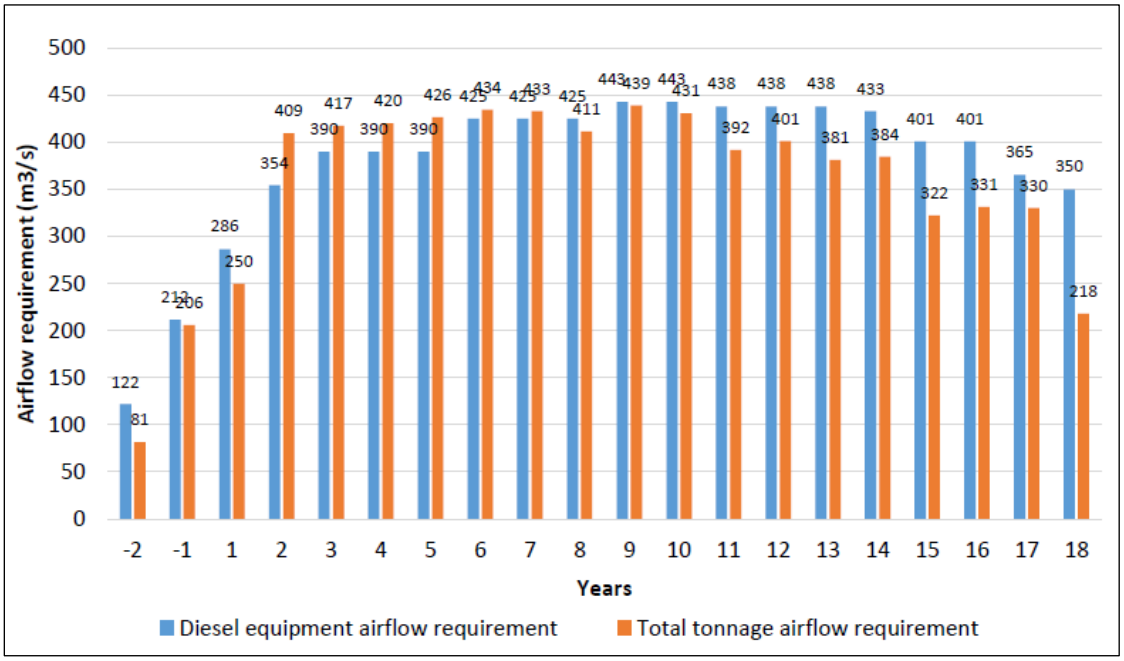


Figure 16-71: Global Airflow Requirements—Diesel Equipment Plus Personnel vs. Total Annual Tonnage

In all but six years, the higher airflow requirement is diesel equipment plus personnel.

To obtain the overall airflow requirement of 487 m^3/s for Years 9 and 10, 10% contingencies were added to the previous airflow requirement, as shown Figure 16-72.

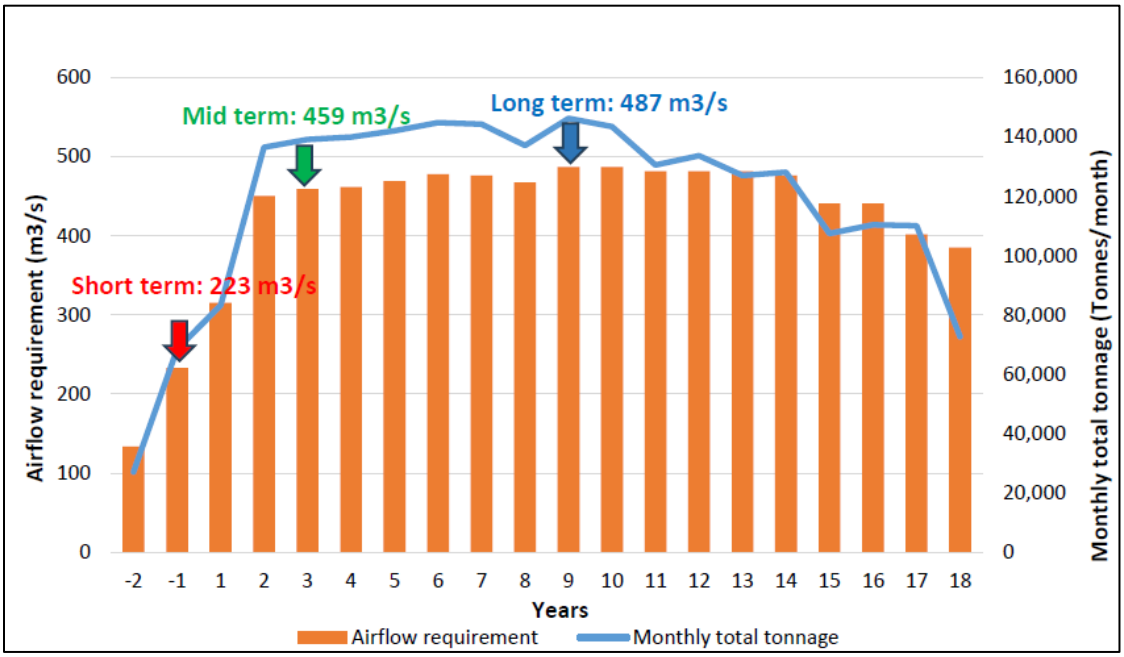


Figure 16-72: Total Airflow Requirement

Local Airflow Requirements

Table 16-51 gives the maximum airflow requirement established based on the most demanding activity in the mine cycle—the loading operation.

Table 16-51: Local Ventilation Airflow Requirement Calculation—Loading Activities

Item	Power (HP)	Utilization (%)	Factor (m^3/min–HP)	Airflow Requirements (m^3/min)
Truck	500	80	2.65	1,060
Loader	348	50	2.65 × 0.75	346
Diesel Airflow Requirement + 3 Personnel (m^3/s)				23.52

Furthermore, since no auxiliary fan will be dedicated to ventilating a single working area at the active levels (excluding primary development), the second-largest airflow demand activity was also assessed:

Table 16-52: Local Ventilation Airflow Requirement Calculation—Explosives Charging Activity

Item	Power (HP)	Utilization (%)	Factor (m^3/min–HP)	Airflow Requirements (m^3/min)
Explosives Truck	150	50	2.65	259
Scissor Lift	131	75	2.65 × 0.75	149
Diesel Airflow Requirement + 3 Personnel (m^3/s)				6.90

For this reason, 30.5 m^3/s local fans will be required to achieve the local airflow requirements (up to two for production or preparation workings, and one for primary development working), this airflow requirement was considered on local-fan duty-point calculations and must address production and preparation activities and primary development.

16.10.3 Ventilation Design

Ventilation System Type

The proposed ventilation system is the pull-type. Intake air will be delivered to active levels through the ramps and intake shafts for both mine sectors, and will be exhausted by fans installed on exhaust-shaft collars at the surface, with connections on each mine level, to reduce recirculation into deepest levels.

Main System Capacity

To comply with ventilation requirements established by local regulations, and the mine advance and production rates indicated in the original Project feasibility study (Horta de Cerqueira Viana et al., 2024, July 11) and by the MGLIT, four active levels were considered for each sector, and the capacity of the main exhaust ventilation system was determined (Table 16-53).

Table 16-53: Main Exhaust System Capacity

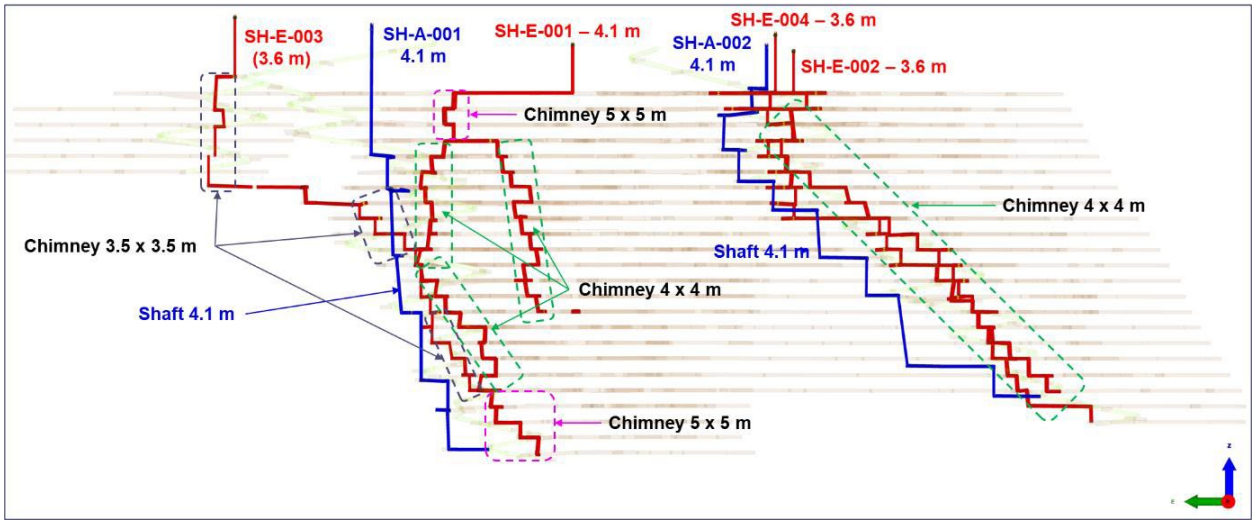
Active Levels		Number Working Areas	Airflow Subtotal (m^3/s)	Airflow +15% Contingencies (m^3/s)
Level 1	Drilling	3 to 4	60	69
Level 2	Production	3 to 4	60	69
Level 3	Preparation	3 to 4	60	69
Level 4	Main Development	1 to 2	60	69
			Airflow Subtotal (m^3/s)	**276**
			Airflow Total = Subtotal + 10% Airflow (m^3/s)	**303.6**

For this reason, each exhaust system must supply 300 m^3/s for the mine's most productive years. The option to merge exhaust systems for both ventilation systems was evaluated.

To ensure each sector of the underground mine has a dedicated ventilation exhaust system, Sector 1 will use the exhaust shaft SH-E-001 from Year 1 through Year 18. Beginning in Year 3, the "Satellite 1" exhaust shaft (SH-E-003) will commence operation, and from Year 6 onward, the combined system will provide a total capacity of 330 m^3/s (Figure 16-73).

Also, three sets of ventilation chimneys will be required for connection to each level. This is because of ore body extension and to maintain an adequate ventilation duct length and avoid local airflow recirculation and lack of air in the working areas

The "Corpo 2" exhaust system will have two shafts. SH-E-002 that will pull air from hanging wall levels, and SH-E-004 that will pull air from footwall levels to minimize airflow recirculation from levels to ramp and improve airflow control, each shaft will be connected to levels through two chimneys system (for each shaft) (Figure 16-73).



Source: Howden (2025).

Figure 16-73: Mine Ventilation System (Exhaust Shafts in Red; Intake Aire in Blue)

According to mine infrastructure presented previously, the mine ventilation system was designed to maintain an airflow coverage higher than 100% during the LOM; ventilation system requirements and capacity are presented in Figure 16-74.

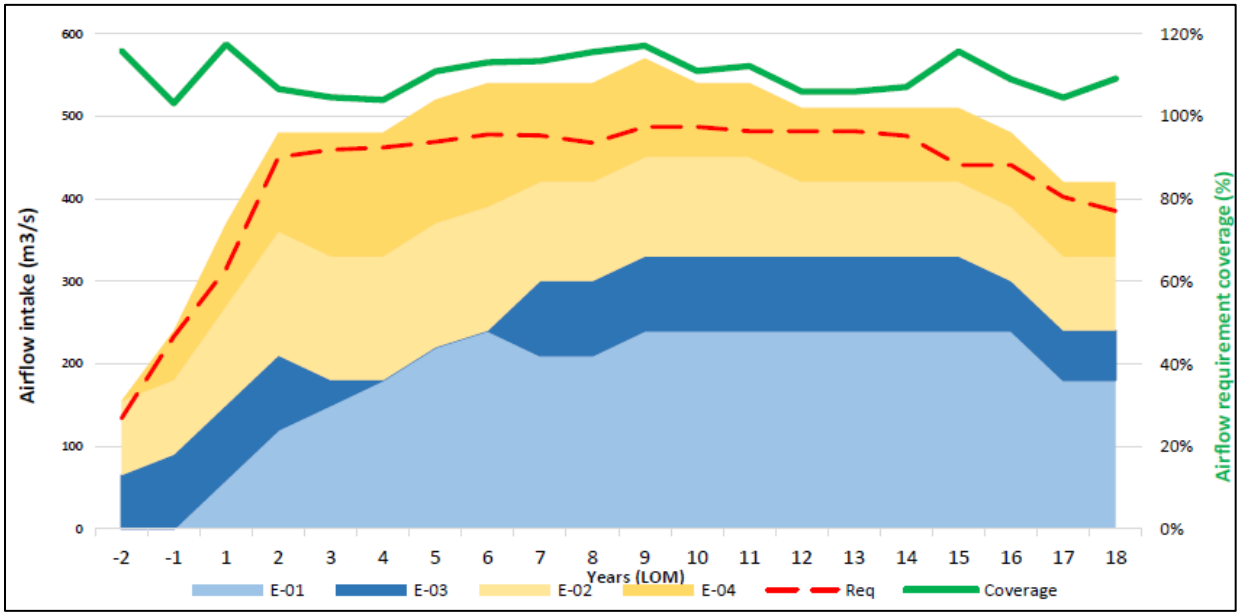


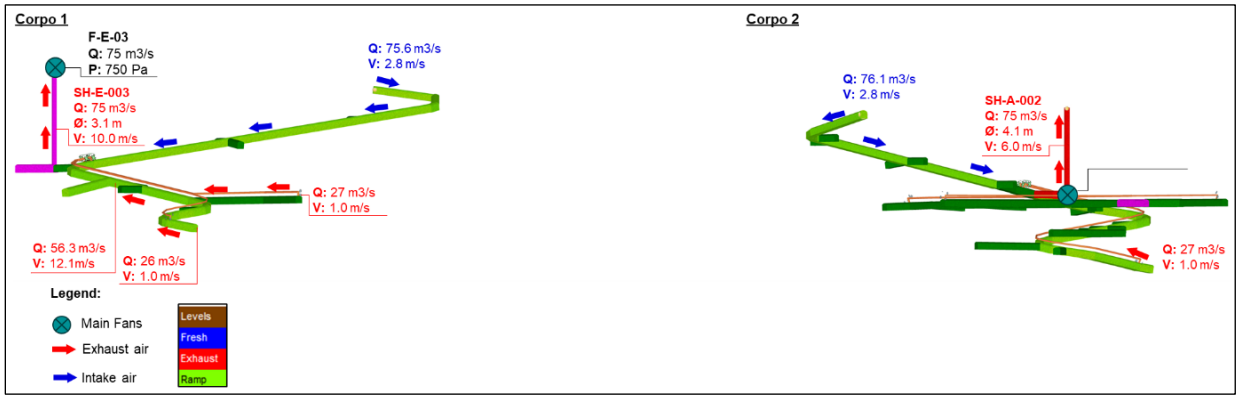
Figure 16-74: Ventilation System Capacity and Requirement for Each Sector Over the LOM

16.10.4 Mine Project Stage—Ventilation Planning

Year −2 Ventilation System

During Year −2, the ventilation system will require two 175 hp local fans, one installed in the main decline portal of each ramp development.

At year's end, ventilation SH-E-003 (exhaust) and SH-A-002 (intake) will be excavated, and main axial exhaust fan F-E-03 will be installed on the SH-E-003 collar (surface) to establish an exhaust circuit for mine development in Sector 1. For Sector 2 development, initially only two 175 hp local fans will be installed on SH-A-002's toe as temporary exhaust fans Figure 16-75 shows the main ventilation system features for the year.



Source: Howden (2025).

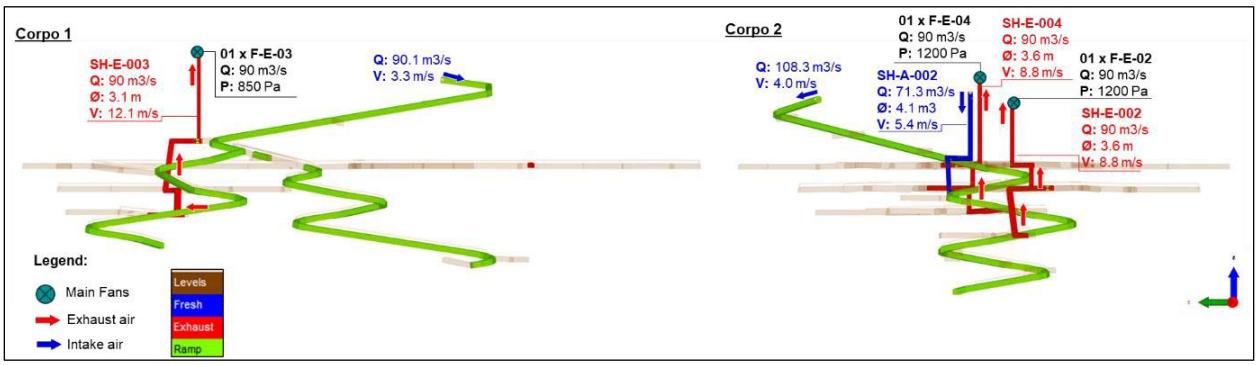
Figure 16-75: Year -2 Ventilation System

Year −1 Ventilation System

In Year −1, the major changes to the ventilation system takes place in Section 2. After excavations for SH-E-002 and SH-E-004 are finished, one of two new 400 hp exhaust fans (F-E-02 and F-E-04) will be installed onto each shaft collar, to achieve the airflow requirements and allow Sector 2 development (with a higher development rate).

For Satellite 1 development, main exhaust fans will operate at higher capacity, and local fans for workings will be located on the ramp connection to active levels.

The exhaust circuit will be shared with Sector 1 primary developments, which will require two local fans installed on each ramp. Figure 16-76 shows the main ventilation system features for this period.



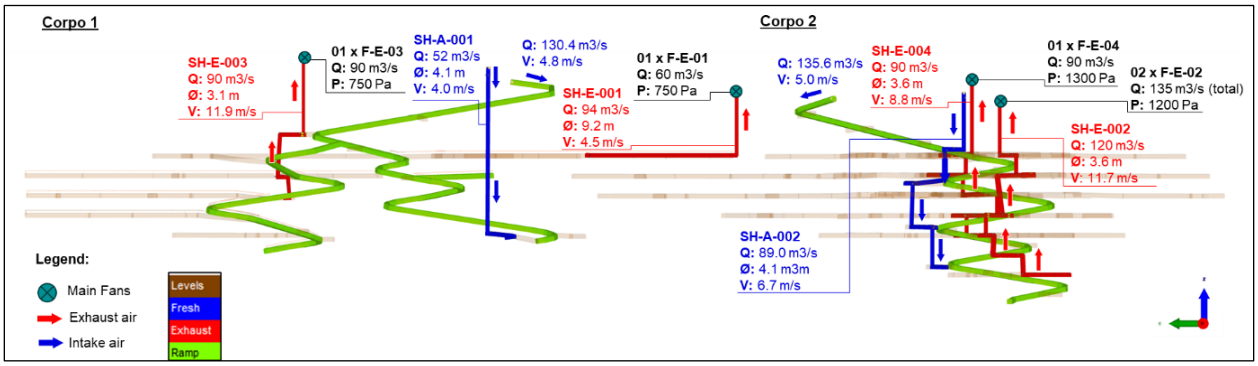
Source: Howden (2025)

Figure 16-76: Year −1 Ventilation System

16.10.5 Mine Production Stage—Ventilation Planning

Year 1

For the mine production-stage start, significant changes will be required in the ventilation system in Sector 1. Air will be drawn through the F-E-01 fan, installed at the surface collar of SH-E-01. Additionally, for primary development and preparation workings, a new intake shaft, SH-A-01 (from Level 156 to surface), will be required to maintain an adequate ventilation duct length for the mine deepening and to provide an emergency escapeway for Sector 1. The start-up of Satellite 1 ore production will require the SH-E-003 exhaust fan to operate at full capacity (100% rpm), with the duty point for F-E-03 calculated based on this year. Sector 2 will require installing a second F-E-02 on the SH-E-02 collar (surface) after shaft excavation finishes during this year, to work in parallel with the F-E-02 previously installed. With the completion of this infrastructure, the total airflow requirement will be reached. Figure 16-77 shows the main ventilation system features for this period.



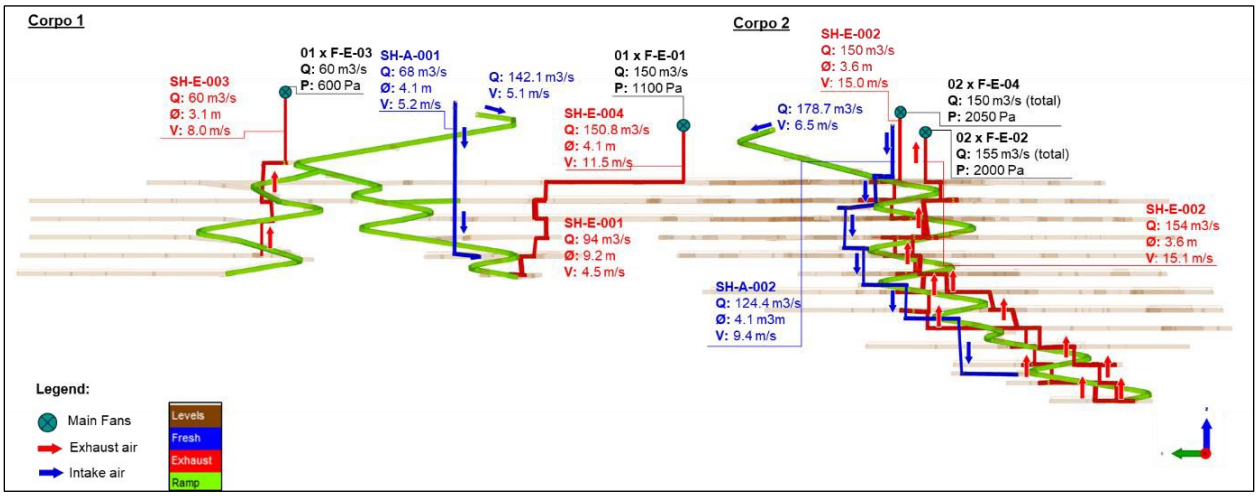
Source: Howden (2025).

Figure 16-77: Year 1 Ventilation System

Years 2 and 3 Ventilation System

For Years 2 and 3, minor infrastructure changes in the ventilation system will be needed, as ventilation circuits direction (intake and exhaust) will be maintained. Sector 1 ore production starts, fan F-E-01 will operate at full capacity (100% rpm) and as Satellite 1 reserves are depleted (Year 3), fan F-E-03's rotation frequency will be gradually decreased.

In addition, in Year 2, Sector 2 will require installation of the second fan on the SH-E-04 collar (surface) after shaft excavation finishes; it will work in parallel with the previously installed fan. With this change, Sector 2's 300 m^3/s ventilation system capacity will be reached. Figure 16-78 shows the main ventilation system features for Year 3.



Source: Howden (2025).

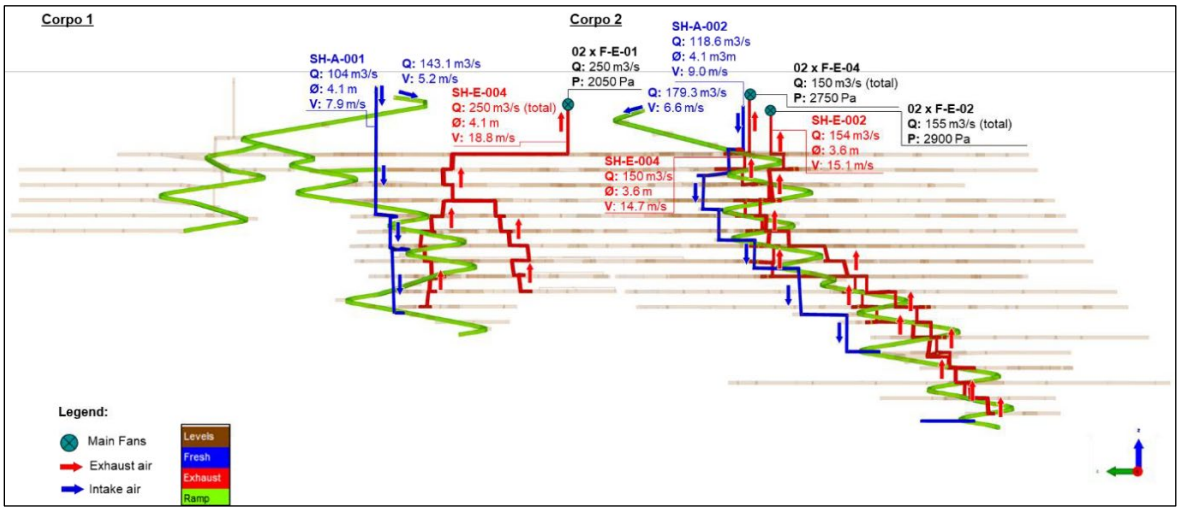
Figure 16-78: Year 3 Ventilation System

Years 4 to 6 Ventilation System

During Years 4 to 6 the ventilation system reaches full design capacity in both sectors. Fan F-E-03 will be turned off, and the SH-E-03 ventilation circuit will be temporarily disabled.

To increase the Sector 1 ventilation capacity, in Year 4 the second F-E-01 fan will be installed on the SH-E-001 collar (surface) after shaft excavation finishes. With this infrastructure completion, the main ventilation infrastructure requirement is reached in each sector.

Sector 2 reaches the maximum airflow requirement during this period, and the main fans in this sector will operate at full capacity (100% rpm). F-E-02's duty point was calculated considering Year 6. Figure 16-79 shows the main ventilation system features for Year 6.



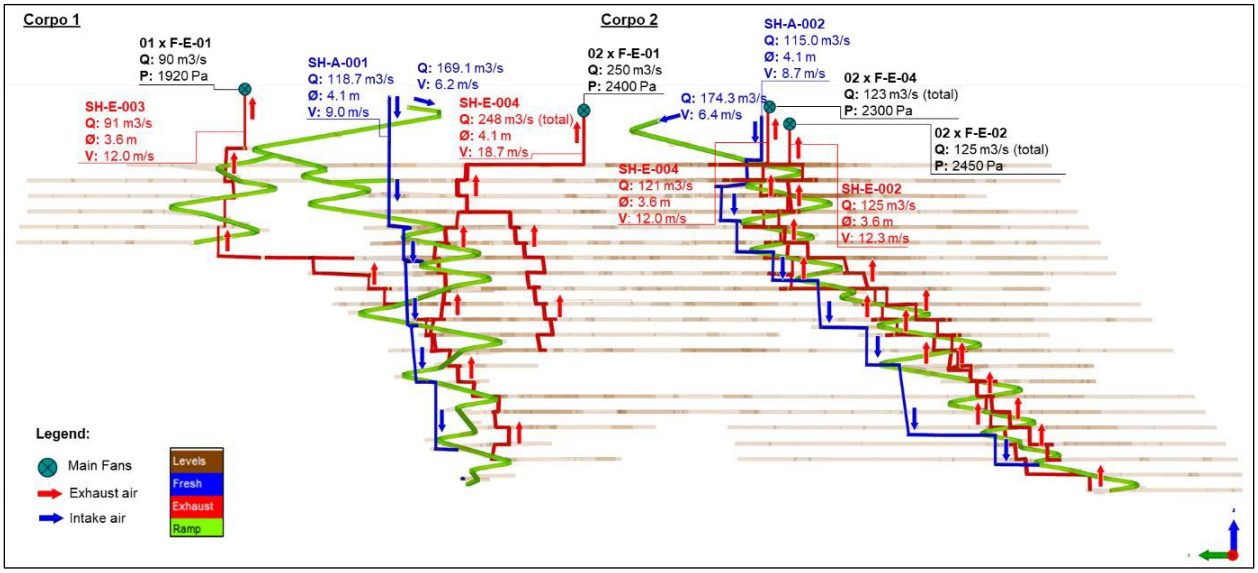
Source: Howden (2025).

Figure 16-79: Year 6, Ventilation System

Years 7 to 9 Ventilation System

During this stage the airflow requirement reaches its peak (487 m^3/s), and Sector 1 will reach full ventilation capacity through an integration with SH-E-003 via a connection with Level 116, which requires additional development to be completed in Year 7. Fan F-E-03 will restart operations to increase the airflow capacity up to 330 m^3/s for Sector 1.

The Sector 2 ventilation system will not see any change, and as airflow will gradually decrease into Year 9 (Figure 16-80), exhaust capacity will be regulated through fan rpm.

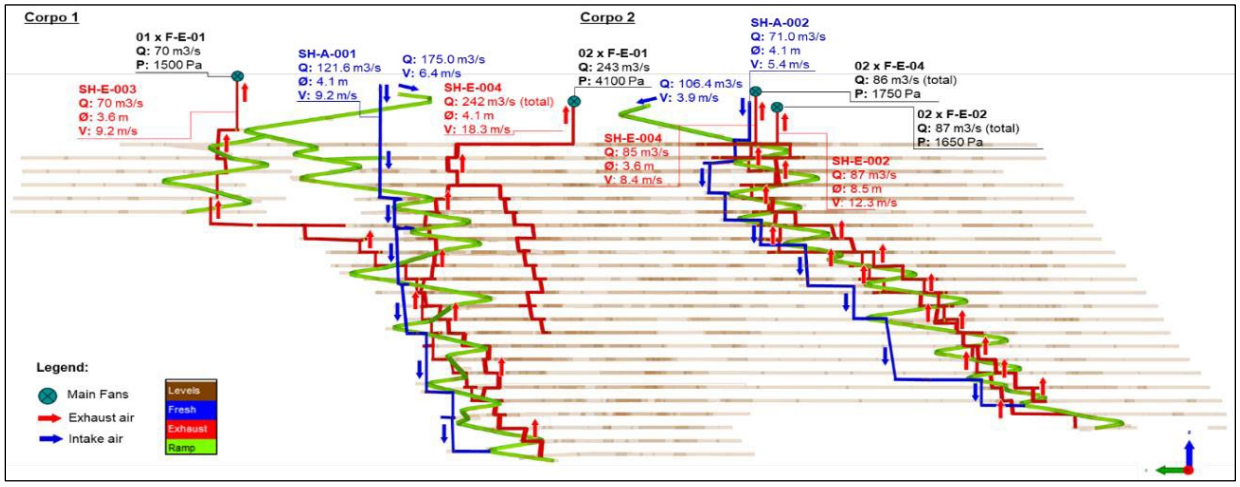


Source: Howden (2025).

Figure 16-80: Year 9 Ventilation System

Years 10 to 18 Ventilation System

During this stage the ventilation system will see no major changes, as Sector 2 production and development will gradually decrease. Sector 1 development will be completed in Year 16, and it will have the highest airflow requirement until that year. For that reason, F-E-01's duty point was calculated considering that Year 16 represents Sector 1's highest airflow and resistance forecast during the LOM. Figure 16-81 shows the main ventilation system features for this period.



Source: Howden (2025).

Figure 16-81: Year 16 Ventilation System

16.11 Electric Power System

The Project electrical design has been developed with a focus on reliability, redundancy, and scalability. The system must not only address current operational requirements but also be adaptable to increasing demands as the mine expands to deeper levels.

16.11.1 Electrical Loads in Underground Mining

Most of the electrical demand in the underground mine will be driven by:

- Main and secondary ventilation fans, which constitute the largest continuous load operating 24 hours a day, 7 days a week, to maintain safe air quality throughout the workings.
- Dewatering pumps, critical for water management and safety, require progressively more energy as pumping depths increase with mine development.
- Air compressors, essential for supplying pneumatic energy to various underground tools and auxiliary equipment.
- Refuge stations, which require uninterrupted power to maintain life-support systems, communication equipment, and lighting.
- General underground lighting, installed in key access routes, working areas, and safety stations.

16.11.2 Surface Substation

The planned surface substation will receive power from the regional transmission grid through a high-voltage overhead line, and will step it down from 138 kV to 13.8 kV. The energy will then be distributed internally between the mine and the processing plant via overhead lines, with each facility having its own step-down substation, to supply medium voltage at 440 V.

The electrical substation receives power from the regional transmission grid through a high-voltage overhead line and steps it down from 138 kV to 13.8 kV. The energy will then be distributed internally between the mine and the processing plant via overhead lines, with each facility having its own step-down substation to medium voltage at 440 V (Figure 16-82 and Figure 16-83).

For the underground mine, two dedicated substations and fans will be installed on the surface near the NATM portals.

The first substation will be responsible for supplying the ventilation system, as the main and secondary fans represent one of the largest and most continuous power demands at the mine. The second substation will supply all other underground loads—production equipment, pumping stations for mine dewatering, refuge chambers, compressors, and lighting. This separation of supply ensures that ventilation, a critical safety system, remains independent from the variable operational loads of the mine, thereby improving overall reliability, redundancy, and operational resilience.

The substation design incorporates:

- Power transformers sized to handle both current demand and projected future loads as the mine deepens and production expands
- Medium-voltage switchgear and protection systems, ensuring safe operation and quick isolation in case of faults
- Integration for real-time monitoring, data collection, and remote operation of all major electrical components
- Redundancy in key equipment, which allows scheduled maintenance or unexpected repairs without compromising the continuity of power supply.

This facility will serve as the central hub of the mine’s electrical system, distributing power to underground feeders and auxiliary surface facilities. The system has been designed to meet the dual objectives of operational efficiency and safety, while also ensuring flexibility to accommodate future increases in electrical demand.

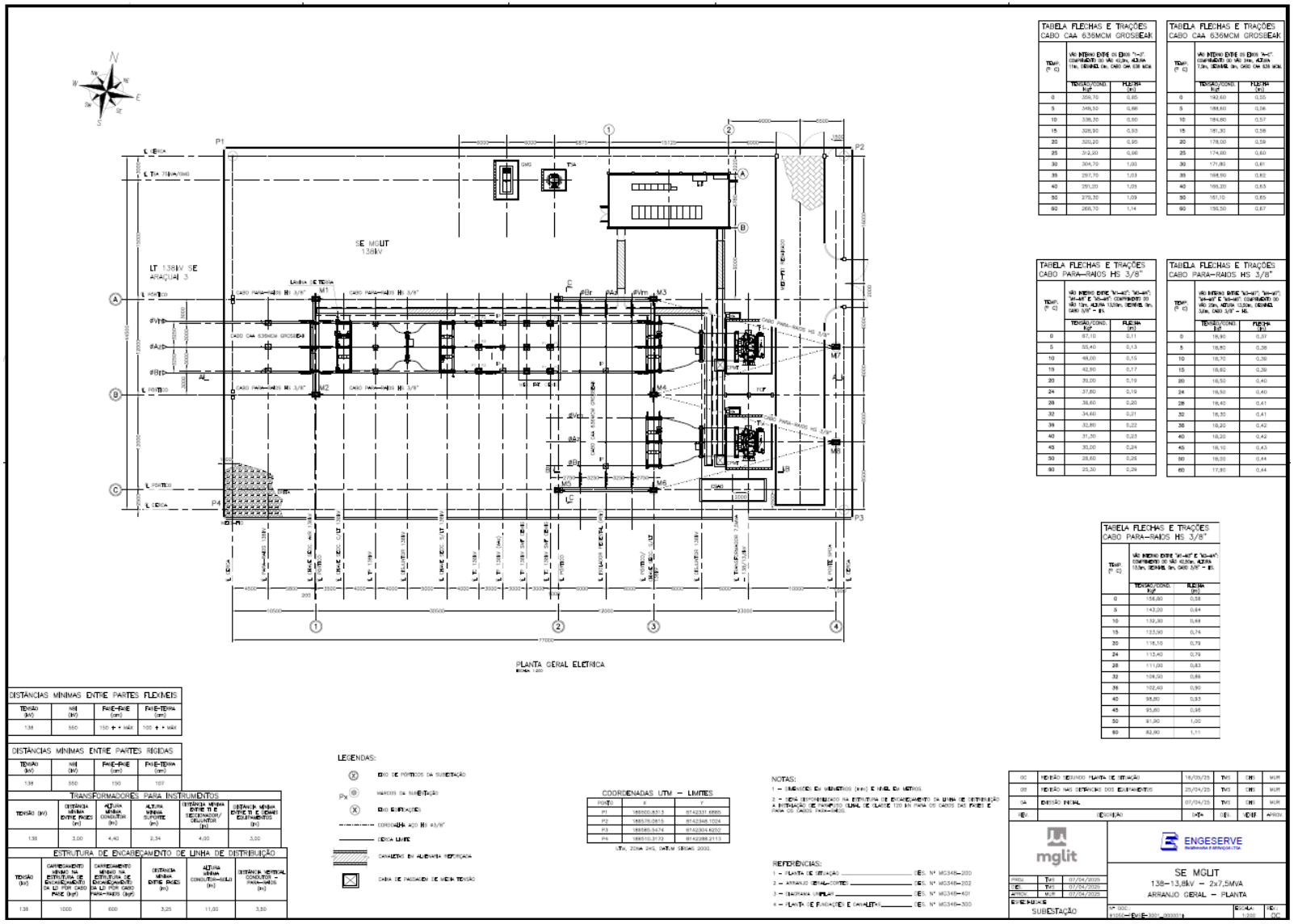


Figure 16-82: Electrical Substation

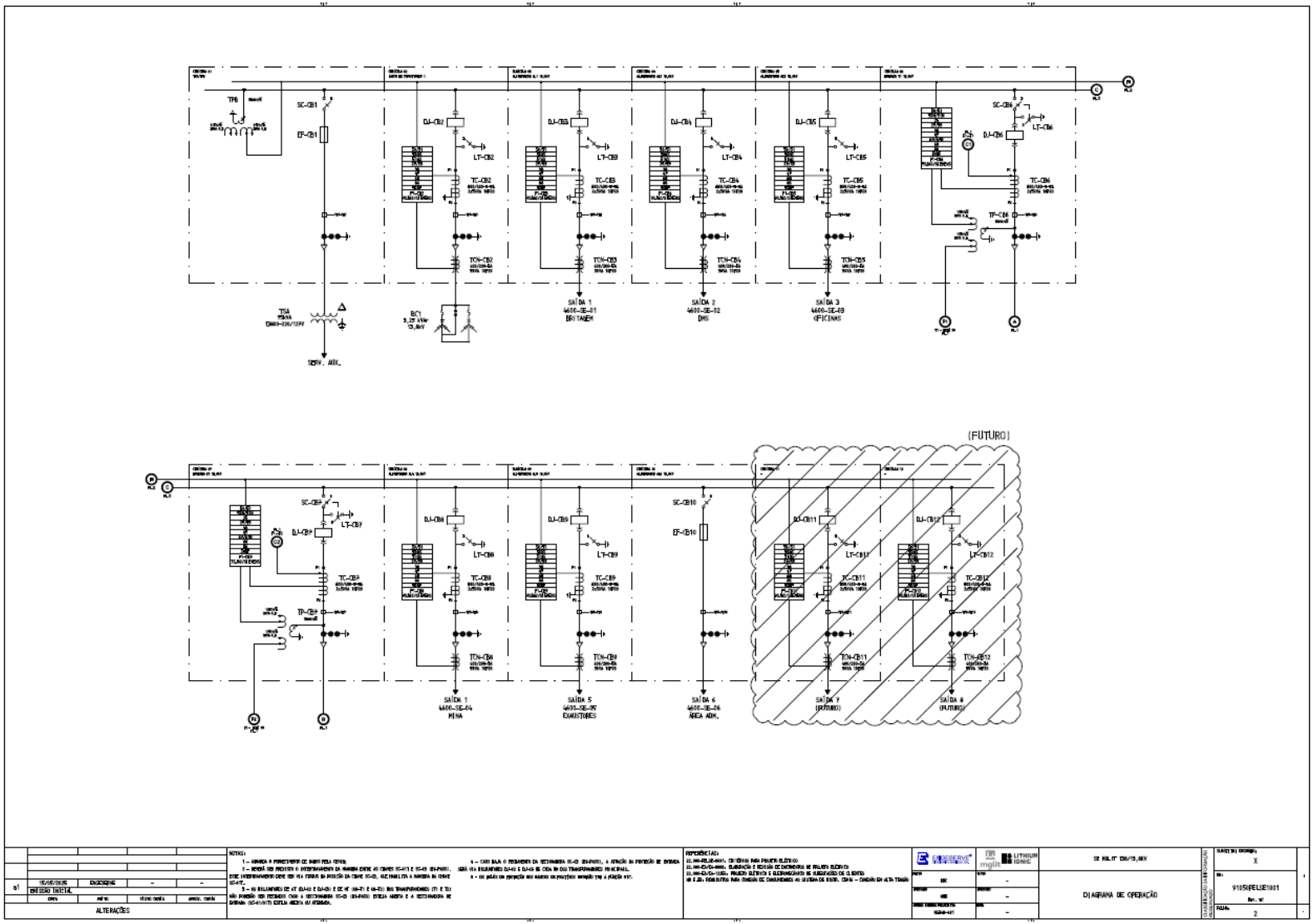


Figure 16-83: Electrical Power Step-Down Diagram

16.11.3 Underground Substations

As mining progresses deeper, electrical distribution efficiency becomes critical. To reduce transmission losses and voltage drops, 440 V underground substations will be installed progressively. These units will:

- Step down medium-voltage supply to levels suitable for equipment operation
- Be strategically located near production areas to minimize cabling distances
- Provide localized redundancy and the ability to isolate sections of the network for maintenance
- Allow staged expansion of the electrical network in line with mine development.

Ventilation System and Electrical Demand

Ventilation is the single largest consumer of electrical power in the mine. Fresh air is introduced through dedicated intake portals and shafts, distributed via drifts and raises, and exhausted through return airways.

- Main fans: installed on surface return airways, operating continuously to provide the required volume flow rate as defined in the Mine's LOM plan. These fans are large-diameter, variable-speed units designed to adapt to changing airflow requirements as the mine deepens.
- Secondary fans: located underground to boost airflow to active headings and stoping areas. These typically operate on a demand basis, turning on and off in coordination with production schedules.

The electrical design ensures that ventilation circuits can handle peak requirements with redundancy. Multiple fans are installed in parallel where necessary, allowing staged operation to optimize energy efficiency. Fan control systems are integrated with the electrical network to enable variable-frequency drive control, reducing energy consumption during periods of lower demand.

Dewatering System and Electrical Demand

Groundwater inflows into the mine present a significant challenge and must be managed through a cascading dewatering system powered by the electrical network. The system is designed as follows:

- Primary pump stations are installed at the lowest active mining levels. These pumps lift water vertically to an intermediate pump station at a higher elevation.
- Intermediate pump stations receive the water and continue lifting it upwards. By cascading water in stages, each station operates within an efficient head range, minimizing pump wear and optimizing power usage.
- This sequence of pumping continues through multiple levels until water reaches the main surface dewatering station.
- From the surface, water is directed to the water treatment facility, where it undergoes sedimentation and treatment before being reintroduced into the closed-loop water system for reuse in the process plant and dust suppression.

Each pump station is electrically supplied by the underground substations, with dedicated switchgear and control systems to allow for automated start and stop sequences, remote monitoring, and emergency shut-off. The stations are designed with redundancy, typically installing multiple pumps in parallel (duty + standby) to ensure continuous operation in case of equipment failure.

The cascading design reduces the risk of a single-point failure: if one pump station goes offline, temporary storage capacity in sumps provides time to bring backup systems online without interrupting operations.

16.11.4 Service Water

The underground mine requires a reliable supply of service water for drilling operations, dust suppression, and other auxiliary activities.

16.11.5 Water Sources

The main source of service water will be a surface reservoir that will be continuously supplied by the site's raw-water system.

As a secondary source, water naturally accumulating in underground collection points will be pumped to the site raw-water system for treatment and consumption, then treated, and reused within the system, reducing freshwater intake and promoting sustainability.

Water Treatment

Before entering the distribution system, all water will undergo a treatment process that includes:

- Sedimentation to remove suspended solids
- Filtration to eliminate fine particles and ensure adequate water quality for use in drilling equipment and dust control.

This process ensures that the water meets operational and environmental standards.

Distribution System

Treated water will be distributed throughout the mine primarily by gravity, minimizing energy requirements.

The distribution network will be constructed using PVC pipelines, selected for durability, corrosion resistance, and ease of installation.

Underground storage facilities (tanks) will be strategically located to:

- Guarantee continuous supply in case of interruptions in the surface system
- Provide localized pressure stabilization.

At the working faces, service water will be delivered through overhead water lines, ensuring accessibility and operational efficiency.

16.11.6 Compressed Air

Compressed air is a vital utility for underground mining, supplying energy to pneumatic drills, and auxiliary systems, and instrumentation. The proposed system will primarily rely on electric-driven compressors installed on the surface, ensuring efficient, low-emission operation and reducing ventilation requirements underground.

System Configuration

To maintain reliability during power interruptions or maintenance shutdowns, two mobile diesel-powered compressors, each rated at approximately 286 ft³/min at 10 bar, will be available as backup units. One will be permanently connected to the surface network, while the second will remain mobile for deployment underground as needed. This dual-source configuration ensures operational continuity and flexibility during different phases of mine development.

Distribution

Compressed air will be distributed through steel piping along the main ramps and drifts, with outlets near working areas. Pressure regulators and safety valves will protect the system and adapt pressure to equipment needs. Preventive maintenance and monitoring of both electric and diesel compressors will ensure system reliability, efficiency, and continuous air supply to support safe underground operations.

Reliability Considerations

The use of two independent compressors provides redundancy, ensuring that failure of one will not result in total loss of the compressed-air supply.

Regular preventive maintenance schedules will be implemented to maximize equipment availability.

16.11.7 Communication

Effective communication is essential for safety, productivity, and coordination of underground mining activities.

System Architecture

The proposed communication solution is based on a private long-term evolution (LTE) telecommunications module (Band 28), ensuring robust connectivity and scalability.

This system integrates voice, data, and monitoring functions in a single network, improving operational efficiency.

Infrastructure Components

- 7/8" Tech RFX radiating cables, installed along main ramps and drifts, to ensure continuous signal coverage underground
- VHF radios operating in the 136 MHz to 174 MHz band range for direct communication between equipment operators and supervisors
- Repeaters and antennas to strengthen the signal in deeper or more remote parts of the mine
- Fibre optic backbone, providing high-capacity data transmission and redundancy
- Supporting hardware for installation, power supply, and environmental protection of communication nodes.

System Capabilities

- Voice communication: reliable two-way voice channels for daily operations
- Dispatching system: centralized control to coordinate equipment, crews, and material flows
- Microseismic monitoring: integration of geotechnical sensors for real-time seismic event detection and analysis
- Atmospheric monitoring: remote measurement of gases and ventilation parameters to detect hazardous conditions
- Worker tracking: real-time positioning system to monitor personnel location and enhance safety during emergencies.

Safety and Redundancy

The system provides continuous communication even in the event of localized failures, due to the redundant design of the fibre optic and LTE backbone.

The integration of monitoring systems (atmospheric + seismic) within the communication framework provides early warning of hazardous conditions, contributing to risk reduction.

16.11.8 Explosives Storage and Handling

Explosives

The underground mining operation will use emulsion explosives for development and ore production activities. Emulsion products are selected for their performance, handling characteristics and suitability for mechanized loading systems. All explosives management (procurement, storage, transport, issue and disposal) will comply with applicable national regulations, industry standards, and the mine’s own explosives management procedures.

Explosives Magazine

Bulk emulsion tanks and the principal explosives magazine will be on the surface in a controlled, secure area. The surface magazine will also accommodate blasting accessories and non-energetic supplies. The design of the surface storage area will incorporate segregation distances, blast walls, controlled

access, lightning protection, and environmental containment measures consistent with regulatory requirements.

Detonators and Initiation Systems

Detonators and initiation devices will always be stored and transported separately from bulk explosive charges. A dedicated, purpose-built detonator magazine will be provided on surface, physically separated from the main explosive tanks and magazines to eliminate the potential for sympathetic initiation.

Blast Outsourcing Services

It is intended that explosives, detonators, blasting accessories, specialist equipment, and blasting services will be supplied by an outsourced qualified contractor. Key contract requirements will include:

- Evidence of regulatory license
- Documented competence and experience in underground blasting operations
- Demonstration of quality and safety management systems, and insurance and indemnity provisions
- Disposal of surplus or expired product.

The contract will define responsibilities for storage, transport, inventory control, issue procedures, and disposal of surplus or expired product.

Security and Access Control

Explosives areas will be secured with multiple layers of protection, including controlled perimeter fencing, restricted entry points, camera monitoring system, and an access-control system tied to authorization lists. Only personnel with valid explosives handler qualifications and current medical clearance will be authorized to access explosives magazines. A chain-of-custody process will be implemented for every movement of explosive products from receipt to issue and return.

Inventory Management and Record Keeping

A strict inventory and records system will be maintained to track all explosives from arrival on site to consumption or disposal. Records will include batch identification, quantity, date of receipt, expiry date (where applicable), storage location, issue logs, return logs, and waste and disposal records. Regular stock reconciliations and audits will be conducted to ensure traceability and regulatory compliance. Inventory systems will be integrated with the mine's central materials management and compliance databases and be auditable for regulatory inspections.

Transport and Internal Logistics

Transport of explosives between surface storage and underground working faces will follow segregated routes and schedules designed to minimize interaction with personnel and other operational traffic. Transport equipment will be purpose-designed and maintained, with electrical components intrinsically safe or located outside classified zones. Movement of explosive materials underground will be

restricted to approved times and escorted by authorized personnel. Where possible, use of mechanized delivery systems (pumping emulsion via approved lines for bulk product) will be preferred to minimize manual handling.

Handling, Issuing, and Charging Controls

All handling, issuing, and charging activities will be managed under written procedures, with defined roles for the supplier, shotfirer, and blasting supervisor, as well as mine operations. Typical controls include pre-issue checks, two-person verification for explosives issue and return, positive identification of shot locations and charge designs, and a sign-off regime. Only certified shotfirers will be permitted to prepare and initiate blast patterns; all other personnel will be trained in exclusion zone awareness, sheltering procedures, and emergency response.

16.11.9 Fuel Storage and Handling

On-site diesel storage will be designed to comply with international standards and national regulatory frameworks governing flammable-liquid storage and handling. These standards will guide the design of tanks, berms, piping, fire protection, and monitoring systems.

The installation will have a storage capacity equivalent to approximately one week of supply, consisting of two tanks placed within a fully lined containment berm. The fuel-dispensing area will be adjacent to the tanks, with impervious paving and graded drainage to a containment dike. This configuration ensures that any accidental fuel spill or runoff is directed into a secure, controlled collection area, mitigating environmental contamination.

Safety and risk-management systems will be incorporated into the design and operation, including:

- Fire detection and suppression systems, such as fixed foam lines, portable extinguishers, and strategically placed hydrants
- Automatic shut-off valves and overfill protection devices on tanks and pumps
- Oil–water separators and spill recovery sumps integrated into drainage to treat any contaminated runoff before release or reuse
- Emergency response equipment, including spill kits, absorbent barriers, and mobile firefighting gear
- Lightning protection and grounding systems for tanks and transfer pumps to eliminate ignition risks
- Access control and surveillance, ensuring that only authorized personnel can enter the fuel facility.

The fuel station construction and operation will be provided under a lease agreement with a specialized third-party fuel supplier. Under this model, the supplier will deliver, install, and maintain the entire infrastructure—tanks, pumps, containment structures, and monitoring systems—in compliance with applicable standards.

16.11.10 Mining Quality Control

A comprehensive sampling and assay program is a critical component for ensuring grade control and supporting the overall resource and reserve models. For this operation, it is planned that approximately 1,200 samples per month will be collected from underground-mine activities. These samples will originate from a variety of sources, ensuring both representativeness and reliability of the data.

The primary sources of samples include:

- Productive development, where systematic channel samples will be taken to verify ore–waste contacts and assist in short-term production decisions
- Grade control drilling, which provides high-density data to refine local ore body geometry and grade distribution
- Exploratory drilling carried out underground, contributing to continuous resource definition and incremental upgrades of confidence categories
- Ore drive-sampling, where chip or channel samples are collected along the sidewalls of development headings to monitor lateral grade variations.

All collected material will be logged, labelled, and transported under chain-of-custody procedures to the mine's sample preparation facilities. Sample preparation will include drying, crushing, splitting, and pulverizing, following industry-standard protocols to ensure homogeneity and minimize contamination. QA/QC protocols will be implemented through the insertion of blanks, standards, and duplicates at regular intervals.

The analytical program will focus primarily on determining lithium oxide concentrations, as these are key indicators for ore quality control and downstream processing performance.

Integrating data with face mapping, resource re-evaluation, grade estimation, mining monitoring, and reconciliation will provide a robust framework for operational decision-making. This will enable the geology team to exercise effective grade control, minimize ore losses and dilution, and ensure that production aligns with the projected LOM schedule.

Furthermore, the reconciliation of mined and milled grades with block model predictions will allow continuous improvement of geological interpretations and resource models. Over time, the systematic collection of samples and integration with mine data will strengthen confidence in production forecasts, reduce variability, and improve metallurgical planning.

In summary, the sampling program represents a fundamental pillar of the Project's technical strategy. By combining consistent data collection, rigorous QA/QC, and integrated geological analysis, the mine will establish the necessary foundation to achieve reliable grade control, maintain product quality, and support long-term operational success.

16.11.11 Mine Personnel

Table 16-54 summarizes the mine personnel requirements for the underground project.

Table 16-54: Underground Mine Administrative and Operations Personnel from Years −2 to 18

	Year-2	Year-1	Year 1	Year 2	Year 3	Year 4	Year 5	Year 6	Year 7	Year 8	Year 9	Year 10	Year 11	Year 12	Year 13	Year 14	Year 15	Year 16	Year 17	Year 18
Technical Services Manager	1	1	1	1	1	1	1	1	1	1	1	1	1	1	1	1	1	1	1	1
Mine Planning Coordinator	1	1	1	1	1	1	1	1	1	1	1	1	1	1	1	1	1	1	1	1
Mine Planning Engineer	1	2	4	4	4	4	4	4	4	4	4	4	4	4	4	4	4	4	4	4
Mine Technician	0	2	4	4	4	4	4	4	4	4	4	4	4	4	4	4	4	4	4	4
Ventilation Engineering	1	1	1	1	1	1	1	1	1	1	1	1	1	1	1	1	1	1	1	1
Auxiliary Ventilation	4	4	4	4	4	4	4	4	4	4	4	4	4	4	4	4	4	4	4	4
Surveying Supervisor	1	1	1	1	1	1	1	1	1	1	1	1	1	1	1	1	1	1	1	1
Surveyor	1	2	4	4	4	4	4	4	4	4	4	4	4	4	4	4	4	4	4	4
Auxiliary Topography	1	2	4	4	4	4	4	4	4	4	4	4	4	4	4	4	4	4	4	4
Geo Manager																				
Geology Coordinator	1	1	1	1	1	1	1	1	1	1	1	1	1	1	1	1	1	1	1	1
Geotechnics Coordinator	1	1	1	1	1	1	1	1	1	1	1	1	1	1	1	1	1	1	1	1
Geotechnical Supervisor	1	1	1	1	1	1	1	1	1	1	1	1	1	1	1	1	1	1	1	1
Geotechnical Engineer	0	1	1	2	2	2	2	2	2	2	2	2	2	2	2	2	2	2	2	2
Geotechnical and Geologist Technicians	0	4	8	8	8	8	8	8	8	8	8	8	8	8	8	8	8	8	8	8
Geology Supervisor	1	2	2	2	2	2	2	2	2	2	2	2	2	2	2	2	2	2	2	2
Geologist of Production, Data Collection, Resource	1	3	3	3	3	3	3	3	3	3	3	3	3	3	3	3	3	3	3	3
Driller	0	1	2	3	3	3	3	3	3	3	3	3	3	3	3	3	3	3	3	3
Geotechnical Assistant	1	2	4	4	4	4	4	4	4	4	4	4	4	4	4	4	4	4	4	4
Drilling Assistant	0	1	2	3	3	3	3	3	3	3	3	3	3	3	3	3	3	3	3	3
Warehouse Assistant	0	1	2	2	2	2	2	2	2	2	2	2	2	2	2	2	2	2	2	2
Sampling Aid	2	4	8	8	8	8	8	8	8	8	8	8	8	8	8	8	8	8	8	8
Maintenance Manager	1	1	1	1	1	1	1	1	1	1	1	1	1	1	1	1	1	1	1	1
Auto Maintenance Coordinator	1	1	1	1	1	1	1	1	1	1	1	1	1	1	1	1	1	1	1	1
Supervisor of Maintenance	2	4	4	4	4	4	4	4	4	4	4	4	4	4	4	4	4	4	4	4
Eng Mec and Electrician	2	2	2	2	2	2	2	2	2	2	2	2	2	2	2	2	2	2	2	2
Planning of man.	1	1	2	2	2	2	2	2	2	2	2	2	2	2	2	2	2	2	2	2
Supervisor Mechanic	1	1	1	1	1	1	1	1	1	1	1	1	1	1	1	1	1	1	1	1
Maintenance Mechanic	8	12	16	20	20	20	20	20	20	20	20	20	20	20	20	20	20	20	16	16
Maintenance Assistant	8	12	16	20	20	20	20	20	20	20	20	20	20	20	20	20	20	20	16	16
Toolmaker	1	1	1	1	1	1	1	1	1	1	1	1	1	1	1	1	1	1	1	1
Rubber Repairer	2	2	2	2	2	2	2	2	2	2	2	2	2	2	2	2	2	2	2	2
Washer	1	2	2	2	2	2	2	2	2	2	2	2	2	2	2	2	2	2	2	2
Welder	2	2	4	4	4	4	4	4	4	4	4	4	4	4	4	4	4	4	4	4

	Year-2	Year-1	Year 1	Year 2	Year 3	Year 4	Year 5	Year 6	Year 7	Year 8	Year 9	Year 10	Year 11	Year 12	Year 13	Year 14	Year 15	Year 16	Year 17	Year 18
Lubricator	4	8	8	8	8	8	8	8	8	8	8	8	8	8	8	8	8	8	8	8
Supervisor Electrotechnical	1	1	1	1	1	1	1	1	1	1	1	1	1	1	1	1	1	1	1	1
Electrotechnical Supervisor	1	1	1	1	1	1	1	1	1	1	1	1	1	1	1	1	1	1	1	1
Electrician	4	6	8	10	10	10	10	10	10	10	10	10	10	10	10	10	10	10	10	10
Operations Manager	0	0	1	1	1	1	1	1	1	1	1	1	1	1	1	1	1	1	1	1
Mining Coordinator	1	1	1	1	1	1	1	1	1	1	1	1	1	1	1	1	1	1	1	1
Mining Supervisor	0	4	4	4	4	4	4	4	4	4	4	4	4	4	4	4	4	4	4	4
Mining Operational Engineer	0	3	3	3	3	3	3	3	3	3	3	3	3	3	3	3	3	3	3	3
Loader Operator	0	8	12	20	20	20	20	20	20	20	20	20	20	20	20	20	20	20	20	20
Truck Operator	20	28	48	56	64	64	64	72	72	72	76	76	76	76	76	76	72	72	64	64
Trainer	1	1	1	1	1	1	1	1	1	1	1	1	1	1	1	1	1	1	1	1
Mine Service Assistant	4	8	16	16	16	16	16	16	16	16	16	16	16	16	16	16	16	16	16	16
CCO Technician	0	4	4	4	4	4	4	4	4	4	4	4	4	4	4	4	4	4	4	4
Dev Manager	0	0	0	0	0	0	0	0	0	0	0	0	0	0	0	0	0	0	0	0
Dev Coordinator	1	1	1	1	1	1	1	1	1	1	1	1	1	1	1	1	1	1	1	1
Sup. Development	4	4	4	4	4	4	4	4	4	4	4	4	4	4	4	4	4	4	4	4
Jumbo Operator	12	16	16	20	20	20	20	20	20	20	20	20	16	16	16	12	0	0	0	0
Fandrill Operator	0	8	12	24	24	24	24	24	24	24	24	24	24	24	24	24	24	24	24	24
Scaler Operator	4	8	12	12	12	12	12	12	12	12	12	12	12	12	12	12	12	12	12	12
Dev Services Assistant	4	8	16	16	16	16	16	16	16	16	16	16	16	16	16	16	16	16	16	16
Infra Manager	0	0	0	0	0	0	0	0	0	0	0	0	0	0	0	0	0	0	0	0
Coord. Infrastructure	1	1	1	1	1	1	1	1	1	1	1	1	1	1	1	1	1	1	1	1
Sup. Infrastructure	2	4	4	4	4	4	4	4	4	4	4	4	4	4	4	4	4	4	4	4
Construction	2	4	8	8	8	8	8	8	8	8	8	8	8	8	8	8	8	8	8	8
Electrician	2	4	8	8	8	8	8	8	8	8	8	8	8	8	8	8	8	8	8	8
Operator Platform truck	4	4	4	4	4	4	4	4	4	4	4	4	4	4	4	4	4	4	4	4
Operator Tractor Platform	4	8	12	16	16	16	16	16	16	16	16	16	16	16	16	16	16	16	16	16
Operator Water Truck	8	8	8	8	8	8	8	8	8	8	8	8	8	8	8	8	8	8	8	8
Operator Truck Convoy	4	4	8	8	8	8	8	8	8	8	8	8	8	8	8	8	8	8	8	8
Operator Grader	4	4	8	8	8	8	8	8	8	8	8	8	8	8	8	8	8	8	8	8
Backhoe Operator	4	4	4	4	4	4	4	4	4	4	4	4	4	4	4	4	4	4	4	4
Aux Services Infra/bit sharpening	4	8	16	16	16	16	16	16	16	16	16	16	16	16	16	16	16	16	16	16
Total	**149**	**250**	**361**	**410**	**418**	**418**	**418**	**426**	**426**	**426**	**430**	**430**	**426**	**426**	**426**	**422**	**406**	**406**	**390**	**390**

16.12 Safety and Emergency

16.12.1 Safety and Emergency Measures

Escape Ladders

The ventilation intake raises at the Project underground mine will be equipped with ladders to serve as an escape route for the miners.

Escape ladders in underground mines are crucial safety features designed to provide a means of egress for miners in the event of an emergency, such as a fire, gas leak, or other life-threatening situations. These ladders will be strategically installed to facilitate a rapid and safe ascent to the surface or a designated escape route.

Key aspects of escape ladders in the underground mine include being:

- Located at some fresh-air ventilation raises that connect different levels of the mine, allowing miners to climb vertically to reach the surface or a safer location
- Constructed using materials that can withstand the specific environmental conditions of the mine, including corrosion resistance, to prevent deterioration
- Provided with adequate lighting to ensure visibility, especially in low-light conditions or during power outages
- Marked with clear and visible signage to guide miners to safety during an emergency.

Refuge Chambers

The installation of refuge chambers at strategic points in the mine is planned for the Project mine.

Refuge chambers play a critical role in enhancing the safety of underground mining operations, providing a secure place for miners to seek shelter and await rescue in the face of unexpected and potentially life-threatening events.

These chambers are specifically designed to offer protection from various hazards, such as fires, explosions, gas leaks, or other life-threatening situations that may occur in underground mining operations.

The Project underground mine will install refuge chambers with a 20-person capacity and 48 hours of independent support capacity, enough to shelter all workers during a shift inside the mine. They will be installed strategically so that each worker must travel no more than 400 m from the working face.

The number of personnel allowed underground each shift will be restricted by the capacity of the refuge chambers and displayed at all the mine entrances.

Key features and aspects of the Projects' refuge chambers include:

- Accessibility
  - Strategically located throughout the mine to ensure easy access for miners in case of an emergency.
  - Situated along main escape routes, at intersections, or in areas prone to higher risks.
- Design
  - Constructed to withstand the specific hazards present in the mines, including fire, blast pressure, and potential structural damage.
  - The walls, roof, and floor will be reinforced and insulated to provide a protective barrier against external hazards.
- Ventilation
  - Equipped with a reliable air supply system to ensure a continuous flow of breathable air.
  - Ventilation systems will include air filtration to remove contaminants and maintain air quality within the chamber.
  - Ventilation system failure will trigger an emergency procedure scenario with proper conditions for full personnel evacuation
- Communication Systems
  - Such as two-way radios or other devices to enable contact with the surface or other parts of the mine.
- Supplies
  - Refuge chambers will be stocked with essential supplies, including food rations, potable water, first aid kits, and other items to sustain occupants until rescue or evacuation is possible.
- Temperature
  - A temperature control system will be integrated to maintain a comfortable environment within the refuge chamber, as extreme temperatures can be a concern in some mining environments.
- Lighting
  - Adequate lighting will be provided within the chamber to ensure visibility and create a safe environment for occupants.
- Control Systems
  - Equipped with monitoring systems to keep track of the conditions inside and outside the chamber, including gas levels, temperature, and structural integrity.
- Training and Drills
  - Miners will receive training on how to use refuge chambers and participate in regular drills to ensure they are familiar with emergency procedures.
- Regulatory Compliance

  The design and installation of refuge chambers with Brazilian industry regulations and safety standards to ensure their effectiveness during emergencies.

17 RECOVERY METHODS

This section describes the processes used to treat the mineral ore extracted from the mines, to produce spodumene concentrate within market specifications.

The Project's objective is to process 1.3 Mt/a of ROM pegmatite ore, with spodumene as the product and source of lithium oxide.

The spodumene beneficiation plant will consist of the following unit operations:

- Primary crushing
- Secondary crushing and screening
- Ore sorter—being evaluated for inclusion after transition to underground mining
- Tertiary crushing and screening
- Wet screening
- Thickening and filtering fines (−0.6 mm) including water recycling
- Primary DMS treating the whole stream
- Two secondary DMS units for coarse and fine fractions
- Recrush of secondary coarse DMS floats
- Recrush DMS
- Magnetic separation of DMS sink products.

The objective is to produce a concentrate with a lithium oxide content of 5.20% and a ferric oxide content of less than 1%. The product stream is the non-magnetic fraction from the combination of DMS sinks from secondary coarse, secondary fines, and recrush.

Fine material (−0.60 mm) with a lithium content of around 0.95% and potential for future use through other concentration processes (such as flotation) will be generated and stored.

A block diagram of unit operations and the flowsheet are shown in Figure 17-1 and Figure 17-2.

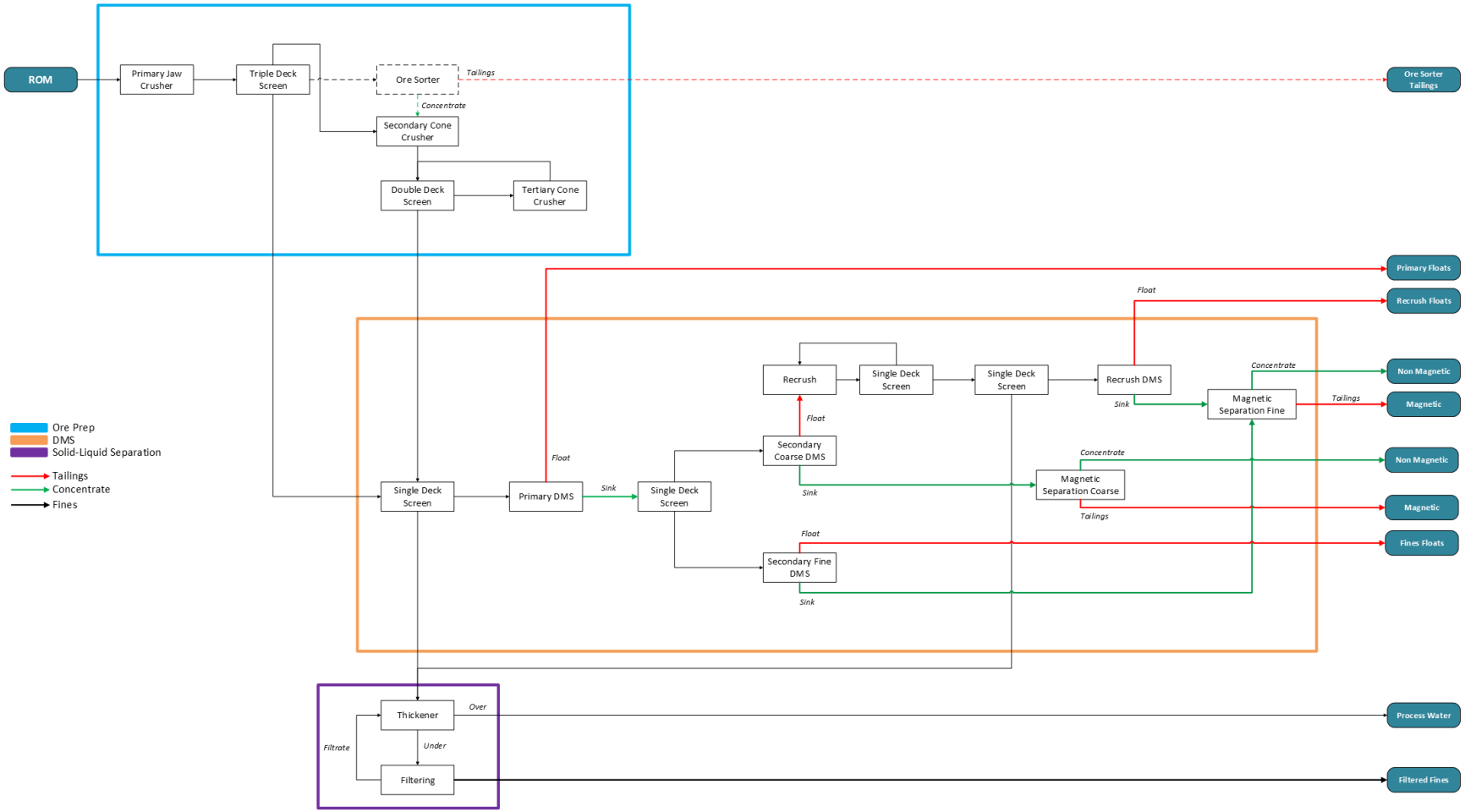


Figure 17-1: Bandeira Simplified Project Flowchart

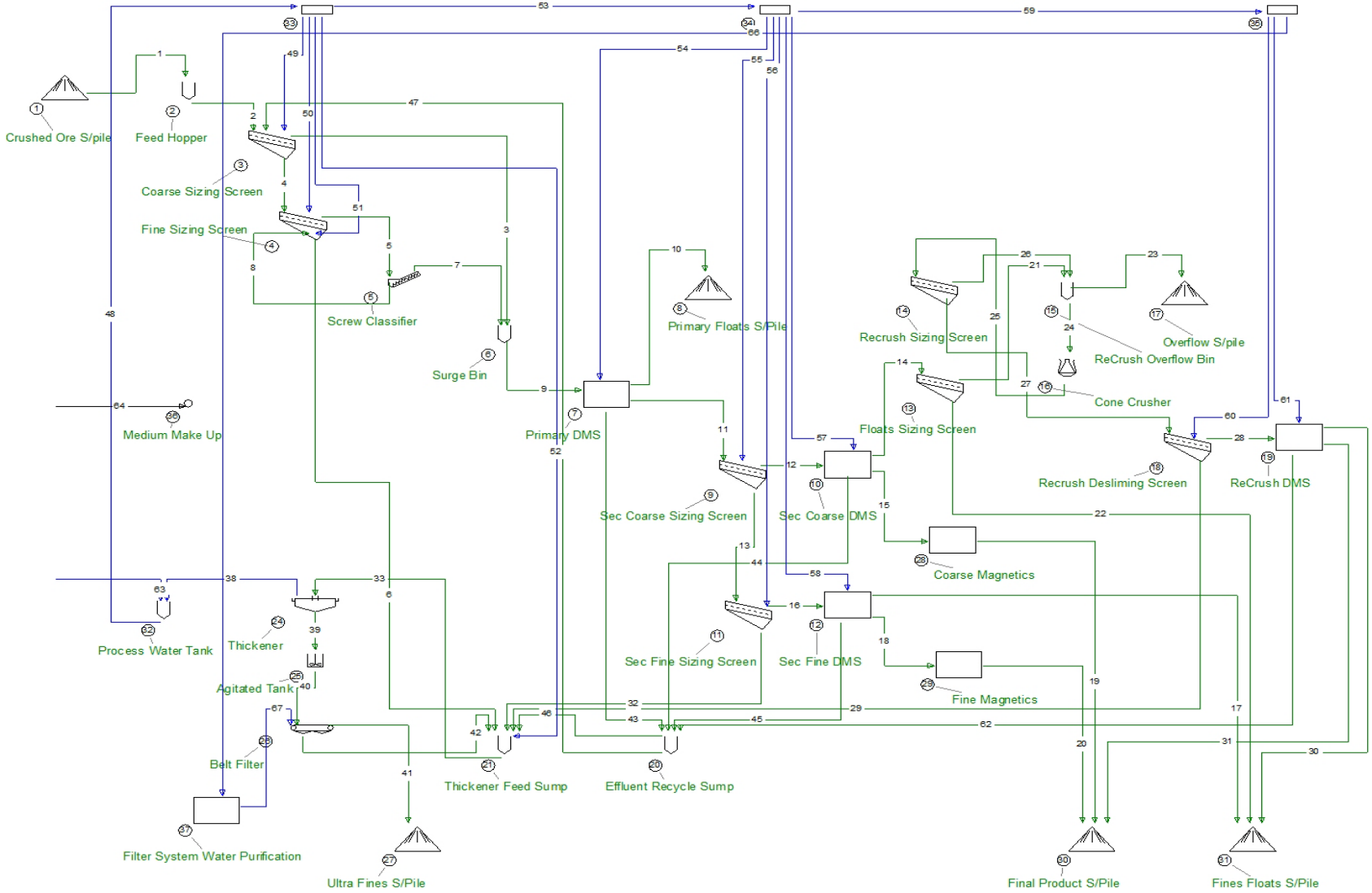


Figure 17-2: Project Flowsheet

The beneficiation plant operating-regime is given in Table 17-1.

Table 17-1: Operational Parameters

Description	Crushing	DMS Circuits, Thickening, and Filtration Circuits
Production Days per Year	365	
Hours per Day	24	
Days per Week	7	
Hours per Calendar Year	8,760	
Scheduled Operating Time (%)	66	85
Scheduled Hours per Year	5,782	7,446
ROM Feed (nominal capacity) (Mt/a)	1.50	
Nominal Hourly Rate of Primary Crushing (t/h)	260	
ROM Feed % Moisture	2	

The particle-size distribution of the ROM is shown in Table 17-2.

Table 17-2: ROM Particle-Size Distribution—Underground and Open Pit

Size (mm)	Underground	Open Pit
	Cumulative Passing (%)	Cumulative Passing (%)
800	100.00	100.00
700	100.00	95.20
600	100.00	90.50
420	96.30	85.60
337	92.30	81.20
230	79.30	76.30
195	68.50	69.20
150	53.50	55.30
130	47.50	51.90
100	39.30	46.80
75	32.60	36.40
50	26.30	28.40
38	22.50	24.50
25	19.80	17.50
19	18.50	14.80
0.85	14.50	9.60

Various scenarios were evaluated to define the best-option process flowsheet, including the use of ore sorting, recrushing secondary coarse DMS floats, and a magnetic-separation step for the final concentrate produced. The results of these scenarios are presented in the Table 17-3.

Table 17-3: Process Flowsheet Scenarios Evaluated

Process Flowsheet Scenarios	Concentrate Production (kt/a)	Mass Recovery (%)	Li_2O Grade (%)	Metallurgical Recovery (%)	Product Quality
Base Zero—no Recrush, no Ore Sorter, no Magnetic Separation	153.61	11.93	5.20	56.32	Iron off spec.
Scenario 1—with Recrush, no Ore Sorter, no Magnetic Separation	179.52	13.94	5.20	65.88	Iron off spec.
Scenario 2—with Recrush and Ore Sorter, no Magnetic Separation	174.44	13.53	5.20	64.00	On spec.
Scenario 3—with Recrush and Mag Sep (for all fractions), no Ore Sorter	177.90	13.81	5.20	65.29	On spec
Scenario 1—with Recrush, Ore Sorter and Magnetic Separation (for all fractions)	173.0	13.43	5.20	63.50	On spec

The best and recommended process flowsheet is Scenario 3, and the mass balance and lithium oxide distribution are presented in the Table 17-4 for this selection. After allowing for fines losses, the global lithium recovery of 5.2% concentrate is 65.3% into a mass of 13.8%.

Table 17-4: Average Mass Balance of Mine Life and Metallic Distribution in Relation to Li_2O

	No Ore Sorter		Magnetic Separation Operating with Full Size Fraction		
Ore Mine Dilution	Mass Flow (kt/a)	Mass Distribution (%)	Li_2O Content (%)	Li_2O (kt/a)	Li_2O Distribution (%)
ROM—Diluted 18%	1,288.00	100	1.10	14.17	100
Ore Sorter Rejects	0	0	0	0	0
Filtered Fines Total (-0.60 mm)	253.99	19.72	0.95	2.41	17.03
DMS Feed	1,034.01	80.28	1.14	11.76	82.97
DMS Primary					
DMS Sinks	423.94	32.91	2.52	10.70	75.50
DMS Floats	610.07	47.37	0.17	1.06	7.47
DMS Secondary					
DMS Coarse Feed	289.00	22.44	2.37	6.85	48.32
DMS Coarse Float	196.52	15.26	1.18	2.33	16.43
DMS Coarse Sink	92.48	7.18	4.89	4.52	31.89
DMS Fines Feed	134.94	10.48	2.85	3.85	27.18
DMS Fines Sinks	61.40	4.77	5.58	3.43	24.19
DMS Fines Floats	73.54	5.71	0.58	0.42	2.99
DMS Recrush					
DMS Recrush Feed	176.87	13.73	1.20	2.12	14.95
DMS Recrush Fine	19.65	1.53	1.07	0.21	1.48
DMS Recrush Sinks	35.37	2.75	3.95	1.40	9.87
DMS Recrush Floats	141.50	10.99	0.51	0.72	5.08
Mag Sep					
Mag Sep Feed	189.25	14.69	4.94	9.34	65.95
Magnetic	11.36	0.88	0.82	0.09	0.66
Non Magnetic	177.90	13.81	5.20	9.25	65.29
Final DMS Product	**177.90**	**13.81**	**5.20**	**9.25**	**65.29**

17.1 Crushing

While the open pit is operating, for approximately the first 12–18 months the ROM will have a top size of 800 mm, which the C130 primary crusher is sized to cope with. (Figure 17-3).

When the transition is made to underground mining, the open-pit ore will have a top size ~600 mm (d50 close to 150 mm) and will be stored in a stockpile with a capacity of 5,200 tonnes, corresponding to 24 h of operation. ROM ore will be reclaimed by a front-end loader and fed to the primary crusher.

A metal detection system will be provided for on the primary crusher product conveyor that goes to feed a triple deck screen. A triple deck screen has been allowed for to cater for a future ore sorter installation. The +16 mm will pass to the secondary crusher, and the fraction −16 mm will go to the crushed ore stockpile.

All of the material passing through the secondary crusher passes by another double-deck screen. The +16 mm fraction passes to the tertiary crusher. The −16 mm fraction passes to the crushed ore stockpile (Figure 17-4). The tertiary crushed product is recirculated over the double-deck screen mentioned above.

The final conveyor to the crushed ore stockpile will be equipped with a belt scale for inventory control, and a cross-belt sampler will also be installed on the same belt.



Figure 17-3: Primary Crushing Circuit



Figure 17-4: Example of Modular Crushing and Classification Plant

17.2 Fines Thickening and Filtration (−0.60 mm)

The fine material (−0.60 mm) from Derrick stack sizer will be pumped to a thickener to thicken the underflow for filtration (Figure 17-5 and Figure 17-6). The thickener overflow reports to the process-water circuit. The underflow of the thickener, containing 55% solids, will feed the filtration.

Filtration will be carried out through a vacuum-belt filter (area 27 m²). The filter cake, with a moisture content of 15% and grade of 0.95% Li_2O, will be stacked in a stockpile with approximately 14 hours residence time, and a sampling point will be provided to generate a metallurgical sample. The filtrate will be pumped back to the thickener for water recovery.

A modular mixing and dosing system is being installed for the supply of flocculant, as required, to the thickener and filter.



Figure 17-5: Thickening Equipment

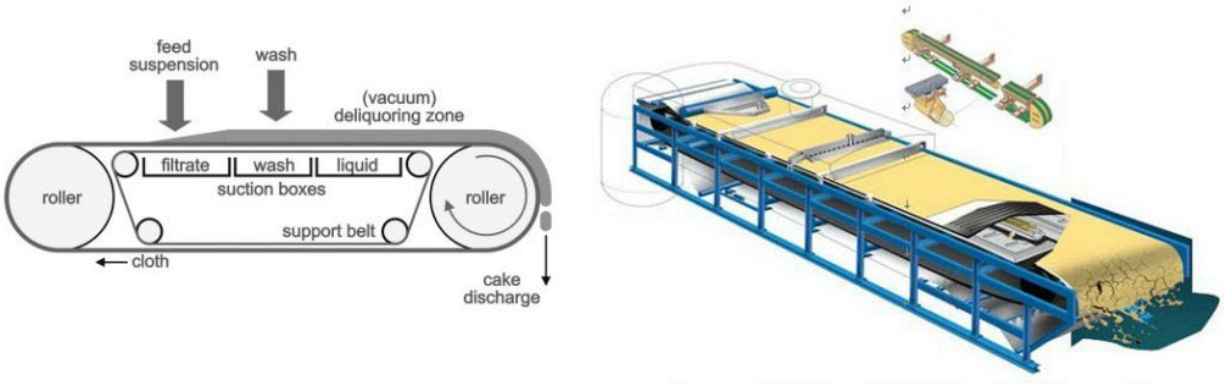


Figure 17-6: Belt Filter

17.3 DMS Modular Circuits

The surge bin for the primary DMS module feed will hold about 40 m^3, corresponding to around 20 minutes of capacity. Figure 17-7 shows a 3-D vision of the entire DMS concentration plant.

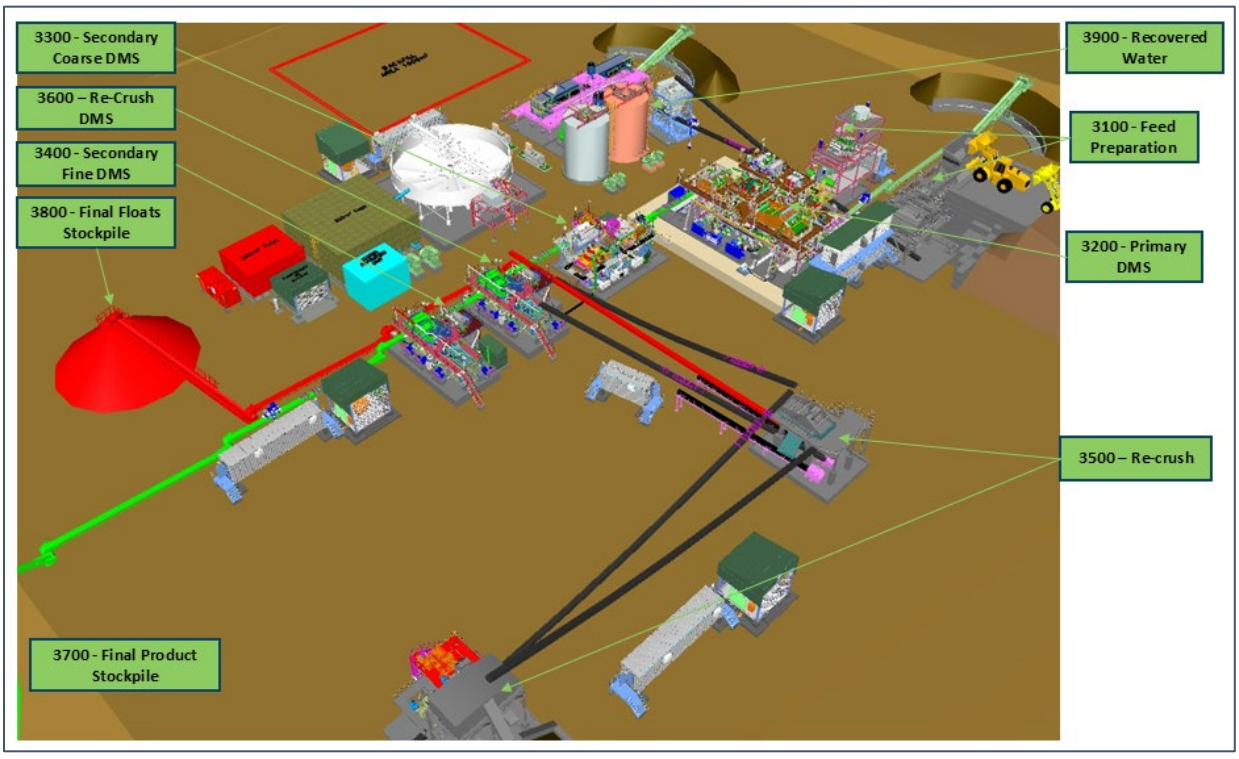


Figure 17-7: 3-D View of the Concentration Plant

The primary DMS plant feed will be withdrawn from the feed bin at a controlled rate and fed to the primary DMS. The floats from the primary DMS will be transferred to the final tailings stockpile. Primary sinks will feed the secondary coarse sizing screen to produce a coarse +3 mm stream for the secondary coarse DMS and the −3 mm material will be pump-fed to the secondary fines DMS. Belt weighers will be fitted on the primary floats and sinks streams.

Density will be controlled and monitored through nuclear density-meters. Water-addition points will also be provided, as well as densifying cyclones and densifier tubes to adjust the density of the dense media.

The −16/+3 mm materials from the screen oversize will feed the secondary coarse DMS. The sinks from this DMS will report to the magnetic separator feed.

Coarse secondary DMS floats will report to the floats sizing screen. This float sizing-screen oversize will be blanked for initial operation, and all material will be fed to two roll crushers. The crushed product passes to the recrush sizing screen, +5 mm oversize from this screen is recycled to the crushers, thus closing the crushing circuit. The −5 mm from the sizing screen is conveyed to the recrush desliming screen that will scalp out −0.6 mm material, and −5/+0.6 mm material will then be fed to the recrush DMS. The −0.6 mm material from the desliming screen will be pumped to the thickener.

Sinks from both the secondary fines and recrush DMS plants will join the secondary, coarse DMS sinks and will be used as magnetic separator feed. The fines DMS's joint float tailings will be conveyed to the fines stockpile.

The dewatered DMS concentrates will go to belt conveyors and be stacked with an average moisture content of 4.5% (6% for the fine fraction and 3% for the coarse fraction). The pile will have an approximate capacity of 450 m^3, ensuring 33 hours of continuous operation. The concentrate will contain 5.2% Li_2O. Metallurgical sampling will be provided for the concentrates through cross-belt samplers installed on the stacking conveyors. Scales will be provided to monitor production.

17.4 Chemical Laboratory

The beneficiation plant will be equipped with a chemical laboratory for preparing and analyzing metallurgical samples. The laboratory demand is expected to be:

- Mine and geology samples: 1,000/month
- Processing plant samples: 1,000/month.

Note that 100 samples/month related to environmental control will not be analyzed at the plant site, and must be transported for analysis at a certified laboratory.

The Project laboratory will occupy an area of approximately 30 m by 30 m, and the concept is to house the sample preparation and analysis equipment in modules. The modules will be installed on concrete floors in a shed.

Tests, analyses, and preparations to be carried out are:

- Physical preparation for plant, geology, and mine operational control samples: receipt and recording; crushing at P_{75} 2 mm; quartering to get an aliquot of 150 g at P_{85} 200 mesh.
- Physical preparation of plant samples for heavy-liquid separation (HLS) tests: receiving and checking; 15.9 mm; 12.7 mm, 9.5 mm, 6.3 mm, 3.4 mm, 1.7 mm, and 0.6 mm screening; homogenization and quartering in rotary splitter for aliquot analysis.

- Physical preparation of samples for granulometry: particle-size analysis in different meshes (according to the plant's comminution process).
- HLS tests using separator hoppers or beaker, depending on the particle size of the sample. The monthly quantity foreseen for the HLS tests is 10 samples per month.

Mineralogical analysis is performed using Fourier-transform infrared spectroscopy (FTIR) technology with Bruker Alpha FTIR equipment or similar equipment.

Quantification of the following minerals is planned:

- Spodumene
- Petalite
- Tantalite
- Quartz
- Feldspar
- Mica
- Chlorite.

The percentages obtained in the mineralogical analysis can also be reported for the chemical analysis, which is calculated based on the stoichiometry of the chemical elements in the minerals.

Chemical analysis of lithium and iron is planned by means of sample decomposition through fusion with sodium peroxide, acid dissolution, and reading by atomic absorption spectrometry (AAS).

The estimated consumption of utilities for the laboratory water and electricity is:

- 5,000 L water tank with a flow rate of 5,000 L/d
- 190 kVA availability.

The liquid effluent generated in the laboratory will be neutralized to be treated later by the wastewater treatment plant (WWTP).

18 PROJECT INFRASTRUCTURE

18.1 Plateaus and Accesses

The on-site roads were designed in accordance with the Brazilian Standards of the Brazilian National Standards Organization (ABNT). For cases not prescribed in the ABNT Standards, the following standards may be used: Brazil's National Department of Transportation Infrastructure (DNIT), Brazil's Department of Highways (DER), and the United States American Association of State Highway and Transportation Officials (AASHTO).

The vehicles considered for the roads in plant and administrative areas of the site for the purposes of design are the three-quarter ton (3T4) and 2-litre 4-cylinder (2C) trucks. It is emphasized that the definition of the design vehicle covers other vehicles, such as buses and cars. For the final product stockpile, scale and dispatch was considered a 9-axle B-train.

As the Bandeira's project area covers a section that crosses a local river, a 56 m-long and 10 m-wide concrete bridge is planned to cross the Piauí River from the site entrance (west side) to the plant and mine area (east side).

18.2 Earthworks

The earthworks mass distribution plan was developed to provide economical solutions seeking a balance between the cut and fill material according to the soil classification and volumes involved, focusing on reducing transport distance and minimizing exhaust emissions from trucks during earthmoving activities. The earthworks strategy is reusing the material during the internal access construction phase, and if any removed soil from the cuts still remain, this material will be used for the piles plateaus within the MGLIT's area.

The requirements for carrying out the earthworks are:

- Removing the top 1.30 m of the natural terrain (soil and organic matter) in 0.3 m cuts, without compaction, then executing the fills defined in the earthwork project to restore the level required
- Compacting in layers no more than 20 cm thick. If manual compaction is necessary due to access restrictions, the layer thickness should not exceed 10 cm
- Minimum compaction degree of 98% using the Proctor standard
- Minimum California Bearing Ratio (CBR) of the final layer is 7%
- Maximum permissible moisture content deviation is ±1.0% from its optimum value determined in compaction tests
- Minimum of six passes to ensure compaction.

In the case of rock cuts, to prevent vibration from moving the surrounding terrain and to reduce noise and dust, the cut areas should be broken and removed gradually, at an angle that allows constructing a

route consisting of a drainage layer and drains to collect and conduct water draining out of the body of the plateau area directing to the natural slope of the terrain.

All plant earthwork slopes will be designed and executed as follows:

- Cuts:
  - Horizontal (H) to vertical (V) slope ratio of 1.0:1.0
  - Maximum slope height of 6.0 m between berms. Maximum slope height of 8.0 m can be adopted when there is no area for a 6.0 m slope height
  - For intermediate berms a minimum slope width of 3.0 m will be adopted.
- Fills:
  - Slope of 1.5 H:1.0 V
  - Maximum slope height of 6.0 m between berms. In exceptional circumstances a maximum height of 8.0 m can be adopted
  - Intermediate berms have a minimum width of 3.0 m.

To integrate with the drainage, minimum sections with routes will be provided along the slope of each plateau area of the plant. The slope will facilitate the flow of surface water toward the natural slopes of the terrain.

If there is any soil left over that needs to be stored in a pile for future use, the slope and slope-height parameters of the piles general parameters will be:

- Embankment slope 2.0 H:1.0 V
- Maximum height between benches 8.0 m
- Bench width: 4.0 m
- Slope width: 16.0 m.

As previously mentioned, the plant and utilities area layouts were designed to reduce cut-and-fill volumes to balance the material removed during filling and reduce excess material.

Civil 3-D software is used to develop pile volumes for storage in natural terrain, where the data from the topographic and altimetric survey were loaded, as well as the results of the soil surveys.

18.2.1 Drainage and Stormwater

The stormwater drainage system will be located above ground whenever possible, to facilitate cleaning and maintenance. This system will follow the natural topography, directing stormwater through a speed reducer into a sump that will capture water from which water trucks will pump the water, to be used to wet roads to suppress dust and for irrigating vegetation on slopes. In the event of heavy rainfall, the sump will have an overflow that directs excess water to the Piauí River.

It is important to note that the water circulating in the DMS plant will not be sent to the stormwater drainage sump, as the plant has its own collection system that recirculates this wastewater.

In the area of the gatehouse and substation, the stormwater system will discharge water to the natural drainage after first passing through a speed reducer.

18.3 Process Plant, Operational Area, and Buildings

18.3.1 Architectural Concept

The architectural concept and construction system adopted for the Project aims to optimize the cost, maintain safety, ensure operability, and reduce construction time.

The buildings were designed with functionality and spatial optimization in mind, being dimensioned to adequately house all users and equipment necessary for the activities carried out in the building, considering the comfort and safety of employees, and complying with the requirements of the applicable standards.

There are two main concepts for buildings, guided by their intended use:

- Administrative buildings, primarily for human use: reception, office, locker room, clinic, cafeteria, etc.
- Industrial buildings, primarily for operational use: workshop, warehouse, battery room, tire repair, etc.

For the Project, modular construction will be adopted for the cafeteria, locker room, administrative building, and industrial support facilities. The workshop and warehouse will use steel and conventional structures; the support rooms for these buildings will be modular; and other areas will be tarpaulin-type roofing.

This type of construction is fast to assemble and reduces waste, as it is prefabricated, with a construction methodology of fitting and fixing, which simplifies the entire construction process so they can be ready for human occupation quickly, avoiding rented containers.

For the laboratory traditional masonry walls will be combined with a steel roof structure. For the explosive magazine, the construction method consists of a concrete foundation, a steel column structure with enclosure concrete block masonry up to the storage height. The walls must, mandatorily, be double, with a minimum spacing of 50 cm between them.

All administrative buildings are accessible in accordance with the ABNT standard NBR 9050—Accessibility to Buildings, Furniture, Spaces and Urban Equipment, prioritizing site safety according to the activities carried out there, defining guardrail installations, fall-arrest barriers, reinforced floors, and other requirements.

18.3.2 Project Areas, Descriptions, and Scope

Gatehouse and Parking Area

The gatehouse and parking plateau buildings (Figure 18-1) comprise the:

- Entrance substation
- Gatehouse and site security
- Uncovered bus and truck stop.

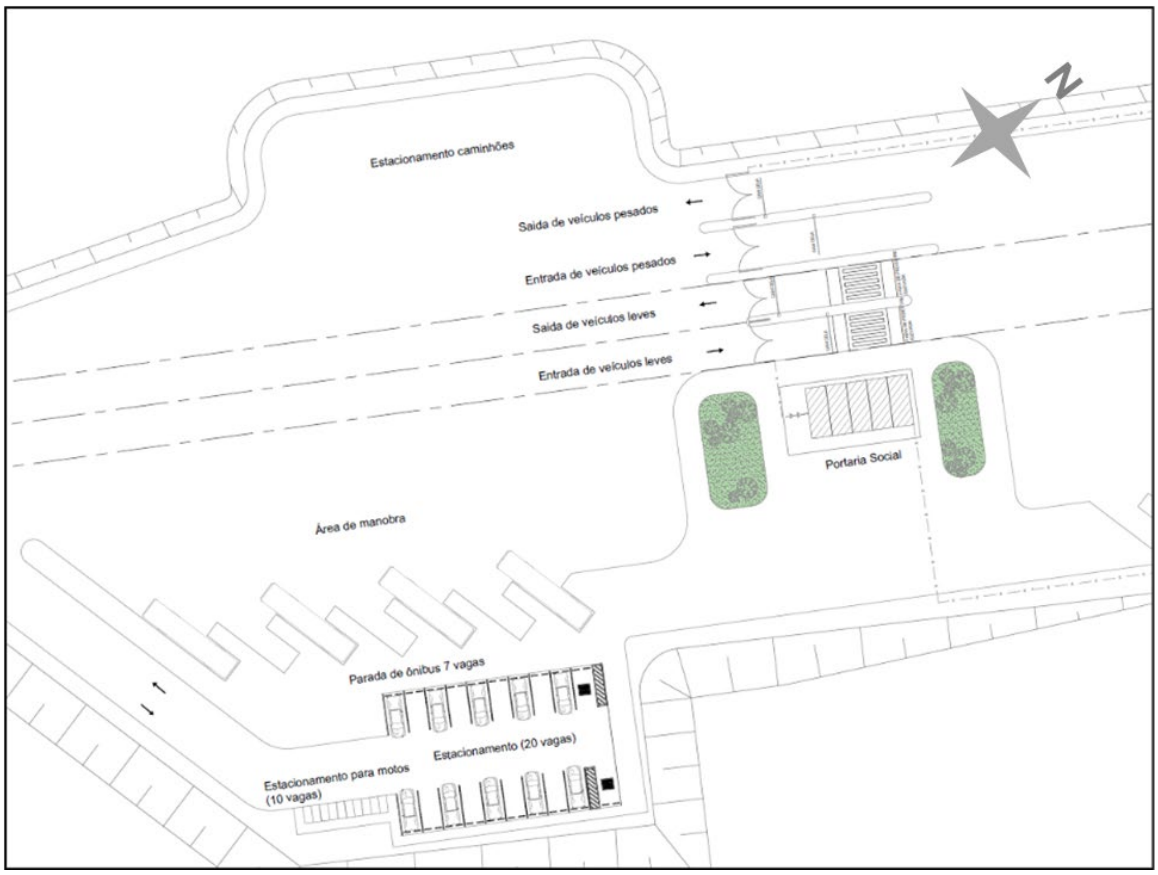


Figure 18-1: Gatehouse (Portaria Social) and Parking Area (Estacionamento)

The main gatehouse is intended to provide access control at a single point of the Project. The building provides an external, covered, access-control area with two turnstiles for personnel. The gatehouse will also control access for light vehicles and trucks on the site in two lanes, one for entry and one for exit—both controlled by gates.

The gatehouse building will consist of a guardhouse where the reception will operate with two workstations for the identification of visitors and suppliers; two more workstations for the security team; employee access control; sanitary facilities, pantry, cleaning material deposit (CMD), and electrical and IT room.

The bus stop will be dimensioned for parking seven buses (or trucks) plus 10 cars simultaneously.

Administrative Plateau

The administrative plateau buildings (Figure 18-2) comprise:

- Administrative office building
- Cafeteria
- Locker room

- Medical centre and fire brigade
- Common living and smoking areas.

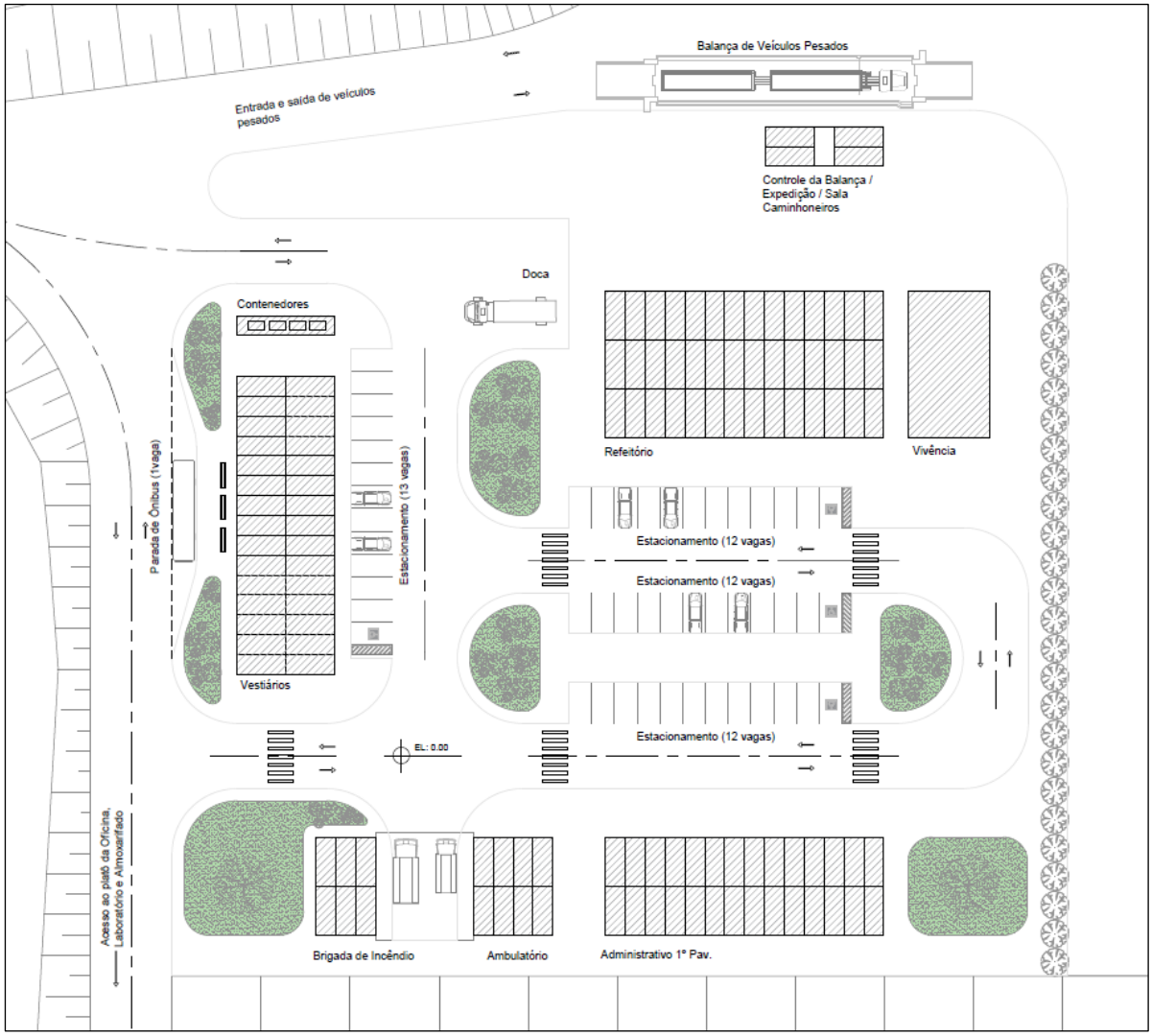


Figure 18-2: Administrative Plateau

Laboratory, Warehouse, Workshop, and Mine Support plateau

Figure 18-3 is a plan of the laboratory, warehouse, workshop, and mine support plateau buildings, comprising:

- Battery room
- Laboratory
- Intermediate waste depot (DIR)
- Plant and mine warehouse
- Plant and mine workshop for mine equipment and vehicles

- Tire repair and tire warehouse
- Gas station
- Core shed (may be located off site)
- Mine control room and operational meeting room.

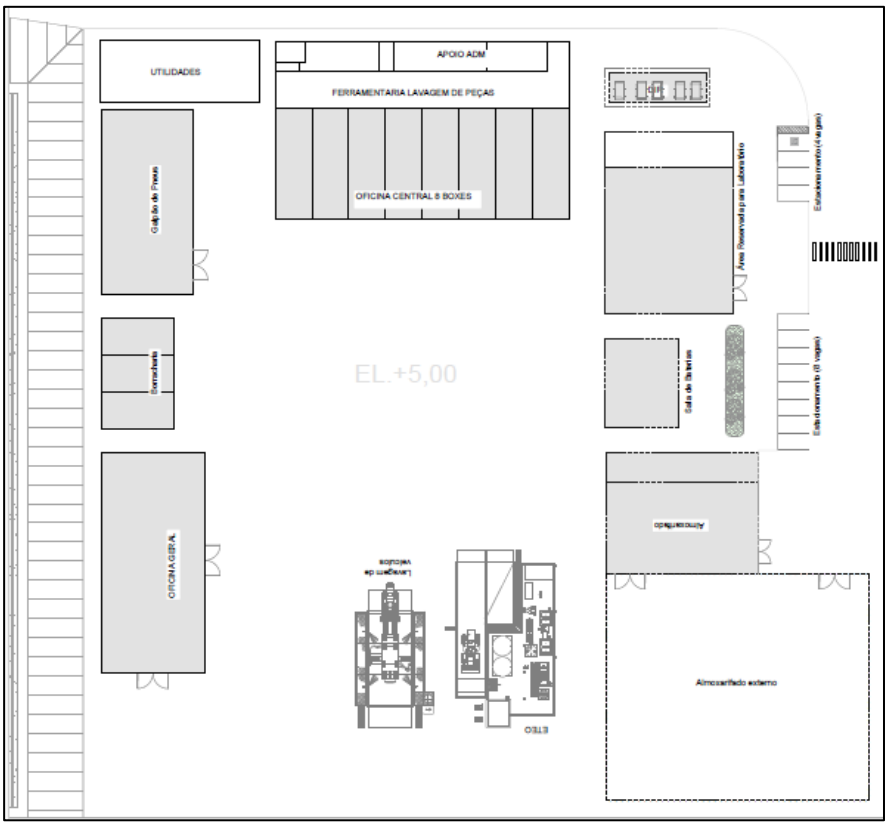


Figure 18-3: Laboratory, Warehouse, Workshop, and Mine Support Plateau

Explosives Magazine Plateau

Figure 18-4 shows the explosives magazine plateau buildings, comprising:

- Office and sentry box
- Accessory deposit
- Emulsion tanks.

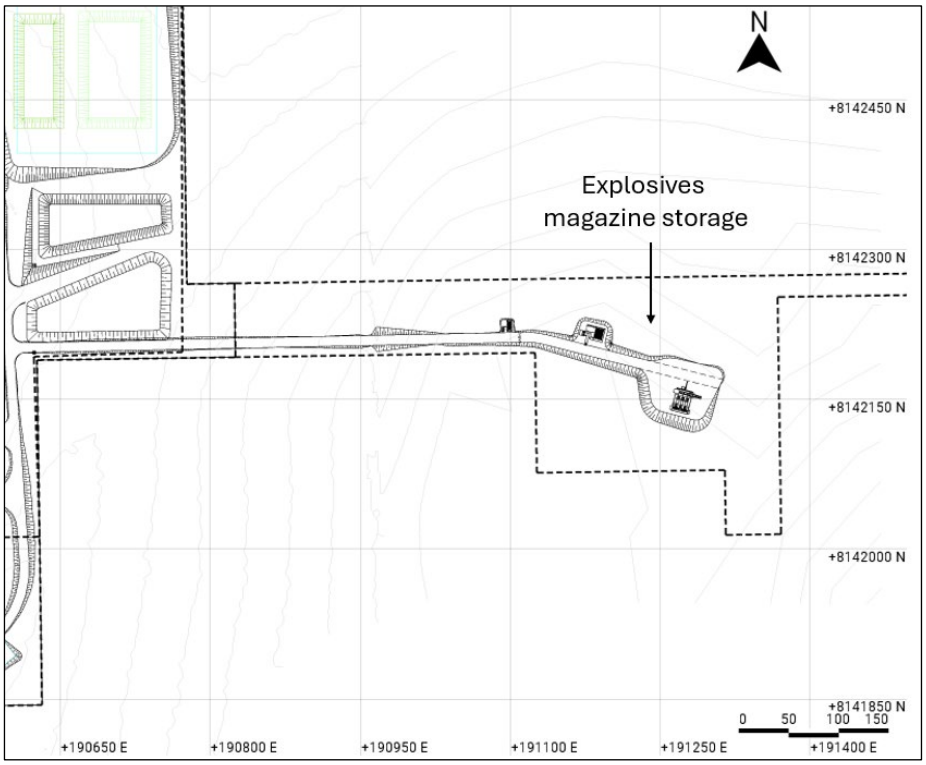


Figure 18-4: Explosives Magazine Plateau

18.3.3 Building Sizing

Plant and Mine Administration Building

The following premises were considered when designing the administrative building:

- 50%/50% male/female ratio adopted for administrative employees
- Maximum number of people using the administrative building is 58; however, there will be four extra tables for visitors.

The administrative building will be modular (Figure 18-5). The building includes the following internal areas and number of workstations per area:

- Plant process and operational control (7)
- Safety and Environmental management team (5)
- Mine planning (13)
- Mine geology (12)
- Mine operation (12)
- Mine infrastructure (5)
- Plant management office (1)
- Mine management office (2)

- Supply Chain Team (1)
- Meeting room (16 people)
- Technical archive
- Cafeteria
- Women's toilet (2)
- Men's toilet (2)
- Toilet for disabled people (1)
- CMD
- Electrical/IT room

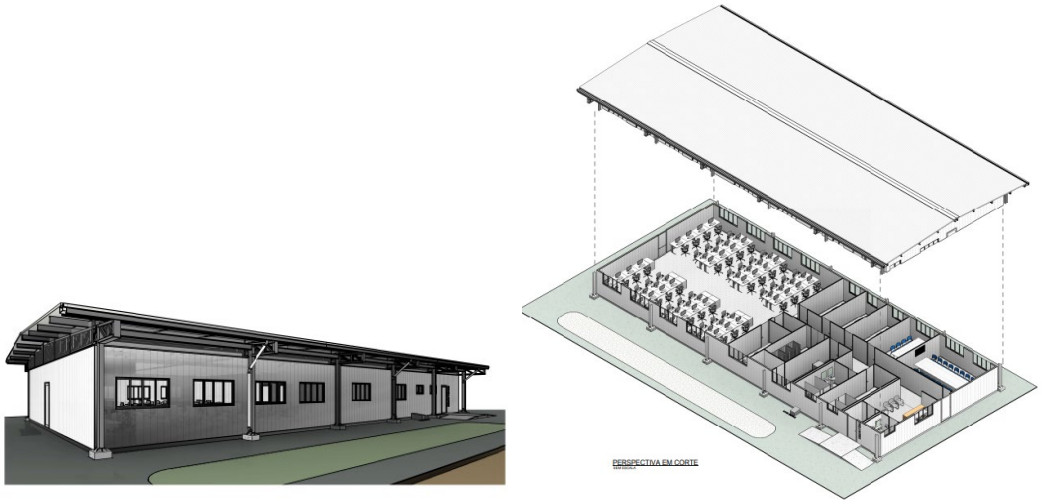


Figure 18-5: Administrative Office Building (Left); 3-D Model External and Internal (Right)

Laboratory

- The laboratory will be designed for four people performing chemical analyses of material collected on site.
- The laboratory's construction system consists of traditional masonry walls with a concrete floor and metal roofing.
- It has an adjacent area for maneuvering and DIR.

Medical Centre and Fire Brigade

- The medical centre will provide low-complexity outpatient care and will have an emergency care station (2 units), nursing (1 workstation), doctor’s room (1 unit), ambulance space (1 unit), and reception (1 person). The support areas will also be considered, consisting of an archive area, storage, changing rooms, electrical room and IT, and an adequate disposal area (common garbage and infectious waste).
- The medical centre project will comply with RDC nº 50/2002 (ANVISA Resolution of the Collegiate Board).

- The fire brigade area will be close to the medical center and consist of an administrative area with five workstations for brigade members, a storage room for SPCI equipment, and a parking space for the emergency vehicle. This area will be in the same building as the medical center, but with a separate entrance.

Scale Control—Dispatch

- The fiscal and shipping booth will be next to the scale control that will be used to weigh the inputs. These areas will have three workstations for dispatch and two for scale control.
- The same building will also have a waiting room for truck drivers, sanitary facilities, pantry, CMD, and electrical and IT room.

Cafeteria

- The cafeteria (Figure 18-6) project will comply with RDC No. 2016/2004 (ANVISA Resolution of the Collegiate Board).
- The cafeteria was sized for a kitchen to produce one meal for 330 people per shift, and a dining area accommodating a maximum of 110 people.
- Infrastructure for the cafeteria workers, with male and female locker rooms and sanitary facilities.
- A depot for cooking tools, bagged food, canned supplies, etc., cold room, a depot for cleaning materials and tools in a segregated area, waste deposit, CMD (an electrical and IT room will also be considered).
- The cafeteria main entrance will have male and female sanitary facilities, as well as one for disabled people, and common areas for handwashing.

Central Locker Room—Changing Room

The following premises were considered when designing the locker room (Figure 18-7):

- 250 lockers, 177 for men and 76 for women.
- 10 showers for men and 5 for women.
- Administrative employees will not be considered in the locker room estimation.
- The locker room will also serve the workshop and warehouse employees.
- The facility design will support people with reduced mobility.

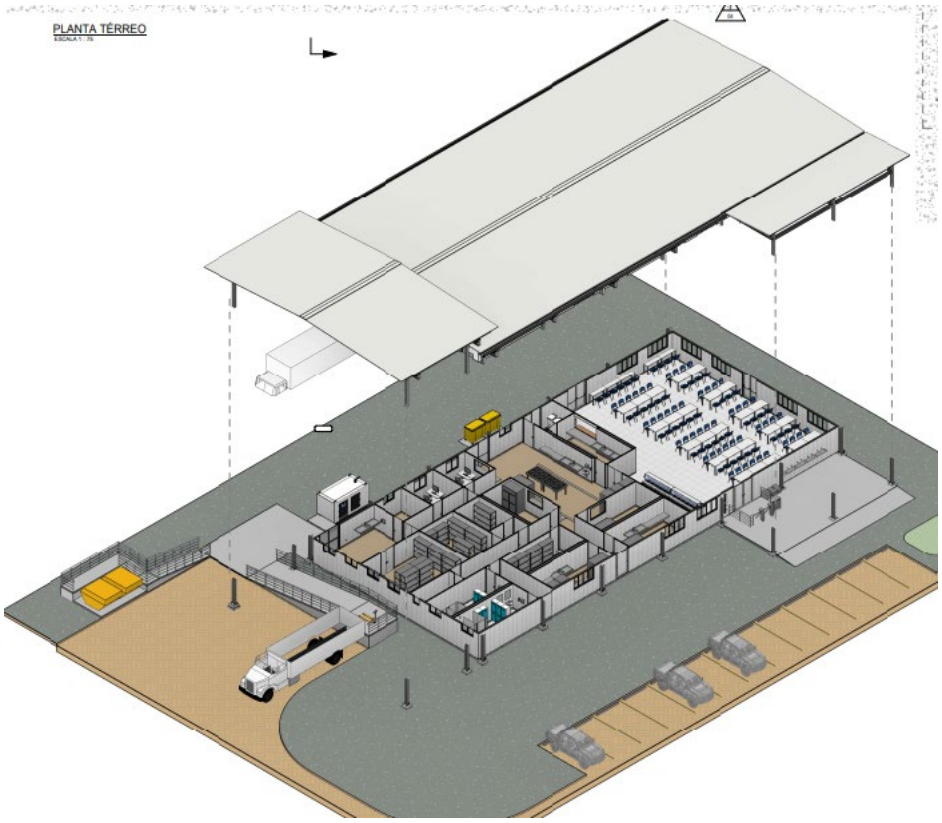


Figure 18-6: Cafeteria Internal Areas—3-D Model

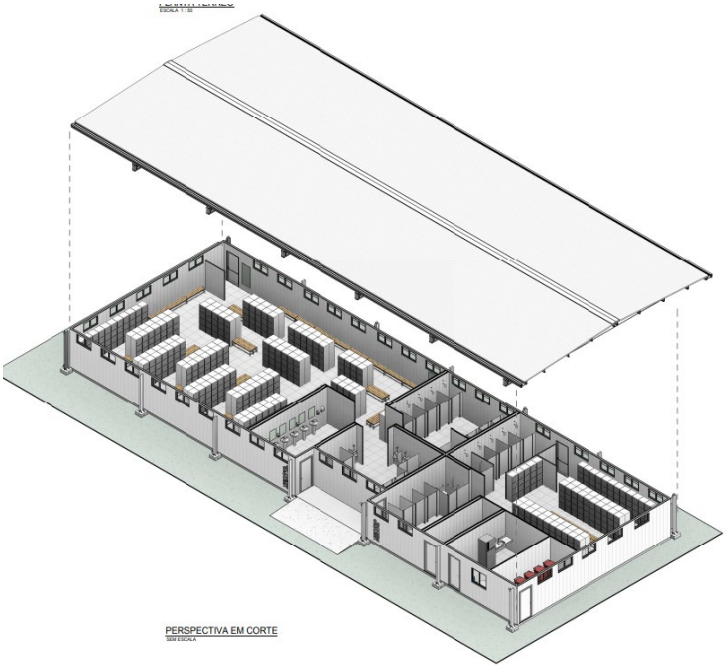


Figure 18-7: Changing Room Internal Area 3-D Model

Warehouse

The warehouse is dimensioned to store parts for plant and mine maintenance.

The construction will consist of metal beams and pillars, with a vinyl canvas roof and lateral closures. It is designed for three workstations and will have a level concrete floor. The floor is designed for an overload of 2.0 tf/m² or a Munck type vehicle with a maximum axle load of 17 short tons.

A large area is planned for storing external items (the entire area is fenced), as well as the positioning of 40-foot containers, for additional storage. Two of these containers will have a higher level of security, one dedicated to storing chemical products, where ventilation shutters should be installed, and the other refrigerated.

Workshop

The workshop (Figure 18-8) was designed with bays for the simultaneous maintenance of seven pieces of heavy equipment, as well as separate areas for boiler-equipment maintenance, machining, instruments, pumps, piping, and welding.

Areas are also provided for washing parts, lubrication, tool and material storage, and overhead crane for moving heavy parts such as engines.

In addition to the areas listed above, it is designed with areas for professional use, such as the pantry, coffee room, and office.

The workshop is designed using high-resistance concrete flooring, modular closure, pillars, and metal roofing.

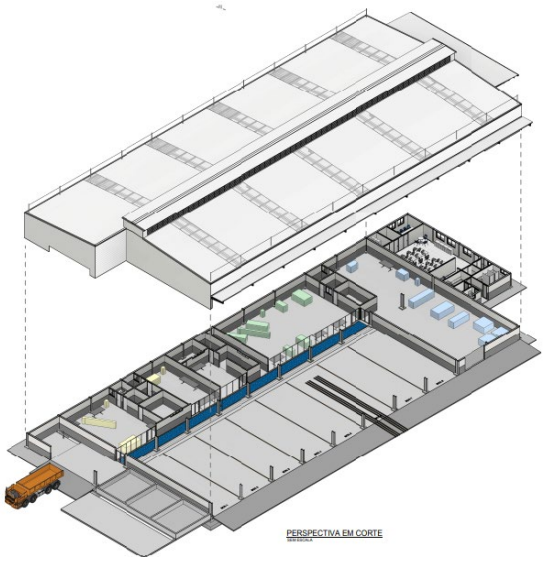


Figure 18-8: 3-D View of the Workshop

18.3.4 Processing Plant Layout

The processing plant master plan (Figure 18-9) was developed adopting normative premises and good engineering practices, with the main ones being:

- Use, whenever possible, the unevenness of the natural terrain to minimize height of structures and power of equipment.
- Make the support area using containers or modular construction, including six workstations plus a break room and sanitary areas.
- Design the conveyor transfer points without roofs and siding.
- Use containers for reagent and storing ferrosilicon.
- Use of concrete floors with drainage channels where it is necessary to dispose of effluent from washing or leakage, and to enable adequate cleaning.
- Plan locations for installing ducts and pipe rack, and electrical trays with their auxiliary structures, such as pipe-racks, pipe ways, cable racks, etc.

Locate a tower crane centrally in the plant for erection and keep it in place for maintenance during operations.

The crushing buildings are designed entirely as modular structures, with the crushers supported on skid-mounted units, to minimize concrete structures and reduce cost.

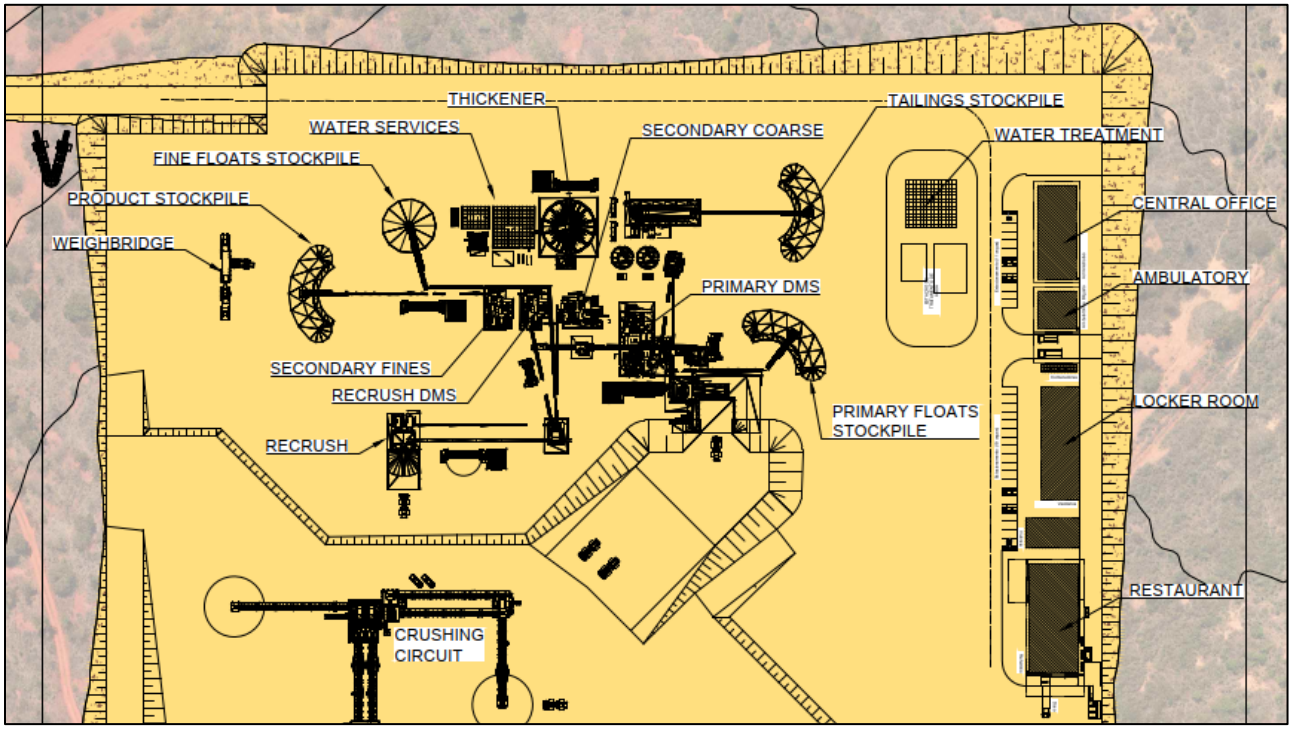


Figure 18-9: Processing Plant Layout (DMS + Crushing + Buildings)

18.3.5 Platework

All the Project platework (tanks, pulp boxes, and chutes) will be made of carbon steel. The liners will be natural rubber for the pulp equipment, ceramic for wet areas, and Hardox 500 for the dry material-handling equipment.

18.3.6 Utility Systems

The following utility systems were studied for the Project

18.3.7 Raw Water Extraction

Raw water from the Jequitinhonha River will be extracted by pump and transported through a pipeline from the intake point to a 1,200 m³ raw-water tank and process-water tank, with a dedicated reserve for fire protection. Additionally, the Project has as a backup secondary water source on the seasonal Piauí River, which will not require a pipeline, as the transport distance is shorter. The estimated plant consumption is 14 m^3/h, and 25 m^3/h for road dust suppression; the remaining raw water will be sent to the water treatment system for filtration.

18.3.8 Water Treatment System

A 69 m^3/h treatment plant will be designed to remove suspended solids and reduce chemical residues from water coming from the Jequitinhonha River; after treatment, most of the water will be sent for mine-equipment make-up water.

The Project will include installing a compact potable water treatment plant (WTP) with a capacity of 6.0 m³/h, which will meet the drinking water demand of the entire operational employees

18.3.9 Reclaimed Process Water System

The 800 m^3 reclaimed process-water tank will be fed by the thickener overflow, and a deficit of 14 m³/h will be replenished by make-up water from the water treatment filter. Recovered water will be pumped through two networks, which will meet the needs for pulping, pre-screen, and DMS screen washing.

18.3.10 Sewage Treatment System

The Project will include installing a compact, 5.0 m^3/h sanitary sewage treatment plant, which will serve the entire operation.

18.3.11 Oily-Effluent Treatment Plant

A 40.0 m³/h oily-effluent treatment plant will be installed near the workshop to treat the effluent generated by heavy-vehicle washing in the wash bays and parts in the workshop.

18.3.12 Fire Control System

The fire protection and firefighting system will have a capacity of 30.0 m³/h and will serve the DMS and building plateaus. Technical instructions from the Mina Gerais Military Fire Brigade and applicable ABNT standards were adopted.

18.3.13 Compressed-Air Generation and Distribution System

The compressed-air generation, treatment, storage, and distribution system will be divided into the plant and workshop areas.

In the plant will be two compressor houses, which will contain the compressors, dryers, coalescing filters, and air reservoirs to meet the consumption for instruments, service and cleaning, and process air.

To serve the workshop support structures, lubricated screw compressors with dryers and integrated vessels will be provided—one operational and one spare.

18.4 Metallic Structures

The steel structure design will be developed using the Brazilian Standards of the ABNT. For cases not prescribed in the ABNT Standards, the following standards may be used: FIB, ACI, DIN, ASTM, AISC, ASCE, EUROCODE, AWS, BS, ANSI, SIS.

According to NBR 8800, Table K4, the outdoor aggressiveness class is defined as C.3, urban and industrial atmospheres with moderate pollution by sulfur dioxide; and the indoor aggressiveness class is defined as C.3, environments such as processing industries.

At this stage of the Project the metallic structures of the operational buildings will be quantified in the Architectural Quantity Worksheet. The DMS structures (Figure 18-10), despite being metallic, will be the scope of the equipment supplier and therefore quantified in the Mechanical Quantity Worksheet.



Figure 18-10: DMS Plant 3-D Model—Steel Structure Equipment

18.5 Concrete

The scope for the reinforced-concrete structures will be defined by the mechanical and architecture discipline.

The concrete structures design criteria call for direct foundations for equipment and operational buildings and slabs for administrative buildings. The structures will be designed and dimensioned in compliance with NBR 6118 Design and Execution of Concrete structures, NBR 6120 Loads for Calculation of Building Structures and NBR 6122 Design and Execution of Foundations.

In the design stage, after receiving the drilling reports, reference or vendor drawings (DR/DF) (provided by the client or suppliers), or load tables provided by the mechanical and steel structures disciplines and suppliers, the foundations and structures were pre-dimensioned, and may undergo changes in dimensions and concept (type of foundation).

The main criteria are:

- Concrete C10—Characteristic compressive strength: fck ≥ 10 MPa
- Application: ballast concrete for foundations, floors and other buried structures. Concrete C30—Characteristic compressive strength: fck ≥ 30 MPa
- Application: foundations (footings, blocks, and lintels) and structures in environmental aggressiveness Class II.

18.6 Electrical

To provide power to the Project, a new 138 kV transmission line will be built. It will begin at the CEMIG Integrator Substation and be approximately 3 km long.

To implement the transmission-line project, it will be necessary to build a new main substation (Figure 18-11), to be fed by the new 138 kV transmission line. The new main substation will lower the voltage from 138 kV to 13.8 kV. A 13.8 kV overhead distribution network will power the secondary substations in e-houses distributed throughout the plant.



Figure 18-11: CEMIG Integrator Substation and New Main Substation from 138 kV to 13.8 kV Layout

The plant will have 11 motor control centers (MCC) to feed the loads from the plant and the mine (Table 18-1):

- Primary DMS
- Feed prep and secondary DMS
- Secondary fine DMS
- Recrush DMS
- Recrush
- Water recovery and fines

- Crushing and ore sorter
- ADM and utilities
- Mine
- Mine exhaust fans
- Workshop.

Table 18-1: Power Demand

System Power	Voltage (kV)	Active Power (kW)	Reactive Power (kVAr)	Apparent Power (kVA)	Power Factor
Main Substation	13.8	8734	2783	9167	0.95

18.7 Instrumentation, Control, and Automation

The instrumentation, control, and automation project will be developed considering the implementation of a fully automated mineral processing plant, with minimal human intervention, based on technologies that allow the best cost–benefit ratio for automated systems.

The system will be based on programmable logic controllers (PLC), which will interface with and control all process equipment. Control of the plant will be carried out from the dedicated control and operation room, where the plant's operation and engineering stations will be located.

The server room for the plant’s automation system will be adjacent to the control room.

The control system will have client-server architecture, with the ability to expand and perform online modification of the software and hot modifications of the hardware while ensuring maximum availability of resources for plant operation. The controllers will be interconnected to the plant servers in a redundant network. The interface with the instruments will be carried out through remote panels, which will be designed according to the communication needs of the process areas.

The plant's instrumentation will be intelligent, with all analog instrumentation interconnected via the industrial network.

18.8 Telecommunications Systems

The telecommunications systems will be subdivided as follows:

- Automation technology (AT) and IT network infrastructure: considers all optical and metallic network infrastructure necessary for communications and interfaces of IT and AT systems, including all racks, servers, radios, switches, patch panel, and other necessary assets.
- Process closed-circuit television (CCTV): The CCTV system for process monitoring is based on a set of cameras installed in the plant process areas, making the images available via network to the CCTV stations, according to the plant's operational needs.
- Property security: The CCTV system for property security is based on a set of cameras installed throughout the plant's administrative facilities, making the images available via network to

security monitors installed in the security room. In addition to the property security CCTV system, the Project will have an access control system, which will enable the control of personnel entry and exit on the plant premises and access control in controlled or restricted areas.

- Data and telephone network: The data and telephone network system will be responsible for data traffic between the plant's IT equipment, in a fully integrated and secure way, providing high connectivity between all network points. This system will meet all the plant needs, through dedicated applications such as telephone, corporate management systems, email, internet, intranet, and integrated maintenance systems.

18.8.1 Underground Communication

Effective communication is essential for safety, productivity, and coordination of underground mining activities.

18.8.2 System Architecture

The proposed communication solution is based on a private long-term evolution (LTE) telecommunications module (Band 28), ensuring robust connectivity and scalability.

This system integrates voice, data, and monitoring functions in a single network, improving operational efficiency.

18.8.3 Infrastructure Components

- 7/8" Tech RFX radiating cables, installed along main ramps and drifts, to ensure continuous signal coverage underground
- VHF radios operating in the 136 MHz to 174 MHz band range for direct communication between equipment operators and supervisors
- Repeaters and antennas to strengthen the signal in deeper or more remote parts of the mine
- Fiber optic backbone, providing high-capacity data transmission and redundancy
- Supporting hardware for installation, power supply, and environmental protection of communication nodes.

18.8.4 System Capabilities

- Voice communication: reliable two-way voice channels for daily operations
- Dispatching system: centralized control to coordinate equipment, crews, and material flows
- Microseismic monitoring: integration of geotechnical sensors for real-time seismic event detection and analysis
- Atmospheric monitoring: remote measurement of gases and ventilation parameters to detect hazardous conditions
- Worker tracking: real-time positioning system to monitor personnel location and enhance safety during emergencies.

18.8.5 Safety and Redundancy

The system provides continuous communication even in the event of localized failures, due to the redundant design of the fiber optic and LTE backbone.

The integration of monitoring systems (atmospheric + seismic) within the communication framework provides early warning of hazardous conditions, contributing to risk reduction.

18.9 Civils Geotechnical

A drill and geotechnical testing plan was completed, comprising 21 mixed drill holes totalling approximately 390 m, along with the extraction of undisturbed samples for laboratory testing. The campaign was conducted between February and March 2025.

A location plan for the mixed drill holes was also received, identified as workmap_26062025, which included 16 additional drill holes totalling approximately 378.50 m. These drill holes were planned for the investigation of soil and weathered rock, with depths ranging from 11 m to 46 m, reaching the fresh rock.

The drill-hole reports provided geological descriptions based on the classification of the drilled material, indicating respective thicknesses, as well as quantitative data on the Standard Penetration Test (SPT), blow count (NSPT), Rock Quality Designation (RQD), core recovery percentage, groundwater level, and drill coordinates and collar elevations.

In addition to mixed drill holes, infiltration tests were carried out to assess soil permeability; direct shear and triaxial tests were performed on soil samples to determine strength parameters; Lugeon (Packer) tests were conducted to evaluate permeability in the fractured rock mass; and uniaxial compression strength (UCS) tests were performed on core samples with varying degrees of consistency and cohesion.

Based on the interpretation of these drill holes, a colluvial layer of reddish-brown sandy clayey soil was identified, ranging from 2.5 m to 6.0 m thick. Beneath this, a saprolitic layer occurs, varying from 1.0 m to 7.0 m thick. Finally, a layer of gray, laminated and mottled biotite schist was encountered, with the contact with the saprolite occurring between elevations 272.00 m and 339.00 m. Most drill holes did not present groundwater levels; in those that did, water was observed between 1 m and 6 m deep.

With the information available at the moment to support the infrastructure and foundation design, the following provisional assumptions may be adopted: for permanent slopes in natural soil cuts, use a slope of 1.0 H:1.0 V up to 6 m high; for higher slopes, include a 3 m wide berm after the first 6 m. For controlled embankments, use a slope of 1.5 H:1.0 V up to 6 m high; for higher slopes, include a 3 m-wide berm after 6 m. Slopes shall be free of blocks or boulders larger than 200 mm in diameter, and the soil moisture content shall allow for proper compaction (±2% of the optimum moisture content). For shallow foundations, an allowable bearing pressure of 150 kPa shall be considered. These parameters must be confirmed following the final layout definition and complementary investigation.

18.10 Piping

The plant utilities and process lines are designed by the mechanical discipline. The materials to be used include carbon steel piping and high-densitypolyethylene (HDPE) piping, reinforced rubber hoses and galvanized piping for air services. Carbon steel piping will generally be schedule STD / schedule 20 / schedule 10 and PN 16 HDPE. Critical process suctions in the DMS modules are ceramic tiled.

The fire system will be an underground network of HDPE pipe with risers at defined locations.

18.11 Construction

18.11.1 Construction Strategy

The Project implementation strategy is structured across four work fronts, each comprising specific activities:

- Front 1: Infrastructure includes earthworks, drainage systems, and bridge construction.
- Front 2: Civil works and electromechanical erection covers the beneficiation plant and utility installations.
- Front 3: Mine opening and development encompasses the development of mine Portals 1 and 2.
- Front 4: South open pit involves preparation and development of the mining area.

18.11.2 General Objectives

Key Project Drivers are:

- Zero harm to people, the community, and the environment
- Positive impact on surrounding communities
- Maximize project value for stakeholders.

Achieve on-specification first production according to the Project schedule.

18.11.3 Project's Main Milestones

The Project's main milestones (Table 18-2) will be revised and further detailed during the Basic and Detailed Engineering phases, once the Project implementation start-up is established.

Table 18-2: Project's Main Milestones

Item	Estimated Date
Financial Investment Decision	March 2026
Field Construction Activities Start	December 2025
Mine Development Start	January 2026
Detailed Engineering Start (Promon)	June 2025
Mine Start (First Production)	November 2027
Transmission Line—Energization	February 2027
Mechanical Completion	May 2027
Commissioning Completion	July 2027
First Product	July 2027

Preliminary Schedule

Figure 18-12 shows the preliminary schedule, which will be updated in the next phase with detailed engineering.

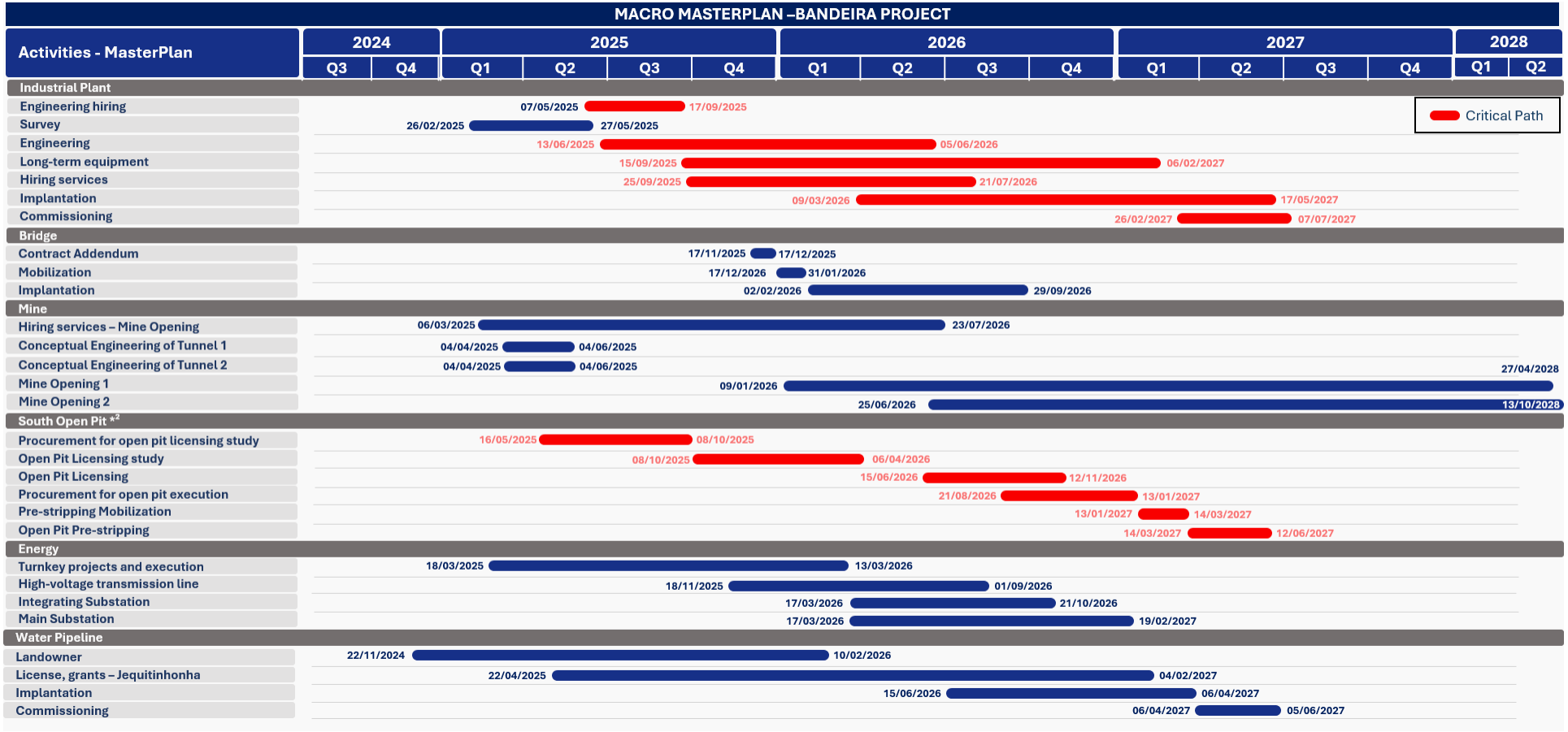


Figure 18-12: Preliminary Schedule

18.12 Bandeira Waste Dump and Tailings Storage Facilities

This section presents the basic design of the two waste rock and tailings disposal structures planned for the Project. The first, referred to as the North Dump, will be located north of the future access ramp to the underground mine, while the second, referred to as the South Dump, will be located south of the remaining project facilities.

Accordingly, two disposal facilities are planned to serve the entire LOM, initially considering the co-disposal of materials generated throughout the Project's operation. The design includes the co-disposal of filtered tailings, dry tailings (DMS), and waste rock. Together, the facilities will provide a total storage capacity of 19.4 Mm³. Each structure consists of a waste rock embankment that functions simultaneously as a drainage and containment element, ensuring geotechnical stability and long-term performance.

The design has been developed in accordance with geotechnical, geometric, hydrological, hydraulic, operational, and environmental criteria, as established by applicable standards, regulations, and resolutions, including:

- Regulatory Standard No. 22—Occupational safety and health in mining
- Mining Regulatory Standard No. 19—Regulation for waste rock and tailings dumps
- ANM Resolution No. 95/2022—Consolidation of regulatory acts concerning the safety of mining dams
- ABNT NBR 13.028/2024—Design and presentation of projects for tailings dams, sediment containment, and water reservoirs
- ABNT NBR 13.029/2024—Design and presentation of projects for waste rock dumps.

The objective of the project is to ensure the controlled and orderly disposal of materials generated from both open-pit and underground mining operations, as well as tailings from processing plant The dumps must remain stable, ensuring the safety of personnel, equipment, and the environment, while constituting safe structures integrated into the surrounding area.

The waste materials generated during mining, understood to be inert based on available data, consist mainly of biotite schist blocks, transitioning from residual soils derived from near-surface weathered rock to fresh rock at depth. As depth increases, the degree of weathering decreases and rock quality improves. Tailings from the concentration plant are mainly coarse, with a mineralogical composition generally comprising feldspar, quartz, and albite, with minor biotite schist mined together with the ore as dilution.

The area designated for disposal of these materials in the North Dump is located west of the concentration plant, while the South Dump will be situated south of the same facility (Figure 18-13).

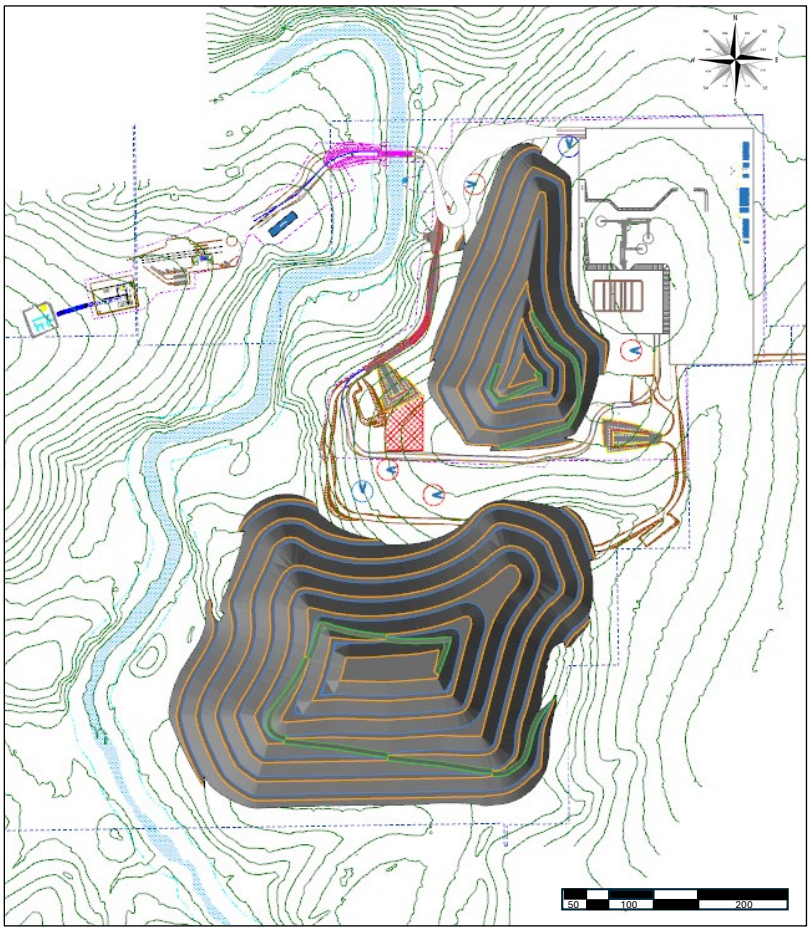


Figure 18-13: Master Plan with North and South Dump Design (Plan View)

18.12.1 Reference Documents

MGLIT provided the following documents and topographic plans used in the work:

- Master Plan: BAN-0300-TS-PD-0002_B, dated 15/09/2024
- Topographic plan without date: executed by MGLIT
- Conceptual project: Tailings Dump P5—Part 1—Bandeira Project, elaborated by MLF Geomechanics, dated 23/04/2024
- Detailed Design: Waste Rock and Tailings Dump Bandeira Project 1, elaborated by Itaaçu Geologia e Engenharia, dated May/2024
- Technical Report ML-2024-002-RL-001 – Technical Feasibility Study for Waste Rock, Ore, Tailings, and Product Deposition Dumps, Surface Drainage System, and Sediment Containment, prepared by Itaaçu Geologia e Engenharia, dated 31/10/2024
- Technical Report SAFF-027.25-059-01-RD-001 - Geotechnical Data consolidation, elaborated by Saff Engenharia.

18.12.2 Geotechnical Aspects

For the foundation designated North Dump, the analysis based on borehole profiles and SPT - Standard Penetration Test, tests revealed a superficial layer with low strength, reaching a maximum depth of approximately 3 m (NSPT <12), interpreted as a possible colluvium layer (COL). This layer discontinuously covers the slopes and is thicker only along the thalwegs of small local drainages.

Beneath this, the subsoil is composed of mature residual soil and residual soil, grouped into the residual soil unit (SR) due to the consistency of the results and the gentle topography of the area. Young residual soil and saprolite were unified into the saprolite unit (SAP). In general, the residual soil and saprolite exhibit medium strength (Class V/III) and extend to approximately 22 m in depth.

Figure 18-14 shows the distribution of NSPT,60 values for the materials reinterpreted from 46 mixed drilling profiles (totalling 999.33 m). SPT tests indicate increasing strength with depth and layer variability.

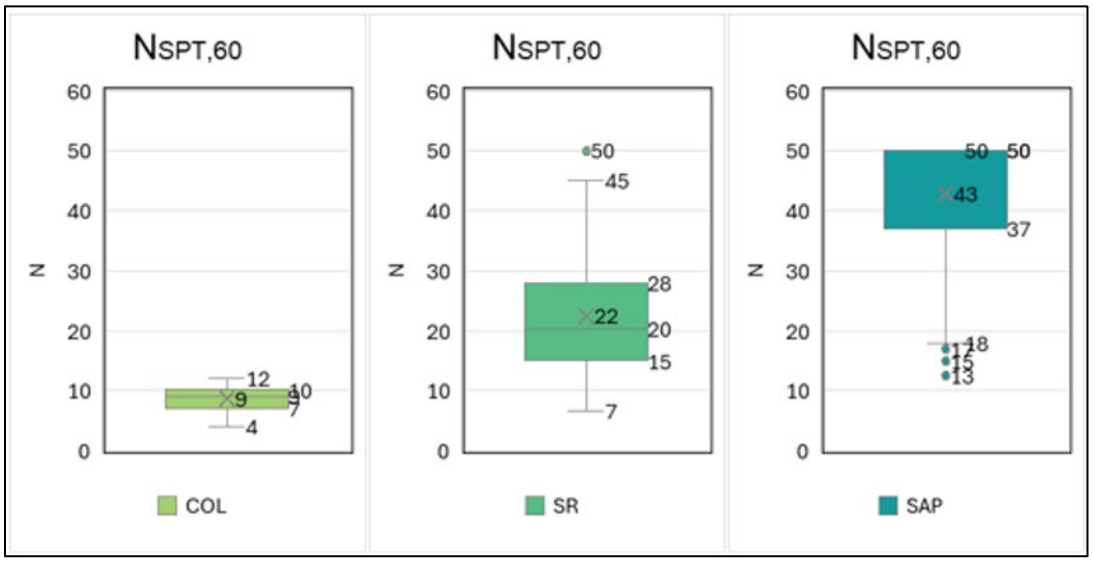


Figure 18-14: Box Plot of the NSPT Values Observed in the Materials Intercepted by the Mided Drilling.

The colluvium has a predominantly clay-silt to clay-sand texture, occurring discontinuously in the superficial layers of the Project area. Its thickness is variable, with average NSPT values between 4 and 12 blows, representing soft soil, for which additional testing may be required to assess the need for removal as foundation treatment.

The residual soil has a predominantly clay-silt to clay-sand texture, with silty-sandy to sandy-silty sections. NSPT values range from 7 to 50 blows, showing a slight increase in resistance with depth, occurring between 0 and 10 m and emerging in some points north of the ADA, coinciding with the North Dump foundation.

The saprolite has a predominantly silty-sandy to sandy-silty texture, occurring between 1 and 15 m in depth. NSPT values range from 13 to 50 (average 43), increasing with depth, indicating competent material.

Based on field and laboratory tests, core logging, and field observations in the Project area, a residual soil to saprolite horizon was identified with relatively homogeneous thickness and composition, low permeability, and adequate mechanical characteristics, considered suitable for the construction of a waste and tailings dump.

18.12.3 Investigations in the Area

To characterize the materials for the waste rock and tailings storage facilities, in situ investigations and laboratory tests were conducted to determine mechanical properties, particle-size distribution, chemical reactivity, geotechnical profiles, and the hydrological and hydraulic characteristics of the foundation materials.

Due to changes in the layout of the industrial area, the Area investigation study was consolidated from previous geotechnical campaigns carried out for the design of industrial structure foundations, the crown pillar, and the underground mine accesses. These analyses included the final geometric arrangement, stability assessment, surface and internal drainage design, sediment containment, and construction sequencing, providing greater robustness and reliability to the results.

Figure 18-15 shows the site plan with all geotechnical investigations carried out in the mining rights area, highlighting that only the mixed drilling were focused on the quantitative characterization of materials and the assessment of foundation conditions (Figure 18-15).

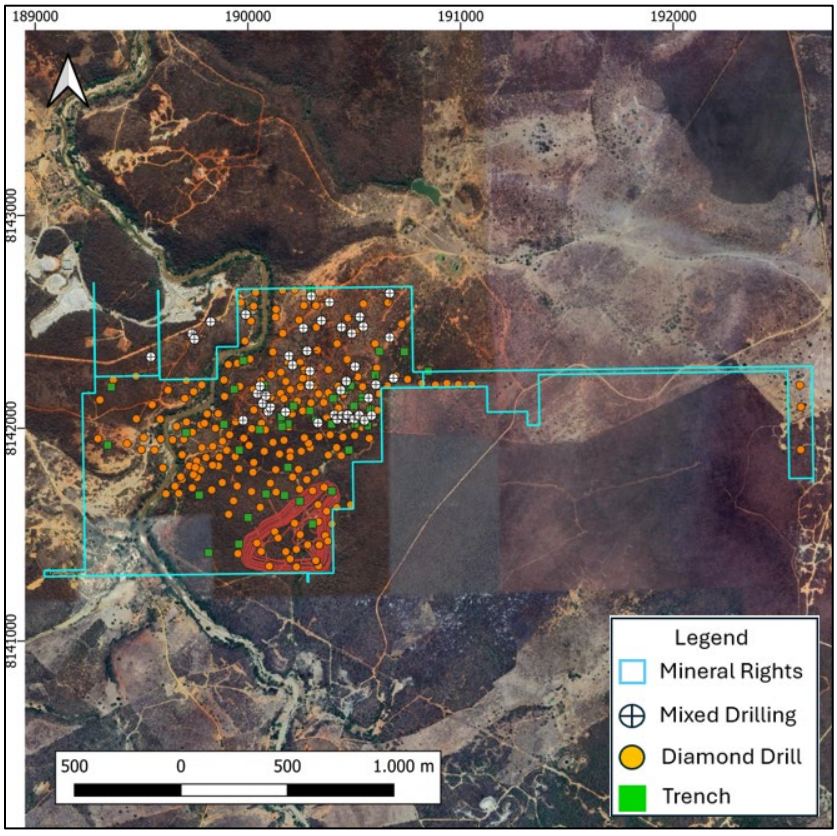


Figure 18-15: Location of the Geotechnical Investigations for the Project

18.12.4 Main Features of the Storage Facility Foundation

The samples collected and tested during the investigation described above generally exhibited well-graded characteristics, with a predominance of sandy materials and moderate amounts of coarse-grained components (coarse sand and gravel), and only minor clay content.

The clay fraction behaves as a low-compressibility inorganic clay (CL), indicating that the soil is not prone to significant settlement. It was classified as having low activity, characteristic of soils with minimal colloidal activity, with kaolinite identified as the dominant clay mineral. Kaolinite's low expansion potential further suggests that the soil poses no risk of structural instability.

No evidence of water seepage, open discontinuities, or instability features was observed on the adjacent slopes. The terrain exhibits good natural drainage and low permeability, providing favorable foundation conditions for the pile and promoting drained behaviour of both the filtered tailings and the stacked waste rock.

Based on this assessment the foundation of both dumps is considered suitable for the combined stacking of filtered tailings and waste rock, offering low deformation risk and high bearing capacity, thus eliminating the need for complex reinforcement or base impermeabilization works at this stage of construction.

18.12.5 Seismic Risk

The Brazilian technical standard ABNT NBR 15421—Design of Structures Resistant to Earthquakes—Procedure (2006) regulates seismic effects on buildings in Brazil.

Both waste and tailings facilities, being situated in the central portion of a tectonic plate, far from its edges, is expected to experience low-frequency and low-magnitude seismic activity.

NBR 15421 divides Brazil into five seismic zones (Figure 18-16, of which most of Brazil, including the Project, lies in Zone 0, characterized by very low seismic danger, with horizontal accelerations of 0.025 g.

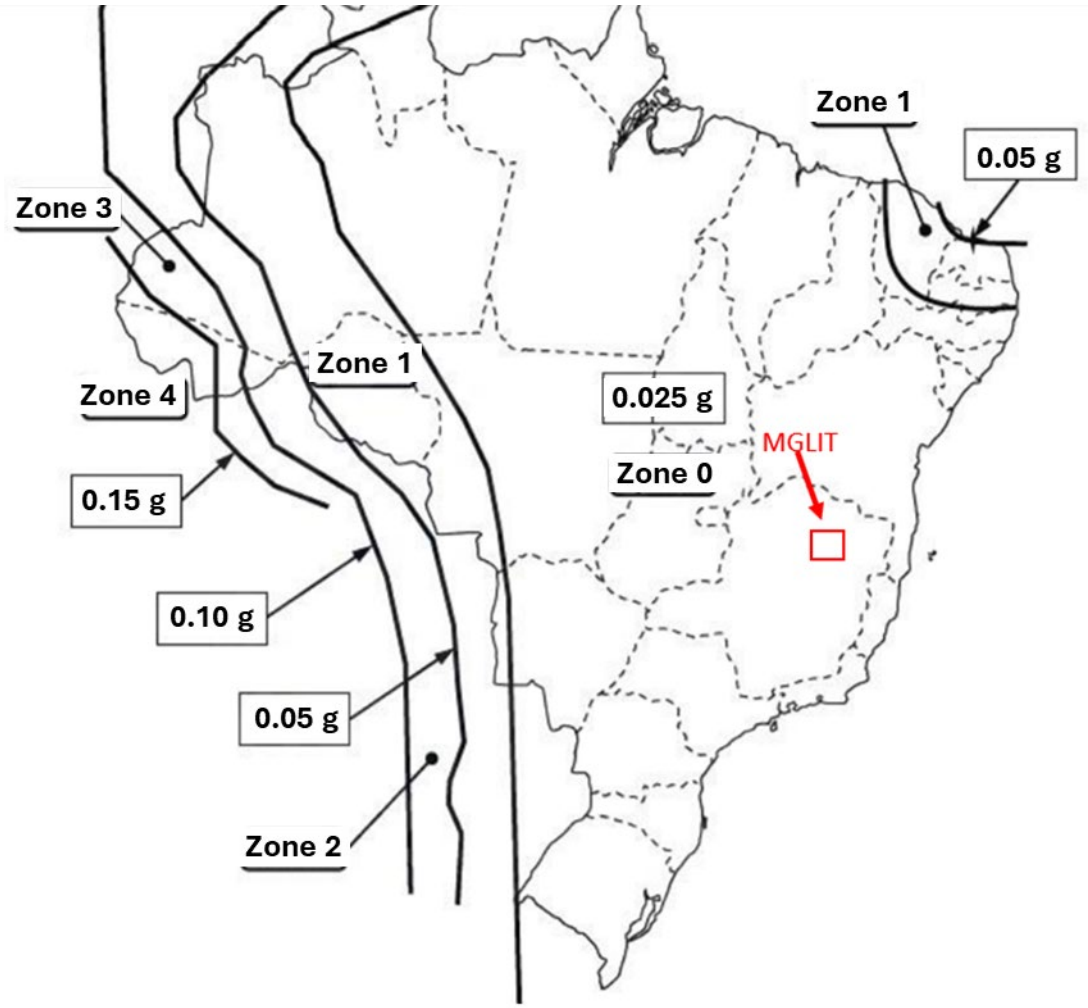
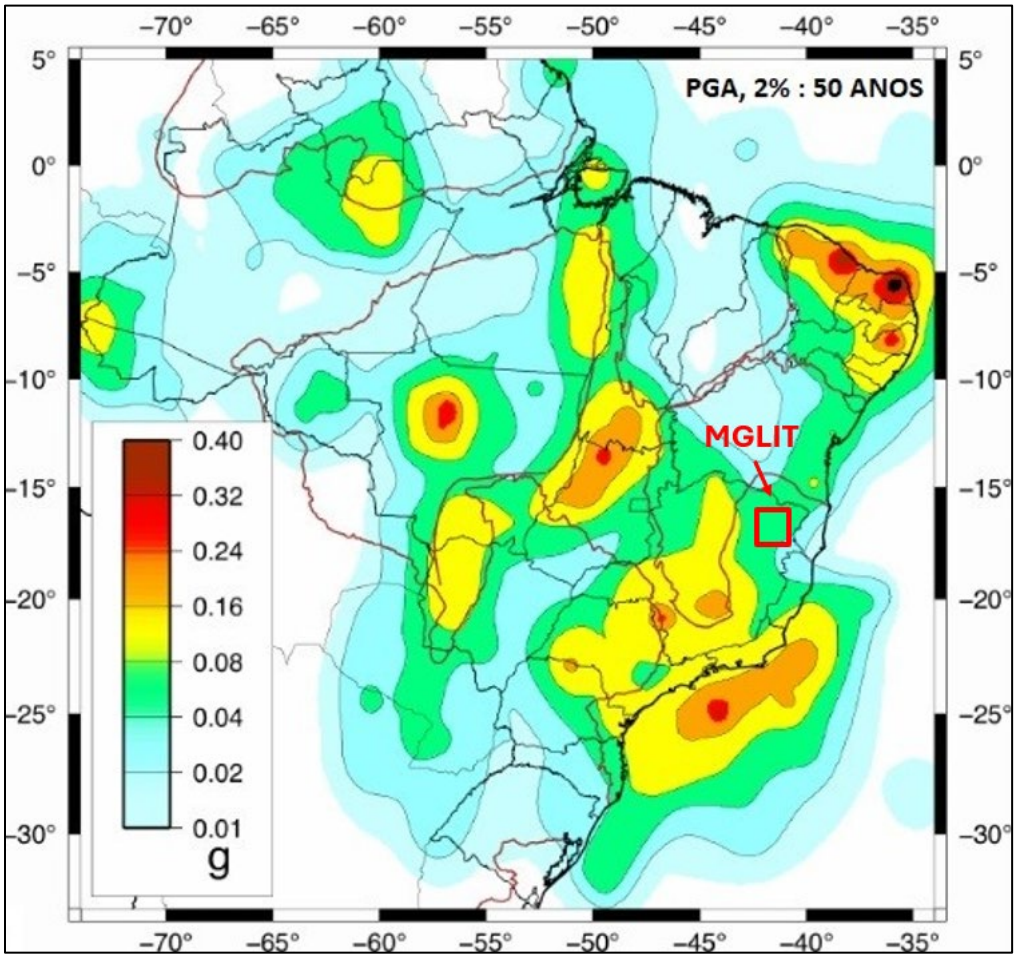


Figure 18-16: ABNT NBR 15421 (2006) Seismic Zones of Brazil

Figure 18-17 gives a more conservative prediction. It contemplates a peak ground acceleration (PGA) with a probability of exceedance of 2% in 50 years, which is equivalent to a return period T = 2,475 years.



Note: PGA in rock, for probabilities of 2% exceedance in 50 years, to a return period of 2,475 years.

Source: Assumpção et al. (2016).

Figure 18-17: Brazil Seismic Hazard Heat Map—Peak Acceleration

Although the use of a value for the vertical seismic coefficient (kv) is a widely accepted concept. Seed and Martin (1966) and Duncan and Wright (2005) suggest adopting a vertical seismic coefficient equal to 0, under the assumption that the movement of shear seismic waves is vertical. In contrast, Papadimitriou et al. (2014) stress that vertical acceleration values in regions of low seismic activity can be considered negligible or of little relevance.

Therefore, the maximum horizontal acceleration identified in Figure 18-14 was 0.04 g.

18.12.6 Cleaning and Treatment of the Foundation

The recommended treatment includes clearing vegetation, removing stumps, and cleaning the topsoil, which can be reused to cover the final slopes of the dump. In addition, the spatial distribution of the colluvium should be thoroughly mapped to assess the need for its removal as a foundation treatment measure for the waste and tailings piles.

18.12.7 Internal Drainage and Superficial Drainage

Despite the draining behaviour of the stacked material, which could allow the omission of internal drainage, the bottom layer of the pile, constructed with the rockfill itself, can potentially function as a bottom drain, as specified in Brazilian standard ABNT NBR 13.029.

Nevertheless, bottom drains were designed to be installed in the thalwegs after leveling the foundation terrain. Each drain consists of a graded gravel layer (D50 = 38 mm) with a 0.50 m thickness, wrapped in 400 g/m² nonwoven geotextile, serving as a filter and separator between the rockfill material and the foundation soil. The main drain converges into a collector gallery using Ø 300 mm HDPE pipe, directing the flow to the downstream outlet of the pile.

The internal drainage system of the North and South piles is designed to capture and convey infiltrated water, originating from both incident precipitation and natural springs located in the foundations or upstream thalwegs.

The surface drainage system was developed to minimize infiltration and prevent erosion on slopes and berms, ensuring structural stability and operational efficiency. It consists of three functional subsections: at the top, trapezoidal soil-cement channels, lined with granular material and capped with concrete in high-energy hydraulic areas, collect surface runoff and convey water to the hydraulic steps.

The integration of bottom drains with the surface drainage system preserves the natural water flow, aligns with the terrain, and reduces environmental impacts. The system is designed to intercept percolated water upon reaching the natural ground and convey it in a controlled manner downstream. The combination of the drained behaviour of the foundation with the surface drainage creates a highly drained and stable geotechnical environment, fully compliant with the safety requirements of ABNT NBR 13.029:2024 and NBR 13.028:2024.

18.12.8 Geometric Design

The geometric design was developed based on the topographic data MGLIT provided, aiming to accommodate the necessary volumes in appropriate geometry, and designed infrastructure, for rapid integration with the environment.

The berms were designed to function as conduits for rainwater, despite the initial high permeability of the embankment. Longitudinally, they should have a slope of 1%. This slope allows water to flow towards the water exits, even in the event of settlement due to block rearrangement. Transversely, the s should have a slope of 5% towards the toe of the upper slope. The main geometric parameters considered for the design are listed in Table 18-3.

Table 18-3: Geometric Parameters of North Dump

Geometric Parameter	Unit	Value
Maximum Height	m	64
Base and Crest Elevation	m	321–400
Maximum Seat Height	m	20
Minimum Width of Shoulders	m	10
Slope (H:V)—Angle Between Berms	°	1.3:1—37.6
Slope (H:V)—General Angle	°	1.8:1—29
Longitudinal Slope	%	1
Cross Slope	%	5
Occupied Area	ha	13.1
Available volume	m³	3 408 625.7

Figure 18-18 presents the arrangement of the north waste and tailings design.

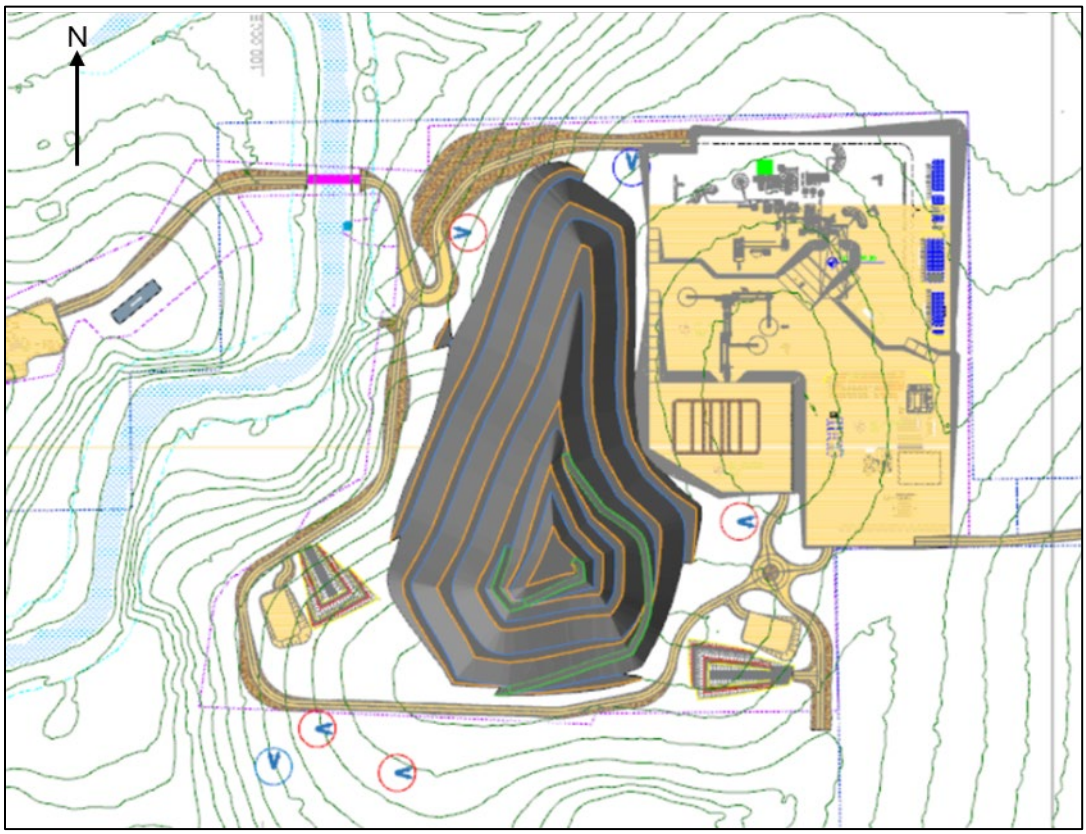


Figure 18-18: North Waste and Tailings Dump

18.12.9 Stack Formation Sequence

The dump will be constructed, following upstream sequencing according to the monthly volumes of waste and tailings material. The dump will be located by prioritizing the least transport distance or the

best transport average and beginning at the lowest point in the dump footprint, where bottom drains with sound rock will be installed.

When disposing of rock in a waste and tailings facilities, the naturally formed angle of repose ranges from 37° to 42° for rockfill, depending on the size of the blocks. As the blocks are made of sound rock, it will not be possible to alter the material's angle of repose, resulting in the slope face with the angle of block arrangement. After reaching the toe of the slope, it will be ready to be revegetated using hydroseeding or another method considered more convenient, as shown in Figure 18-19.

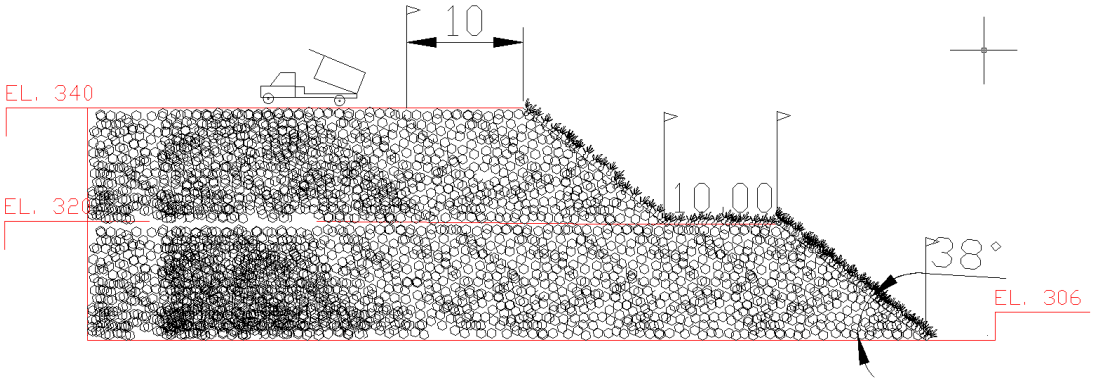


Figure 18-19: Geometries for Forming the Bank Edge

The construction sequence of the benches should be executed according to the specifications shown in Figure 18-20 and Figure 18-21.

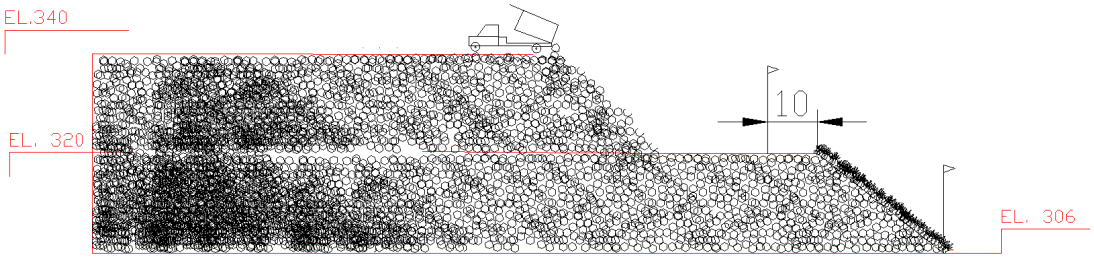


Figure 18-20: Reached at El. 320 m, Place a Line of Flags 10 m from the Crest, which will be the Edge of Bank 320

The first line of flags marks the dumping disposal limit at the edge of the embankment, with the blocks remaining at their angle of repose (Figure 18-21).

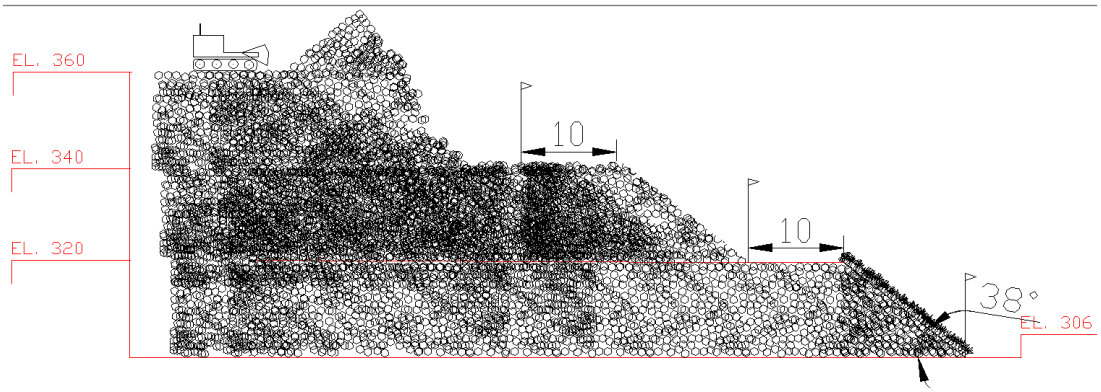


Figure 18-21: Construction Sequence of the Benches—Once the Position of the Berm Is Reached, Mark the Next Berm, Until the Dump is Complete

The pile rehabilitation through planting for surface protection and drainage of the lower bench should always commence once it is completed.

The first stage of work will include:

- Clearing all vegetation of medium and large size from dumping site
- Removing low-consistency materials such as vegetal soils, organic clays, and plastics, if present
- Constructing downstream sump
- Commencing block disposition for constructing the bottom drain.

The second stage will consist of:

- Continuing construction of the bottom drains
- Constructing peripheral drainage channels

The third stage will consist of:

- Waste rock and tailings disposition
- Revegetating
- Install instrumentation during the construction sequence, involving both the stacked material and the foundation.

18.12.10 Stability Analysis

A stability analysis section was prepared, passing through the highest points of the embankment, considering the hypothesis of any type of failure. The Slide program was used, employing the simplified Bishop Method, GLE, and Spencer methods, with resistance parameters typically used in rockfill waste rock dumps.

For the foundation, the resistance parameters from CIU triaxial tests conducted in neighbouring regions of the Project were adopted, which will be adjusted subsequently by laboratory tests being conducted for the area. The adopted geotechnical parameters are listed in Table 18-4.

Table 18-4: Geotechnical Parameters

Materials	γ (kN/m³)	C' (kPa)	Φ (graus)
Fill 1 (Barren Rock Fill)	19	1	40
Fill 2 (Coarse Waste)	20	10	37
Foundation 1 (Shale Saprolite)	16.9	9.6	26.9
Foundation 2 (Biotite Shale)	21	50	34

Notes: γ = Unit weight, C' = cohesion, Φ = friction angle

As the dump is composed of blocks, a simulation was not conducted with the water level positioned at half the height of the dump because there will be no loss of internal drainage, as the dump will drain naturally.

The geometric arrangement was designed to incorporate a structural waste rock mass placed along the edges and at the base of the main body of the pile. This arrangement aims to absorb stresses and interrupt potential critical failure surfaces, ensuring the overall stability of the system. This configuration also provides greater construction and operational flexibility, allowing the pile to be built in layers without the need for excessive compaction of the filtered tailings.

The evaluation of safety factors follows the guidelines outlined in ABNT NBR 13029 of July 2017, Mining—Preparation and Presentation of Waste Disposal Dump Project, as well as other related standards and decrees, and international practices, as shown in Table 18-5 and Table 18-6.

Table 18-5: ABNT—NBR 13029-2017—Mining—Preparation and Presentation of Waste Disposal in Dump Project

Rupture	Condition	Security Factor
General Slope	Normal Phreatic Surface	1.5
General Slope	Critical Phreatic Surface	1.3
Slope between Berms	Predominantly Soil Face	1.5
Slope between Berms	Predominantly Rock Face	1.3

Table 18-6: Waste Dump Stability Acceptance Criteria

Consequence	Confidence	Static Analysis		Pseudo-Static Analysis	Maximum Acceptable Voltage (%)
		Minimal Security Factor	Maximum Probability of Failure	Minimal Security Factor	
Low	Low	1.3–1.4	10–15	1.05–1.1	≤1
	Moderate	1.2–1.3	15–25	1.0–1.05	≤1.5
	High	1.1–1.2	25–40	1.0	≤2
Moderate	Low	1.4–1.5	2.5–5	1.1–1.15	≤0.75
	Moderate	1.3–1.4	5–10	1.05–1.1	≤1
	High	1.2–1.3	10–15	1.0–1.05	≤1.5
High	Low	≤1.5	≥1	1.15	≤0.5
	Moderate	1.4–1.5	1–2.5	1.1–1.16	≤0.75
	High	1.3–1.4	2.5–5	1.05–1.1	≤1

Source: Hawley & Cunning (2017).

The results of the stability analysis are summarized in Table 18-7 and in Figure 18-22 and Figure 18-23.

Table 18-7: Results of Stability Analyses

Section	FOS Minimal	FOS Pseudo-Static
BB	1.26/1.43	0.61/1.12

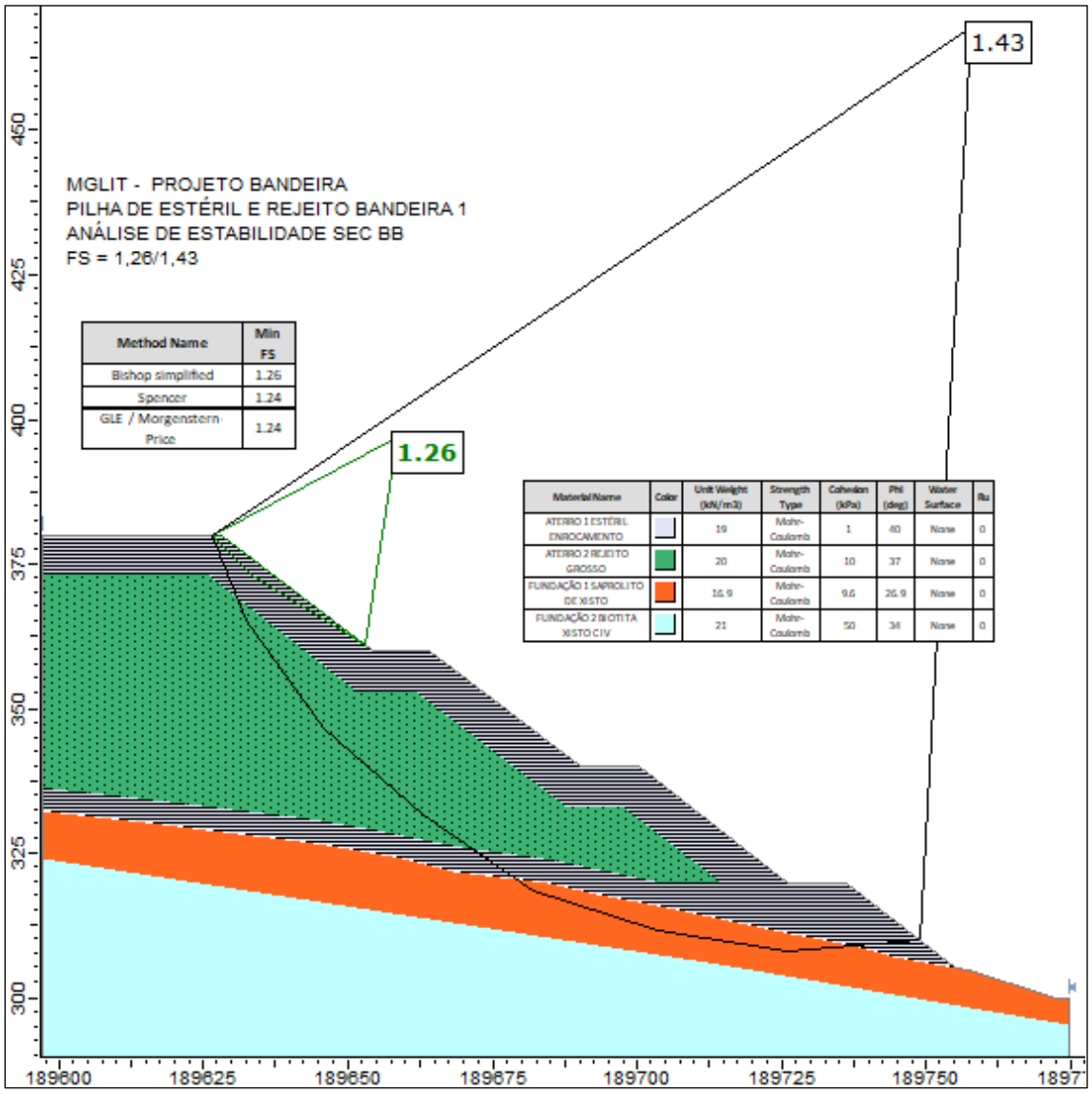


Figure 18-22: Stability Analysis of Cross-Section B–B, FOS = 1.26/1.43

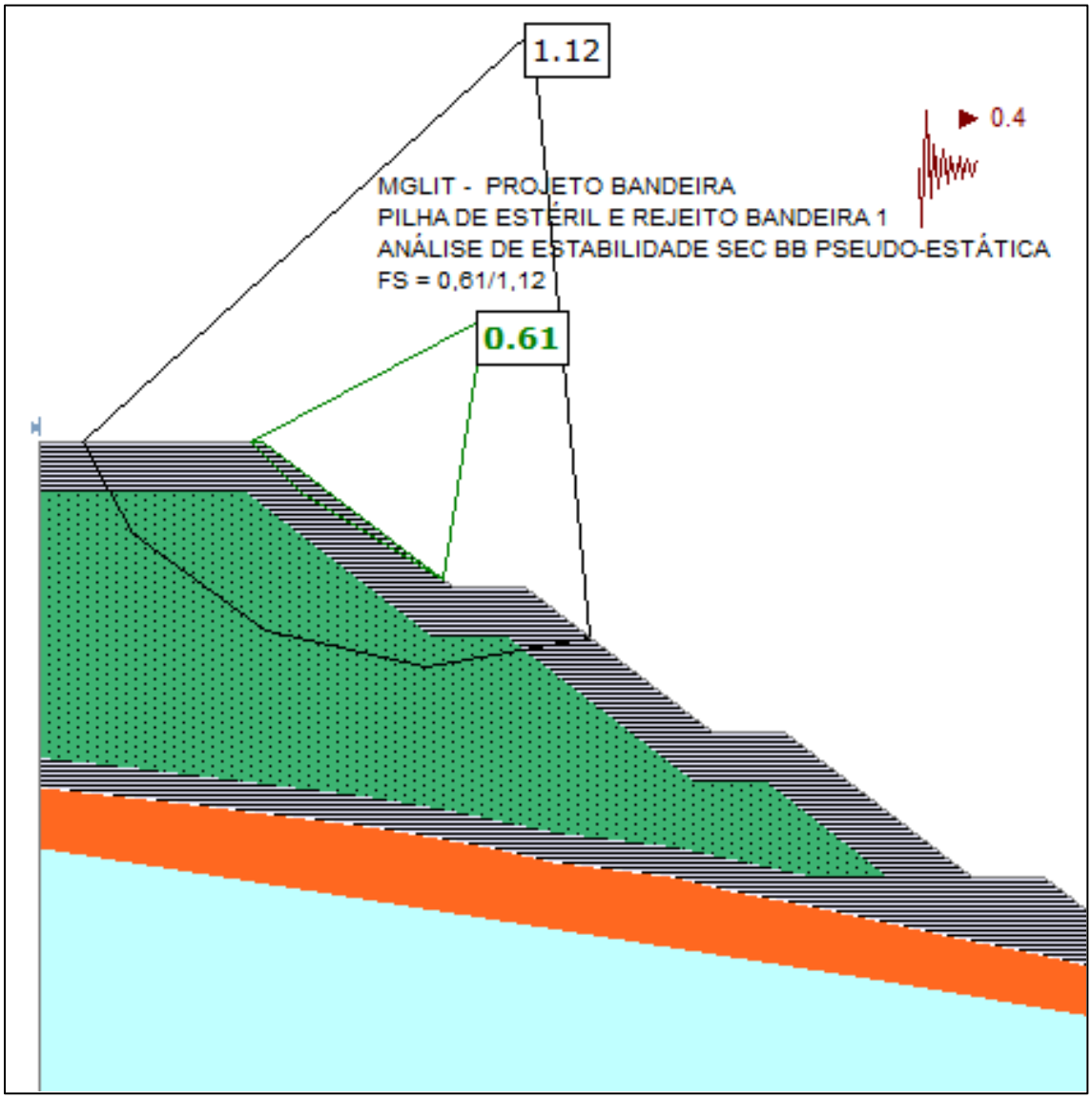


Figure 18-23: Stability Analysis of Cross-Section B–B Seismic Load, FOS = 0.61/1.12

The results indicate that the factors of safety (FOS) are in accordance with the factors typically adopted for similar structures, which are considered safe when the safety factor exceeds the values presented in Table 18-5 and Table 18-6. The critical failure surfaces with the lowest FOS were observed between berms, a behaviour typical of piles composed of materials with contrasting grain sizes (filtered tailings + waste rock).

With a seismic loading of 0.04 g, the safety factors remain above the stipulated value of FOS = 1.10.

The safety factors found for the theoretical rupture surface passing close to the slope face and presenting results with FOS <1.3 are a function of the software, which assumes that materials without cohesion, only with friction angle, tend to roll off the slope face, without considering the interlocking of the blocks that prevent rolling. The increases in resistance due to compaction and rearrangement

resulting from self-weight over the life of the deposit are not quantified, as they are difficult to quantify but do exist.

The alternative adopted for the disposal of waste rock and tailings at the Project ensures technical feasibility and operational safety, in accordance with current standards and aligned with best engineering practices.

18.12.11 Instrumentation

The instrumentation sections are designed to monitor deformations, verify the efficiency of internal drainage, and support corrective measures if necessary. They may include water level indicators, although no water level rise is expected due to the inherent drainage of the piles.

The geotechnical instrumentation plan, integrated into the monitoring program, aims to continuously assess the structural and geotechnical performance of the piles, validate stability and drainage analyses, and provide data for operational control and safety, in accordance with ABNT NBR 13.029:2024.

Monitoring will be conducted at two levels—visual and instrumented—allowing the early detection of changes or anomalies that could affect stability.

18.12.12 Sediment Containment Ponds

The waste rock and tailings facilities will be constructed using granular material and will incorporate fine containment sumps, integrated into the surface drainage system. Trapezoidal rockfill channels at the base of the pile will convey rainfall runoff and surface exudates to the sumps, retaining particles larger than 75 µm and allowing fine material to settle, while preserving natural flow and minimizing environmental impacts.

Given the co-disposal operation of waste rock and filtered tailings at the Project, which presents a moderate potential for sediment generation due to surface erosion, a containment system based on excavated sumps has been implemented. This solution eliminates the risk of Potential Associated Damage and simplifies both operation and maintenance.

The design complies with regulatory criteria (ABNT NBR 13.028:2024), considering: a 1,000-year return period for structural stability; 24-hour rainfall for a 2-year return period; minimum sediment removal efficiency of 85%; annual sediment generation estimated at 300 m³/ha for rock areas and 30 m³/ha for vegetated areas; and annual inspections prior to the rainy season.

Six sumps were positioned along the main thalwegs downstream of the pile, with volumes sized to store annual sediments and accommodate the designed runoff. This arrangement ensures stability, preserves natural drainage, and allows operational access, maintaining elevations above the local water table and harmonizing the infrastructure with the existing terrain.

All waste disposals will be done using the mining equipment already sized for mining, transportation, and the spreading operation, and there will be no construction of a sediment-containment dam (usually the largest expenditure of waste rock dumps).

Project Description of the Surface Drainage System—North Dump

The proposed surface drainage system for North Dump includes a surface-water management and sediment-containment system. The surface-water management system consists of peripheral channels around the dumps, which collect surface runoff from the Projected area of the dumps and direct it to the draining heaps at the lowest points of the valleys.

Approximately 93% of the surface flow from the drainage area of North Dump will be collected and directed to channels CP-01 and CP-02, which will discharge upstream of the draining heap to be placed at the northwest end of the dump. The effluent flow from this draining heap will be discharged into a valley that drains to the right bank of the Piauí River.

The remaining surface-flow produced in the drainage area of North Dump will be collected and directed to Channels CP-03 and CP-04, which will discharge upstream of the draining heap to be constructed at the southeast end of the dump. The effluent flow from this draining heap will be discharged into an unnamed tributary on the right bank of the Piauí River.

Table 18-8 shows the arrangement of the surface drainage and sediment containment system designed for North Dump, while typical cross-sections of the hydraulic devices are illustrated in Figure 18-24. The synthesis of the geometric characteristics of the surface drainage devices designed for North Dump can be found in Figure 18-25.

Table 18-8: Geometric Characteristics of Designed Surface Drainage Devices—North Dump

Structure	Description	Minimum Dimensions (m)	D50 (mm)
CT-01 Top Channel	Trapezoidal section excavated in soil and/or dump. Rockfill covering, with a minimum thickness equal to twice the D50 of the block. Transition is composed of 20 cm of granular material and non-woven polyester geotextile blanket. Needled, with tensile strength of 21 kN/m (type Bidim RT 21—former OP40). In sections with a steep slope, equal to or greater than 5%, concrete must be applied.	(0.5 x 0.5) m 1V:1.5H	200
CT-02 Top Channel		(0.5 x 0.5) m 1V:1.5H	200
CP-01 Peripheral Channel		(1.0 x 1.0) m 1V:1.5H	400
CP-02 Peripheral Channel		(1.0 x 1.0) m 1V:1.5H	400
CP-03 Peripheral Channel		(0.5 x 0.5) m 1V:1.5H	200
CP-04Peripheral Channel		(0.5 x 0.5) m 1V:1.5H	200
DA-01 Water Runoff		(1.0 x 0.5) m 1V:1.5H	400
DA-02 Water Runoff		(1.0 x 0.5) m 1V:1.5H	400

Notes: CP = Canal Periférico (peripheral channel); DA = Descida de água (water runoff); CT = Canal de topo (top channel).

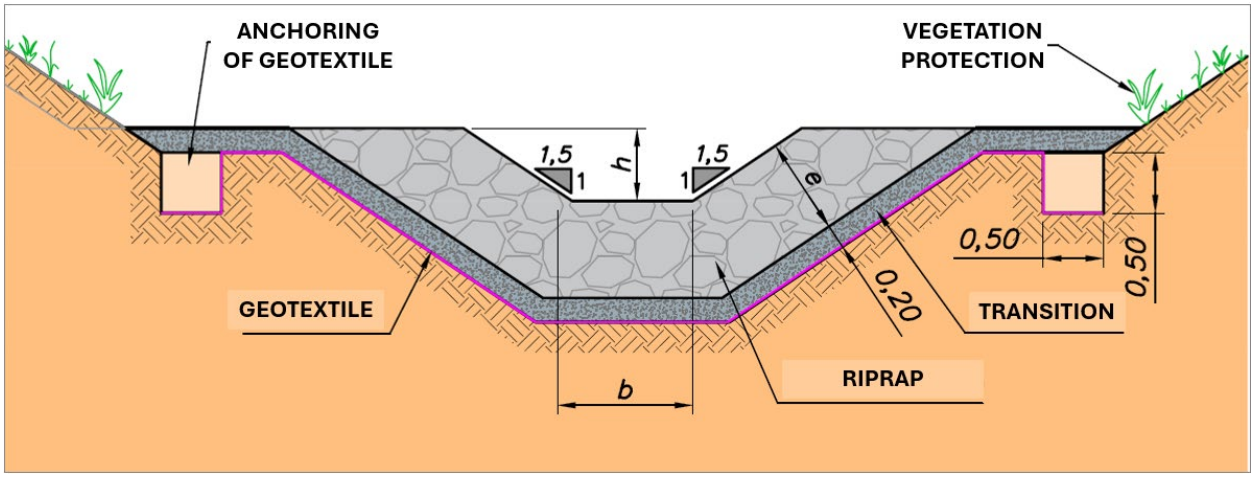


Figure 18-24: Typical Cross-Section of Hydraulic Devices Consisting of a Trapezoidal Channel with Rockfill Lining

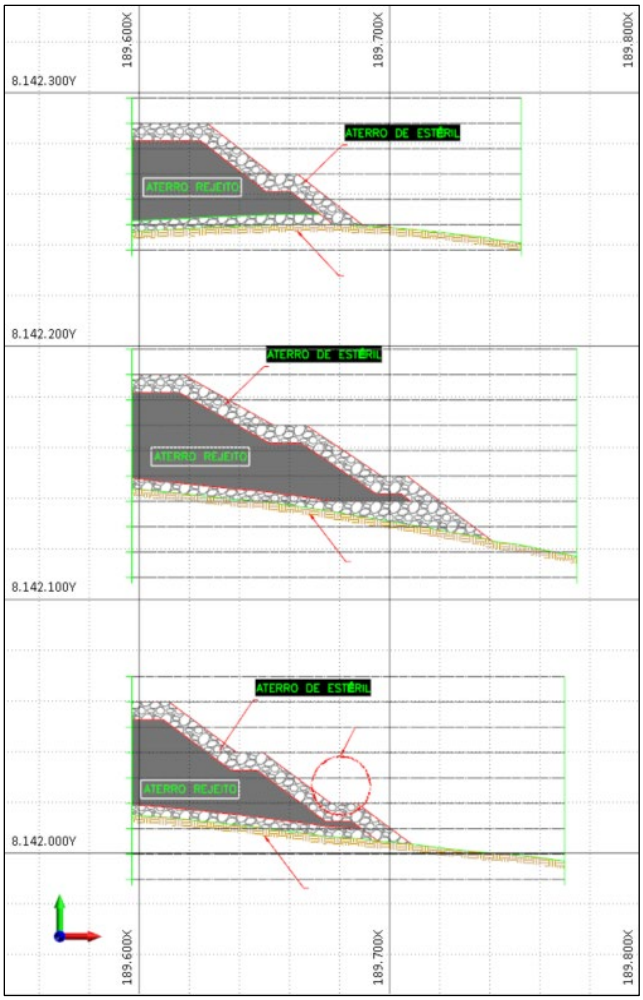


Figure 18-25: Waste Dump North Cross-Section—Arrangement

Sediment Containment Pond System Project Description

The arrangement of the surface drainage and sediment containment system designed for North Dump is presented here. The containment of coarse sediments will be carried out through draining heaps, with a maximum height of 2 m, to be constructed at the northwest and southeast ends of the dump. It is recommended that at least two draining heaps be constructed at each end. The first heap should be positioned at least 5 m downstream from the foot of the dump, and the second, at least 5 m downstream from the foot of the upstream heap.

There should be no water accumulation upstream of the draining heaps. If it occurs, the geotextile on the upstream face should be replaced, as it may be clogged. Cleaning the area upstream of the draining heaps should be performed regularly, always after rainy periods or when the accumulated sediments reach a height of 1 m.

Figure 18-26 presents the typical section of the draining heaps.

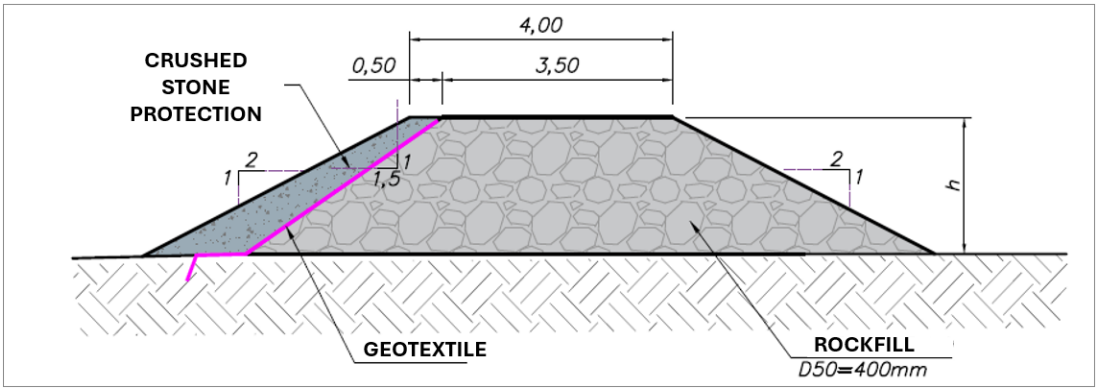


Figure 18-26: Typical Drainage Heap

18.12.13 Description of the Bottom Drainage System Project

The proposed bottom drainage system for North Dump consists of two rockfill drains to be installed in the existing valleys beneath the projection of the dump. These drains are intended to collect the percolated flows from the waste material to be deposited, thereby preventing the formation of saturation points within the dump body and ensuring the geotechnical safety of the structure. The designed drains will discharge into the dump's surface drainage system (Channels CP-01 and CP-02).

The arrangement of the bottom drainage system designed for Dump 1 is shown in Figure 18-28, the typical cross-sections of the drains in Figure 18-29, and the typical longitudinal section of the toe drain. A summary of the geometric characteristics of the bottom drainage device is presented in Table 18-9.

Table 18-9: Summary of Geometric Characteristics of the Designed Bottom Drainage Device

Structure	Drainage Section Dimensions (m)		
	Base (Smaller)	Base (Higher)	Height
DF-01	0.5	2.0	0.5
DF-02	0.5	2.0	0.5

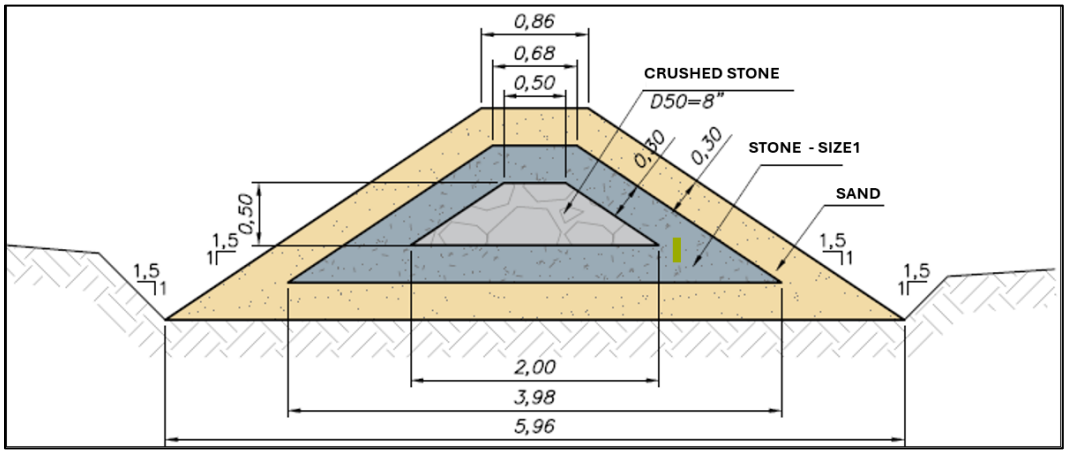


Figure 18-27: Typical Bottom Drain Device Cross-Section

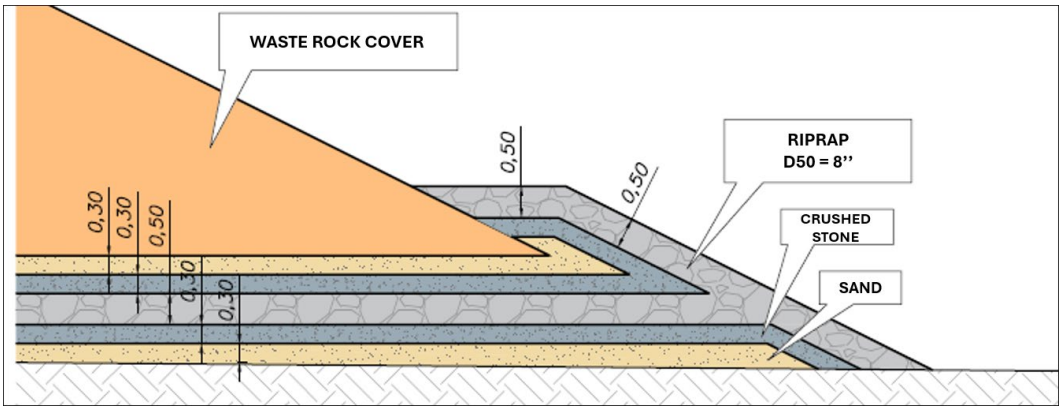


Figure 18-28: Typical Foot Drain Cross-Section

Waste and Tailings Facilities—South Dump

In addition to North Dump, there are plans for South Dump, which will be constructed mainly using tailings from the concentration plant, with construction initiated after stacking in North Dump is completed. Table 18-10 presents the geometric parameters of South Dump.

Table 18-10: Geometric Parameters of South Dump

Geometric Parameter	Value
Maximum Height (m)	155
Base and Crest Elevation (m)	275-430
Maximum Seat Height (m)	20
Minimum Width of Shoulders (m)	10
Slope—Angle Between Berms (°)	1.3:1—37.6
Slope—General Angle (°)	1.8:1—29
Longitudinal Slope (%)	1
Cross Slope (%)	5
Occupied Area (ha)	37.2
Available Volume (Mm^3)	15.9

The selected deposition site comprises an area with an average slope of approximately 17%. The foundation is characterized by the presence of weathered rock at greater depth and soil alteration in the shallower portion (residual soil) up to about 20 m.

The dump will be shaped on natural terrain, covering an approximate total area of 10.45 ha and with a final accumulation capacity of 2,270 km^3. The deposited material will be tailings consisting of sandy material.

The construction method will be the same as described for Dump 1, as well as the general premises for the design of the internal and external drainage systems of the dump.

Figure 18-29 presents the South Dump design.

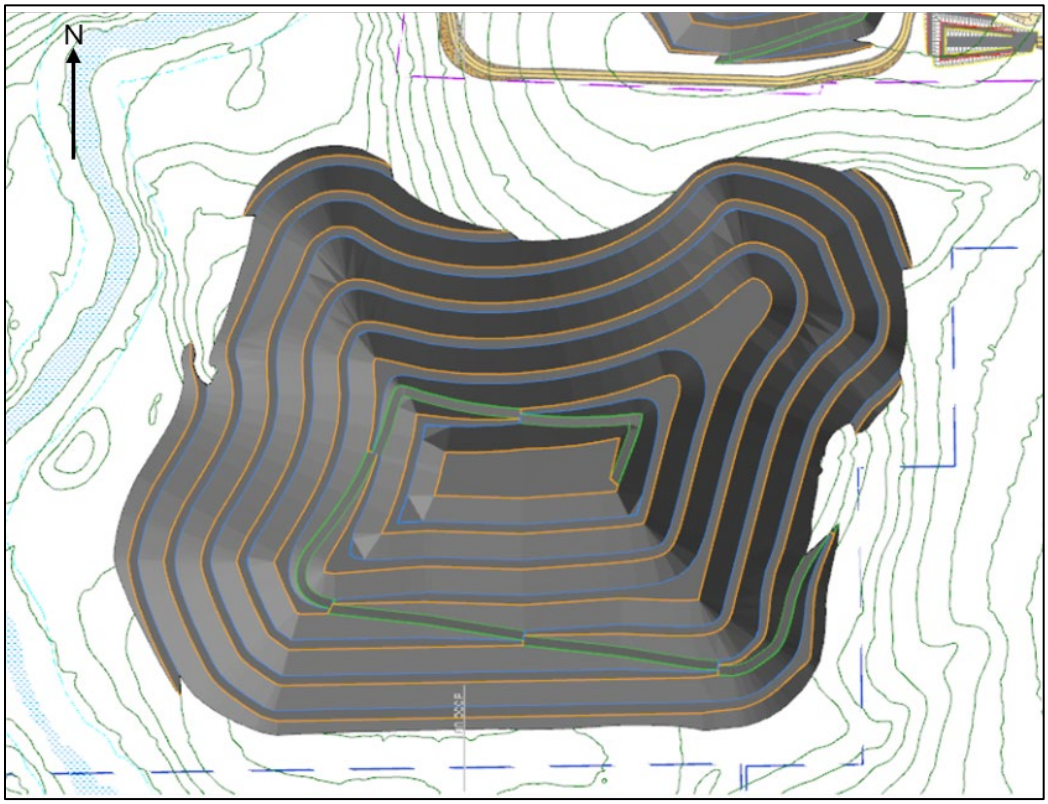


Figure 18-29: South Dump Design (Plan View)

18.13 Waste Dumps—Conclusions and Recommendations

The Master Plan for Waste Rock and Filtered Tailings Disposal demonstrates full technical, geotechnical, and environmental feasibility under the conditions of the Project. The studies conducted show that:

- Geotechnical conditions at the site are favorable, with dense residual soils and high-strength rock, allowing safe stacking without the need for structural reinforcement.

- Global and local stability analyses indicate safety factors above the minimum regulatory requirements under all evaluated conditions (drained, critical, and seismic), ensuring stable performance of the pile throughout its operational life.
- The surface and internal drainage system ensures efficient runoff, erosion control, and absence of saturation, maintaining drained conditions during all phases of operation.
- Sediment sumps are sized for hydraulic efficiency and operational simplicity, reducing the risk of Potential Associated Damage and facilitating the management and reuse of sedimented material.
- The closure design ensures stable conditions, with a vegetated final cover and minimal need for additional interventions, promoting environmental reintegration and mitigating geotechnical and erosive risks.

In conclusion, the Waste Rock Piles of the Project were designed in accordance with best practices in tailings and waste engineering, providing high technical reliability, low environmental impact, and compliance with national and international dam safety and dry disposal standards.

Additionally, vegetative residues from preparatory site clearing can be used to revegetate the initial benches of the landfill, contributing to the project's sustainability and environmental restoration of the area.

19 MARKET STUDIES AND CONTRACTS

MGLIT engaged Fastmarkets to provide a basis for the long-term price forecast. Fastmarkets is a cross-commodity price-reporting agency for metals and mining.

19.1 Macroeconomic Outlook and Lithium

Global lithium demand tracks the electrification trend in transport and stationary storage, reinforced by decarbonization policy and purchase subsidies. Between 2018 and 2024, demand expanded at an approximate 25% compound annual growth rate (CAGR). Fastmarkets expects growth to continue at a moderated approximately 18% CAGR as electric vehicle (EV) markets mature, and policy support becomes more selective.

Prices and balances reflect this push–pull. Production cuts are helping to rebalance the market, yet there is a risk that prices will remain too low to incentivize all the investment required. Larger lithium supply deficits are expected from about 2032, although higher prices later in the decade should draw supply back. For 2025 specifically, Fastmarkets expects carbonate to average about $0.50/kg above hydroxide, with convergence thereafter; a strong nickel cobalt manganese (NCM)-led EV recovery could briefly invert that spread as the downstream lithium conversion plants restart idle capacity. China's rapid 2021–2023 supply response will be harder to repeat as demand scales. By 2027, total demand is projected to be more than two-and-a-half times that of 2022, keeping conditions generally tight as annual tonnage-needs compound.

19.2 Lithium Price Forecast

Fastmarkets expects a period of near-term balance that gradually gives way to tighter conditions later in the decade. Production cuts have helped slow the price slide and rebalance the market, and the outlook is broadly balanced until around 2027. However, the 2024 low-price environment delayed or cancelled a number of projects, raising the risk that future prices will need to work harder to attract new capacity when demand accelerates.

From approximately 2032, larger supply deficits are expected as lithium project certainty diminishes. Fastmarkets notes that higher prices toward the end of the decade should incentivize a supply response, moderating tightness as electrification compounds annual tonnage requirements.

Fastmarkets forecast average prices (2025–2032):

- Lithium hydroxide: $21.61/kg
- Lithium carbonate: $21.66/kg
- Spodumene concentrate: $1,716/t.

Taken together, the forecast implies a range-bound, but investable environments Spodumene Price History (2018–2024) and Forecast (2025–2032)

19.3 Contracts

MGLIT expects that terms within sales contracts, including spodumene off-take agreements, that could be entered into would be typical of, and consistent with standard industry practices, and be similar to contracts for the supply of spodumene concentrate elsewhere in the world.

Other than for product sales, the largest contracts will cover items such as mine equipment, drill-and-blast operations, mining contract services, and other contracts that are typical of a hard rock spodumene mine. It is expected that terms within any contracts that could be entered into would be typical of, and consistent with standard industry practices. MGLIT is currently negotiating contract terms. Contracts will be renegotiated and renewed as needed throughout the LOM.

MGLIT is currently negotiating contract terms for the open-pit mining and construction contracts. The mining contract would likely comprise a fixed administration fee per month; costs associated with mobilization and demobilization at the start and end; a volume-based rate per tonne of ore; and a rate per tonne of waste. The construction contract will also be typical of, and consistent with, standard industry contracts. Contracts will be renegotiated and renewed as needed throughout the LOM.

19.4 Qualified Person's Comment

The QP reviewed the Fastmarkets report, agreed with the content, and did not find any significant factors or risks.

20 ENVIRONMENTAL STUDIES, PERMITTING, AND COMMUNITY IMPACTS

This section presents the environmental and social baseline, the permitting framework, and the status of the Project's regulatory processes. The analyses comply with applicable federal, state, and municipal legislation covering environmental protection, water resources, biodiversity, land use, cultural heritage, and social-economic assessment of surrounding communities.

The environmental studies were developed in accordance with the National Environmental Policy (Federal Law No. 6,938/1981) and its regulatory Decree No. 99,274/1990, which establish the principles and instruments for environmental licensing in Brazil. The mining regulatory framework follows the Brazilian Mining Code and related decrees under the supervision of the Ministry of Mines and Energy (MME) and the National Mining Agency (ANM).

20.1 Regulatory and Permitting Framework

The Project is subject to a coordinated regulatory framework that integrates both mining and environmental permitting processes, involving federal, state, and municipal institutions.

At the federal level, mining activities are regulated by the National Mining Agency (ANM), linked to the Ministry of Mines and Energy (MME). ANM manages mineral rights, evaluates technical and economic feasibility, and grants concessions for mineral exploitation.

The Project follows the sequential mining permitting process defined by the Brazilian Mining Code, which includes:

- Exploration Authorization—granting the right to conduct geological investigations and sampling.
- Final Exploration Report (RFP)—submission of exploration results demonstrating the deposit's geological and economic potential, currently under ANM review.
- Economic Exploitation Plan (PAE)—submission of the detailed plan for mining, processing, infrastructure, environmental and social management, and closure; the Bandeira PAE for the underground mine was submitted on September 4, 2024.
- Mining Concession Ordinance (Portaria de Lavra)—issued after approval of the PAE and confirmation of environmental licensing, granting the legal right to extract and sell the mineral resource.
- Concession Possession (Imissão de Posse)—formal handover of operational control of the deposit, authorizing the start of production.

The Mining Concession Ordinance depends on the issuance of the Project's environmental license, a procedure conducted by the State of Minas Gerais, ensuring integration between ANM and the environmental authorities.

At the state level, the State Secretariat for Environment and Sustainable Development (SEMAD) is the competent environmental licensing authority. SEMAD evaluates and issues licenses through its

regional branches, in the case of Project, the Eastern Minas Gerais Regional Environmental Unit (URA-Leste) was designated for the licensing process.

The State Council for Environmental Policy (COPAM) is the deliberative body that provides final approval for environmental licenses following SEMAD's technical review. COPAM operates through specialized chambers that assess projects according to classification criteria established in state regulations.

Environmental licensing in Brazil generally follows a three-stage process, as established by CONAMA Resolution No. 237/1997:

- The Preliminary License (Licença Prévia—LP) attests to the environmental feasibility of the project and approves its basic design and location.
- The Installation License (Licença de Instalação—LI) authorizes construction and installation of facilities in accordance with approved plans and mitigation measures.
- The Operating License (Licença de Operação—LO) authorizes operation of the project after verification of environmental compliance with the LP and LI conditions.

In Minas Gerais, environmental licensing is regulated by State Decree No. 47,383/2018 and COPAM Normative Deliberation No. 217/2017 (ND 217/2017), which modernized and consolidated state procedures.

Under ND 217/2017, projects are classified according to:

- Project Size, determined by production capacity, physical footprint, and complexity
- Potential Environmental Impact, defined as low, medium, or high
- Locational Criteria, based on environmental sensitivity of the area and vegetation type and succession stage.

The combination of these criteria determines the applicable licensing modality, ranging from simplified to concurrent procedures.

For the Project, SEMAD determined that the appropriate modality is the Concurrent Environmental License (Licenciamento Ambiental Concomitante [LAC]), as the activities occur mainly in previously altered areas with limited vegetation suppression in an early regeneration stage of the Atlantic Forest biome.

The LAC, introduced by ND 217/2017, can merge the Preliminary (LP), Installation (LI) and Operation (LO) stages into a single process that allows project construction once feasibility and mitigation measures are approved.

The State Forestry Institute (IEF) supports SEMAD by evaluating vegetation suppression and intervention requests in Permanent Preservation Areas (APPs) and Legal Reserves (RLs). It analyzes the Environmental Intervention Project (PIA) and Native Vegetation Planting Plan, as required under SEMAD/IEF Joint Resolution No. 1,914/2013.

The Minas Gerais Water Management Institute (IGAM) manages state water resources, issuing Water Rights (Outorgas) for abstraction or discharge in accordance with State Water Resources Policy.

At the federal level, the National Water Agency (Agência Nacional de Águas [ANA]) authorizes the use of water from inter-state or federal rivers, such as the Jequitinhonha River, ensuring alignment with the National Water Resources Policy.

Cultural heritage is overseen by the National Institute of Historic and Artistic Heritage (IPHAN), responsible for archaeological and intangible assets of federal relevance, and the State Institute of Historic and Artistic Heritage of Minas Gerais (IEPHA-MG), responsible for state-level heritage evaluation. Both agencies issue technical opinions that are incorporated into SEMAD's licensing process.

Other technical entities, such as the State Environmental Foundation (FEAM) and the Rural Environmental Registry (CAR) system, support SEMAD in pollution control, legal reserve validation, and monitoring of restoration commitments.

At the municipal level, the Municipalities of Araçuaí and Itinga verify zoning compatibility and issue Land-Use and Occupation Certificates, ensuring that project facilities comply with local land-use and urban development regulations.

20.2 Mining and Environmental Licensing Approvals

The permitting pathway of the Project follows a coordinated sequence of environmental and mining approvals that advance in parallel and are interdependent. In Brazil, environmental authorization is a prerequisite for the federal concession of mining rights, ensuring that all environmental and social management plans are in place before mineral extraction begins.

The process began with the exploration stage, when MGLIT obtained mineral exploration licenses authorizing geological investigations, drilling and sampling in the project area. The data collected were consolidated into Final Exploration Reports (RFPs), submitted to ANM's review to confirm the technical and economic viability of the lithium pegmatite deposit.

Following acceptance of the RFPs, MGLIT prepared the Economic Exploitation Plan (PAE) for the underground operation. Submitted to ANM on September 4th, 2024, the PAE describes the mining method, process flowsheet, production capacity, economic justification, environmental management, and conceptual closure strategy. A consolidated PAE covering both the underground and open-pit operations will be filed subsequently to ensure full integration of the mining and environmental scopes.

In parallel, MGLIT initiated the Concurrent Environmental Licensing (Licenciamento Ambiental Concomitante—LAC) with SEMAD on November 20, 2023. The application was supported by the Environmental Control Report (RCA) and Environmental Control Plan (PCA) prepared by Neo AgroAmbiental, which characterized the site conditions, identified potential impacts, and proposed mitigation and monitoring programs.

According to ND 217/2017, the Project's underground activities are classified under the following codes:

- Tailings/waste rock piles from ornamental and cladding rocks, pegmatites, gems, and non-metallic minerals (A-05-04-6): usable area of 20.67 ha, medium polluting/degrading potential, large size, corresponding to Class 04.
- Underground mining of pegmatites and gems (A-01-01-5): gross production >787,800 m³/a, medium polluting/degrading potential, large size, also corresponding to Class 04.
- Ore Treatment Unit (UTM), with wet processing (A-05-02-0): installed capacity of ≤1,300,000 t/a, considerable polluting/degrading potential, medium size, classified as Class 05.
- Resale stations, supply stations, supply points, retail system installations, floating stations, and aviation fuel resale stations (F-06-01-7): storage capacity ≤14.9 m³, activity classified as non-passible—Class 02.

Following a technical inspection by SEMAD in September 2024, the licensing process was re-classified as a Corrective Installation and Operation License under the same LAC framework. Upon completion of the Project's assessment, on February 13, 2025, the multidisciplinary technical team of the State Environmental Foundation (FEAM), entity subject to SEMAD, issued the Technical Opinion No. 14, recommending Project approval, which is still pending. Upon COPAM approval, the Project LAC will authorize both the construction and operation of the underground mine and process plant, marking a key regulatory milestone.

Complementary authorizations have also been secured. The Minas Gerais Water Management Institute (IGAM) issued a ten-year Water Rights authorizing abstraction of 101.6 m³/h from the Piauí River, and a River-Crossing Authorization for installation of the bridge over the same river, and the National Water Agency (ANA) issued a Water Rights authorizing abstraction of 386 m³/h from the Jequitinhonha River for civil works, dust control, and other implementation activities. An Authorization for Vegetation Suppression was obtained for areas in an early regeneration stage within the Atlantic Forest biome, including limited interventions in Permanent Preservation Areas (APPs). This vegetation clearance authorization is directly linked to the main LAC and will be issued concurrently with the environmental license.

At the municipal level, Land-Use and Occupation Certificates issued by the municipalities of Araçuaí and Itinga confirm compatibility with local zoning and land-use regulations.

Once the LAC is approved by SEMAD and ratified by COPAM, the federal mining procedures will proceed. ANM will review and approve the PAE, issue the Mine Servitude Rights (Servidão Minerária) authorizing access to and use of land for mining purposes, and subsequently grant the Mining Concession Ordinance (Portaria de Lavra). The final step, the Concession Possession (Imissão de Posse) will confer legal possession and allow MGLIT to commence full-scale extraction and commercialization of the mineral resource.

Parallel licensing processes are underway for complementary infrastructure. The 138 kV transmission line and Integrating Substation are under state review, requiring vegetation-suppression authorization from the State Forestry Institute (IEF) and grid-connection approval by CEMIG.

MGLIT also plans to construct a dedicated pipeline connecting the Jequitinhonha River to the project site. This additional water source is being developed as a risk mitigation measure, since the Piauí River, a smaller, seasonal tributary, may experience low flow or dry conditions during the dry season. The Jequitinhonha River, with greater flow regularity and availability, will therefore ensure a reliable year-round water supply for both construction and operation.

A new LAC process will subsequently be initiated for the open-pit expansion, which will increase production capacity to approximately 1.5 Mt per year and include a tailings storage facility of about 38 ha.

MGLIT continues to actively engage with all relevant regulatory agencies, community stakeholders, ensuring full compliance with Brazilian law and addressing evolving expectations transparently and proactively.

The following summarizes the environmental licenses and authorizations already issued, under analysis, and planned to be initiated for the Project:

- Water Rights (ANA): for abstraction of 386 m³/h from the Jequitinhonha River during construction and infrastructure installation activities
- Water Rights (IGAM): authorizing abstraction of 101.6 m³/h from the Piauí River for a 10-year term
- River crossing authorization (SEMAD/IGAM): permitting installation of the bridge across the Piauí River
- Land-Use and Occupation Certificates (Municipalities of Araçuaí and Itinga): confirming compliance with municipal zoning and land-use requirements.

Ongoing environmental licensing process:

- Archaeological technical opinion (IPHAN): confirm compliance with the archaeological assessment and impacts evaluation related to the project construction and operation, as well as the associated management plan of cultural assets within the Project area.
- Cultural Heritage opinion (IEPHA): confirm compliance with the state cultural heritage assessment and mitigation measures related to the impacts of the project construction and operation.
- Concurrent Environmental License (LAC) (SEMAD): license for construction and operation of the process plant and underground mine.
- Authorization for Vegetation Suppression (IEF): for removal of native vegetation in early regeneration stage within the Atlantic Forest biome, including limited interventions in Permanent Preservation Areas (APPs). This authorization is directly linked to the LAC and will be issued concurrently with the license.
- Fauna Rescue (SEMAD/IEF): Fauna rescue and management during the construction phase.
- Environmental Intervention Project (IEF): submitted to IEF for review, addressing vegetation clearance and restoration measures for the 3km transmission line.

- Environmental Intervention Project (IEF): submitted to IEF for review, addressing vegetation clearance and restoration measures for the 100m connection between the CEMIG substation and project substation.

Planned licensing process:

- Concurrent Environmental License (LAC – Expansion) (SEMAD): expansion license for implementation and operation of the open pit, which will increase production capacity to approximately 1.5 Mt/a, and include a tailings storage facility of about 38 hectares.
- Environmental Intervention Project (IEF): submitted to IEF for review, addressing vegetation clearance and restoration measures for water pipeline.
- Water Rights (ANA): water abstraction for the operational phase in the Jequitinhonha River.
- Road-Crossing Permits (Municipality of Araçuaí): for two crossings associated with the water pipeline, to be requested before the start of civil works.
- Authorization for Vegetation Suppression (IEF): for removal of native vegetation in early regeneration stage within the Atlantic Forest biome, including limited interventions in Permanent Preservation Areas (APPs). This authorization is directly linked to the LAC of the open pit and will be issued concurrently with the license.

20.2.1 Land Access and Occupation

The surface-rights owner is legally obligated to grant access to mining rights holders for the conduct of exploration and mining activities. If the holder of mining rights or mining concessions does not own the surface property where the mining interests or mining-related infrastructure are situated, they may obtain access or occupy the land through mining easements granted by the ANM under the Brazilian Mining Code, or assert their access rights through Brazilian courts.

Holders of mining rights must compensate the surface rights owner for access to and use of the surface, and indemnify them for any property damage. The fee amount can be negotiated between the parties within the parameters defined by the Mining Code, with subsequent notification to the ANM of the agreement. However, if no agreement is reached, entities, after obtaining an exploration authorization or a mining concession, may petition a court to determine compensation values.

The Directly Affected Area (ADA) that the Project will impact encompasses rural properties in the municipalities of Araçuaí and Itinga (Table 20-1). MGLIT has a private agreement for the assignment of rights with Valitar Participações S.A. (Valitar), owner of the Brejos, Piauí (Part 1), and Boa Vista farms (Parts 1 and 2), for the conduct of mining activities on their properties.

Table 20-1: Rural Properties in the Project's ADA

Name/Identification	Title Holder	Area (ha)	Municipality MG	Registry No.	Title
Part 01 da Fazenda Piauí-Boa Vista	Valitar	2.0063	Araçuaí	038968.2.00 35875-88	Land Ownership MGLIT–Usufructuary)
Part 02 da Fazenda Piauí-Boa Vista	Valitar	14.5620	Araçuaí	038968.2.00 35876-85	Land Ownership (MGLIT–Usufructuary)
Fazenda Brejos, Monte Belo, Floresta Piauí Part 01A	Valitar	52.1089	Itinga	038968.2.00 36783-80	Land Ownership (MGLIT–Usufructuary)
Fazenda Piauí	Valitar	17.9315	Itinga	038968.2.00 41148-80	Land Ownership (MGLIT–Usufructuary)
Fazenda Piauí-Barreiro, Part 01	Valitar	42.5549	Itinga	038968.2.00 36330-81	Lang Ownership MGLIT–Usufructuary

Source: Neo AgroAmbiental (2023).

Legal Reserve and Conservation Units

In accordance with the Brazilian Forest Code (Law No. 12,651/2012), rural properties must maintain a portion of their native vegetation as a Legal Reserve (RL) to promote sustainable land use, conserve biodiversity, and protect native fauna and flora. For rural areas located within the Atlantic Forest biome, Article 12 of the Forest Code requires that at least 20% of each property be preserved as RL, duly registered with the competent environmental authority through the Rural Environmental Registry (CAR).

The properties designated for the future development of the Project—the Brejos, Piauí (Part 1), and Boa Vista (Parts 1 and 2) farms—are owned by Valitar Participações S.A. (Valitar) and registered jointly in the CAR as a single rural property. The RL areas within these properties fully comply with the requirements of Federal Law No. 12,651/2012. Importantly, the RL polygons do not overlap with the Directly Affected Area (ADA) of the Project, ensuring that all legally protected vegetation is preserved and excluded from mining activities.

Regarding regional environmental protection, the National System of Nature Conservation Units (SNUC), established by Law No. 9,985/2000, defines Conservation Units (UCs) as territorially delimited areas and their environmental resources, legally designated for conservation and subject to specific protection measures. The Project is not located within any Conservation Unit or its buffer zone, nor does it lie within 3 km of any UC boundary.

Although the Project is not situated in a formally protected area, it is within a region classified by the Ministry of the Environment (MMA) as having "very high biological importance" for conservation due to its elevated species richness, presence of endemic and threatened species, and unique ecological characteristics typical of the Atlantic Forest biome. This classification underscores the ecological relevance of the region and has been duly considered in the environmental studies and in the design of the Project's mitigation and monitoring programs.

20.3 Mine Closure

In Brazil, under Federal Decree No. 97,632/1989, mineral extraction projects must submit a Degraded Areas Recovery Plan (PRAD) together with the Environmental Impact Assessment (EIA) and Environmental Impact Report (RIMA) during the environmental licensing process. Accordingly, the recovery of areas degraded by mining must be planned from the outset. Mining companies must present their PAE to the National Mining Agency (ANM) to obtain the mining concession. These studies must include recovery and decommissioning measures to prevent degradation and minimize environmental impacts throughout the mining process. The ANM approves mine closure once the applicant demonstrates compliance with the decommissioning plan and environmental requirements.

The recovery of degraded areas seeks to restore ecological balance and reintegrate altered environments into the natural landscape, correcting disturbances caused by mining through mandatory revegetation. The conceptual strategy for the Project focuses on facilitating ecological succession to accelerate native vegetation establishment and continuously reintegrate rehabilitated areas into the surrounding environment.

The Conceptual Mine Closure Plan for the underground portion of the Project (Neo AgroAmbiental, 2023) defines corporate guidelines, closure activities, and technical and financial conditions approved by the ANM and the State Secretariat for Environment and Sustainable Development (SEMAD). The plan addresses final waste pile configurations with stable slopes, a drainage network for water control, and vegetation measures to reduce erosion and visual impacts. The closure strategy aligns with regulatory expectations and international best practices.

Mine closure planning begins well before the end of mining operations and is integrated into the project lifecycle. It involves setting clear objectives, defining methods, and establishing a realistic timeline for implementation. The plan considers environmental and social impacts, post-mining land use, and financial responsibilities, and includes stakeholder engagement with authorities, communities, and employees. Financial mechanisms, such as trust funds or guarantees, are established to secure future closure obligations.

Upon completion of underground operations, decommissioning will involve removing surface and underground infrastructure, sealing shafts to prevent access, managing air circulation, and backfilling mined areas to improve geotechnical stability and minimize subsidence risks.

Environmental rehabilitation will restore disturbed areas to a safe, stable, and productive post-mining condition. For the underground mine, this includes reshaping the terrain, re-establishing vegetation to control erosion and support habitat recovery, and, where necessary, implementing water treatment systems to manage water quality risks.

Following closure, a post-closure monitoring and maintenance program will track environmental performance and ensure long-term stability. This includes periodic inspections, water and air quality monitoring, subsidence control, and maintenance of drainage and residual infrastructure to ensure ongoing safety and environmental protection.

This feasibility study includes preliminary estimates of direct closure costs for the underground mine (Table 20-2). The main objective is to close the underground mine in a way that ensures public safety,

restores environmental integrity, and supports future land use opportunities aligned with local development objectives.

Table 20-2: Bandeira's Mine Closure Activities and Cost Estimate

Activities	Cost Estimate ($M)
Preparing a Detailed Mine Closure Plan	0.17
Removing Equipment and Underground Structures	0.25
Removing Mine Structures on the Surface (office, workshop, washer, tire shop, explosive preparation yard)	0.65
Reshaping and Revegetating the Land Surface	0.95
Stabilizing and Revegetating Remnant Waste Piles	0.34
Closing and Sealing All Mine Openings (e.g., portal, decline, ventilation raise)	0.20
Monitoring of Structure Stabilization Conditions, Surface and Underground Water Quality, and Mine Effluents	0.28
Total	**2.83**

This amount of $2.83 million was increased to $10 million in the sustaining CAPEX plan to include additional contingency.

For the open-pit mine, MGLIT has also proposed a closure plan integrated into the updated PAE for submission to ANM. After operations cease, the pit will be progressively filled with waste and tailings to restore topography and stabilize the terrain. This filling will support future waste stacking and optimize land use throughout the LOM. No additional closure costs are anticipated, as these activities are incorporated into site operating costs.

20.4 Summary of Socio-Environmental Diagnosis

The Project is within the Jequitinhonha River basin, specifically in the Piauí River sub-basin, an area characterized by gently undulating terrain with slopes between 0° and 5° and low susceptibility to erosion. Groundwater occurs in fractured aquifers of limited productivity, and the Piauí River is the main surface watercourse near the project site. The regional climate is semi-arid tropical (Aw), marked by distinct wet and dry seasons, average annual rainfall below 1,000 mm, and high evapotranspiration rates, making seasonal water scarcity an important environmental consideration for project development and water management.

The vegetation in the project area is mainly Seasonal Deciduous Forest (FED) in a submontane formation within the Atlantic Forest biome. The landscape has been largely modified by pasture and small-scale agriculture, leaving fragmented patches of secondary vegetation interspersed with open areas. Field surveys indicate a low degree of naturalness, with flora and fauna communities adapted to anthropized environments. The local fauna includes species from the transition zone between the Atlantic Forest, Cerrado, and Caatinga biomes, reflecting regional ecological diversity, although most species identified are widely distributed and tolerant to human activity.

From a socioeconomic perspective, the project is situated between the municipalities of Araçuaí and Itinga, in the Jequitinhonha Valley, a region of strong cultural identity, known for its artisanal traditions, folklore, and community ties, and historically characterized by limited economic diversification. The

closest rural communities are Barreiros and Fazenda Velha, both within Araçuaí's rural zone. Residents depend primarily on subsistence agriculture, livestock farming, and government social programs. There are no permanent residents within the project area itself. The municipalities' main urban centers provide education, health, and public services. The project is expected to generate employment, income, and local supplier opportunities, supporting the economic revitalization of the Jequitinhonha Valley while preserving its cultural and social fabric.

For detailed baseline data, refer to the Environmental Control Report (RCA) and Environmental Control Plan (PCA) prepared by Neo AgroAmbiental (2023).

20.5 Environmental and Social Management Plan

The environmental and social assessment identified potential impacts on the physical environment, including waste generation, soil and water contamination risks, erosion processes, noise, and increased vehicle traffic. Regarding the biotic environment, the main impacts relate to vegetation suppression and faunal disturbance during construction. In the socioeconomic context, potential impacts include landscape changes, pressure on local infrastructure, and community expectations associated with employment opportunities.

To mitigate these impacts, the Environmental Control Plan (PCA) developed by Neo AgroAmbiental (2023) includes preventive, corrective, and monitoring measures organized into thematic programs, such as:

- Atmospheric and Sound Quality Maintenance Program
- Solid and Liquid Waste Management Program
- Erosion Control and Surface Water Quality Monitoring Programs
- Vegetation Suppression Control and Fauna Monitoring Programs
- Recovery Plan for Degraded Areas (PRAD)
- Maintenance and Conservation of Permanent Preservation Areas and Legal Reserves
- Social Communication Program and Program to Prioritize Local Labour
- Occupational Health, Safety, and Risk Management Programs.

According to the conclusions of the RCA/PCA, the Project is considered environmentally viable, as the potential impacts identified can be effectively mitigated through the implementation of appropriate management programs and continuous environmental monitoring throughout the construction and operational phases. The Project does not directly affect any communities or households, and there are no families residing within the Project footprint or in the areas designated for mining and associated infrastructure. The land required for implementation is privately owned, previously utilized for rural and pasture activities, and free from permanent human occupation. Consequently, no physical or economic displacement is anticipated, and no resettlement measures are required. Environmental assessments further indicate that the Project's physical and biological impacts are low in magnitude, as activities are concentrated in previously modified areas characterized by early-stage regeneration vegetation, limited fauna occurrence, and the absence of sensitive habitats or protected ecosystems.

21 CAPITAL AND OPERATING COSTS

21.1 Basis of Estimates

CAPEX and OPEX estimates were developed to support the Project's feasibility study. These estimates are calculated within a range of −20% to +30%.

The base date of the estimates is the second quarter (Q2) 2025, with a reference exchange rate of R$5.85:$1.

The reference exchange rate of R$5.85:$1 is the median 2026 forecast of the ten largest brokers by market capitalization that provide 2026 forecasts.

These estimates are based on the feasibility-study conceptual sizing of the main mine, process, mechanical, and electrical equipment, which were costed through consultations with traditional market suppliers. Mechanical equipment was priced from recent quotes from a preliminary equipment list. Earthworks and civils costs were determined from estimative quantities and priced using data base figures. Mechanical erection was priced using a database and comparing to similar projects recently undertaken. Mine development and mining costs were estimated based on real quotations obtained from contractors currently operating in Brazil and benchmarked against similar underground mining projects developed in recent years. The estimates include detailed evaluations for development, production, and services, considering unit costs for drilling, blasting, mucking, and hauling operations. Labour, consumables, and maintenance costs were also derived from recent contracts and supplier quotations, ensuring realistic and up-to-date pricing aligned with local market conditions.

Mine equipment costs were established through direct quotations obtained from suppliers for the main units of the production and support fleet. Labour costs were determined by a third-party consulting company that conducted a market survey in the project region, identifying current salary levels, Labour charges, and employee benefits applicable to the mining sector.

Other items (instrumentation, automation, electrical materials, and smaller-diameter piping) were estimated from similar installations and benchmarking, applying an appropriate estimate factor in each case.

21.1.1 Estimate Price Source

PROMON and MGLIT prepared cost estimates for process and mechanical equipment, design criteria, process flowchart, mass balance, descriptive process sheets, master layout/plan, conveyor information, general earthmoving plan, quantity sheets for the disciplines of metal structures, boiler making, and piping. The sources of costs are presented in Table 21-1.

Table 21-1: Sources of Direct and Indirect Cost Estimates

Description	Responsibility	Source
Mine Equipment Supply	MGLIT	Supplier—Market Quotes
Process, Mechanical and Electrical Equipment Supply	R-Tek	Supplier—Market Quotes
Equipment Installation—Process and Mechanical	R-Tek	Database
Supply and Installation of Structural Steel, Platework and Piping >4"	R-Tek	Database
Supply and Installation of Electrical, Piping <4", and Instrumentation and Telecom Equipment	R-Tek	Database
Civil	Promon	Database
Production Support Infrastructure	Promon	Database
Infrastructure	Promon	Quotes—Database
Freight	R-Tek	Database
Mobilization—Demobilization—Camp	Promon	Database
Spares	R-Tek	Market quotes Factored
Erection Supervision	R-Tek	Database
Commissioning	R-Tek	Database
QA/QC	R-Tek	Database
Pre-OPEX—Mine	MGLIT	Estimated
Pre-OPEX—Plant	MG Lit	Quotes
EPCM	R-Tek	Database
Owner´s Team	MGLIT	Estimated
Insurance / Risk	MGLIT	Factored
Contingency	R-Tek	Factored

21.2 Work Breakdown Structure

Costs were classified according to the Project's work breakdown structure (WBS) (Table 21-2).

Table 21-2: Work Breakdown Structure

Area	Description
0000	General
1000	Mine
2000	Crushing
3000	Beneficiation Plant
4000	Dry Disposition
5000	Utilities
6000	Operational Support Facilities
7000	Administrative Support Facilities
8000	Infrastructure
9000	Construction Site and Temporary Facilities

21.3 Estimate Plan

MGLIT, R-Tek and PROMON developed costing for the mine development, beneficiation plant and infrastructure, where the main process steps are crushing, ore sorting, classification, DMS, fines filtration, and all general infrastructure for administrative and operational support of the facilities.

The prices adopted in the estimate preserved the source currencies; conversion rates from US dollars and Euros to Brazilian reals are given in Table 21-3.

Table 21-3: US Dollar and Euro Conversion Rates

Currency	Conversion Rate
$	US$1.00 = R$5.85
€	€1.00 = R$6.88

21.4 Capital Cost

21.4.1 Capital Cost Estimation

The CAPEX summary is presented in Table 21-4. The total initial CAPEX is estimated at $191 million inclusive of equipment financing.

This value considers the initial CAPEX for the mine, surface, contingency, and Owner's costs. The mine CAPEX is net of a $9.6 million deferral resulting from financing a portion of initial mine fleet equipment, as explained in Section 21.4.2. The principal, including interest, will be paid during the first five years of operation. The owner’s costs include a team dedicated to following project development, environmental costs, social project costs, and hired services.

The tax analysis on the CAPEX and OPEX was based on the general rules of the Mercosul (Southern Common Market) TEC (Common External Tariff) and on the TIPI as defined in legislation. Basic incidence of taxes at federal, state, and municipal levels was applied, as well as tax benefits provided-for by legislation, considering the activity and location of the Project.

In the update of the tax analysis L&M Advisory conducted on the CAPEX file, two tax benefits were considered:

- At the federal level: the Regime Especial de Aquisição de Bens de Capital para Empresas Exportadoras (RECAP) (Special Regime for the Acquisition of Capital Goods for Exporting Companies) suspends the collection of PIS and COFINS on the acquisition of machinery, instrumentation, and equipment during the construction phase. A total reduction of $2.3 million was determined for the Project.
- At the state level, the collection of ICMS on imports and acquisitions in the state from suppliers of machinery, instrumentation, and equipment will be exempted, as well as the DIFAL on acquisitions from outside the State of Minas Gerais from suppliers of machinery, instrumentation, and equipment during the construction phase. A total reduction of $4.5 million was determined.

Table 21-4: Initial Capital Cost Summary

	Cost ($M)
Initial CAPEX	**191.0**
Mine	**59.2**
Mining Equipment	18.5
Equipment Purchase	27.2
Equipment Financing	(9.6)
Capitalized Interest on Equipment Financing	0.9
Underground Development and Infrastructure	37.9
Mining Pre-Operational Costs	2.8
Surface	**107.3**
Services	66.9
Supply	35.2
Surface Pre-Operational Costs	5.2
Owner's Cost	**4.9**
Contingency	**19.6**

21.4.2 Financial Operation—ECA Equipment Financing (SANDVIK)

Equipment financing will be in monthly installments, with pre-fixed interest for the mine's main equipment. Disbursements are expected during the construction period, Years -2 and -1, with interest capitalized during this time. Repayment of the principal plus interest would be paid back in Years 1 through 4.

Table 21-5: ECA Equipment Financing Cashflow

	Total ($M)	-2 ($M)	-1 ($M)	1 ($M)	2 ($M)	3 ($M)	4 ($M)	5 ($M)
ECA Equipment Financing	**(2.0)**	4.5	5.1	(2.8)	(3.3)	(3.4)	(2.0)	(0.1)
Drawdown	**9.6**	4.5	5.1	-	-	-	-	
Principal Repayment	**(9.6)**	-		(2.4)	(2.6)	(2.9)	(1.7)	-
Interest Payment	**(2.0)**	-		(0.4)	(0.7)	(0.5)	(0.3)	(0.1)

21.4.3 Summary of Main Quantities

Table 21-6 and Table 21-7 present the main quantities for each area of investment estimation.

Table 21-6: Summary of Quantities—Start-Up and Replacement Equipment Capital Purchases

Year	-2	-1	1	2	3	4	5	6	7	8	9	10	11	12	13	14	15	16	17	18
Haul Truck	2	2	4	4	4	2	2	2	0	2	1	0	1	0	0	0	0	0	0	0
Jumbo	3	1	0	1	0	0	0	0	0	3	1	0	0	0	0	0	0	0	0	0
LHD	0	1	2	2	0	0	0	0	0	2	1	2	0	0	0	0	2	1	0	0
Wheel loader	2	0	0	0	0	0	0	0	0	0	0	0	0	0	0	0	0	0	0	0
FanDrill	0	2	1	3	0	0	0	0	0	0	0	0	2	1	3	0	0	0	0	0
Slot Raise Borer	0	0	1	0	0	0	0	0	0	0	0	0	0	0	0	0	0	0	0	0
C. Bolter	1	1	0	0	0	0	0	0	0	0	0	0	0	1	0	0	0	0	0	0
Boltec	0	1	1	1	0	0	0	0	0	0	0	0	0	0	0	0	0	0	0	0
Scaler	1	1	1	0	2	0	0	0	0	2	0	0	0	0	2	0	0	0	0	0
Scissor Lift	1	0	0	0	0	0	3	0	0	0	0	3	0	0	0	0	3	0	0	0
JCB 540-170	1	1	1	1	0	4	0	0	0	0	4	0	0	0	0	4	0	0	0	0
Fuel and Lube Truck	1	0	1	0	2	0	0	0	0	2	0	0	0	0	2	0	0	0	0	0
Personnel Carrier	1	0	1	0	0	2	0	0	0	0	2	0	0	0	0	2	0	0	0	0
Maintenance Truck	1	0	1	0	0	0	2	0	0	0	0	2	0	0	0	0	2	0	0	0
Jackleg Drill	1	1	2	0	2	1	1	0	0	2	1	1	0	0	2	1	1	0	0	0
Stoper Drill	1	0	1	0	2	0	0	0	0	2	0	0	0	0	2	0	0	0	0	0
Air Compressor	1	0	1	0	0	2	0	0	0	0	2	0	0	0	0	2	0	0	0	0
Grader	1	0	1	0	0	0	2	0	0	0	0	2	0	0	0	0	2	0	0	0
Ventillation Fan	2	7	2	0	3	3	3	0	0	3	3	3	0	0	3	3	3	0	0	0
Exhaustor	2	2	0	0	2	0	0	0	0	2	0	0	0	0	2	0	0	0	0	0
Dewatering Pump	2	2	2	0	0	3	0	0	0	0	3	0	0	0	0	3	0	0	0	0
Diesel Generator	1	1	1	0	0	0	2	0	0	0	0	2	0	0	0	0	2	0	0	0
Utility Vehicle	4	4	2	0	2	2	2	0	0	2	2	2	0	0	2	2	2	0	0	0

Table 21-7: Project Main Quantities

	Unit	Quantities
Buildings	No.	15
Plant Total Area	m^2	173,800
DMS Modules	No.	4
Earthworks (Cut)	m^3	539,137
Earthworks (Fill)	m^3	212,614
Concrete Structures	m^3	2,332
Steel Structures	t	363
Platework	t	274
Piping	m	12,515
Electrical Cables	m	29,748
Distribution Line	m	10,500
Instruments	unit	641

21.4.4 Contingency

The contingency used in this Technical Report totals $19.6 million and was estimated at 15% for the mine and 9% for the surface, $10.3 million and $9.3 million, respectively. A lower value was used for surface equipment due to R-Tek and Promon having database pricing for two similar sized processing plants and associated infrastructure in the past year.

The deferral of $9.6 million related to mobile equipment financing with Sandvik was excluded from the calculation of the mine contingency.

21.4.5 Taxes

The tax analysis for the Bandeira Project is detailed in Section 22.

21.4.6 Exclusions

The following expense items were not included in the CAPEX estimate:

- Those incurred by the owner to September 2025
- Any related to obtaining licenses, or any others related to regulatory agencies
- Those related to the closure at the end of the useful life of the facilities
- Those related to obtaining funds for the venture, if necessary
- Entrepreneur's implementation overhead
- Those related to any impact on the shortening or lengthening of the implementation period
- Possible exchange-rate variations
- Escalation
- Technological characterization
- Impacts on costs intended to cover any type of risk.

21.4.7 Mine Capital Cost Estimation

The initial and sustaining mining CAPEX considered for the Project mine operations are as follows:

- Purchase of major production equipment by financial loan supplied by the manufacturer bank
- Purchase of auxiliary mine equipment
- Mine equipment maintenance facilities—workshop, warehouse, equipment washer, tire repair shop
- Mine buildings—office, dispatch and communication room, battery and security equipment room, changing room
- Surface infrastructure—vegetation removal, access roads, water tank, electrical substation, preparation of waste piles and temporary ore stockpiles, sedimentation dikes
- Systems, hardware and software—mine management, communication, topography, geology and mine planning

- Underground infrastructure—Mine entrance, decline, ventilation system, electrical substation
- Purchase of service materials and accessories—roof support, ventilation, water, electrical, compressed air.

21.4.8 Underground Development and Infrastructure

The initial CAPEX considers $37.9 million of underground development and infrastructure costs. During the development period, $10.9 million is categorized as capitalized underground development costs. This is comprised of diesel, electricity, labour, and other consumables associated with the underground development mining in the period.

Other Mine CAPEX items are illustrated in Table 21-8 and include underground infrastructure and costs associated with the contract open-pit mining that occurs within the construction period.

Table 21-8: Project Initial CAPEX—Underground Development and Infrastructure

	Total ($M)	Year -2 ($M)	Year -1 ($M)
Underground Development and Infrastructure	**37.9**	**19.9**	**18.1**
Capitalized Underground Development Costs	10.9	6.4	4.5
Other Mine CAPEX Items	27.0	13.4	13.6
Mine Entrance	10.3	10.3	-
Electric Substation (inside mine)	1.5	0.7	0.7
Electric Cable	0.3	0.0	0.3
Refuge Chamber	1.0	0.5	0.5
Mine Exhaust system	1.9	1.9	-
Open Pit Mining (Contractor)	10.2	-	10.2
Open Pit Diesel	1.9	-	1.9

21.4.9 Surface Capital Cost

The initial CAPEX considers $107.3 million of surface costs. During the construction period, $66.9 million is categorized as surface service costs and $35.2 million as surface supply costs (Table 21-9 and Table 21-10) for a detailed breakdown. An additional $5.2 million is associated with process costs (including labour, electricity, consumables) during the construction and ramp-up period of the concentrator.

Table 21-9: Initial CAPEX—Surface Services

	Total ($M)	Year -2 ($M)	Year -1 ($M)
Surface Services	**66.9**	**26.8**	**40.1**
E / EP / Consultancy / Management	10.5	4.2	6.3
Civil Construction	13.1	5.2	7.8
Electromechanical Assembly	18.3	7.3	11.0
Construction Site and Temporary Installations	7.1	2.8	4.3
Commissioning / training and startup	1.1	0.4	0.7
Indirect Cost	7.3	2.9	4.4
Additional Project Consultancy and Studies	9.5	3.8	5.7

Table 21-10: Initial CAPEX—Surface Supply

	Total ($M)	Year -2 ($M)	Year -1 ($M)
Surface Supply	**35.2**	**14.1**	**21.1**
Mechanical Equipment	23.1	9.2	13.9
Electrical Equipment	4.5	1.8	2.7
Instruments	0.3	0.1	0.2
Electrical Materials	1.7	0.7	1.0
Instrumentation Materials	0.1	0.0	0.1
Piping Materials	0.7	0.3	0.4
Steel Structures (Supply)	1.9	0.8	1.2
Environment—Services	2.0	0.8	1.2
Environment—Supply	0.8	0.3	0.5

21.4.10 Sustaining Capital Cost

Table 21-11 illustrates the sustaining CAPEX was estimated at $100.2 million to cover mine and plant equipment reinvestments during the LOM, including tailings disposal. End-of-life mine closure was estimated at $10 million.

Table 21-11: Sustaining CAPEX

	Total ($M)	1	2	3	4	5	6	7	8	9	10	11	12	13	14	15	16	17	18
Sustaining CAPEX	**100.2**	12.6	13.7	4.7	4.7	4.8	0.9	0.5	11.5	7.3	7.3	4.6	5.3	9.5	3.9	7.1	1.7	0.1	0.0

21.5 Operating Costs

21.5.1 Operating Cost Summary

The mine OPEX estimate includes the operation of the underground and open-pit mine; the processing plant estimate, which includes the operation of a crushing plant, and modular DMS units.

The operating cost summary for the main areas is presented in Table 21-12. It is presented on the basis of 5.2% spodumene concentrate produced.

Table 21-12: LOM Operating Cost Summary—Per Tonne of Spodumene Concentrate

Description	SPO Concentrate (5.2%, $/t)
Mining	190
Processing	98
General and Administrative (G&A) Sales	19
Subtotal	**307**
Capitalized Mining	70
Total Including Capitalized Mining	**378**
Transportation Costs (CIF China Port)	119
Royalties and Deductions	81
Sustaining CAPEX and Closure	34
All-In Sustaining Cost (AISC)	**613**

21.5.2 Operating Cost Detail

The breakdown of the mining OPEX and capitalized mining cost is presented in Table 21-13.

Table 21-13: LOM Mining Operating Costs

	Total ($M)	ROM ($/t)	(SPO) ($/t)
Mining	**607.0**	**26.16**	**189.85**
Underground Mining			
Diesel	20.7	0.89	6.47
Electrical Energy	16.5	0.71	5.16
Tires	19.9	0.86	6.23
Lubricants	3.3	0.14	1.02
Maintenance Parts	37.3	1.61	11.66
Wear Parts	9.5	0.41	2.98
Labour	171.3	7.38	53.58
Blasting	173.7	7.48	54.31
Roof Support	20.1	0.87	6.29
Drilling Wear Parts	74.8	3.22	23.40
Other Mining Costs	33.1	1.43	10.35
Open Pit Mining			
Contract Mining	22.5	0.97	7.02
Diesel	4.4	0.19	1.37
Capitalized Mining	**225.0**	**9.70**	**70.4**

Note: SPO = Spodumene. Values shown on LOM basis

The mining OPEX was calculated from first principles, based on the project's mine plan. Inputs were sourced from a combination of current quotations and historical data (Table 21-14). Industry standard consumption rates for consumables such as diesel, tires, lubricants, maintenance parts, and wear parts, were utilized.

Several notable costs are being outsourced to mining contractors and have been recently quoted accordingly: the drilling and blasting, raise boring (part of the capitalized underground development) and the open pit mining.

Table 21-14: LOM Processing OPEX

	Total ($M)	ROM ($/t)	(SPO) ($/t)
Processing	**314.2**	**13.54**	**98.26**
Labour	82.3	3.54	25.72
External Services	97.7	4.21	30.56
Electrical Energy	21.3	0.92	6.67
Consumables	39.0	1.68	12.21
Maintenance	45.3	1.95	14.17
Other Processing Costs	28.6	1.23	8.93

Note: SPO = Spodumene. Values shown on LOM basis

Table 21-15: LOM Other OPEX including Sustaining CAPEX and Closure

	Total ($M)	ROM ($/t)	(SPO) ($/t)
G&A Sales	61.5	2.65	19.23
Transportation CIF China	380.4	16.39	118.95
Sustaining Capital	100.2	4.32	31.34
Closure	10.0	0.43	3.13

Note: SPO = Spodumene. Values shown on LOM basis

Table 21-16 summarizes the Project's annual operating costs.

Table 21-16: Summary of the Project's Annual Operating Costs ($M)

Year	-2	-1	1	2	3	4	5	6	7	8	9	10	11	12	13	14	15	16	17	18	Total
Mine Operating Cost	0.0	23.4	32.4	35.8	34.2	33.9	32.5	35.8	34.5	36.9	35.1	35.1	34.9	32.9	32.4	31.9	26.7	29.5	24.2	25.0	607.0
Capitalized Underground Development	0.0	6.3	11.9	15.0	16.0	15.6	13.4	10.6	12.3	9.1	10.2	10.8	10.1	12.4	11.8	11.9	17.3	14.1	13.7	2.7	225.0
Processing Operating Cost	0.0	4.7	17.4	17.4	17.4	17.4	17.4	17.4	17.4	17.4	17.4	17.4	17.4	17.4	17.4	17.4	17.4	17.4	15.9	15.5	314.2
SG&A Operating Cost	0.0	2.2	2.8	3.5	3.4	3.4	3.4	3.5	3.5	3.5	3.5	3.5	3.5	3.5	3.5	3.4	3.4	3.4	2.8	1.9	61.5
Total	**0.0**	**36.6**	**64.4**	**71.6**	**70.9**	**70.3**	**66.7**	**67.3**	**67.6**	**66.9**	**66.1**	**66.8**	**65.9**	**66.1**	**65.1**	**64.6**	**64.7**	**64.4**	**56.5**	**45.1**	**1,207.8**

21.5.3 Labour

Labour costs were defined based on the estimated labour employees (Table 21-17) and average wage values.

Table 21-17: Site Employees—Labour

Year	-2	-1	1	2	3	4	5	6	7	8	9	10	11	12	13	14	15	16	17	18
Mine	140	241	351	400	408	408	408	416	416	416	420	420	416	416	416	412	396	396	380	380
Plant	4	86	110	110	110	110	110	110	110	110	110	110	110	110	110	110	110	110	71	71
G&A	24	41	45	45	45	45	45	45	45	45	45	45	45	45	45	45	45	45	38	37
Total	**168**	**368**	**506**	**555**	**563**	**563**	**563**	**571**	**571**	**571**	**575**	**575**	**571**	**571**	**571**	**567**	**551**	**551**	**489**	**488**

21.5.4 Consumables

Plant consumables costs were defined based on annual consumption and unit values (Table 21-18).

Table 21-18: Plant Consumables

	Unit	
Specific Consumption		
Flocculant	(g/t ROM)	25
Ferrosilicon	(g/t ROM)	400
Liners	(g/t ROM)	250
Fuel	(L/h)	213
Price		
Flocculant	($/kg)	4.60
Ferrosilicon	($/kg)	1.66
Liners	($/kg)	0.85
Fuel	($/L)	0.99
Average Annual Consumption		
Flocculant	(kg/a)	32,200
Ferrosilicon	(kg/a)	515,201
Liners	(kg/a)	322,001
Fuel	(L/a)	858,072
Average Annual Cost		
Flocculant	($/a)	148,120
Ferrosilicon	($/a)	855,234
Liners	($/a)	273,701
Fuel	($/a)	852,086

Notes: The price of all plant consumables includes taxes and freight to the site.
The price of ferrosilicon (FeSi) was obtained through consultation of the two main suppliers from South Africa and U.S.A. Estimated value of $1.66/kg, already considering the applicable tax incidence under the drawback regime.
Flocculant, liners and fuel price were estimated through supplier consultation in Brazil.

21.5.5 Electrical Energy

CEMIG provided the cost of electricity. It presented a unit value of R$296.76/MWh (off-peak hours) and R$465.84/MWh for peak hours. The Project considered purchasing energy in the free market for R$250/MWh.

Figure 21-1 presents the average price of electrical energy in Brazil for the last 18 years. The price ranges from R$12.20 to R$822.83, with average price in this period of R$183.59. The use of R$250 for this Project was a recommendation from Grid Energia—energy consultant for the Project.

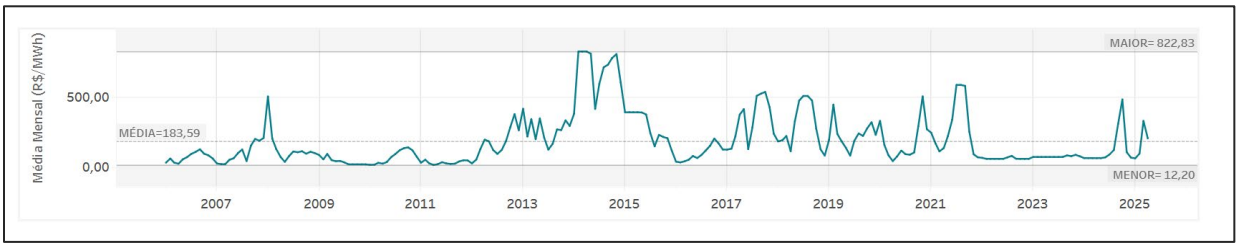


Figure 21-1: Câmara de Comercialização de Energia Elétrica (CCEE)—Average Free Market Power Price in the Last 18 Years in Brazil

Table 21-19 shows the plant and mine-estimated consumption.

Table 21-19: Annual Plant and Mine Estimated Consumption

Area	Description	kW	h/a	kWh/a
4600-SE-01	Crushing substation	1058	6,135	6487575
4600-SE-02	DMS substation	2456	7,447	18287055
4600-SE-03	Workshops substation	458	5,184	2375568
Unit 6	Administrative area	29	3,220	94187
4600-SE-04	Mine substation	13950	8,760	122182792
4600-SE-05	Ventilation substation	3321	8,760	29096075
Total				**178523252**

21.5.6 Plant Maintenance

Plant maintenance cost is estimated at 6.75% of the mechanical equipment cost, equal to approximately $2.5 million per year of operation.

21.5.7 Plant Services

For chemical analysis an outsourced proposal was received to process around 2,000 samples per month, within nine sampling points. The estimated cost is $0.47/t ROM.

The leased plant equipment cost is based on a proposal for the first five years of operation (Table 21-20).

Table 21-20: Equipment Leasing Cost

Equipment	Model	Quantity	Hourly Cost (R$/h)	Monthly Unit Value (R$/month)	Total Annual Value (R$/a)	Function
Tanker Truck	FMX 540 8X4	1	602	120,540	1,446,486	Roads and surface accesses wetting (1 turn)
Truncated Dump Truck	FMX 540 8X4	4	397	695,712	8,348,544	Waste transport, products, tailings (2 shifts)
Backhoe	416F	1	300	60,066	720,802	(1 shift)
Crawler Tractor	D8	1	1,760	352,170	4,226,044	Dry stacking (1 Shift)
Winch Truck	VM360	1	459	91,872	1,102,465	General Maintenance (1 shift)
Ambulance	Fiat Ducato	1	324	48,630	583,566	Emergency ambulance. (1 shift)
Forklift	GDP170VX	1	725	108,818	1,305,826	Workshop spare parts handing (1 shift)
Mobile Crane on Tires	RT540E	1	684	136,913	1,642,963	General maintenance (1 shift)
Lighting Tower		2	50	15,010	180,121	Waste rock and rejects stockpile (1 shift)
Pickup Truck	Hilux	4	4	12,000	144,000	Mine (1 shift)
Pickup Truck	Hilux	4	4	12,000	144,000	Plant (1 shift)
Scissor Lift	S105 4WD	1	724	144,900	1,738,808	General maintenance (1 shift)
Subtotal (R$/a)					**21,583,631**	
Total (R$/a) % Accredited Operator + mobilization/demobilization (5%)					**26,614,117**	

For other non-dimensioned costs, 10% was estimated on top of the plant's other OPEX values.

22 ECONOMIC ANALYSIS

L&M Assessoria Empresarial (L&M Advisory) prepared the economic analysis for the Bandeira Lithium Project the feasibility study update.

This analysis was based on information provided by Promon and the technical teams from MGLIT and R-Tek, using the following files developed by the companies:

- Promon:
  - CapEx Basico_MGLit_Sent_2025_09_02_Tributos.xlsx
- MGLIT and R-Tek technical teams:
  - 20250824-MGlit-Mine Cost v5.1–low grade.xlsx
  - Plant OPEX–Feasibility Study update 2025_Rev05.1
  - LM_Equipment Financing (ECA) Leasing SANDVIK_08Sep25 v5.1.xlsx
  - 0915–Updated Economics v5.1–FINAL–Feasibility Study_15Set25.xlsx.

PROMON was responsible for the initial CAPEX estimates for the processing plant, surface infrastructure, and indirect costs. Technical teams from MGLIT and R-Tek oversaw the production plan, initial CAPEX estimates for both open-pit and underground mines, as well as development and operational costs, sustaining CAPEX, and mine closure. Additionally, MGLIT provided product sales price projections from Fastmarkets Global Limited.

L&M Advisory was responsible for the estimation of tax impacts on the Project, including revenue, CAPEX and OPEX, and profits. The tax rates adopted are those is the current Brazilian tax legislation, and applicable tax benefits at federal and state level.

The main tool used for the analyses is a Microsoft Excel-based discounted cash-flow model L&M Advisory developed. This model updates the key economic metrics to identify and assess the key Project value-drivers. From a technical and operational point of view it is a high-level model focused on detailed tax implications and resulting Project economics appropriate for this phase of the Project's development.

22.1 Main Assumptions and Parameters

The following sections outline the main assumptions and parameters used for this economic analysis.

22.1.1 Production

The annual production rate varies from year to year and is based on a nominal capacity of 1.3 Mt/a of ore feed. The expected LOM is 18.5 years, including ramp-up and -down. The average spodumene concentrate at 5.20% Li_2O is estimated to be 177 kt/a.

The ore feed to the plant and lithium oxide grades and concentrate produced along the LOM period are presented in Figure 22-1, and Figure 22-2, respectively.

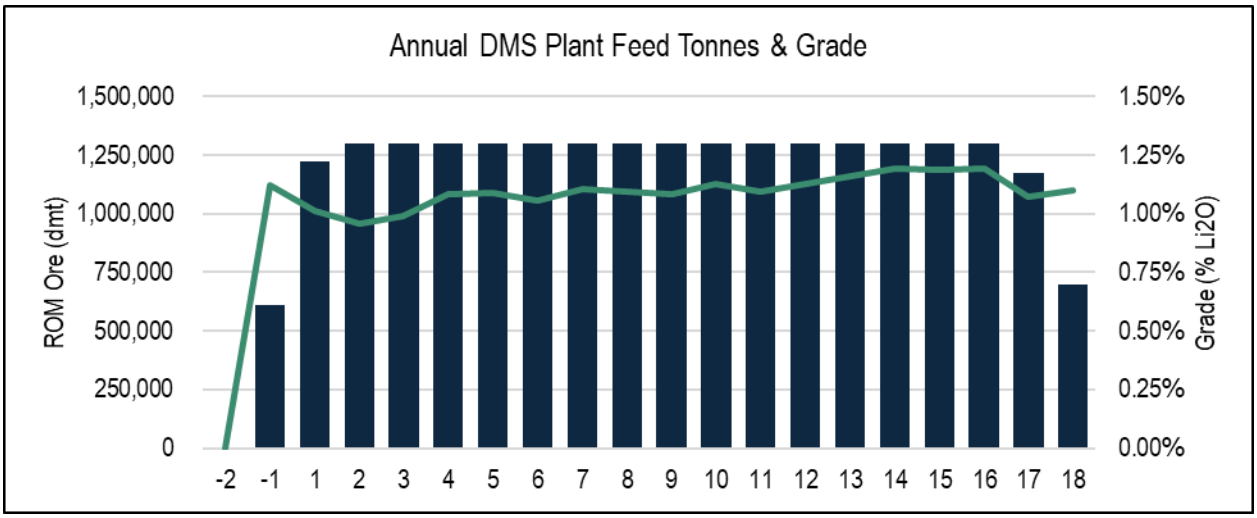


Figure 22-1: ROM Feed to Plant over LOM

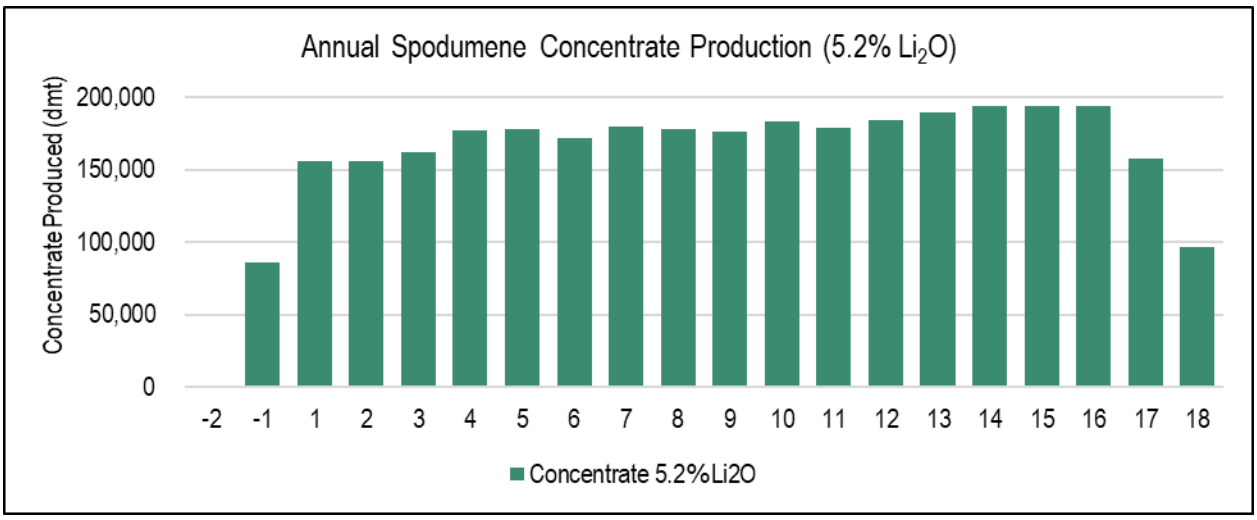


Figure 22-2: Spodumene Concentrate Production (5.2% Li_2O) over LOM

Detailed projections of the ore and waste mined; plant feed and respective mineral grades; metallurgical recoveries; and concentrate production are presented in Section 22.5.

22.1.2 Initial Capital Cost

The initial after-tax CAPEX is $191.0 million, including a $19.6 million allowance for contingencies, equivalent to 9.8% of the total initial CAPEX. The CAPEX disbursement schedule is shown in Table 22-1.

Table 22-1: Initial CAPEX ($M)

Year	CIF + Non-Recoverable Taxes	Recoverable Taxes	Total
−2	83.0	4.2	87.2
−1	107.0	6.4	113.4
Initial CAPEX Subtotal	190.0	10.6	200.6
Equipment Financing Net Cash Flow	0	0	(9.6)
Initial CAPEX Total	**190.0**	**10.6**	**191.0**

Note: CIF = cost, insurance, and freight.

For the initial CAPEX phase, MGLIT has opted to finance some of the main mining equipment. A scenario was prepared based on quotations from a major European domiciled supplier supported by seller arranged financing.

The cash-flow projections for the drawdown and repayment of the financing are presented in Table 22-2. The positive balance related to financing provides a reduction of $9.6 million in the total disbursement during the initial CAPEX phase.

Table 22-2: Mining Equipment Financing ($M)

	Implementation Phase				Operations Phase		Total Financing Cash Flow
Year	Drawdown	Amortization	Drawdown-Amortization	Capitalized Interest	Amortization	Interest Paid	
−2	5.4	(0.9)	4.5	(0.4)	0.0	0.0	4.1
−1	7.3	(2.2)	5.1	(0.5)	0.0	0.0	4.6
1	0.0	0.0	0.0	0.0	(2.4)	(0.4)	(2.8)
2	0.0	0.0	0.0	0.0	(2.6)	(0.7)	(3.3)
3	0.0	0.0	0.0	0.0	(2.9)	(0.5)	(3.4)
4	0.0	0.0	0.0	0.0	(1.7)	(0.3)	(2.0)
	12.7	**(3.1)**	**9.6**	**(0.9)**	**(9.6)**	**(2.0)**	**(2.9)**

22.1.3 Sustaining CAPEX and Mine Closure

LOM sustaining CAPEX is estimated at $100.2 million, including increase and replacement of mining mobile equipment. The sustaining CAPEX annual schedule and the recoverable taxes incurred, are detailed in Table 22-3.

The total estimated mine closure costs amount to $10.0 million, planned to be spent in Year 19, starting immediately after commercial production shuts down.

Table 22-3: Sustaining CAPEX ($M)

Year	Sustaining CAPEX CIF + Non-Recoverable Taxes	Recoverable Taxes	Total Sustaining CAPEX
1	12.2	0.4	12.6
2	13.3	0.4	13.7
3	4.3	0.4	4.7
4	4.3	0.3	4.7
5	4.6	0.3	4.8
6	0.8	0.1	0.9
7	0.3	0.1	0.5
8	11.0	0.5	11.5
9	7.0	0.4	7.3
10	7.0	0.3	7.3
11	4.5	0.2	4.6
12	5.1	0.2	5.3
13	9.1	0.43	9.5
14	3.7	0.3	3.9
15	6.8	0.2	7.1
16	1.6	0.1	1.7
17	0.1	0.0	0.1
Total	**95.7**	**4.5**	**100.2**

Note: CIF = cost, insurance, and freight.

22.1.4 Operating Costs

The average LOM OPEX of ore feed to plant is estimated to be $42.35/t. The annual average of the mine site OPEX is $51.7 million. The OPEX percent contribution by activity is presented in Table 22-4. Figure 22-3 shows the evolution of the Mine site OPEX along the LOM period.

Table 22-4: OPEX—Run-of-Mine Feed ($/t)

Activity	Annual Cost (LOM avg. $M)	Unit Cost (LOM avg. $/t)	Participation (%)
Mining	31.95	26.16	61.77
Processing	16.54	13.54	31.97
General & Administrative	3.24	2.65	6.26
Total OPEX	**51.73**	**42.35**	**100.00**

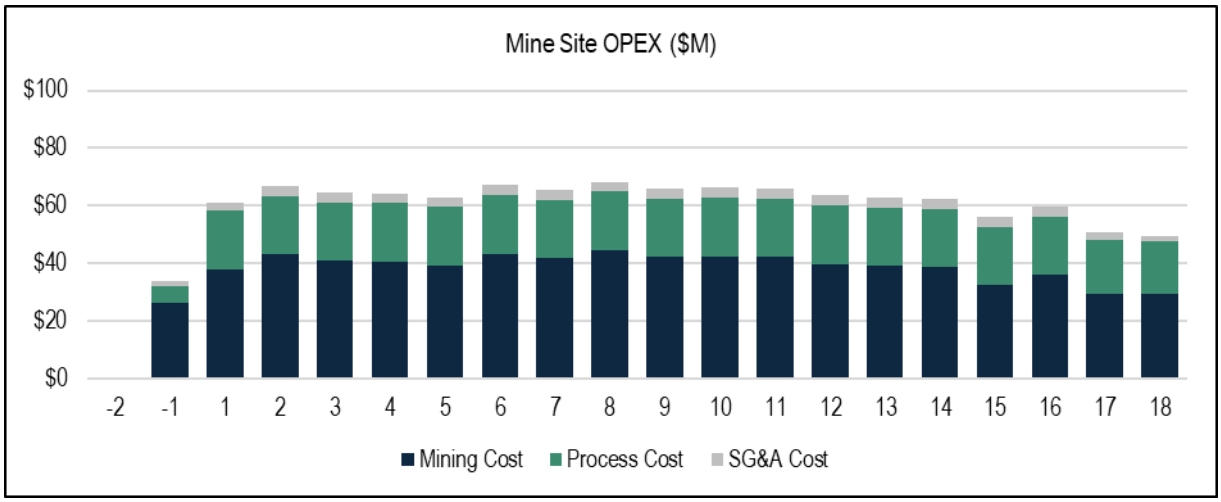


Figure 22-3: Annual OPEX ($M)

The site OPEX of producing 5.2% Li_2O spodumene concentrate is $378/t, including capitalized costs associated with primary development. Table 22-5 presents the average unit costs per tonne and the average total costs over the mine's lifespan. The Figure 22-4 illustrates the evolution of total OPEX, including the capitalized underground development costs.

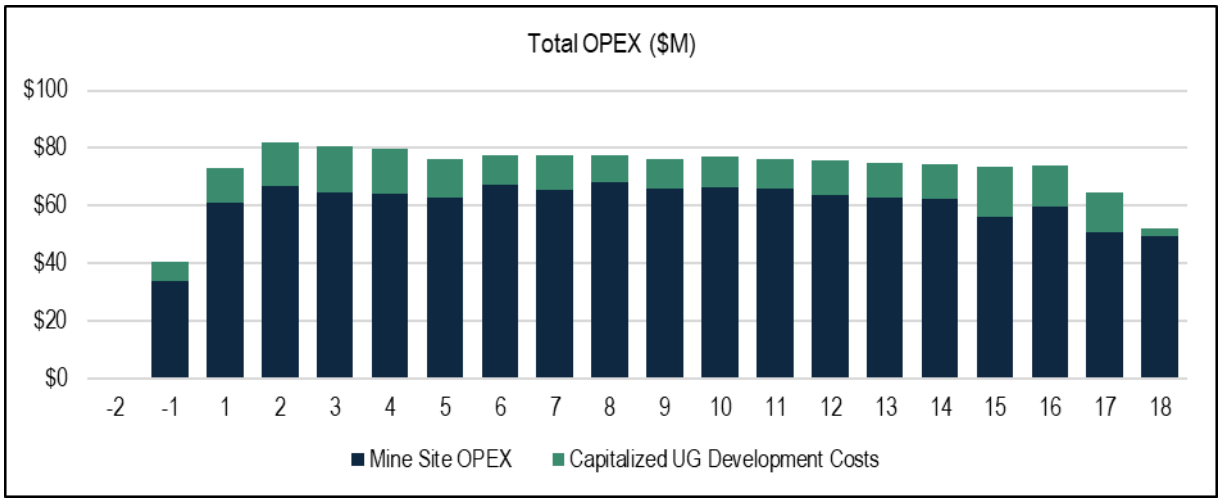


Figure 22-4: Total OPEX ($M)

Table 22-5: OPEX per Tonne of 5.2% Li_2O Spodumene Concentrate (SC)

Activity	Annual Cost (LOM avg. $M)	Unit Cost (LOM avg. $/t of SC)	Participation (%)
Mining	31.95	189.85	50.27
Processing + Tailings Handling	16.54	98.26	26.01
General & Administrative	3.24	19.23	5.09
Capitalized Mining and Underground Primary Development	11.84	70.38	18.63
Total OPEX	**63.57**	**377.72**	**100.00**

22.1.5 Spodumene Concentrate Transportation

The unit cost for transporting spodumene concentrate from the plant site to Shanghai Port is $118.95/t. The annual average of all logistics costs is $20.0 million, which includes road transport from the plant site to Ilhéus Port, loading and port costs on vessels, and sea-freight from Ilhéus to Shanghai Port. A brokerage fee of 1.5% on the total value of the concentrate sold is due from the start of the operations until 2032.

22.1.6 Royalties and Deductions

The following royalties and fees are owed by the Project:

- Financial Compensation for the Exploration of Mineral Resources (CFEM): 2% royalty payable to the Brazilian government on spodumene concentrate sales.
- Taxa de Controle, Monitoramento e Fiscalização das Atividades de Pesquisa, Lavra, Exploração e Aproveitamento de Recursos Minerários (TFRM): a fee payable to the State of Minas Gerais according to State Law 19,976, December 27, 2011. However, Item III of Art. 7° states that the TFRM is exempted for research, extraction, exploration, and utilization activities of mineral resources in the mining area of the Superintendência do Desenvolvimento do Nordeste (SUDENE) (Superintendence for the Development of the Northeast).
- Private royalty: A royalty of 2.25% on the gross sales of spodumene concentrate is due to Appian Capital.
- Landholder royalty: A royalty of 1.00% on the gross sales of spodumene concentrate is payable to the surface rights holder. As the landholder, Valitar Participações S.A., is an affiliate of the operating entity, this payment is effectively internal and cashflows are consolidated within the project ownership structure.

22.1.7 Revenue

The projections of gross revenue are based on the quantity of spodumene concentrate to be sold at the price forecast for the Project's life period. The prices are expressed in 2025 real dollars on the basis of cost, insurance, and freight (CIF) Shanghai.

Table 22-6 shows yearly prices for the 5.2% Li_2O spodumene concentrate to be produced by MGLIT, based on Fastmarkets' 2025 long-term spodumene concentrate (SC6) price forecast, CIF China. Fastmarkets methodology underpins the projections of sales volumes and prices, presented in Section 19.

Table 22-6: Spodumene Concentrate Price (CIF Shanghai)

Project Year	Concentrate 6% Li_2O (SC6) ($/t)	Concentrate 5.2% Li_2O ($/t)
2027	1,400.0	1,213.3
2028	1,600.0	1,386.7
2029	1,900.0	1,646.7
2030	2,100.0	1,820.0
2031	2,300.0	1,993.3
Long-term price: 2032 to 2045	2,300.0	1,993.3

Source: Fastmarkets Global Limited (2025).

The projected average annual gross revenue between 2028 and 2044 is $343.1 million. The average annual net revenue, after royalties and deductions is $328.5 million, detailed in Section 22.2.5. Figure 22-5 shows the evolution of gross and net revenue over the LOM.

The detailed, year-by-year LOM projections of gross revenue and deductions are detailed in Section 22.5.

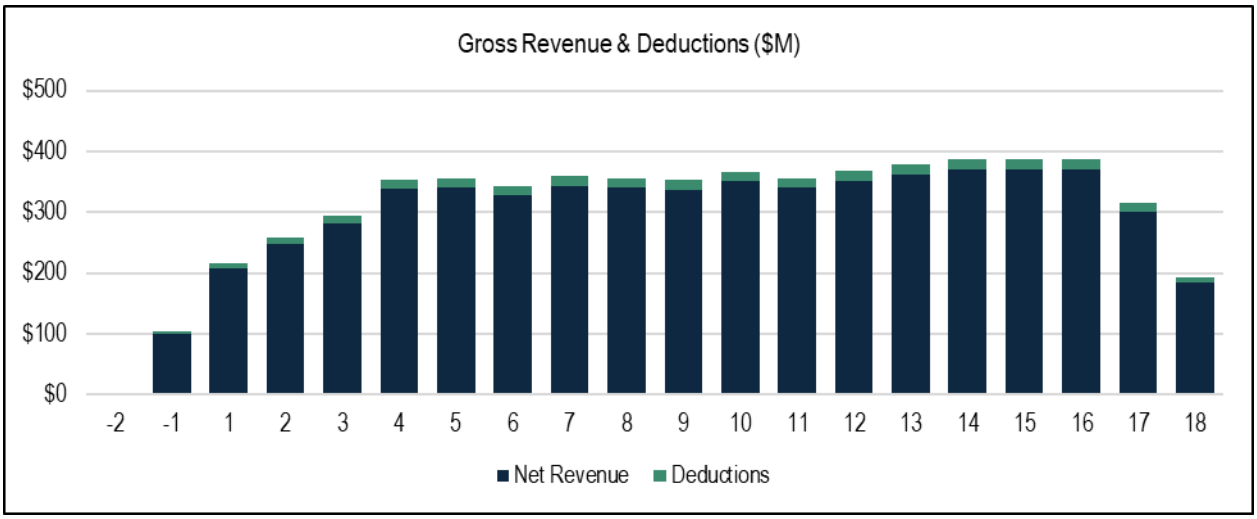


Figure 22-5: Gross Revenue and Deductions

22.1.8 Taxation

The tax analysis for the Project takes into consideration current tax laws applied to CAPEX, OPEX, spodumene concentrate sales, and profits. This work was developed from the identification and analysis of the basic taxes applicable to the various Project activities and respective tax benefits provided for each tax as legislated, whether at the federal, state, or municipal level.

The relevant taxes included in the analysis are summarized in Table 22-7.

Table 22-7: List of Taxes

Federal	
II	Import Tax
IPI	*Tax on Industrialized Products*
IRPJ	Corporate Income Tax
CSLL	Social contribution on net income
COFINS	Contribution to social security financing
PIS	Social integration program
CFEM	Financial compensation for the exploration of mineral resources
AFRMM	Additional to freight for merchant marine renewal
IOF	Financial operation tax

State—Minas Gerais	
ICMS	Tax on operations relating to the circulation of goods and on the provision of interstate and intermunicipal transport and communication services
DIFAL	Supplement related to the ICMS rate differential
TFRM	Control, monitoring and inspection fee for research, mining, exploration, and use of mining resources activities

Municipal	
ISSQN	Services Tax

Taxes on Spodumene Concentrate Sales

Federal Taxes: PIS, COFINS, IPI, and CFEM

Spodumene concentrate is classified as NT, not taxed by the IPI, according to the Tabela de incidência do Imposto sobre produtos industrializados (TIPI) (Table of Incidence of the Tax on Industrialized Products), classification code: NCM 2530.90.10. Export sales are not taxed by PIS or COFINS.

CFEM rate is 2% incident on gross sales revenue.

State Tax: ICMS

Tax legislation for the ICMS in Minas Gerais follows the national legislation applied since 1988 and its subsequent amendments. Exports are not taxed by ICMS. The state legislation ensures the maintenance of all ICMS credits on the purchase of equipment, inputs, and electricity.

Financial Contribution for Mineral Extraction Royalty

The Contribuição Financeira para Extração Mineral (CFEM) (Financial Contribution for Mineral Extraction) is a 2% royalty paid to the federal government, based on sales revenue.

Taxes on CAPEX and OPEX

The tax analysis on the CAPEX and OPEX was developed using cost estimates that Promon prepared. Tax classification requires detailed work, based on the General Rules of the Tarifa Externa Comum (TEC) (Common External Tariff) of Mercosul (Southern Common Market) and on the TIPI, as defined in legislation. Basic incidence of taxes at federal, state, and municipal levels was applied, as well as tax benefits provided-for by legislation, considering the activity and location of the Project. Taxation on the CAPEX and OPEX estimates, on Project revenue and profits, including applicable tax benefits, was updated according to 2025 tax legislation.

Recoverable Tax Credits

- The amounts of recoverable tax credits identified in the initial CAPEX were as follows: ICMS/DIFAL credits totalling $3.6 million.
- PIS/COFINS credits totalling $10.5 million.

Tax Benefits Adopted for the Federal Taxes

In the update of the tax analysis L&M Advisory conducted on the CAPEX file, two tax benefits were considered:

- At the federal level: the Regime Especial de Aquisição de Bens de Capital para Empresas Exportadoras (RECAP) (Special Regime for the Acquisition of Capital Goods for Exporting Companies) suspends the collection of PIS and COFINS on the acquisition of machinery, instrumentation, and equipment during the construction phase. A total reduction of $2.3 million was determined for the Project.
- At the state level, the collection of ICMS on imports and acquisitions in the state from suppliers of machinery, instrumentation, and equipment will be exempted, as well as the DIFAL on acquisitions from outside the State of Minas Gerais from suppliers of machinery, instrumentation, and equipment during the construction phase. A total reduction of $4.5 million was determined.

Impact of the Tax Reform

With the approval of the new National Tax System, the objective was to simplify five taxes on consumption, currently existing, namely: PIS, COFINS, ICMS, ISSQN, and gradually the IPI. These taxes will be replaced by a dual value-added tax (VAT) system—the newly created IBS (Tax on Goods and Services) and CBS (Contribution on Goods and Services)—that will be levied on goods, services and rights, both tangible and intangible.

To make such measures official, on January 16, 2025, Complementary Law 214 was enacted, which institutes the new taxes, but even with the sanction of the first law related to the tax reform, the rates must still be defined, and other regulatory rules need to be prepared and approved.

The main characteristics of the new dual VAT tax model starting from January 1, 2033, are:

- Unification of taxes: reduces tax complexity by integrating all previous taxes into two.

- Standard reference: to be applied clearly and proportionally to the price of goods and services, with an initial projection of 26.5% (as a general rule, dividing (4.92% + 13.70% = 17.87%) of IBS and 8.80% of CBS). The idea with this is to improve predictability for companies when calculating the tax impacts on prices and margins.
- Appropriation of 100% of the credits: eliminates cascading taxation. It allows companies to deduct taxes paid in previous stages of the production chain.

Taxes on Profits

The federal tax corporate income tax, IRPJ, is payable at a basic rate of 15.0%, with a surplus of 10.0% on the annual income, totalling 25.0%.

The CSLL is taxed at a rate of 9.0% on a similar calculation basis as defined for IRPJ.

SUDENE Incentives

The project is in the municipality of Araçuaí, Jequitinhonha valley, northeast region of Minas Gerais, within the area covered by Superintendency for the Development of the Northeast (SUDENE) and is eligible for a granted benefit of a 75% reduction in the IRPJ payable. The initial benefit period spans ten years, from 2027 to 2036, with the possibility of applying for an additional term beginning in 2037, which is expected to remain in effect until the end of the mine's operational life in 2045. Two 10-year periods with a 75% reduction in income tax payable were considered in this study. The first period awarded is expected to start in 2027, during the last year of the ramp-up phase of the Project, and end in 2036. A second ten-year benefit period, if granted, would be based on the modernization of the plant, expected to take place early in 2037 and remain in place until the end of the mine life in 2045.

22.1.9 Evaluation Base-Date and Exchange Rate

The evaluation base-date is December 31, 2025. All financial modelling and analysis work is based in real terms as of 2025, using real, ungeared discount rates, the economic model projections exclude any Project debt financing, but do include equipment financing. For the purposes of this report, the Project funding is assumed to be through equity.

Economic projections are reported in 2025 dollars using a base-case exchange rate of R$5.85:$1.00. This exchange rate was used for the initial capital estimation, as well as the long-term rate during operation of the mine including OPEX, sustaining CAPEX, and mine closure costs. Project economics at a range of exchange rates (±30%) are assessed as part of Project sensitivity analysis in Section 22.4.

The base-case exchange rate of R$5.85:$1.00 is within the range of historical actual rates over the past five years, as shown in Figure 22-6.

The forecast exchange rate adopted is in accordance with the median of the long-term forecasts (2028) of the top five Brazilian independent market analysts listed in the Banco Central do Brasil weekly publication: Focus Market Readout (May 16, 2025).

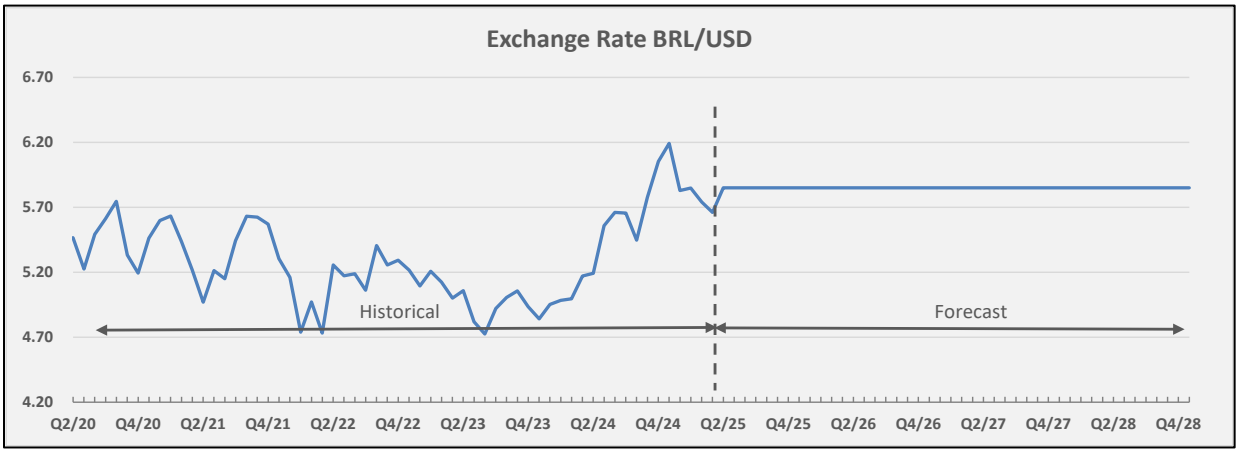


Figure 22-6: Exchange Rate BRL:USD

22.2 Cash-Flow Analysis

The Project's estimated post-tax, unlevered net present value (NPV) is $1,447.5 million using a discount rate of 8.0%. The post-tax, unlevered internal rate of return (IRR) is 61.2%, and the average annual earnings before interest, taxes, depreciation, and amortization (EBITDA) is $253.9 million. The total undiscounted, free cash-flow generated over the life of the Project is $3,391.3 million, and the payback period after the start-up of operations is 2.2 years (26 months). Table 22-8 summarizes the financial results.

Based on the assumptions used in this Technical Report, the Project is economically viable, given the significantly positive NPV and IRR as compared to the discount rate adopted.

Table 22-8: Financial Results Summary

Financial Analysis	Unit	Post-Tax
NPV at 8%	$M	1,447.5
Payback[1]	year	2.2
IRR	%	61.2
Profitability Ratio	%	753.2
EBITDA[2]	$M	253.9
Total Cash Flow	**$M**	**3,391.6**

Notes: [1] Undiscounted, after start-up.
[2] Annual average, full production years.

22.3 Sensitivity Analysis

The sensitivity analysis shows the impact of adjusting key input variables on the Project's NPV and IRR.

In assessing the sensitivity of the Project returns, each of these inputs is varied independently of the others. Scenarios combining beneficial or adverse variations simultaneously in two or more variables will have a more marked effect on the economics of the Project than will the individual variations

considered. The sensitivity analysis has been conducted assuming no change to the mine plan or schedule.

Section 22.3.1 shows sensitivity analyses of the Project´s NPV and IRR to key input variables. A sensitivity analysis showing the Project's NPV in a range of discount rates between 6% and 10% is presented in Section 22.3.2.

22.3.1 Sensitivity Analysis to Key Input Variables—After Tax, Unlevered NPV, and IRR

The sensitivity analysis for the NPV and IRR was conducted considering a range of ±30% in the key input variables of the Project's cash flow, as follows:

- Spodumene concentrate price
- Exchange rate BRL/USD
- OPEX
- CAPEX.

Table 22-9 and Figure 22-7 present the results of the sensitivity analysis for the Project's NPV on an after-tax unlevered basis, and for each of the critical variables. NPV results are reported at a discount rate of 8%. Table 22-10 and Figure 22-8 present the same for the IRR. As can be seen, the Project's returns are highly sensitive to the spodumene concentrate sales price. The exchange rate represents the second-most significant factor, as its fluctuations affect both CAPEX and OPEX. In contrast, individual variations in OPEX and CAPEX have relatively minor impacts when compared to shifts in the selling price.

Table 22-9: Sensitivity for Post-Tax NPV at 8%

Δ%	SC 5.2% Li_2O Price		Exchange Rate		OPEX		Initial CAPEX	
(%)	$/t (CIF Shanghai)	NPV at 8% ($M)	BRL/USD	NPV at 8% ($M)	Total ($/t Ore)	NPV at 8% ($M)	($M)	NPV at 8% ($M)
-30	1,341.9	747.3	4.10	1,163.8	29.64	1,607.9	140.4	1,496.1
-20	1,533.6	981.1	4.68	1,282.2	33.88	1,554.5	160.5	1,480.0
-10	1,725.3	1,214.6	5.27	1,374.1	38.11	1,501.1	180.5	1,463.8
0	1,917.0	1,447.5	5.85	1,447.5	42.35	1,447.5	200.6	1,447.5
+10	2,108.7	1,680.3	6.44	1,507.5	46.58	1,394.0	220.7	1,431.3
+20	2,300.3	1,913.0	7.02	1,557.4	50.82	1,340.4	240.7	1,415.1
+30	2,492.0	2,145.6	7.61	1,599.7	55.05	1,286.7	260.8	1,398.9

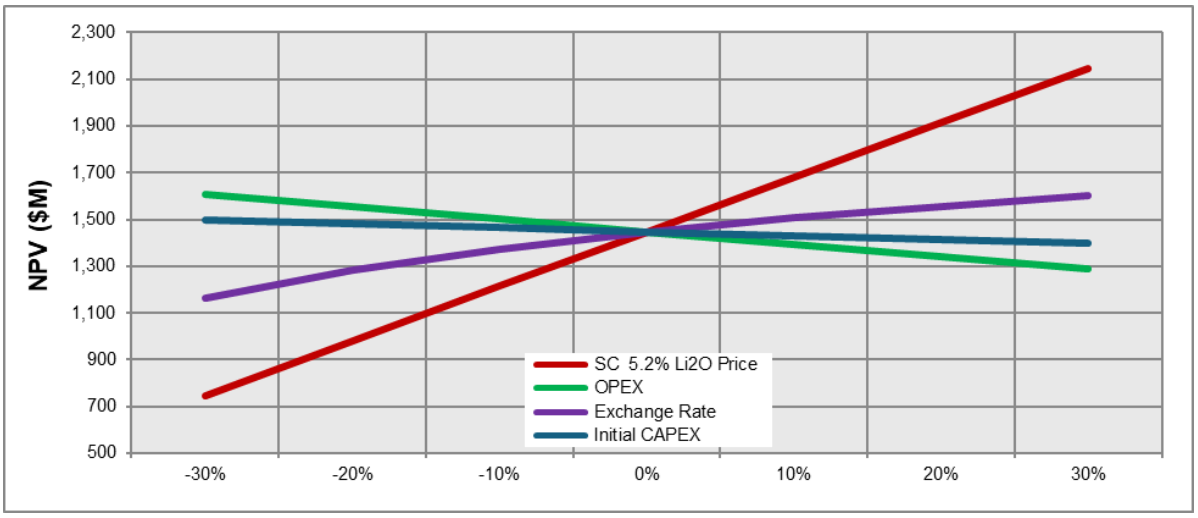


Figure 22-7: Sensitivity for Post-Tax NPV at 8%

Table 22-10: Sensitivity Post-Tax IRR

Δ%	SC 5.2% Li_2O Price		Exchange Rate		OPEX		Initial CAPEX	
(%)	$/t (CIF Shanghai)	IRR (%)	BRL/USD	IRR (%)	Total $/t Ore	IRR (%)	($M)	IRR (%)
-30	1,341.9	36.3	4.10	40.3	29.64	70.3	140.4	81.0
-20	1,533.6	44.7	4.68	47.5	33.88	67.2	160.5	72.9
-10	1,725.3	53.0	5.27	54.5	38.11	64.2	180.5	66.5
0	1,917.0	61.2	5.85	61.2	42.35	61.2	200.6	61.2
+10	2,108.7	69.4	6.44	67.8	46.58	58.3	220.7	56.9
+20	2,300.3	77.4	7.02	74.0	50.82	55.5	240.7	53.2
+30	2,492.0	85.5	7.61	80.1	55.05	52.7	260.8	50.1

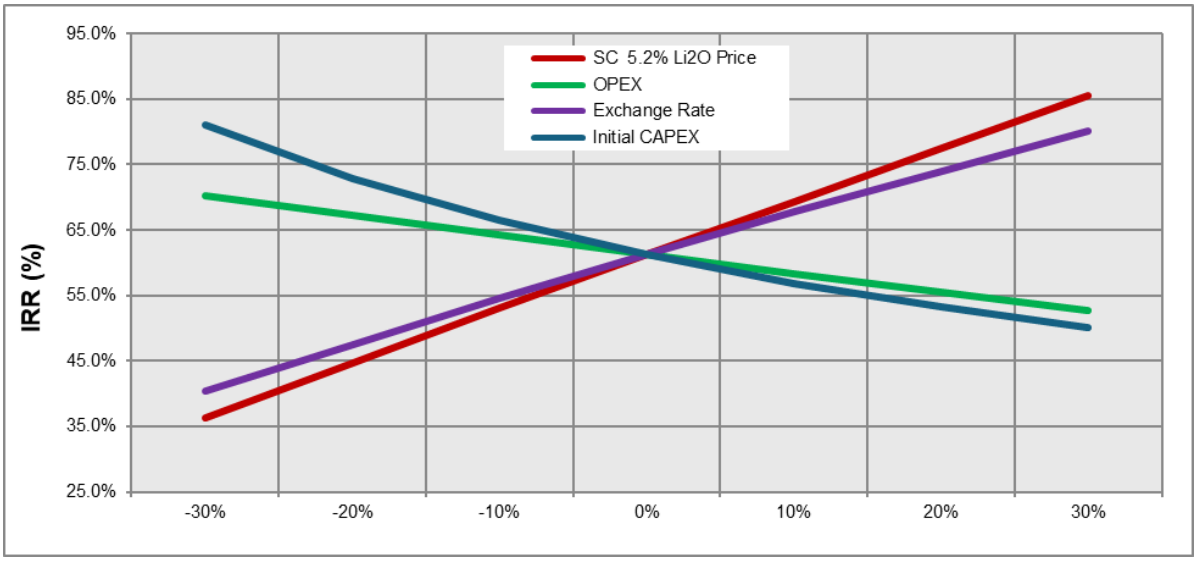


Figure 22-8: Sensitivity for Post-Tax IRR

22.3.2 Sensitivity Analysis—NPV x Discount Rate

Table 22-11 and Figure 22-9 present a sensitivity analysis showing the Project's NPV in a range of discount rates between 6% and 10%.

Table 22-11: Sensitivity for Post-Tax, Unlevered NPV x Discount Rate

Discount Rate	
%	NPV ($M)
6.0	1,763.7
6.5	1,677.2
7.0	1,595.9
7.5	1,519.5
8.0	1,447.5
8.5	1,379.7
9.0	1,315.8
9.5	1,255.5
10.0	1,198.6

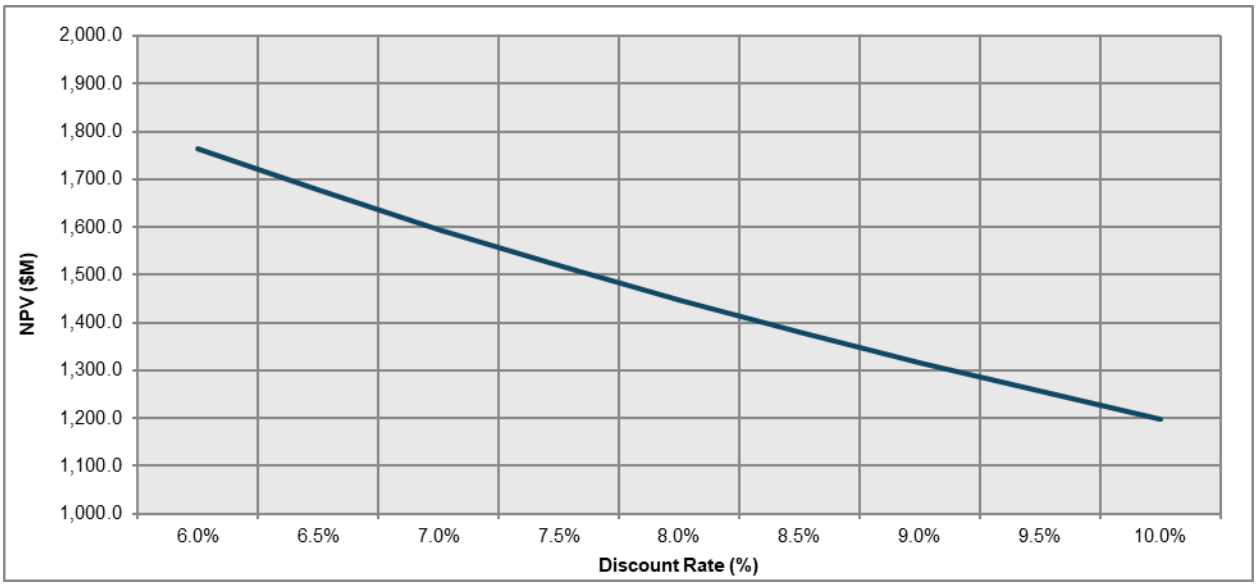


Figure 22-9: Sensitivity Post-Tax, Unlevered NPV x Discount Rate

22.4 Financial Projections

Table 22-12 to Table 22-15 present the production flow, OPEX and all-in sustaining cost (AISC), profit and loss statement, and Project free cash-flow, respectively.

Table 22-12: Annual Projections—Production Flow

	Unit	Total LOM	2026 -2	2027 -1	2028 1	2029 2	2030 3	2031 4	2032 5	2033 6	2034 7	2035 8	2036 9	2037 10	2038 11	2039 12	2040 13	2041 14	2042 15	2043 16	2044 17	2045 18	2046 19
MINING																							
Ore Mined																							
Open Pit	k dmt	1,099	-	794.7	304.2	-	-	-	-	-	-	-	-	-	-	-	-	-	-	-	-	-	-
Ore Grade	% Li_2O	1.12	0.00	1.13	1.06	0.00	0.00	0.00	0.00	0.00	0.00	0.00	0.00	0.00	0.00	0.00	0.00	0.00	0.00	0.00	0.00	0.00	0.00
Underground	k dmt	22,108	-	19	755	1,314	1,278	1,296	1,300	1,321	1,325	1,326	1,304	1,303	1,314	1,303	1,319	1,291	1,289	1,300	1,049	701	-
Ore Grade	% Li_2O	1.10	0.00	0.84	0.97	0.96	0.99	1.09	1.09	1.05	1.10	1.09	1.08	1.13	1.10	1.13	1.16	1.20	1.19	1.19	1.06	1.10	0.00
Waste Mined	k dmt	19,007	13.7	10,957	2,815	581	548	491	384	395	365	343	324	314	268	264	203	191	217	190	141	3	-
Open Pit	k dmt	12,838	-	10,565	2,273	-	-	-	-	-	-	-	-	-	-	-	-	-	-	-	-	-	-
Underground	k dmt	6,169	13.7	391	542	581	548	491	384	395	365	343	324	314	268	264	203	191	217	190	141	3	-
PROCESSING																							
Ore Processed																							
ROM to Plant Feed	k dmt	23,207	-	610.5	1,224	1,300	1,300	1,300	1,300	1,300	1,300	1,300	1,300	1,300	1,300	1,300	1,300	1,300	1,300	1,300	1,172	701	-
Ore Grade	% Li_2O	1.10	0.00	1.12	1.02	0.96	0.99	1.08	1.09	1.05	1.10	1.09	1.08	1.13	1.10	1.13	1.16	1.19	1.19	1.19	1.07	1.10	0.00
Concentrate Produced																							
Overall Recovery	%	65.3	0.0	65.3	65.3	65.3	65.3	65.3	65.3	65.3	65.3	65.3	65.3	65.3	65.3	65.3	65.3	65.3	65.3	65.3	65.3	65.3	0.0
Spodumene Concentrate 5.2% Li_2O	k dmt	3,197.5	-	86.2	156.0	156.5	162.1	177.1	178.2	172.0	180.1	178.6	176.8	183.9	178.9	184.2	189.5	194.4	194.0	194.4	158.0	96.7	-
Transportation																							
Output to Shanghai																							
Spodumene Concentrate 5.2% Li_2O	k dmt	3,197.5	-	86.2	156.0	156.5	162.1	177.1	178.2	172.0	180.1	178.6	176.8	183.9	178.9	184.2	189.5	194.4	194.0	194.4	158.0	96.7	-
Moisture Content	%	3.0	0.0	3.0	3.0	3.0	3.0	3.0	3.0	3.0	3.0	3.0	3.0	3.0	3.0	3.0	3.0	3.0	3.0	3.0	3.0	3.0	0.0
SC 5.2% Li_2O (wet)	k wmt	3,293.5	-	88.8	160.7	161.2	166.9	182.4	183.5	177.2	185.5	183.9	182.1	189.4	184.2	189.7	195.2	200.3	199.9	200.2	162.8	99.6	-

Table 22-13: Annual Projections—OPEX, Spodumene Concentrate Transportation, and Other Costs

	Unit	Total LOM	2026 -2	2027 -1	2028 1	2029 2	2030 3	2031 4	2032 5	2033 6	2034 7	2035 8	2036 9	2037 10	2038 11	2039 12	2040 13	2041 14	2042 15	2043 16	2044 17	2045 18	2046 19
MINE SITE COSTS																							
Annual Costs	$ M	982.7	0.0	30.3	52.6	56.6	54.9	54.7	53.3	56.7	55.4	57.8	55.9	56.0	55.8	53.7	53.3	52.7	47.5	50.3	42.9	42.4	0.0
Mining	"	607.0	0.0	23.4	32.4	35.8	34.2	33.9	32.5	35.8	34.5	36.9	35.1	35.1	34.9	32.9	32.4	31.9	26.7	29.5	24.2	25.0	0.0
Processing	"	314.2	0.0	4.7	17.4	17.4	17.4	17.4	17.4	17.4	17.4	17.4	17.4	17.4	17.4	17.4	17.4	17.4	17.4	17.4	15.9	15.5	0.0
SG&A	"	61.5	0.0	2.2	2.8	3.5	3.4	3.4	3.4	3.5	3.5	3.5	3.5	3.5	3.5	3.5	3.5	3.4	3.4	3.4	2.8	1.9	0.0
Unit Costs	$/t ROM	42.35	0.00	49.58	42.94	43.57	42.26	42.06	41.03	43.60	42.60	44.44	43.02	43.05	42.93	41.33	40.97	40.57	36.51	38.71	36.59	60.49	0.00
Mining	"	26.16	0.00	38.30	26.45	27.52	26.29	26.05	25.01	27.54	26.53	28.37	26.99	27.03	26.88	25.31	24.92	24.57	20.51	22.69	20.65	35.68	0.00
Processing	"	13.54	0.00	7.75	14.20	13.37	13.36	13.37	13.37	13.37	13.37	13.37	13.37	13.37	13.37	13.37	13.37	13.37	13.37	13.37	13.57	22.15	0.00
SG&A	"	2.65	0.00	3.53	2.29	2.68	2.60	2.64	2.65	2.69	2.70	2.70	2.66	2.66	2.68	2.66	2.69	2.63	2.63	2.65	2.37	2.65	0.00
ALL-IN SUSTAINING COSTS																							
Annual Costs																							
Mine Site Costs	$ 000	982.7	0.0	30.3	52.6	56.6	54.9	54.7	53.3	56.7	55.4	57.8	55.9	56.0	55.8	53.7	53.3	52.7	47.5	50.3	42.9	42.4	0.0
Royalties & Deductions	$ 000	260.5	0.0	4.4	9.2	11.0	12.5	15.0	15.1	14.6	15.3	15.1	15.0	15.6	15.2	15.6	16.1	16.5	16.4	16.5	13.4	8.2	0.0
SC Transportation Costs	$ 000	380.4	0.0	11.1	20.6	21.2	22.4	24.9	25.0	19.2	20.1	20.0	19.8	20.6	20.0	20.6	21.2	21.7	21.7	21.7	17.7	10.8	0.0
Total Cash Cost	$ 000	1,623.6	0.0	45.9	82.3	88.8	89.8	94.6	93.5	90.5	90.8	92.9	90.7	92.1	91.0	89.9	90.5	91.0	85.6	88.5	73.9	61.4	0.0
Capitalized Mining	$ 000	225.0	0.0	6.3	11.9	15.0	16.0	15.6	13.4	10.6	12.3	9.1	10.2	10.8	10.1	12.4	11.8	11.9	17.3	14.1	13.7	2.7	0.0
Sustaining Capital & Closure	$ 000	110.2	0.0	0.0	12.6	13.7	4.7	4.7	4.8	0.9	0.5	11.5	7.3	7.3	4.6	5.3	9.5	3.9	7.1	1.7	0.1	0.0	10.0
All-In Sustaining Cost	$ 000	1,958.9	0.0	52.1	106.8	117.5	110.5	114.9	111.7	102.0	103.5	113.5	108.2	110.2	105.7	107.6	111.9	106.8	109.9	104.3	87.7	64.1	10.0
Unit Costs																							
Minesite Costs	$/t SC	307.3	0.0	351.3	336.9	361.9	339.0	308.8	299.3	329.4	307.5	323.5	316.3	304.3	312.0	291.7	281.0	271.2	244.6	258.9	271.4	438.5	0.0
Royalties & Deductions	$/t SC	81.5	0.0	51.6	58.9	70.0	77.4	84.7	84.7	84.7	84.7	84.7	84.7	84.7	84.7	84.7	84.7	84.7	84.7	84.7	84.7	84.7	0.0
SC Transportation Costs	$/t SC	119.0	0.0	129.3	131.8	135.5	138.0	140.5	140.5	111.8	111.8	111.8	111.8	111.8	111.8	111.8	111.8	111.8	111.8	111.8	111.8	111.8	0.0
Total Cash Cost	$/t SC	507.8	0.0	532.1	527.6	567.4	554.3	534.0	524.5	526.0	504.1	520.1	512.9	500.9	508.6	488.3	477.6	467.8	441.2	455.5	467.9	635.0	0.0
Capitalized Mining	$/t SC	70.4	0.0	72.9	76.1	95.7	98.6	88.3	75.1	61.8	68.1	51.1	57.5	58.8	56.7	67.2	62.4	61.2	88.9	72.3	86.5	27.7	0.0
Sustaining Capital & Closure	$/t SC	34.5	0.0	0.0	80.9	87.5	28.7	26.4	27.0	5.3	2.5	64.4	41.6	39.5	25.9	28.8	50.4	20.2	36.4	8.6	0.8	0.1	0.0
All-In Sustaining Cost	$/t SC	612.6	0.0	605.0	684.6	750.6	681.6	648.7	626.6	593.1	574.7	635.6	612.0	599.1	591.2	584.2	590.4	549.2	566.5	536.4	555.2	662.8	0.0

Table 22-14: Profit and Loss Statement

	Unit	Total LOM	2026 -2	2027 -1	2028 1	2029 2	2030 3	2031 4	2032 5	2033 6	2034 7	2035 8	2036 9	2037 10	2038 11	2039 12	2040 13	2041 14	2042 15	2043 16	2044 17	2045 18	2046 19
PRODUCTION SUMMARY																							
ROM	kdmt	23,207.3	-	610.5	1,224	1,300	1,300	1,300	1,300	1,300	1,300	1,300	1,300	1,300	1,300	1,300	1,300	1,300	1,300	1,300	1,172	700.7	-
Li_2O Grade in ROM	%	1.10	0.00	1.12	1.02	0.96	0.99	1.08	1.09	1.05	1.10	1.09	1.08	1.13	1.10	1.13	1.16	1.19	1.19	1.19	1.07	1.10	0.00
Overall Recovery	%	65.3	0.0	65.3	65.3	65.3	65.3	65.3	65.3	65.3	65.3	65.3	65.3	65.3	65.3	65.3	65.3	65.3	65.3	65.3	65.3	65.3	0.0
Spodumene Concentrate 5.2% Li_2O	kdmt	3,197.5	-	86.2	156.0	156.5	162.1	177.1	178.2	172.0	180.1	178.6	176.8	183.9	178.9	184.2	189.5	194.4	194.0	194.4	158.0	96.7	-
PROFIT & LOSS																							
GROSS REVENUE	$ 000	6,129.5	0.0	104.6	216.4	257.7	294.9	353.0	355.2	342.9	358.9	356.0	352.4	366.6	356.5	367.2	377.8	387.6	386.8	387.4	315.0	192.7	0.0
Sales Volume	kdmt	3,197.5	0.0	86.2	156.0	156.5	162.1	177.1	178.2	172.0	180.1	178.6	176.8	183.9	178.9	184.2	189.5	194.4	194.0	194.4	158.0	96.7	0.0
Concentrate Price																							
SC6 Price - 2025 Fastmarkets	*$/t*	*2,211.9*	*0.0*	*1,400*	*1,600*	*1,900*	*2,100*	*2,300*	*2,300*	*2,300*	*2,300*	*2,300*	*2,300*	*2,300*	*2,300*	*2,300*	*2,300*	*2,300*	*2,300*	*2,300*	*2,300*	*2,300*	*2,300*
Spodumene Concentrate 5.2% Li_2O	*$/t*	*1,917.0*	*0.0*	*1,213*	*1,387*	*1,647*	*1,820*	*1,993*	*1,993*	*1,993*	*1,993*	*1,993*	*1,993*	*1,993*	*1,993*	*1,993*	*1,993*	*1,993*	*1,993*	*1,993*	*1,993*	*1,993*	*1,993*
(-) Royalties & Deductions	$ 000	(260.5)	0.0	(4.4)	(9.2)	(11.0)	(12.5)	(15.0)	(15.1)	(14.6)	(15.3)	(15.1)	(15.0)	(15.6)	(15.2)	(15.6)	(16.1)	(16.5)	(16.4)	(16.5)	(13.4)	(8.2)	0.0
CFEM	"	*(122.6)*	*0.0*	*(2.1)*	*(4.3)*	*(5.2)*	*(5.9)*	*(7.1)*	*(7.1)*	*(6.9)*	*(7.2)*	*(7.1)*	*(7.0)*	*(7.3)*	*(7.1)*	*(7.3)*	*(7.6)*	*(7.8)*	*(7.7)*	*(7.7)*	*(6.3)*	*(3.9)*	*0.0*
Appian Royalty		*(137.9)*	*0.0*	*(2.4)*	*(4.9)*	*(5.8)*	*(6.6)*	*(7.9)*	*(8.0)*	*(7.7)*	*(8.1)*	*(8.0)*	*(7.9)*	*(8.2)*	*(8.0)*	*(8.3)*	*(8.5)*	*(8.7)*	*(8.7)*	*(8.7)*	*(7.1)*	*(4.3)*	*0.0*
(=) Net Revenue	$ 000	5,869.0	0.0	100.1	207.2	246.7	282.4	338.0	340.1	328.4	343.7	340.8	337.5	351.0	341.4	351.6	361.7	371.1	370.3	371.0	301.6	184.5	0.0
(-) OPERATING COSTS	$ 000	(1,363.1)	0.0	(41.4)	(73.1)	(77.8)	(77.3)	(79.6)	(78.4)	(75.9)	(75.5)	(77.8)	(75.7)	(76.5)	(75.8)	(74.3)	(74.5)	(74.5)	(69.2)	(72.1)	(60.6)	(53.2)	0.0
Minesite Costs	"	(982.7)	0.0	(30.3)	(52.6)	(56.6)	(54.9)	(54.7)	(53.3)	(56.7)	(55.4)	(57.8)	(55.9)	(56.0)	(55.8)	(53.7)	(53.3)	(52.7)	(47.5)	(50.3)	(42.9)	(42.4)	0.0
Transportation Costs	"	(380.4)	0.0	(11.1)	(20.6)	(21.2)	(22.4)	(24.9)	(25.0)	(19.2)	(20.1)	(20.0)	(19.8)	(20.6)	(20.0)	(20.6)	(21.2)	(21.7)	(21.7)	(21.7)	(17.7)	(10.8)	0.0
(=) EBITDA	$ 000	4,505.9	0.0	58.7	134.1	168.9	205.1	258.4	261.7	252.4	268.2	263.1	261.8	274.5	265.6	277.2	287.3	296.6	301.2	298.9	241.0	131.3	0.0
EBITDA Margin	*%*	*73.5*	-	*56.1*	*62.0*	*65.5*	*69.5*	*73.2*	*73.7*	*73.6*	*74.7*	*73.9*	*74.3*	*74.9*	*74.5*	*75.5*	*76.0*	*76.5*	*77.9*	*77.1*	*76.5*	*68.1*	-
(-) Depreciation	$ 000	(526.1)	0.0	(1.5)	(67.6)	(70.4)	(28.7)	(20.3)	(19.6)	(8.6)	(15.1)	(19.2)	(18.2)	(18.7)	(18.8)	(23.5)	(25.4)	(27.6)	(31.8)	(34.6)	(36.2)	(30.2)	(10.0)
(=) EBIT	$ 000	3,979.8	0.0	57.2	66.4	98.5	176.4	238.1	242.1	243.9	253.1	243.9	243.6	255.8	246.8	253.8	261.8	269.0	269.4	264.3	204.8	101.1	(10.0)
Interest Paid on ECA Financing	$ 000	(2.0)	0.0	0.0	(0.4)	(0.7)	(0.5)	(0.3)	(0.1)	0.0	0.0	0.0	0.0	0.0	0.0	0.0	0.0	0.0	0.0	0.0	0.0	0.0	0.0
(=) EBT	$ 000	3,977.8	0.0	57.2	66.0	97.8	175.9	237.8	242.1	243.9	253.1	243.9	243.6	255.8	246.8	253.8	261.8	269.0	269.4	264.3	204.8	101.1	(10.0)
(-) Corporate Tax Payable	$ 000	(598.2)	0.0	(6.1)	(8.8)	(14.9)	(26.8)	(36.3)	(30.9)	(37.2)	(38.6)	(37.2)	(37.1)	(39.0)	(37.6)	(38.7)	(39.9)	(41.0)	(41.1)	(40.3)	(31.2)	(15.4)	0.0
IRPJ	"	(980.6)	0.0	(10.0)	(14.4)	(24.4)	(44.0)	(59.5)	(50.6)	(61.0)	(63.3)	(61.0)	(60.9)	(63.9)	(61.7)	(63.4)	(65.5)	(67.3)	(67.3)	(66.1)	(51.2)	(25.3)	0.0
CSLL	"	(353.0)	0.0	(3.6)	(5.2)	(8.8)	(15.8)	(21.4)	(18.2)	(21.9)	(22.8)	(21.9)	(21.9)	(23.0)	(22.2)	(22.8)	(23.6)	(24.2)	(24.2)	(23.8)	(18.4)	(9.1)	0.0
SUDENE Benefit	"	735.5	0.0	7.5	10.8	18.3	33.0	44.6	38.0	45.7	47.5	45.7	45.7	48.0	46.3	47.6	49.1	50.4	50.5	49.5	38.4	19.0	0.0
(=) Net Profit After Taxes	$ 000	3,379.6	0.0	51.1	57.2	82.9	149.1	201.5	211.2	206.7	214.5	206.7	206.4	216.8	209.1	215.1	221.9	228.0	228.3	224.0	173.6	85.7	(10.0)

Table 22-15: Project Free Cash Flow—Annual Projections

	Unit	Total LOM	2026 -2	2027 -1	2028 1	2029 2	2030 3	2031 4	2032 5	2033 6	2034 7	2035 8	2036 9	2037 10	2038 11	2039 12	2040 13	2041 14	2042 15	2043 16	2044 17	2045 18	2046 19
Net Profit After Taxes	$ 000	3,379.6	0.0	51.1	57.2	82.9	149.1	201.5	211.2	206.7	214.5	206.7	206.4	216.8	209.1	215.1	221.9	228.0	228.3	224.0	173.6	85.7	(10.0)
(+) Depreciation	$ 000	526.1	0.0	1.5	67.6	70.4	28.7	20.3	19.6	8.6	15.1	19.2	18.2	18.7	18.8	23.5	25.4	27.6	31.8	34.6	36.2	30.2	10.0
(-) INITIAL CAPEX	$ 000	(191.0)	(82.7)	(108.3)	0.0	0.0	0.0	0.0	0.0	0.0	0.0	0.0	0.0	0.0	0.0	0.0	0.0	0.0	0.0	0.0	0.0	0.0	0.0
Total Initial CAPEX	"	(200.6)	(87.2)	(113.4)	0.0	0.0	0.0	0.0	0.0	0.0	0.0	0.0	0.0	0.0	0.0	0.0	0.0	0.0	0.0	0.0	0.0	0.0	0.0
Initial CAPEX Cost	*"*	*(190.0)*	*(83.0)*	*(107.0)*	*0.0*	*0.0*	*0.0*	*0.0*	*0.0*	*0.0*	*0.0*	*0.0*	*0.0*	*0.0*	*0.0*	*0.0*	*0.0*	*0.0*	*0.0*	*0.0*	*0.0*	*0.0*	*0.0*
Recoverable Taxes	*"*	*(10.6)*	*(4.2)*	*(6.4)*	*0.0*	*0.0*	*0.0*	*0.0*	*0.0*	*0.0*	*0.0*	*0.0*	*0.0*	*0.0*	*0.0*	*0.0*	*0.0*	*0.0*	*0.0*	*0.0*	*0.0*	*0.0*	*0.0*
ECA Equipment Financing	"	9.6	4.5	5.1	0.0	0.0	0.0	0.0	0.0	0.0	0.0	0.0	0.0	0.0	0.0	0.0	0.0	0.0	0.0	0.0	0.0	0.0	0.0
Drawdown	"	*12.7*	*5.4*	*7.3*	*0.0*	*0.0*	*0.0*	*0.0*	*0.0*	*0.0*	*0.0*	*0.0*	*0.0*	*0.0*	*0.0*	*0.0*	*0.0*	*0.0*	*0.0*	*0.0*	*0.0*	*0.0*	*0.0*
Repayment	"	*(3.1)*	*(0.9)*	*(2.2)*	*0.0*	*0.0*	*0.0*	*0.0*	*0.0*	*0.0*	*0.0*	*0.0*	*0.0*	*0.0*	*0.0*	*0.0*	*0.0*	*0.0*	*0.0*	*0.0*	*0.0*	*0.0*	*0.0*
(-) CAPEX OPERATIONS	$ 000	(344.9)	0.0	(6.3)	(26.9)	(31.3)	(23.5)	(22.0)	(18.2)	(11.6)	(12.7)	(20.6)	(17.5)	(18.1)	(14.8)	(17.7)	(21.4)	(15.8)	(24.3)	(15.7)	(13.8)	(2.7)	(10.0)
Sustaining Capital	"	(100.2)	0.0	0.0	(12.6)	(13.7)	(4.7)	(4.7)	(4.8)	(0.9)	(0.5)	(11.5)	(7.3)	(7.3)	(4.6)	(5.3)	(9.5)	(3.9)	(7.1)	(1.7)	(0.1)	(0.0)	0.0
Sustaining Capital Cost	"	(95.7)	0.0	0.0	(12.2)	(13.3)	(4.3)	(4.3)	(4.6)	(0.8)	(0.3)	(11.0)	(7.0)	(7.0)	(4.5)	(5.1)	(9.1)	(3.7)	(6.8)	(1.6)	(0.1)	(0.0)	0.0
Recoverable Taxes	"	(4.5)	0.0	0.0	(0.4)	(0.4)	(0.4)	(0.3)	(0.3)	(0.1)	(0.1)	(0.5)	(0.4)	(0.3)	(0.2)	(0.2)	(0.4)	(0.3)	(0.2)	(0.1)	(0.0)	(0.0)	0.0
Mine Closure	"	(10.0)	0.0	0.0	0.0	0.0	0.0	0.0	0.0	0.0	0.0	0.0	0.0	0.0	0.0	0.0	0.0	0.0	0.0	0.0	0.0	0.0	(10.0)
Capitalized Mine Development Costs	"	(225.0)	0.0	(6.3)	(11.9)	(15.0)	(16.0)	(15.6)	(13.4)	(10.6)	(12.3)	(9.1)	(10.2)	(10.8)	(10.1)	(12.4)	(11.8)	(11.9)	(17.3)	(14.1)	(13.7)	(2.7)	0.0
ECA Financing Repayment	"	(9.6)	0.0	0.0	(2.4)	(2.6)	(2.9)	(1.7)	0.0	0.0	0.0	0.0	0.0	0.0	0.0	0.0	0.0	0.0	0.0	0.0	0.0	0.0	0.0
(-/+) WORKING CAPITAL MOVEMENTS	$ 000	0.0	0.0	(14.7)	(16.5)	(6.5)	(6.3)	(9.6)	(0.3)	2.1	(2.7)	0.7	0.6	(2.5)	1.6	(1.9)	(1.6)	(1.8)	(0.3)	0.1	11.4	19.9	28.2
Working Capital	"		0.0	14.7	31.2	37.7	44.0	53.5	53.9	51.7	54.5	53.8	53.2	55.7	54.0	55.9	57.6	59.4	59.7	59.5	48.1	28.2	0.0
Receivables	"		*0.0*	*17.2*	*35.5*	*42.4*	*48.5*	*58.0*	*58.2*	*56.4*	*59.0*	*58.5*	*57.8*	*60.3*	*58.6*	*60.4*	*61.9*	*63.7*	*63.6*	*63.7*	*51.6*	*31.7*	*0.0*
Payables	"		*0.0*	*(2.5)*	*(4.3)*	*(4.7)*	*(4.5)*	*(4.5)*	*(4.4)*	*(4.7)*	*(4.6)*	*(4.7)*	*(4.6)*	*(4.6)*	*(4.6)*	*(4.4)*	*(4.4)*	*(4.3)*	*(3.9)*	*(4.1)*	*(3.5)*	*(3.5)*	*0.0*
(+/-) Recoverable Taxes Cash Flow and Offsets	$ 000	21.7	0.0	3.4	1.2	(2.6)	(4.3)	(4.1)	(4.3)	(5.0)	2.2	1.9	2.6	2.3	2.3	2.5	2.6	2.8	3.6	3.1	3.9	2.6	4.9
Recoverable Taxes Payable on OPEX	"	(179.3)	0.0	(3.9)	(8.7)	(10.4)	(9.9)	(9.8)	(9.9)	(10.6)	(10.3)	(10.8)	(10.3)	(10.4)	(10.4)	(10.1)	(9.9)	(9.9)	(9.0)	(9.6)	(8.1)	(7.2)	0.0
PIS/COFINS/CBS	"	(80.0)	0.0	(2.7)	(4.2)	(4.5)	(4.3)	(4.3)	(4.3)	(4.6)	(4.5)	(4.7)	(4.5)	(4.6)	(4.6)	(4.4)	(4.4)	(4.4)	(4.0)	(4.3)	(3.5)	(3.1)	0.0
ICMS/IBS	"	(99.3)	0.0	(1.2)	(4.5)	(5.8)	(5.6)	(5.5)	(5.5)	(6.0)	(5.8)	(6.1)	(5.8)	(5.9)	(5.9)	(5.6)	(5.5)	(5.5)	(5.0)	(5.4)	(4.6)	(4.1)	0.0
PIS/COFINS Offsets	"	110.9	0.0	7.3	10.0	7.8	5.6	5.7	5.5	5.6	5.5	5.6	5.5	5.5	5.5	5.5	5.4	5.5	5.4	5.6	4.7	3.5	0.0
Against Corporate Taxes Payable	"	*22.8*	*0.0*	*1.2*	*1.2*	*1.2*	*1.2*	*1.2*	*1.2*	*1.2*	*1.2*	*1.2*	*1.2*	*1.2*	*1.2*	*1.2*	*1.2*	*1.2*	*1.2*	*1.2*	*1.2*	*1.2*	*0.0*
Against Other Federal Taxes Payable	"	*88.0*	*0.0*	*6.1*	*8.8*	*6.6*	*4.4*	*4.5*	*4.3*	*4.4*	*4.3*	*4.4*	*4.3*	*4.3*	*4.3*	*4.3*	*4.2*	*4.3*	*4.2*	*4.4*	*3.5*	*2.3*	*0.0*
IBS Credits Refund	"	90.1	0.0	0.0	0.0	0.0	0.0	0.0	0.0	0.0	6.9	7.2	7.5	7.2	7.3	7.1	7.1	7.2	7.2	7.1	7.3	6.3	4.8
(=) FREE CASH FLOW	$ 000	3,391.6	(82.7)	(73.3)	82.7	112.9	143.8	186.1	207.9	200.9	216.3	207.9	210.3	217.2	217.1	221.5	227.0	240.8	239.1	246.1	211.4	135.7	23.0
Accumulated Free Cash Flow	$ 000		(82.7)	(156.0)	(73.3)	39.6	183.3	369.5	577.4	778.3	994.6	1,202.5	1,412.8	1,630.0	1,847.1	2,068.5	2,295.5	2,536.3	2,775.4	3,021.5	3,232.8	3,368.5	3,391.6
Average Periods			*1-7-26*	*1-7-27*	*1-7-28*	*1-7-29*	*1-7-30*	*1-7-31*	*1-7-32*	*1-7-33*	*1-7-34*	*1-7-35*	*1-7-36*	*1-7-37*	*1-7-38*	*1-7-39*	*1-7-40*	*1-7-41*	*1-7-42*	*1-7-43*	*1-7-44*	*1-7-45*	*1-7-46*
Number of Payback Periods	Years	2.2	0.0	0.5	1.0	0.6	0.0	0.0	0.0	0.0	0.0	0.0	0.0	0.0	0.0	0.0	0.0	0.0	0.0	0.0	0.0	0.0	0.0
Post-tax NPV	$ M	1,447.5																					
Internal Rate of Return (IRR)	%	61.2																					
PRE-TAX CASH FLOW	$ 000	3,989.8	(82.7)	(67.2)	91.5	127.8	170.6	222.4	238.8	238.1	254.9	245.1	247.5	256.2	254.7	260.2	266.9	281.8	280.2	286.4	242.6	151.1	23.0
Post-tax NPV	$ M	1,721.3																					
Internal Rate of Return (IRR)	%	68.4																					

23 ADJACENT PROPERTIES

The Araçuaí Pegmatitic District, in the northeastern sector of the Brazil's Eastern Pegmatitic Province, covers the region of the Minas Gerais municipalities of Salinas, Araçuaí, and Capelinha, to the west, and Itinga and Caraí, to the east. In this district, Brazil's largest lithium-producing area, hundreds of pegmatites occur, including litiniferous pegmatites, gemological pegmatites, and pegmatites producing ceramic minerals and ornamental rocks, many of which have been exploited by mineral exploration and mining companies, and prospectors, for more than a century.

The Bandeira lithium ore deposit, under ANM mining right 832439/2009, is adjacent to the spodumene-bearing pegmatite minerals of CBL's Cachoeira mine, and the Barreiro, Murial, and Lavra do Meio deposits of Sigma Lithium Corporation.

24 OTHER RELEVANT INFORMATION

24.1 Cooperation Agreement with the Government of Minas Gerais

On July 19, 2023, the Minas Gerais government and MGLIT signed a cooperation agreement, an MOU, to prioritize and speed requests with state government secretariats and agencies regarding lithium ore exploration and deployment projects in MGLIT's Jequitinhonha Valley (Lithium Ionic, 2023, July 19).

24.2 Electric Power Connection Agreement

On October 31, 2023, MGLIT signed a contract with Centrais Elétricas de Minas Gerais (CEMIG) to connect electricity to the Project. MGLIT foresees the construction of the 138 kV transmission line and a substation to connect to the industrial unit's distribution substation. The substation is expected to be energized by February 19, 2027 (Lithium Ionic, 2025, September 02).

24.3 Minas Gerais State Tax Exemption

The Memorandum of Understanding signed between the State of Minas Gerais and MGLIT Empreendimentos Ltda. aims to enable the maintenance and expansion of the company’s operations in the municipalities of Araçuaí and Itinga, with planned investments of R$ 1.4 billion between 2025 and 2027. The agreement provides for job creation, training of local labor, compliance with environmental standards, and prioritization of suppliers from Minas Gerais. MGLIT commits to submitting annual reports on the progress of the project and to maintaining its establishment in the state for the legally required period.

In return, the State grants tax benefits, such as deferral of ICMS on imports and acquisitions of machinery, equipment, and raw materials, as well as institutional support through Invest Minas. The memorandum establishes compliance rules, data protection (LGPD), and provides mechanisms for renegotiation or termination in case of non-compliance or legal changes. The document was published on July 4, 2025, and follows the principles of public administration and current legislation.

24.4 Lithium Decree of 1997

The lithium decree was created on December 4, 1997, benefiting Brazilian companies that explore and produce lithium compounds in Brazil. The decree ensures their priority in the national market.

Decrees No. 4,338, dated August 19, 2002, No. 5,473 dated June 21, 2005, and No. 10,577 dated December 14, 2020, renewed the objective of maintaining the Brazilian lithium market for domestic producers.

On July 5, 2022, through Decree No. 11,120, the Brazilian market was opened for import and export for lithium ores and minerals and their compounds.

25 INTERPRETATION AND CONCLUSIONS

This Technical Report outlines the requirements for operating an open pit and an underground mine equipped with two ramps, with a spodumene DMS concentration plant that produces 5.20% Li_2O concentrate. The design capacity of the plant is 1.5 Mt/a of ore, production capacity is 1.3 Mt/a ore. This Technical Report describes all the infrastructure necessary for removing ore from the mine, and its processing, including producing concentrate within the technical specifications for supply to the international market. The LOM mining plan (18.5 years) defined an ore mass of 23.4 Mt with an average grade of 1.10% Li_2O after operational dilution. All production of spodumene concentrate is expected to be exported through the port of Ilhéus or Vitoria to downstream lithium chemical compound conversion facilities globally.

25.1 Geology and Mineral Resources

Mineral Resources are estimated in this Technical Report, limited to the areas outlined using the mining rights polygon, which comprises the Bandeira Property and the reasonable prospect for eventual economic extraction.

The MGLIT Bandeira database contains 10,298 assays, comprising 247 from trenches and 10,051 intervals from drill holes.

The Project employed advanced technology, with a set of solid-grade shells for estimation domains created using a 0.3% Li_2O threshold. These interpretations were then transformed into a series of implicit 3-D models aligned with the dominant strike directions of 235° and 140°. Additionally, weathering modelling was performed, considering the information provided in the core logs. The model was built from implicit modelling using Leapfrog Edge 2024.1.3 software.

Based on the structural analysis results, the ordinary kriging (OK) estimation method was used on the Li_2O% and density variables.

The mathematical and geostatistical criterion for classifying the resource was based on the following:

- The Measured Mineral Resource classification referenced the 50 m of the average Euclidean distance to sample (AvgD) used in OK estimation with a minimum of seven composites in at least three different drill holes.
- The Indicated Mineral Resource classification referenced the 100 m of the AvgD used in OK with a minimum of seven composites in at least three different drill holes.
- The Inferred Mineral Resource classification contains all remaining estimated blocks.

The Mineral Resource estimate is limited to the area delimited by the polygon of the ANM mining rights 832.439/2009, 831.116/2016, and 831117/2016, that makes up the Project and the reasonable prospect for eventual economic extraction.

The Bandeira Mineral Resource estimates are summarized in Table 25-1.

Table 25-1: Bandeira Mineral Resource Estimates (0.5% Li_2O Cut-Off)

Deposit/Cut-Off Grade	Category	Resource (Mt)	Grade % Li_2O	Contained LCE (kt)
Bandeira (0.5% cut-off)	Measured	3.36	1.38	115
	Indicated	23.91	1.33	786
	Measured + Indicated	27.27	1.34	901
	Inferred	18.55	1.34	615

Source: GE21 (2025).
Notes:

- The Mineral Resource estimate's effective date is November 20, 2024.
- Carlos J. E. Silva (MAIG #7868) prepared the Mineral Resource estimate using CIM (2014).
- The report meets the Canadian Securities Administrators' NI 43-101 requirements.
- Mineral Resources are not Mineral Reserves and have no economic viability. There is no certainty that any portion of the Mineral Resource will be converted into a Mineral Reserve.
- Figures are rounded to appropriate levels of precision, and discrepancies may occur due to rounding.
- The spodumene pegmatite domains were modelled using composites with Li_2O grades exceeding 0.3%.
- Grade estimation was conducted using OK within Leapfrog Edge 2024.1.3 software.
- The Mineral Resource estimate is confined to the MGLIT Bandeira mining right (ANM) and includes only fresh-rock domains.
- The Mineral Resource estimate was restricted by interpreting suitable-grade shells using a 0.5% Li_2O cut-off for underground resources.
- Inferred Mineral Resources are conceptual in nature and can only form the basis for economic analyses with further drilling and evaluation.
- The Mineral Resource estimate may be materially affected by environmental, legal, tax, sociopolitical, permitting, title, marketing, and other relevant factors.

25.2 Industrial Plant

The process flowchart developed for the Project is based on the commonly used practice of using DMS to produce spodumene concentrate, which has been used worldwide for many years.

Metallurgical tests performed with core samples from geological boreholes resulted in spodumene concentrates that comply with the minimum specifications of 5.20% Li_2O and a maximum of 1.00% Fe_2O_3, with a metallurgical recovery of 65.3%.

The process flowchart includes three-stage crushing, screen classification, pre-concentration by ore sorter (future), DMS concentration of four stages (primary, secondary coarse and fines, and recrush).

The process design criteria are well supported, with multiple rounds of bench- and pilot-scale testwork complete with mineralogy for understanding the deposit. This was done on composite and individual samples to de-risk deposit variability. The selected process flowsheet is demonstrated by adjacent operations, and the low complexity presents a low-risk and low-cost solution to processing ore from the Bandeira deposit.

25.3 Infrastructure

The infrastructure required to keep the industrial unit in operation with the necessary utilities, services, and access, consists of the main and secondary substations, unpaved roads, weighbridge,

administrative buildings, (cafeteria, industrial kitchen, medical clinic, warehouse, mine office, change house) maintenance workshop, compressed-air distribution, and fire suppression system.

The site is well supported by regional infrastructure, external to the site, providing paved road access, low-carbon power, access to bulk ports, and a locally residing workforce.

25.4 Water Management

Water drawn from the Piauí and Jequitinhonha rivers will be received directly in the raw-water tank and will be of sufficient quantity for the construction and operation of all the units that make up the Project industrial plant. Rainwater runoff within the industrial areas will be directed through channels, and a speed reducer into a sump that will capture water from which water trucks will pump the water to be used to wet roads to suppress dust and for irrigating lawns on slopes. In the event of heavy rainfall, the sump will have an overflow that directs excess water to the Piauí River.

It is important to note that the water circulating in the DMS plant will not be sent to the stormwater drainage sump, as the plant has its own collection system that recirculates this wastewater. All underground mine-affected water is collected and treated prior to reuse or discharge at permitted discharge points.

25.5 Underground Mine

The Bandeira underground mine will be accessed by two ramps, which together should have a maximum mining capacity of 1.3 Mt/a of ore out of a calculated reserve of 23.4 Mt, with an average grade of 1.10% Li_2O after the total dilution of 21%. In the northern part of the mine, sublevel stoping mining is to be adopted, and in the southeastern part, the process will be open-pit (approx. 1 Mt ROM). All ore from the mine will be extracted by blasting, and transported from the mine to the plant using 40-tonne conventional trucks

25.6 Geotechnical and Hydrogeology

The Project's geotechnical, structural, and hydrogeological studies confirm the technical feasibility and operational safety of both open-pit and underground mining, providing a solid foundation for advancement to the basic engineering stage.

The sublevel open stope method was identified as the most suitable for the local conditions, with the schist rock mass exhibiting good stability and low dilution risk. Key design parameters indicate a robust and stable structural behaviour, effectively controlled through anchored support and mesh systems—including maximum spans limited to 50 m and a crown pillar safety factor above 1.5.

The open-pit operation is considered technically sound and strategically transitional, enabling early revenue generation and ensuring a gradual and safe transition to underground production.

From a hydrogeological perspective, the project is in a semi-arid region, characterized by strong seasonal rainfall and the predominance of fractured aquifers with low productivity. The conceptual hydrogeological model indicates that groundwater flow is structurally controlled, with intermittent drainage and limited natural recharge.

In summary, the Project exhibits geotechnical and hydrogeological conditions compatible with the proposed mining plan, demonstrating technical viability, operational safety, and sufficient project maturity to advance to subsequent development phases, provided that continuous monitoring and refinement of design parameters are maintained.

25.7 Mineral Reserves Estimate and Mining Methods

The estimated Mineral Reserves for the Project include underground and open-pit mine methods deemed adequate for the deposit. Required modifying factors have been applied for the Mineral Reserves estimate to demonstrate its technical and economic feasibility in accordance with the CIM Definition Standards.

The open-pit mining operation is strategically designed to efficiently supply ore to processing in parallel with the underground production ramp-up and will be operated by a contractor. By employing conventional methods and optimizing haul distances, the plan aims to maximize productivity within its limited LOM.

The mining method involves sublevel stoping, with ore drives planned to follow the ore-body's strike, ensuring the necessary capacity for the planned extraction of 1.3 Mt/a of ore. To achieve this production rate, the mine will be accessed through two declines for the transportation of ore, waste, equipment, and personnel, while also serving as part of the mine's ventilation system. The decline section was properly sized for stability and to accommodate 40-tonne trucks and infrastructure components.

Underground mining services include all required infrastructure such as power, pumping, water, compressed air, backfill, and communication, and were defined as preliminary.

Proven and Probable Mineral Reserves for the mine as of the resource effective date of November 20, 2024, are estimated in 23.2 Mt grading 1.1% Li_2O for 628.5 kt LCE.

A 10% dilution and 100% of mining recovery have been assumed for open-pit Mineral Reserves.

For the ore from the underground development, Mineral Reserve volumes and tonnages assume 100% of mine recovery, 31% of planned dilution, and 10% of operational dilution due to overbreaking. For the stopes, mining recovery is 90% and 21% of planned dilution.

Given the presence of ore lenses interspersed with waste rock, a minimum pillar of 4 meters has been established for stope optimization. Pillar between parallel stopes is sensitive to the geotechnical conditions and its integrity can be affected by the operation conditions, impacting in the mining dilution and mining recovery.

To effectively execute mining as planned under these conditions, and mitigate associated risks, it is crucial to implement rigorous controls over the ore-drivers development and support execution and ensure high efficiency in drilling, blasting, and backfilling operations.

25.8 Environment

The environmental licensing process was filed with SEMAD on November 20, 2023. On January 26, 2024, MGLIT received notification from the responsible body that the documentation filed met the requirements, and that the analysis of the process was beginning.

After a field inspection carried out by the environmental agency on September 25, 2024, the process was reclassified as a Corrective Installation License process, concurrently with the Operating License, maintaining the LAC modality.

Upon completion of the Project's assessment, on February 13, 2025, the multidisciplinary technical team of the State Environmental Foundation (FEAM), entity subject to SEMAD, issued the Technical Opinion No. 14, recommending Project approval. MGLIT is awaiting COPAM approval to secure the LP, LI, and LO to commence construction activities.

25.9 Capital Cost Estimate

The estimated CAPEX was developed using the concept of the American Association Cost Estimation (AACE) Class III for an underground mine equipped with two ramps and an industrial spodumene concentration unit. The contingencies adopted for the mine were 15% and 10% for the plant .The total estimated cost is $191 million, with an assumed accuracy of −20% to +30% (Table 25-2).

Table 25-2: Initial Capital Cost Summary

	Cost ($M)
Initial CAPEX	191.0
Mine	59.2
Surface	107.3
Owner's Cost	4.9
Contingency	19.6

25.10 Operating Cost Estimate

The underground mine and industrial spodumene concentration unit OPEX is shown in Table 25-3, with a maximum processing capacity of 1.5 Mt/a of lithium ore. The planned ROM production is 1.3 Mt/a of ore from the mine. Production of 177 kt/a of SPO with a grade of 5.2% Li_2O. Production cost of the mine and plant are calculated at $190/t and $98/t of SPO, respectively. Also added is $19/t of SPO for general and administrative (G&A); environmental, social, and governance (ESG); and insurance; totalling $307/t of SPO. Further, $70/t of SPO for capitalized underground mining brings the total OPEX to $378/t of SPO.

Table 25-3: LOM Operating Cost Summary—Per Tonne of Spodumene Concentrate

Description	SPO Concentrate (5.2%, $/t)
Mining	190
Processing	98
General and Administrative (G&A) Sales	19
Subtotal	307
Capitalized Mining	70
Total Including Capitalized Mining	378
Transportation Costs (CIF China Port)	119
Royalties and Deductions	81
Sustaining Capital CAPEX and Closure	34
All-In Sustaining Cost (AISC)	613

In addition, on a Life-of-Mine basis, $119/t, $81/t and $34/t of SPO for illustrative transportation costs, royalties and deductions, and sustaining CAPEX and closure bring the total All-In Sustaining Cost (AISC) to $613/t of SPO.

These costs are benchmarked with regional and global peer producers and are in line with industry estimates.

25.11 Economic Analysis

The economic analysis of the estimated cash flow for the Project indicates the potential for an economic project across a broad range of input assumptions. The NPV calculated at an 8% discount rate is positive, and the IRR calculated for the Project is within a favourable range.

The sensitivity analysis demonstrated that Project outcomes are significantly impacted by price fluctuations, more so than by other input variables. Nonetheless, the findings indicate that the results remain robust, even when applying the most conservative price series outlined in the market analysis.

26 RECOMMENDATIONS

26.1 Geology and Mineral Resource Estimate

GE21 proposes the following recommendations for the continuous improvement of the Mineral Resource estimate:

- Carry out a 50 m x 50 m infill-drilling program in the domain of the Indicated resource classification to focus on improving resource delineation.
- Carry out a 100 m x 100 m infill-drilling program in the domain of the Inferred resource classification to focus on resource delineation improvement.
- Conduct an on-site density survey in the weathered zone.

26.2 Mineral Reserves Estimate and Mining Methods

GE21 recommends that the following activities related to the mine area to be carried out during the development of the next engineering phase:

- Conduct a dilution study in the mine to determine the optimal block size, and confirm the value of diluted content in the model for open-pit and underground mining methods.
- Conduct geotechnical feasibility studies to determine the optimal pillar size between parallel stopes.
- Detail the sequential mining plans on a monthly or quarterly basis for the first three years of Project operation.
- Develop standard operating procedures for grade control, geotechnical, and mining operations to ensure that the ore quality meets the specifications required for supply to the processing plant.
- Conduct hydrogeological investigations, including monitoring with the installation of piezometers and INAs; a network of streamflow monitoring in watercourses; and aquifer tests in underground instruments to estimate, at the feasibility level, the hydrodynamic parameters and gain a better understanding of water flow behaviour.
- Develop basic and detailed engineering studies for underground services, including pumping, power, water, air compressed, backfill, and communication.

26.3 Project Infrastructure

26.3.1 Bridge Over the Piauí River

Start the construction of the bridge over the Piauí River in the dry season of 2026 to improve access to construction and laydown areas during the site development phase.

26.4 Processing Plant

The following activities need to be conducted to progress the processing plant:

- Complete a Project Execution Plan (PEP) including:
  - Detailed project schedule
  - Site safety and entry control
  - Logistics and storage for equipment purchased
  - Study and application for Project Ex Tarifario (duty exemptions)
  - Construction staging area
  - Project insurance.
- Study outbound logistics, including port access, storage, and infrastructure.
- Commence a conceptual project design for fines flotation.

26.4.1 Processing Alternatives

- Continue to evaluate alternatives for processing the fines below 0.6 mm to increase spodumene recovery with the use of flotation.
- Investigate the possibility to recover separated heavy minerals like tantalite, cassiterite from the flotation concentrate.
- Study flotation recovery methods as a future process expansion.

26.5 Environmental Feasibility Assessment

Socio-environmental studies (RCA/PCA) confirm that the Project lies outside Indigenous Lands, Quilombola Community, and Cultural Heritage sites.

To support the transition from feasibility to implementation, the following actions are recommended:

- Advance the environmental licensing process for the open-pit expansion, including the preparation of the EIA and environmental impact report (RIMA) required for the increased capacity (1.5 Mt/a) and expanded area of influence.
- Monitor and ensure the timely conclusion of pending authorizations, particularly those related to the water abstraction (adutora), bridge construction, and native vegetation suppression, maintaining close coordination with the environmental agency.
- Consolidate and implement the environmental and social management system (ESMS), integrating the environmental programs already defined in the PCA, such as water and waste management, biodiversity monitoring, occupational health and safety, social communication, and emergency response.
- Formalize stakeholder engagement and consultation plans, ensuring inclusive and well-documented participation of local communities, landowners, and the Baú Quilombola community.

- Advance the Mine Closure and Rehabilitation Plan defining clear post-closure monitoring indicators.
- Maintain proactive coordination with regulatory and heritage agencies to streamline technical reviews and ensure procedural consistency.

27 REFERENCES

Afgouni, K., & Marques, F. F. (1997). Depósitos de lítio, berílio e césio de Araçuaí/Itinga, Minas Gerais. In C. Schobbenhaus, E. T. Queiroz, & C. E. S. Coelho (Coords.), *Principais Depósitos Minerais do Brasil* (pp. 373–388). Departamento Nacional da Produção Mineral, Companhia Vale do Rio Doce.

Alkmim, F. F., Marshak, S., Pedrosa-Soares, A. C., Peres, G. G., Cruz, S. C. P., & Whittington, A. (2006). Kinematic evolution of the Araçuaí-West Congo orogen in Brazil and Africa: Nutcracker tectonics during the Neoproterozoic assembly of Gondwana. *Precambrian Research*, *149*, 43–64.

Aquino, J. A., Oliveira, M. L. M., & Braga, P. F. A. (2007). Ensaios em meio denso. In J. A. Sampaio, S. C. Alves França, & P. F. Almeida Braga (Eds.), *Tratamento de Minérios: práticas laboratoriais* (pp. 297–318). Centro de Tecnologia Mineral/Ministério da Ciência, Tecnologia e Inovação.

Arenare, D. S., Rodrigues, O. M. S., Araujo, A. C., & Viana, P. R. M. (2009). Espirais concentradoras no tratamento de minérios de ferro: uma breve revisão. *Tecnologia em Metalurgia, Materiais e Mineração, 5*, 224–228.

Associação Brasileira de Geologia e Engenharia Ambiental (ABGE) (1983). Métodos para descrição quantitativa de descontinuidades em maciços rochosos. São Paulo, Brasil.

Assumpção, M. S., Pirchiner M., Dourado J. C., & Barros L.V. (2016). Terremotos no Brasil: preparando-se para eventos raros. Boletim SBGf, 96, 25-29.

Bamber, A. S. (2008). Integrated mining, pre-concentration and waste disposal systems for the increased sustainability of hard rock metal mining [Unpublished doctoral dissertation]. University of British Columbia.

Bazzana, A., & Parkes, T. (2023, July 7). *Lithium Ionic Dense Media Separation Testwork Report*. Sepro Laboratories Inc.

Bradley, D., & McCauley, A. (2013). *A Preliminary Deposit Model for Lithium-Cesium-Tantalum (LCT) Pegmatites*. U.S. Geological Survey, Open-File Report 2013–1008 Version 1.1.

Brady, B. H. G., BROWN, E. T. (1985). Rock Mechanics for underground mining. 3rd ed. Springer Science.

Carter, T. G. (2014). Guidelines for use of the Scaled Span Method for Surface Crown Pillar Stability Assessment. Ontario: Ontario Ministry of Northern Development and Mines.

Conselho Nacional do Meio Ambiente (CONAMA). (1997). Resolução nº 237, de 19 de dezembro de 1997. Regulamenta os aspectos de licenciamento ambiental estabelecidos na Política Nacional do Meio Ambiente. Diário Oficial da União: seção 1, Brasília, DF.

Conselho Nacional do Meio Ambiente (CONAMA). (2006). Resolução nº 369, de 28 de março de 2006. Dispõe sobre os casos excepcionais de utilidade pública, de interesse social ou de baixo impacto ambiental, que possibilitam a intervenção ou supressão de vegetação em Área de Preservação Permanente - APP. Diário Oficial da União: seção 1, Brasília, DF.

Constituição. (1988). Constituição da República Federativa do Brasil. Brasília, DF.

Decreto nº 6.660, de 21 de novembro de 2008. Regulamenta dispositivos da Lei nº 11.428, de 22 de dezembro de 2006, que dispõe sobre a utilização e proteção da vegetação nativa do Bioma Mata Atlântica. Diário Oficial da União, Brasília, DF.

Decreto nº 97.632, de 10 de abril de 1989. Dispõe sobre a regulamentação do Artigo 2°, inciso VIII, da Lei n° 6.938, de 31 de agosto de 1981, e dá outras providências. Diário Oficial da União, Brasília, DF.

Decreto nº 99.274, de 6 de junho de 1990. Regulamenta a Lei nº 6.902, de 27 de abril de 1981, que dispõe sobre a criação de Estações Ecológicas e Áreas de Proteção Ambiental, e a Lei nº 6.938, de 31 de agosto de 1981, que dispõe sobre a Política Nacional do Meio Ambiente, e dá outras providências. Diário Oficial da União: seção 1, Brasília, DF.

Hawley, M., & Cunning, J. (2017). Guidelines for Mine Waste Dump and Stockpile Design. Csiro Publishing.

Hoek, E. and Bray, J. (1981). Rock Slope Engineering, 3rd ed. Inst. Mining and Metallurgy, London, UK.

Instituto Brasileiro do Meio Ambiente e dos Recursos Naturais Renováveis (IBAMA). Instrução Normativa nº 146, de 10 de janeiro de 2007. Estabelece os critérios para procedimentos relativos ao manejo de fauna silvestre em áreas de influência de empreendimentos e atividades consideradas efetiva ou potencialmente causadoras de impactos à fauna sujeitas ao licenciamento ambiental, como definido pela Lei n° 6938/81 e pelas Resoluções Conama n° 001/86 e n° 237/97. Diário Oficial da União, Brasília, DF.

Instituto do Patrimônio Histórico e Artístico Nacional (IPHAN). Instrução Normativa nº 001, de 25 de março de 2015. Estabelece procedimentos administrativos a serem observados pelo IPHAN nos processos de licenciamento ambiental nos quais participe. Diário Oficial da União, Brasília, DF.

Lei nº 11.903, de 6 de setembro de 1995. Cria a Secretaria de Estado de Meio Ambiente e Desenvolvimento Sustentável, Altera a Denominação da Secretaria de Estado De Ciência, Tecnologia e Meio Ambiente e da Outras Providências. Diário Oficial da União: seção 1, Brasília, DF.

Lei nº 12.651, de 25 de maio de 2012. Dispõe sobre a proteção da vegetação nativa; altera as Leis nºs 6.938, de 31 de agosto de 1981, 9.393, de 19 de dezembro de 1996, e 11.428, de 22 de dezembro de 2006; revoga as Leis nºs 4.771, de 15 de setembro de 1965, e 7.754, de 14 de abril de 1989, e a Medida Provisória nº 2.166-67, de 24 de agosto de 2001; e dá outras providências. Diário Oficial da União: seção 1, Brasília, DF.

Lei nº 12.725, de 16 de outubro de 2012. Dispõe sobre o controle da fauna nas imediações de aeródromos. Diário Oficial da União, Brasília, DF.

Lei nº 6.938, de 31 de agosto de 1981. Dispõe sobre a Política Nacional do Meio Ambiente, seus fins e mecanismos de formulação e aplicação, e dá outras providências. Diário Oficial da União: seção 1, Brasília, DF.

Lei nº 9.433, de 8 de janeiro de 1997. Institui a Política Nacional de Recursos Hídricos, cria o Sistema Nacional de Gerenciamento de Recursos Hídricos, regulamenta o inciso XIX do art.

21 da Constituição Federal, e altera o art. 1º da Lei nº 8.001, de 13 de março de 1990, que modificou a Lei nº 7.990, de 28 de dezembro de 1989. Diário Oficial da União: seção 1, Brasília, DF, 9 jan. 1997.

Lei nº 9.985, de 18 de julho de 2000. Regulamenta o art. 225, § 1o, incisos I, II, III e VII da Constituição Federal, institui o Sistema Nacional de Unidades de Conservação da Natureza e dá outras providências. Diário Oficial da União: seção 1, Brasília, DF, 19 jul. 2000.

Burt, R. O., & C. Mills. (1984). *Gravity concentration technology*. Elsevier. p.139–183.

Campos, A. R., Luz, A. B., & Braga, P. F. A. (2018). Separação em meio denso. In A. R. Campos, A. B. Luz, & P. F. A. Braga (Eds.), *Tratamento de minérios* (6th ed., pp. 303–338). Rio de Janeiro, CETEM/MCTIC.

Canadian Institute of Mining, Metallurgy and Petroleum (CIM) Standing Committee on Reserve Definitions. (2014). *CIM Definition Standards for Mineral Resources & Mineral Reserves*. https://mrmr.cim.org/media/1128/cim-definition-standards_2014.pdf

Canadian Institute of Mining, Metallurgy and Petroleum (CIM) Mineral Resource & Mineral Reserve Committee. (2019). *Estimation of Mineral Resources and Mineral Reserves Best Practice Guidelines*. https://mrmr.cim.org/media/1129/cim-mrmr-bp-guidelines_2019.pdf

Cerný, P. (1991). Rare-element granite pegmatites. Part I: anatomy and internal evolution of pegmatite deposits. *Geoscience Canada, 18*, 49–67.

Cerný, P. (1991). Rare-element granite pegmatites. Part II: regional to global relationships and petrogenesis. *Geoscience Canada, 18*, 68–81.

Cerný, P., & Ercit, T. (2005). The classification of granitic pegmatites revisited. *The Canadian Mineralogist, 43*, 2005–2026.

Cerný, P., London, D., & Novak, M. (2012). Granitic pegmatites as reflections of their sources. *Elements, 8*, 289–294.

Chaves, M. L. S. C., Dias, C. H., & Cardoso, D. K. (2018). Lítio. In A. C. Pedrosa-Soares, E. Voll, & E. C. Cunha (Orgs.), *Recursos Minerais de Minas Gerais* (pp. 1–21). Companhia de Desenvolvimento de Minas Gerais. http://recursomineralmg.codemge.com.br

Correia-Neves, J. M., Pedrosa-Soares, A.C., & Marciano, V.R. (1986). A Província Pegmatítica Oriental do Brasil à luz dos conhecimentos atuais. *Revista Brasileira de Geociências*, *16*(1), 106–118.

Costa Sena, J. C. de (1982). Notícia sobre a mineralogia e geologia de uma parte do norte e nordeste da Província de Minas Gerais. *Annaes da Escola de Minas de Ouro Preto, 2*, 113–136.

Costa, A. G. (1990). Evolução petrológica para uma sequência de rochas metamórficas regionais do tipo baixa pressão, Itinga, NE de MG. *Revista Brasileira de Geociências, 19*, 440–448.

Costa, A. G., Neves, J. M. C., & Mueller, G. (1984). Feições polimetamórficas de metapelitos da região de Itinga (Minas Gerais, Médio Jequitinhonha). In *Anais do XXXIII Congresso Brasileiro de Geologia, Rio de Janeiro* (pp. 3166–3180). Sociedade Brasileira de Geologia.

Delboni Jr., H., Laporte, M-A, Quinn, J., Rodriguez, P. C., & O'Brien, N. (2023). *Grota do Cirilo Lithium Project, Updated Technical Report Araçuaí and Itinga regions, Minas Gerais, Brazil*.

Deluca, C., Pedrosa-Soares, A., Lima, S., Cordani, U., & Sato, K. (2019). Provenance of the Ediacaran Salinas Formation (Araçuaí Orogen, Brazil): Clues from lithochemical data and zircon U-Pb (SHRIMP) ages of volcanic clasts. *Brazilian Journal of Geology, 49*, 1–19. https://doi.org/10.1590/2317-4889201920190017.

Dias, C. H. (2015). Mineralogia, tipologia e causas de cor de espodumênios da Província Pegmatítica Oriental do Brasil e química mineral de Nb-tantalatos da mina da Cachoeira (Minas Gerais) [Master's thesis, Universidade Federal de Minas Gerais]. Repositório Institucional da UFMG. https://repositorio.ufmg.br/handle/1843/BUBD-9ZWPNA

Duncan, J.M., & Wright, S.G. (2005). Soil Strength and Slope Stability. John Wiley & Sons Inc.

Dupéré, M., & Sayeed, F. (2023, August 10). T*echnical Report on the Mineral Resource Estimated for Lithium Ionic, Itinga Project, Neae Araçuai Village, Minas Gerais State, Brazil* (Effective date June 24, 2023). Prepared by SGS Geological Services for Lithium Ionic Corp.

Ferraz, L. C. (1928). *Compêndio dos minerais do Brasil*. Imprensa Nacional.

Handley, M. F. (2013). Pre-mining stress model for subsurface excavations in southern Africa. *Journal of the Southern African Institute of Mining and Metallurgy, 113*(6), 449–471.

Horta de Cerqueira Viana, B., Silva, C, Lipiec, I. A., Hilário, J. A., Cabaleiro Rodriguez, P. & Mendonça, R. (2024, July). *Bandeira Lithium Project Araçuaí–Itinga, NI 43-101 Feasibility Study Technical Report, Minas Gerais, Brazil*.

IDE SISEMA/IBGE. (2022). https://idesisema.meioambiente.mg.gov.br/webgis

Lithium Ionic Corp. (2023, July 19). *Lithium Ionic signs MOU with local government authority Invest Minas; obtains priority status to facilitate acceleration of licensing and development for its Itinga and Salinas lithium projects, Brazil* [Press release]. https://lithiumionic.com/news/lithium-ionic-signs-mou-with-local-government-authority-invest-minas-obtains-priority-status-to-facilitate-acceleration-of-licensing-and-development-for-its-itinga-and-salinas-lithium-projects-brazil

London, D. (1984). Experimental Phase Equilibria in the System $LiAlSiO_4$- SiO_2-H_2O; a Petrogenetic Grid for Lithium-rich Pegmatites. *American Mineralogist, 69*(11–12), 995–1004.

London, D. (2008). *Pegmatites*. *Canadian Mineralogist* Special Publication 10. Mineralogical Association of Canada.

Luiz, C.R. (2023). *Como garantir segurança geotécnica em minas subterrâneas: O exemplo da Mina da Cachoeira da Companhia Brasileira de Lítio*. Invited lecture in Lithium Business 2023, Vale do Rio Jequitinhonha, Araçuaí, Brazil. https://www.youtube.com/watch?v=5QKjPYJtV8k

Melo, A. (2025, August). *Testes de sedimentação, reologia e filtragem a vácuo para amostra de rejeito de minério de lítio*. Delkor.

MGLIT Empreendimentos Ltda (2022, April). *QA/QC Protocol for Diamond Drilling, Itinga Project*.

MGLIT Empreendimentos Ltda (2023, July 10). *Relatorio dos Testes com Ore Sorter TOMRA Solutions*—Alemanha.

Minas Gerais. Conselho Estadual de Política Ambiental (COPAM). Deliberação Normativa COPAM nº 217, de 6 de dezembro de 2017. [Título da deliberação se houver]. Diário Oficial de Minas Gerais: seção [seção], Belo Horizonte, MG.

Minas Gerais. Conselho Estadual do Patrimônio Cultural; Instituto Estadual do Patrimônio Histórico e Artístico de Minas Gerais. Deliberação Normativa CONEP nº 007, de 3 de dezembro de 2014. Estabelece normas para a realização de estudos de impacto no patrimônio cultural no Estado de Minas Gerais. Diário do Executivo – Minas Gerais, Belo Horizonte, 12 dez. 2014.

Minas Gerais. Decreto nº 47.383, de 2 de março de 2018. Estabelece normas para licenciamento ambiental, tipifica e classifica infrações às normas de proteção ao meio ambiente e aos recursos hídricos e estabelece procedimentos administrativos de fiscalização e aplicação das penalidades. Diário do Executivo – "Minas Gerais", Belo Horizonte, 03 mar. 2018.

Minas Gerais. Decreto nº 47.749, de 11 de outubro de 2019. Dispõe sobre os processos de autorização para intervenção ambiental e sobre a produção florestal no âmbito do Estado de Minas Gerais e dá outras providências. Diário Oficial do Estado, Belo Horizonte, 11 out. 2019.

Minas Gerais. Lei nº 20.922, de 16 de outubro de 2013. Dispõe sobre a proteção à flora nativa no Estado de Minas Gerais, e dá outras providências. Diário Oficial de Minas Gerais: seção 1, Belo Horizonte, MG.

Minas Gerais. Lei nº 21.972, de 21 de janeiro de 2016. Dispõe sobre o Sistema Estadual de Meio Ambiente e Recursos Hídricos – Sisema – e dá outras providências. Diário do Executivo – "Minas Gerais", Belo Horizonte, 22 jan. 2016.

Minas Gerais. Secretaria de Estado de Meio Ambiente e Desenvolvimento Sustentável; Fundação Estadual do Meio Ambiente; Instituto Estadual de Florestas; Instituto Mineiro de Gestão das Águas. Resolução Conjunta SEMAD/FEAM/IEF/IGAM nº 2.466, de 13 de fevereiro de 2017. Institui a Infraestrutura de Dados Espaciais do Sistema Estadual de Meio Ambiente e Recursos Hídricos e cria seu Comitê Gestor. Diário do Executivo – Minas Gerais, Belo Horizonte, 14 fev. 2017.

Minas Gerais. Secretaria de Estado de Meio Ambiente e Desenvolvimento Sustentável; Instituto Estadual de Florestas. Resolução Conjunta SEMAD/IEF nº 1914, de 05 de setembro de 2013. Estabelece procedimentos para o cumprimento e a fiscalização da Reposição Florestal no Estado de Minas Gerais. Diário do Executivo – "Minas Gerais", Belo Horizonte, 06 set. 2013.

Minas Gerais. Secretaria de Estado de Meio Ambiente e Desenvolvimento Sustentável; Instituto Estadual de Florestas. Resolução Conjunta SEMAD/IEF nº 3.102, de 26 de outubro de 2021. Dispõe sobre os processos de autorização para intervenção ambiental no âmbito do Estado de Minas Gerais e dá outras providências. Diário do Executivo – "Minas Gerais", Belo Horizonte, 04 nov. 2021.

Neo Ambiental (2023). *Plano de Controle Ambiental*. Araçuaí. Minas Gerais.

Neo Ambiental (2023). Plano de Intervenção Ambiental-PIA Araçuaí. Minas Gerais.

Neo Ambiental (2023). Programa de Afugentamento, Resgate e Destinação da Fauna. Araçuaí. Minas Gerais.

NeoAgro Ambiental (2023, November). Relatório de Controle Ambiental, Projeto Bandeira, Araçuaí MG, novembro 2023.

Paes, V. J. C., Heineck, C. A., & Drumond, J. B. V. (2010). Folha SE.24-V-A-IV Itaobim. Programa Geologia do Brasil, 1:100000. Belo Horizonte: CPRM

Paes, V. J. C., Santos, L. D., Tedeschi, M. F. (2016). *Avaliação do Potencial do Lítio no Brasil: Área do Médio Rio Jequitinhonha, Nordeste de Minas Gerais*. Programa Geologia do Brasil. CPRM.

Paiva, G. (1946). Províncias Pegmatíticas do Brasil. *Boletim DNPM/DFPM, 78*, 13–21.

Papadimitriou, A. G., Bouckovalas, G. D., Andrianopoulos, K. I. (2014). Methodology for estimating seismic coefficients for performance-based design of earthdams and tall embankments. Soil Dynamics and Earthquake Engineering, 56, 57-73.

Paulo F. A., Braga A., Sílvia C. A., França A., & dos Santos, R. L. C. (2010). Panorama da indústria do lítio no Brasil. In *II simpósio de minerais industriais do Nordeste* (pp. 237–247). CETEM Centro de Tecnologia Mineral, Ministério de Ciência e Tecnologia.

Pedrosa-Soares A. C., Correia-Neves J. M., & Leonardos O. H. (1990). Tipologia dos pegmatitos de Coronel Murta—Virgem da Lapa, Médio Jequitinhonha, MG. *Revista Escola de Minas,* 44–54.

Pedrosa-Soares, A. C. (1997). *Mapa Geológico da Folha Araçuaí, Minas Gerais, Brasil*. Belo Horizonte, Projeto Espinhaço, 1:100.000. Mapa e relatório, CODEMIG. http://www.portalgeologia.com.br/index.php/mapa

Pedrosa-Soares, A. C., Alkmim, F. F., Tack, L., Noce, C. M., Babinski, M., Silva, L. C., & Martins-Neto, M. A. (2008). Similarities and differences between the Brazilian and African counterparts of the Neoproterozoic Araçuaí-West Congo orogen. *Geological Society, London, Special Publications, 294*, 153–172. https://doi.org/10.1144/SP294.9

Pedrosa-Soares, A. C., Baars, F. J., Lobato, L. M., Magni, M. C. V., & Faria, L. F. (1993). Arquitetura tectono-metamórfica do setor central da Faixa Araçuaí e suas relações com o Complexo Guanhães. In *4 Simpósio Nacional de Estudos Tectônicos, Belo Horizonte* (pp. 176–182). SBG Núcleo MG.

Pedrosa-Soares, A. C., Chaves, M., & Scholz, R. (2009). Eastern Brazilian Pegmatite Province. *PEG 2009, Fieldtrip Guide*. https://www.researchgate.net/publication/234037120EasternBrazilian_PegmatiteProvince

Pedrosa-Soares, A. C., de Campos, C. P., Noce, C., Silva, L. C., Novo, T., Roncato, J., Medeiros, S., Castañeda, C., Queiroga, G., Dantas, E., Dussin, I., & Alkmim, F. (2011). Late Neoproterozoic-Cambrian granitic magmatism in the Araçuaí orogen (Brazil), the Eastern Brazilian Pegmatite Province and related mineral resources. *Geological Society, London, Special Publications, 350*, 25–51. https://doi.org/10.1144/SP350.3

Pedrosa-Soares, A. C., Deluca, C., Araujo, C. S., Gradim, C. S., Lana, C. C., Dussin, I., Silva, L. C., & Babinski, M. (2020). Capítulo 11: O Orógeno Araçuaí à luz da Geocronologia: um tributo a Umberto Cordani. In A. Bartorelli, W. Teixeira, & B. V. Brito Neves (Orgs.), *Geocronologia e evolução tectônica do Continente Sul-Americano: a contribuição de Umberto Giuseppe Cordani* (pp. 250–272). Solaris Edições Culturais.

Pedrosa-Soares, A. C., Diniz, H. B., Costa, C. H. C., Victoria, A., Guimarães, A., Guimarães, F., Silva, G., Wisniowski, L. & Serrano, P. (2025). Lithium in the Eastern Brazilian Pegmatite Province: A synthesis highlighting spodumene-rich deposits. *Economic Geology*, *120* (5), 1331–1370. https://doi.org/10.5382/econgeo.5175

Pedrosa-Soares, A. C., Leonardos, O. H., & Correia-Neves, J. M. (1984). Aspectos metamórficos de sequências supracrustais da Faixa Araçuaí em Minas Gerais. In *Congresso Brasileiro de Geologia, 33, Rio de Janeiro, Anais, 6* (pp. 3056–3065). Sociedade Brasileira de Geologia.

Pedrosa-Soares, A. C., Leonardos, O. H., Ferreira, J. C. H., & Reis, L. B. (1996). Duplo Regime Metamórfico na Faixa Araçuaí: Uma reinterpretação à luz de novos dados. In *XXXIX Congresso Brasileiro De Geologia, 1996, Salvador* (Volume 6, pp. 5–9). SBG Núcleo Bahia-Sergipe.

Pedrosa-Soares, A. C., Monteiro, R., Correia-Neves, J. M., Leonardos, O. H., & Fuzikawa, K. (1987). Metasomatic evolution of granites, Northeast Minas Gerais, Brazil. *Revista Brasileira de Geociências, 17*, 512–518.

Pedrosa-Soares, A. C., Noce, C. M., Wiedemann, C. M., & Pinto, C. P. (2001). The Araçuaí-West-Congo Orogen in Brazil: an overview of a confined orogen formed during Gondwanaland assembly. *Precambrian Research, 110*, 307–323. https://doi.org/10.1016/S0301-9268(01)00174-7

Pedrosa-Soares, A. C., Pinto, C. P., Custódio Netto, Araújo, M. C., Castañeda, C., Achtschin, A. B., & Basilio, M. S. (2001). A Província Gemológica Oriental do Brasil. In C. Castañeda, J. E. Addad, & A. Liccardo (Orgs.), *Gemas de Minas Gerais* (1st ed., pp. 16–33). Sociedade Brasileira de Geologia-Núcleo Minas Gerais.

Pedrosa-Soares, A. C., Romeiro, J. C. P., Castañeda, C. (1997). Papel do Controle Estrutural de Pegmatitos Graníticos em suas Mineralizações. In *VI Simpósio Nacional de Estudos Tectônicos* (pp. 357–359). SBG-Núcleo Brasília.

Pedrosa-Soares, A., Chavez, M., &Scholz, R. (2009). *Field Trip Guide Eastern Brazilian Pegmatite Provinces*. 4th International Symposium on Granitic Pegmatite.

Peixoto, A., Ferreira, D., & Mattos, I. (2016). *Catálogo de minerais do laboratório de mineralogia. Universidade Federal do Ceará*. Centro de Ciências, Departamento de Geologia. https://geologia.ufc.br/wp-content/uploads/2017/05/catalogo-mineralogia.pdf

Peixoto, E., Alkmim, F. F., Pedrosa-Soares, A., Lana, C., & Chaves, A. O. (2017). Metamorphic record of collision and collapse in the Ediacaran-Cambrian Araçuaí orogen, SE-Brazil: Insights from P-T pseudosections and monazite dating. *Journal of Metamorphic Geology, 3*.

Planvale (1994). Plano diretor de recursos hídricos para os vales do rio Jequitinhonha e Pardo. Governos MG e BA/Geotécnica/Consultants. R1 Relatório de Diagnóstico, an. B-Hidrogeologia.

Potvin, Y. (1988). Empirical open stope design in Canada. Ph.D. Thesis, Dept. Mining and Mineral Processing, University of British Columbia, 343 p.

Pöllmann, H., & König, U. (2021). Monitoring of Lithium Contents in Lithium Ores and Concentrate-Assessment Using X-ray Diffraction (XRD). *Minerals, 11*, 1058. https://doi.org/10.3390/min11101058

Quemeneur, J., & Lagache, M. (1999). Comparative Study of Two Pegmatitic Field from Minas Gerais, Brazil, using the Rb and Cs Contents of Mica and Feldspars. *Revista Brasileira de Geociencias, 29*(1), 27–32.

Read, J., & Stacey, P. (2009). *Guidelines for open pit slope design*. CRC Press/Balkema.

Revuelta, M. B., (2018). *Mineral resources: from exploration to sustainability assessment*. Springer.

Romeiro, J. C. P. (1998). Controle da mineralização de lítio em pegmatitos da Mina da Cachoeira, Companhia Brasileira de Lítio, Araçuaí, MG [Unpublished Master's thesis]. Instituto de Geociências, UFMG.

Romeiro, J. C., & Pedrosa-Soares, A. C. (2005). Controle do minério de espodumênio em pegmatitos da Mina da Cachoeira, Araçuaí, MG. *Geonomos, 13*, 75–85.

Sá, J. H. Silva, & Afgouni, K. (1978). Lithium Ore in Brazil. *Energy, 3*, 247–253.

Sá, J. H. S. (1977). Pegmatitos litiníferos da região de Itinga-Araçuaí, Minas Gerais [Unpublished doctoral dissertation]. Universidade de São Paulo.

Saadi., A., & Pedrosa-Soares, A. C. (1990). Um graben cenozóico no Médio Jequitinhonha, Minas Gerais. In *Workshop sobre Neotectônica e Sedimentação Cenozoica Continental no Sudeste Brasileiro* (Boletim, Sociedade Brasileira de Geologia Nucleo Minas Gerais, n.11 pp. 101–124). Sociedade Brasileira de Geologia Nucleo Minas Gerais.

Sahoo, S. K., Tripathy, S. K., Nayak, A., Hembrom, A. C, Dey, S., Rath, R. K., & Mohanta, M. K. (2022). Beneficiation of lithium bearing pegmatite rock: a review. *Mineral Processing and Extractive Metallurgy Review, 45*, 1–27.

Sampaio, J. A., & Braga, P. F. A. (2007). Ensaios em espirais concentradoras. In J. A. Sampaio, S. C. A. França, & P. F. A. Braga (Eds.), *Tratamento de Minérios: práticas laboratoriais* (pp. 281–293). CETEM/MCTI.

Santos, R. F., Alkmim, F. F., & Pedrosa-Soares, A. C. (2009). A Formação Salinas, Orógeno Araçuaí, MG: História deformacional e significado tectônico. *Revista Brasileira de Geociências, 39*, 81–100.

Sarubbi, A. (2025). Magnetic Separation—Amenability Tests. Steinert, July 14, 2025.

Seed, H. B., & Martin, G. R. (1966). The Seismic Coefficient in Earth Dam Design. Journal of the Soil Mechanics and Foundations Division, 92(3), 25-58.

Amaral, R., Ferreira, R., & Savassi, O. (2025, October 3). *Ensaios de flotação aberta e LCT*. SGS Prepared by SGS Geosol for MGLIT Empreendimentos Ltda.

de Faria, A. A. (2022). *Preliminary testwork, Final Report Rev 01*, Lithium Ionic/MGLIT, Lithium Project, December 22, 2022. SGS Geosol.

SGS Geosol: de Faria, A. A. (2025). *Variability Study 2025 – Projeto Bandeira*, Lithium Ionic/MGLIT, Lithium Project, October 10, 2025.

Silva Santos Rocha, L. (2023, January 25). QA/QC *Assessment: Lithium Ionic Corp 2022 Diamond Drilling Campaign Results—Draft Technical Memo*. Project 220210. Prepared by GE21 Consultoria Mineral Ltda. for Lithium Ionic.

Silva, C. J. E., Abrantes, B. H. A., Ferreira, G. G., & Bergman, P. (2023, November 30). *Bandeira Project, Araçuaí and Itinga, Minas Gerais State, Brazil, Independent Technical Report—Preliminary Economic Assessment Independent Technical Report* (Effective date: August 30, 2023). Prepared by GE21 Ltda. for Lithium Ionic Corp.

Silva, C. J. E., Rocha, L., & Bergman, P. (2024, May 27). *NI 43-101 Technical Report—Mineral Resource Update on Bandeira Project, Araçuaí and Itinga, Minas Gerais State, Brazil* (Effective date: March 5, 2024). Prepared by GE21 Consultoria Mineral Ltda. for Lithium Ionic.

Silva, C. J. E., & Bergmann, P. R. (2025, March 26). *NI 43-101 Independent Technical Report—Mineral Resource Update on Bandeira Project, Araçuaí and Itinga, Minas Gerais State, Brazil* (Effective date: November 20, 2024). Prepared by GE21 Consultoria Mineral Ltda. for Lithium Ionic Corp.

Simmons, W. B., Webber, K. L., Falster, A. U., & Nizamoff, J. W. (2003). *Pegmatology: Pegmatite Mineralogy, Petrology and Petrogenesi*s. Rubellite Press.

Sistema Estadual de Meio Ambiente e Recursos Hídricos (2024). IDE - Sisema. https://idesisema.meioambiente.mg.gov.br/webgis

Spix, J. B. von, & Martius, C. F. P., von. (1823). *Viagem pelo Brasil*, Volume 2. Imprensa Nacional.

Stevanato, R., Intergeo Comércio E Serviços Em Geofísica Aplicada Ltda – Me. (2022). *Projeto Lítio – Araçuaí-MG (Polarização Induzida e Resistividade na Exploração Mineral)*. Prepared for MGLIT Empreendimentos Ltda & Grupo GE21.

Veras, M. M. (2018). *Detecção de minério portador de elementos de terras raras do depósito de Pitinga/AM, Brasil assistido por tecnologia de* sensor-based sorting [Master's thesis, Universidade Federal do Rio Grande do Sul, Porto Alegre]. https://1library.org/document/z3j6068y-deteccao-minerio-portador-elementos-deposito-pitinga-assistido-tecnologia.html

Veras, M. M., Young, A. S., Sampaio, C. H., & Petter, C. O. (2016). A mining breakthrough: preconcentration by sensor-based sorter. *Mining Engineering Magazine, 1*, 38–42.

Viana, R. R., Manttari, I., Kunst, H., & Jordt-Evangelista, H. (2003). Age of Pegmatites from Eastern Brazil and Implication of Mica Intergrowths on Cooling Rates and Age Calculation. *Journal of South American Earth Sciences, 16*, 493–501.

Villaescusa, E. (2014). *Geotechnical Design for Sublevel Open Stoping*. CRC Press.

Wills, B. A. (1988). *Mineral Processing Technology* (4th ed.). Pergamon Press.

Wills, B. A., & Napier-Munn, T. J. (2006*). Wills' mineral processing technology: an introduction to the practical aspects of ore treatment and mineral recovery* (7th ed.). Elsevier.

Wotruba, H., & Harbeck, H. (2010). *Sensor-Based Sorting. Ullmann's Encyclopedia of Industrial Chemistry* (Volume 32, pp. 395–404). Wiley.

Young, A. S. (2017). Uso da separação automática por sensor de raio X na pré-concentração de minérios: ferro e zinco [Master's thesis, Universidade Federal do Rio Grande do Sul, Porto Alegre]. LUME Repositorio Digital. https://www.lume.ufrgs.br/bitstream/handle/10183/178315/001064746.pdf?sequence=1

28 CERTIFICATE OF AUTHORS

28.1 Brian Colin Talbot, Chemical Engineer, BSc (Hons), FAusIMM

I, Brian Colin Talbot, Chemical Engineer, as a Qualified Person of this report titled *Bandeira Lithium Project, National Instrument 43-101 Technical Report—Definitive Feasibility Study Update, Araçuaí–Itinga, Minas Gerais, Brazil* (the Technical Report), with an effective date of September 17, 2025, prepared for Lithium Ionic and dated October 31, 2025, do hereby certify that:

1. I am a Chemical Engineer, with a business address at Unit No: 643, DMCC Business Centre, Level No 1, Jewellery and Gemplex 3, Dubai, United Arab Emirates
2. I am a graduate of University of Witwatersrand, Johannesburg, South Africa (1994) with a degree of bachelor's in chemical engineering (Honours). I am Fellow 3001296 of the Australasian Institute of Mining and Metallurgy.
3. I have practiced my profession for 30 years since the beginning of my Bachelor's degree.
4. I have read the definition of "qualified person" set out in National Instrument 43-101 (NI 43-101)and certify that by reason of my education, affiliation with a professional association (as defined in NI 43-101) and past relevant work experience, I fulfill the requirements to be a "qualified person "for the purposes of NI 43-101.
5. I visited the Bandeira Lithium Project on August 22 and 23, 2024.
6. I am responsible for Section 1.21, 1.25, 21.1, 21.2, 21.3, 21.4.1, 21.4.3, 21.4.9, 21.4.10, 21.5,25.9 and 25.10 of the Technical Report.
7. I am independent of the Issuer applying all the tests set out in Section 1.5 of the Instrument.
8. I have had no prior involvement with the property that is the subject of the Technical Report.
9. I have read NI 43-101, and the Technical Report has been prepared in compliance with NI 43-101and Form 43-101F1.
10. At the effective date of the Technical Report, to the best of my knowledge, information, and belief, the Technical Report contains all scientific and technical information that is required to be disclosed to make the Technical Report not misleading.
11. I have read the News Release dated September 17, 2025, and confirm it is a fair and accurate summary of my sections of this report.
12. I consent to the filing of the Technical Report with any stock exchange and other regulatory authority and any publication by them for regulatory purposes, including electronic publication in the public company files on their websites accessible by the public, of the Technical Report.

Dated this 31st day of October 2025, at Toronto, Ontario, Canada.

Original Signed and Sealed
Brian Colin Talbot, Chemical Engineer,
BSc (Hons), FAusIMM

28.2 Carlos José Evangelista Silva, P.Geo., MSc, AIG

I, Carlos José Evangelista Silva, Geologist, MSc., AIG, as a Qualified Person of this report titled Bandeira Lithium Project, National Instrument 43-101 Technical Report—Definitive Feasibility Study Update, Araçuaí–Itinga, Minas Gerais, Brazil (the Technical Report), with an effective date of September 17, 2025, prepared for Lithium Ionic and dated October 31, 2025, do hereby certify that:

1. I am a geologist at GE21 Consultoria Mineral, whose business address is on the 12th floor, 3130 Afonso Pena Ave, Belo Horizonte, Brazil.
2. I am a graduate of the Federal University of Minas Gerais (UFMG) in Belo Horizonte, Brazil (2005) with Bachelor´s degree in Geology and have a master's degree in engineering in Mineral Technology from the Postgraduate Program in Mining, Metallurgical and Materials Engineering (PPGE3M) at the Federal University of Rio Grande do Sul, Brazil (2020). I have been Fellow 7868 of the Australian Institute of Geoscientists since 2021.
3. I have practiced my profession for 18 years since my graduation.
4. I have read the definition of "qualified person" set out in National Instrument 43-101 (NI 43-101) and certify that by reason of my education, affiliation with a professional association (as defined in NI 43-101) and past relevant work experience, I fulfill the requirements to be a "qualified person" for the purposes of NI 43-101.
5. I visited the Bandeira Lithium Project on September 13 and 14, 2023; December 12, 2023; and November 26 and 27, 2024.
6. I am responsible for Sections 1.4, 1.5, 1.6, 1.7, 1.8, 1.9, 1.10, 1.11, 1.12, 1.14, 1.23, 1.24, 1.25, 1.26, 4, 5, 6, 7, 8, 9, 10, 11, 12, 14, 23, 24, 25.1 and 26.1 of the Technical Report.
7. I am independent of the Issuer applying to all of the tests set out in Section 1.5 of the Instrument.
8. I have had no prior involvement with the property that is the subject of the Technical Report.
9. I have read NI 43-101, and the Technical Report has been prepared in compliance with NI 43-101 and Form 43-101F1.
10. At the effective date of the Technical Report, to the best of my knowledge, information, and belief, the Technical Report contains all scientific and technical information that is required to be disclosed to make the Technical Report not misleading.
11. I have read the News Release Dated September 17, 2025, and confirm it is a fair and accurate summary of my sections of this report.
12. I consent to the filing of the Technical Report with any stock exchange and other regulatory authority and any publication by them for regulatory purposes, including electronic publication in the public company files on their websites accessible by the public, of the Technical Report.

Dated this 31st day of October 2025, at Toronto, Ontario, Canada.

Original Signed and Sealed
Carlos José Evangelista Silva, MSc, AIG, Geologist
GE21 Consultoria Mineral

28.3 Hugo Ribeiro de Andrade Filho, P.Eng., FAusIMM

I, Hugo Ribeiro de Andrade Filho, FAusIMM(CP), Mining Engineer and Project Manager, as an author of this report titled Bandeira Lithium Project, National Instrument 43-101 Technical Report—Definitive Feasibility Study Update, Araçuaí–Itinga, Minas Gerais, Brazil (the Technical Report), with an effective date of September 17, 2025, prepared for Lithium Ionic and dated October 31, 2025, do hereby certify that:

1. I am a Senior Mining Engineer Consultant, with a business address on 9th Floor, Room 909, 1222, Tancredo Neves Avenue, CEP 41.820-020, Salvador, Bahia, Brazil.
2. I am a graduate of the Federal University of Bahia (UFBA), Araújo Pinho Avenue, Canela, Salvador, Bahia, Brazil (1997) with a bachelor's degree in mining engineering and a postgraduate certificate (MBA) in Project Management from IBMEC (2022).
3. I am a registered member in good standing of the Regional Council of Engineering and Agronomy (CREA 29-862/D) in the state of Bahia.
4. I am a Fellow of the Australian Institute of Mining and Metallurgy (AusIMM) and accredited as a Chartered Professional (Membership Nº 323096).
5. I have over 25 years of experience in mine design, planning, evaluation, mining regulatory review and reporting, Mineral Reserve estimation, and development of precious and base metal projects.
6. I have read the definition of Qualified Person set out in NI 43-101 and certify that by reason of education, affiliation with a professional association, and past relevant work experience, I fulfill the requirements to be a Qualified Person for NI 43-101.
7. I am responsible for Section 1.15, 1.16, 1.25, 1.26, 15, 16, 21.4.2, 21.4.7, 21.4.8, 25.5, 25.6, 25.7 and 26.2 of this Technical Report.
8. I am independent of the Issuer applying to all of the tests set out in Section 1.5 of the Instrument.
9. I have had no prior involvement with the property that is the subject of the Technical Report.
10. I have read NI 43-101, and the Technical Report has been prepared in compliance with NI 43-101 and Form 43-101F1.
11. At the effective date of the Technical Report, to the best of my knowledge, information, and belief, the Technical Report contains all scientific and technical information that is required to be disclosed to make the Technical Report not misleading.
12. I have read the News Release Dated September 17, 2025, and confirm it is a fair and accurate summary of my sections of this report.
13. I consent to the filing of the Technical Report with any stock exchange and other regulatory authority and any publication by them for regulatory purposes, including electronic publication in the public company files on their websites accessible by the public, of the Technical Report.

Dated this 31st day of October 2025, at Toronto, Ontario, Canada.

Original Signed and Sealed

Hugo R. A Filho, P.Eng.
Senior Mining Engineer

28.4 Juliano Felix de Lima, MAIG (CP)

I, Juliano Felix de Lima, MAIG (CP), Geological Engineer and Project Manager, as a Qualified Person of this report titled *Bandeira Lithium Project, National Instrument 43-101 Technical Report—Definitive Feasibility Study Update, Araçuaí–Itinga, Minas Gerais, Brazil* (the Technical Report), with an effective date of September 17, 2025, prepared for Lithium Ionic and dated October 31, 2025, do hereby certify that:

1. I am a Senior Geological Engineer, with a business address on 12th Floor, 3130, Afonso Pena Avenue, CEP 30130-910, Belo Horizonte, Minas Gerais, Brazil.
2. I am a graduate of the Federal University of Ouro Preto (UFOP), Ouro Preto, Minas Gerais, Brazil (1999) with a Bachelor's degree in Geological Engineering, and a postgraduate certificate (MBA) in Project Management from Fundação Getúlio Vargas (2015).
3. I am Registered with the Regional Council of Engineering and Agronomy (CREA 71.382/D) in the state of Minas Gerais, and a Member of the Australian Institute of Geology and accredited as a Chartered Professional (Membership Nº 9180).
4. I have over 25 years of experience in exploration, mine geology, mine design, mining sequencing, mine management, regulatory review and reporting, Mineral Resources estimation, and development of industrial, precious and base metal projects.
5. I have read the definition of Qualified Person set out in NI 43-101 and certify that by reason of education, affiliation with a professional association, and past relevant work experience, I fulfill the requirements to be a Qualified Person for NI 43-101.
6. I am responsible for Section 1.18, 1.25, 1.26, 18, 25.3 and 26.3 related to mining geology and rock mechanics, this Technical Report.
7. I am independent of the Issuer applying all the tests set out in Section 1.5 of the Instrument.
8. I have had no prior involvement with the property that is the subject of the Technical Report.
9. I have read NI 43-101, and the Technical Report has been prepared in compliance with NI 43-101 and Form 43-101F1.
10. At the effective date of the Technical Report, to the best of my knowledge, information, and belief, the Technical Report contains all scientific and technical information that is required to be disclosed to make the Technical Report not misleading.
11. I have read the News Release dated September 17, 2025, and confirm it is a fair and accurate summary of my sections of this report.
12. I consent to the filing of the Technical Report with any stock exchange and other regulatory authority and any publication by them for regulatory purposes, including electronic publication in the public company files on their websites accessible by the public, of the Technical Report.

Dated this 31st day of October 2025, at Toronto, Ontario, Canada.

Original Signed and Sealed
Juliano Felix de Lima, MAIG (CP)
Senior Geological Engineer

28.5 Porfirio Cabaleiro Rodriguez, P.Eng., BSc, FAIG

I, Porfirio Cabaleiro Rodriguez, P.Eng., BSc, FAIG, as a Qualified Person of this report titled *Bandeira Lithium Project, National Instrument 43-101 Technical Report—Definitive Feasibility Study Update, Araçuaí–Itinga, Minas Gerais, Brazil* (the Technical Report), with an effective date of September 17, 2025, prepared for Lithium Ionic and dated October 31, 2025, do hereby certify that:

1. I am a Technical Director of GE21 Consultoria Mineral, with a business address at 12th floor, 3130, Afonso Pena Avenue, CEP 30.130-190, Belo Horizonte, Brazil.
2. I am a graduate in Mining Engineer of the Federal University of Minas Gerais (UFMG), in Belo Horizonte, Brazil, and I have been Fellow 3708 of the Australian Institute of Geoscientists since 2008.
3. I have practiced my profession for 47 years since my graduation.
4. I have read the definition of “qualified person” set out in National Instrument 43-101 (NI 43-101) and certify that by reason of my education, affiliation with a professional association (as defined in NI 43-101) and past relevant work experience, I fulfill the requirements to be a "qualified person" for the purposes of NI 43-101.
5. I have not visited the Bandeira Lithium Project site.
6. I am responsible for Section 1.1, 1.2, 1.3, 1.19, 2, 3, and 19 of the Technical Report.
7. I am independent of the Issuer applying to all the tests set out in Section 1.5 of the Instrument.
8. I have had no prior involvement with the property that is the subject of the Technical Report.
9. I have read NI 43-101, and the Technical Report has been prepared in compliance with NI 43-101 and Form 43-101F1.
10. At the effective date of the Technical Report, to the best of my knowledge, information, and belief, the Technical Report contains all scientific and technical information that is required to be disclosed to make the Technical Report not misleading.
11. I have read the News Release dated September 17, 2025, and confirm it is a fair and accurate summary of my sections of this report.
12. I consent to the filing of the Technical Report with any stock exchange and other regulatory authority and any publication by them for regulatory purposes, including electronic publication in the public company files on their websites accessible by the public, of the Technical Report.

Dated this 31st day of October 2025, at Toronto, Ontario, Canada.

Original Signed and Sealed
Porfirio Cabaleiro Rodriguez, P.Eng., BSc, FAIG
GE21 Consultoria Mineral
Technical Director, Mining Engineer

28.6 João Augusto Hilário de Souza, B.A.Sc., MBA

I, João Augusto Hilário de Souza, B.A.Sc., MBA, (MAIG) #4084, as a Qualified Person of this report titled *Bandeira Lithium Project, National Instrument 43-101 Technical Report—Definitive Feasibility Study Update, Araçuaí–Itinga, Minas Gerais, Brazil* (the Technical Report), with an effective date of September 17, 2025, prepared for Lithium Ionic and dated October 31, 2025, do hereby certify that:

1. I am a senior Mining Engineer and Associate Consultant at L&M Assessoria, with a business address at Rua Senhora das Graças, 99/1002, Belo Horizonte, MG, Brasil, CEP 30.310-130.
2. I am a graduate of the Federal University of Minas Gerais (UFMG), in Belo Horizonte, Brazil (1976), with a Bachelor´s degree in Mining Engineering; completed a Geostats Specialization at the Federal University of Ouro Preto (UFOP), Brazil (1979); Master Business Administration at USP, Brazil (2002). I am a Registered Mining Engineer in the Conselho Regional de Engenharia e Agronomia (Crea–MG 16.917 and National–140610073-0) in the state of Minas Gerais. I have been a member of the Australian Institute of Geoscientists (AIG) since 2009 and of the Sociedade Mineira dos Engenheiros (SME) since 1977.
3. I have practiced my profession for more than 40 years since graduation.
4. I have read the definition of “qualified person” set out in National Instrument 43-101 (NI 43-101) and certify that by reason of my education, affiliation with a professional association (as defined in NI 43-101) and past relevant work experience, I fulfill the requirements to be a "qualified person" for the purposes of NI 43-101.
5. I visited the Bandeira Lithium Project from January 17 to 19, 2024.
6. I am responsible for Sections 1.22, 1.25, 21.4.4, 21.4.5, 21.4.6, 22 and 25.11 of the Technical Report.
7. I am independent of the Issuer applying all of the tests set out in Section 1.5 of the Instrument.
8. I have had no prior involvement with the property that is the subject of the Technical Report.
9. I have read NI 43-101, and the Technical Report has been prepared in compliance with NI 43-101 and Form 43-101F1.
10. At the effective date of the Technical Report, to the best of my knowledge, information, and belief, the Technical Report contains all scientific and technical information that is required to be disclosed to make the Technical Report not misleading.
11. I have read the News Release Dated September 17, 2025, and confirm it is a fair and accurate summary of my sections of this report.
12. I consent to the filing of the Technical Report with any stock exchange and other regulatory authority and any publication by them for regulatory purposes, including electronic publication in the public company files on their websites accessible by the public, of the Technical Report.

Dated this 31st day of October 2025, at Toronto, Ontario, Canada.

Original Signed and Sealed
João Augusto Hilario de Souza, B.A.Sc., MBA
Associate Consultant
L&M Assessoria Empresarial S.S. Ltda (L&M)

28.7 Noel Mark O'Brien, BE(Met), MBA, FAusIMM

I, Noel Mark O'Brien, BE(Met), Metallurgical Engineer, as a Qualified Person of this report titled *Bandeira Lithium Project, National Instrument 43-101 Technical Report—Definitive Feasibility Study Update, Araçuaí–Itinga, Minas Gerais, Brazil* (the Technical Report), with an effective date of September 17, 2025, prepared for Lithium Ionic and dated October 31, 2025, do hereby certify that:

1. I am a Metallurgical Consultant, with a business address of 76 Stockdale Crescent, Wembley Downs, 6019, Perth, Western Australia.
2. I am a graduate of University of Melbourne, Victoria, Australia (1972) with a bachelor's degree in metallurgical engineering, and a Master of Business Administration degree from The University of the Witwatersrand, South Africa (1982). I am Fellow 226758 of the Australasian Institute of Mining and Metallurgy.
3. I have practiced my profession for 50 years, since the beginning of my bachelor's degree.
4. I have read the definition of "qualified person" set out in National Instrument 43-101 (NI 43-101) and certify that by reason of my education, affiliation with a professional association (as defined in NI 43-101) and past relevant work experience, I fulfill the requirements to be a "qualified person" for the purposes of NI 43-101.
5. I have not visited the Bandeira Lithium Project site.
6. I am responsible for Sections 1.13, 1.17, 1.25, 1.26, 13, 17, 25.2, and 26.4 of this Technical Report.
7. I am independent of the Issuer applying to all of the tests set out in Section 1.5 of the Instrument.
8. I have had no prior involvement with the property that is the subject of the Technical Report.
9. I have read NI 43-101, and the Technical Report has been prepared in compliance with NI 43-101 and Form 43-101F1.
10. At the effective date of the Technical Report, to the best of my knowledge, information, and belief, the Technical Report contains all scientific and technical information that is required to be disclosed to make the Technical Report not misleading.
11. I have read the News Release Dated September 17, 2025, and confirm it is a fair and accurate summary of my sections of this report.
12. I consent to the filing of the Technical Report with any stock exchange and other regulatory authority and any publication by them for regulatory purposes, including electronic publication in the public company files on their websites accessible by the public, of the Technical Report.

Dated this 31st day of October 2025, at Toronto, Ontario, Canada.

Original Signed and Sealed
Noel Mark O'Brien, BE(Met), MBA, FAusIMM
Metallurgical Consultant

28.8 Bernardo Horta de Cerqueira Viana, MBA, FAIG

I, Bernardo Horta de Cerqueira Viana, Geologist, MBA, as a Qualified Person of this report titled *Bandeira Lithium Project, National Instrument 43-101 Technical Report—Definitive Feasibility Study Update, Araçuaí–Itinga, Minas Gerais, Brazil* (the Technical Report), with an effective date of September 17, 2025, prepared for Lithium Ionic and dated October 31, 2025, do hereby certify that:

1. I am a Geologist, with a business address at GE21 Consultoria Mineral, 12th Floor, 3130, Afonso Pena Avenue, CEP 30.130-910, Belo Horizonte, Minas Gerais, Brazil.
2. I am a graduate of the Federal University of Minas Gerais (UFMG, 2001), and I am registered with the Regional Council of Engineering and Agronomy (83150/D) in the state of Minas Gerais. I am a Fellow of the Australian Institute of Geoscientist (FAIG) (# 3709). I have been the CEO of GE21 Mineral Consulting Group (www.grupoge21.com.br) since 2015.
3. I have practiced my profession for 22 years since graduation.
4. I have read the definition of Qualified Person set out in NI 43-101 and certify that by reason of education, affiliation with a professional association, and past relevant work experience, I fulfill the requirements to be a Qualified Person for NI 43-101.
5. I have not visited the Bandeira Lithium Project site.
6. I am responsible for Section 1.20, 1.25, 1.26, 20, 25.4, 25.8 and 26.5 of the Technical Report.
7. I am independent of the Issuer applying all of the tests set out in Section 1.5 of the Instrument.
8. I have had no prior involvement with the property that is the subject of the Technical Report.
9. I have read NI 43-101, and the Technical Report has been prepared in compliance with NI 43-101 and Form 43-101F1.
10. At the effective date of the Technical Report, to the best of my knowledge, information, and belief, the Technical Report contains all scientific and technical information that is required to be disclosed to make the Technical Report not misleading.
11. I have read the News Release dated September 17, 2025, and confirm it is a fair and accurate summary of my sections of this report.
12. I consent to the filing of the Technical Report with any stock exchange and other regulatory authority and any publication by them for regulatory purposes, including electronic publication in the public company files on their websites accessible by the public, of the Technical Report.

Dated this 31st day of October 2025, at Toronto, Ontario, Canada.

Original Signed and Sealed
Bernardo Horta de Cerqueira Viana, MBA, FAIG
CEO of GE21 Group